Triggered Pluripotency During *Kalanchoë* Plantlet Development

A thesis submitted to the University of Manchester for the degree of

Doctor of Philosophy

in the Faculty of Biology, Medicine and Health

2021

JOO PHIN OOI

SCHOOL OF BIOLOGICAL SCIENCES

DIVISION OF MOLECULAR AND CELLULAR FUNCTION

TABLE OF CONTENTS

Final word count: 58, 323 words

LIST OF FIGURES

LIST OF TABLES

LIST OF ABBREVIATIONS

ABA	Abscisic acid
ABCG11	ATP-BINDING CASSETTE G11
ABI3	ABSCISIC ACID INSENSITIVE3
AFL	ABI3, FUS3, LEC2
AG	AGAMOUS
AHP1/2/3/4/5	ARABIDOPSIS THALIANA HISTIDINE-CONTAINING PHOSPHOTRANSFER PROTEIN 1/2/3/4/5
AHP6	ARABIDOPSIS THALIANA PSEUDP HISTIDINE-CONTAINING PHOSPHOTRANSFER PROTEIN
AIL6	AINTEGUMENTA-LIKE 6
AP2	APETALA2
APM1	AMINOPEPTIDASE M1
ARF	AUXIN RESPONSE FACTOR
ARRs	ARABIDOPSIS RESPONSE REGULATOR
AUX1	AUXIN-RESISTANT 1
BAM	BARELY ANY MERISTEM
BAP	6-Benzylaminopurine
BBM	BABYBOOM
BP	BREVIPEDICELLUS
C2	C2 DOMAIN PROTEIN
CAM	Crassulacean Acid Metabolism
CAM5	CALMODULIN 5
CIPK11	CBL-INTERACTING SERINE/THREONINE-PROTEIN KINASE 11
CKI	CYTOKININ INSENSITIVE
CLV1/2/3	CLAVATA 1/2/3
COL	CONSTANS-LIKE
CUC1/2/3	CUP-SHAPED COTYLEDON 1/2/3
DEG	Differentially Expressed Genes
DREB2C	DEHYDRATION-RESPONSIVE ELEMENT-BINDING 2CP
EDE1	ENDOSPERM DEFECTIVE 1
EDTA	Ethylenediaminetetraacetic Acid
FDR	False Discovery Rate
FON1	FLORAL ORGAN NUMBER
FUS3	FUSCA 3
GA	Giberrelic Acid
GAPDH	GLYCERALDEHYDE 3-PHOSPHATE DEHYDROGENASE
GFP	Green Fluorescent Protein
GO	Gene Ontology
GOS1	GASSHO1
GPAT1	GLYCEROL-3-PHOSPHATE SN-2-ACYLTRANSFERASE
GUS	B-Glucuronidase

HAM1/2	HAIRY MERISTEM
HAP3	HEME-ACTIVATED PROTEIN3
HP1/2/3/4/5	HISTIDINE-CONTAINING PHOSPHOTRANSFER PROTEIN
IAA	Indole-3-Acetic Acid
IPA	Indole-3-Pyruvic Acid
JA	Jasmonic Acid
JMT	JASMONIC ACID CARBOXYL METHYLTRANSFERASE
Kd	*Kalanchoë daigremontiana*
KN1	KNOTTED1
KN5	KNOX5
KNAT1	KNOTTED-1 LIKE FROM ARABIDOPSIS THALIANA 1
KNOX/KNOX1	KNOTTED1-LIKE HOMEOBOX 1
Kp	*Kalanchoë pinnata*
L1L	LEC1-LIKE
LAFL	LEC1, LEC2, L1L, ABI3, FUS3
LAX1	LIKE AUX 1
LEC1/2	LEAFY COTYLEDON 1/2
MAP	MITOGEN-ACTIVATED PROTEIN
MAPK	MITOGEN-ACTIVATED PROTEIN KINASE
MIR164A	microRNA164a
MP	MONOPTEROS
MYB94	MYB DOMAIN PROTEIN 94
NAA	1-Naphthaleneacetic Acid
NF-YB	Nuclear Transcription Factor Y Subunit Beta
NOS	NOPALINE SYNTHASE
NTPII	NEOMYCIN PHOSPHOTRANSFERASE II
OC	Organising Centre
PATL5	PATELLIN PROTEIN 5
PCA	Principal Component Analysis
PEG	Polyethylene glycol
PGA6	PLANT GROWTH ACTIVATOR 6
PHP1/2/5/6	PSEUDO HISTIDINE-CONTAINING PHOSPHOTRANSFER PROTEIN
PID	PINOID
PIN1/2/4/5/7/8	PIN-FORMED 1/2/4/5/7/8
PLT1/2/3/4	PLETHORA 1/2/3/4
PP2C5	PROTEIN PHOSPHATASE 2C FAMILY PROTEIN 5
PR3	PATHOGENESIS-RELATED PROTEIN 3
PVP	Polyvinylpyrrolidone
PYL4	PYRABACTIN RESISTANCE-LIKE 4
QC	Quiescent Center
qRT-PCR	quantitative Real Tme-Polymerase Chain Reaction
RAM	ROOT APICAL MERISTEM
RAV1	RELATED TO ABI3/VP1 1

RDUF1	RING AND DOMAIN OF UNKNOWN FUNCTION 1
RHA2A	RING-H2 FINGER A2A
RL1	RAV-LIKE
SAM	Shoot Apical Meristem
SCR	SCARECROW
SEM	Scanning Electron Microscope
SHR	SHORT ROOT
SOC1	SUPPRESSOR OF CONSTANS OVEREXPRESSION 1
SRS5/7	SHI-RELATED SEQUENCE 5/7
SSP	SHORT-SUSPENSOR
STM	SHOOTMERISTEMLESS
STY1	STYLISH 1
TAA	TRYPTOPHAN AMINOTRANSFERASE OF ARABIDOPSIS
TCSn	Two Component Signalling Sensor new
TIBA	2,3,5-Triiodobenzoic Acid
TPL	TOPLESS
TRN1	TORNADO 1
Trp	Tryptophan
UNE15	UNFERTILISED EMBRYO SAC 15
VAL1	VIVIPAROUS ABI3-LIKE1
VP1	VIVIPAROUS 1
WOX2/5/8/9/13	WUSCHEL-RELATED HOMEOBOX 2/5/8/9
WRKY2/23	WRKY DNA-BINDING PROTEIN 2
WUS	WUSCHEL
YPD1	PHOSPHORELAY INTERMEDIATE PROTEIN
YUC1/3/4/9	YUCCA1/3/4/9

THESIS ABSTRACT

In contrast to animal cells, plant cells demonstrate incredible plasticity in terms of cell fate changes. A differentiated plant cell can be triggered to de-differentiate and regain its pluripotency. *Kalanchoë* plants evolved to have a distinctive asexual reproductive strategy by forming plantlets, miniature versions of adult plant on the leaf margin. Previous studies have shown that plantlet formation in *Kalanchoë daigremontiana* involves the process of ectopic embryogenesis, in which differentiated leaf cells de-differentiate and regain totipotent potential to develop into an embryo. However, molecular mechanism(s) underlying this cell fate change during plantlet formation remains elusive. This project aims to uncover genetic mechanisms and hormonal control of plantlet formation through expression analyses of candidate genes, phenotype analyses of transgenic plants and RNA-sequencing analysis. It was found that a late embryogenesis gene, *FUSCA3* has the potential to replace embryogenesis functions of *LEAFY COTYLEDON 1* needed for *K. daigremontiana* plantlet formation. In addition, two key meristem genes, *WUSCHEL* and *CLAVATA1* were required for plantlet formation as these genes were expressed during plantlet development and reduced expression of these genes affected plantlet number and morphology. Auxin was also involved in regulating plantlet formation. Changes in expression of an auxin biosynthesis enzyme gene *YUCCA1* were in seen in transgenic plants with reduced plantlets, and the auxin efflux transporter PIN1 was present at the leaf notches prior to pedestal and plantlet formation. Furthermore, a complex auxin-cytokinin crosstalk might be involved in regulating plantlet formation as plants with reduced expression of a putative cytokinin signalling inhibitor, *KdaHP*, exhibited irregular plantlet formation and was also accompanied by changes in *YUCCA1* expression. Moreover, *KdaHP* was highly expressed during wild-type plantlet development and novel cytokinin activity was observed during early plantlet formation. *K. daigremontiana* forms plantlets constitutively whereas *K. pinnata* forms plantlets only upon stress induction. RNA-sequencing showed that there were more unique than shared biological processes involved in regulating *K. daigremontiana* and *K. pinnata* plantlet formation. Although further studies are required, this work has illustrated novel insights into the molecular mechanisms of plantlet formation. Transcriptome analysis of *Kalanchoë* plantlet formation and molecular experiments presented in this study will be pioneering sources of information for future studies on plant triggered pluripotency and developmental plasticity.

DECLARATION

I declare that no portion of the work referred to in the thesis has been submitted in support of an application for another degree or qualification of this or any other university or other institute of learning, excluding images in Figure 5.1A that have been submitted by Victoria Spencer for a Doctor of Philosophy (PhD) degree in the Faculty of Biology, Medicine and Health, University of Manchester, 2018.

COPYRIGHT STATEMENT

ACKNOWLEDGMENTS

I wish to express my sincere appreciation and gratitude to those who have supported me academically and personally throughout this PhD. First and foremost, I would like to thank my supervisor, Dr. Minsung Kim, who has patiently and professionally supported me throughout my PhD. Secondly, I would like to thank my advisor, Dr. Patrick Gallois for his exceptional guidance and helpful response in supporting my personal development. I am also thankful to a former PhD student in our lab, Dr. Victoria Spencer, who taught me most of the technical skills needed for my PhD.

I am grateful for the opportunities to supervise undergraduate and masters students in our lab, from which I rediscovered my passion in teaching. Of these students, I would like to thank Tanda Qi for her positivity, Aisha Khan for her encouragement and Joey Lau for her hardwork in supporting my research. I am also thankful to a PhD student in our lab, Paco Jácome Blásquez, for sharing his RNA-sequencing data and for maintaining the lab and the plants. I would also like to acknowledge the helpful scientific discussions with other PhD students and post-docs in the department.

I would also like to thank the faculty's Genomic Technologies Core Facility and Bioinformatics Core Facility for performing RNA-sequencing and data analysis; Bioimaging staff for training and support with microscopy; the Histology Core Facility for tissue embedding equipment and a laboratory technician from the Stopford labs for the WIFI camera. I am also incredibly grateful for the Doctoral Academy Research Scholarship offered by the faculty.

I would like to thank my parents for the financial support; my faith community mentors, Fey Toh and Yichin Dai; my sister, Joo Enn Ooi and my friends, James Dinsley, Franciska Urszuly and Qin-Ferng Wong for their words of encouragement. Last but not least, without the unconditional love of my partner, Jun Qi Lau, I would not have completed this piece of work.

CHAPTER 1

GENERAL INTRODUCTION

1. INTRODUCTION

1.1. General view of *Kalanchoë*

1.1.1. Nomenclature of the genus *Kalanchoë*

*Kalancho*ë plants belong to the subfamily Kalanchoideae of the Crassulaceae family (Smith et al., 2019). The name *Kalanchoë* was first coined by a French naturalist, Michel Adanson in 1763 (Baldwin, 1938). Most *Kalancho*ë plants are native to Southern Africa (Eggli, 2003), but the name derived from *Kalanikoe spathulata*, a species originated from China. This plant was called "Kalan Chauhuy" in Chinese, meaning "that which falls and grows", this name was then phonetically transcribed into the scientific name *Kalanchoë* (Boiteau and Allorge-Boiteau, 1995). The sound of the name may have referred to its ability to reproduce asexually via plantlet formation. However, none of the plantlet-producing species is native to China (Chernetskyy, 2011). Consequently, this points to other possible sources of the name, such as "kalanka" and "chaya", ancient Indian words that respectively means "rust" and "gloss", perhaps referring to the shiny, reddish leaves of Indian *K. laciniata* (Eggli, 2003). The introduction of another two genera *Bryophyllum* and *Kitchingia*, and significant increase in new species of the subfamily Kalanchoideae complicated the use of nomenclature (Chernetskyy, 2011). This is because different scientists classified the plants into these three genera depending on only a few factors such as morphological traits, phylogenetic relationships or embryological evidence (Chernetskyy, 2011). The most consistent taxonomic classification is to group all species into one genus *Kalanchoë* with three sub-divisions of *Bryophyllum, Kalanchoë* and *Kitchingia* (Chernetskyy, 2011).

1.1.2. The role of *Kalancho*ë in research

Due to the origin of *Kalanchoë* plants from arid and dry regions, these plants have succulent and waxy leaves that are designed to respectively store large amounts of water and prevent transpirational water loss (Eggli, 2003; Rabas and Martin, 2003). In addition, *Kalanchoë* plants also depend on their unique water-conserving photosynthesis mechanism, Crassulacean acid metabolism (CAM) to perform photosynthetic carbon assimilation at night. The lower atmospheric pressure and higher humidity at night reduces transpirational water loss via stomatal opening (Fanourakis et al., 2017; Rabas and Martin, 2003). Apart from its long-standing role as a model plant for CAM studies (Amin, 2019; Garcês and Sinha, 2009a; Osmond

and Allaway, 1974), *Kalanchoë* is also well-known for its use as traditional medicine in Africa (Abebe and Ayehu, 1993; Veale et al., 1992), North America (Balick et al., 2000) and Asia (Heyne, 1988). Recent research on the medicinal use of *Kalanchoë* has provided scientific basis for its use as traditional medicine, revealing that the metabolites in *Kalanchoë* exhibit antiviral, antioxidant and anticancer properties (Agarwal and Shanmugam, 2019; Joshi et al., 2020; Yusuf, 2017). Apart from its medicinal uses, *Kalanchoë* plants are also promising sources of compounds for synthesis of magnetic nanoparticles for water treatment (Morales et al., 2019) and corrosion inhibitors for metals (Al-Nami, 2020).

The distinctive asexual reproductive strategy in *Kalanchoë* has also sparked great research interest. Asexual reproduction of *Kalanchoë* occurs *via* formation of plantlets on the edges of the leaves. These plantlets are like miniature version of the adult plant and are also known as "epiphyllous buds" (Houck and Rieseberg, 1983), "adventitious buds" (Broertjes et al., 1968), "propagules" (Batygina et al., 1996), "foliar embryos" (Yarbrough, 1932), "marginal buds" (Dostál, 1970) and "pseudo-bulbils" (Johnson, 1934) . For the purpose of consistency and clarity, the term "plantlets" will be used to describe these structures formed on the leaf margin of the plants. The ability of plantlet formation varies depending on the *Kalanchoë* species (See Fig. 1.1). There are species that do not produce plantlets such as *K. marmorata, K. rhombopilosa, K. tomentosa and K. thyrsiflora* and there are those that produce plantlets only upon stress induction such as *K. pinnata, K. prolifera, K. strepthantha and K. fedstchenkoi*. Species such as *K. daigremontiana* produces plantlets constitutively at almost all indentations of mother leaves whereas *K. gastoni-bonnieri* produces one plantlet on each mother leaf constitutively but produces plantlets on other leaf indentations under stress induction (Garcês and Sinha, 2009a; Garcês et al., 2007). The capability of plantlet formation in *Kalanchoë* plants varies greatly despite their close phylogenetic relationships. Hence *Kalanchoë* plants are ideal for studying the evolution and detailed mechanism of plantlet formation (Garcês and Sinha, 2009a; Garcês et al., 2007).

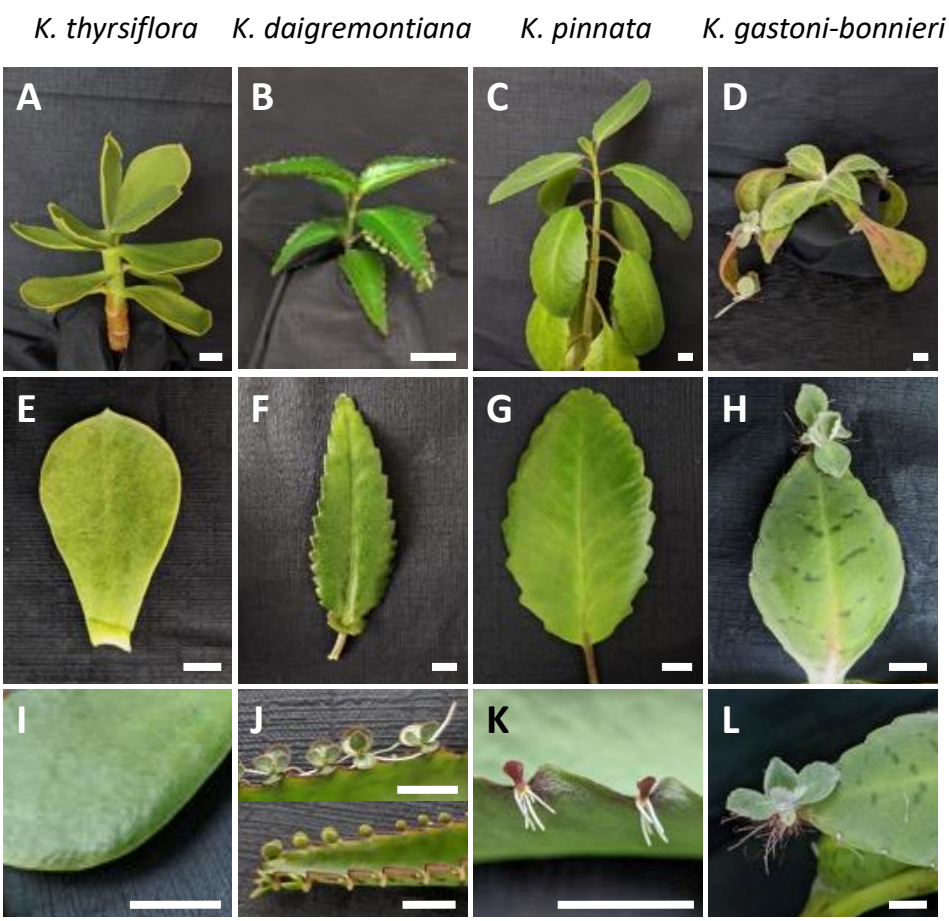

Figure 1.1 Examples of *Kalanchoë* species with different mode of plantlet formation.
(A-D) Whole plant and (E-H) leaf of *K. thyrsiflora*, *K. daigremontiana*, *K. pinnata* and *K. gastoni-bonnieri* respectively. (I) Close-up image of *K. thyrsiflora* leaf margin. (J-L) Plantlet(s) of *K. daigremontiana*, *K. pinnata* and *K. gastoni-bonnieri* respectively. From left to right, each species represents the *Kalanchoë* species that do not make plantlet; make plantlets constitutively; make plantlets under stress induction and make plantlet constitutively and also when induced by stress. Scale bar in (A-D) represents 1 cm; in (E-L) represents 0.5 cm.

1.2. Plant reproduction

1.2.1. Asexual reproduction in plants

The meaning of asexual reproduction has long been debated but here, asexual or clonal reproduction refers to production of genetically identical offspring or clones of the mother plant without gametes fusion (de Meeûs et al., 2007). In contrast to sexual reproduction, clonal offspring can avoid loss of adaptive alleles *via* meiotic recombination and maintains adaptive genotypes that confer fitness to its species (Niklas and Cobb, 2017). In addition, asexual reproduction is rapid, allowing replication and propagation of adaptive genotypes and quick colonisation in a new environment (Klimeš et al., 1997; Rautiainen et al., 2004). This behaviour allows these plants to respond to its environment swiftly to escape nutrient-poor locations and thrive in desirable conditions, enabling clonal plants to exploit resource-rich microhabitats and environments with patchy distribution of resources (Hutchings, 1988; Klimeš et al., 1997). In certain modes of asexual reproduction, a physical connection between mother plant and offspring is maintained. This implies that offspring can obtain supply from mother plants until independence is achieved, and the clonal plants can share resources and spread the mortality risks, thereby increasing the survival rate of the population (Callaghan, 1984; Doust, 1981; Klimeš et al., 1997; Savini et al., 2008). Nonetheless, clonal propagation is short-distant, resulting in competition between the clonal plants (Rautiainen et al., 2004). Furthermore, with the absence of genetic recombination, asexual plants thrive only at relatively stable environments due to inability to acquire adaptive mutations within a short timeframe to cope with fluctuating conditions (Neiman et al., 2014). The lack of genetic diversity also heightens the susceptibility of the clonal population to diseases and insect infestation (Lei, 2010). To combat the trade-offs between sexual and asexual reproduction, many plants have opted for both to maximise its output by shifting from one mode of reproduction to another depending on the conditions (Eckert, 2002; Lei, 2010; Silvertown, 2008; Winkler and Fischer, 2001).

The modes of asexual reproduction in plants are very diverse and can be generally classified into two types; type 1 forms complete progeny on existing organs of a mother plant and type 2 forms specialised structures that only serve to facilitates clonal propagation. Type 1 plants such as *Kalanchoë* produce individual plantlets with their own vasculature system and roots on the indentation of leaf margin (Garcês and Sinha, 2009a; Garcês et al., 2007; Laura et al.,

2013). After the plantlet is fully formed, the plantlet detaches from the mother leaf, and in the case of *K. gastoni-bonnieri*, plantlets remain attached until the mother leaf dies (Garcês and Sinha, 2009a). Apart from *Kalanchoë,* other plants in the same family of *Crassulaceae*, *Graminaceae*, *Orchidaceae* and *Liliaceae* also produce plantlets, but from several origins such as base of the leaves, leaf vein and stem nodes (Gorelick, 2015; Laura et al., 2013). Similarly, a particular species of *Begonia* also reproduces by producing plantlets on veins of attached leaves (Chlyah-Arnason and Van, 1968; de Meeûs et al., 2007).

Type 2 plants form bulbs, corm, stolon (or runners), rhizomes, tubers, gemmae cups (fragmentation) and seeds (apomixis) during asexual reproduction. Plants in the genus *Gladiolus* and *Crocus* grow from corms, while plants such as garlic, tulips and lilies grow from bulbs (Bell and Bryan, 2008). These underground structures provide nutrients during plant growth and when nutrient supply is exhausted, a new corm or bulb replaces the old ones and simultaneously giving rise to daughter corms (cormels) or bulbs (Grace, 1993). When the old corm or bulb dies, the daughter corm or daughter bulb separates from the mother plant and grows into an individual plant. The difference between these two structures is that new bulbs or daughter bulbs grow inside the mother bulb, and new corms and cormels are formed externally (Berg, 1972; Putz, 1996). Stolons and rhizomes are elongated stem structures that usually grow horizontally above and under the ground, respectively (Bell and Bryan, 2008; Savini et al., 2008). Plants such as strawberries make stolons that produce one or more offspring known as a ramet. The stolons provide supports until the ramets achieve independence by transferring resources and aid communication between ramets (Savini et al., 2008). In comparison to stolons, rhizomes are thicker, more fleshy, woody and are usually wrapped with scale leaves. A rhizome naturally separates to form two ramets whenever a proximal portion decays (Bell and Bryan, 2008). Reproductive tubers are swollen, modified root or stem structures that are connected to mother plant *via* thin roots or stem and when the connection decays, shoots germinate from tubers (Bell and Bryan, 2008). Gametophyte plants reproduce *via* fragmentation of leaf-like structures (thallus) of the mother plant, forming structures called gemma cups that then produces numerous gemmae. These gemmae grow after dispersal *via* water droplets that fill the gemma cups (Eklund et al., 2015). Recent research revealed that more than half of all angiosperms reproduce *via* apomixis, a mode of

asexual reproduction achieved through formation of a clonal seed from an unfertilised egg (León-Martínez and Vielle-Calzada, 2019; Schmidt, 2020). As meiosis and fertilisation are bypassed, creation of apomictic crops might facilitate crop production through preservation of heterosis (Ozias-Akins and Conner, 2020). This mode of reproduction has also attracted attention as seed formation normally depends on fertilization but here is part of an asexual reproduction strategy (Ozias-Akins and Conner, 2020).

1.2.2. Plant pluripotency and cell fate determination

Plants are well-known for their developmental plasticity, and the molecular mechanisms behind regeneration of different plant organs have been extensively studied (Ikeuchi et al., 2019). However, the molecular mechanisms behind the formation of whole plantlets from mature organs remains unresolved (Guo et al., 2015; Radoeva and Weijers, 2014). It has been proposed that plantlet formation is a product of somatic embryogenesis in which the somatic leaf cell dedifferentiates, regaining totipotency to become an embryo and then develop into a plantlet (Buchanan et al., 2015; Garcês et al., 2007; Nick and Opatrny, 2014). These processes are remarkable as it was long assumed that differentiation is irreversible as in animal cells and as a cell differentiates, differentiation potential is progressively and permanently lost (Grafi, 2004). Nonetheless, decades of *in vitro* cell and tissue culture have proved against this concept, showing that differentiation is reversible (Espinosa-Leal et al., 2018; Haberlandt, 2003; Liu et al., 2020a). Intense research on cell pluripotency also contributed to generation of induced pluripotent stem cells and scientists are only beginning to understand the origin and mechanisms behind innate organ or whole-body regeneration that is only limited to basal bilaterian animals (Liu et al., 2020a; Slack, 2017; Sogabe et al., 2019). For plantlets to develop via somatic embryogenesis, *Kalanchoë* plant cells will require efficient mechanisms to regulate determination of cell fate and control of cell potency. To dissect the mechanisms that govern cell pluripotency in plants, particularly in *Kalanchoë*, we need to examine existing research on the impact of genetics, environmental cues and plant hormones on embryogenesis, meristematic tissues activity and *Kalanchoë* plantlet formation.

1.2.2.1. Zygotic embryogenesis: morphogenesis

During sexual reproduction, a diploid zygotic cell is formed upon fusion of gametes (Radoeva and Weijers, 2014; de Vries and Weijers, 2017). From this stage onwards and up until germination, the developmental process of this zygote is known as zygotic embryogenesis (Tian et al., 2020a; Tvorogova and Lutova, 2018). This zygotic cell is the undifferentiated initial cell of a new individual and is capable of dividing, proliferating and differentiating into any cell type of whole adult plant. Due to these capabilities and its differentiation potential, the zygotic cell is described as totipotent (Condic, 2013). The zygotic embryo first undergoes morphogenesis, which establishes its body plan through determination of apical-basal polarity and specification of meristems (Hove et al., 2015; Smet et al., 2010).

Upon fertilisation, *SHORT-SUSPENSOR* (*SSP*) transcripts from the sperm cell are translated and transiently produced in the *Arabidopsis* zygote (Bayer et al., 2009; Neu et al., 2019). SSP proteins then activates the *YODA* signalling pathways that are responsible for determination of the zygote's apical-basal polarity. *YODA* encodes a mitogen-activated protein kinase (MAPKKK) that initiates a MAP kinase cascade with the downstream MAPKKs and MAPKs (Wang et al., 2007; Zhang et al., 2017b) to result in zygote elongation and development of the basal cell lineage (Lukowitz et al., 2004; Musielak and Bayer, 2014). *YODA* also phosphorylates and activates WRKY DNA-BINDING PROTEIN (WRKY2) that in turn upregulates expression of *WUSCHEL-RELATED HOMEOBOX* (*WOX*) transcription factors, *WOX8* and *WOX9* (Ueda et al., 2017). During early embryo development, *WOX2* and *WOX8* are co-expressed in the zygote but after asymmetrical division of the zygote, *WOX2* expression is restricted to the smaller apical cell whilst *WOX8* and *WOX9* are localised in the bigger basal cell (Haecker et al., 2004; Ueda et al., 2011). The apical cell eventually develops into the embryo proper that subsequently give rise to the embryo. The basal cell divides transversely to generate tandemly-arranged cells, in which by globular stage, the uppermost cell forms the hypophysis, and the rest develops into the extraembryonic suspensor (Wang et al., 2020b).

The proper development of these apical and basal cell fates also requires auxin signalling, which commences from the 2-cell embryo stage (Friml et al., 2003). At the 2-cell and 8-cell stage, auxin is transported from the basal to the apical region *via* PIN7 auxin efflux transporter

(Friml et al., 2003). The auxin is synthesised at the basal region by YUCCA (YUC) type flavin-containing monooxygenase, YUC3, YUC4 and YUC9 (Robert et al., 2013). At the 16 to 32-celled stages, auxin is distributed basipetally through relocation of PIN7. This reverses flow of auxin which is maternally supplied from the integument and biosynthesised by YUC1, YUC4 and TRYPTOPHAN AMINOTRANSFERASE OF ARABIDOPSIS (TAA) in the apical region (Friml et al., 2003; Robert et al., 2013, 2018). The basal auxin accumulation is also established through auxin influx transporters AUXIN-RESISTANT 1 (AUX1) and LIKE AUX1 (LAX1) (Robert et al., 2015a). In addition, auxin efflux transporters PIN1 and PIN4 also supports directional auxin flow to the hypophysis and upper suspensor, creating a auxin maximum at this region (Friml et al., 2003; Robert et al., 2013), which later give rise to the root apical meristem (RAM).

1.2.2.2. Zygotic embryogenesis: meristem establishment

During early embryogenesis, three pluripotent stem cell niches, (i) the shoot apical meristem (SAM), (ii) the RAM and (iii) lateral meristem (Aichinger et al., 2012), are specified, and set aside for post-embryonic development (Gaillochet and Lohmann, 2015). The SAM is responsible for the formation of above-ground structures such as stems and lateral organs (Bowman and Eshed, 2000), whereas the RAM maintains and regulates root growth (Perilli et al., 2012). The lateral meristem is responsible for formation of vascular cambium and phellogen (cork cambium) (Aichinger et al., 2012; Jura-Morawiec et al., 2015; Pavlović and Radotić, 2017). The lateral meristem is sometimes referred to as secondary meristem because it gives rise to vascular cambium that regulates secondary growth of plants (Jura-Morawiec et al., 2015; Nieminen et al., 2015). The vascular cambium produces the secondary tissues of plants, phloem and xylem, which are responsible for the transport of minerals and water in plants; whilst the cork cambium produces the protective outer layer of roots (Aichinger et al., 2012; Nieminen et al., 2015). These pluripotent meristematic stem cells can differentiate into most but not all cell types of the adult plant. Hence, pluripotency refers to a lower differentiation potential relative to totipotency. The fate specification and maintenance of pluripotent stem cells are regulated by spatial and temporal action of different transcription factors (Wang and Schiefelbein, 2014). This suggests that pluripotent stem cells are non-autonomous due to dependency on communication between neighbouring cells *via* intercellular signals. These intercellular signals confer positional information and timing of

differentiation that specifies cell identity (Verdeil et al., 2007). These properties are illustrated by determination and development of pluripotent stem cells in the SAM and the RAM.

RAM specification initiates at the octant (8-cell) stage, reflected by expression of the *PLETHORA* (*PLT*) genes, *PLT1* and *PLT2* in the lower tier of the apical cells (Aida et al., 2004). Following this, at the dermatogen stage, the hypophysis expresses *WOX5*, which functions to maintain and act as marker of the quiescent center (QC) (Haecker et al., 2004). Later, at the globular (32-64) stages, the hypophysis divides asymmetrically to form a smaller lens-shaped cell and a larger basal cell which is a precursor of the distal root meristem cells (Laux et al., 2004). The lens-shaped cell is the QC precursor, and at this stage, *PLT1* and *PLT*2 expression is present at and around the region. At the heart stage, *PLT3* (*AINTEGUMENTA-LIKE6*, *AIL6*) and *PLT4* (*BABYBOOM*, *BBM*) expression replace expression of *PLT1* and *PLT2* at the provascular cells and lens-shaped cells. (Aida et al., 2004; Galinha et al., 2007). *PLT1* and *PLT2* expression is regulated by the activity of an auxin-responsive gene, *MONOPTEROS* (*MP*) (Aida et al., 2004; Schlereth et al., 2010) and a transcriptional corepressor encoded by *TOPLESS* (*TPL*) (Long et al., 2006; Smith and Long, 2010). When *PLT1* and *PLT2* were ectopically expressed at apical and basal regions of *Arabidopsis* embryo, formation of hypocotyl, root and root stem cell niche were induced. Thus, providing evidence for the role of *PLT1* and *PLT2* as determinants of the basal cell fate (Aida et al., 2004). The post-embryonic maintenance of the RAM and QC also requires SHORT ROOT (SHR) and SCARECROW (SCR) in addition to *PLT1* and *PLT2.* Provascular cylinder cells above the root stem cells produce SHR protein that moves into the QC to induce *SCR* expression, which is essential for maintenance of QC and its progeny (Nakajima et al., 2001; Sabatini et al., 2003). *SCR* expression is maintained *via* a positive autoregulatory feedback loop, stabilising lineage specification and QC maintenance (Heidstra et al., 2004; Helariutta et al., 2000; Nakajima et al., 2001).

The SAM formation during embryogenesis was thought to have initiated at the globular stage as expression of *WUSCHEL* (*WUS*), marker of shoot organising centre and key regulator of stem cell homeostasis in the SAM is observed (Mayer et al., 1998). However, a recent study showed that stem cell initiation during embryogenesis by *WUS* function is dispensable, but depends on the early embryo patterning gene *WOX2* to inhibit differentiation of stem cell progenitors

(Zhang et al., 2017a). *WOX2* exerts this function by upregulating class III HD-ZIP transcription factors such as *PHABULOSA*, *PHAVOLUTA* and *REVOLUTA* that determines the SAM identity, and maintaining balance between cytokinin and auxin pathways (Brandt et al., 2012; Prigge et al., 2005; Reinhart et al., 2013; Zhang et al., 2017a). Cytokinin signalling aids initiation of shoot stem cells through a positive regulatory feedback induction of a *KNOTTED1-LIKE HOMEOBOX* (*KNOX*) gene, *SHOOTMERISTEMLESS* (*STM*), which specifies the centre region of the embryonic SAM (Jasinski et al., 2005; Long et al., 1996; Takada et al., 2001; Yanai et al., 2005). On the other hand, *STM* is also regulated by a negative feedback loop in which CUP-SHAPED COTYLEDON 1 (CUC1) and CUC2 induce *STM* expression but *CUC1* and *CUC2* are repressed by microRNA164a, which is activated by STM (Aida et al., 1999; Hibara et al., 2006; Spinelli et al., 2011; Takada et al., 2001).

At mid-stage embryogenesis, a three-layered SAM consisting the central zone, the peripheral zone and the rib zone (Laux and Mayer, 1998) is histologically visible between the cotyledons (Jürgens et al., 1994) (See Fig. 1.2). From this stage onwards, including post-embryogenic development, *WUS* is vital for stem cell homeostasis (Brand et al., 2002). Fate specification and maintenance of the SAM is very similar to the RAM as in the case of the RAM, QC like the organizing centre in shoot meristem produces an unknown signal that maintains a reservoir of stem cells surrounding it by inhibiting differentiation and promoting continuous division of the surrounding cells (Berg et al., 1997; Dolan et al., 1993). Within the central zone, there is a group of cells termed the organizing centre (OC) which is localised below three layer of stem cells (See Fig. 1.2). To maintain the stem cell population, the OC expresses *WUS* that causes production of an unknown signal that signals overlying cells to maintain its pluripotency (Aichinger et al., 2012; Williams and Fletcher, 2005). WUS moves from the central zone and bind to *CLAVATA* (*CLV*) 3 promoter of peripheral zone daughters cells that produce CLV3 ligand, which binds to CLV1 receptor kinase and CLV2 accessory protein (Clark et al., 1997; Jeong et al., 1999; Yadav et al., 2011). This interaction subsequently leads to activation of signal transduction pathways that transcriptionally inhibits expression of *WUS* to promote organ initiation (Schoof et al., 2000). This is reinforced by the maintenance of *CLV*1 expression through *STM* expression (Gallois et al., 2002).

The role of *WUS* in the SAM identity specification was elucidated when recessive *wus* *Arabidopsis* mutants do not have recognisable stem cells in the SAM and form a premature terminated SAM (Laux et al., 1996). Moreover, ectopic *WUS* expression resulted in formation of an enlarged SAM (Schoof et al., 2000). This phenotype was also observed in *clv1* and *clv3* mutants, indicating that these *CLV* genes transcriptionally inhibit *WUS* expression to promote organ initiation (Schoof et al., 2000). Double mutants of *wus* and *clv* genes revealed that the SAM is maintained *via* a negative regulatory feedback loop mediated by *CLV* and *WUS* genes (Schoof et al., 2000). Apart from fate specification and maintenance of pluripotent meristem cells, existing evidence suggests that action of these genes might trigger dedifferentiation conferring relatively greater differentiation potential. For example, overexpression of PLANT GROWTH ACTIVATOR 6 (PGA6), a gene similar to WUS led to formation of somatic embryos in the absence of external plant hormones (Zuo et al., 2002). In addition, somatic embryogenesis in different species exhibited elevated *WUS* induction (Arroyo-Herrera et al., 2008; Chen et al., 2009; Santa-Catarina et al., 2012; Xiao et al., 2018; Zheng et al., 2014). On the other hand, mutants that overexpress *CLV1* also showed signs of cellular differentiation (Elhiti et al., 2010), indicating repression of somatic embryogenesis. Given the participation of *WUS* and *CLV* in regulation of pluripotency, it is plausible to observe activity of these genes in plantlet initiation of *Kalanchoë* plants but this is yet to be investigated.

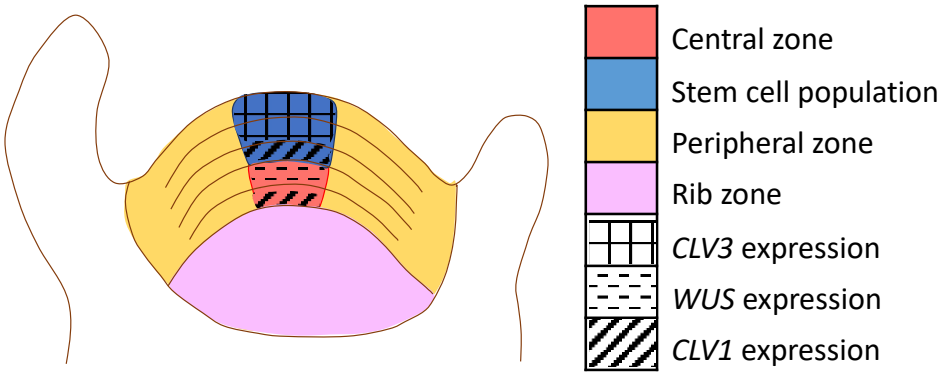

Figure 1.2 Different regions of the shoot apical meristem and *WUSCHEL* (*WUS*) and *CLAVATA* (*CLV*) expression. Each division of the shoot apical meristem is colour-coded. The horizontal lines in the peripheral zone roughly correspond to division of rows of cells. Localisation of *CLV3*, *WUS* and *CLV1* expression is also shown in the diagram. Adapted from (Aichinger et al., 2012; Bowman and Eshed, 2000).

1.2.2.3. Zygotic embryogenesis: maturation & dormancy

After morphogenesis, the final phase of embryogenesis occurs, in which the embryo matures and transitions to dormancy. The *LAFL* genes, *LEAFY COTYLEDON 1* (*LEC1*), *LEC1-LIKE* (*L1L*), *ABSCISIC ACID INSENSITIVE3* (*ABI3*), *FUSCA3* (*FUS3*) and *LEC2*, are known to initiate and contribute to embryo maturation (Fatihi et al., 2016; Santos-Mendoza et al., 2008). During embryogenesis, these genes exhibit the highest expression levels (Le et al., 2010; Winter et al., 2007); and are expressed sequentially, with *LEC1*, *L1L* and *ABI3* expressed at very early stages, followed by *LEC2* at the globular stage, and *FUS3* during late globular or early heart stage (Kroj et al., 2003; Kwong et al., 2003; Lotan et al., 1998; O'Neill et al., 2019; Parcy et al., 1994; Stone et al., 2001; Tsuchiya et al., 2004). Although *LEC1* expression continues to decrease throughout embryogenesis, its importance during maturation is evident as loss-of-function *lec1 Arabidopsis* mutants show reduced storage nutrients and loss of desiccation tolerance, which are typical traits of seeds (Meinke, 1992). In contrast to *LEC1*, *L1L* has the highest transcript expression during maturation, and constitutive *L1L* expression can trigger embryo-specific programs in leaves and rescue desiccation intolerance of *lec1* mutants (Kwong et al., 2003). Similar to constitutive *L1L* mutants, seedlings with inducible *LEC2* expression can activate embryo programs (Braybrook et al., 2006; Feeney et al., 2013; Stone et al., 2008). Nonetheless, constitutive expression of *LEC1* or *LEC2* were sufficient to induce somatic embryogenesis of vegetative cells (Lotan et al., 1998; Stone et al., 2001). Like *lec1* and *lec2* mutants, loss-of-function *fus3* mutants are also desiccation intolerant but *FUS* over-expressor seedlings only exhibited cotyledon-like leaves and were unable to produce somatic embryos (Gazzarrini et al., 2004; Keith et al., 1994; Meinke et al., 1994). *ABI3* has the highest expression level during maturation, and *abi3* seeds were also desiccation intolerant (Casson et al., 2005; Klepikova et al., 2016; Nakabayashi et al., 2005; Nambara et al., 1992; Schmid et al., 2005; To et al., 2006). When *ABI3* was ectopically expressed, some embryo programs were activated, resulting in transcript accumulation of seed storage proteins (Parcy et al., 1994). Based on these findings, the participation of *LAFL* genes in embryo development is obvious. Molecular mechanisms in regulation and function of these genes were studied extensively (Lepiniec et al., 2018) but a detailed regulatory map of these genes in controlling germination, seedling, and vegetative development remains to be investigated (Yamamoto et al., 2014; Yoshii et al., 2015).

1.2.2.4. Somatic embryogenesis

In contrast to zygotic embryogenesis, somatic embryogenesis refers to the development of embryos from somatic cells that are non-dividing differentiated cells and not involved in sexual reproduction (Verdeil et al., 2007). During this process, the somatic cells dedifferentiate and acquire embryogenic competence, which confers the capability to develop into an embryo (Fehér, 2006). Upon induction of embryogenic competency, the switching of cell fate from somatic to embryogenic is accompanied by reprogramming of the genome architecture, which is achieved *via* epigenetic modification and chromatin remodelling (De-la-Peña et al., 2015; Kumar and Staden, 2017). Consequently, the somatic cells acquire an open chromatin configuration with increased accessibility that allows large-scale transcriptional activation of embryogenic genes (Florentin et al., 2013; Wang et al., 2020a). An open chromatin configuration is a shared feature among all stem cells (Grafi et al., 2011). However, somatic cells in somatic embryogenesis are totipotent stem cells that have a greater differentiation potential, compared to pluripotent stem cells in meristematic tissues. This difference might be the consequence of different degree of chromatin condensation (Grafi et al., 2011; Verdeil et al., 2007).

Apart from difference in origin, the nutrient resources of zygotic and somatic embryo were also shown to vary (Alexandra Pila Quinga et al., 2018). In addition, after maturation, a zygotic embryo would enter developmental arrest, whereas a somatic embryo does not acquire desiccation intolerance and would initiate seedling development (Smertenko and Bozhkov, 2014). Nonetheless, somatic embryos also undergo morphogenetic stages like zygotic embryos, though specific morphological changes are distinct between monocotyledonous and dicotyledonous plants (Winkelmann, 2016; Zhao et al., 2017). Despite these differences, similarity in morphological features between somatic and zygotic embryogenesis particularly during the initial stages and before maturation imply that similar genes are expressed in both processes. This was proven to be the case through comparative transcriptome analysis, which showed that more than a half of highly expressed genes were shared between somatic and zygotic embryogenesis (Jin et al., 2014). Some of these genes include *LEC* genes, *BBM* and *WUS* that are sufficient to induce somatic embryogenesis upon overexpression (Arroyo-Herrera et al., 2008; Boutilier et al., 2002; Horstman et al., 2017a; Lotan et al., 1998; Stone et al., 2001).

Most of the transcription factors with altered expressions during somatic embryogenesis were found to be involved in regulation of phytohormones and stress responses (Gliwicka et al., 2013). To date, it is known that the embryogenic competence of somatic cells is triggered by cellular stress and that *BBM* and *LEC* genes are vital in the molecular network of somatic embryogenesis (Gulzar et al., 2020).

Plant tissue culture that occurs *via in vitro* somatic embryogenesis has proven to be a useful tool in biotechnological applications. Some examples are the production of crops with desirable characteristics such as improved productivity, adaptation and drought tolerance, and to engineer plants for biosynthesis of specific metabolites such as vitamins, anthocyanins and terpenoids (Altman and Hasegawa, 2012). Hence, further research into molecular and cellular control of cell fate determination in plants will improve the progress of biotechnology and aid the understanding of plant development. Intensive research and use of *in vitro* plant tissue culture has revealed much of the molecular mechanisms behind somatic embryogenesis (Gulzar et al., 2020; Rocha and Carnier Dornelas, 2013; Yang and Zhang, 2010). However, these details should serve solely as a reference for the study of plantlet formation in *Kalanchoë* plants as *in vitro* somatic embryogenesis is induced artificially. Nonetheless, specific mechanism behind these processes is expected to overlap significantly due to similarities between zygotic and somatic embryogenesis.

Table 1.1 A glossary of certain terms discussed in this literature review.

Term	Definition
Dedifferentiation	The process in which a differentiated cell returns to its previous undifferentiation state
Differentiation	The process in which a cell becomes more specialised in terms of its structure and function
Meristematic Cell	Pluripotent stem cells that can continue to differentiate into cell types of more specialised form and function
Somatic Cell	A non-dividing differentiated cell that has a specialised structure and function
Somatic Embryogenesis	The process in which a somatic cell acquires and exhibits embryogenic competency
Zygotic Cell	A cell formed upon fusion of gametes

1.3. **Plantlet formation of *K. daigremontiana***

Kalanchoë daigremontiana (*K. daigremontiana*) or *Bryophyllum daigremontianum* is a *Kalanchoë* species that produces plantlets constitutively under the long day condition (Garcês et al., 2007). *K. daigremontiana* is commonly known as the mother of thousands, Mexican hat plant and devil's backbone. *K. daigremontiana* is native to Madagascar (Baldwin, 1938) but is widely distributed in tropical and subtropical regions such as South-Eastern USA, Australia, islands on North Pacific Ocean and countries around the Mediterranean Sea due its introduction as ornamental plant (Herrera and Nassar, 2009). As a result of its introduction, *K. daigremontiana* can also be readily purchased for research purposes (Garcês and Sinha, 2009a). The genome sequence of *K. daigremontiana* is not available but the genomes of closely related species in the same genus (*K. fedtschenkoi, K. laxiflora*) have been sequenced and are available on Phytozome 2020. Moreover, among known CAM species, *Kalanchoë* is the most closely related to *Arabidopsis* (Garcês and Sinha, 2009a). Hence, *K. daigremontiana* is still genetically amenable with the current technology (Innis et al., 2012).

Apart from laboratory research, the life cycle and reproductive strategies of *K. daigremontiana* have been well-studied in the wild due to its invasive and toxic effects to its surrounding animal and plant species (Guerra-García et al., 2015; Herrera and Nassar, 2009). Based on these investigations, *K. daigremontiana* is an autogamous species that generates more than 16,000 seeds per fruits through self-pollination and fertilisation (Herrera et al., 2012). However, the seeds have a low viability and germination rate; and the plants require at least 3 years before reproducing sexually (Herrera and Nassar, 2009; Herrera et al., 2012). In contrast, *via* asexual plantlet formation, a *K. daigremontiana* plant can generate about 200 plantlets in one month and its offspring can reproduce asexually in less than a year (Herrera and Nassar, 2009; Herrera et al., 2012). Typically, *K. daigremontiana* goes through a complete life cycle of 2 years that includes a vegetative phase and a flowering phase (Baldwin, 1938; Herrera and Nassar, 2009). During the vegetative phase, growth and maturation occurs and adult plants reproduce by plantlet formation; during the flowering phase, adult plants reproduces sexually and die (Baldwin, 1938; Herrera and Nassar, 2009) but occasionally, the flowering phase delays when the vegetative phase extends beyond 2 years (Groner, 1974; Hannan-Jones and Playford, 2011). *K. daigremontiana* can also be grown in growth chambers, green houses and *in vitro* culture

with the ideal vegetative growth conditions of 23°C to 29°C with a photoperiod of 16 hour light/8 hour dark (Garcês and Sinha, 2009a). Apart from asexual reproduction *via* plantlet formation, these plants can also be propagated easily by stem cuttings and leaf rooting (Garcês and Sinha, 2009a).

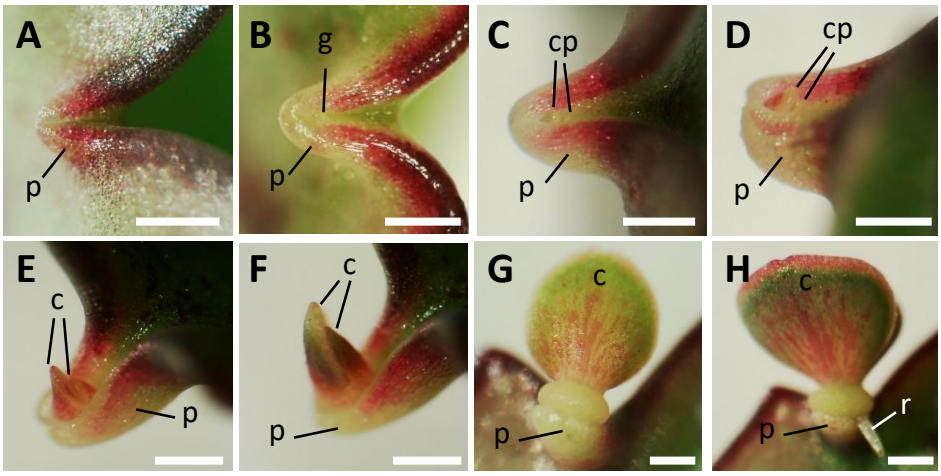

Figure 1.3 Chronological development of *Kalanchoë daigremontiana* plantlets.
(A) Top view of a pedestal without plantlet. (B) Top view of a globular-stage plantlet. (C) Heart-stage plantlet. (D) Side view of a more mature heart-stage plantlet. (E) Cotyledons emerging from the pedestal. (F) Cotyledons continue to grow and develop green colour. (G) Young plantlet with cotyledon still attached onto the pedestal. (H) Plantlet with mature cotyledon with roots emerging from its base. Scale bar represents 0.5mm. c, cotyledon; cp, cotyledon primordium; p, pedestal; r, root.

When *K. daigremontiana* plants are provided with at least 12 hours of light, plantlets are formed sequentially and symmetrically from the leaf tip to the leaf base on indentations of the leaf (Garcês et al., 2007; Hershey, 2002; Johnson, 1934). Plantlets are formed on the indentations at basal region of the leaf only when detached (Guo et al., 2015). Plantlets are formed as the leaf matures, hence, if the leaf reaches maturity before the condition is suitable for plantlet formation (e.g. move plants from short day to long day condition), no plantlet will be formed (Henson and Wareing, 1977). If the conditions for plantlet formation are met, pedestals start to develop at each indentation, serving as the site of plantlet formation (Fig. 1.3A) (Batygina et al., 1996). Then, dome-like structures protrude from the centre of the pedestal, resembling globular-stage zygotic embryos (Fig. 1.3B) (Batygina et al., 1996; Garcês et al., 2007). The plantlet develops into a heart-shaped structure (Fig. 1.3C, D) that then produces cotyledon-like leaves at its later stage of development (Fig. 1.3E-G) (Garcês et al., 2007). Adventitious roots eventually grow out of the basal "hypocotyl" of the plantlet (Fig.

1.3H) (Garcês et al., 2007; Johnson, 1934). Scanning electron images showed an abscission zone was formed on the pedestal site once the root system is mature (Garcês et al., 2007). The plantlets remain seated on the pedestal sometimes even after production of secondary plantlets, and they only detaches when a mechanical force is applied (Batygina et al., 1996; Garcês et al., 2007; Johnson, 1934). Once plantlet formation is initiated, excision of mother leaf or changes in photoperiod does not inhibit plantlet formation (Henson and Wareing, 1977). However, if the plantlet is removed prior to a certain maturation stage (before the stages shown in Fig. 1.3G), it does not continue to develop (Henson and Wareing, 1977). This indicates that there are certain signals present on the mother leaf that are required for plantlet growth (Henson and Wareing, 1977). It is still not known whether the plantlets originated from dedifferentiation of differentiated somatic cells or from differentiation of a group cells that remain undifferentiated during leaf organogenesis. Many authors assume that *Kalanchoë* plantlet formation occurs *via* the former mechanism through somatic embryogenesis (Radoeva and Weijers, 2014; Rodríguez-Garay et al., 2014; Zhu et al., 2017). Nonetheless, a study observed origination of plantlet from a group of G2 phase arrested stem cell-like cells that are localised at leaf notches of very small *K. daigremontiana* leaf of only about 600 µm (Guo et al., 2015). The study concluded that plantlets arise from this group of pre-existing stem-cells (Guo et al., 2015). However, it is still unclear whether these cells were dedifferentiated somatic leaf cells or were retained as pluripotent stem cells from the SAM before leaf organogenesis or from earlier stages of leaf development.

1.3.1. Genetic control of plantlet formation

As described previously, morphological development of plantlets greatly resembles zygotic embryo and shoot development. Hence, the first genetic study of plantlet formation investigated key regulators of organogenesis and embryogenesis, *SHOOTMERITSTEMLESS* (*KdSTM*) and *LEAFY COTYLEDON1* (*KdLEC1*) in *K. daigremontiana* (Garcês et al., 2007), which showed the recruitment of embryogenesis and organogenesis programs into plantlet formation (Garcês et al., 2007). Almost a decade later, a study on *K.* x *houghtonii* showed that changes in expression of *KNOX5* (*KN5*), a gene in the same class as *STM* affected plantlet formation, supporting the use of organogenesis molecular mechanisms in plantlet formation (Laura et al., 2013). Nonetheless, the most surprising recent finding was participation of a

flowering gene, *SUPPRESSOR OF CONSTANS OVEREXPRESSION 1* (*KdSOC1*) in plantlet formation (Liu et al., 2016; Zhu et al., 2017), provoking further interest in genetic control of plantlet formation.

STM is a class I *KNOTTED1-LIKE HOMEOBOX* (*KNOX*) gene that encodes homeodomain transcription factors responsible for SAM establishment and maintenance during organogenesis (Clark et al., 1996; Endrizzi et al., 1996; Scofield et al., 2014). As its name suggests, *Arabidopsis* homozygous *stm* seedlings lacked SAM but were otherwise normal (Barton and Poethig, 1993). Overexpression of *STM* led to ectopic meristem development on the adaxial leaf surface of *Arabidopsis* (Gallois et al., 2002; Lenhard et al., 2002). In *Arabidopsis*, *STM* mRNA is localised in embryonic SAM progenitor cells, and main shoot, axillary, inflorescence and floral meristems (Long et al., 1996). *KNOTTED1* (*KN1*), the *STM* homolog in maize also exhibited similar expression pattern (Jackson et al., 1994; Smith et al., 1992), and the loss of *KN1* resulted in defective meristem maintenance (Kerstetter et al., 1997). Enhanced *STM* expression was present in maize and *Medicago* somatic embryo (Ma et al., 1994; Orłowska and Kępczyńska, 2018). In addition, *STM* was consistently expressed in embryonic competent vanilla orchids tissues (Ramírez-Mosqueda et al., 2018) and altered *STM* expression caused deformation of SAM in habanero pepper somatic embryos (Regla-Márquez et al., 2019). *STM* overexpression in *Brassica* explants also induced embryonic cell formation with low auxin requirement (Elhiti et al., 2010). From these observations, the participation of *STM* during somatic embryogenesis is evident. In *K. daigremontiana*, *in situ* hybridisation showed localisation of *KdSTM* transcripts in the SAM and axillary buds of wild-type plantlets (Garcês et al., 2007) and similar expression was observed for most simple-leaved plants (Bharathan et al., 2002). *KdSTM* transcripts was observed in plantlet initiation sites and in the early heart-shape plantlet. There were increased *KdSTM* transcripts in the vascular bundles and upper half of the plantlet and its leaf primordia (Garcês et al., 2007). This expression pattern resembles *STM* expression in maize somatic embryos, but in *Arabidopsis* embryo *STM* expression is not present in its leaf primordia (Long and Barton, 1998; Zhang et al., 2002). Transgenic *K. daigremontiana* plants in which *KdSTM* was down-regulated produced deformed or aborted plantlets, accompanied by formation of altered leaf margin (Garcês et al., 2007). High expression of *KdSTM* at the plantlet-initiation site and complete inhibition of plantlet

formation when the transcripts were down-regulated led the authors to propose that *KdSTM* was essential for plantlet formation by maintaining or initiating undifferentiated cells at the leaf notches (Garcês et al., 2007).

The recruitment of organogenesis molecular mechanisms into plantlet formation was further demonstrated by another class I *KNOX* gene, *KN5* in *K. x houghtonii* (Laura et al., 2013). *K. x houghtonii* is a hybrid species resulted from crossing two constitutive plantlet-forming *Kalanchoë* species, *K. daigremontiana* and *K. tubiflora* (Garcês et al., 2007; Houghton, 1935). *K. x houghtonii* plantlet formation is also induced under long-day condition and its plantlet morphogenesis is similar to *K. daigremontiana* in which plantlets are formed basipetally on the leaf and the plantlet is formed on a pedestal that envelopes the plantlet at globular-stage (Laura et al., 2013). In wild-type *K. x houghtonii*, *KxhKN5* is expressed in the adaxial side of leaf primordia and is absent from plantlets (Laura et al., 2013). The up- and down-regulation of *KxhKN5* expression in *K. x houghtonii* resulted in varied alterations in leaf and plant traits without a clear consistent pattern but due to impact on leaf morphology, plantlet formation was also impacted (Laura et al., 2013). The irregularity of leaf margin morphology was accompanied by reduced number of leaf notches and subsequently reduced plantlets frequency in plants with down-regulated *KxhKN5* expression (Laura et al., 2013). In contrast, plants with increased *KxhKN5* expression exhibited a novel plantlet development phenotype in which plantlets were formed directly on the leaf notch in absence of pedestal formation (Laura et al., 2013). In some of these plants, plantlets developed into shoots with strong vascularisation with the mother leaf, remaining strongly attached and resembling lateral branch (Laura et al., 2013).

Phylogenetic analysis of KNOX protein sequences from different dicot species revealed that KxhKN5 shares 49% similarity with *Arabidopsis* KNOTTED-1 LIKE FROM ARABIDOPSIS THALIANA 1 (KNAT1) but shares 94.3% similarity within the homeodomain sequences (Lütken et al., 2011). In *Arabidopsis*, KNAT1 is expressed in SAM peripheral zone and subepidermal cells of the stem and pedicel (Lincoln et al., 1994; Long et al., 1996). KNAT1 is also known as BREVIPEDICELLUS (BP) through identification of *Arabidopsis bp* mutants with affected pedicel development and inflorescence architecture (Venglat et al., 2002). *KNAT1* acts downstream of

STM and has partially redundant function with *STM,* as *knat1* caused stronger *stm* phenotype and its overexpression partially rescues *stm* (Byrne et al., 2002; Scofield et al., 2007). Previous studies showed that overexpression of *KNAT1* resulted in lobed leaves with ectopic meristems and that loss of *KNAT1* caused deformation of abscission zone at joints between the siliques and pedicels of *Arabidopsis* plants (Chuck et al., 1996; Wang et al., 2006). These explain the changes in leaf morphology and formation of ectopic shoots with strong attachment to mother leaf in *K. x houghtonii* with *KxhKN5* overexpression (Laura et al., 2013).

Apart from organogenesis, evidence has pointed towards participation of embryogenesis programs in *Kalancho*ë plantlet formation (Garcês et al., 2007). LEC1 is a pleiotropic central regulator of seed development as it interacts with distinct gene sets during embryogenesis to regulate endosperm development, embryo morphogenesis, maturation, photosynthesis and chloroplast development (Jo et al., 2019; Pelletier et al., 2017). *LEC1* encodes a transcriptional activator with evolutionary conserved B domain in the HEME-ACTIVATED PROTEIN3 (HAP3) subunit, allowing DNA binding and interaction with other transcription factors (Li et al., 1992; Lotan et al., 1998). *LEC1* was first shown to regulate late embryogenesis as *Arabidopsis lec1* mutant embryos bypassed embryo maturation and developed morphological and molecular vegetative characteristics (Meinke, 1992; West et al., 1994). *LEC1* is expressed only during embryogenesis in *Arabidopsis* and other higher plants (Lotan et al., 1998). In addition, ectopic *LEC1* expression in *lec1* mutant seedlings were sufficient to induce embryogenic development while repressing vegetative growth (Lotan et al., 1998) This indicates the importance of *LEC1* as a marker and regulator of embryogenesis. These findings suggest that ectopic *LEC1* expression might contribute to plantlet formation by inducing somatic embryogenesis of leaf cells at the leaf notches of *Kalancho*ë leaf.

In situ hybridisation showed that *KdLEC1* was expressed in *K. daigremontiana* seed embryo and pre-globular and heart-stage plantlet, suggesting that embryogenesis may be recruited in plantlet formation (Garcês et al., 2007). However, the B domain of *KdLEC1* that confers its activity in embryogenesis (Lee et al., 2003) was truncated and non-functional as the truncated protein was unable to rescue the *lec1* Arabidopsis mutant (Garcês et al., 2007). When *KdLEC1* was downregulated in *K. daigremontiana*, the formation of plantlets was similar to wild-type

plants, confirming that wild-type *KdLEC1* was not required for plantlet formation (Garcês et al., 2014). When functional *Arabidopsis* LEC1 was expressed in *K. daigremontiana*, it resulted in deformation of plantlets with features of dormant seeds such as accumulation of oil bodies and response to abscisic acid biosynthesis inhibitor fluridone (Garcês et al., 2014). This explained that loss of *LEC1* was vital to bypass the dormancy stage typically observed in seeds to allow formation of plantlets (Meinke, 1992). Phylogenetic analysis of LEC1 protein sequences from different *Kalanchoë* species showed a switch in mode of reproduction from seed to plantlet formation in *Kalanchoë* over evolutionary time (Garcês et al., 2007). *Kalanchoë* species that do not produce plantlets share similar protein sequences with *Arabidopsis* LEC1 and produce viable seeds, but species that produce plantlet constitutively and cannot produce viable seed express LEC1 protein with mutation in the B domain (Garcês et al., 2014). *K. gastonis-bonnieri,* a semi-constitutive plantlet formation species that produces only on plantlet on each leaf constitutively and produces plantlets on other leaf indentations when induced by stress contains LEC1 similar to *Arabidopsis* LEC1, making it intermediate species between the transition from seed production to plantlet formation (Garcês et al., 2007). Further research on this species might provide valuable insights regarding evolution of *Kalanchoë* reproduction at molecular level.

Given the importance of *LEC1* in embryogenesis, it was intriguing to observe a defective copy of KdLEC1 in *K. daigremontiana* (Garcês et al., 2014). Hence, Garcês et al., 2007 examined another embryogenesis marker and *LEC* class protein containing B-domain, *KdFUS3* which showed high expression during plantlet development and in pollinated ovaries. This provided further evidence of embryogenesis recruitment during plantlet formation (Garcês et al., 2007; Jia et al., 2013; Luerßen et al., 1998; Stone et al., 2001). Nonetheless, this evidence is insufficient to answer the question regarding whether other genes, perhaps the ones in *LAFL* network have evolved and replaced the original function of *LEC1* in *K. daigremontiana*. Further investigation should also be performed on other *LAFL* network genes in *Kalanchoë* to study whether the mechanism of plantlet initiation and formation is similar to induced somatic embryogenesis and if these genes are responsible for embryo-like morphological features in constitutive plantlet-forming *Kalanchoë* plants (Garcês et al., 2007).

The most recent research on plantlet formation of *Kalanchoë* investigated the role of *KdSOC1* gene in plantlet formation (Liu et al., 2016; Zhu et al., 2017). *SOC1* codes for a MADS-box transcription factor that plays a central role of integrating signals from multiple flowering pathways to control temporal differentiation of floral meristem (Lee and Lee, 2010; Moon et al., 2003). Similarly to flowering, plantlet formation is influenced by environmental factors such as photoperiod (Hershey, 2002), hormones (Kulka, 2006, 2008) and desiccation, hence, it is not surprising to observe recruitment of gene involved in flowering regulation into plantlet formation (Liu et al., 2016; Zhu et al., 2017). Apart from that, *Arabidopsis SOC1* was found to modulate determination of inflorescence meristem and secondary meristems (Melzer et al., 2008). The participation of *KdSOC1* in plantlet formation was first presented through upregulation of *KdSOC1* under long-day condition and drought stress in *K. daigremontiana* (Liu et al., 2016). *GUS* expression driven by *KdSOC1* promoter activity in *K. daigremontiana* revealed localisation of *KdSOC1* expression only at leaf notches prior to formation of pedestal (Zhu et al., 2017). When *KdSOC1* was overexpressed, *K. daigremontiana* transgenic plants exhibited inconsistent formation of pedestals, which resulted in asymmetrical plantlet formation (Zhu et al., 2017). The upregulation of *KdSOC1* was accompanied by increased auxin and auxin transporter *KdPIN1* and decreased zeatin concentration but the expression level of *KdCUC1*, *KdSTM* and *KdWUS* remained similar compared to wild-type and negative control samples (Zhu et al., 2017). The authors postulated that *KdSOC1* upregulates expression of *KdPIN1*, causing changes in directional flow of auxin, eventually affecting formation of leaf serrations and thus plantlet formation (Zhu et al., 2017). Attempt to generate transgenic *K. daigremontiana* with down-regulation of *KdSOC1* failed as most regenerated calli arrested at globular-stage; and any cotyledons eventually desiccated. This indicates an essential role for *KdSOC1* in somatic embryogenesis (Zhu et al., 2017).

The family of MADS-box genes are divided into two major protein classes; type I proteins consist of only highly conserved DNA-binding MADS-domain (M), and type II proteins are typically characterised by four domains, M-domain, I-domain, K-domain and a C-terminus (Smaczniak et al., 2012; Theissen et al., 1996). The presence of these domains categorised *Arabidopsis* SOC1 as type II protein (van Dijk et al., 2010) but in the case of *K. daigremontiana* KdSOC1, the gene lacks I-domain, C-terminus and has an M-domain that overlaps with the K-

domain (Liu et al., 2016). The I-domain specifies dimer interaction with DNA (van Dijk et al., 2010), the keratin-like K domain enables higher order protein complex formation and the highly variable C-terminus regulates transcription (Kaufmann et al., 2005). The regulation and interaction of *SOC1* is extremely complex (Immink et al., 2012; Richter et al., 2019), hence, changes in *KdSOC1* domains might have conferred novel biological function in a flowering gene in plantlet formation. In the case of *Kalanchoë*, *SOC1* might have evolved over time to divert its function in flowering or meristem determination towards plantlet formation, explaining the loss of sexual reproduction and gain of plantlet formation capability in *Kalanchoë* over evolutionary time (Garcês et al., 2007).

The existing literature have shown very few genes that play a role in *Kalanchoë* plantlet formation. Nonetheless, these studies have provided a general overview on genetic control of plantlet formation and have paved the way into understanding the detailed molecular mechanisms regulating plantlet formation and development. Based on this evidence, the mechanisms of embryogenesis, organogenesis and flowering development seem to be recruited during plantlet formation, particularly in constitutive plantlet-forming *Kalanchoë* species. Continued investigation into the role of these genes in other species might reveal differences and evolution into the mechanisms of plantlet formation. Understanding the sequence of temporal and spatial expression of these genes will reveal possible interaction and adaptation of different pathways during the plantlet formation. Nevertheless, the action of genetic control is dependent on changes in the plant's environment, which will be discussed in the following section.

1.3.2. Environmental cues on plantlet formation

The effect of duration of light on flowering is well studied in *Kalanchoë* genus as plants in the genus are often propagated for ornamental purposes (Currey and Erwin, 2011; Lopes Coelho et al., 2015; Resende, 1949; Schwabe, 1954). According to the induction of flowering in response to daylight, *Kalanchoë* species are classified into two categories: short-day species and and long-short day species. Short-day species require only short length of daylight to induce flowering, while long-short day species must be exposed to a specific sequence of long-day and short-day conditions to stimulate flowering. Examples of short-day *Kalanchoë* species

include *K. blossfeldiana* and *K. porphyrocalyx,* while *K. daigremontiana, K. pinnata* and *K. prolifera* are long-short day species (Lopes Coelho et al., 2015). Apart from induction of flowering, light also affects the formation of plantlets in *Kalanchoë* species. Plantlet formation in *K. daigremontiana* is induced only when exposed to a long-day condition for an extended period of time (Henson and Wareing, 1977), and the critical photoperiod for plantlet formation induction is known to be at least 12 hours of day light (Hershey, 2002). Nonetheless, photoperiodism of plantlet formation is only applicable to the initiation phase of plantlet formation as initiated plantlets continue to develop independently of day length (Henson and Wareing, 1977). Detached leaves of *K. daigremontiana* without axillary bud was also proven to develop plantlet under short day condition (Heide, 1965). The detailed mechanism behind the regulation of plantlet formation by light has yet to be demonstrated. However, with the long-standing role of phytohormones in responding to environment cues, it is expected that phytohormones are mediating the perception of light intensity to regulate changes in gene expression during plantlet development (Gupta and Nath, 2020; Vaishak et al., 2019).

Apart from the light condition, plants are also capable of detecting myriad environmental changes that ultimately cause a response by altering the genetic programs implemented (Gilroy, 2008). Nonetheless, plant response is not only limited to external factors but is also dependent on mechanical pressure created intrinsically. Mechanical stress is critical for normal growth and development of plants as movement of plant cells is very limited (Hernández-Hernández et al., 2014; Mirabet et al., 2011). Mechanical properties at the cellular, tissue and organ level of plants have been characterised with timed photographs tracking movement of cells (Poethig and Sussex, 1985), computer simulations (Rolland-Lagan et al., 2003), scanning electron microscopy and stereoscopy (Dumais and Kwiatkowska, 2002), atomic force microscopy (Oberhauser et al., 1998), 4D digital reconstruction (Fernandez et al., 2010) and others (Vogler et al., 2015). The current technology is so advanced that the mechanical properties of several parameters can be resolved at cellular resolution with three or four dimensions (Dumais and Kwiatkowska, 2002; Fernandez et al., 2010).

At the cellular level, a plant cell experiences mechanical stress from membrane tension due to turgor pressure on the cell wall. Turgor pressure is the build-up of pressure that is higher than

atmospheric pressure due to accumulation of hydrostatic fluid within a cell. It has been suggested that high turgor pressure causes high membrane tension, aiding the process of exocytosis (Fricke et al., 2000). To create a high turgor pressure, however, also requires regulation of the rigidity of the cell wall. The plant cell wall is a complex matrix of polysaccharides like pectin, hemicellulose and cellulose (Cosgrove, 2005). The ease of expansion of cell wall depends on the activity of cell wall enzymes such as expansins and pectin methylesterases and plant cytoskeleton (Cosgrove, 2005; Hernández-Hernández et al., 2014; Mirabet et al., 2011; Paredez et al., 2006). Plant hormones like auxin can also regulate cell wall expansion flexibility. The movement of auxin is then mediated by the localisation of its transporters PIN proteins, which in turn relies on membrane tension for its localisation (Nakayama et al., 2012). One study showed that when the SAM of *K. daigremontiana* was removed, leaf acidity and osmotic value of leaf sap increased along with rate of plantlet formation (Yazgan and Vardar, 1977). In a more recent study, a higher sucrose concentration was able to counteract inhibition of plantlet formation by cytokinin in *K. marnierianum* (Kulka, 2006). Mechanical pressure generated *via* these mechanisms mentioned above can regulate cell growth and shape alteration, which contribute to growth and shaping of tissues and organs that then confers its specification and identity (Hernández-Hernández et al., 2014; Mirabet et al., 2011).

Changes in individual cell due to mechanical stress are important to build a functional tissue or organ but are also critical for the identity and functionality at the scale of single cells. A perfect example in this case would be the guard cell. The guard cells are paired to form a stomatal pore between the cells with opening and closure regulated by turgor changes within each guard cell (Carter et al., 2017; Yi et al., 2019). Maintaining the turgor pressure beyond a certain threshold drives opening of stomatal pore, allowing gaseous exchange for photosynthesis and transpiration (Yi et al., 2019). Delicate control of stomatal opening is required to ensure sufficient gaseous exchange has taken place for photosynthesis and that water does not get loss excessively through transpiration (Negi et al., 2014). Another example is the regulation of the SAM and formation of primordial protrusion by localisation of different auxin concentrations and changes in cell wall elasticity (Murray et al., 2012). However, it was also suggested that the cell wall elasticity is affected by changes in orientation of microtubules

due to mechanical stresses (Hamant and Haswell, 2017). The buckling model explains that stress is more concentrated near the tip of concave shaped structures such as shoot apex and primordia, leading to changes in cytoskeleton organisation and stimulating organ initiation and elongation (Green, 1999). Even though the structure of apical meristem is different compared to xylem, it has been postulated that similar mechanism applies to radial growth of xylem tissues (Hernández-Hernández et al., 2014). Mechanical stress also participates in regulating below-ground structures of plants, particularly initiation and development of lateral roots. Mechanical stress that arise from rigid endodermis blocks lateral root growth and endodermal cell ablation triggered division of pericycle cells (Marhavý et al., 2016; Vermeer et al., 2014).

In order to execute different responses upon stimulation of these mechanical forces, plants require mechanisms to sense these forces, relay the signal to modify gene expression programs and induce physical or biochemical changes in the cell. One way that plants might sense these forces is through mechanosensors, which are proteins that change their conformation upon exertion of mechanical forces (Monshausen and Haswell, 2013; Orr et al., 2006). This converts physical force into a biochemical force that then can be relayed to other parts of the cell. In plants, mechanosensing occurs *via* changes in ion channels or extracellular matrix. Mechanosensing has been implicated in lateral root formation and response to touch stimulation (Monshausen and Gilroy, 2009). In the case of plantlet formation, mechanosensing might be involved in detection of pressure between leaf serrations, stimulating development of plantlets. However, this remains as a hypothesis to be confirmed. To bring about significant changes in the cell, the signal would have to be targeted to alter gene expressions. It has been shown that *STM* expression correlates with the curvature of the SAM and as mentioned above, the curvature exerts mechanical stress. Moreover, *STM* expression can be induced through the use of microvice and ablation to exert mechanical stress on the SAM (Landrein et al., 2015). Apart from *STM,* the promoter activity of *CUC3* gene was also found to be affected in the presence of mechanical stress (Fal et al., 2015). Gathering these information, mechanical stress due to concave structure of leaf notches of *Kalanchoë* plants might result in initiate of plantlet formation, in addition to change in cell wall elasticity due to membrane tension and auxin distribution in response to light stimulation.

1.3.3. Hormonal control on plantlet formation

Plant hormones, sometimes referred to as plant growth regulators, are chemical molecules that in extremely small amounts, regulate proper development and physiological processes in plants (Bhattacharya, 2019; Dilworth et al., 2017). The six major phytohormones are auxin, cytokinin, gibberellin, abscisic acid, brassinosteroids and ethylene (Dilworth et al., 2017; Yamaguchi et al., 2010). The others include jasmonic acid-related compounds and salicylic acid (Jiménez, 2005; Yamaguchi et al., 2010) and the increasingly well-known hormones karrikins, melatonin and strigolactones (Arnao and Hernández-Ruiz, 2020; Yao and Waters, 2020; Zwanenburg and Blanco-Ania, 2018). Apart from governing sustained growth and development of plants, these hormones can interact or independently regulate one or multiple processes in plants to allow detection and response to environment, reproduction, regeneration and senescence (Ahammed and Yu, 2016; Gerashchenkov and Rozhnova, 2013; Ikeuchi et al., 2019; Tamaki et al., 2020; Wojciechowska et al., 2018). Given the evident role of phytohormones in plant development, it is expected that *Kalanchoë* plantlet initiation, formation and growth will also depend on the action of phytohormones.

1.3.3.1. Auxin

To date, auxin hormone treatment experiments have not yield conclusive findings on the role of auxin on *Kalanchoë* plantlet formation. One of these experiments performed decades ago showed that exogenous application of auxin inhibited plantlet formation in *K. daigremontiana* and *K. pinnata* (Heide, 1965). In the case of *K. daigremontiana*, the inhibitory effect was observed on intact leaves of long day plants but its effect varied depending on leaf maturity (Heide, 1965). Auxin treatment on mature leaves with serrations resulted in reduction of plantlet number and delayed plantlet formation; but on young leaves, it caused these leaves to exhibit few to no serrations on the leaf margin, leading to inability to form plantlet due to absence of plantlet formation site (Heide, 1965). These results showed that under the long day condition, intact leaves with axillary bud developed plantlets normally whereas externally applied auxin inhibited plantlet formation (Heide, 1965). This suggests that perhaps under short day condition, a higher endogenous auxin concentration in intact leaves prohibited plantlet formation. A later study showed that the transfer of *K. daigremontiana* plants from short to long day condition, resulted in initial increase of the level of auxin IAA which then

rapidly declined and remained at a higher level than the initial level (Henson and Wareing, 1977). Nonetheless, this finding was insufficient to eliminate this speculation as whole leaves extract was used for the measurement and plantlet initiation might be a consequence of a more localised change of auxin concentration (Henson and Wareing, 1977). In contrast to intact leaves, leaves detached from *K. daigremontiana* plants develop plantlets independent of day length (Heide, 1965; Yazgan and Vardar, 1977). In addition, auxin treatment of detached leaves from *K. daigremontiana* plants grown under long day condition stimulated plantlet formation; but beyond a threshold concentration, auxin exerted an inhibitory effect (Yazgan and Vardar, 1977). Another study also showed that auxin treatment of leaves detached from plants grown under short day condition increases number of plantlets formed (Heide, 1965). If axillary buds are present on detached leaves from plants grown under short day condition, plantlet formation was also inhibited (Heide, 1965).

A more recent study support the previous findings that high concentrations of auxin inhibits plantlet formation (Zhu et al., 2017). There was elevated auxin content and increased expression of auxin transporter *KdPIN1* in *K. daigremontiana* leaves with *KdSOC1* overexpression that displayed inconsistent pedestal and plantlet formation (Zhu et al., 2017). This study suggests that upregulation of *KdSOC1* affects *KdPIN1* distribution, which in turns disrupts directional auxin flow that shapes the leaf serration and formation of pedestal sites (Zhu et al., 2017). However, the results presented are not conclusive as whole leaves were harvested for measurement of auxin accumulation and *KdPIN1* expression, and based on existing evidence, auxin seems to be acting locally at the site of leaf indentation. Although the mechanism of auxin activity has not been clearly illustrated, there is increasing evidence pointing towards the involvement of auxin in plantlet formation. A recent example is the chronological increase of auxin concentration from formation of leaf serration, to division of plantlet-initiating cells at the leaf notches and then until shoot formation (Guo et al., 2015). A fluorescence reporter line of synthetic auxin promoter DR5 in *K. daigremontiana* also showed fluorescence at the leaf serration (Guo et al., 2015). Nonetheless, the fluorescence spots were inconsistently distributed and faint, thus a more robust reporter line is needed to provide a clearer illustration of auxin participation in plantlet formation.

For auxin to act locally near or at the site of plantlet formation to influence plantlet initiation and development, auxin needs to be synthesised locally or be transported to the site of action. Auxin can be synthesised *via* two major pathways: (i) Tryptophan(Trp)-dependent and (ii) Trp-independent pathway (Cohen et al., 2003; Strader and Bartel, 2008). Trp-dependent pathways are further categorised into four pathways in which the indole-3-pyruvic acid (IPA) pathway is the most well-categorised and known to be the primary auxin biosynthesis pathway in plants (Mashiguchi et al., 2011; Zhao, 2010). According to this pathway, TAA mediates the conversion of Trp to IPA, which is then directly converted into IAA through a rate-limiting step catalysed by YUC type flavin-containing monooxygenase (Mashiguchi et al., 2011; Tao et al., 2008). *YUC1* is the first gene in the *YUC* gene family that was identified through gain-of-function mutants that exhibited auxin overproduction phenotypes, such as long hypocotyl and epinastic cotyledons (Zhao et al., 2001). Explants from these mutants contained sufficient endogenous auxin to be propagated in hormone-free media, and to induce and up-regulate expression of auxin-inducible genes and auxin reporters (Zhao et al., 2001). Overexpression of other *YUC* genes resulted in similar phenotypes but inactivation of a single *YUC* gene does not cause significant developmental defects, indicating functional redundancy of *YUC* genes (Cheng et al., 2006, 2007; Kim et al., 2007; Marsch-Martinez et al., 2002; Woodward et al., 2005; Zhao et al., 2001). However, each *YUC* gene was shown to localise and function in specific organs, and auxin synthesised in one organ cannot replace auxin deficiency in another organ (Blakeslee et al., 2019; Cheng et al., 2006; Matthes et al., 2019; Zhao, 2018). These findings imply that *YUC* genes are responsible for regulation of local auxin dynamics. The presence of *YUC* gene family in various plant species proves that *YUC* genes are evolutionarily conserved (Cao et al., 2019). Hence, it is possible that *YUC* genes are involved in local auxin biosynthesis required for plantlet formation.

Apart from *de novo* synthesis, local auxin level is also regulated by auxin transport proteins such as PIN-FORMED (PIN) polar auxin transporters. In general, PIN transporters can be categorised into two groups based on subcellular localisation, molecular structure and auxin facilitation (Bennett et al., 2014; Blakeslee et al., 2005). Most PIN proteins, including PIN1, PIN2, PIN4 and PIN7 contain a highly conserved long central hydrophilic loop and are localised on the plasma membrane, aiding influx and efflux of auxin (Ganguly et al., 2014; Luschnig and

Vert, 2014). Other PIN proteins, PIN5 and PIN8 with a short central hydrophilic loop, are located at intracellular compartments and are responsible for auxin homeostasis in the cells (Bennett et al., 2014; Dal Bosco et al., 2012; Ganguly et al., 2014; Mravec et al., 2009). In the *PIN* gene family, PIN1 is the first protein identified from the *Arabidopsis pin1* mutant which was characterised by missing or abnormal inflorescence axes, flowers, and leaves due to failure in formation of lateral organ primordia (Adamowski and Friml, 2015; Křeček et al., 2009; Okada et al., 1991). As dramatic phenotypic changes resulted from the loss of only PIN1, it was recognised as the least redundant protein in the PIN protein family. Expression analysis also revealed that PIN1 is expressed in *Arabidopsis* shoot and root meristems, vasculature and apical region of embryo at early stages, providing evidence that PIN1 is required for normal development of these structures (Guenot et al., 2012; Izhaki and Bowman, 2007; Omelyanchuk et al., 2016; Scarpella et al., 2006). Given the role of PIN1 in organogenesis and embryogenesis and recruitment of these processes in plantlet formation, it would not be surprising if PIN1 was involved in plantlet initiation and development. To confirm its participation in *K. daigremontiana* plantlet formation, it would be useful to visualise localisation of PIN1 specifically at the site of plantlet formation.

1.3.3.2. Cytokinin

Over the past few decades, it has been suggested that cytokinin might be the hormone responsible for breaking the dormancy of plantlet primordia (Heide, 1965; Houck and Rieseberg, 1983; Yazgan and Vardar, 1977). However, the existing literatures have presented contradictory evidence on the possible functions of cytokinin on plantlet formation. For example, in contrast to auxin, cytokinin seemed to exert an opposite effect, as external application of cytokinin on long-day *K. daigremontiana* and *K. pinnata* plants stimulated plantlet formation (Heide, 1965; Houck and Rieseberg, 1983; Yazgan and Vardar, 1977). In addition, short-day grown *K. daigremontiana* plants treated with cytokinin resulted in the same rate of plantlet formation as non-treated long-day grown plants (Heide, 1965). This evidence implies that plantlet formation might be triggered by increase in cytokinin due to increase in day length. Nonetheless, when plants are transferred from short day to long day condition, the changes in endogenous level of cytokinin in leaves exhibited similar trend to auxin, displaying a sharp increase which was followed by a decline (Henson and Wareing, 1977).

However, increase in cytokinin level was more gradual than auxin (Henson and Wareing, 1977). This data does not show consistent correlation between cytokinin level and plantlet formation. The limitations of the study include the use whole leaf extracts that might masks localised changes in cytokinin level, and the long time period between each measurement might fail to capture immediate change in hormone level, straight after moving the plant from short to long day or the exact moment in which plantlet formation is initiated.

Other evidence showed that similar to auxin, the detachment of leaf also affects the influence of cytokinin on *K. daigremontiana* plantlet formation. When detached leaves from plants grown under long day condition were treated with increasing concentration of cytokinin, the number of plantlets formed decreases (Yazgan and Vardar, 1977) but the opposite was observed when the treatment was performed on detached leaves from plants grown under short day condition (Heide, 1965). When auxin and cytokinin were both applied in different combinations of concentrations, the inhibitory effect of cytokinin on plantlet formation masked the stimulatory effect of auxin on plantlet formation as shown by lower plantlet number compared to non-treated plants (Yazgan and Vardar, 1977). The inhibition of plantlet formation by cytokinin was also observed in detached leaves from *K. marnierianum* long-day grown plants (Kulka, 2006). The author tested various cytokinin (zeatin, kinetin and BAP), and all showed strong inhibitory effect albeit at different concentrations, possibly due to inability to mimic *in vivo* conditions (Kulka, 2006). When a cytokinin antagonist was applied to detached leaves with stem, plantlets were formed (Kulka, 2006). The restoration of plantlet formation was then partially reversed by application of BAP cytokinin (Kulka, 2006). Based on these findings, it is very clear that cytokinin has an inhibitory effect on plantlet formation of detached leaves in *K. daigremontiana* and *K. marnierianum.* Nonetheless, it was interesting to observe how similar observations on the action of cytokinin was obtained for *K. daigremontiana* and *K. marnierianum*, which have different modes of plantlet formation (Garcês and Sinha, 2009a; Kulka, 2006); and that *K. pinnata*, which has the same mode of plantlet formation as *K. marnierianum*, exhibited the opposite effect of cytokinin on plantlet formation (Heide, 1965; Houck and Rieseberg, 1983).

The participation of cytokinin in plantlet formation will depend on its regulation at different levels, which includes biosynthesis and metabolism, transport and signal transduction (Kieber and Schaller, 2018). Among these three aspects of cytokinin regulation, the signal transduction pathway of cytokinin is the most well-illustrated, as synthesis and degradation of cytokinin are affected by multiple factors and the information on cytokinin transport is still limited (Durán-Medina et al., 2017a; Sakakibara, 2005; Werner et al., 2006). Cytokinin signal transduction involves phosphotransfer from His residue of the histidine kinase cytokinin receptors to Asp residue of the response regulator proteins (Schaller et al., 2008). This process is mediated by histidine-containing phosphotransfer proteins (Hutchison et al., 2006). In *Arabidopsis,* there are six *Arabidopsis thaliana* histidine-containing phosphotransfer proteins (AHP1-6). AHP1-AHP5 contain conserved amino acids that confer their function as partially redundant positive regulators of cytokinin signalling. However, AHP6 has a mutation at its conserved histidine residue that renders it impossible to be phosphorylated and act as a true phosphotransfer protein (Mähönen et al., 2006; Suzuki et al., 2000). Hence, AHP6 is known as a pseudo histidine-containing phosphotransfer protein, which acts as a negative regulator of cytokinin responsiveness (Mähönen et al., 2006). *ahp6* mutants showed defects in vascular patterning, suggesting that AHP6 specifies protoxylem cell fate through spatial control of cytokinin signalling (Mähönen et al., 2006). The importance of AHP6 in confining cytokinin signalling was also demonstrated through the requirement of AHP6 induction for proper gynoecium development, particularly formation of outer carpel tissue (Durán-Medina et al., 2017b; Müller et al., 2017; Reyes-Olalde et al., 2017). Apart from that, AHP6 mediates auxin-cytokinin crosstalk; through influencing localisation of auxin transporter PIN1 and specific spatio-temporal expression of auxin downstream genes to regulate lateral root patterning and organ initiation at shoot apex (Besnard et al., 2014a; Moreira et al., 2013). These studies also showed direct impact of cytokinin on AHP6 expression (Besnard et al., 2014a; Durán-Medina et al., 2017b; Mähönen et al., 2006; Moreira et al., 2013; Reyes-Olalde et al., 2017). Given the role of AHP6 in organ initiation, cell fate specification and its direct relationship with cytokinin, AHP6 seems to be a good candidate for studying the role of cytokinin in plantlet formation.

1.3.3.3. Other hormones

Studies of the effect of other plant hormones on plantlet formation are not limited to *K. daigremontiana* and mostly were performed more than a decade ago. Previous studies showed that when a late embryogenesis gene, *LEC1*, was lost, dormancy of plantlet growth is removed (Garcês et al., 2014; Jo et al., 2019). Hence, exogenous application of gibberellic acid (GA), which is known to release seed dormancy, is expected to trigger plantlet formation in constitutive plantlet-forming *Kalanchoë* species. However, external application of GA around the stem or leaves of *K. tubiflora* inhibited plantlet formation (Dostál, 1970). *K. tubiflora*, like *K. daigremontiana* also forms plantlets constitutively, hence, a similar effect by GA on *K. daigremontiana* is expected. Nonetheless, GA treatment of *K. daigremontiana* resulted in elongation of the adult plant and plantlets (Garcês et al., 2014). Application of GA biosynthesis inhibitor, uniconazole, on the other hand, inhibited plantlet development and retarded growth of *K. daigremontiana* (Garcês et al., 2014; Izumi et al., 1984). When GA was applied to *K. daigremontiana* with functional *KdLEC1*, the arrested plantlets could not be restored (Garcês et al., 2014).

In the case of ethylene, a plant hormone known to affect organ senescence, induction of stem and petiole growth and pathogen infection has exhibited different responses when applied on different *Kalanchoë* species (Bleecker and Kende, 2000). *K. marierianum* initiates plantlet formation upon excision of leaves, and when ethylene was externally applied to excised leaves and explants of *K. marierianum*, root induction occurred earlier (Kulka, 2008). In addition, ethylene treatment resulted in development of smaller and more roots and premature plantlet detachment (Kulka, 2008). When ethylene is exogenously applied to explants previously treated with auxin transport inhibitor TIBA, root induction was not restored. However, the addition of ethylene lowered the concentration threshold of auxin NAA required to restore root formation (Kulka, 2008). In *K. pinnata,* the use of ethrel, an ethylene-releasing compound promoted plantlet growth (Jaiswal and Sawhney, 2006a).

1.4. **Conclusion**

Kalanchoë plants have contributed greatly to the understanding of CAM and have also provided valuable compounds to the research and medical community. However, the innate and fascinating asexual reproductive strategy of *Kalanchoë* plants, plantlet formation, remained minimally investigated. The method in which *Kalanchoë* plants reproduce *via* plantlet formation is remarkable as the plantlets are suggested to have formed from somatic cells on leaves. Existing literature on mechanisms behind totipotency and pluripotency of cells during zygotic embryogenesis, somatic embryogenesis and specification and maintenance of meristematic tissues has provided clues on physiological and molecular control during plantlet initiation and development. Changes in gene expression, plant hormones and responses to environmental cues have shown to play a role in plantlet formation. Nonetheless, the majority of existing evidence on these aspects has remained controversial. Detailed information on the mechanism of plantlet formation illustrating development of whole plants from existing plant organs will certainly accelerate our understanding of plant developmental plasticity and in turn aid the production of better crops and plants that are of economic importance to the society.

CHAPTER 2

RESULTS 1

MD generated qRT-PCR data in Fig. 2.4H and Fig. 2.5C, D. FJB stained *KdFUS3::GUS* for GUS activity and took the GUS staining images presented in Fig. 2.1H-J. JPO produced all text in this chapter and prepared samples for RNA-sequencing. University of Manchester Genomic Technologies Core Facility and Bioinformatics Core Facility performed and analysed the RNA-sequencing data from which JPO obtained expression data presented in Fig. 2.4A-G and Fig. 2.5A, B. All other data were generated by HG. All final figures were produced by MK and JPO.

2. Participation of *FUSCA3* During *Kalanchoë daigremontiana* Plantlet Formation

Joo Phin Ooi[1], Helena Gârces[1], Marco D'Ario[1], Francisco Jácome Blásquez[1] and Minsung Kim[1]*

[1]School of Biological Sciences, Faculty of Biology, Medicine and Health, University of Manchester, Manchester, M13 9PT, United Kingdom

*Corresponding author: Minsung.kim@manchester.ac.uk

Key Words: Asexual Reproduction, *Kalanchoë*, plantlet formation, embryogenesis

2.1. Abstract

Plant species in the genus *Kalanchoë* have varying capacity in reproducing asexually *via* plantlet formation. Previous studies suggest that plantlet development in *K. daigremontiana* morphologically resembles *Arabidopsis* zygotic embryo development. Late embryogenesis genes such as *LEAFY COTYLEDON1* (*LEC1*) and *FUSCA3* (*FUS3*) are expressed during *K. daigremontiana* plantlet formation. However, *K. daigremontiana* LEC1 homolog KdLEC1 was non-functional. As LEC1 homologs are master regulators of late embryogenesis, this suggest that the embryogenesis program is recruited in plantlet formation but with some alterations. Here we show that *KdFUS3* is required for plantlet formation, and it may share a part of *KdLEC1* function in plantlet development due to overlapping expression domains. *KdFUS3* was expressed during plantlet formation, and downregulation of *KdFUS3* led to reduction of plantlets on leaves. These *KdFUS3* antisense transgenic plants also exhibited defective pedestal formation and plantlet initiation, indicating early participation of *KdFUS3* in plantlet formation. Downregulation of organogenesis genes in these *KdFUS3* antisense transgenic plants and phenotypic similarities between *KdFUS3* and *KdSHOOTMERISTEMLESS* (*KdSTM*) antisense transgenic plants suggest that embryogenesis and organogenesis pathways might be integrated to regulate plantlet formation. These findings show that key embryogenesis and organogenesis genes have been recruited but may exhibit tinkering in their mechanisms to establish asexual reproduction in *Kalanchoë*.

2.2. Introduction

In contrast to animal cells, plant somatic cells have great regeneration capacity (Ikeuchi et al., 2016). Plants can repair or regenerate new structures upon wounding (Ikeuchi et al., 2016; Pulianmackal et al., 2014). *Via* somatic embryogenesis, plant somatic cells can even de-differentiate, regain embryonic potency and develop into a whole plant (Elhiti et al., 2013; Yang and Zhang, 2010). However, this is often artificially achieved by external applications of plant hormones in *in vitro* tissue culture (Horstman et al., 2017b; Jiménez, 2005). Certain *Kalanchoë* species have exploited the ability to regain embryonic competence through stimulation of somatic embryogenesis to reproduce asexually by forming plantlets on its leaf serrations (Garcês and Sinha, 2009a; Garcês et al., 2007). These *Kalanchoë* plantlets resemble a miniature version of an adult plant, and the morphology and the physiology of plantlet formation have been characterised in great detail (Batygina et al., 1996; Dostál, 1970; Howe, 1931). The capability to produce plantlets varies among different species in the genus *Kalanchoë*. For example, some basal species such as *K. marmorata, K. rhombopilosa, K. tomentosa* and *K. thyrsiflora* do not produce plantlets. Species such as *K. pinnata, K. prolifera, K. strepthantha* and *K. fedstchenkoi* produce plantlets only upon stress, whereas *K. daigremontiana* produces plantlets constitutively under a long day condition. Another species, *K. gastoni-bonnieri* can form one plantlet on each leaf constitutively, and when induced by stress, forms plantlets on other indentations of the leaves (Garcês and Sinha, 2009a; Garcês et al., 2007). As the range of plantlet production ability of *Kalanchoë* species varies considerably despite their close phylogeny, *Kalanchoë* serves as an ideal model to study development and evolution of the molecular mechanism of plantlet formation (Garcês et al., 2007).

Previous scanning electron microscopy studies showed that plantlet formation in *K. daigremontiana* closely resembles developmental stages of *Arabidopsis* zygotic embryo (Garcês et al., 2007). In addition, the homologous late embryogenesis gene, *LEAFY COTYLEDON 1* (*LEC1*) in *K. daigremontiana* (*KdLEC1*) was expressed in developing plantlet (Garcês et al., 2007). This suggests zygotic embryogenesis pathways may be involved in plantlet formation. However, sequence analysis revealed a 20-nucleotide deletion in *KdLEC1* sequence, which resulted in formation of a truncated protein (Garcês et al., 2007). The truncated KdLEC1 could not rescue *lec1 Arabidopsis* mutants, and knock-out of *KdLEC1* from *K. daigremontiana* did not

affect plantlet formation (Garcês et al., 2007). Introducing an *Arabidopsis* LEC1 copy into *K. daigremontiana* resulted in defective plantlets that exhibit typical characteristics of a dormant seed. This indicates that changes in KdLEC1 relative to *Arabidopsis* LEC1 was required to bypass the seed dormancy phase and to allow plantlet formation (Garcês et al., 2014). Phylogenetic analyses revealed a consistent co-relationship between LEC1 protein truncation, seed viability and plantlet formation ability across different *Kalanchoë* species. Species that do not produce plantlets share similar protein sequences with Arabidopsis LEC1 and produce viable seeds, while species that produce plantlet constitutively and cannot produce viable seed expresses the non-functional truncated LEC1 protein (Garcês et al., 2007). These findings were perplexing; as non-functional LEC1 appeared to be involved in plantlet formation, it is not clear how embryogenesis-like developmental processes are regulated during plantlet development (Pelletier et al., 2017). Hence, this led to a hypothesis that the other genes are recruited to replace essential functions of LEC1 in *Kalanchoë* species that produce plantlets.

LEC1 was first identified as a master regulator of late embryogenesis as *lec1 Arabidopsis* mutant embryos lacked features of embryo maturation (Meinke, 1992; West et al., 1994). However, *lec1* mutant embryos also prematurely exhibited morphological and molecular characteristics of the post-germination *Arabidopsis* seedling such as leaf-like cotyledons (Meinke, 1992; West et al., 1994). On the other hand, seedlings overexpressing *LEC1* developed embryo-like structures on leaves whilst vegetative growth were repressed (Huang et al., 2015; Lotan et al., 1998; Meinke, 1992; West et al., 1994). This suggests that *LEC1* is required to specify cotyledon identity during embryogenesis. *LEC1* is also sufficient to induce somatic embryo development in several species (Guo et al., 2013; Ledwoń and Gaj, 2011; Lotan et al., 1998; Nic-Can et al., 2013; Orłowska et al., 2017; Yang and Zhang, 2010), indicating the role of *LEC1* in embryo morphogenesis. Moreover, *LEC1* regulates expression of embryo morphogenesis genes such as *PHAVOLUTA* and *SCARECROW* (Hu et al., 2018; Junker et al., 2012; Pelletier et al., 2017). The role of *LEC1* in early embryogenesis is also consistent with its expression within 24 hours after fertilisation (Lotan et al., 1998). During seed development, *LEC1* is also known to regulate photosynthesis, chloroplast biogenesis and endosperm development (Junker et al., 2012; Meinke, 1992; Pelletier et al., 2017; West et al., 1994; Xu et

al., 2016; Zhang et al., 2008). These studies show that *LEC1* is involved in not only seed maturation, but also other aspects of seed development.

LEC1 is a NF-YB subunit of the CCAAT box-binding protein in the *LAFL* network of genes that regulates seed maturation (Cagliari et al., 2014; Lotan et al., 1998). The LAFL network encompasses LEC1, LEC1-LIKE (L1L) and three B3 domain proteins ABSCISIC ACID INSENSITIVE3 (ABI3), FUSCA3 (FUS3) and LEC2 (Giraudat et al., 1992; Jia et al., 2013; Kwong et al., 2003; Lotan et al., 1998; Luerßen et al., 1998; Stone et al., 2001). These genes are expressed during embryogenesis and interact with each other to activate maturation-related genes (Kroj et al., 2003; Kwong et al., 2003; Lepiniec et al., 2018; Lotan et al., 1998; O'Neill et al., 2019; Parcy et al., 1994; Stone et al., 2001; Tsuchiya et al., 2004). *L1L* is the closest related gene to *LEC1* but *l1l* mutants displayed different defects in embryo development compared to *lec1* mutants, suggesting that L1L play a different role in embryogenesis (Cagliari et al., 2014; Lotan et al., 1998). Unlike other LAFL genes, *abi3* mutants do not have leafy cotyledons, hence, do not belong to the *LEC* class family (*LEC1, LEC2, FUS3*) (Giraudat et al., 1992; Meinke et al., 1994). *lec1*, *fus3* and *abi3* mutants are desiccation-intolerant and embryonic lethal, whereas *lec2* mutants are only partially desiccation-intolerant (Harada et al., 2001; Nambara et al., 1992). *Arabidopsis fus3* mutants, like *Arabidopsis lec1* mutants, displayed premature vegetative features in embryos such as leaf-like cotyledons, implying that *FUS3* is also involved in specification of cotyledon identity (Bäumlein et al., 1994; Keith et al., 1994; Meinke, 1992). Furthermore, the downstream embryo maturation genes that FUS3 and LEC1 directly target, overlap (Pelletier et al., 2017; Wang and Perry, 2013). In addition to that, *FUS3* is directly transcriptionally regulated by LEC1, which coincides with up- and down-regulation of *FUS3* in *lec1* mutants and in *LEC1* overexpression mutants, respectively (Kagaya et al., 2005; Mu et al., 2008; Parcy et al., 1997; Pelletier et al., 2017; To et al., 2006). FUS3 also directly upregulates VIVIPAROUS ABI3-LIKE1 (VAL1) that represses LEC1 activity *via* chromatin structure modification (Wang and Perry, 2013). From these observations, *FUS3* is a possible candidate to compensate for the loss of *LEC1* essential functions in plantlet-forming *Kalanchoë* species.

A previous study has identified the FUSCA ortholog in *K. daigremontiana* (KdFUS3) that shares high protein sequence similarity with *Arabidopsis* FUS3. KdFUS3 was grouped in the same clade

with B3 domain family proteins (Garcês et al., 2007). The same study also showed *KdFUS3* transcripts were highly expressed across different plantlet developmental stages and in pollinated ovaries but were absent in the shoot apical meristem (SAM) (Garcês et al., 2007). These support the recruitment of the embryogenesis program during plantlet formation. Similarity in expression pattern of *KdFUS3* and *KdLEC1* in *K. daigremontiana* also suggests that KdFUS3 may replace the necessary embryogenesis role that the truncated KdLEC1 cannot execute (Garcês et al., 2007). To determine whether this is true, we further analysed KdFUS3 sequence and showed that KdFUS3 sequence is clustered with other angiosperm FUS3 sequences. *In situ* hybridisation of *KdFUS3* and GUS staining of *KdFUS3*::*GUS* in *K. daigremontiana* also suggest that *KdFUS3* transcripts and activity are present during early plantlet development. *KdFUS3* downregulation led to defective pedestal formation, plantlet initiation and formation of plantlets with altered phenotypes, which resemble *KdSTM* RNAi plants. In *KdFUS3* antisense lines, *KdSTM* and *KdWUSCHEL* (*WUSCHEL*) were also downregulated. Hence, *KdFUS3* function might be integrated with organogenesis pathways. Although functional characterisation of *KdFUS3* is still required to confirm that KdFUS3 can replace embryogenesis functions of LEC1, our results has shown that temporal and spatial expression of *KdFUS3* overlaps with *KdLEC1.* In addition, other LAFL genes also exhibited differences in expression compared to their corresponding orthologs in *Arabidopsis*, indicating that LAFL network of genes might have been co-opted with some alteration to aid *Kalanchoë* plantlet formation. Our findings suggest that the evolution of the LAFL network might have contributed to different modes of plantlet formation strategies in the *Kalanchoë* genus, and that embryogenesis pathways might have integrated with organogenesis pathways to regulate *K. daigremontiana* plantlet development.

2.3. **Materials & Methods**

2.3.1. Phylogenetic and sequence analysis

19 B3-domain protein sequences were obtained from GenBank database and were aligned using ClustalX 2.1. The sequences were trimmed to isolate only B3-domain sequences. All sequences contained 72 amino acids apart from AtRL1 and AtRAV1, which contained 74 amino acids. The phylogenetic tree of these sequences was constructed using maximum parsimony and neighbour-joining analysis in PAUP program (version 4.0 beta10, David L. Swofford, Sinauer Associates) with a bootstrap value of 1000. The multiple sequence alignment of FUS3 B3-domain sequences in Supplementary Fig 2.1 was created using Jalview 2.11.1.2. See http://www.jalview.org/help/html/colourSchemes/clustal.html for information of the colour scheme used. The secondary structural information was incorporated using ESPript 3.0 at https://espript.ibcp.fr/ESPript/ESPript/index.php (Robert and Gouet, 2014).

Table 2.1 The list of species and proteins used for phylogenetic analysis.

Symbol	Species Name	Protein	Accession number
AtRL1	*Arabidopsis thaliana*	RAV-LIKE 1	AAM65499.1
AtRAV1	*Arabidopsis thaliana*	RELATED TO ABI3/VP1	NP_172784.1
GrLEC2	*Gossypium raimondii*	LEAFY COTYLEDON 2	XP_012445413.1
CsLEC2	*Camelina sativa*	LEAFY COTYLEDON 2	XP_010460618.1
AtLEC2	*Arabidopsis thaliana*	LEAFY COTYLEDON 2	AAL12004.1
AtABI3	*Arabidopsis thaliana*	ABSCISIC ACID INSENSITIVE3	BAD93896.1
PtABI3	*Populus tomentosa*	ABSCISIC ACID INSENSITIVE3	AGM20671.1
OsVP1	*Oryza sativa*	VIVIPAROUS1	XP_015629311.1
ZmVP1	*Zea mays*	VIVIPAROUS1	ONM35246.1
NnFUS3	*Nelumbo nucifera*	FUSCA3	XP_010249172.1
EgFUS3	*Eucalyptus grandis*	FUSCA3	XP_039173749.1
CsFUS3	*Citrus sinensis*	FUSCA3	ARK19654.1
AtFUS3	*Arabidopsis thaliana*	FUSCA3	AAC35246.1
CmFUS3	*Cucumis melo*	FUSCA3	XP_016903652.1
MdFUS3	*Malus domestica*	FUSCA3	XP_008341665.1
KdFUS3	*Kalanchoë daigremontiana*	FUSCA3	ABP01773.1
MtFUS3	*Medicago truncatula*	FUSCA3	XP_003624470.1
GaFUS3	*Gossypium arboretum*	FUSCA3	KHG24234.1
TcFUS3	*Theobroma cacao*	FUSCA3	XP_007031992.2

2.3.2. Plant material and growth conditions

K. daigremontiana wild-type and transgenic plants were grown in a 29˚C growth chamber with a photoperiod of 16 hour light/8 hour dark. The first mature whole leaves from wild-type *K. daigremontiana* were used for plant transformation. For RNA-sequencing analysis, wild-type *K. daigremontiana* plants were grown in a 23˚C growth chamber with a photoperiod of 16 hour light/8 hour dark.

2.3.3. Histology and *in situ* hybridisation

Plant tissues fixation and preparation for scanning electron microscope (SEM) analysis and tissue sectioning were performed as described in (Garcês and Sinha, 2009b). The sense and antisense *KdFUS3* sequences were used as probes for *in situ* hybridisation. Preparation of probes and *in-situ* hybridisation were performed as described in (Garcês and Sinha, 2009c) on only wild-type samples. The images of developed *in situ* hybridisation sections were captured using Leica DMR microscope (Leica Microsystems, Germany). GUS staining solution containing final concentration of 100 mM Sodium phosphate buffer pH 7.2, 10 mM EDTA pH 8.0, 0.1% Triton X-100, 1 mM Potassium Ferricyanide, 1 mM Potassium Ferrocyanide and 2 mM X-gluc were used for GUS staining. All GUS staining images were taken using Leica S8 APO microscope (Leica Microsystems, Germany) with a GX-CAM Eclipse camera (GT Vision, UK) attached.

2.3.4. Transgenic plants

To generate plants with reduced expression of *KdFUS3*, a construct containing the antisense strand of *KdFUS3* (GenBank: ABP01773.1) driven by 35S promoter and terminator were inserted into a modified plasmid *pBi121*. *KdFUS3* was previously isolated as shown in (Garcês et al., 2007). Photographs of the antisense plants were captured with Digital D3100 Nikon digital camera (Nikon, Japan). The 1581 bp *KdFUS3* promoter, GUS gene and NOS terminator were used to generate a complete reporter construct, which was inserted into a modified plasmid *pBi121*. All constructs were formed *via* golden gate assembly, then transformed into *Agrobacterium tumefaciens* strain *LBA4404* through electroporation. The protocol from (Garcês and Sinha, 2009d) was used to transform wild-type plant tissues to generate the transgenic plants.

2.3.5. Genotyping PCR and expression analyses

Approximately 2mm wide margin of 1-2 cm long leaves from wild-type and *KdFUS3* antisense plants were harvested for genomic DNA and RNA extraction. Genomic DNA were extracted as described in (Garcês and Sinha, 2009e). The genomic DNA was used for amplification of *35S::*antisense-*KdFUS3* with the primers 5'-GTGGTCTCAGGAGGCTAGAGCAGCTTGCCAAC-3' and 5'-GGAGACCTTTCTCCCTG-3'. For *NEOMYCIN PHOSPHOTRANSFERASE II* (*NPTII*) gene, the primers 5'-CACAACAGACAATCGGCTGC-3' and 5'-GCACGAGGAAGCGGTCAG-3' were used. RNA was extracted as described in (Garcês and Sinha, 2009f). cDNA was synthesised using Tetro cDNA Synthesis Kit (Bioline, UK). For reverse-transcriptase PCR (RT-PCR), an annealing temperature of 60 °C with 35 cycles was used. *KdFUS3* primers were 5'GAGACCTTTCTCCCTGTGCTTG-3' and 5'GGCCAGTACCTGTATTTGAAGC-3'. Quantitative real-time PCR (qRT-PCR) primers for *KdSTM* were 5'-GGATCAGTTCATGGAGGCTTAC-3' and 5'-CTTGAACTGGGACTCAATCCTC-3'; for *KdLEC1*, the primers were 5'-GTCGGAGTATATCGGCTTCATC-3' and 5'-TGTATCGGTGCAGGTACAGAG T-3'; for *KdWUS*, the primers were 5'-GAGCAGATAAGAATACTCAAAGATCTTTA-3' and 5'-TAGAAGACATTTTTGCCCTCGATCT-3'. StepOne™ Real-Time PCR System (Applied Biosystems, UK) and sensiFAST SYBR® Hi-ROX Mix (Bioline, UK) was used to perform qRT-PCR. StepOne™ and StepOnePlus™ Software v2.3 (Thermo Fisher Scientific, UK) was used for template design and analysis. *KDGLYCERALDEHYDE 3-PHOSPHATE DEHYDROGENASE* (*KdGAPDH*) were used as a reference gene for both RT-PCR and qRT-PCR; its primers were 5'GGAGCAGAGATAACAACCTTC-3' and 5'-TCCATTCATCAACACAGACTAC-3'. An annealing temperature of 60 °C with 40 cycles was used for qRT-PCR. All graphs and statistical tests (non-parametric Kruskal-Wallis statistical tests and Dunn's multiple comparison tests) were performed by GraphPad Prism 8.

2.3.6. Total RNA isolation & sequencing

Four plantlet stages in wild-type *K. daigremontiana* were identified to include stages of initiation of plantlet formation (See Supplementary Fig. 2.2). Leaves exhibiting at least three of these plantlet stages along its leaf margin were selected for use. 0.3 cm^2 tissues at the leaf notches were harvested. The control samples were margin of 1-2 cm young leaves of measured from the base to tip. Total RNAs was extracted using Qiagen RNeasy Plant Mini Kit (Qiagen, UK)

according to the manufacture's protocol with modification. 600 µl RLC buffer with 10 mg Polyvinylpyrrolidone (PVP), molecular weight 40,000 was used for a maximum of 100 mg tissue powder. The mixed solution was then vortexed and incubated for 1 minute at 56 °C before following the protocol. The purified RNA samples were sent for paired-end Sanger sequencing by Illumina RNA-sequencing technology (The University of Manchester Sequencing Facility). The average number of reads for each biological replicate was 24,930,858, with each read being 75 base pairs and varying coverage for each transcript.

2.4. **Results**

2.4.1. KdFUS3 protein sequence is conserved within the angiosperm family

Garcês et al., 2007 identified the FUS3 ortholog in *K. daigremontiana* and revealed that among *Arabidopsis* B3 domain-containing transcription factors such as auxin-response factors, ABSCISIC ACID INSENSITIVE3/VIVIPAROUS1 (ABI3/VP1), RELATED TO ABI3/VP1 (RAV) and RAV-LIKE (RL), KdFUS3 shares the same phylogeny and has high sequence identity with *Arabidopsis* FUS3. Plant-specific B3 domain transcription factors recognise and bind to conserved DNA sequences of six base pairs (Kagaya et al., 1999; Suzuki et al., 1997; Ulmasov et al., 1997a), and have varied functions particularly in vegetative and reproductive growth (Swaminathan et al., 2008). The *ABI3*, *LEC2* and *FUS3* (*AFL*) B3 domain transcription factor subfamily is known specifically to activate embryo maturation program (Giraudat et al., 1992; Luerßen et al., 1998; Meinke et al., 1994). To examine the evolutionary relationship of B3 domain sequences of KdFUS3 among B3 domain proteins of angiosperms, we aligned B3 domain sequences from KdFUS3 and known AFL proteins from different angiosperm species (Fig. 2.1A). The phylogenetic analysis showed that the AFL B3 domain originated from the same ancestor, distinct from *Arabidopsis* RAV and RL. FUS3 B3 domains branched out into its own clade, whereas ABI3 and LEC2 B3 domains continued to share an ancestry before branching out to its respective cluster. ABI3 and LEC2 clusters showed consistently high bootstrap values of above 70 at each branching, which is in contrast with FUS3 cluster that exhibited bootstrap values of below 55, except for the clustering of GaFUS3 and TcFUS3. KdFUS3 B3 domain was positioned within the monophyletic group of all FUS3 B3 domains and was grouped more specifically with MtFUS3. Multiple sequence alignment of only B3 domain from the FUS3 proteins (Supplementary Fig. 2.1) showed that the majority of the amino acid bases were conserved. Within these B3 domain sequences, the region from position 40 to 54 (position 127 to 141 based on whole *Arabidopsis* FUS3 sequence) was the least conserved. KdFUS3 B3 domain also displayed a few differences in amino acid at this region. However, KdFUS3 also uniquely exhibited amino acid N, asparagine at position 15, which was unlike other FUS3 B3 domain sequences with amino acid S, serine at this position. Comparative sequence analysis also showed that KdFUS3 B3 domain was at least 81.9% similar to other FUS3 B3 domain, and shared 84.7% sequence similarity with *Arabidopsis* FUS3 B3 domain.

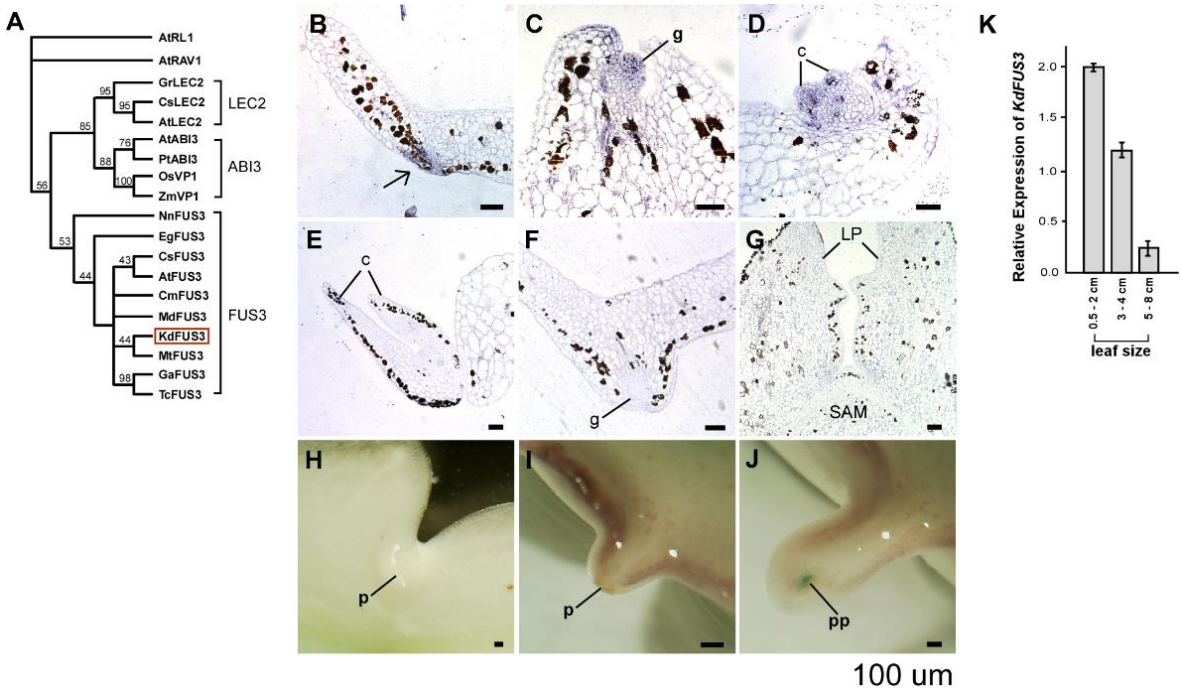

Figure 2.1 Phylogeny of FUSCA3 (FUS3) B3 domains and *KdFUS3* promoter and gene expression analyses.
(A) Phylogenetic tree showing the phylogeny of FUS3 B3 domains of *K. daigremontiana* and other angiosperm species. The bootstrap values were produced using 1,000 replicates. (B-G) *In situ* hybridisation showed that *KdFUS3* transcripts were present at (B) site of plantlet formation before pedestal was formed, (C) globular-stage plantlet and (D) heart-stage plantlet. *KdFUS3* transcript was absent at (E) cotyledons of plantlet emerged from pedestal, (F) negative control using sense probes on globular-stage plantlet and (G) the shoot apical meristem of a mature plantlet. (H-J) GUS staining showed that *KdFUS3* promoter activity was absent during (H) initial and (I) mature pedestal, but its activity was present at (J) emerging plantlet primordium. (K) qRT-PCR showing relative *KdFUS3* transcript levels in leaves of three different sizes, 0.5-2 cm, 3-4 cm and 5-6 cm. g, globular plantlet; c, cotyledon; LP, leaf primordia, p, pedestal; pp, plantlet primordium.

2.4.2. KdFUS3 expression was present during early plantlet formation

Semi-quantitative measurement showed that *KdFUS3* transcripts are present at the margins of young *K. daigremontiana* leaves containing plantlets at early developmental stages (Garcês et al., 2007). To understand localisation of *KdFUS3* expression at these stages, its expression was visualised *via in situ* hybridisation (Fig. 2.1B-G). *KdFUS3* transcripts were present at and around the site of pedestal formation before maturation of pedestal (Fig. 2.1B, arrow) which is the structure that a plantlet emerges from. *KdFUS3* expression was also visible at the globular-stage plantlet, showing more intense localisation at apical half of the plantlet (Fig. 2.1C). At heart-stage, *KdFUS3* also seemed to be present at top half of the plantlet, with stronger expression at cotyledon primordia (Fig. 2.1D). *KdFUS3* expression was absent at later stages when plantlet cotyledons emerged from the pedestal (Fig. 2.1E) and at the SAM of

mature plantlet (Fig. 2.1G). GUS activity of *KdFUS3* promoter was absent during initial and mature pedestal formation (Fig. 2.1H, I), but present at the plantlet primordium (Fig. 2.1J).

The formation of pedestal and plantlet on a leaf occurs basipetally and symmetrically on both sides of the leaf along the vein axis (Garcês and Sinha, 2009a). When the leaves are of 0.5 to 2.0 cm, pedestals or plantlets are forming on each indentation (Garcês et al., 2007). When the leaves reach the size of 3.0 to 4.0 cm, most indentations on the leaf would have completed the embryogenesis-equivalent stages of plantlet formation, and almost all of the indentation on leaves of 5.0 to 8.0 cm would have a mature plantlet formed. Previously, *KdFUS3* expression was present in increasing level in margin of leaves from 0.4 cm to 3.0 cm, which corresponded to plantlets at embryogenesis stages (Garcês et al., 2007). As *FUS3* is known to be expressed until later stages of embryogenesis even after completion of germination, we decided to examine *KdFUS3* level in margin of leaves from 0.5 up to 8.0 cm (Luerßen et al., 1998). Semi-quantitative RT-PCR (Fig. 2.1K) showed that 0.5 to 2.0 cm young leaves exhibited the highest level of *KdFUS3*, followed by 3.0 to 4.0 cm leaves and 5.0 to 8.0 cm leaves had the lowest *KdFUS3* expression. This expression pattern was in accordance with the *KdFUS3* expression pattern seen in *in situ* hybridisation, which reflected decrease in *KdFUS3* transcripts expression intensity in mature plantlets.

2.4.3. Reduced KdFUS3 Expression Disrupted Plantlet Formation

To investigate the specific role of *KdFUS3* in plantlet formation, transgenic *K. daigremontiana* plants with reduced expression of *KdFUS3 via* antisense suppression were generated. PCR amplification of genomic DNA confirmed the presence of the transgenes and *NPTII* gene that was located on the plasmid transformed in six independent *35S*::*antisense-KdFUS3* lines (Fig. 2.2A). However, out of the six antisense lines, four line exhibited more severely affected plantlet phenotype. Semi-quantitative RT-PCR analysis was then performed and confirmed the reduction of *KdFUS3* transcripts in these lines (Fig. 2.2B).

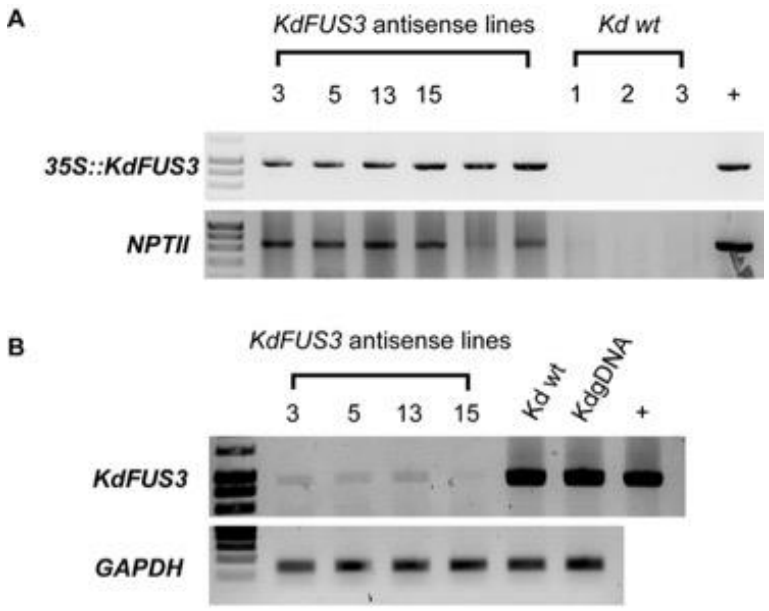

Figure 2.2 PCR amplification to screen transgenic *KdFUS3* antisense plants.
(A) Genomic PCR amplification showing presence and absence of transgene *35S::antisense-KdFUS3* and *NEOMYCIN PHOSPHOTRANSFERASE II* (*NPTII*) in *KdFUS3* antisense lines and wild-type *K. daigremontiana*. (B) Semi-quantitative reverse transcriptase-PCR showing reduced *KdFUS3* transcripts in four *KdFUS3* antisense lines compared to wild-type. Kd, *K. daigremontiana*; wt, wild-type; gDNA, genomic DNA; +, positive control using plasmid containing *35S::antisense-KdFUS3*::*35S* construct.

Phenotypic analysis showed that in general, *KdFUS3* antisense plants (Fig. 2.3B) exhibited very irregular leaf shape compared to wild-type (Fig. 2.3A). In wild-type, plantlets were formed at evenly spaced leaf indentations along the leaf margin (Fig. 2.3C). In contrast, *KdFUS3* antisense plants formed only very few plantlets (Fig. 2.3D), which was reflected by reduction in number of plantlets by more than 80 %, compared to wild-type, from about 45 plantlets to less than 5 plantlets per pair of leaves (Fig. 2.3Q). Some plantlets formed on *KdFUS3* antisense plants failed to mature and was aborted (Fig. 2.3D). In some cases, pedestal and plantlet formation were absent (Fig. 2.3E). Scanning electron microscope (SEM) images revealed stark differences between the leaf notches and plantlet morphology between wild-type and transgenic plants (Fig. 2.3F-M). In wild-type, the site of plantlet formation localised between the leaf serrations was not visible prior to formation of pedestal (Fig. 2.3F). Then, the pedestal emerged as it enveloped the globular-stage plantlet (Fig. 2.3G) and also the heart-stage plantlet (Fig. 2.3H). However, the transgenic plants exhibited exposed plantlet formation sites and defective pedestal formation, which failed to form plantlets (Fig. 2.3J, K). In wild-type *K. daigremontiana*, plantlets formed and matured sequentially in a basipetal order (base to tip) along the leaf

margin. This gradual formation of plantlets was lost in *KdFUS3* antisense plants as shown by the presence of two plantlets and then an absence of a plantlet at the following leaf notch (Fig. 2.3L). As the wild-type plantlet matures, serrated leaves were formed after formation of cotyledons (Fig. 2.3I) but in some cases of *KdFUS3* antisense plants, plantlets stopped developing after partial formation of cotyledons (Fig. 2.3M). These aborted plantlets also displayed multiple fleshy cotyledons-like organs (Fig. 2.3N). Apart from the number of plantlets, depth of indentations on the leaf margin and number of lobes per leaf in *KdFUS3* antisense plants was significantly reduced (Fig. 2.3O, P). The number of lobes per leaf in wild-type was about 50, but in *KdFUS3* antisense plants, it was only about 18 which was less than half of wild-type leaves.

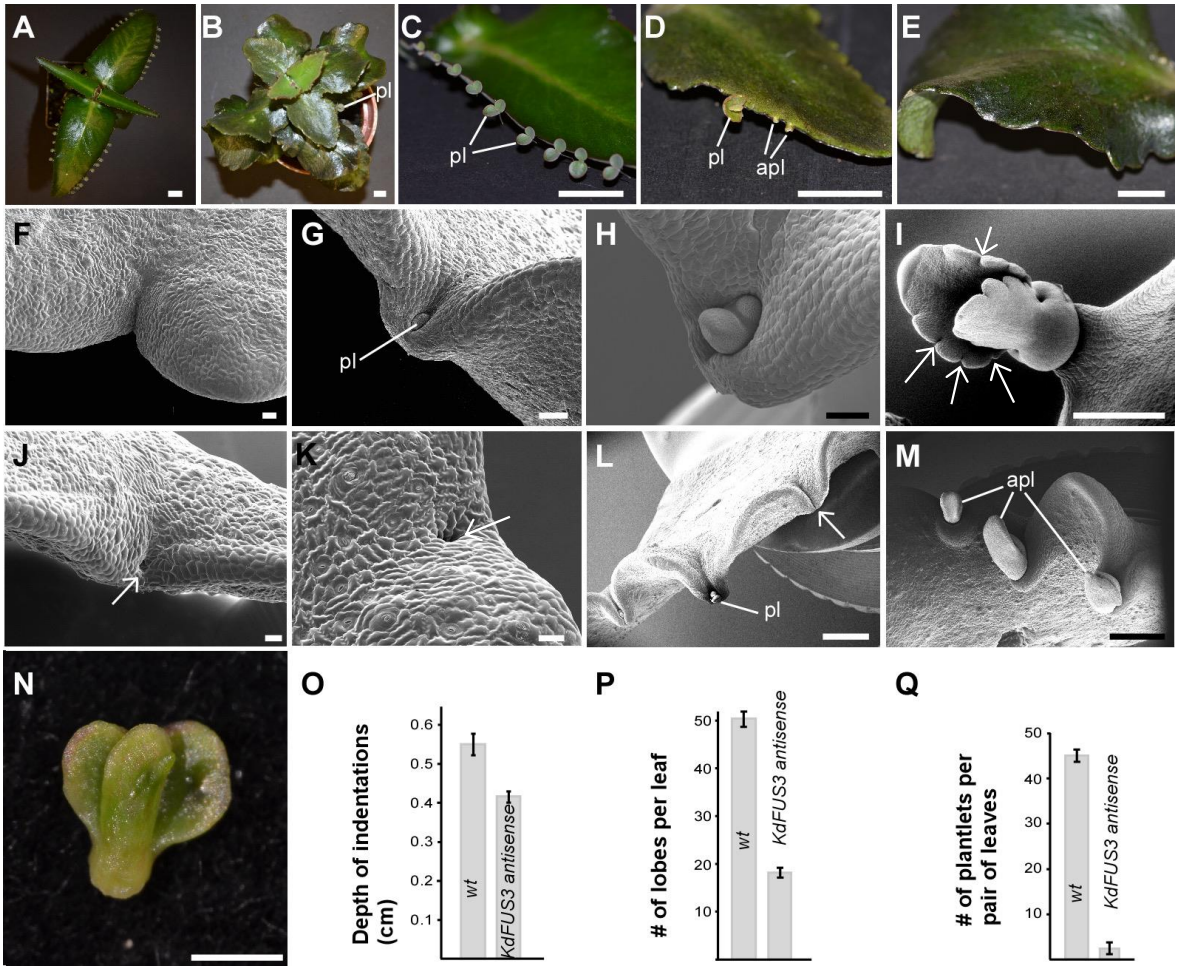

Figure 2.3 Phenotypes of *KdFUS3* antisense transgenic plants.

(A) Wild-type (wt) non-transformed plant. (B) Whole *KdFUS3* antisense plant with irregular leaf shape. (C) Consistent plantlet formation along leaf margin of non-transformed leaf. (D, E) Irregularly-shaped *KdFUS3* antisense leaves showing reduced plantlet formation; plantlets formed and aborted (D) and no plantlet formation (E). (F-H) Scanning electron microscope (SEM) images of wild-type leaf notches showing (F) leaf indentation before pedestal formation; (G) globular-stage plantlet and (H) heart-stage plantlet enveloped in pedestal. (I) SEM image of a wild-type plantlet with serrated leaves, arrows pointing towards indentations. (J-M) SEM images of *KdFUS3* antisense transgenic plants leaf notches. (J, K) Exposed plantlet formation site without pedestal nor plantlet formation (arrows). (L) Inconsistent plantlet formation along the leaf margin showing no plantlet formed on an indentation (arrow). (M) Plantlets with aborted development. (N) Close-up image of an aborted plantlet. Graphs comparing indentation depth (O), number of lobes per leaf (P) and number of plantlets (Q) in wild-type and *KdFUS3* antisense plants. Two-sample tailed Student's t tests were performed for each graph and the differences between wt (n=15) and *KdFUS3* antisense (n=15) in each graph was significant, $P \leq 0.05$. pl, plantlet; apl, aborted plantlet.

2.4.4. Expression analyses of embryogenesis and organogenesis genes

Previous studies showed that *K. daigremontiana KdSTM*, *KdLEC1* and *KdFUS3* are expressed during plantlet formation and that *KdSTM* and *KdFUS3* might be participating in the process (Garcês et al., 2007, 2014). To determine whether other embryogenesis or organogenesis genes are involved in *K. daigremontiana* plantlet formation, RNA-sequencing analysis was performed to measure expression of these genes. Tissues were harvested from leaves containing at least three different selected stages of plantlet development; S1, S2, S3 and S4 (Supplementary Fig. 2.2A). Stage S1 referred to leaf notches without pedestal formation; stage S2 is when pedestal have formed but without morphologically visible plantlet emergence; stage S3 samples were plantlet primordium emerging from pedestal whereas stage S4 were plantlets more mature than stage S3 that formed cotyledons (Supplementary Fig. 2.2). The control samples (Ctrl) were margins of young 1 to 2 cm leaves. We inspected expression levels of *Kalanchoë* homologs of early embryogenesis genes, *WRKY DNA-BINDING PROTEIN* 2 (*WRKY2*), *WUSCHEL-RELATED HOMEOBOX 2* (*WOX2*), *WOX8*, *WOX9*; and late embryogenesis genes *LEC1*, *L1L*, *ABI3*, *FUS3*, *LEC2* (*LAFL*) across these plantlet stages. We also recorded expression level of organogenesis genes, *STM* and *WUSCHEL* (*WUS*). Of these genes, *KdWOX2* and *KdLEC2* were not expressed at any of the plantlet stages examined. The changes in expression level of most genes were not statistically significant suggesting that the expression levels of each gene across plantlet development were similar (Fig. 2.4, 2.5).

KdLEC1 expression was absent at the last two plantlet stages S3 and S4 (Fig. 2.4A). Its expression was the highest in Ctrl samples but dropped at plantlet stage S1 and then slightly increased in plantlet S2. For *KdL1L*, its expression was the highest at plantlet stages S3 and S4, followed by S2, Ctrl and then S1 (Fig. 2.4B). Expression of *ABI3* was present only at plantlet stage S1 (Fig. 2.4C). *KdFUS3* expression was the highest in the Ctrl samples, followed by a slight decrease at S1 and a sharp drop in expression at S2 (Fig. 2.4D). Though its expression at S3 and S4 was higher than at S2, the level remained a lot lower compared to S1 and Ctrl. Expression of *KdWOX8* fluctuated across the plantlet stages as it was upregulated from Ctrl to S1, then its expression dropped to its lowest at S2, followed by an increase in expression at S3 which remained fairly similar to stage S4 (Fig. 2.4E). *KdWOX9* expression was present at very low levels at Ctrl and S3, and was absent at S1 and S2; however, its expression rose sharply to its

highest at S4 and was statistically significant (P≤0.05) compared to stage S1 and S2 (Fig. 2.4F). *KdWRKY2* exhibited the highest expression level compared to all other genes examined, but its expression remained relatively similar across all stages of plantlet formation and in Ctrl (Fig. 2.4G). In the case of *KdSTM,* there was a gradual increase in expression level from Ctrl and across plantlet developmental stages (Fig. 2.5A) but the increase in expression was statistically significant (P≤0.005) only at S4 when compared to Ctrl. As for *KdWUS*, there was a steep increase in expression from Ctrl to S1 and there was no significant change in expression at S2. A drop in expression was followed at S3 and then it was upregulated at S4. With the exception of *KdWRKY2*, the expression of *KdSTM* was substantially higher during plantlet development and the change in expression between stages were very dramatic compared to other genes examined.

The expression pattern of *KdFUS3* and the impact of *KdFUS3* downregulation on plantlet formation suggest that *KdFUS3* participates in regulating plantlet formation. To understand the interaction of *KdFUS3* with other genes in regulating plantlet formation, after *KdFUS3* antisense lines were generated and confirmed showing reduced *KdFUS3* expression, three lines were selected for examination of other genes' expression. Quantitative measurement showed that *KdLEC1* expression (Fig. 2.4H) was very high in wild-type compared to *KdSTM* and *KdWUS* (Fig. 2.5C, D). In the three *KdFUS3* antisense lines, *KdLEC1* expression was dramatically reduced to almost 80 times less than in wild-type (Fig. 2.4H) but the results were not statistically significant. As for *KdSTM* and *KdWUS*, their expression was lower than in wild-type but the differences in expression was statistically significant (P≤0.05) only between wild-type and *KdFUS3* antisense line 3 (Fig. 2.5C, D). For all three genes examined, their expression was not significantly different among the *KdFUS3* antisense lines.

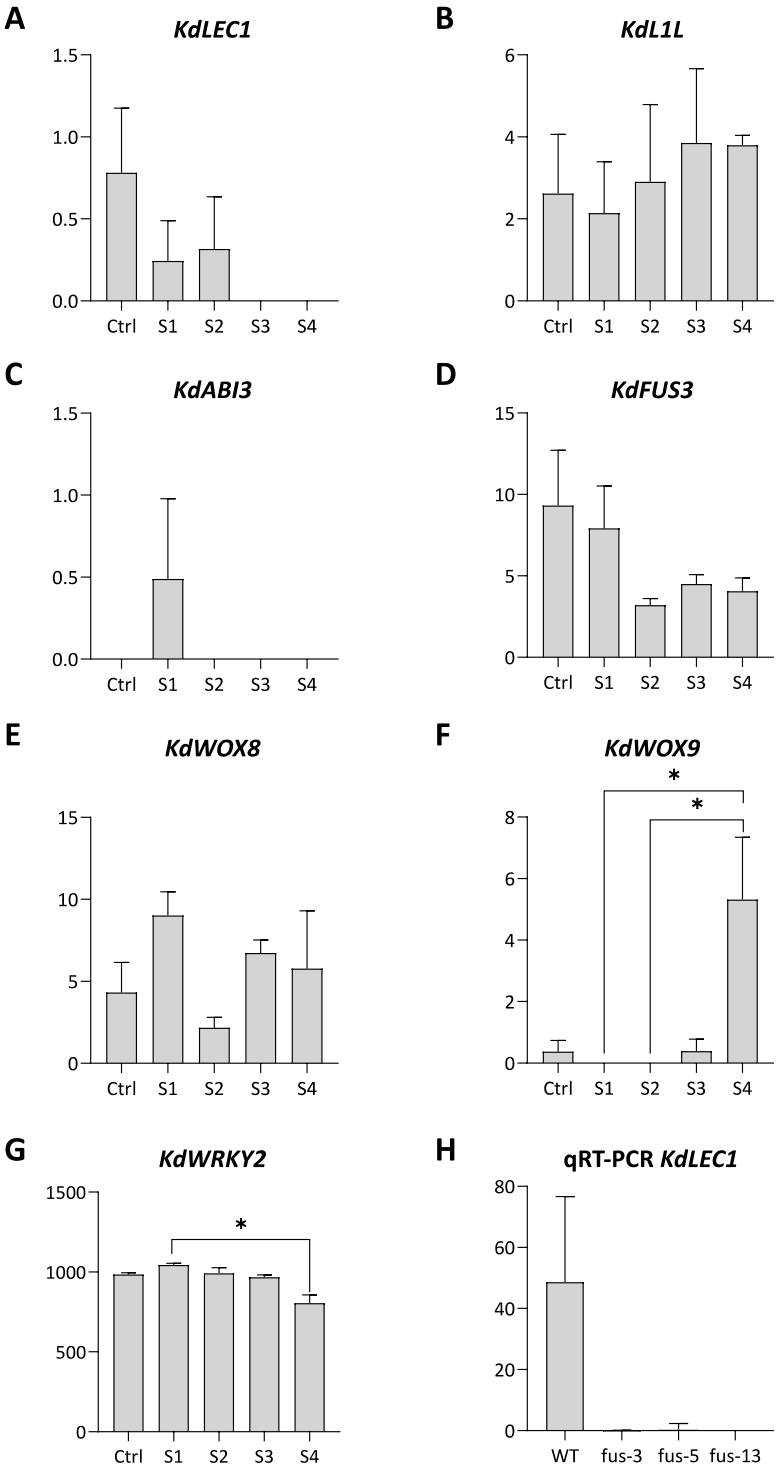

Figure 2.4 Relative expression of embryogenesis genes in *K. daigremontiana* during plantlet formation.
The relative change in expression of (A) *KdLEAFY COTYLEDON 1* (*KdLEC1*), (B) *KdLEC1-LIKE* (*KdL1L*), (C) *KdABSCISIC ACID INSENSITIVE3* (*KdABI3*), (D) *KdFUSCA3* (*KdFUS3*), (E) *KdWUSCHEL-RELATED HOMEOBOX 8* (*KdWOX8*), (F) *KdWOX9* and (G) *KdWRKY DNA-BINDING PROTEIN 2* (*KdWRKY2*) in wild-type *K. daigremontiana* according to RNA-sequencing analysis. (H) Relative expression of *KdLEC1* in wild-type *K. daigremontiana* (WT) and in *KdFUS3* antisense lines 3, 5, and 13 obtained from quantitative RT-PCR. Ctrl, control samples using leaf margin of 1-2 cm young leaves; S1, stage 1; S2, stage 2; S3, stage 3; S4, stage 4 (Supplementary Fig. 2.2). Y-axis refers to relative change in expression. Kruskal Wallis test with Dunn's multiple comparison test indicate statistical significance, *P≤0.05. Error bar represents standard error.

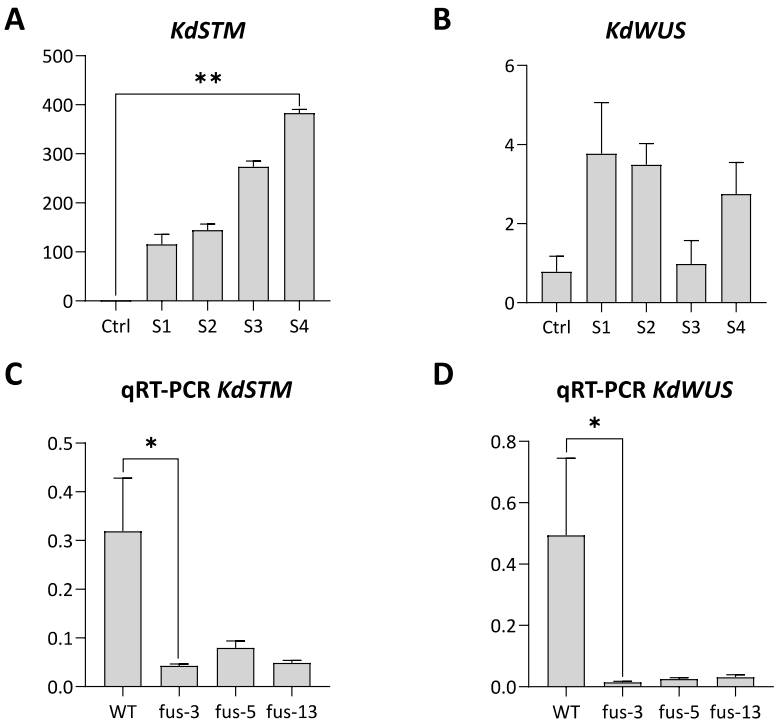

Figure 2.5 Relative expression of organogenesis genes in *K. daigremontiana* during plantlet formation.
RNA-sequencing analysis of relative (A) *KdSHOOTMERISTEMLESS* (*KdSTM*) and (B) *KdWUSCHEL* (*KdWUS*) expression across plantlet developmental stages. qRT-PCR measurement of (C) *KdSTM* and (D) *KdWUS* expression in wild-type *K. daigremontiana* (WT) and in *KdFUS3* antisense lines 3, 5, and 13. Ctrl, control samples, margin of 1-2 cm young leaves; S1, stage 1; S2, stage 2; S3, stage 3; S4, stage 4 (Supplementary Fig. 2.2). Y-axis refers to relative change in expression. Kruskal Wallis test with Dunn's multiple comparison test indicate statistical significance, *P≤0.05, **P≤0.005. Error bar represents standard error.

2.5. **Discussion**

K. daigremontiana plantlet develops morphologically similarly to a zygotic embryo (Garcês et al., 2007). Moreover, embryogenesis genes *LEC1* and *FUS3* are expressed during plantlet development, suggesting that embryogenesis pathways are recruited during *K. daigremontiana* plantlet formation (Garcês et al., 2007). However, KdLEC1 has a defective B domain, which rendered it non-functional (Garcês et al., 2007). For KdFUS3 to replace KdLEC1's functions, it has to retain its activity conferred by its B3 domain. A previous study showed that KdFUS3 clustered with *Arabidopsis* FUS3 among *Arabidopsis* B3 domain-containing transcription factors. However, it was not known whether KdFUS3 activity is conserved among the angiosperm family. To determine this, we aligned B3 domain sequences from KdFUS3 and AFL proteins of different angiosperm species (Fig. 2.1A). The AFL proteins clustered with its corresponding protein subfamilies ABI3, LEC2 and FUS3 as expected because of differences in their B3 domain DNA-binding sequences. The sharing of a common ancestor between ABI3 and LEC2 was consistent with a previous study that investigated evolution of LAFL genes in land plants (Han et al., 2017). Although KdFUS3 B3 domain clustered with FUS3 B3 domains from different angiosperm plants, most phylogenetic branches within the cluster had low bootstrap values of below 55. This might be due to a lack of characters as plant-specific B3 domain sequences are highly conserved (Han et al., 2017; Soltis and Soltis, 2003). Typically, a bootstrap value of at least 70 is required to indicate accuracy, but some studies showed that bootstrap value below 70 is usually an underestimation (Efron et al., 1996; Felsenstein and Kishino, 1993; Hillis and Bull, 1993; Newton, 1995). In addition, multiple sequence alignment showed high conservation of KdFUS3 B3 domain sequence identity compared to other angiosperm FUS3. Nonetheless, no evidence has shown differences in B3 domains among the AFL protein family contributed to functional differentiation. Instead, their functions are more likely to depend on three factors: 1) temporal and spatial expression; 2) mutual regulatory interactions at the same expression site and 3) functions of other protein domains (Suzuki and McCarty, 2008). Multiple sequence alignment also unexpectedly showed variation at position 40 to 54 that contributes to formation of two secondary structures, but no literature has reported variation in FUS3 structure or function due to these changes. The change from amino acid S, serine to N, asparagine at position 15 of KdFUS3 B3 domain may be caused by mutation of the second nucleotide in the amino acid codon from G to A. In nature, change in second

position of the amino acid codon is less likely compared to a change in the third position (Bofkin and Goldman, 2007). However, as this position does not contribute to formation of KdFUS3 B3 domain secondary structure (Supplementary Fig. 2.1), this amino acid might not be subjected to selective constraints of maintaining the same amino acid. To determine if FUS3 has evolved to replace LEC1 functions in constitutive plantlet-forming *Kalanchoë* species, future studies need to investigate whether FUS3 in *Kalanchoë* species with different modes of plantlet formation exhibit differences in the three factors mentioned.

To understand KdFUS3 function in *K. daigremontiana* plantlet formation, we performed *in* situ hybridisation and GUS staining to visualise localisation of *KdFUS3* transcripts and *KdFUS3* promoter activity respectively. *In situ* hybridisation showed that *KdFUS3* expression is very similar to *KdLEC1* (Garcês et al., 2007) in that both genes are expressed at the apical half of the globular and heart stage plantlet, but absent from the SAM (Fig. 2.1C, D, G). *KdFUS3* promoter activity was also observed at the plantlet primordium (Fig. 2.1J). The *in situ* hybridisation data also correlated to *KdFUS3* expression obtained from RNA-sequencing analysis (Fig. 2.4D). *LEC1* expression is visible early during *Arabidopsis* embryogenesis at the two-celled embryo, at the embryo proper and suspensor of an eight-celled proembryo (Lotan et al., 1998). Then, *LEC1* exhibited its highest expression at globular and heart stages, localising at the *Arabidopsis* embryo periphery (Lotan et al., 1998). This is quite similar to *KdLEC1* and *KdFUS3* expression in *K. daigremontiana* plantlet that displayed the highest intensity at the boundary of globular-staged plantlet and at cotyledon primordia of heart-stage plantlet (Garcês et al., 2007) but their expression was much weaker at basal half of the plantlet (Fig. 2.1C, D). According to RNA-sequencing data, *KdLEC1* expression was also the highest at young leaf margins, similar to *KdFUS3* but its magnitude of expression was much smaller than *KdFUS3* (Fig. 2.4A, D). Unlike *KdLEC1* expression that was absent at later stages of plantlet formation, *KdFUS3* was still expressed, similar to *Arabidopsis FUS3* expression that persists until relatively late during embryogenesis, compared to *LEC1* (Tian et al., 2020a).

In contrast to *LEC1* expression, *FUS3* is not expressed during early embryogenesis and is expressed in protodermal tissues of embryo at globular and heart-stage of *Arabidopsis* embryo (Tsuchiya et al., 2004). In *Arabidopsis*, *FUS3* expression is visible in provascular tissues and

mature epidermis (Tsuchiya et al., 2004); and after completion of germination, *FUS3* expression is still present at low levels (Luerßen et al., 1998). However, in our case, these were not observed in plantlets *via KdFUS3 in situ* hybridisation. The similarity in temporal and spatial expression of *KdLEC1* and *KdFUS3* showed that *KdFUS3* has fulfilled one aspect of the requirements for it take over KdLEC1 embryogenesis functions. The slight differences in expression of *KdLEC1* and *KdFUS3* compared to their corresponding orthologs in *Arabidopsis* also suggest that *KdLEC1* and *KdFUS3* might have functionally deviated over evolutionary time. The similarity in expression pattern between Arabidopsis *FUS3* and *KdFUS3* transcripts and restriction of *KdFUS3* expression only at embryogenesis-equivalent stages of plantlet formation suggests that *KdFUS3* may be involved in embryogenesis-like process during plantlet formation. This is further supported by increase in relative expression of *KdFUS3*, which correlates to decreased leaf size and higher number of indentations undergoing plantlet formation and development (Fig. 2.1K). The residual *KdFUS3* expression in leaves sized 5–8 cm may have reflected its expression in the indentations at the base of each leaf which had much delayed pedestal and plantlet development, due to basipetal developmental sequence along the leaf margin.

Our results showed that *KdFUS3* is essential for normal development of plantlets and initiation of pedestal and plantlet formation. The presence of *KdFUS3* at the site of pedestal and plantlet formation in wild-type (Fig. 2.1B); defective pedestal formation and dramatic reduction in plantlet number in *KdFUS3* antisense plants (Fig. 2.3J, K) implies that KdFUS3 is active during pedestal formation and plantlet initiation (Fig. 2.3O, P). In addition, these plants exhibited inconsistent leaf serration as shown by decrease in indentation number and depth of leaf notches (Fig. 2.3P, Q). Pedestal formation might be linked to leaf serration formation which was defective possibly due to downregulation of *KdSTM* (Fig. 2.5C). *KdSTM* downregulation in *K. daigremontiana* also led to irregular pedestal formation and leaf serration (Garcês et al., 2007). In *Arabidopsis*, continuous *STM* expression was known to upregulate *CUP-SHAPED COTYLEDON 2* (*CUC2*) and *microRNA-164a* (MIR164A) that are responsible for regulating *Arabidopsis* leaf serration (Nikovics et al., 2006; Spinelli et al., 2011). After leaf serration patterning is specified, differences in temporal expression of MIR164A and CUC2 at the leaf sinuses and post-transcriptional regulation of CUC2 by MIR164A determine the depth of

serrations (Laufs et al., 2004; Nikovics et al., 2006). *CUC2* is expressed at leaf sinuses to repress growth at these regions and promotes PIN-FORMED1 (PIN1) that leads to localisation of auxin maxima at serration tips (Bilsborough et al., 2011). In *Arabidopsis*, downregulation of *CUC2, MIR164A* or *PIN1* resulted in leaves with smooth margin (Nikovics et al., 2006). The study showed that *CUC2* is expressed very strongly at leaf indentations during early leaf development, which seems similar to our RNA-sequencing data that showed increasing *KdCUC2* expression across plantlet developmental stages S1 to S4 as the plantlets develop new leaves (Nikovics et al., 2006). The expression of *MIR164A* largely overlaps with *CUC2* expression in *Arabidopsis* but the corresponding homolog of *MIR164A* was not detected in our RNA-sequencing data (Nikovics et al., 2006). If this mechanism was indeed defective in *KdFUS3*, we expect to observe downregulation of *CUC2* or *MIR164A* in *KdFUS3* antisense leaves.

KdFUS3 antisense plants only formed from none to a few plantlets (Fig. 2.3Q), possibly due to incomplete penetrance of the antisense transgene. This observation is similar to incomplete suppression of *KdSTM* in *KdSTM* RNAi plants (Garcês et al., 2007), suggesting that defective plantlet initiation of *KdFUS3* antisense plants might also be related to *KdSTM* function. Similarly, *KdSTM* and *KdWUS* downregulation (Fig. 2.5C, D) might have caused abortion of plantlet development (Fig. 2.3M) in *KdFUS3* antisense plants because these aborted plantlets are similar to *stm* and *wus Arabidopsis* mutants that still develop cotyledons but terminated SAM prematurely (Laux et al., 1996; Long et al., 1996). How *KdFUS3* caused downregulation of *KdSTM*, however, is unclear as no link was reported between LAFL genes and *STM*. Perhaps *KdWUS* is involved in the link between *KdSTM* and *KdFUS3* as *WUS* is known to regulate *STM* expression and can promote embryo development when ectopically expressed (Gallois et al., 2002; Su et al., 2020; Zuo et al., 2002). RNA-sequencing data also showed that *KdWUS* was expressed during plantlet formation, with higher expression during early plantlet formation stage S1 and S2 (Fig. 2.5B). RNA-sequencing data showed gradual increase in *KdSTM* expression during plantlet formation (Fig. 2.5A). This is consistent with *in situ* hybridisation of *KdSTM* expression (Garcês et al., 2007), similar to a broader expression of *KNOX1* genes in maize somatic embryogenesis (Smith et al., 1995; Zhang et al., 2002). Similar to what was previously reported, spatial expression of *KdSTM* was different compared to *Arabidopsis STM.* And based on expression data from Arabidopsis eFP Browser 2.0, *KdSTM* expression pattern during

plantlet formation is the complete opposite of *Arabidopsis STM* which gradually decreases during embryogenesis. These observations provided further evidence that unlike in *Arabidopsis* embryogenesis, *KdSTM* might be involved in not only during plantlet initiation but also during its development.

Interestingly, some of the aborted plantlets were morphologically similar (Fig. 2.3N) to *Arabidopsis* mutants with *LEC1* ectopic expression (Lotan et al., 1998). This observation was unexpected because even though FUS3 transcriptionally regulates *LEC1*, KdLEC1 is non-functional in *K. daigremontiana* plantlet formation (Garcês et al., 2007; Wang and Perry, 2013). Hence, this observation is unlikely to be the consequence of *KdLEC1* upregulation. Moreover, *KdLEC1* expression was downregulated in *KdFUS3* antisense plants (Fig. 2.4H). A plausible explanation is that perhaps *KdFUS3* is required for cotyledon specification similar to *FUS3*, as evident by development of vegetative characteristics on cotyledons *fus3* mutants (Keith et al., 1994; Meinke et al., 1994). In contrast to *KdFUS3* antisense plants, *fus3* mutant embryos are desiccation intolerant and does not remain dormant; thus, when mature, resembles germinating seedling (Keith et al., 1994; Meinke et al., 1994). This stark difference suggests that *KdFUS3* does not contribute to maintenance of dormancy and again, suggests that *KdFUS3* has acquired different functions compared to *Arabidopsis FUS3*. This is supported by difference in expression level of *FUS3* and *KdFUS3*, which unlike *FUS3* that increases in expression across embryogenesis (Tian et al., 2020a), *KdFUS3* expression was the highest during early plantlet development and remained lower in expression at later stages of plantlet formation (Fig. 2.4D).

As mentioned above, although *KdLEC1* and *KdFUS3* spatial expression during plantlet development overlaps with *Arabidopsis LEC1* and *FUS3* expression in zygotic embryogenesis, their expression level are different compared to their corresponding orthologs (Tian et al., 2020a). Interestingly, *KdLEC2* expression was undetected during plantlet development, unlike in Arabidopsis eFP Browser 2.0 that shows high *LEC2* expression in transition to torpedo stage *Arabidopsis* embryo. *KdABI3* expression was very different compared to *Arabidopsis* embryo that shows gradual increase in *ABI3* expression across embryogenesis and seed development. *KdABI3* expression (Fig. 2.4C) was solely detected at very low level in stage S1 plantlet. *KdL1L* expression (Fig. 2.4B), however was quite similar to *Arabidopsis* embryo, exhibiting fairly high

expression across plantlet formation (S1 to S4) which is roughly equivalent to globular to cotyledon stage of *Arabidopsis* embryo. The only difference is that *KdL1L* expression level was quite similar across these stages and has a narrower range of expression. As LAFL genes works in the same regulatory network and share extensive interaction with each other (Boulard et al., 2018; Pelletier et al., 2017; Tian et al., 2020b; Wang and Perry, 2013), it was not unexpected to observe changes in expression of these genes as *KdLEC1* and *KdFUS3* expression showed clear differences compared to *Arabidopsis LEC1* and *FUS3*. We also examined expression of early embryogenesis genes, *WRKY2*, *WOX2, WOX8* and *WOX9* that establish apical-basal embryo polarity (Breuninger et al., 2008; Haecker et al., 2004; Ueda et al., 2011; Wu et al., 2007). *WOX2* is expressed in *Arabidopsis* zygote and localises to the apical cell from the 2-cell stage to specify the shootward embryonic lineage (Breuninger et al., 2008; Haecker et al., 2004). However, *KdWOX2* expression was undetected during plantlet formation, possibly due to its low expression levels, similar to low *WOX2* expression during embryogenesis prior to cotyledons formation according to Arabidopsis eFP Browser 2.0. In contrast to *WOX2*, *WOX8* and *WOX9* establishes suspensor development and rootward embryonic lineage (Breuninger et al., 2008; Ueda et al., 2011; Wu et al., 2007). The fluctuating *WOX8* expression according to Arabidopsis eFP Browser 2 is similar to *KdWOX8* expression pattern (Fig. 2.4E), whereas consistent *WOX9* expression during *Arabidopsis* embryogenesis is different to *KdWOX9* expression (Fig. 2.4F). *KdWOX9* expression was very low or absent until plantlet stage S4. Interestingly, during plantlet formation, *WRKY2*, a gene required for *WOX8* transcription, exhibited the highest expression level among all the genes examined (Ueda et al., 2011). This contradicts *WRKY2* expression data from Arabidopsis eFP Browser 2 that shows *WRKY2* has a relatively low expression. The expression of these early embryogenesis genes in *K. daigremontiana* is inconsistent with expression data of *Arabidopsis* embryo, probably due to inconsistent grouping of specific stages of plantlet as the samples were selected using naked eyes. Moreover, these genes are expressed only in a few cells during early embryogenesis, hence, inconsistent grouping of stages might significantly change the expression level. Alternatively, *K. daigremontiana* plantlet development might be different compared to *Arabidopsis* zygotic embryo development. Nonetheless, expression of these genes during plantlet formation suggests that similar mechanisms are also used for patterning early *K. daigremontiana* plantlet formation.

2.6. **Conclusion**

In this study, our results agree with previous finding that embryogenesis is recruited not only during the initiation of pedestal and plantlet formation but also during plantlet development. This is evident from defective formation of pedestal and plantlet throughout plantlet development of plants with reduced *KdFUS3* expression. These phenotypes observed also correlates with temporal and spatial expression of *KdFUS3* during plantlet formation. We have yet to confirm that *FUS3* is the gene that has evolved to replace essential *LEC1* functions during plantlet formation in *K. daigremontiana*. Nonetheless, *KdFUS3* expression overlaps with *KdLEC1*, which contrasts with the situation where *Arabidopsis FUS3* is different from *Arabidopsis LEC1* expression. This suggests that *KdFUS3* might have functionally deviated and can replace essential *KdLEC1* due to overlapping expression domains. Preliminary data showed that expression patterns of other *Kalanchoë* LAFL genes are also different from those of *Arabidopsis* orthologs, which is not unexpected due to mutual regulation of LAFL genes. In addition, expression of early embryogenesis genes showed that same mechanisms might be used to pattern early plantlet formation. Similarity in defective phenotypes seen in *KdFUS3* antisense and *KdSTM* RNAi plants, and downregulation of some organogenesis genes in *KdFUS3* antisense plants indicates that *KdFUS3* or embryogenesis function might be integrated with organogenesis pathway. Our data have shed light on the gain of pluripotency by somatic leaf cells *via* turning on the embryogenesis and organogenesis programs in which components in both programs might interact to regulate plantlet formation and development. Further experiments on the action of embryogenesis genes and regulation and interaction between embryogenesis and organogenesis programs need to be conducted to build a more complete picture on the molecular mechanisms behind plantlet initiation and development. These experiments will contribute to our knowledge on asexual reproduction of plants and plant cells dedifferentiation and pluripotency, which will be useful for improving production and cultivation of plant crops in the long term as many crop plants reproduce asexually and plant cultivation through tissue culture depends on pluripotency of plant tissues.

CHAPTER 3

RESULTS 2

JPO produced all data, figures and text in this chapter. This excludes the RNA-sequencing performed and analysed by the University of Manchester Genomic Technologies Core Facility and Bioinformatics Core Facility; and isolation of *WUSCHEL*, *CLAVATA 1* and *CLAVATA 2* genes from *Kalanchoë pinnata* by FJB.

3. The Role of Meristematic Genes During *Kalanchoë daigremontiana* Plantlet Formation

Joo Phin Ooi[1], Francisco Jácome Blásquez[1] and Minsung Kim[1]*

[1]School of Biological Sciences, Faculty of Biology, Medicine and Health, University of Manchester, Manchester, M13 9PT, United Kingdom

*Corresponding author: Minsung.kim@manchester.asc.uk

Key Words: Asexual Reproduction, *Kalanchoë*, plantlet formation, organogenesis, shoot apical meristem, *WUSCHEL, CLAVATA*

3.1. Abstract

Asexual reproduction of *Kalanchoë* plants involves formation of plantlets on leaves that were speculated to be a product of somatic embryogenesis. Previous molecular studies have shown that apart from embryogenesis, organogenesis is also recruited into plantlet formation. Hence, this study investigated whether key organogenesis genes *WUSCHEL* (*WUS*), *CLAVATA1* (*CLV1*) and *CLV2* are involved in *K. daigremontiana* plantlet formation. Our results showed that conserved regions of *Kalanchoë WUS*, *CLV1* and *CLV2* were distinct enough to be grouped into a separate clade. Furthermore, at different stages of plantlet development, these genes exhibited high expression, which was not reflected by previous studies. Reduction in *KdWUS* and *KdCLV1* expression also led to a range of irregular phenotypes in *K. daigremontiana* transgenic plants. Our data suggests that *KdWUS* and *KdCLV1* are involved in *K. daigremontiana* plantlet formation, supporting that idea that key organogenesis pathways are recruited for plantlet formation. However, future studies are required to confirm the specific mechanisms in which *KdWUS* and *KdCLV1* genes contribute to plantlet formation. These information will reveal how plantlet formation is initiated and regulated by organogenesis and possibly add to our knowledge of mechanisms behind various asexual reproduction strategies in plants.

3.2. Introduction

Plants exhibit incredible plasticity as evident from regeneration of plant organs and the development of whole plants from tissue culture (Fehér, 2019; Ikeuchi et al., 2019). The capability of plants to achieve these impressive feats derive primarily from maintenance of pluripotent meristem cells at different parts of plants and its competency to respond to hormone signalling (Fehér, 2019; Ikeuchi et al., 2019; Mozgová et al., 2017; Novák et al., 2017; Wójcik et al., 2020). In tissue culture, whole plants are developed as a consequence of somatic embryogenesis, which is stimulated when an ideal ratio of different hormones is present (Skoog and Miller, 1957). In the case of the *Kalanchoë* genus, some species are able to make plantlets, miniature adult plants on its leaf margin, possibly through triggering somatic embryogenesis of leaf cells without artificial applications of plant hormones (Garcês et al., 2007). There is evidence of stem cell localisation in the region of plantlet formation in *Kalanchoë* and other species that produce plantlets (Guo et al., 2015). Recent genetic studies have also revealed participation of embryogenesis, flowering and organogenesis genes in plantlet formation (Garcês et al., 2007, 2014).

Of the plantlet-forming *Kalanchoë* species, *K. daigremontiana* is one of the species that produces plantlets constitutively under a continuous long-day condition (Garcês et al., 2007; Hershey, 2002). The development of *K. daigremontiana* plantlet morphologically resembles *Arabidopsis* zygotic embryo development (Garcês et al., 2007). Further examination revealed that late embryogenesis genes, *LEAFY COTYLEDON 1* (*LEC1*) and *FUSCA3* are expressed during *K. daigremontiana* plantlet development (Garcês et al., 2007). This suggests that embryogenesis pathways were recruited during plantlet formation. However, reduction of *KdLEC1* expression did not affect *K. daigremontiana* plantlet formation (Garcês et al., 2014). This was because KdLEC1 protein was non-functional due to a 20-nucleotide deletion that resulted in formation of a truncated protein (Garcês et al., 2014). When a functional copy of *Arabidopsis* LEC1 was inserted into *K. daigremontiana*, plantlets with seed dormancy characteristics developed, indicating that loss of LEC1 function is vital for bypassing dormancy to allow plantlet development (Garcês et al., 2014). Nonetheless, this mechanism of plantlet formation is applicable only to constitutive plantlet-forming species. *Kalanchoë* species that

do not make plantlets or make plantlets only under stress conditions still contain intact LEC1 proteins, similar to *Arabidopsis* LEC1 (Garcês et al., 2007).

The most recent molecular study on plantlet formation studied the role of a flowering signals integrator gene, *SUPPRESSOR OF CONSTANS OVEREXPRESSION 1* (*KdSOC1*) during plantlet development (Lee and Lee, 2010; Moon et al., 2003; Zhu et al., 2017). The study showed that *KdSOC1* was expressed between two leaf serrations before formation of pedestals, the structure from which *K. daigremontiana* plantlets emerge from (Zhu et al., 2017). Attempt to generate transgenic *K. daigremontiana* with the knockdown of *KdSOC1* was unsuccessful because the calli induced in *in vitro* tissue culture could not survive beyond formation of globular-staged somatic embryos or beyond development of cotyledons (Zhu et al., 2017). This suggests that somatic embryogenesis requires *KdSOC1* activity. In contrast, *KdSOC1* overexpression led to formation of irregular leaf shape, inconsistent pedestal formation and asymmetrical plantlet formation in *K. daigremontiana* (Zhu et al., 2017). These plants also exhibited increased auxin and auxin efflux transporter *KdPIN1* in its leaves, suggesting that changes in *KdPIN1* localisation affected auxin distribution and resulted in abnormal leaf serration formation (Zhu et al., 2017). Furthermore, drought stress and long-day condition stimulated *KdSOC1* expression, which was accompanied by rapid plantlet formation (Liu et al., 2016). In addition, KdSOC1 has different structural domains compared to *Arabidopsis* SOC1, suggesting that KdSOC1 might have evolved novel biological functions in plantlet formation or have evolve to divert flowering pathways to plantlet formation (Liu et al., 2016).

In the case of an organogenesis gene, *SHOOTMERISTEMLESS* (*STM*), high levels of its expression was observed at the shoot apical meristem (SAM) and axillary buds in *K. daigremontiana* (Garcês et al., 2007). In addition, *KdSTM* transcripts were present at *K. daigremontiana* early and heart-shaped plantlets, similar to *KNOX1* gene expression during maize somatic embryogenesis (Garcês et al., 2007; Zhang et al., 2002). When *KdSTM* was downregulated in *K. daigremontiana*, plantlet formation was completely inhibited (Garcês et al., 2007). These findings suggest that *KdSTM* is crucial for plantlet formation, and that organogenesis is likely to contribute to plantlet formation through initiation or maintenance of stem cells at site of plantlet formation. *KxhKN5*, another class I *KNOX* gene, was studied in

K. x houghtonii (Laura et al., 2013), a hybrid *Kalanchoë* species that has the same mode of plantlet formation as *K. daigremontiana* (Garcês et al., 2007; Houghton, 1935). In comparison to *K. daigremontiana KdSTM* RNAi plants, downregulation of *KxhKN5* in *K. x houghtonii* only reduced number of plantlets as a result of reduced number of leaf indentations (Laura et al., 2013). However, when *KxhKN5* was overexpressed, plantlets were formed at the indentation in absence of pedestal (Laura et al., 2013). In some cases, *KxhKN5* overexpression plantlets formed strong vascularisation with the mother leaf, developing as shoots that resembled lateral branch (Laura et al., 2013). The *KxhKN5* overexpression phenotypes were similar to overexpression of its homolog *KNOTTED-1 LIKE FROM ARABIDOPSIS THALIANA1* (*KNAT1*) that induced formation of lobed leaves with ectopic meristems (Chuck et al., 1996; Moulton et al., 2020). As *KNAT1* is known to act downstream of *STM* (Byrne et al., 2002), these observations provided further evidence that pathways regulating organogenesis might be participating in plantlet formation.

In contrast to the *KdSTM* expression in *K. daigremontiana* plantlets (Garcês et al., 2007), Arabidopsis *STM* was present only in a few cells of globular and heart-stage zygotic embryo (Jurkuta et al., 2009; Long et al., 1996). But in later stages, including post-embryonic development, *STM* was expressed throughout the SAM to repress cell differentiation, but was downregulated in developing organ primordia (Long et al., 1996). Apart from *STM*, another pathway that regulates the homeostasis of shoot meristem cells is governed by *WUSCHEL* (*WUS*) (Mayer et al., 1998). *WUS* is expressed at the organising centre (OC) of the SAM central zone and functions to maintain the stem cell niche above the OC. *WUS* specifies undifferentiated stem cell identity and promotes proliferation, by ensuring presence of appropriate number of pluripotent stem cells in the SAM (Laux et al., 1996; Mayer et al., 1998). From the OC, WUS protein is transported to the three outermost cell layers of the SAM central zone (Daum et al., 2014; Yadav et al., 2011) where WUS represses differentiation programs. WUS binds directly to promoter of *CLAVATA3* (*CLV3*) to activate its expression exclusively in the outermost apical layer of SAM (Busch et al., 2010; Yadav et al., 2010, 2011, 2013). Subsequently, the stem cells produce non-autonomous small ligand peptide, CLV3, that is extracellularly secreted and directly binds to ectodomain of CLV1 receptor kinases (Fletcher et al., 1999; Ogawa et al., 2008; Rojo et al., 2002). Previously, the stability of CLV1 was known to

depend on the presence of CLV2, a receptor-like protein that forms a heterodimer receptor complex with CLV1 (Jeong et al., 1999). However, more recent studies revealed that maintenance of shoot stem cells can act through receptor complexes such as CLAVATA1 (CLV1) homomers and CLV1/CLV2/CORYNE multimers (Bleckmann et al., 2010; Guo et al., 2010; Müller et al., 2008; Shinohara and Matsubayashi, 2015; Zhu et al., 2010). Activation of CLV1 through these receptor complexes induces a cascade of MITOGEN ACTIVATED PROTEIN (MAP) kinase signalling that leads to WUS repression (Betsuyaku et al., 2011). A negative regulatory feedback loop is reinforced by direct transcriptional activation of *CLV1* and *CLV3* expression by WUS and STM respectively (Busch et al., 2010; Su et al., 2020). In the presence of HAIRY MERISTEM1/2 (HAM1/2) proteins, WUS proteins also repress CLV3 expression in the rib zone of SAM. In addition, *STM* expression is dependent on WUS and STM also interacts with WUS to enhance WUS binding to the same *CLV3* promoter (Su et al., 2020).

As outlined above, WUS is vital for the post-embryonic maintenance of the SAM. Even though *WUS* expression is present as early as at the 16-cell stage *Arabidopsis* embryo (Capron et al., 2009; Mayer et al., 1998; Tucker et al., 2008), WUS is dispensable for stem cell initiation during embryogenesis (Zhang et al., 2017a). The CLV-WUS regulatory pathway in SAM maintenance is employed only after formation of a histologically visible three-layered SAM at mid-stage embryogenesis (Brand et al., 2002; Jürgens et al., 1994; Laux and Mayer, 1998). Nonetheless, studies have shown that overexpression of *WUS* is sufficient to induce somatic embryogenesis (Arroyo-Herrera et al., 2008; Bouchabké-Coussa et al., 2013; Kadri et al., 2021; Zuo et al., 2002). The interaction between STM and WUS was also observed during somatic embryogenesis as STM up-regulates *WUS* transcription and promotes somatic embryogenesis through WUS expression (Elhiti et al., 2010; Gallois et al., 2002). The same study also showed that ectopic CLV1 expression suppresses *WUS* expression and significantly reduced responsiveness of *in vitro* tissues to somatic embryogenesis stimuli (Elhiti et al., 2010). Apart from that, the CLV-WUS signalling was also functioning in early floral stages (stage 1–6) to regulate spatial distribution and maintenance of floral stem cells, but WUS works with AGAMOUS to terminate stem cell activity at floral stage 6 (Ikeda et al., 2009; Sun and Ito, 2015). Moreover, CLV1 was found to interact with BARELY ANY MERISTEM (BAM) receptor kinases to regulate shoot stem cell proliferation independent from WUS (Nimchuk et al., 2015). In contrast to *CLV1* and *WUS*,

CLV2 is expressed more broadly at the SAM. *CLV2* is also expressed in many other tissues and is affected by external stimuli such as heat and osmotic stress (Kayes and Clark, 1998; Wang et al., 2008, 2010a; Wu et al., 2016). This corresponds to the multiple functions of CLV2, which is not only limited to control of proliferation and differentiation of stem cells in the SAM but also includes distinct physiological programs such as defence against microbes and nematode infections (Hanemian et al., 2016; Replogle et al., 2011; Wang et al., 2010b).

Previous studies have shown that organogenesis was recruited during plantlet formation of *K. daigremontiana* and that *STM* seems to regulate organogenesis in cooperation with *WUS* and *CLV* genes in *Arabidopsis*. We therefore decided to study if *WUS* and *CLV* genes also play a role in plantlet formation. We successfully isolated *WUS*, *CLV1* and *CLV2* genes from *K. daigremontiana* and confirmed the orthologies of these genes through sequence alignment and phylogenetic analyses. Immunolocalisation showed strong KdWUS activity present and sustained from prior to heart-stage plantlet to cotyledons formation. Expression analyses showed that *KdCLV1* expression was gradually upregulated across plantlet developmental stages, but *KdCLV2* expression was consistent throughout plantlet development. Both *KdWUS* and *KdCLV1* antisense plants exhibited reduction in number of leaf indentations, number of plantlets and reduced indentation depths. Plantlets from these plants also formed irregular cotyledon and leaf shape, inconsistent phyllotaxy and multiple meristems. In some plantlets of a *KdWUS* antisense line, two plantlets were present on a single pedestal, probably due to stimulation of ectopic plantlet formation via ectopic somatic embryogenesis. Both *KdWUS* and *KdCLV1* antisense plants showed altered expression of *KdYUCCA1* (*KdYUC1*) but in *KdCLV1* antisense plants, expression of genes such as *KdWUS, KdCLV2, KdLEC1*, *KdSTM* were also reduced. These results indicate that *KdWUS* and *KdCLV1* play a role during plantlet formation. However, these data still require extensive experiments to confirm molecular mechanisms behind these phenotypic changes and whether *WUS-CLV* signalling is functional during formation of *K. daigremontiana* plantlets.

3.3. **Materials & Methods**

3.3.1. Sequence analysis and phylogenetic analysis

Apart from *K. daigremontiana* and *K. pinnata* sequences, all sequences were downloaded from NCBI or Phytozome version 12. For species without annotated *WUS*, *CLV1* or *CLV2* sequence, sequence from the top results of blast search using annotated sequences from closely related species in the tree were used. The isolated *K. daigremontiana* and *K. pinnata* nucleotide sequences were translated into amino acid sequences using ApE plasmid editor version 3. The sequences were trimmed following the length of *K. daigremontiana* and *K. pinnata* isolated sequences. The fasta sequences from alignment of the trimmed sequences using ClustalX version 2.1 were used to construct the multiple sequence alignment. ESPript 3.0 at https://espript.ibcp.fr/ESPript/ESPript/index.php was used to generate the final multiple sequence alignment figure containing secondary structural information (Robert and Gouet, 2014). Sequence Identity And Similarity calculator (SIAS) at http://imed.med.ucm.es/Tools/sias.html with default settings and mean length of sequences was used to calculated percentage sequence identity. Prior to construction of phylogenetic trees, full and trimmed sequences were aligned using ClustalX version 2.1. The phylogenetic trees were constructed using RAxML Black Box, https://raxml-ng.vital-it.ch/#/. The default settings for datatype DNA were used for nucleotide sequences whilst default settings for datatype Protein/AA were used for amino acid sequences. Bootstraping was selected to apply automated bootstopping of 0.03. Dendroscope version 3.7.2. was used to visualise, edit and generate final phylogenetic analysis figures. Sequences from *Physcomitrium patens* were used as the root for all phylogenetic trees.

Table 3.1 List of species name, gene or protein that each symbol represents in all phylogenetic trees and its corresponding sequence identifier.
WUS, WUSHCEL; CLV; CLAVATA. All accession numbers or transcript ID correspond to its record on Genbank database or Phytozome database.

Symbol	Species	Gene/ Protein	Accession number/Transcript ID
AtrWUS	*Amborella trichopoda*	WUS	XP_011624486.2, XM_011626184.2
AcomWUS	*Ananas comosus*	WUS	XP_020114973.1, XM_020259384.1
AcoWUS	*Aquilegia coerulea*	WUS	KZ305021.1, PIA59942.1
AthWUS	*Arabidopsis thaliana*	WUS	NP_565429.1, NM_127349.4
CpaWUS	*Carica papaya*	WUS	XP_021908316.1, XM_022052624.1
CmiWUS	*Cinnamomum micranthum*	WUS	RWR79206.1, QPKB01000003.1
EguWUS	*Erythranthe guttata*	WUS	XM_012989541.1, XP_012844995.1

GmaWUS	*Glycine max*	WUS	XM_006590661.4, XP_006590724.1
HanWUS	*Helianthus annuus*	WUS	XM_022151273.2, XP_022006965.1
KdaWUS	*Kalanchoë daigremontiana*	WUS	
KfeWUS	*Kalanchoë fedtschenkoi*	WUS	Kaladp0040s0534.1
KlaWUS	*Kalanchoë laxiflora*	WUS	Kalax.0129s0063.1
KpiWUS	*Kalanchoë pinnata*	WUS	
MtrWUS	*Medicago truncatula*	WUS	XM_003612110.3, XP_003612158.1
MacWUS	*Musa acuminata*	WUS	XP_009408701.1, XM_009410426.1
NnuWUS	*Nelumbo nucifera*	WUS	XP_010268704.1, XM_010270402.2
NthWUS	*Nymphaea thermarum*	WUS	KAF3794921.1, JAANDH010000022.1
OsaWUS	*Oryza sativa*	WUS	XM_015779885.2, XP_015635371.1
PpaWUS	*Physcomitrium patens*	WUS	AB699867.1, BAM76366.1
PabWUS	*Picea abies*	WUS	JX512364.1, AGL54197.1
PtrWUS	*Populus trichocarpa*	WUS	XP_006383114.1, XM_006383052.2
PpeWUS	*Prunus persica*	WUS	XP_007203178.1, XM_007203116.1
SmoWUS	*Selaginella moellendorffii*	WUS	XP_002962413.1, XM_002962367.2
SlyWUS	*Solanum lycopersicum*	WUS	NP_001234015.2, NM_001247086.3
TcaWUS	*Theobroma cacao*	WUS	XP_007046708.1, XM_007046646.2
VviWUS	*Vitis vinifera*	WUS	XP_002266323.1, XM_002266287.3
AtrCLV1	*Amborella trichopoda*	CLV1	XM_006856682.3, XP_006856744.3
AcomCLV1	*Ananas comosus*	CLV1	XP_020112369.1, XM_020256780.1
AcoCLV1	*Aquilegia coerulea*	CLV1	PIA57392.1, KZ305023.1
AthCLV1	*Arabidopsis thaliana*	CLV1	NP_177710.1, NM_106232.4
CpaCLV1	*Carica papaya*	CLV1	XM_022047056.1, XP_021902748.1
CmiCLV1	*Cinnamomum micranthum*	CLV1	RWR92326.1, QPKB01000009.1
EguCLV1	*Erythranthe guttata*	CLV1	XP_012835707.1, XM_012980253.1
GmaCLV1	*Glycine max*	CLV1	NP_001238576.1, NM_001251647.1
HanCLV1	*Helianthus annuus*	CLV1	XM_022141913.2, XP_021997605.2
KdaCLV1	*Kalanchoë daigremontiana*	CLV1	
KfeCLV1	*Kalanchoë fedtschenkoi*	CLV1	Kaladp0068s0368.1
KlaCLV1	*Kalanchoë laxiflora*	CLV1	Kalax.0183s0036.1
KpiCLV1	*Kalanchoë pinnata*	CLV1	
MtrCLV1	*Medicago truncatula*	CLV1	XP_003606988.2, XM_003606940.4
MacCLV1	*Musa acuminata*	CLV1	XP_009418700.1, XM_009420425.2
NnuCLV1	*Nelumbo nucifera*	CLV1	XM_010268510.2, XP_010266812.1
NthCLV1	*Nymphaea thermarum*	CLV1	KAF3796441.1, JAANDH010000004.1
OsaCLV1	*Oryza sativa*	CLV1	XP_015642501.1, XM_015787015.1
PpaCLV1	*Physcomitrium patens*	CLV1	XP_024392526.1, XM_024536758.1
PabCLV1	*Picea glauca*	CLV1	ABF73316.1, DQ530597.1
PtrCLV1	*Populus trichocarpa*	CLV1	XP_002307734.1, XM_002307698.2
PpeCLV1	*Prunus persica*	CLV1	XP_007225356.2, XM_007225294.2
SmoCLV1	*Selaginella moellendorffii*	CLV1	EFJ13721.1, GL377631.1
SlyCLV1	*Solanum lycopersicum*	CLV1	XM_004238322.4, XP_004238370.1
TcaCLV1	*Theobroma cacao*	CLV1	XP_017981861.1, XM_018126372.1
VviCLV1	*Vitis vinifera*	CLV1	FN595227, CCB46051.1
ZmaCLV1	*Zea mays*	CLV1	GRMZM2G300133_T01
AtrCLV2	*Amborella trichopoda*	CLV2	XP_006852121.2, XM_006852059.3

AcomCLV2	*Ananas comosus*	CLV2	OAY84350.1, LSRQ01000224.1
AcoCLV2	*Aquilegia coerulea*	CLV2	PIA30817.1, KZ305071.1
AthCLV2	*Arabidopsis thaliana*	CLV2	NP_176717.1, NM_105212.3
CpaCLV2	*Carica papaya*	CLV2	XP_021890931.1, XM_022035239.1
CmiCLV2	*Cinnamomum micranthum*	CLV2	RWR96860.1, QPKB01000012.1
EguCLV2	*Erythranthe guttata*	CLV2	XP_012833350.1, XM_012977896.1
GmaCLV2	*Glycine max*	CLV2	XP_003533585.3, XM_003533537.5
HanCLV2	*Helianthus annuus*	CLV2	XP_021984324.1, XM_022128632.1
KdaCLV2	*Kalanchoë daigremontiana*	CLV2	
KfeCLV2	*Kalanchoë fedtschenkoi*	CLV2	Kaladp0007s0037.1
KlaCLV2	*Kalanchoë laxiflora*	CLV2	Kalax.0189s0047.1
KpiCLV2	*Kalanchoë pinnata*	CLV2	
MtrCLV2	*Medicago truncatula*	CLV2	XP_003624130.1, XM_003624082.4
MacCLV2	*Musa acuminata*	CLV2	XP_009379932.1, XM_009381657.2
NnuCLV2	*Nelumbo nucifera*	CLV2	XP_010275969.1, XM_010277667.2
NthCLV2	*Nymphaea thermarum*	CLV2	KAF3788586.1, JAANDH010000154.1
OsaCLV2	*Oryza sativa*	CLV2	XP_015623374.1, XM_015767888.2
PpaCLV2	*Physcomitrium patens*	CLV2	XP_024374702.1, XM_024518934.1
PabCLV2	*Picea sitchensis*	CLV2	ABR18056.1, EF678290.1
PtrCLV2	*Populus trichocarpa*	CLV2	XP_002319815.2, XM_002319779.2
PpeCLV2	*Prunus persica*	CLV2	XP_007206423.1, XM_007206361.2
SmoCLV2	*Selaginella moellendorffii*	CLV2	EFJ12600.1, GL377638.1
SlyCLV2	*Solanum lycopersicum*	CLV2	NP_001234824.2, NM_001247895.2
TcaCLV2	*Theobroma cacao*	CLV2	XP_007029405.2, XM_007029343.2
VviCLV2	*Vitis vinifera*	CLV2	XP_002272643.1, XM_002272607.4
ZmaCLV2	*Zea mays*	CLV2	PWZ25737.1, NCVQ01000005.1

3.3.2. Immunolocalisation

The protocol from (Garcês and Sinha, 2009b) was used to fix and section the plant materials for KdWUS immunolocalisation. Subsequent preparation of samples and antibodies treatment were performed as described in (Kim et al., 2003). The primary antibody WUS (aE-17): sc-12587 (Santa Cruz Biotechnology, Inc; United States) with 1:250 dilution was used. For the secondary antibody, AP-conjugated Donkey Anti-Goat IgG (Promega, United States) of 1:400 dilution was used. The staining of samples developed under 20 minutes. Images of immunolocalization was taken using Leica DMR microscope (Leica, Germany) and with SPOT Software version 5.5 (SPOT Imaging, United States).

3.3.3. Plant materials

Wild-type *K. daigremontiana* plants were grown in growth chambers at 23 ^{o}C under continuous long day cycle of 16 hours day and 8 hours dark condition. The potting mixture contained 6

parts Levington® F2 Seed & Modular Compost (The Scotts Company, UK), 1 part Vermiculite V3 medium (Sinclair Pro, UK) and 1 part Perlite P35 standard (Sinclair Pro, UK).

Table 3.2 Description of leaves and plantlets harvested for RNA-sequencing and quantitative real-time PCR.

Stages	Description
SAM	Shoot apical meristem tissues
Ctrl	Whole leaf margin of 1-2 cm young leaves
S0	Basal leaf notches (no pedestal formation) of leaves showing 1-2 leaf notches developing pedestal
S1	Leaf notches without pedestal formation harvested from leaves showing plantlets at S2 and S3
S2	Leaf notches with formed pedestal but without plantlet formation
S3	Leaf notches with emerging plantlet primordium
S4	Leaf notches showing plantlets with visible cotyledons

3.3.4. RNA-sequencing and expression analysis

RNA was extracted using RNeasy® Plant Mini kit (Qiagen, UK) following the kit manual using RLC buffer. 10 mg polyvinylpyrrolidone (PVP, molecular weight 40,000) for each 100 mg plant tissues was dissolved at 56 ^{o}C in the RLC buffer before use. After addition of RLC buffer, the mixture was incubated at 56 ^{o}C for 1 minute and then vortexed before following the subsequent procedures. Purified RNA samples were sequenced at the University of Manchester Sequencing Facility using Sanger sequencing by Illumina HiSeq 2000 technology. For reverse-transcriptase PCR (RT-PCR), the RNA was treated with RQ1 RNase-free DNase (Promega, UK) and Tetro cDNA Synthesis Kit (Bioline, UK) was used to synthesise cDNA. Q5® High-Fidelity DNA Polymerase (New England Biolabs, USA) and BIOTAQ™ DNA Polymerase were used to perform the RT-PCR. The reactions were setup following the instructions in BIOTAQ polymerase datasheet. *Kda18s* were amplified at 58 ^{o}C with 32 cycles and the other genes were amplified at 56 ^{o}C with 40 cycles. *K. daigremontiana 18S ribosomal RNA* (*Kd18s*) gene was used as a reference gene for RT-PCR. StepOne™ Real-Time PCR System (Applied Biosystems, UK) and SensiFAST SYBR® Hi-ROX Mix (Bioline, UK) were used to perform quantitative real-time PCR (qRT-PCR). The software used for template design and analysis was StepOne™ and StepOnePlus™ Software v2.3 (Thermo Fisher Scientific, UK). An annealing temperature of 60 °C was used, with 40 cycles and *KdGAPDH* as a reference gene. GraphPad Prism 8 was used to generate all graphs and to perform non-parametric Kruskal-Wallis statistical tests and Dunn's multiple comparison tests.

Table 3.3 List of primers used for semi-quantitative reverse transcriptase PCR and quantitative real-time PCR. The table includes expected band size for the PCR products amplified using either cDNA or genomic DNA for each gene. Kd, *K. daigremontiana*; *GAPDH, GLYCERALDEYHDE-3-PHOSPHATE DEHYDROGENASE*; *STM*, SHOOT *MERISTEMLESS*; *LEC1*, *LEAFY COTYLEDON 1*; *WUS*, *WUSCHEL*; *CLV1*, *CLAVATA1*; *CLV2*, *CLAVATA2*; *YUC1*, *YUCCA1*; *TPL*, *TOPLESS.*

Gene	5' to 3' primer sequence	With cDNA (bp)	With gDNA (bp)
KdGAPDH	GGAGCAGAGATAACAACCTTC TCCATTCATCAACACAGACTAC	290	290
Kd18s	AGAAACGGCTACCACATCCAAG GACTCATTGAGCCCGGTATTGT	104	104
KdSTM	GGATCAGTTCATGGAGGCTTAC CTTGAACTGGGACTCAATCCTC	112	112
KdLEC1	GTCGGAGTATATCGGCTTCATC TGTATCGGTGCAGGTACAGAGT	135	135
KdWUS	CCTCCAAATACTCAGACATCAACAA CATCCCTCCTTTAGCCCAAC	146	930
KdCLV1	ATTGCTCTCCGCCGATTCT CTTCCGACCCGTTATCAGC	248	339
KdCLV2	GGTGTTTCCAGTTACTCGCTTTG TTGGCAATGGCGTCGTTC	217	217
KdYUC1	GAGCATTCAAGAAACAGAGCATC GAAGTTCATCAGCGGGAGC	277	277
KdTPL	GACGACATTTATGCCTCCTCC AGCCCCTGATGAAACTAGAACA	211	302

3.3.5. Generation and phenotypic analysis of transgenic plants

KdWUS, KdCLV1 and *KdCLV2* genes were isolated using genomic DNA of wild-type *K. daigremontiana* using the primers listed in Table 4. The genomic DNA were extracted as described in (Garcês and Sinha, 2009e). Antisense sequence of each *KdWUS*, *KdCLV1* and *KdCLV2* gene was ligated with a cauliflower mosaic virus (CaMV) 35S Promoter and Terminator into a modified *pBI121* vector. All antisense constructs were assembled using golden-gate technique and then transformed into *K. daigremontiana* plants as shown in (Garcês and Sinha, 2009d). iPhone 8 or Leica S8 APO microscope (Leica Microsystems, Germany) with a GX-CAM-Eclipse camera (GT Vision, UK) attached was used to photograph live plants. Graphical representation of quantitative measurement of plant phenotypes were generated using GraphPad Prism 8. The same software was used to perform non-parametric Kruskal-Wallis statistical tests and Dunn's multiple comparison tests.

Table 3.4 List of primer sequences used for isolating the stated gene or gene construct.

Gene/Construct	Primer sequence 5'-3'
KdWUS	GTGGTCTCTAAGCATGATGGGTGATGACCTTGG
	GTGGTCTCTGGTGTTGTTGATGTCTGAGTATTTGG
KdCLV1	GTGGTCTCTAAGCCATCTGCTGTTTCCTCCGTA
	GTGGTCTCTGGTGCCGTTCCGTCCGAGATTC
KdCLV2 (gene construct)	GTGGTCTCTAAGCTTTAGAGGGTCCTTTGCCG
	GTGGTCTCTGGTGAATCTCCAGCGATCTACAC
KdCLV2 (sequence alignment & phylogenetic analysis)	GTGGTCTCTAAGCCTCGATGTCAGCAGGAAC
	GTGGTCTCTGGTGAATCTCCAGCGATCTACAC
p35S::antisense-*KdWUS*	GTGGTCTCAGGAGGCTAGAGCAGCTTGCCAAC
	GTGGTCTCTAAGCATGATGGGTGATGACCTTGG
antisense-*KdCLV1*::*35ST*	GTGGTCTCTGGTGCCGTTCCGTCCGAGATTC
	GTGGTCTCAAGCGGGTGATCTGGATTTTAGTACTGG
antisense-*KdCLV2*::*35ST*	GTGGTCTCTGGTGAATCTCCAGCGATCTACAC
	GTGGTCTCAAGCGGGTGATCTGGATTTTAGTACTGG
NPTII	CACAACAGACAATCGGCTGC
	GCACGAGGAAGCGGTCAG

3.3.6. Genotype Analysis

Genomic DNA was extracted following the protocol "Quick DNA Prep for PCR" from (Weigel and Glazebrook, 2002). Transgene in each construct and *NEOMYCIN PHOSPHOTRANSFERASE II* (*NPTII*) gene in each plasmid containing the construct were amplified using the primers listed in Table 2.4. Q5® High-Fidelity DNA Polymerase (New England Biolabs, USA) and BIOTAQ™ DNA Polymerase were used to perform the genotyping PCR at 56 ^{o}C in a T100™ Thermal Cycler (Biorad, UK). The concentrations of reagents in the reaction mixture used were as described in the BIOTAQ polymerase datasheet. All electrophoresis gels were visualised using ChemiDoc™ XRS+ Imager (Bio-Rad, UK) and Image Lab 5.1 (Bio-Rad, UK).

3.4. **Results**

3.4.1. Conservation and evolution of WUS, CLV1 and CLV2 sequences in *Kalanchoë*

The genome of *K. daigremontiana* and *K. pinnata* genome has not yet been sequenced. Hence, *Arabidopsis WUS*, *CLV1* and *CLV2* sequences were used to blast search for the gene orthologs in *K. laxiflora* and *K. fedtschenkoi*. Sequences with the highest scores were aligned and used to design primers to isolate *WUS*, *CLV1* and *CLV2* from *K. daigremontiana* and *K. pinnata.* Upon isolation of *WUS*, *CLV1* and *CLV2* from *K. daigremontiana* and *K. pinnata*, their sequences were aligned and analysed to examine whether sequences of these genes are conserved in *Kalanchoë* and in the angiosperm kingdom. Translated *K. daigremontiana* and *K. pinnata* WUS, CLV1 and CLV2 sequences were aligned with trimmed sequences of the same orthologs from two other *Kalanchoë* species and other angiosperm plants (Fig. 3.1). The 62-residue region of WUS protein sequences isolated from *K. daigremontiana* and *K. pinnata* were highly conserved across all angiosperm species, including the basal angiosperm species and also gymnosperms and lower plants such as *Picea abies*, *Physcomitrium patens* and *Selaginella moellendorffii* (Fig. 3.1A). All *Kalanchoë* nucleotide (Fig. 3.2A) and protein sequences (Fig. 3.2B) were 100 % identical and shared 81.12 % and 83.87 % identity with *Arabidopsis WUS* nucleotide sequences and protein sequences, respectively. The trimmed WUS protein sequences and their corresponding nucleotide sequences were used to generate a gene tree and a protein tree (Fig. 3.3A, B). Both trees grouped the *Kalanchoë* sequences together as this region of sequences is identical within the genus but contain sufficient differences to be distinguished from sequences of other species outside of the *Kalanchoë* clade (Fig. 3.3A, B). Similar observation was obtained when whole sequences of WUS were used, however, due to the lack of *K. daigremontiana* and *K. pinnata* whole sequences, only *K. laxiflora* and *K. fedtschenkoi* sequences were used for the phylogenetic analysis (Fig. 3.3G, H).

All *Kalanchoë CLV1* nucleotide and protein sequences shared at least 64 % identity with the corresponding *Arabidopsis* orthologs. In contrast to the WUS *Kalanchoë* sequences, isolated CLV1 sequences from *K. daigremontiana* and *K. pinnata* were 100 % identical but trimmed CLV1 sequences from *K. laxiflora* and *K. fedtschenkoi* were 99.33 % identical (Fig. 3.2D). This also resulted in *K. daigremontiana* and *K. pinnata* sequences sharing 97 % sequence identity to *K. laxiflora* and *K. fedtschenkoi* sequences (Fig. 3.2D). As for nucleotide sequences, *K.*

daigremontiana and *K. pinnata CLV1* were 100 % identical, but trimmed *CLV1* sequences from *K. laxiflora* and *K. fedtschenkoi* were 99.66 % identical (Fig. 3.2C). However, *K. daigremontiana* and *K. pinnata CLV1* sequences were 98.55 % identical to *K. laxiflora* and 98.55 % identical to *K. fedtschenkoi CLV1* sequences (Fig. 3.2C). The differences between *Kalanchoë* sequences were also reflected in the phylogenetic analysis of trimmed sequences, which showed *K. daigremontiana* and *K. pinnata* in a separate clade from *K. laxiflora* and *K. fedtschenkoi* sequences (Fig. 3.3C, D).

A different relationship between CLV2 *Kalanchoë* sequences was exhibited, in which trimmed *K. laxiflora* and *K. fedtschenkoi* nucleotide and protein sequences shared 99.37 % and 100 % identity (Fig. 3.2E, F). *K. daigremontiana* and *K. pinnata* nucleotide and protein sequences only shared 95.77 % and 97.65 % identity respectively (Fig. 3.2E, F). *K. daigremontiana* shared 96.4 % and 96.55 % identity with nucleotide sequence of trimmed *K. fedtschenkoi* and *K. laxiflora* (Fig. 3.2E) but shared 99.53 % identity with their protein sequences (Fig. 3.2F). *K. pinnata* shared 97.49 % and 98.12 % identity with trimmed nucleotide and protein sequences of *K. fedtschenkoi* and *K. laxiflora* respectively (Fig. 3.2E, F). *Kalanchoë CLV2* nucleotide and protein sequences shared at least 67.6 % and 71.36 % identity with the corresponding *Arabidopsis CLV2* sequences. The evolutionary relationship between CLV2 *Kalanchoë* sequences was once again demonstrated in the phylogenetic analysis of trimmed CLV2 sequences (Fig. 3.3E, F). In both nucleotide and protein trees, *K. laxiflora* and *K. fedtschenkoi* sequences were grouped together but based on the nucleotide tree (Fig. 3.3E), *K. daigremontiana CLV2* sequence was the most evolutionary distant, followed by *K. pinnata CLV2* sequence. However, based on the protein tree, *K. daigremontiana* and *K. pinnata* CLV2 sequences were equally distant from *K. laxiflora* and *K. fedtschenkoi* sequences (Fig. 3.3F).

Unlike the WUS sequences (Fig. 3.1A), CLV1 (Fig. 3.1B) and CLV2 (Fig. 3.1C) sequences did not share global similarity score of more than 0.7 (black framed) across the entire trimmed sequences. This score indicates that more than 70% of the residues in the framed region have similar physico-chemical properties. However, most regions in the trimmed sequences still share a similarity global score of more than 0.7. Both CLV1 (Fig. 3.1B) and CLV2 (Fig. 3.1C) sequence alignment also displayed some gaps of 1 or 2 amino acid residues and one region

containing a longer gap. For CLV1 sequence alignment, the region in which there was a greater gap of more than 5 amino acid residues was due to the rice, *Oryza sativa* sequence OsaCLV1 that showed additional amino acids at that region (Fig. 3.1B). As for CLV2, the region showing a gap of almost 50 residues was due to *P. sitchensis* and *S. moellendorffii* containing additional amino acids at that region (Fig. 3.1C). Phylogeny of whole *CLV1* and *CLV2* nucleotide and protein sequences showed that the grouping of *K. laxiflora* and *K. fedtschenkoi* sequences indicates differences in its sequences compared to other species (Fig. 3.3I-L), similar to as shown in whole sequences WUS phylogeny (Fig. 3.3G, H). In addition, phylogenetic analyses of whole sequences also showed that the relationship between sequences from angiosperm species were more distinguishable, reflected by separation of clades (Fig. 3.3G-L).

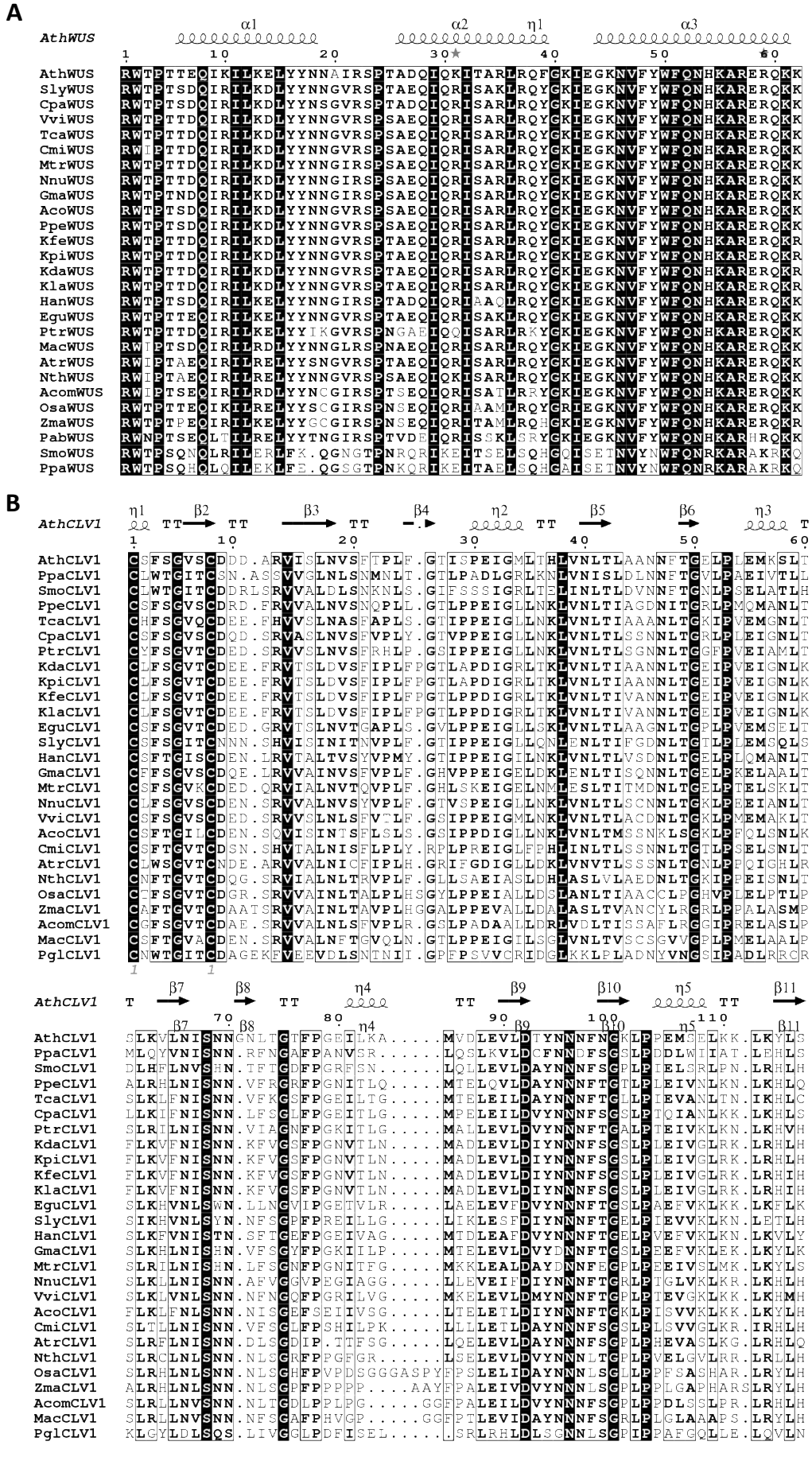
A
AthWUS
α1
α2
η1
α3
AthWUS RWTPTTEQIKILKELYYNNAIRSPTADQIQKITARLRQFGKIEGKNVFYWFQNHKARERQKK
SlyWUS RWTPTSDQIRILKDLYYNNGVRSPTAEQIQRISAKLRQYGKIEGKNVFYWFQNHKARERQKK
CpaWUS RWTPTSDQIRILKDLYYNSGVRSPTADQIQRISARLRQYGKIEGKNVFYWFQNHKARERQKK
VviWUS RWTPTTDQIRILKDLYYNNGVRSPSAEQIQRISARLRQYGKIEGKNVFYWFQNHKARERQKK
TcaWUS RWTPTTDQIRILKDLYYNNGVRSPSAEQIQRISARLRQYGKIEGKNVFYWFQNHKARERQKK
CmiWUS RWIPTTDQIRILKDLYYNNGVRSPSAEQIQRISARLRQYGKIEGKNVFYWFQNHKARERQKK
MtrWUS RWTPTTDQIRILKDLYYNNGIRSPSAEQIQRISARLRQYGKIEGKNVFYWFQNHKARERQKK
NnuWUS RWTPTTDQIRILKDLYYNNGIRSPSAEQIQRISARLRQYGKIEGKNVFYWFQNHKARERQKK
GmaWUS RWTPTNDQIRILKDLYYNNGIRSPSAEQIQRISARLRQYGKIEGKNVFYWFQNHKARERQKK
AcoWUS RWTPTSDQIRILKDLYYNNGVRSPSAEQIQRISARLRQYGKIEGKNVFYWFQNHKARERQKK
PpeWUS RWTPTSDQIRILKDLYYNNGVRSPSAEQIQRISARLRQYGKIEGKNVFYWFQNHKARERQKK
KfeWUS RWTPTTDQIRILKDLYYNNGVRSPTAEQIQRISARLRQYGKIEGKNVFYWFQNHKARERQKR
KpiWUS RWTPTTDQIRILKDLYYNNGVRSPTAEQIQRISARLRQYGKIEGKNVFYWFQNHKARERQKR
KdaWUS RWTPTTDQIRILKDLYYNNGVRSPTAEQIQRISARLRQYGKIEGKNVFYWFQNHKARERQKR
KlaWUS RWTPTTDQIRILKDLYYNNGVRSPTAEQIQRISARLRQYGKIEGKNVFYWFQNHKARERQKR
HanWUS RWTPTSDQIRILKELYYNNGIRSPTADQIQRIAAQLRQYGKIEGKNVFYWFQNHKARERQKK
EguWUS RWTPTTEQIRILKELYYNNGVRSPTAEQIQRISAKLRQYGKIEGKNVFYWFQNHKARERQKK
PtrWUS RWTPTTDQIRILKELYYIKGVRSPNGAFIQQISARLRKYGKIEGKNVFYWFQNHKARERQKK
MacWUS RWIPTSDQIRILRDLYYNNGLRSPNAEQIQRISARLRQYGKIEGKNVFYWFQNHKARERQKK
AtrWUS RWIPTAEQIRILRELYYSNGVRSPTAEQIQRISARLRQYGKIEGKNVFYWFQNHKARERQKK
NthWUS RWIPTAEQIRILRELYYNNGVRSPSAEQIQKISARLRQYGKIEGKNVFYWFQNHKARERQKK
AcomWUS RWIPTSEQIRILRDLYYNCGIRSPTSEQIQRISATLRRYGKIEGKNVFYWFQNHKARERQKK
OsaWUS RWTPTTEQIKILRELYYSCGIRSPNSEQIQRIAAMLRQYGRIEGKNVFYWFQNHKARERQKK
ZmaWUS RWTPTPEQIRILKELYYGCGIRSPNSEQIQRITAMLRQHGKIEGKNVFYWFQNHKARERQKR
PabWUS RWNPTSEQLTILRELYYTNGIRSPTVDEIQRISSKLSRYGKIEGKNVFYWFQNHKARHRQKK
SmoWUS RWTPSQNQLRILERLFK.QGNGTPNRQRIKEITSELSQHGQISETNVYNWFQNRKARAKRKQ
PpaWUS RWTPSQHQLQILEKLFE.QGSGTPNKQRIKEITAELSQHGAISETNVYNWFQNRKARAKRKQ
B
AthCLV1
η1
β2
β3
β4
η2
β5
β6
η3
AthCLV1 CSFSGVSCDDD.ARVISLNVSFTPLF.GTISPEIGMLTHLVNLTLAANNFTGELPLEMKSLT
PpaCLV1 CLWTGITCSN.ASSVVGLNLSNMNLT.GTLPADLGRLKNLVNISLDLNNFTGVLPAEIVTLL
SmoCLV1 CLWTGITCDDRLSRVVALDLSNKNLS.GIFSSSIGRLTELINLTLDVNNFTGNLPSELATLH
PpeCLV1 CSFSGVSCDRD.FRVVALNVSNQPLL.GTLPPEIGLLNKLVNLTIAGDNITGRLPMQMANLT
TcaCLV1 CHFSGVQCDEE.FHVVSLNASFAPLS.GTIPPEIGLLNKLVNLTIAAANLTGKIPVEMGNLT
CpaCLV1 CSFSGVSCDQD.SRVASLNVSFVPLY.GTVPPEIGLLNKLVNLTLSSNNLTGRLPLEIGNLT
PtrCLV1 CYFSGVTCDED.SRVVSLNVSFRHLP.GSIPPEIGLLNKLVNLTLSGNNLTGGFPVEIAMLT
KdaCLV1 CLFSGVTCDEE.FRVTSLDVSFIPLFPGTLAPDIGRLTKLVNLTIAANNLTGEIPVEIGNLK
KpiCLV1 CLFSGVTCDEE.FRVTSLDVSFIPLFPGTLAPDIGRLTKLVNLTIAANNLTGEIPVEIGNLK
KfeCLV1 CLFSGVTCDEE.FRVTSLDVSFIPLFPGTLPPDIGRLTKLVNLTIVANNLTGEIPVEIGNLK
KlaCLV1 CLFSGVTCDEE.FRVTSLDVSFIPLFPGTLPPDIGRLTKLVNLTIVANNLTGEIPVEIGNLK
EguCLV1 CSFSGVTCDED.GRVTSLNVTGAPLS.GVLPPEIGLLSKLVNLTLAAGNLTGPLPVEMSELT
SlyCLV1 CSFSGITCNNN.SHVISINITNVPLF.GTIPPEIGLLQNLENLTIFGDNLTGTLPLEMSQLS
HanCLV1 CSFTGISCDEN.LRVTALTVSYVPMY.GTIPPEIGILNKLVNLTLVSDNLTGELPLQMANLT
GmaCLV1 CFFSGVSCDQE.LRVVAINVSFVPLF.GHVPPEIGELDKLENLTISQNNLTGELPKELAALT
MtrCLV1 CSFSGVKCDED.QRVIALNVTQVPLF.GHLSKEIGELNMLESLTITMDNLTGELPTELSKLT
NnuCLV1 CLFSGVSCDEN.SRVVALNVSYVPLF.GTVSPEIGLLNKLVNLTLSCNNLTGKLPEEIANLT
VviCLV1 CSFSGVSCDED.SRVVSLNLSFVCLF.GSIPPEIGMLNKLVNLTLACDNLTGKLPMEMAKLT
AcoCLV1 CSFTGILCDEN.SQVISINTSFLSLS.GSIPPDIGLLNKLVNLTMSSNKLSGKLPFQLSNLK
CmiCLV1 CSFTGVTCDSN.SHVTALNISFLPLY.RPLPREIGLFPHLINLTLSSNNLTGTLPSELSNLT
AtrCLV1 CLWSGVTCNDE.ARVVALNICFIPLH.GRIFGDIGLLDKLVNVTLSSSNLTGNLPPQIGHLR
NthCLV1 CNFTGVTCDQG.SRVIALNLTRVPLF.GLLSAEIASLDHLASLVLAEDNLTGKIPPEISNLT
OsaCLV1 CTFSGVTCDGR.SRVVAINLTALPLHSGYLPPEIALLDSLANLTIAACCLPGHVPLELPTLP
ZmaCLV1 CAFTGVTCDAAT.SRVVAINLTAVPLHGGALPPEVALLDALASLTVANCYLRGRLPPALASMP
AcomCLV1 CGFSGVTCDAE.SRVVALNLSFVPLR.GSLPADAALLDRLVDLTISSAFLRGGIPRELASLP
MacCLV1 CSFTGVACDEN.SRVVALNFTGVQLN.GTLPPEIGILSGLVNLTVSCSGVVGPLPMELAALP
PglCLV1 CNWTGITCDAGEKFVEEVDLSNTNII.GPFPSVVCRIDGLKKLPLADNYVNGSIPADLRRCR
1 1
AthCLV1
β7
β8
η4
β9
β10
η5
β11
AthCLV1 SLKVLNISNNGNLTGTFPGEILKA.....MVDLEVLDTYNNNFNGKLPPEMSELKK.LKYLS
PpaCLV1 MLQYVNISNN.RFNGAFPANVSR.....LQSLKVLDCFNNDFSGSLPDDLWIIAT.LEHLS
SmoCLV1 DLHFLNVSHN.TFTGDFPGRFSN.....LQLLEVLDAYNNNFSGPLPIELSRLPN.LRHLH
PpeCLV1 ALRHLNISNN.VFRGRFPGNITLQ.....MTELQVLDAYNNNFTGTLPLEIVNLKN.LKHLQ
TcaCLV1 SLKLFNISNN.VFKGSFPGEILTG.....MTELEILDAYNNNFTGLLPIEVANLTN.IKHLC
CpaCLV1 LLKIFNISNN.LFSGLFPGEITLG.....MPELEILDVYNNNFSGSLPTQIANLKK.LKHLS
PtrCLV1 SLRILNISNN.VIAGNFPGKITLG.....MALLEVLDVYNNNFTGALPTEIVKLKN.LKHVH
KdaCLV1 FLKVFNISNN.KFVGSFPGNVTLN.....MADLEVLDIYNNNFSGSLPLEIVGLRK.LRHLH
KpiCLV1 FLKVFNISNN.KFVGSFPGNVTLN.....MADLEVLDIYNNNFSGSLPLEIVGLRK.LRHLH
KfeCLV1 FLKVFNISNN.KFVGSFPGNVTLN.....MADLEVLDIYNNNFSGSLPLEIVGLRK.LRHIH
KlaCLV1 FLKVFNISNN.KFVGSFPGNVTLN.....MADLEVLDIYNNNFSGSLPLEIVGLRK.LRHIH
EguCLV1 SLKHVNLSWN.LLNGVIPGETVLR.....LAELEVFDVYNNNFTGSLPAEFVKLKK.LKFLK
SlyCLV1 SIKHVNLSYN.NFSGPFPREILLG.....LIKLESFDIYNNNFTGELPIEVVKLKN.LETLH
HanCLV1 SLKFVNISTN.SFTGEFPGEIVAG.....MTDLEAFDVYNNNFTGELPVEFVKLKN.LKVLY
GmaCLV1 SLKHLNISHN.VFSGYFPGKIILP.....MTELEVLDVYDNNFTGSLPEEFVKLEK.LKYLK
MtrCLV1 SLRILNISHN.LFSGNFPGNITFG.....MKKLEALDAYDNNFEGPLPEEIVSLMK.LKYLS
NnuCLV1 SLKLLNISNN.AFVGGVPEGIAGG.....LLEVEIFDIYNNNFTGRLPTGLVKLKR.LKHLH
VviCLV1 SLKLVNLSNN.NFNGQFPGRILVG.....MKELEVLDMYNNNFTGPLPTEVGKLKK.LKHMH
AcoCLV1 FLKLFNLSNN.NISGEFSEIIVSG.....LTELETLDIYNNNFTGKLPISVVKLKK.LKYLH
CmiCLV1 SLTLLNISNN.VFSGLFPSHILPK.....LLLLETLDAYNNNFSGSLPLSVVGLKR.IRHLH
AtrCLV1 SLRFLNISNN.DLSGDIP.TTFSG.....LQELEVLDAYNNNFSGPLPHEVASLKG.LRHLQ
NthCLV1 SLRCLNLSNN.NLSGRFPPGFGR.....LSELEVLDVYNNNLTGPLPVELGVLRR.LRLLH
OsaCLV1 SLRHLNLSNN.NLSGHFPVPDSGGGASPYFPSLELIDAYNNNLSGLLPPFSASHAR.LRYLH
ZmaCLV1 ALRHLNLSNN.NLSGPFPPPPP....AAYFPALEIVDVYNNNLSGPLPPLGAPHARS.LRYLH
AcomCLV1 SLRLLNVSNN.NLTGDLPPLPG.....GGFPALEILDVYNNNFSGPLPPDLSSLPR.LRHLH
MacCLV1 SLRLLNVSNN.NFSGAFPHVGP.....GGFPTLEVIDAYNNNFSGRLPLGLAAAPS.LRYLH
PglCLV1 KLGYLDLSQS.LIVGGLPDFISEL.....SRLRHLDLSGNNLSGPIPPAFGQLLE.LQVLN

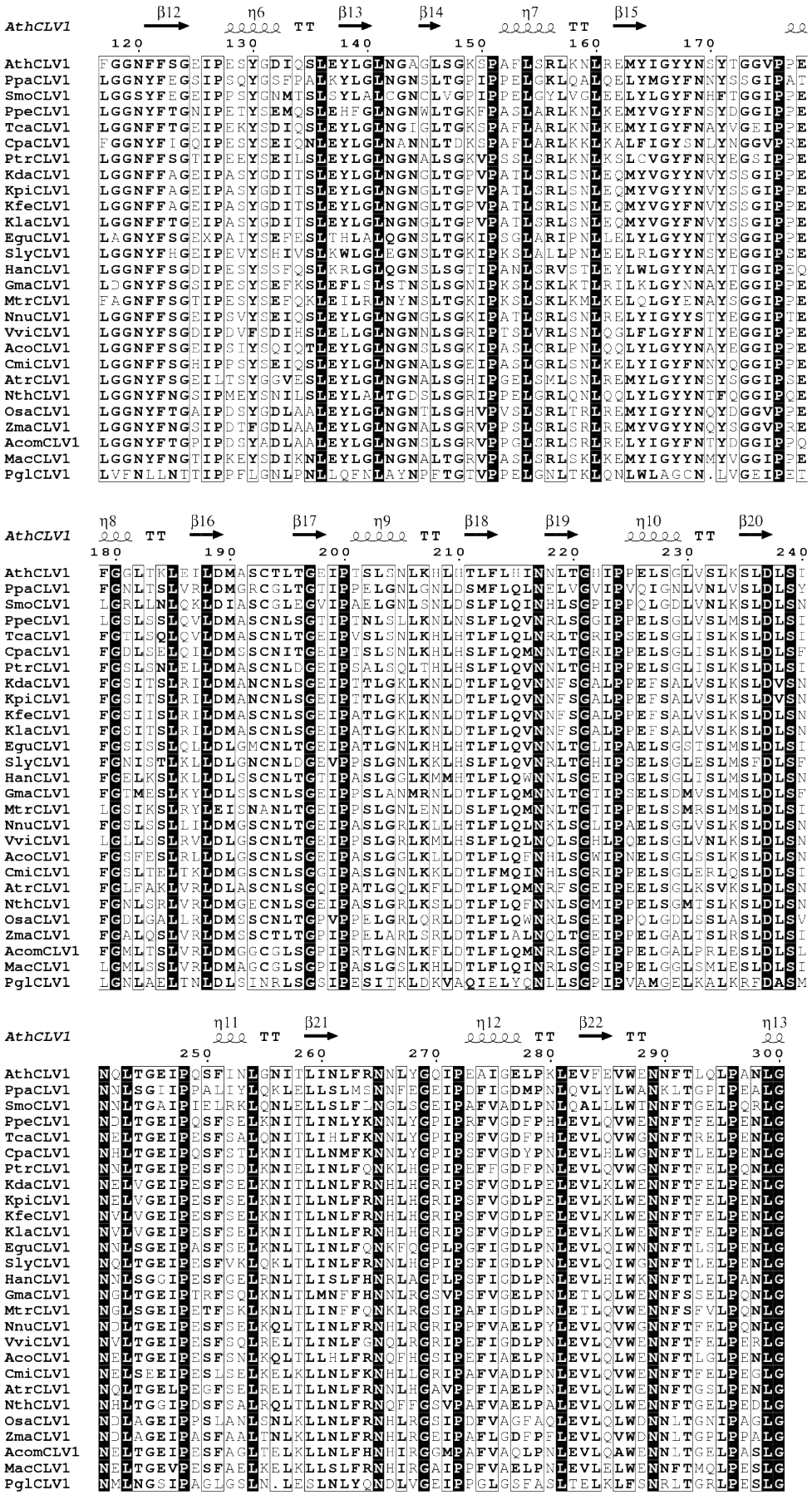
AthCLV1
β12 η6 TT β13 β14 η7 TT β15
120 130 140 150 160 170
AthCLV1 FGGNFFSGEIPESYGDIQSLEYLGLNGAGLSGKSPAFLSRLKNLRELMYIGYYNSYTGGVPPE
PpaCLV1 LGGNYFEGSIPSQYGSFPALKYLGLNGNSLTGPIPPELGKLQALQELYMGYFNNYSSGIPAT
SmoCLV1 LGGSYFEGEIPPSYGNMTSLSYLALCGNCLVGPIPPELGYLVGLEELYLGYFNHFTGGIPPE
PpeCLV1 LGGNYFTGNIPETYSEMQSLEHFGLNGNWLTGKFPASLARLKNLKEMYVGYFNSYDGGIPPE
TcaCLV1 LGGNFFTGEIPEKYSDIQSLEYLGLNGIGLTGKSPAFLARLKNLKEMYIGYFNAYVGEIPPE
CpaCLV1 FGGNYFIGQIPESYSEIQNLEYLGLNANNLTDKSPAFLARLKKLKALFIGYSNLYNGGVPRE
PtrCLV1 LGGNFFSGTIPEEYSEILSLEYLGLNGNALSGKVPSSLSRLKNLKSLCVGYFNRYEGSIPPE
KdaCLV1 LGGNFFAGEIPASYGDITSLEYLGLNGNGLTGPVPATLSRLSNLEQMYVGYYNVYSSGIPPE
KpiCLV1 LGGNFFAGEIPASYGDITSLEYLGLNGNGLTGPVPATLSRLSNLEQMYVGYYNVYSSGIPPE
KfeCLV1 LGGNFFAGEIPASYGDITSLEYLGLNGNGLTGPVPATLSRLSNLEQMYVGYFNVYSSGIPPE
KlaCLV1 LGGNFFTGEIPASYGDITSLEYLGLNGNGLTGPVPATLSRLSNLEQMYVGYFNVYSSGIPPE
EguCLV1 LAGNYFSGEXPAIYSEFESLTHLALQGNSLTGKIPSGLARIPNLLELYLGYYNTYSGGIPPE
SlyCLV1 LGGNYFHGEIPEVYSHIVSLKWLGLEGNSLTGKIPKSLALLPNLEELRLGYYNSYEGGIPSE
HanCLV1 LGGNFFSGDIPESYSSFQSLKRLGLQGNSLSGTIPANLSRVSTLEYLWLGYYNAYTGGIPEQ
GmaCLV1 LDGNYFSGSIPESYSEFKSLEFLSLSTNSLSGNIPKSLSKLKTLRILKLGYYNAYEGGIPPE
MtrCLV1 FAGNFFSGTIPESYSEFQKLEILRLNYNSLTGKIPKSLSKLKMLKELQLGYENAYSGGIPPE
NnuCLV1 LGGNFFSGEIPSVYSEIQSLEYLGLNGNGLSGKIPATLSRLSNLRELYIGYYSTYEGGIPTE
VviCLV1 LGGNYFSGDIPDVFSDIHSLELLGLNGNNLSGRIPTSLVRLSNLQGLFLGYFNIYEGGIPPE
AcoCLV1 LGGNFFSGEIPSIYSQIQTLEYLGLNGNSLSGKIPASLCRLPNLQQLYLGYYNAYEGGIPPE
CmiCLV1 LGGNFFSGHIPPSYSEIQSLEYLGLNGNALSGEIPASLGRLSNLKELYIGYFNNYQGGIPPE
AtrCLV1 LGGNYFSGEILTSYGGVESLEYLGLNGNALSGHIPGELSMLSNLREMYLGYYNSYSGGIPSE
NthCLV1 LGGNYFNGSIPMEYSNILSLEYLALTGDSLSGRIPPELGRLQNLQQLYLGYYNTFQGGIPQE
OsaCLV1 LGGNYFTGAIPDSYGDLAALEYLGLNGNTLSGHVPVSLSRLTRLREMYIGYYNQYDGGVPPE
ZmaCLV1 LGGNYFNGSIPDTFGDLAALEYLGLNGNALSGRVPPSLSRLSRLREMYVGYYNQYSGGVPREE
AcomCLV1 LGGNYFTGPIPDSYADLAALEYLGLNGNSLSGRVPPGLSRLSRLRELYIGYFNTYDGGIPPQ
MacCLV1 LGGNYFNGTIPKEYSDIKNLEYLGLNGNALTGRVPPASLSRLSKLKEMYIGYYNMYVGGIPPE
PglCLV1 LVFNLLNTTIPPFLGNLPNLLQFNLAYNPFTGTVPPELGNLTKLQNLWLAGCN.LVGEIPET
η8 TT β16 β17 η9 TT β18 β19 η10 TT β20
180 190 200 210 220 230 240
AthCLV1 FGGLTKLEILDMASCTLTGEIPTSLSNLKHLHTLFLHINNLTGHIPPELSGLVSLKSLDLSI
PpaCLV1 FGNLTSLVRLDMGRCGLTGTIPPELGNLGNLDSMFLQLNELVGVIPVQIGNLVNLVSLDLSY
SmoCLV1 LGRLLNLQKLDIASCGLEGVIPAELGNLSNLDSLFLQINHLSGPIPPQLGDLVNLKSLDLSN
PpeCLV1 LGSLSSLQVLDMASCNLSGTIPTNLSLLKNLNSLFLQVNRLSGGIPPELSGLVSLMSLDLSI
TcaCLV1 FGTLSQLQVLDMASCNLTGEIPVSLSNLKHLHTLFLQLNRLTGRIPSELSGLISLKSLDLSI
CpaCLV1 FGDLSELQILDMSSCNITGEIPTSLSNLKHLHSLFLQMNNLTGRIPPELSGLISLKSLDLSF
PtrCLV1 FGSLSNLELLDMASCNLDGEIPSALSQLTHLHSLFLQVNNLTGHIPPELSGLISLKSLDLSI
KdaCLV1 FGSITSLRILDMANCNLSGEIPTTLGKLKNLDTLFLQVNNFSGALPPEFSALVSLKSLDVSN
KpiCLV1 FGSITSLRILDMANCNLSGEIPTTLGKLKNLDTLFLQVNNFSGALPPEFSALVSLKSLDVSN
KfeCLV1 FGSIISLRILDMASCNLSGEIPATLGKLKNLDTLFLQVNNFSGALPPEFSALVSLKSLDLSN
KlaCLV1 FGSITSLRILDMASCNLSGEIPATLGKLKNLDTLFLQVNNFSGALPPEFSALVSLKSLDLSN
EguCLV1 FGSISSLQLLDLGMCNLTGEIPATLGNLKHLHTLFLQVNNLTGLIPAELSGSISLMSLDLSI
SlyCLV1 FGNISTLKLLDLGNCNLDGEVPPSLGNLKKLHSLFLQVNRLTGHIPSELSGLESLMSLDLSF
HanCLV1 FGELKSLKLLDLSSCNLTGTIPASLGGLKMMHTLFLQWNNLSGEIPGELSGLISLMSLDLSN
GmaCLV1 FGTMESLKYLDLSSCNLSGEIPPSLANMRNLDTLFLQMNNLTGTIPSELSDMVSLMSLDLSF
MtrCLV1 LGSIKSLRYLEISNANLTGEIPPSLGNLENLDSLFLQMNNLTGTIPPELSSMRSLMSLDLSI
NnuCLV1 FGSLSSLLILDMGSCNLTGEIPASLGRLKLLHTLFLQLNKLSGLIPAELSGLVSLKSLDLSN
VviCLV1 LGLLSSLRVLDLGSCNLTGEIPPSLGRLKMLHSLFLQLNQLSGHLPQELSGLVNLKSLDLSN
AcoCLV1 FGSFESLRLLDLGSCNLSGEIPASLGGLKLLDTLFLQFNHLSGWIPNELSGLSSLKSLDLSN
CmiCLV1 FGSLTELTKLDMGSCNLSGGIPASLGNLKKLDTLFMQINHLSGRIPPELSGLERLQSLDLSI
AtrCLV1 FGLFAKLVRLDLASCNLSGQIPATLGQLKFLDTLFLQMNRFSGEIPEELSGLKSVKSLDLSN
NthCLV1 FGNLSRLVRLDMGECNLSGEIPASLGRLKSLDTLFLQFNNLSGMIPPELSGMTSLKSLDLSN
OsaCLV1 FGDLGALLRLDMSSCNLTGPVPPELGRLQRLDTLFLQWNRLSGEIPPQLGDLSSLASLDLSV
ZmaCLV1 FGALQSLVRLDMSSCTLTGPIPPELARLSRLDTLFLALNQLTGEIPPELGALTSLRSLDLSI
AcomCLV1 FGMLTSLVRLDMGGCGLSGPIPRTLGNLKFLDTLFLQMNRLSGPIPPELGALPRLESLDLSL
MacCLV1 LGMLSSLVRLDMAGCGLSGPIPASLGSLKHLDTLFLQINRLSGSIPPELGGLSMLESLDLSI
PglCLV1 LGNLAELTNLDLSSINRLSGSIPESITKLDKVAQIELYQNLLSGPIPVAMGELKALKRFDASM
η11 TT β21 η12 TT β22 TT η13
250 260 270 280 290 300
AthCLV1 NQLTGEIPQSFINLGNITLINLFRNNLYGQIPEAIGELPKLEVFEVWENNFTLQLPANLG
PpaCLV1 NNLSGIIPPALIYLQKLELLSLMSNNFEGEIPDFIGDMPNLQVLYLWANKLTGPIPEALG
SmoCLV1 NNLTGAIPIELRKLQNLELLSLFLNGLSGEIPAFVADLPNLQALLLWINNFTGELPQRLG
PpeCLV1 NDLTGEIPQSFSELKNITLINLYKNNLYGPIPRFVGDFPHLEVLQVWENNFTFELPENLG
TcaCLV1 NELTGEIPESFSALQNITLIHLFKNNLYGPIPSFVGDFPHLEVLQVWGNNFTRELPENLG
CpaCLV1 NHLTGEIPQSFSTLKNITLLNMFKNNLYGPIPSFVGDYPNLEVLHLWGNNFTLELPENLG
PtrCLV1 NNLTGEIPESFSDLKNIELINLFQNKLHGPIPEFFGDFPNLEVLQVWGNNFTFELPQNLG
KdaCLV1 NELVGEIPESFSELKNITLLNLFRNNHLHGRIPSFVGDLPELEVLKLWENNFTFELPENLG
KpiCLV1 NELVGEIPESFSELKNITLLNLFRNNHLHGRIPSFVGDLPELEVLKLWENNFTFELPENLG
KfeCLV1 NVLVGEIPESFSELKNITLLNLFRNNHLHGRIPSFVGDLPELEVLKLWENNFTFELPENLG
KlaCLV1 NVLVGEIPESFSELKNITLLNLFRNNHLHGRIPSFVGDLPELEVLKLWENNFTFELPENLG
EguCLV1 NNLSGEIPASFSELKNLTLINLFQNKFQGPLPGFIGDLPNLEVLQIWNNNFTLSLPENLG
SlyCLV1 NQLTGEIPESFVKLQKLTLINLFRNNLHGPIPSFIGDLPNLEVLQIWGNNFTLELPENLG
HanCLV1 NNLSGGIPESFGELRNLTLISLFHNRLAGPLPSFIGDLPNLEVLHIWKNNFTLELPANLG
GmaCLV1 NGLTGEIPTRFSQLKNLTLMNFFHNNLRGSVPSFVGELPNLETLQLWENNFSSELPQNLG
MtrCLV1 NGLSGEIPETFSKLKNLTLINFFQNKLRGSIPAFIGDLPNLETLQVWENNFSFVLPQNLG
NnuCLV1 NDLTGEIPESFSELKQLTLINLFRNNHLRGRIPPFVAELPYLEVLQVWGNNFTFELPQNLG
VviCLV1 NVLTGEIPESFSQLRELTLINLFGNQLRGRIPEFIGDLPNLEVLQVWENNFTFELPERNLG
AcoCLV1 NELTGEIPESFSNLKQLTLLHLFRNQFHGSIPEFIAELPNLEVLQLWENNFTLGLPENLG
CmiCLV1 NELSEEIPESLSELKELKLLNLFKNHLLGRIPAFVADLPNLEVLQVWENNFTFELPEGLG
AtrCLV1 NQLTGELPEGFSELRELTLLNLFRNNLHGAVPPFIAELPNLEVLQLWENNFTGSLPENLG
NthCLV1 NHLTGGIPDSFSALRQLTLLNLFRNQFFGSVPAFVAELPALEVLQLWENNFTGELPEDLG
OsaCLV1 NDLAGEIPPSLANLSNLKLLNLFRNNHLRGSIPDFVAGFAQLEVLQLWDNNLTGNIPAGLG
ZmaCLV1 NDLAGEIPASFAALTNLKLLNLFRNNHLRGEIPAFLGDFPFLEVLQVWDNNLTGPLPPALG
AcomCLV1 NELTGEIPESFAGLTELKLLNLFHNNHIRGGMPAFVAQLPNLEVLQAWENNLTGELPASLG
MacCLV1 NELTGEVPESFAELKELKLLSLFRNNHIRGAIPPFVAELPNLEVLELWENNFTMQLPESLG
PglCLV1 NMLNGSIPAGLGSLN.LESLNLYQNDLVGEIPPGLGSFASLTELKLFSNRLTGRLPESLG

C

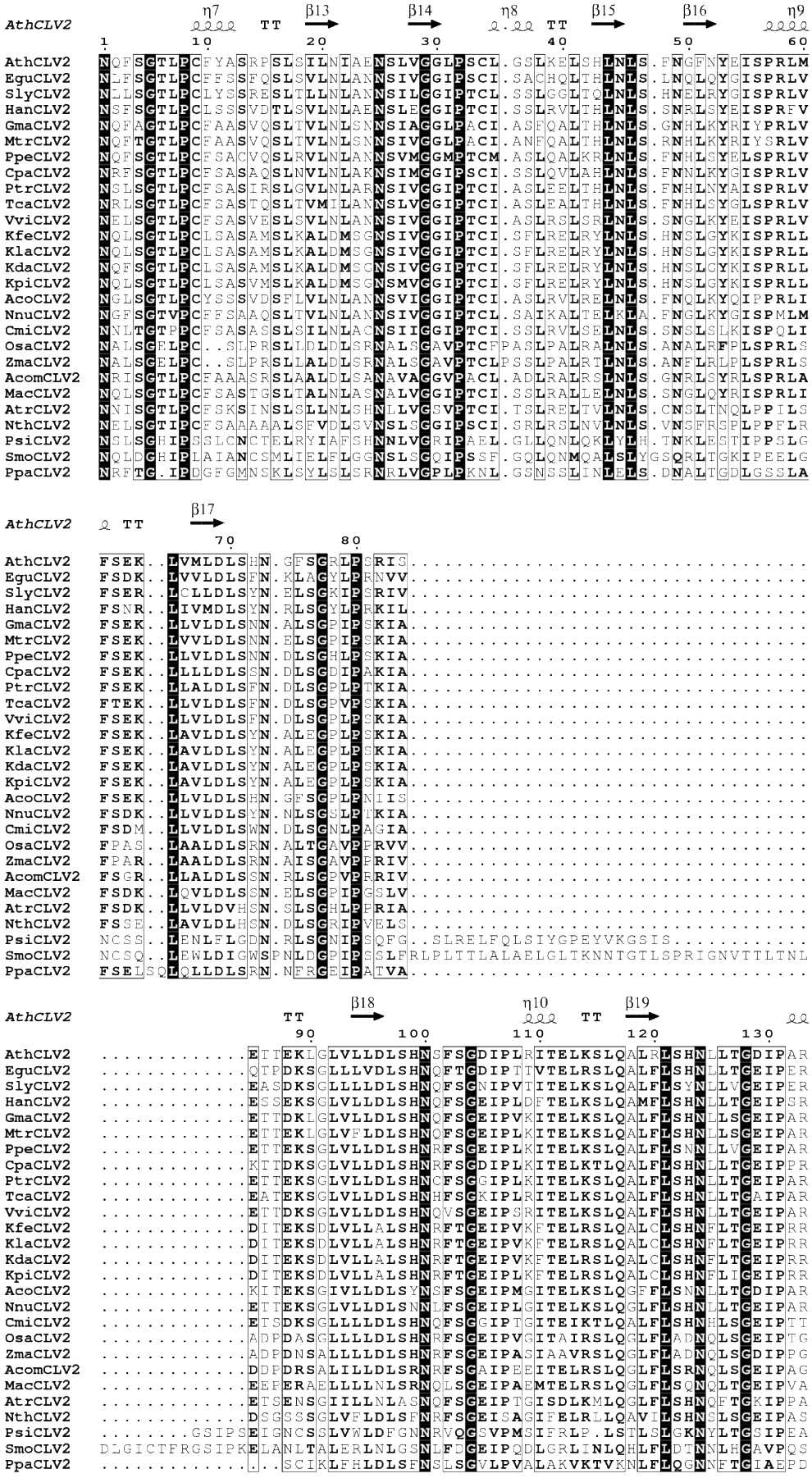
AthCLV2
η7 TT β13 β14 η8 TT β15 β16 η9
1 10 20 30 40 50 60
AthCLV2 NQFSGTLPCFYASRPSLSILNIAENSLVGGLPSCL.GSLKELSHLNLS.FNGFNYEISPRLM
EguCLV2 NLFSGTLPCFFSSFQSLSVLNLANNSIVGGIPSCI.SACHQLTHLNLS.LNQLQYGISPRLV
SlyCLV2 NLLSGTLPCLYSSRESLTLLNLANNSILGGIPTCL.SSLGGLTQLNLS.HNELRYGISPRLV
HanCLV2 NSFSGTLPCLSSSVDTLSVLNLAENSLEGGIPTCI.SSLRVLTHLNLS.SNRLSYEISPRFV
GmaCLV2 NQFAGTLPCFAASVQSLTVLNLSNNSIAGGLPACI.ASFQALTHLNLS.GNHLKYRIYPRLV
MtrCLV2 NQFTGTLPCFAASVQSLTVLNLSNNSIVGGLPACI.ANFQALTHLNLS.RNHLKYRIYSRLV
PpeCLV2 NQFSGTLPCFSACVQSLRVLNLANNSVMGGMPTCM.ASLQALKRLNLS.FNHLSYELSPRLV
CpaCLV2 NRFSGTLPCFSASAQSLNVLNLAKNSIMGGIPSCI.SSLQVLAHLNLS.FNNLKYGISPRLV
PtrCLV2 NSLSGTLPCFSASIRSLGVLNLARNSIVGGIPTCI.ASLEELTHLNLS.FNHLNYAISPRLV
TcaCLV2 NRLSGTLPCFSASTQSLTVMILANNSLVGGIPTCI.ASLEALTHLNLS.FNHLSYGLSPRLV
VviCLV2 NELSGTLPCFSASVESLSVLNLANNSIVGGIPTCI.ASLRSLSRLNLS.SNGLKYEISPRLV
KfeCLV2 NQLSGTLPCLSASAMSLKALDMSGNSIVGGIPTCI.SFLRELRYLNLS.HNSLGYKISPRLL
KlaCLV2 NQLSGTLPCLSASAMSLKALDMSGNSIVGGIPTCI.SFLRELRYLNLS.HNSLGYKISPRLL
KdaCLV2 NQFSGTLPCLSASAMSLKALDMSGNSIVGGIPTCI.SFLRELRYLNLS.HNSLGYKISPRLL
KpiCLV2 NQLSGTLPCLSASVMSLKALDMSGNSMVGGIPTCI.SFLRELRYLNLS.HNSLGYKISPRLL
AcoCLV2 NGLSGTLPCYSSSVDSFLVLNLANNSVIGGIPTCI.ASLRVLRELNLS.FNQLKYQIPPRLI
NnuCLV2 NGFSGTVPCFFSAAQSLTVLNLANNSIVGGIPTCL.SAIKALTELKLA.FNGLKYGISPMLM
CmiCLV2 NNLTGTPPCFSASASSLSILNLAGNSIIGGIPTCI.SSLRVLSELNLS.SNSLSLKISPQLI
OsaCLV2 NALSGRLPC..SLPRSLLDLDLSRNALSGAVPTCFPASLPALRALNLS.ANALRFPLSPRLS
ZmaCLV2 NALSGELPC..SLPRSLLALDLSRNALSGAVPTCLPSSLPALRTLNLS.ANFLRLPLSPRLS
AcomCLV2 NRISGTLPCFAAASRSLAALDLSANAVAGGVPACL.ADLRALRSLNLS.GNRLSYRLSPRLA
MacCLV2 NQLSGTLPCFSASTGSLTALNLASNALVGGIPTCI.SSLRALLELNLS.SNGLQYRISPRLI
AtrCLV2 NNISGTLPCFSKSINSLSLLNLSHNLLVGSVPTCI.TSLRELTVLNLS.CNSLTNQLPPILS
NthCLV2 NELSGTIPCFSAAAAALSFVDLSVNSLSGGIPSCI.SRLRSLNVLNLS.VNSFRSPLPPFLR
PsiCLV2 NSLSGHIPSSLCNCTELRYIAFSHNNLVGRIPAEL.GLLQNLQKLYLH.TNKLESTIPPSLG
SmoCLV2 NQLDGHIPLAIANCSMLIELFLGGNSLSGQIPSSF.GQLQNMQALSLYGSQRLTGKIPEELG
PpaCLV2 NRFTG.IPDGFGMNSKLSYLSLSRNRLVGPLPKNL.GSNSSLINLELS.DNALTGDLGSSLA

AthCLV2 β17
70 80
AthCLV2 FSEK..LVMLDLSHN.GFSGRLPSRIS.....
EguCLV2 FSDK..LVVLDLSFN.KLAGYLPRNVV.....
SlyCLV2 FSER..LCLLDLSYN.ELSGKIPSRIV.....
HanCLV2 FSNR..LIVMDLSYN.RLSGYLPRKIL.....
GmaCLV2 FSEK..LLVLDLSNN.ALSGPIPSKIA.....
MtrCLV2 FSEK..LVVLDLSNN.ELSGPIPSKIA.....
PpeCLV2 FSEK..LLVLDLSNN.DLSGHLPSKIA.....
CpaCLV2 FSEK..LLLLDLSSN.DLSGDIPAKIA.....
PtrCLV2 FSEK..LLALDLSFN.DLSGPLPTKIA.....
TcaCLV2 FTEK..LLVLDLSFN.DLSGPVPSKIA.....
VviCLV2 FSEK..LLVLDLSFN.DLSGPLPSKIA.....
KfeCLV2 FSEK..LLAVLDLSYN.ALEGPLPSKIA.....
KlaCLV2 FSEK..LLAVLDLSYN.ALEGPLPSKIA.....
KdaCLV2 FSEK..LLAVLDLSYN.ALEGPLPSKIA.....
KpiCLV2 FSEK..LLAVLDLSYN.ALEGPLPSKIA.....
AcoCLV2 FSEK..LLVLDLSHN.GFSGPLPNIIS.....
NnuCLV2 FSDK..LLVLDLSYN.NLSGSLPTKIA.....
CmiCLV2 FSDM..LLVLDLSWN.DLSGNLPAGIA.....
OsaCLV2 FPAS..LAALDLSRN.ALTGAVPPRVV.....
ZmaCLV2 FPAR..LAALDLSRN.AISGAVPPRIV.....
AcomCLV2 FSGR..LLALDLSSN.RLSGPVPRRIV.....
MacCLV2 FSDK..LQVLDLSSN.ELSGPIPGSLV.....
AtrCLV2 FSDK..LLVLDVHSN.SLSGHLPPRIA.....
NthCLV2 FSSE..LAVLDLHSN.DLSGRIPVELS.....
PsiCLV2 NCSS..LENLFLGDN.RLSGNIPSQFG..SLRELFQLSIYGPEYVKGSIS.....
SmoCLV2 NCSQ..LEWLDIGWSPNLDGPIPSSLFRLPLTTLALAELGLTKNNTGTLSPRIGNVTTLTNL
PppaCLV2 FSELSQLQLLDLSRN.NFRGEIPATVA.....

AthCLV2 TT β18 η10 TT β19
90 100 110 120 130
AthCLV2 .....ETTEKLGLVLLDLSHNSFSGDIPLRITELKSLQALRLSHNLLTGDIPAR
EguCLV2 .....QTPDKSGLLLVDLSHNQFTGDIPTTVTELRSLQALFLSHNLLTGEIPER
SlyCLV2 .....EASDKSGLLLLDLSHNQFSGNIPVTITELKSLQALFLSYNLLVGEIPER
HanCLV2 .....ESSEKSGLVLLDLSHNQFSGEIPLDFTELKSLQAMFLSHNLLTGEIPSR
GmaCLV2 .....ETTDKLGLVLLDLSHNQFSGEIPVKITELKSLQALFLSHNLLSGEIPAR
MtrCLV2 .....ETTEKLGLVFLDLSHNQFSGEIPLKITELKSLQALFLSHNLLSGEIPAR
PpeCLV2 .....ETTEKSGLVLLDLSHNRFSGEIPLKITELKSLQALFLSNNLLVGEIPAR
CpaCLV2 .....KTTDKSGLVLLDLSHNRFSGDIPLKITELKTLQALFLSHNLLTGEIPPR
PtrCLV2 .....ETTEKSGLVLLDLSHNCFSGGIPLKITELKSLQALFLSHNLLTGEIPAR
TcaCLV2 .....EATEKSGLVLLDLSHNHFSGKIPLRITELKSLQALFLSHNLLTGAIPAR
VviCLV2 .....ETTDKSGLVLLDLSHNQVSGEIPSRITELKSLQALFLSHNLLTGEIPAR
KfeCLV2 .....DITEKSDLVLLALSHNRFTGEIPVKFTELRSLQALCLSHNFLTGEIPRR
KlaCLV2 .....DITEKSDLVLLALSHNRFTGEIPVKFTELRSLQALCLSHNFLTGEIPRR
KdaCLV2 .....DITEKSDLVLLALSHNRFTGEIPVKFTELRSLQALCLSHNFLTGEIPRR
KpiCLV2 .....DITEKSDLVLLALSHNRFTGEIPLKFTELRSLQALCLSHNFLIGEIPRR
AcoCLV2 .....KITEKSGIVLLDLSYNSFSGEIPMGITELKSLQGFFLSNNLLTGDIPAR
NnuCLV2 .....ETTEKSGLVLLDLSNNLFSGEIPLGITELKSLQGLFLSHNLLTGEIPAR
CmiCLV2 .....ETSDKSGLLLLDLSHNQFSGGIPTGITEIKTLQALFLSHNHLSGEIPTT
OsaCLV2 .....ADPDASGLLLLDLSHNRFSGEIPVGITAIRSLQGLFLADNQLSGEIPTG
ZmaCLV2 .....ADPDNSALLLLDLSHNRFSGEIPASIAAVRSLQGLFLADNQLSGDIPPG
AcomCLV2 .....DDPDRSALILLDLSRNRFSGAIPEEITELRSLQGLFLSRNQLSGEIPAG
MacCLV2 .....EEPERAELLLLNLSRNQLSGEIPAEMTELRSLQGLFLSQNQLTGEIPVA
AtrCLV2 .....ETSENSGIILLNLASNQFSGEIPTGISDLKMLQGLFLSHNQFTGKIPPA
NthCLV2 .....DSGSSSGLVFLDLSFNRFSGEISAGIFELRLLQAVILSHNSLSGEIPAS
PsiCLV2 .....GSIPSEIGNCSSLVWLDFGNNRVQGSVPMSIFRLP.LSTLSLGKNYLTGSIPEA
SmoCLV2 DLGICTFRGSIPKELANLTALERLNLGSNLFDGEIPQDLGRLINLQHLFLDTNNLHGAVPQS
PppaCLV2 .....SCIKLFHLDLSFNSLSGVLPVALAKVKTVKNLFLQGNNFTGIAEPD

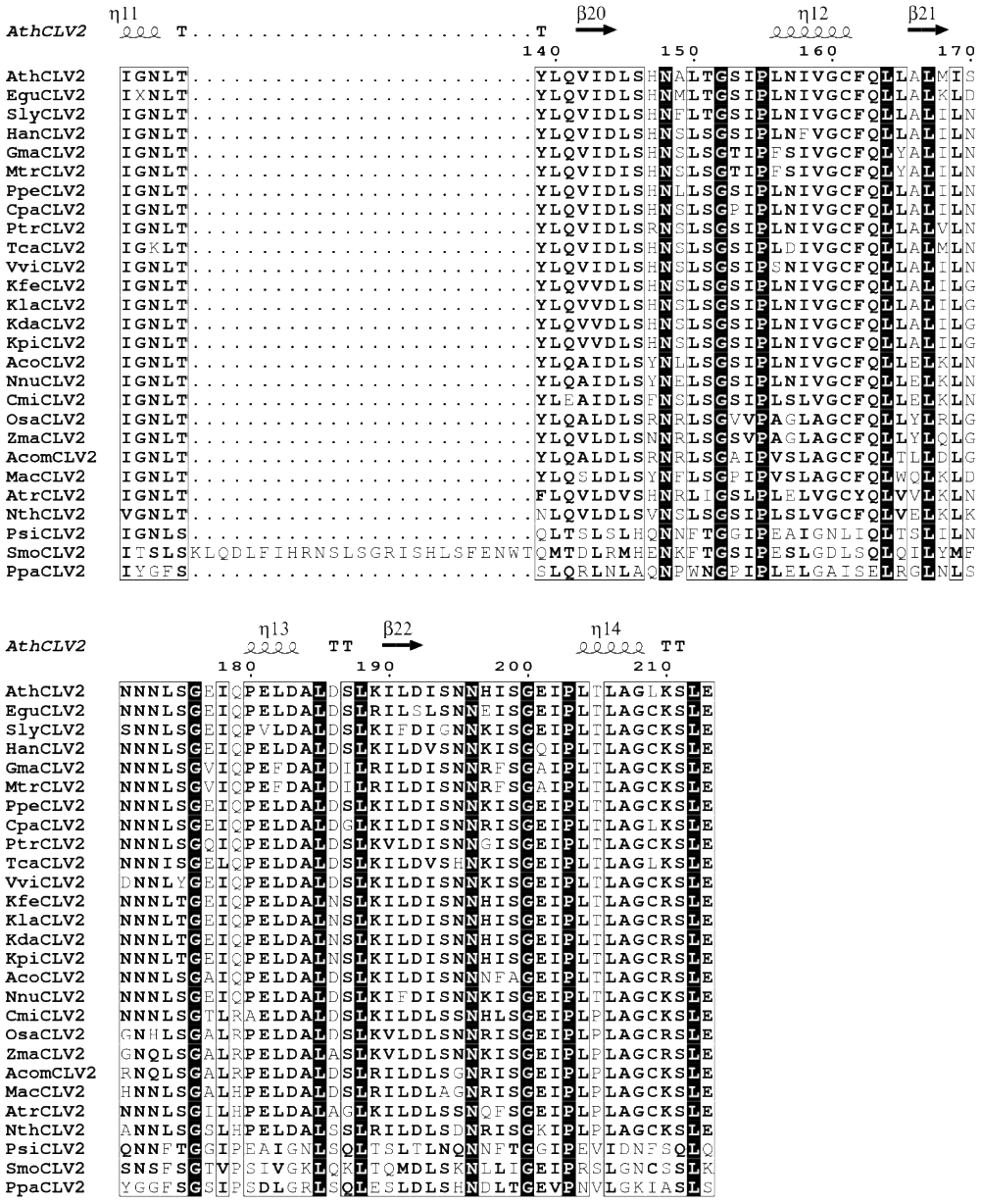

Figure 3.1 Multiple sequence alignment and secondary structure of trimmed WUS, CLV1 and CLV2 proteins from four *Kalanchoë* species and other angiosperm species.

(A) WUSCHEL (WUS) protein sequences of 62 residues; (B) CLAVATA1 (CLV1) protein sequences of about 300 residues and (C) CLV2 protein sequences of about 213 residues were isolated and aligned. Annotation of secondary structure is based on known structural information of the corresponding *Arabidopsis thaliana* protein. Number across the top indicates amino acid position; Bold text with black frame indicates residues with SimilarityGlobalScore > 0.7; Normal text indicates residues identity not conserved; White text with black background indicates residues strictly conserved in the column; Grey star indicates residues with alternate conformations; Digits at the bottom indicates disulphide bridges.

A

	KdaWus	*KpiWus*	*KfeWus*	*KlaWus*
KdaWus	100			
KpiWus	100	100		
KfeWus	100	100	100	
KlaWus	100	100	100	100

B

	KdaWUS	KpiWUS	KfeWUS	KlaWUS
KdaWUS	100			
KpiWUS	100	100		
KfeWUS	100	100	100	
KlaWUS	100	100	100	100

C

	KdaClv1	*KpiClv1*	*KfeClv1*	*KlaClv1*
KdaClv1	100			
KpiClv1	100	100		
KfeClv1	98.66	98.66	100	
KlaClv1	98.55	98.55	99.66	100

D

	KdaCLV1	KpiCLV1	KfeCLV1	KlaCLV1
KdaCLV1	100			
KpiCLV1	100	100		
KfeCLV1	97	97	100	
KlaCLV1	97	97	99.33	100

E

	KdaClv2	*KpiClv2*	*KfeClv2*	*KlaClv2*
KdaClv2	100			
KpiClv2	95.77	100		
KfeClv2	96.4	97.49	100	
KlaClv2	96.55	97.49	99.37	100

F

	KdaCLV2	KpiCLV2	KfeCLV2	KlaCLV2
KdaCLV2	100			
KpiCLV2	97.65	100		
KfeCLV2	99.53	98.12	100	
KlaCLV2	99.53	98.12	100	100

Figure 3.2 Percentage identity of isolated and trimmed *Kalanchoë* WUS, CLV1 and CLV2 sequences.
(A, C, E) Nucleotide and (B, D, F) amino acid sequences of WUS; CLV1 and CLV2 respectively. All values are expressed in percentages. Kda, *K. daigremontiana*; Kpi, *K. pinnata; Kfe, K. fedtschenkoi*; Kla, *K. laxiflora*.

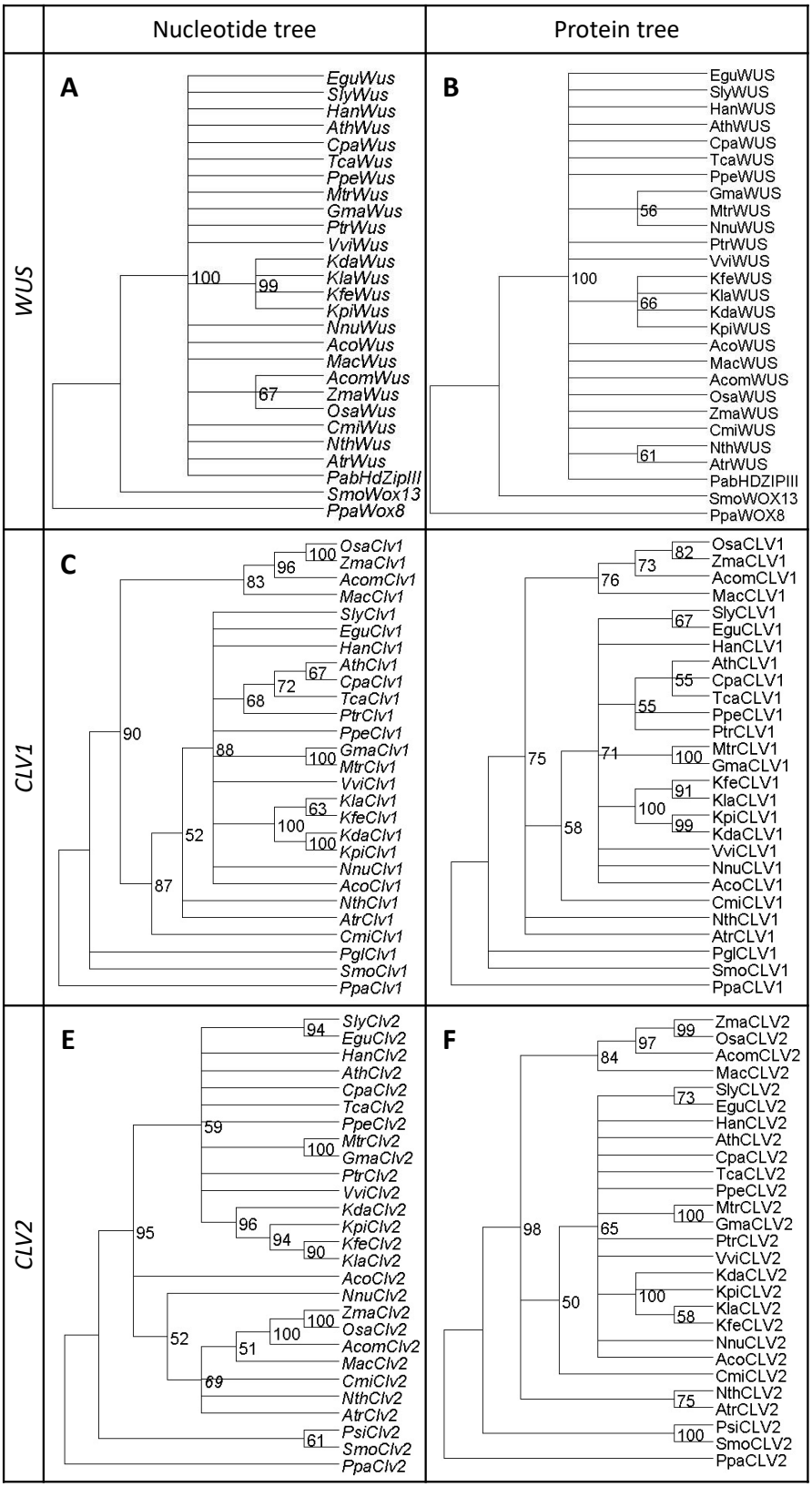
Nucleotide tree
Protein tree
WUS
CLV1
CLV2
A
EguWus
SlyWus
HanWus
AthWus
CpaWus
TcaWus
PpeWus
MtrWus
GmaWus
PtrWus
VviWus
KdaWus
KlaWus
KfeWus
KpiWus
NnuWus
AcoWus
MacWus
AcomWus
ZmaWus
OsaWus
CmiWus
NthWus
AtrWus
PabHdZipIII
SmoWox13
PpaWox8
B
EguWUS
SlyWUS
HanWUS
AthWUS
CpaWUS
TcaWUS
PpeWUS
GmaWUS
MtrWUS
NnuWUS
PtrWUS
VviWUS
KfeWUS
KlaWUS
KdaWUS
KpiWUS
AcoWUS
MacWUS
AcomWUS
OsaWUS
ZmaWUS
CmiWUS
NthWUS
AtrWUS
PabHDZIPIII
SmoWOX13
PpaWOX8
C
OsaClv1
ZmaClv1
AcomClv1
MacClv1
SlyClv1
EguClv1
HanClv1
AthClv1
CpaClv1
TcaClv1
PtrClv1
PpeClv1
GmaClv1
MtrClv1
VviClv1
KlaClv1
KfeClv1
KdaClv1
KpiClv1
NnuClv1
AcoClv1
NthClv1
AtrClv1
CmiClv1
PglClv1
SmoClv1
PpaClv1
OsaCLV1
ZmaCLV1
AcomCLV1
MacCLV1
SlyCLV1
EguCLV1
HanCLV1
AthCLV1
CpaCLV1
TcaCLV1
PpeCLV1
PtrCLV1
MtrCLV1
GmaCLV1
KfeCLV1
KlaCLV1
KpiCLV1
KdaCLV1
VviCLV1
NnuCLV1
AcoCLV1
CmiCLV1
NthCLV1
AtrCLV1
PglCLV1
SmoCLV1
PpaCLV1
E
SlyClv2
EguClv2
HanClv2
AthClv2
CpaClv2
TcaClv2
PpeClv2
MtrClv2
GmaClv2
PtrClv2
VviClv2
KdaClv2
KpiClv2
KfeClv2
KlaClv2
AcoClv2
NnuClv2
ZmaClv2
OsaClv2
AcomClv2
MacClv2
CmiClv2
NthClv2
AtrClv2
PsiClv2
SmoClv2
PpaClv2
F
ZmaCLV2
OsaCLV2
AcomCLV2
MacCLV2
SlyCLV2
EguCLV2
HanCLV2
AthCLV2
CpaCLV2
TcaCLV2
PpeCLV2
MtrCLV2
GmaCLV2
PtrCLV2
VviCLV2
KdaCLV2
KpiCLV2
KlaCLV2
KfeCLV2
NnuCLV2
AcoCLV2
CmiCLV2
NthCLV2
AtrCLV2
PsiCLV2
SmoCLV2
PpaCLV2

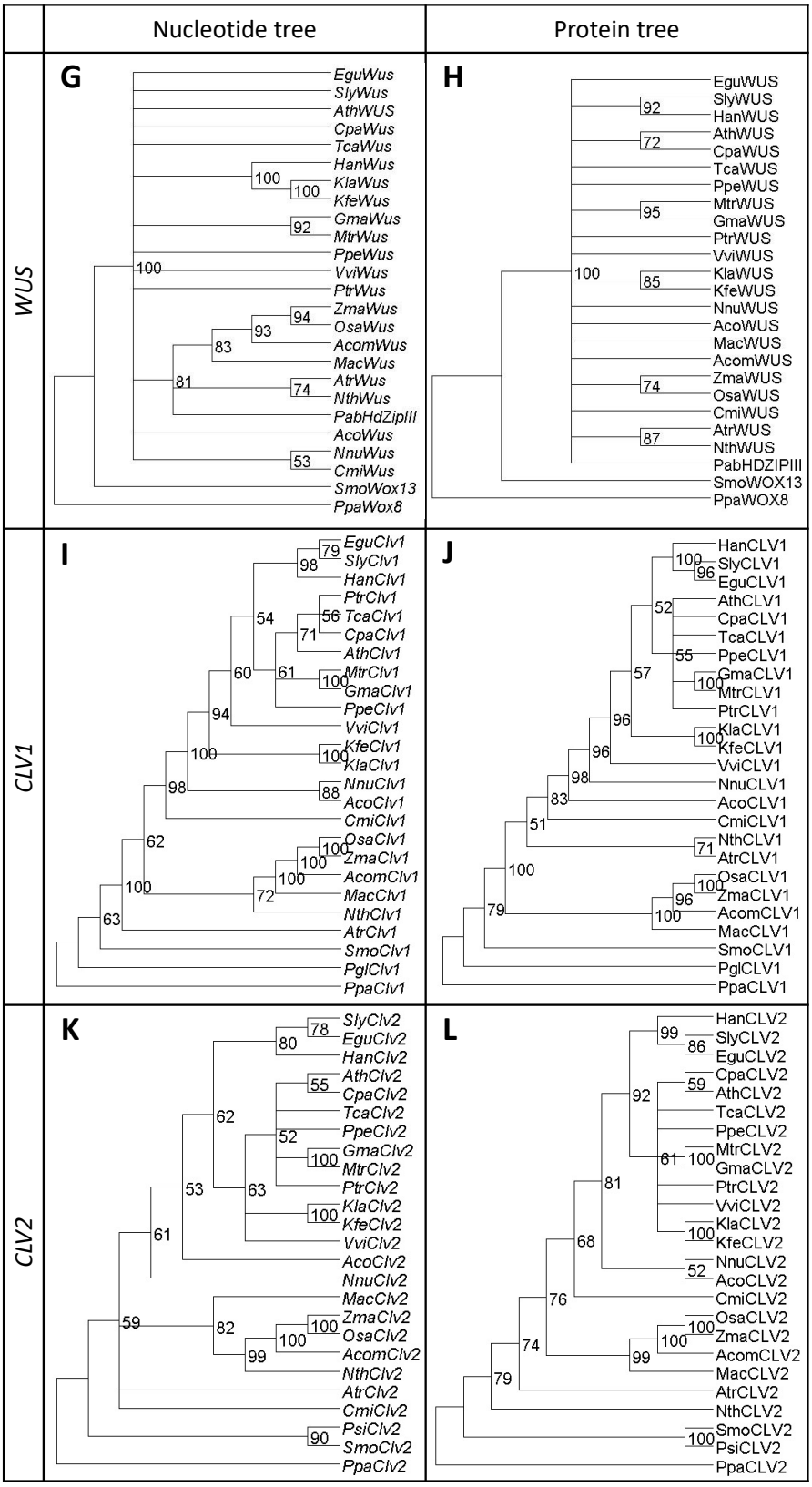

Figure 3.3 Phylogeny of WUSCHEL (WUS), CLAVATA1 (CLV1), CLV2 sequences from different angiosperm and lower plant species.

(A, C, E, G, I, K) Nucleotide trees and (B, D, F, H, J, L) protein trees constructed using maximum-likelihood estimate model with 0.03 bootstopping cutoff value. Trimmed sequences were used for (A-F); full length sequences were used for (G-L). Only phylogenetic trees (A-F) include isolated sequences from *K. daigremontiana* and *K. pinnata*. Bootstrap values are annotated on edges of the trees. Edges with bootstrap value lower than 50 was collapsed.

3.4.2. *KdWUS*, *KdCLV1* and *KdCLV2* are expressed during plantlet development

KdWUS, *KdCLV1* and *KdCLV2* expression were examined to determine whether activity of these genes is present during plantlet initiation and development. Immunolocalisation analysis showed that KdWUS expression was absent at the plantlet primordia, prior to formation of pedestal (Fig. 3.4A). At transitioning from globular-stage to heart-stage, KdWUS expression was detected at the cotyledon primordia (Fig. 3.4B). Later, KdWUS expression was exhibited in a distinctive pattern only at the top-half of the inner cotyledon primordium and the whole outer cotyledon primordium of heart-stage plantlet (Fig. 3.4C). This was in stark contrast compared to the negative sample lacking the primary antibody treatment as KdWUS was completely absent (Fig. 3.4F). As the cotyledons grew bigger, KdWUS expression became stronger across the whole plantlet but began to gradually recede towards basal half of the plantlet (Fig. 3.4D). As the plantlet cotyledons emerged and matured, judging from the presence of the SAM, KdWUS expression diminished (Fig. 3.4E). High KdWUS expression at heart-stage plantlets (Fig. 3.4C, D) correlated with the high *KdWUS* transcripts at plantlet stage S2 from RNA-sequencing analysis (Fig. 3.4G). However, low KdWUS expression as shown from immunolocalization (Fig. 3.4A) at plantlet stage S1 and S4 was not consistent with high *KdWUS* transcript expression from RNA-sequencing analysis (Fig. 3.4G). Nonetheless, *KdWUS* transcript expression was not significantly different across plantlet developmental stages. RNA-sequencing analysis showed that changes in *KdCLV2* transcript expression across plantlet developmental stages was also insignificant, but its expression level compared to *KdWUS* was more consistent across these stages (Fig. 3.4H). *KdCLV2* exppression was also relatively higher than *KdWUS* (Fig. 3.4G, H). Based on RNA-sequencing analyses, *KdCLV1* expression was the highest relative to *KdWUS* and *KdCLV2* (Fig. 3.4G-I). RNA-sequencing analysis showed that *KdCLV1* increased steadily across plantlet developmental stages Ctrl to S3 (Fig. 3.4I), and the same expression pattern was reflected by quantitative real-time PCR showing gradual increase of *KdCLV1* from Ctrl to S2 (Fig. 3.4J). However, the difference in *KdCLV1* expression from Ctrl to S3, based on RNA-sequencing analysis, was significantly different ($P \leq 0.05$), whereas changes in *KdCLV1* expression measured by real-time quantitative PCR was insignificant across plantlet developmental stages compared to the SAM. Nonetheless, these data showed that *KdWUS*, *KdCLV1* and *KdCLV2* were expressed during plantlet formation and development.

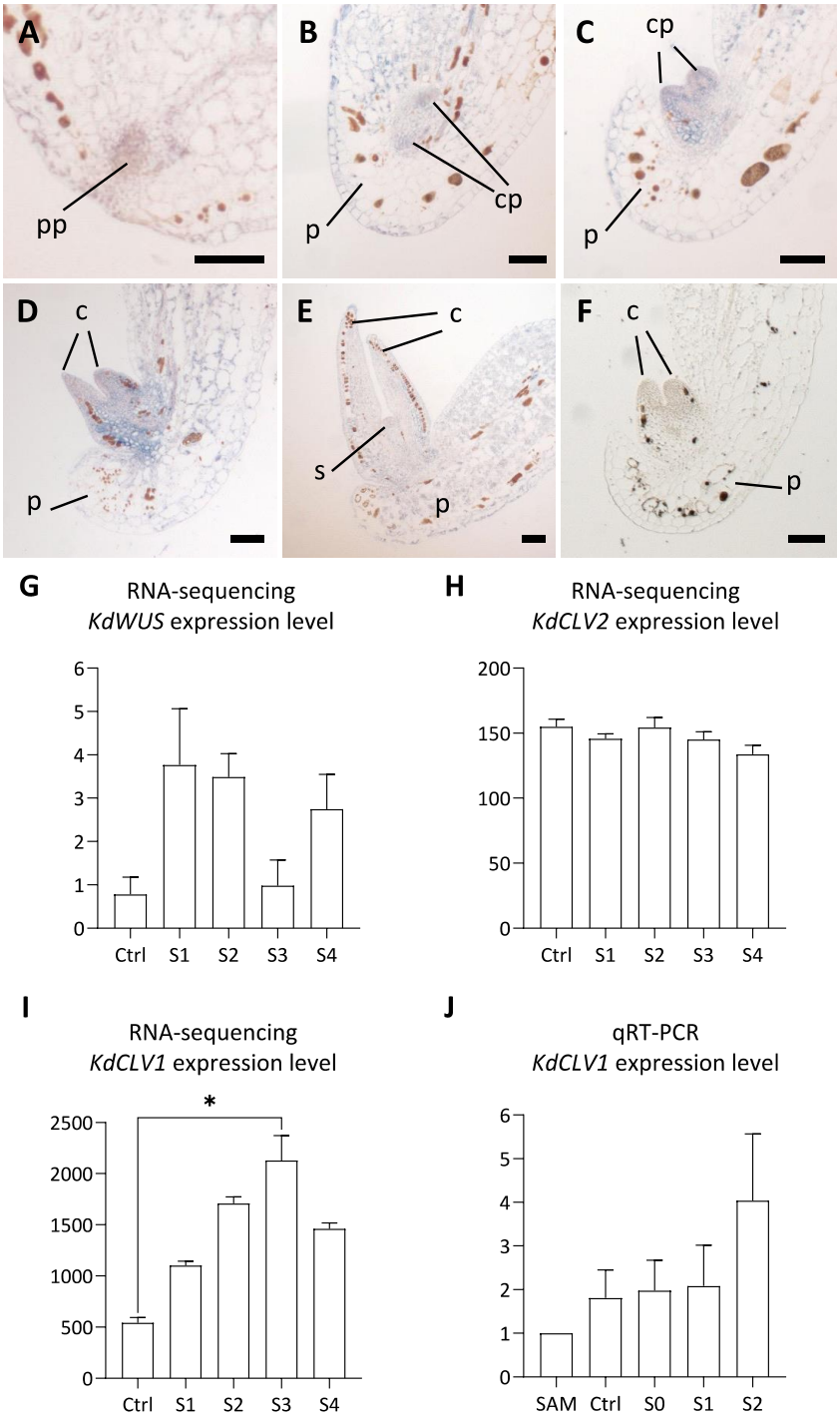

Figure 3.4 Expression analyses of *WUS*, *CLV1* and *CLV2* during *K. daigremontiana* plantlet development. Immunolocalisation (A-F) showing KdWUSCHEL (KdWUS) expression not visible at (A) plantlet primordia prior to pedestal formation. Strong KdWUS expression was present at (B) plantlet transitioning from globular to heart-stage; (C) heart-stage plantlet; (D) more mature heart-stage plantlet. (E) *KdWUS* expression was absent from developing plantlet showing distinguishable shoot apical meristem. c, cotyledon; cp, cotyledon primordia; p, pedestal; pp, plantlet primordium; s, shoot apical meristem. (F) Negative control of immunolocalisation showing a heart-stage plantlet without primary antibody treatment. (G-I) Normalised expression levels of *KdWUS*, *KdCLAVATA1* (*KdaCLV1*) and *KdCLV2* obtained from RNA-sequencing analysis of transcript expression of margin of 1-2 cm leaves (Ctrl) and plantlet stages S1-S4. Kruskal Wallis test with Dunn's multiple comparison test indicate statistical significance, *P≤0.05. (J) Quantitative real-time PCR (qRT-PCR) data showing expression level of *KdCLV1* in the shoot-apical meristem (SAM), margin of 1-2 cm leaves (Ctrl) and plantlet stages S0 to S2. All error bars represent standard error.

3.4.3. Slight reduction in *KdWUS* and *KdCLV1* expression contributed to abnormal phenotypes

To examine whether other organogenesis genes apart from *STM* participates in plantlet formation (Garcês et al., 2007), we generated antisense plants with reduced expression of *KdWUS*, *KdCLV1* and *KdCLV2.* Genotyping analyses showed that transformation of constructs into *K. daigremontiana* were successful (Fig. 3.5A-F). This was verified through successful amplification of a section of the antisense constructs (Fig. 3.5A, C, E) and the *NEOMYCIN PHOSPHOTRANSFERASE II* (*NPTII*) gene in the plasmid containing the antisense constructs (Fig. 3.5B, D, F). From the four *KdWUS* antisense lines that were genotyped successfully, only three independent lines that showed abnormal phenotypes compared to wild-type were selected for semi-quantitative expression analysis (Fig 3.5G).

Semi-quantitative expression analysis of *KdWUS* antisense lines showed that only line H exhibited a very slight reduction in *KdWUS* expression, whereas line C and J had *KdWUS* expression similar to that of wild-type (Fig 3.5G). In addition, line J showed reduced expression of *KdYUC1* whilst line C and H seemed to have a higher *KdYUC1* expression compared to wild-type (Fig 3.5G). The expression of other genes *KdCLV1*, *KdCLV2*, *KdSTM*, *KdLEC1* and *Kalanchoë daigremontiana TOPLESS* (*KdTPL*) in *KdWUS* antisense lines were similar to wild-type (Fig 3.5G). In the case of *KdCLV1* antisense plants, *KdCLV1* expression was lower in all lines compared to wild-type but lines F and K had lower *KdCLV1* expression compared to line E and G (Fig 3.5H). The expression of *KdYUC1* was also affected in *KdCLV1* antisense lines, showing reduced *KdYUC1* expression in lines F and G compared to wild-type (Fig. 3.5H). Moreover, *KdSTM*, *KdLEC1*, *KdWUS* and *KdCLV2* expression were also reduced in all four *KdCLV1* antisense lines (Fig. 3.5H). The expression of *KdTPL* remained similar in the *KdCLV1* antisense lines compared to wild-type (Fig. 3.5H).

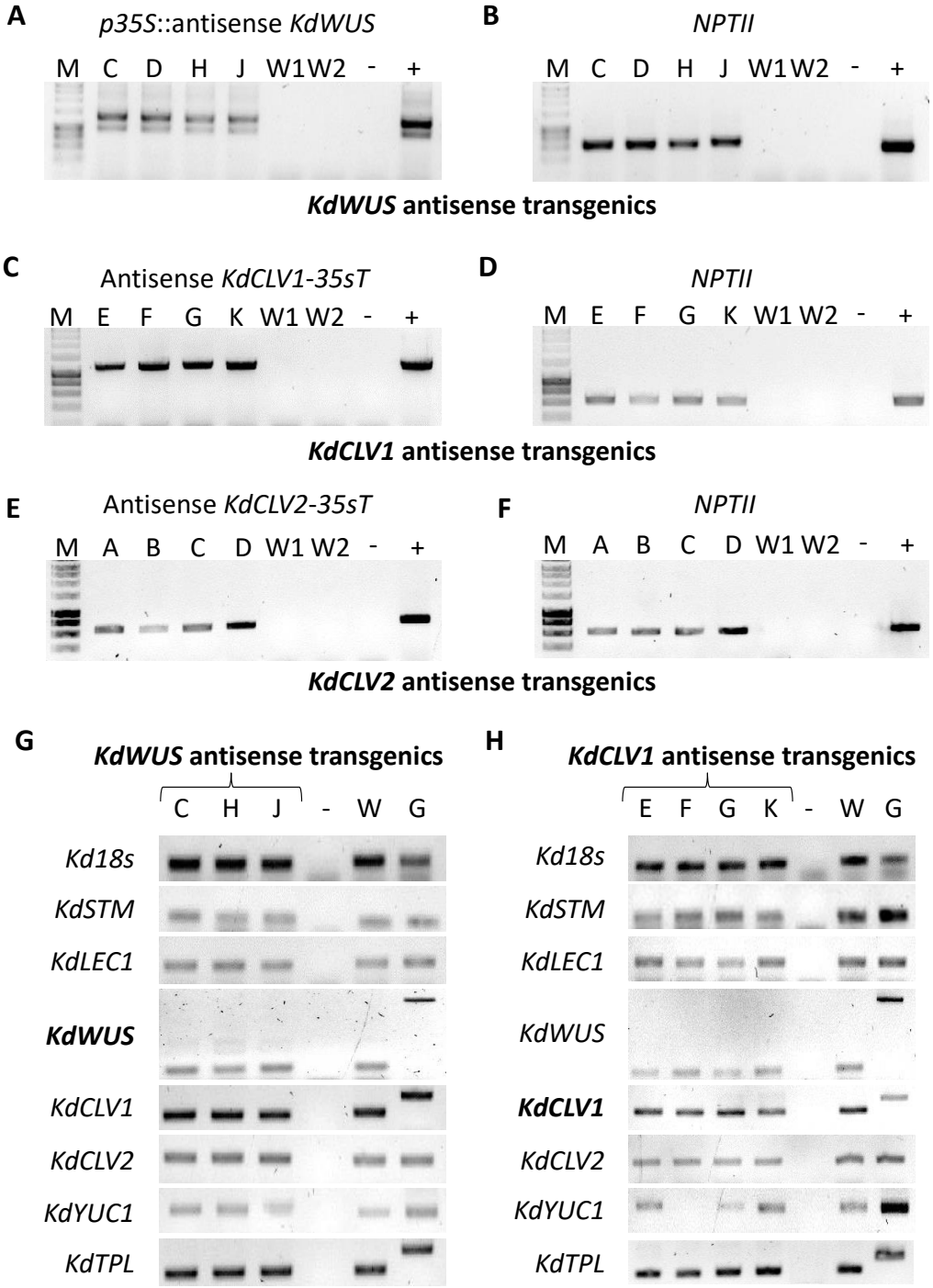

Figure 3.5 Genotyping and transcript expression analysis of *KdWUS*, *KdCLV1* and *KdCLV2* antisense plants.
Gel electrophoresis showing amplification of a part of the antisense constructs (A, C, E) and the *NEOMYCIN PHOSPHOTRANSFERASE* II (*NPTII*) of the transformation vector (B, D, F) in genomic DNA of the transgenic plants. M, molecular marker; W1, wild-type sample 1; W2, wild-type sample 2; -, negative control using water; +, positive control using the transformation vector. Other alphabets represent independent lines of the transgenic plants. (G, H) Gel electrophoresis images showing expression analysis of different genes using semi-quantitative reverse-transcriptase PCR in *KdWUS* antisense plants (G) and *KdCLV1* antisense plants (G). M, molecular marker; -, water; W, wild-type; G, wild-type genomic DNA. *STM*, SHOOT *MERISTEMLESS*; *LEC1*, *LEAFY COTYLEDON 1*; *WUS*, *WUSCHEL*; *CLV1*, *CLAVATA 1*; *CLV2*, *CLAVATA 2*; *YUC1*, *YUCCA 1*; *TPL*, *TOPLESS.*

In contrast to wild-type plants (Fig. 3.6A), *KdWUS* and *KdCLV1* antisense plants were shorter and had shorter internodes (Fig. 3.6B, C). Wild-types plants always show an apical dominance thus one main shoot per plant (Fig. 3.6A). In *KdWUS* and *KdCLV1* plants this apical dominance was lost and had several side shoots growing simultaneously (Fig. 3.6B, C). In wild-type, *K. daigremontiana* leaves are oblong triangular in shape, exhibiting clearly marked mid-vein on the leaf surface and form plantlets symmetrically in both sides of the leaf blade (Fig. 3.6D). *KdWUS* and *KdCLV1* antisense plants, in contrast, had irregularly-shaped and smaller leaves; leaves had uneven surfaces and inconsistent distribution of plantlets along the leaf margin (Fig. 3.6E, F). These leaves also had significantly reduced number of lobes per leaf, with the exception of line K *KdCLV1* antisense plants (Fig. 3.6H, K). Apart from *KdCLV1* antisense line F, the number of plantlets per leaf pair in both *KdWUS* and *KdCLV1* antisense plants was also lower than the wild type by at least 30 plantlets, a significant reduction (Fig. 3.6G, J). In the case of leaf indentation depth, out of three lines, only line H of *KdWUS* antisense plants showed significant reduction, compared to wild-type (Fig. 3.6I). For *KdCLV1* antisense plants, three out of four lines showed significant reduction of leaf indentation depth (Fig. 3.6L).

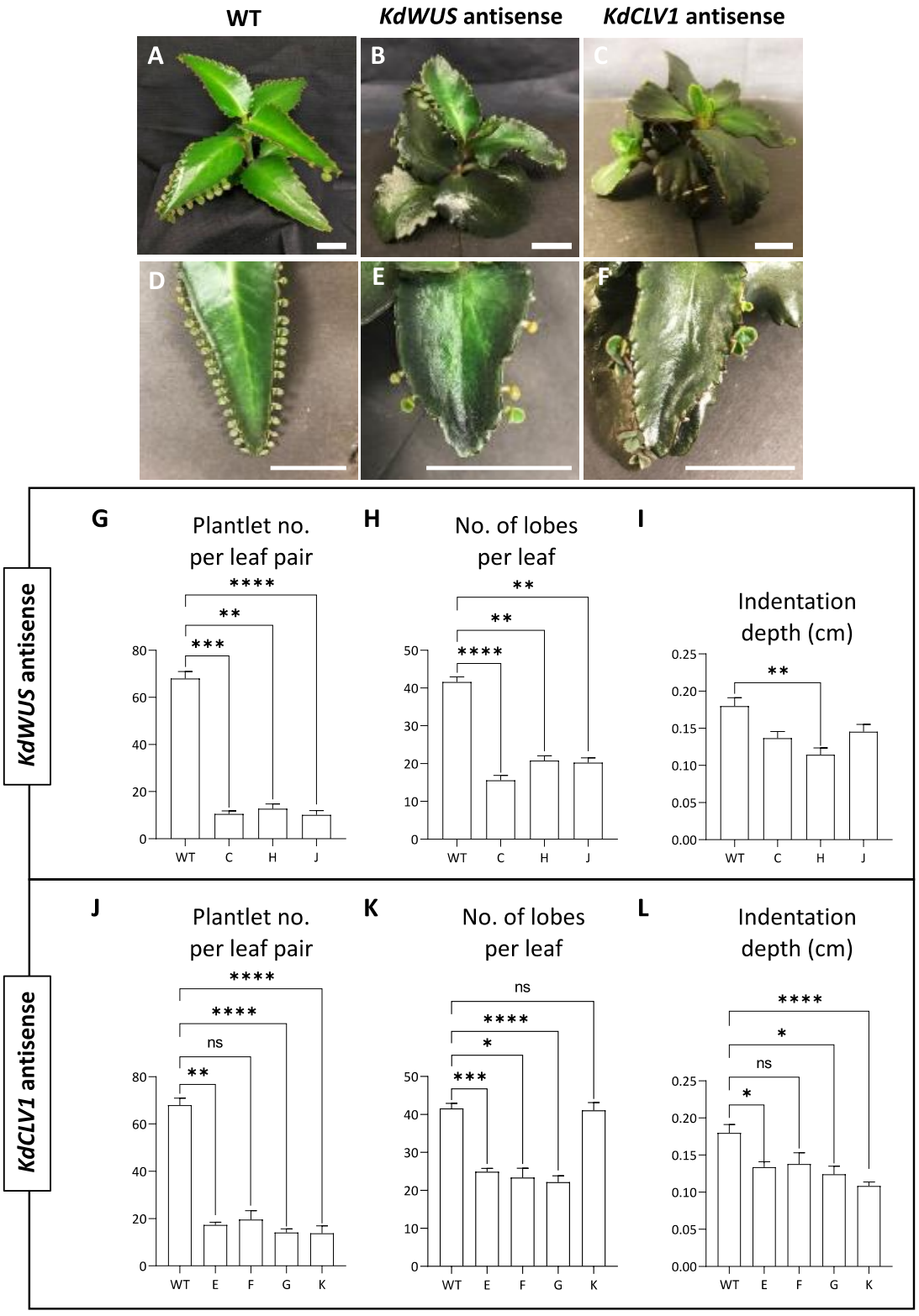

Figure 3.6 Phenotype analyses of *KdWUS* and *KdCLV1* antisense transgenic plants.
Whole plant of (A) wild-type (WT) *K. daigremontiana*; (B) *KdWUSCHEL* (*KdWUS*) antisense and (C) *KdCLAVATA1* (*KdCLV1*) antisense plants; scale bar represents 1 cm. Whole leaf of (D) WT *K. daigremontiana*; (E) *KdWUS* antisense and (F) *KdCLV1* antisense transgenic plants; scale bar represents 1 mm. (G-L) Graphs showing the average (G, J) number of plantlets per leaf pair; (H, K) number of lobes per leaf and (I, L) Indentation depth of notches on the leaves in *KdWUS* and *KdCLV1* antisense transgenic plants, respectively. C, H, J, *KdWUS* antisense plants; E, F, G, K, *KdCLV1* antisense plants. Kruskal Wallis test with Dunn's multiple comparison test indicate statistical significance, *P≤0.05; **P≤0.005; ***P≤0.0005; ****P≤0.0001. Error bar represents standard error.

Wild-type *K. daigremontiana* plantlets usually make a pair of almost equally-sized cotyledons or leaves (Fig. 3.7A). However, some *KdWUS* and *KdCLV1* antisense plantlets only made a single cotyledon (Fig. 3.7J) or leaf (Fig. 3.7I), whereas some produced three cotyledons or leaves (Fig. 3.7M). The feature of three cotyledons could already be observed under the microscope before reaching maturation (Fig. 3.7O). In some cases, the antisense plantlets displayed unequally sized cotyledons (Fig. 3.7L). Apart from the number and size, the shape of cotyledon and leaves was very irregular (Fig. 3.7K) compared to wild-type plantlet (Fig. 3.7A, B). Wild-type plantlets produced leaf pairs perpendicular to each other (Fig. 3.7C) and only maintained one SAM (Fig. 3.7D). In contrast, some antisense plantlets produced two SAM (Fig. 3.7N) and some *KdCLV1* antisense plants also eventually started branching (Fig. 3.6C). Examination of *KdWUS* and *KdCLV1* antisense plantlets using scanning electron microscope showed that pedestal formation of antisense plantlets was irregular and was less organised (Fig. 3.7P-T) compared to wild-type (Fig. 3.7E-H). In wild-type, plantlet primordium was enclosed in a developing pedestal (Fig. 3.7E) but this was not the case for the antisense plantlet primordia (Fig. 3.7P). The developing pedestals remained flat, exposing the plantlet primordia (Fig. 3.7P). As the pedestal continued developing during which the plantlet reached transition phase from globular to heart-stage, the pedestal (Fig. 3.7Q) was shallower compared to wild-type (Fig. 3.7F). At heart-stage, wild-type plantlet started to emerge from the pedestal (Fig. 3.7G), however, the pedestals of antisense plantlets remained extremely shallow and almost flat (Fig. 3.7R, S). Some antisense pedestal also exhibited irregular shape, particularly at the apex (Fig. 3.7S). At later stages, wild-type plantlet cotyledons emerge from pedestal that remained visible and thick around the site of plantlet emergence (Fig. 3.7H). In contrast, pedestal structure around the antisense plantlets at a similar stage was thinner and again shallower (Fig. 3.7T). *KdWUS* antisense plantlets displayed a few unique phenotypes that were not present in *KdCLV1* plantlets (Fig. 3.7U-X). Wild-type plants only produce one plantlet per pedestal at each leaf notch (Fig. 3.7B), however, some pedestals of *KdWUS* antisense plants were presented with two plantlets on the same pedestal (Fig. 3.7U, V). These *KdWUS* antisense plantlets also exhibited extremely deformed cotyledons and leaves of cylinder-shaped (Fig. 3.7U), cone-shaped (Fig. 3.7W) and unusually curved cotyledon and leaves (Fig. 3.7V, X). These cone-shaped cotyledons and leaves terminated the SAM, thus no further growth was observed.

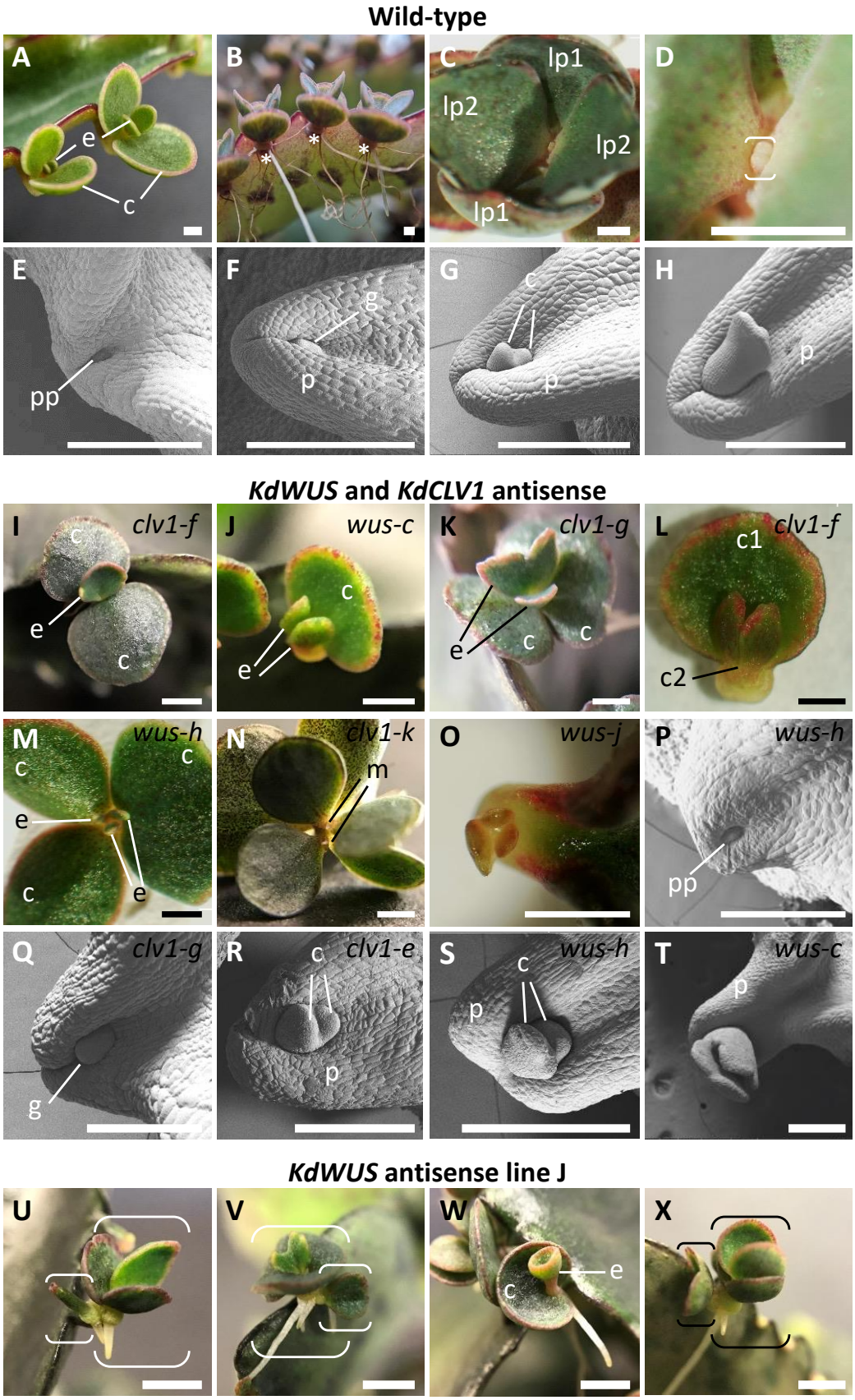

Figure 3.7 Images of wild-type *K. daigremontiana*, antisense *KdWUS* and *KdCLV1* transgenic plantlets.

Figure 3.8 Images of wild-type *K. daigremontiana*, antisense *KdWUS* and *KdCLV1* transgenic plantlets.
(A) Developing wild-type plantlets with equally-sized pairs of cotyledons and leaves. (B) Mature wild-type plantlets on equidistant pedestals and (C) bearing two leaf pairs and visible shoot apical meristem (SAM). (D) Close-up image of wild-type plantlet SAM. (E-H) Scanning electron microscope (SEM) images of wild-type plantlets. (E) Enclosed plantlet primordium at the leaf notch prior to formation of full-sized pedestal. (F) Plantlet enclosed in the pedestal transitioning from globular to heart stage. (G) Heart-stage plantlet showing developing cotyledons. (H) Plantlet with cotyledon already emerged from pedestal. (I-T) Plantlets with phenotypes present in both *KdWUS* and *KdCLV1* antisense plantlets. Antisense plantlet with (I) only one leaf; (J) one cotyledon; (K) irregularly-shaped cotyledons and leaves; (L) unequal-sized cotyledons; (M) 3 cotyledons and leaves; (N) two SAM; (O) abnormally-shaped cotyledons growing out from shallow pedestal. (P-T) SEM images of representative plantlets displaying features shared between *KdWUS* and *KdCLV1* antisense plantlets. (P) Plantlet primordia; (Q) plantlet transitioning from globular to heart stage; (R) heart-stage plantlet; (S) more mature heart-stage plantlet with abnormally shaped pedestal; (T) plantlet with irregularly shaped mature cotyledons. (U-X) Unique phenotypes present only in *KdWUS* antisense plantlets. (U,V,X) Two plantlets on the same pedestal, each bracket highlights an individual plantlet (U) one plantlet with deformed cylinder-shaped cotyledon and another plantlet seems to have only one leaf. (V) One plantlet displaying only one cotyledon and another with irregularly-shaped cotyledons and unequally-sized leaves. (W) Plantlet with deformed cone-shaped cotyledon or leaf formation. (X) Plantlets with curved-shaped cotyledon and leaves. c, cotyledon; e, leaf; g, globular-stage plantlet; lp, leaf pair; m, meristem, p; pedestal; pp; plantlet primordium. Scale bars are 1mm for A-D, I-N and U-X; 0.5 mm for E-H, O, P-T.

3.5. **Discussion**

Plants develop post-embryonically by maintaining stem cells at meristems such as SAM (Aichinger et al., 2012; Murray et al., 2012). From SAM, plants can trigger organogenesis to form above-ground aerial organs. Early molecular study on *Kalanchoë* plantlet formation revealed participation of an organogenesis gene *STM* during plantlet formation (Garcês et al., 2007) and suggest that *STM* maintains pluripotent stem cells for plantlet formation. To better understand how organogenesis functions during plantlet formation, this study examined other genes (*WUS*, *CLV1*, *CLV2*) involved in SAM homeostasis and organogenesis. Comparative sequence identity analysis of isolated *WUS*, *CLV1* and *CLV2* sequences from *K. daigremontiana* and *K. pinnata* confirmed that the sequences are homologs from *K. laxiflora* and *K. fedtschenkoi*. This is because the sequences shared high sequence identity (Fig. 3.2) of far above the requirement of at least 30% similarity for nucleotides and at least 40% similar for protein to be recognised as a homolog (Do and Katoh, 2008; Pearson, 2013). Moreover, the *WUS*, *CLV1* and *CLV2* sequences from *K. laxiflora* and *K. fedtschenkoi* were of the highest scores when blast searched with the *Arabidopsis* homologs. Phylogenetic analysis of trimmed *WUS*, *CLV1* and *CLV2* nucleotide and protein sequences (Fig. 3.3A-F) failed to distinguish and infer the evolutionary relationship of most sequences, probably as a consequence of high sequence conservation and similarity (Grundy and Naylor, 1999). Hence, when whole sequences were used, additional regions present provided more information to infer phylogenetic relationship of the sequences and resulted in formation of more clades (Fig. 3.3G-L).

However, phylogenetic trees of trimmed *WUS* nucleotide and protein sequences contained far fewer (Fig. 3.3A, B) clades compared to *CLV1* and *CLV2* sequences (Fig. 3.3C-F). Apart from the possibility of isolating a shorter sequence, the isolated region for *WUS* sequences happened to be homeodomain region in which WUS protein recognise and bind to diverse DNA sequences to confer its activity as a homeodomain transcription factor (Sloan et al., 2020). Due to its function, this homeodomain region sequences are highly conserved among *WUSCHEL-RELATED HOMEOBOX* (*WOX*) genes not only in plants, but also in diverse organisms including mammals, insects and yeast (Lian et al., 2014; Sloan et al., 2020; Truscott and Nepveu, 2006; Wu et al., 2019). However, gymnosperms such as *Picea abies* and lower plants such as *Physcomitrium patens* and *Selaginella moellendorffii* lack the WUS clade (Palovaara and

Hakman, 2008). The WUS sequences used for these three species *P. abies*, *P. patens* and *S. moellendorffii* were sequences with the highest scores when blast search using WUS sequences from other angiosperm WUS species. The WUS sequences used for *P. abies*, *P. patens* and *S. moellendorffii* are class III homeodomain leucine zipper protein, WOX8-LIKE and WOX13 respectively. Even though *P. patens* WOX8-like and *S. moellendorffii* WOX13 sequences were annotated by automated computational analysis, it is likely to be true WOX genes because studies have shown that gymnosperms such as *P. abies* have WOX members conserved in the same clade as angiosperm species WOX genes (Palovaara and Hakman, 2008; Palovaara et al., 2010).

Despite the high conservation of homeodomain sequences, *K. laxiflora* and *K. fedtschenkoi WUS* sequences were unique enough to be separated into a distinct clade regardless of whether trimmed or whole sequences were used (Fig. 3.3G, H). However, WUS sequences of some species still collapse into the same clade even when whole sequences were used. This contrasts with phylogenetic trees obtained using whole sequences of *CLV1* and *CLV2* that resulted in almost all sequences belonging to a distinct clade (Fig. 3.3I-L). The CLV1 ortholog in rice (*Oryza sativa*) known as *FLORAL ORGAN NUMBER* (*FON1*) is involved in several pathways in regulating stem cells, depending on the type of meristems (Fletcher, 2018; Suzaki et al., 2004). *FON1* restricts stem cell accumulation specifically in floral meristems, without affecting vegetative or inflorescence meristem activity (Nagasawa et al., 1996). Hence, the region with additional residues in CLV1 ortholog of rice and other monocots *e.g.*, pineapple (*Ananas comosus*), banana (*Musa acuminata*) and maize (*Zea mays*) might be the region that is important for its functional activity in regulating floral meristem. On the other hand, that region of sequences might be selected in CLV1 orthologs of other species for its function in regulating SAM. As for the additional sequences presented in the putative CLV2 ortholog in *P. sitchensis* and *S. moellendorffii*, it might be due to absence of a functionally identical CLV2 ortholog. This is supported by the fact that WUS proteins which functions in the same signalling pathway as CLV2 to regulate SAM are absent in gymnosperms (Palovaara and Hakman, 2008).

In an *Arabidopsis* embryo, *WUS* expression is first detected at the 16-cell stage (Capron et al., 2009; Mayer et al., 1998; Tucker et al., 2008). However, KdWUS expression was not detected

in the *K. daigremontiana* plantlet primordia of early globular stage (Fig. 3.4A). This might be due to the weak strength of signal and that, if similar to *Arabidopsis*, KdWUS expression might also be localised underneath the apical cells of the protoderm (Capron et al., 2009; Mayer et al., 1998; Tucker et al., 2008). In addition, the developing pedestal structure might also hinder clear visualisation of KdWUS expression. Hence, to visualise KdWUS expression at this stage, sectioning of samples need to be done at different angles and an image with higher resolution is needed. The observation also indicates that KdWUS might not be expressed, which is not unexpected because WUS was found to be dispensable for stem cell initiation during embryogenesis (Zhang et al., 2017a). In contrast to *Arabidopsis* heart-stage embryo that expresses *WUS* mRNA only at the putative OC and distributes WUS protein across the whole SAM (Capron et al., 2009; Fuchs and Lohmann, 2020; Mayer et al., 1998; Tucker et al., 2008), KdWUS expression was visible at cotyledon primordia of *K. daigremontiana* heart-stage plantlet (Fig. 3.4B). At a later heart-stage, KdWUS expression was still visible at cotyledon primordia but was arranged in a distinctive pattern; the basal region of cotyledon primordium also exhibited KdWUS expression (Fig. 3.4C). KdWUS expression at cotyledon primordia was reminiscent to Arabidopsis WUS expression at floral meristem outgrowth from inflorescence meristem during early flower formation (Yadav et al., 2011). As the cotyledons grew bigger, KdWUS expression started receding towards the basal half of the plantlet (Fig. 3.4D). These observations suggest that KdWUS activity might be assisting the outgrowth of cotyledon. However, whether KdWUS protein is functional at this stage has yet to be confirmed. When the SAM was structurally visible at the emerging plantlet, KdWUS expression was not present, probably due to the fact that its expression is typically only localised at a few cells of OC (Mayer et al., 1998). The expression of KdWUS as shown by immunolocalization was not entirely consistent with *KdWUS* expression obtained from RNA-sequencing analysis. For example, plantlet stage S1 was expected to include plantlets of stages shown in Fig. 3.4A but RNA-sequencing analysis displayed very high *KdWUS* expression. On the other hand, plantlet stage S3 was expected to include plantlets of stages as shown from Fig. 3.4D to Fig. 3.4E, hence, *KdWUS* expression at S3 was expected to be lower than at S2 as observed. This inconsistency might be due to difficulty in isolating specific stages of plantlet formation based on its histological structure when harvesting samples for RNA-sequencing analysis. In addition, this discrepancy between KdWUS protein and *KdWUS* transcripts may be partially due to the cell

autonomy of WUS protein action; WUS protein is able to move between cells and WUS protein and *WUS* transcripts show different expression patterns in *Arabidopsis* embryo (Capron et al., 2009; Fuchs and Lohmann, 2020; Mayer et al., 1998; Tucker et al., 2008).

Based on statistical analysis, qRT-PCR expression analysis showed that level of *KdCLV1* expression is similar across plantlet development. However, based on the expression trend observed, *KdCLV1* expression is lower in the SAM, compared to *K. daigremontiana* plantlets (Fig. 3.4J). This was unexpected as *CVL1* is one of key genes regulating the SAM (Fletcher et al., 1999; Long and Barton, 1998). In addition, *Arabidopsis clv1* mutants displayed defects only at the SAM and floral meristem or flower structures (Clark et al., 1993; DeYoung and Clark, 2008). Apart from that, both RNA-sequencing analysis and qRT-PCR analysis showed increasing *KdCLV1* expression during plantlet developmental from Ctrl (1-2 cm young leaf margin) to stage S3 (Fig. 3.4I, J). Since *CLV1* expression was known to be directly activated by WUS (Busch et al., 2010), perhaps *CLV1* might be expressed in a similar pattern as KdWUS. This may explain *KdCLV1* expression increasing during plantlet development (Fig. 3.4A-E, I, J). On the other hand, *CLV2* expression was expected to be similar to *CLV1* due to participation in CLV signalling by formation of CVL1-CLV2 receptor complexes. Nonetheless, this was not observed in our data; *CLV2* expression stayed the same throughout plantlet development. CLV1 can act independently by forming homomers (Bleckmann et al., 2010), thus, this might explain the difference in *KdCLV1* and *KdCLV2* expression. Previous studies have also shown that *CLV2* was also expressed in multiple tissues (Kayes and Clark, 1998; Wang et al., 2008, 2010a; Wu et al., 2016), hence, the RNA-sequencing analysis might have captured *CLV2* expression in other tissues included during harvesting samples, such as pedestal and leaf margin. To confirm the expression pattern of *CLV1* and *CLV2*, visualisation of their expression at cellular and tissue levels, using rigorous quantitative measurement such as qRT-PCR accompanied by immunolocalisation or *in-situ* hybridisation, is required.

We attempted to generate *KdWUS* and *KdCLV1* antisense plants with reduced expression in the respective genes (Fig. 3.5G, H). Semi-quantitative RT-PCR was not strong enough to confirm downregulation of *KdWUS* and *KdCLV1* in the antisense plants, but it is expected to be so as these plants exhibited obvious plantlet developmental defects. A more robust

measurement technique such as qRT-PCR would provide a more reliable result on expression level of these genes. However, these experiments could not be conducted as university was forced to close due to the Covid-19 pandemic. More detailed phenotyping of these antisense plant also could not be conducted due to the same reason. It was expected to obtain few leaky antisense lines with only slight reduction of *KdWUS* because of its functional importance in the SAM and its role in inducing somatic embryogenesis in *in vitro* tissue culture (Arroyo-Herrera et al., 2008; Bouchabké-Coussa et al., 2013; Kadri et al., 2021; Laux et al., 1996; Mayer et al., 1998; Zuo et al., 2002). Calli with severe downregulation of *KdWUS* expression might not have survived as *Arabidopsis wus* mutants were unable to maintain the stem cell niche of the SAM and terminated after formation of very limited number of organs (Laux et al., 1996). This explains modest levels of downregulation of *KdWUS* seen in the *KdWUS* antisense plants. Interestingly, although only one antisense line exhibited reduction in *KdWUS* expression, the expression of auxin biosynthesis flavin monooxygenase enzyme gene, *KdYUC1* (Stepanova et al., 2011) was either upregulated or downregulated in three of the phenotypic *KdWUS* antisense lines. A previous study showed that ARABIDOPSIS RESPONSE REGULATORs (ARRs) activated *WUS* transcription and repressed *YUC1* and *YUC4* in precursor region of OC, which in turn restricted the expression of YUC1 and YUC4 to the surrounding region (Meng et al., 2017). *yuc1* mutants exhibited attenuated shoot regeneration and enhanced adventitious root formation, and when *YUC1* was overexpressed, *WUS* transcripts were markedly reduced (Meng et al., 2017). Expression of *YUC1* under the control of *WUS* promoter (*proWUS::YUC1*) also resulted in reduced shoot regeneration, suggesting that *YUC1* represses *WUS* expression (Meng et al., 2017). Based on the results presented in the same study, the author also speculated that *YUC1* and *YUC4* was repressed in precursor region of OC and *WUS* expression was repressed by cytokinin signalling (Meng et al., 2017). Previously, WUS was shown to directly regulate cytokinin-inducible response regulators (Leibfried et al., 2005). Hence, in *KdWUS* antisense plants, *KdWUS* downregulation might upregulate cytokinin signalling, which in turn repressed *KdYUC1* signalling. However, our data showed that *KdYUC1* expression was different in each *KdWUS* antisense line. This might be due to the multiple roles of *KdYUC1* and the complexity of auxin-cytokinin cross-talk (Cao et al., 2019; Chen et al., 2016; Müller and Sheen, 2008; Uc-Chuc et al., 2020).

In the case of *KdCLV1* antisense plants, based on semi-quantitative analysis, *KdCLV1* downregulation resulted in downregulation of *KdWUS*, *KdCLV2, KdSTM*, *KdLEC1* and *KdYUC1* (Fig. 3.5H). Given that CLV1 signalling leads to WUS repression (Betsuyaku et al., 2011), reduced *KdCLV1* expression was expected to relieve *KdWUS* repression and cause an increase in *KdWUS* expression (Schoof et al., 2000). A previous study demonstrated that *clv1* null mutants displayed ectopic expression of CLV1-related receptor kinases and buffered stem cell proliferation through the auto-repression of their own expression (Nimchuk, 2017). Moreover, the study showed that regulation of stem cell proliferation through CLV1 signalling can be independent from WUS (Nimchuk, 2017). As the suppression of *KdCLV1* was incomplete in *KdCLV1* antisense plants, hence, the reduction of expression of other genes such as *KdWUS* and *KdCLV2* might be the result of changes in signalling pathways downstream of *KdCLV1*. The downregulation of *KdSTM* might be a result of *KdWUS* downregulation because *STM* expression was shown to be dependent on WUS (Su et al., 2020). The presence of the late embryogenesis gene *KdLEC1* expression, once again confirmed that embryogenesis is recruited into plantlet formation. Moreover, downregulation of *KdLEC1* in *KdCLV1* antisense lines suggests that there may be an interaction between the SAM regulatory WUS-CLV pathway and embryogenesis pathway(s) during *K. daigremontiana* plantlet formation.

Both *KdWUS* and *KdCLV1* antisense plants exhibited a range of phenotypes such as decreased plant height, irregular leaf shape and surface, reduced number of lobes per leaf, number of plantlets and indentation depth (Fig. 3.6). Given the role of WUS-CLV signalling in regulating stem cells that give rise to the formation of all aerial plant organs, it was expected to observe reduction of *KdWUS* and *KdCLV1* expression contributing to reduced plant height, similar to *Arabidopsis wus* and *clv1* mutants (Clark et al., 1993; Laux et al., 1996; Mayer et al., 1998). In addition, previous studies showed that *wus* and *clv1* mutants displayed irregular leaf morphology and phyllotaxy (Ottoline Leyser and Furner, 1992) which were also exhibited by *KdWUS* and *KdCLV1* antisense plants and plantlets (Fig. 3.6, 3.7). The irregular leaf morphology in *KdWUS* and *KdCLV1* antisense plants might be the result of auxin biosynthesis gene *KdYUC1* disruption, which was presented in these plants (Fig. 3.5G, H). Auxin regulates different aspects of leaf development including leaf initiation, leaf shape and leaf serration. It has been shown that local auxin maxima established through auxin efflux transporter PIN1 at incipient leaf

primordia initiates leaf formation (Jönsson et al., 2006; Reinhardt et al., 2003; de Reuille et al., 2006; Smith et al., 2006; Vernoux et al., 2011). Wild-type SAM treated with auxin transport inhibitor and *pin1* mutants displayed failure of organ formation (Gälweiler et al., 1998; Okada et al., 1991; Vernoux et al., 2000). When exogenous auxin was applied, organ formation in these two circumstances was restored (Reinhardt et al., 2000). YUCCA enzymes and transcription factors such as PLETHORA that controls *YUC1* and *YUC4* expression were found to stabilise phyllotaxis (Cheng et al., 2007; Galvan-Ampudia et al., 2018; Pinon et al., 2013). Hence, formation of single cotyledon or single leaf in *KdWUS* and *KdCLV1* antisense plantlets (Fig. 3.7I,J) might be a consequence of change in *KdYUC1* expression.

In terms of reduced leaf serrations in *KdWUS* and *KdCLV1* antisense plants, *KdYUC1* might be contributing to biosynthesis of auxin that is required to form evenly spaced auxin maxima at specific points of leaf margin, which will form tips of serrations (Bilsborough et al., 2011). The respective maintenance of auxin maxima at serration tips and along the leaf margin requires the activity of *CUP-SHAPED COTYLEDONS* (*CUC*) genes (Bilsborough et al., 2011). The region of auxin maxima coincide with outgrowth of serration tips whereas CUC2 maxima coincide with regions of retarded growth, forming a pattern of serrations along the leaf margin (Bilsborough et al., 2011). As *KdYUC1* expression level was inconsistent in each antisense lines that exhibited defective leaf morphology, the *WUS-CLV* pathway might be regulating *CUC* activity. Although there is no evidence of *CUC* regulation by WUS, other members of the same *WUSCHEL-RELATED HOMEOBOX* (*WOX*) clade control *CUC* expression in the cotyledon boundary (Lie et al., 2012). Formation of cup-shaped cotyledon or leaf in *KdWUS* antisense plants (Fig. 3.7U-W) provided support that *CUC* genes were affected as *cuc* mutants are known to display similar phenotypes (Aida et al., 1997; Hibara et al., 2006; Takada et al., 2001).

Changes in *KdYUC1* might also have altered sources of auxin to maintain auxin gradient that contributes to symmetrical basipetal leaf outgrowth and pedestal formation along the leaf margin (Zhang et al., 2020). Basipetal gradient of auxin biosynthesis mediated by local activation of *YUC* genes such as *YUC1* near the leaf margin is needed for proper outgrowth and shape of *Arabidopsis* leaves (Zhang et al., 2020). *Arabidopsis yuc* mutants exhibited abnormal leaf margin development and narrower leaves (Wang et al., 2011; Zhang et al., 2020), similar

to *KdWUS* and *KdCLV1* antisense plants that displayed smaller leaves with uneven leaf surface and shape (Fig. 3.6E). Plantlet formation occurs only during leaf growth and maturation, hence, inconsistent auxin sources due to changes in *KdYUC1* expression might have affected basipetal leaf outgrowth, pedestal formation and the signal required for plantlet initiation. This might also explain the unique feature presented only in *KdWUS* antisense line J plants; the formation of two plantlets on a single pedestal (Fig. 3.7U, V, X). As a consequence of loss of serrations and pedestals, there were loss of asymmetrical and basipetal formation of plantlets along the leaf margin (Fig. 3.6E, F). If auxin maxima were indeed recruited for formation of pedestals, disruption of auxin sources might also provide explanation for inconsistent structural formation of pedestals as observed from SEM images (Fig. 3.7P-T). However, not all loss of plantlets on the leaf margin was due to the defects in serrations and pedestals; some normal serrations failed to initiate plantlets. This suggests that normal plantlet formation requires two key steps: normal serration and plantlet initiation. Our data showed that meristem (*WUS-CLV*) and auxin pathways are involved in both steps.

Although *WUS* and *CLV1* can operate in the same WUS-CLV signalling pathway to maintain SAM, *WUS* and *CLV1* act differently to do so (Schoof et al., 2000). *WUS* acts to maintain the stem-cell population and in *wus* mutants, SAM formation was defective, resulting in only a few rounds of leaf initiation (Laux et al., 1996). In contrast, *CLV1* inhibits *WUS* to restrict the size of the stem-cell population (Schoof et al., 2000). In *Arabidopsis clv1* mutants, enlargement of the SAM and formation of many flowers at the periphery of inflorescence meristem were typically observed, whereas in *wus* mutants, shoot and floral meristems terminated prematurely and resulted in formation of a flat apex (Clark et al., 1993; Laux et al., 1996; Schoof et al., 2000). The phenotypes presented by *clv1* mutants were due to expansion of *WUS* in which its expression promoted ectopic formation of stem cells within the meristem (Clark et al., 1993; Schoof et al., 2000). Due to the opposing functions of *CLV1* and *WUS*, it was surprising to observe common phenotypes in *KdWUS* and *KdCLV1* antisense plants, including the formation of two meristems in a single *KdWUS* or *KdCLV1* antisense plantlet (Fig. 3.7N). Based on known function of *WUS*, downregulation of *KdWUS* should result in fewer meristematic tissues. As for *KdCLV1* antisense plants, downregulation of *KdCLV1* was expected to be accompanied by *KdWUS* upregulation. However, semi-quantitative expression analysis showed that *KdWUS*

expression was reduced in *KdCLV1* antisense plants. This suggests that the phenotypes observed in *KdCLV1* antisense plants might be caused by *CLV1* signalling independent from *WUS* or due to the result of changes in CLV1-related receptor kinases (Nimchuk, 2017). As the full sequences of *K. daigremontiana* WUS and CLV1 homolog is yet to be available and investigated, perhaps *KdWUS* and *KdCLV1* have different functions compared to the *Arabidopsis* counterparts. For example, in liverwort *Marchantia polymorpha*, the *CLV3-CLV1* signalling pathway promotes accumulation of undifferentiated haploid meristem cells, unlike in *Arabidopsis* in which *CLV3-CLV1* signalling acts to inhibit *WUS* to restrict the stem-cell population size (Hirakawa et al., 2020). A ligand-receptor signalling pathway TDIF (TRACHEARY ELEMENT DIFFERENTIATION INHIBITORY FACTOR) peptide and TDR (TDIF RECEPTOR) that shares high similarity to CLV3 and CLV1 exists to maintain the *Arabidopsis* vascular meristem (Hirakawa et al., 2008). The phloem and its neighbouring cells release TDIF, which binds to the TDR receptor kinases on the plasma membrane of procambial cells. This results in proliferation of procambial cells and suppression of their differentiation into xylem cells (Hirakawa et al., 2008). The TDIF-TDR interaction also upregulates *WOX4* that promotes proliferation of procambial cells but not to prevent their differentiation (Hirakawa et al., 2010). This shows another example of how components in a similar signalling pathway can exert different functions, which might be the case for the WUS-CLV signalling in *K. daigremontiana.* As both *KdWUS* and *KdCLV1* antisense plants shared changes in *KdYUC1* expression, it is likely that *KdYUC1* was involved in generating two meristems in a single plantlet (Fig. 3.5G, H). However, *yuc1* mutants still retained near wild-type meristem development and *YUC1* overexpression also did not exhibit meristem abnormality in *Arabidopsis* (Cheng et al., 2007; Zhao et al., 2001). Hence, other genes or pathways that might be contributing to this observation instead. Quantitative expression analysis is required to confirm the changes in expression of *KdYUC1* and other genes in *KdWUS* and *KdCLV1* antisense plants. Formation of double meristem might have then contributed to shoot branching in *KdCLV1* antisense plants (Fig. 3.6C). This observation was reminiscent of the phenotypes observed when *KNAT1* homolog, *KxhKN5*, was overexpressed in *K. x houghtonii*, in which plantlets are formed as ectopic shoots that developed into lateral branch (Laura et al., 2013). This suggests that perhaps *KdKN5* was upregulated in *KdWUS* and *KdCLV1* antisense plants to trigger formation of ectopic meristems in plantlets.

3.6. **Conclusion**

In general, the irregularity in phenotypes shown by *KdWUS* and *KdCLV1* antisense transgenic plants seemed to suggest participation of these genes in *K. daigremontiana* plantlet formation. The difference in expression pattern of *KdWUS*, *KdCLV1* and *KdCLV2* across plantlet developmental stages compared to known expression of *WUS*, *CLV1* and *CLV2* also suggest novel functions of these genes during plantlet formation. Further studies are needed to visualise expression of *KdWUS*, *KdCLV1* and *KdCLV2* at a tissue level. In addition, isolation of whole sequences of *KdWUS*, *KdCLV1* and *KdCLV2* might be necessary to determine whether significant changes were evolved in these genes to confer novel functions in plantlet formation. Quantitative expression analyses are also required to provide a more robust measurement of *KdWUS*, *KdCLV1* and *KdCLV2* and other genes that might have contribute to in phenotypes developed in *KdWUS* and *KdCLV1* antisense plants and plantlets. These future studies would provide greater details into regulation of plantlet formation through organogenesis and possibly other regulatory pathways that are involved in organogenesis.

CHAPTER 4

RESULTS 3

All data, figures and text in this chapter were generated by JPO with the exception of RNA-sequencing data and generation of *PIN1*::*PIN1-GFP* construct. University of Manchester Genomic Technologies Core Facility and Bioinformatics Core Facility sequenced and analysed the RNA samples prepared by JPO. FJB produced the *PIN1*::*PIN1-GFP* construct which was transformed into plant tissues by JPO.

4. Auxin and Cytokinin Activity in Early Stages of *Kalanchoë daigremontiana* Plantlet Formation.

Joo Phin Ooi[1], Francisco Jácome Blásquez[1] and Minsung Kim[1]*

[1]School of Biological Sciences, Faculty of Biology, Medicine and Health, University of Manchester, Manchester, M13 9PT, United Kingdom

*Corresponding author: Minsung.kim@manchester.asc.uk

Key Words: Asexual Reproduction, *Kalanchoë*, plantlet formation, auxin, cytokinin

4.1. Abstract

Certain species of plants in the *Kalanchoë* genus can reproduce asexually through a unique strategy known as plantlet formation. One of these species is *Kalanchoë daigremontiana* which form plantlets constitutively under normal conditions. To date, studies on the hormonal control of *K. daigremontiana* plantlet formation have shown inconsistent results due to limited molecular tools. Hence, this study aims to make use of advanced molecular technologies to create transgenic plants and study the role of two major plant hormones, auxin and cytokinin in plantlet formation. Transgenic *K. daigremontiana* reporter lines showed novel presence of cytokinin and auxin activity during early plantlet formation and similarity in activity to zygotic embryogenesis during plantlet development. The attempt to search for a cytokinin signalling inhibitor in *Kalanchoë* also revealed independent evolution of components involved in cytokinin signalling. We isolated a putative cytokinin signalling inhibitor gene that was highly expressed during plantlet development and showed that reduced expression of this gene resulted in irregular plantlet formation. Our study also discussed the possibility of complex auxin-cytokinin crosstalk during plantlet formation and interaction between different plant developmental processes. These observations shed light onto how these hormones are involved in stimulation of somatic embryogenesis.

4.2. Introduction

Asexual reproduction in plants produces genetically identical offspring in the absence of gametic fusion (de Meeûs et al., 2007). The benefits associated with the development and evolution of asexual reproduction has long been disputed (de Meeûs et al., 2007). Nonetheless, populations that reproduce asexually have increased survival probability. Through asexual reproduction, the species and their adaptive alleles can be replicated and propagated rapidly. This in turns allow the population to respond quickly to environmental changes. Asexually-reproducing populations also tend to share resources to reduce mortality risks (Callaghan, 1984; Doust, 1981; Hutchings, 1988; Klimeš et al., 1997; Rautiainen et al., 2004; Savini et al., 2008). With these advantages, it is not surprising to observe a great diversity of asexual reproduction methods in plants (de Meeûs et al., 2007). In particular, some plant species of the *Kalanchoë* genus reproduce asexually *via* plantlet formation (Garcês et al., 2007). Plantlet formation in *Kalanchoë* involves the emergence of plantlets from leaf notches of the mother leaf. The plantlet goes through embryo-like developmental stages to grow into a mini adult plant (plantlet) (Garcês et al., 2007). Different *Kalanchoë* species has different capability of plantlet formation (Garcês et al., 2007). There are species that do not make plantlets; make plantlets only upon stress induction; and make plantlets constitutively and upon stress inductions. There are also constitutive plantlet-forming species such as *Kalanchoë daigremontiana* (*K. daigremontiana*) which continuously produce plantlets in favourable conditions (Garcês and Sinha, 2009a; Garcês et al., 2007). The existence of different modes of plantlet formation strategies within the genus makes *Kalanchoë* species ideal for studying the evolution and mechanisms of plantlet formation (Garcês and Sinha, 2009a; Garcês et al., 2007).

The earliest molecular study showed that plantlet development involves embryogenesis and organogenesis (Garcês et al., 2007). Studies on a late embryogenesis gene, *LEAFY COTYLEDON 1* (*LEC1*) showed that even though *K. daigremontiana LEC1* (*KdLEC1*) is expressed in the seed embryo and asexual plantlets of *K. daigremontiana*, the protein is not functional (Garcês et al., 2007, 2014; Jo et al., 2019). Moreover, the loss of *KdLEC1* function is needed to bypass seed dormancy and allow formation of plantlets (Garcês et al., 2014). In the case of *SHOOTMERISTEMLESS* (*STM*) gene, a key regulator of organogenesis, *K. daigremontiana STM* (*KdSTM*) was expressed in *K. daigremontiana* shoot apical meristem (SAM), axillary buds and

plantlets from initiation stage to heart-like stage (Garcês et al., 2007). Suppression of *KdSTM* expression led to complete inhibition of plantlet formation (Garcês et al., 2007). Hence, it was speculated that *KdSTM* might be maintaining and establishing pluripotent cells at the leaf notches for plantlet development (Garcês et al., 2007). The most recent genetic study showed that *K. daigremontiana SUPPRESSOR OF CONSTANS OVEREXPRESSION 1* (*KdSOC1*), a flowering signal integrator, was expressed at the leaf notches prior to formation of pedestal which acts as a base for plantlet development (Garcês et al., 2007; Zhu et al., 2017). Attempt to generate transgenic *K. daigremontiana* plants with reduced *KdSOC1* through *in vitro* tissue culture resulted in formation of only few calli that developed into cotyledons (Zhu et al., 2017). Moreover, these cotyledons eventually dried out and failed to develop further (Zhu et al., 2017). Hence, it was proposed that *KdSOC1* is essential for *K. daigremontiana* somatic embryogenesis (Zhu et al., 2017). Overexpression of *KdSOC1* in *K. daigremontiana* also resulted in asymmetrical formation of plantlets along the leaf margin, without affecting plantlet morphology (Zhu et al., 2017). Taken together, these studies suggest that plantlet formation involve complex integration of embryogenesis, organogenesis and flowering pathways.

Apart from genetics regulation, embryogenesis, organogenesis and flowering induction in plants also depend on proper action of hormones such as auxin and cytokinin. During zygotic embryogenesis, auxin signalling is present from as early as the asymmetrical 2-cell embryo stage (Friml et al., 2003). Through PIN-FORMED 7 (PIN7) efflux transporters, auxin is transferred to and accumulates at the apical region of 2-cell to 8-cell embryo stage to specify the fate of embryo proper (Friml et al., 2003). Then, from 16-cell to 32-cell embryo stage, PIN7 relocates to reverse auxin flow from the apical to the basal region (Friml et al., 2003). With the aid of PIN1 and PIN4 efflux transporters, auxin flow is directed towards the upper suspensor cell which eventually develop into the RAM (Friml et al., 2002, 2003). In the case of the shoot apical meristem (SAM), a low auxin level is needed for its formation and maintenance (Shi et al., 2018; Zhang et al., 2017d). This was supported by the fact that increased auxin led to an enlarged SAM with defective stem cells (Shi et al., 2018; Zhang et al., 2017d). In contrast to the SAM, floral meristem is initiated as a lateral organ under high level of auxin (Galvan-Ampudia et al., 2020; Kwiatkowska, 2008; Reinhardt et al., 2000) of which accumulation and polar transport is again dependent on PIN1 (Okada et al., 1991). PIN1 is also in charge of auxin

gradient establishment for the initiation of axillary meristem (Wang et al., 2014a, 2014b). However, axillary meristem initiation requires a low auxin environment as restricted auxin supply through inhibitors or transporter mutant resulted in supernumerary axillary buds (Wang et al., 2014a, 2014b).

Auxin is also known to induce somatic embryogenesis (Wójcik et al., 2020), which is the likely mechanism of *Kalanchoë* plantlet initiation. To date, extensive studies on auxin-mediated somatic embryogenesis revealed similarities in auxin accumulation and function during zygotic embryogenesis. During early stages of zygotic embryogenesis and induction of somatic embryogenesis, there is an increase in endogenous auxin level in different plant species (Awada et al., 2019; Ayil-Gutiérrez et al., 2013; Cheng et al., 2016; Márquez-López et al., 2018; Michalczuk et al., 1992; Pasternak et al., 2002; Pescador et al., 2012; Ribnicky et al., 2002; Thomas et al., 2002; Vondrakova et al., 2018). In addition, most of the *YUCCA* (*YUC*) auxin biosynthesis enzymes associated with somatic embryogenesis are active in zygotic embryogenesis (Bai et al., 2013; Radoeva et al., 2019; Robert et al., 2015b; Wickramasuriya and Dunwell, 2015; Wójcikowska et al., 2013). Majority of *AUXIN RESPONSE FACTOR* (*ARF*) and *AUXIN/INDOLE-3-ACETIC ACID* (*Aux/IAA*) genes were also found to be active during *Arabidopsis* zygotic and somatic embryogenesis (Gliwicka et al., 2013; Rademacher et al., 2011). Similar to zygotic embryogenesis, PIN1 is also needed to establish auxin gradients during somatic embryogenesis (Friml et al., 2003; Liu et al., 1993; Su et al., 2009). The importance of polar auxin transport is evident from development of abnormal zygotic and somatic embryo when auxin transport is disturbed (Abrahamsson et al., 2012; Hadfi et al., 1998).

Early research identified that a high cytokinin level induces formation of shoots from *in vitro* culturing of plant tissues (Skoog and Miller, 1957). However, mutants with defective cytokinin signalling still develop a shoot meristem, leading to debates about whether cytokinin is essential for proper embryo shoot formation (Miyawaki et al., 2004; Riefler et al., 2006). This is in contrast to induction of lateral root primordium trans-differentiation into shoot meristem through exogenous cytokinin treatment (Chatfield et al., 2013; Rosspopoff et al., 2017). Recent studies also revealed that wounding of tissues up-regulates cytokinin biosynthesis and signalling, that then triggers cell proliferation and callus formation (Ikeuchi et al., 2017; Iwase

et al., 2017, 2018). In addition, the role of cytokinin in post-embryonic shoot meristem homeostasis also remains evident from aberrant SAM formation in cytokinin deficient mutants (Chickarmane et al., 2012; Kurakawa et al., 2007; Leibfried et al., 2005; Werner et al., 2003; Yanai et al., 2005). From these studies, we now know that during post-embryonic SAM homeostasis, cytokinin action is achieved through binding of cytokinin response regulator proteins to the *WUSCHEL* (*WUS*), a meristem master regulator (Meng et al., 2017; Wang et al., 2017; Xie et al., 2018). Cytokinin activity upregulates *WUS* expression in the organizing centre of the SAM to maintain stem cell niche needed for organ formation (Wang et al., 2017).

Apart from maintaining the stem cell niche for meristems, cytokinin was shown to spatially and temporally regulate SAM organ initiation through the action of cytokinin signalling inhibitor, PSEUDO-HISTIDINE PHOSPHOTRANSFER PROTEIN 6 (PHP6) (Besnard et al., 2014a). In comparison to other HISTIDINE-CONTAINING PHOSPHOTRANSFER PROTEIN (HP) paralogs, such as Arabidopsis PHOSPHOTRANSFER PROTEIN 1-5 (AHP1-5), PHP6 is non-functional; substitution in one of its conserved histidine residues causes inability of the PHP6 protein to be phosphorylated and therefore relay cytokinin signalling (Mähönen et al., 2006; Suzuki et al., 2000). Through the action of PHP6, cytokinin signalling is spatially and temporally confined to regulate bilateral symmetry of vascular tissues and lateral root initiation (Mähönen et al., 2006; Moreira et al., 2013). Moreover, cytokinin was also shown to control longitudinal size of root meristem by repressing auxin activity (Dello Ioio et al., 2008; Moubayidin et al., 2010). Cytokinin is also involved in flower development, specifically in development of floral meristem, gynoecium and female gametophyte (Wybouw and Rybel, 2019). During flower development, cytokinin induces expression of *AGAMOUS* (*AG*), a floral homeotic gene which terminates meristematic activity in the centre of floral meristem and ultimately leads to specification of carpel identity (Rong et al., 2018). The integration of *AG* and another floral homeotic gene *APETALA2* (*AP2*) is also necessary for flower determinacy (Liu et al., 2014). Later during the gynoecium development, AG and PHP6 activity are again observed, controlling cytokinin signalling to ensure that cytokinin level is sufficient for proper proliferation of gynoecium medial tissues (Durán-Medina et al., 2017b; Marsch-Martínez et al., 2012; Müller et al., 2017; Ó'Maoiléidigh et al., 2018; Reyes-Olalde et al., 2017). Within the gynoecium, cytokinin is employed to specify female gametophyte cell fates (Liu et al., 2017; Yuan et al., 2016). This is

achieved *via* activation or repression of *CYTOKININ INSENSITIVE* (*CKI*) gene in response to the presence or absence of cytokinin levels (Leibfried et al., 2005; Liu et al., 2017; Yuan et al., 2016).

Early studies on the role of auxin and cytokinin in plantlet formation were dependent on the quantification of auxin and cytokinin in leaves or observation of changes in timing and morphology of plantlet development upon external application of auxin and cytokinin (Heide, 1965; Henson and Wareing, 1977; Houck and Rieseberg, 1983; Kulka, 2006; Yazgan and Vardar, 1977). The earliest study showed that auxin has an inhibitory effect on *K. daigremontiana* plantlet formation (Heide, 1965). When young leaves were treated with auxin, formation of leaf serration was abolished but treated mature leaves displayed reduced plantlet number and delayed plantlet formation (Heide, 1965). However, this inhibition on plantlet formation by auxin appears to be concentration-dependent. Whist external application of auxin at low concentrations on detached leaves stimulated plantlet formation, application of auxin at higher concentrations had an inhibitory effect on plantlet formation (Yazgan and Vardar, 1977). The impact of auxin application on plantlet formation also depended on whether the plants were grown under long or short day condition (Heide, 1965; Yazgan and Vardar, 1977). The same concept applies to the effect of cytokinin on plantlet formation as some studies showed that cytokinin treatment of *K. daigremontiana* and *K. pinnata* plants grown under long-day condition stimulated plantlet formation (Heide, 1965; Houck and Rieseberg, 1983; Yazgan and Vardar, 1977). When the same treatment was performed on *K. daigremontiana* grown under short-day condition, the treated plants produced plantlets at similar rate as long-day plants (Heide, 1965). Quantification of cytokinin in leaves of plants transferred from short-day to long-day condition also revealed a sharp rise in cytokinin, which eventually declined (Henson and Wareing, 1976). These results suggest that cytokinin triggers the initiation or increase the rate of plantlet formation. However, the opposite effect was observed; external application of cytokinin on detached *K. daigremontiana* leaves decreased the number of plantlets formed (Yazgan and Vardar, 1977). The inhibitory effect of cytokinin on plantlet formation was also observed on detached leaves of *K. marnierianum*, a species that forms plantlet upon leaf detachment or aging (Kulka, 2006). Based on these results, the role of auxin and cytokinin in plantlet formation is yet to be clearly illustrated.

This study aims to study whether auxin and cytokinin is involved in plantlet initiation and formation and what is the specific endogenous auxin and cytokinin distribution that contributes to the process. To do so, we generated *K. daigremontiana* synthetic cytokinin sensor *TCSn*::*GUS* reporter lines and synthetic auxin response *DR5*::*H2B-GFP* reporter lines to observe localisation of cytokinin and auxin expression respectively across different stages of plantlet development. *PIN1*::*PIN1-GFP* transgenic plants were also created to visualise localisation of auxin efflux transporter PIN1 and study transport of auxin during plantlet formation. This study also detailed the search for a homologous cytokinin signalling inhibitor PHP6 protein in *K. daigremontiana*. Our data suggests that HP paralogs and PHP proteins in *Kalanchoe* might have evolved independently from a primitive group of HP as none of the putative HP sequences clade with existing HP paralogs from various angiosperm species. We isolated a putative *KdaHP* gene in which its *Kalanchoë* homologs exhibited the highest similarity to existing HP paralogs. *KdaHP* gene showed high expression across all stages of plantlet formation based on RNA-sequencing analysis but this was inconsistent with expression data from quantitative real-time PCR (qRT-PCR). This gene might be important for plantlet formation as reduced expression of *KdaHP* caused a range of irregular plantlet phenotypes. These phenotypes might be explained by changes in expression an auxin biosynthesis gene, *KdaYUC1*, suggesting complex auxin-cytokinin crosstalk in regulating plantlet formation. *KdaWUS* and *KdaCLV2* expression were also affected in *KdaHP* antisense plants, providing further evidence of organogenesis recruitment during plantlet development. This study also shows similarity in auxin and cytokinin activity during plantlet development and *Arabidopsis* embryogenesis, suggesting mechanism in zygotic embryogenesis were reused for plantlet formation. There were novel observations such as the expression of auxin efflux transporter PIN1 during the plantlet initiation and cytokinin activity during early plantlet formation. Further investigation into the evolution of cytokinin signalling inhibitor, function of cytokinin in plantlet development and directionality transport of auxin are needed to provide more detailed explanation regarding hormonal control of plantlet formation. Nonetheless, this study has shed light onto induction of somatic embryogenesis by endogenous auxin and cytokinin activity.

4.3. **Materials & Methods**

4.3.1. Sequence alignment & phylogenetic analysis

All sequences were downloaded from NCBI or Phytozome version 12 and aligned using ClustalX version 2.1. The final figure for multiple sequence alignment was created using Jalview 2.11.1.2. The colour scheme used for alignment of protein sequence can be found here: http://www.jalview.org/help/html/colourSchemes/clustal.html. The percentage of sequence identity is calculated using Sequence Identity And Similarity calculator (SIAS) at http://imed.med.ucm.es/Tools/sias.html with default settings and mean length of sequences. Phylogenetic analysis was performed using RAxML Black Box, which can be accessed at https://raxml-ng.vital-it.ch/#/. The default settings with automated bootstrapping were used to generate all phylogenetic trees. The phylogenetic trees were visualised and edited using Dendroscope version 3.7.2.

Table 4.1 The names of species, genes or proteins used for phylogenetic analyses.
Each symbol represents its corresponding sequence identifier. HP, HISTIDINE-CONTAINING PHOSPHOTRANSFER PROTEIN; PHP, PSEUDO HISTIDINE-CONTAINING PHOSPHOTRANSFER PROTEIN; YPD; PHOSPHORELAY INTERMEDIATE PROTEIN

Symbol	Species	Gene/ Protein	Accession number/Transcript ID
AcomPHP6	*Ananas comosus*	PHP6	XP_020098465.1, XM_020242876.1
AthHP1	*Arabidopsis thaliana*	HP1	NP_188788.1, NM_113046.4
AthHP2	*Arabidopsis thaliana*	HP2	NP_189581.1, NM_113860.4
AthHP3	*Arabidopsis thaliana*	HP3	NP_001318703.1, NM_001344287.1
AthHP4	*Arabidopsis thaliana*	HP4	NP_566544.1, NM_112507.1
AthHP5	*Arabidopsis thaliana*	HP5	NP_563684.1, NM_100225.3
AthPHP6	*Arabidopsis thaliana*	PHP6	NP_178127.2, NM_106659.3
AtrHP1	*Amborella trichopoda*	HP1	XP_006830280.2, XM_006830217.3
AtrHP2	*Amborella trichopoda*	HP2	XP_011625967.1, XM_011627665.2
AtrHP4	*Amborella trichopoda*	HP4	XP_006853683.1, XM_006853621.3
AtrPHP6	*Amborella trichopoda*	PHP6	XP_006842046.1, XM_006841983.2
AtrYPD1	*Amborella trichopoda*	YPD1	ERM97696.1, KI395898.1
CmiPHP6	*Cinnamomum micranthum*	PHP6	RWR77400.1, QPKB01000002.1
EguHP1	*Erythranthe guttata*	HP1	XP_012858512.1, XM_013003058.1
EguHP4	*Erythranthe guttata*	HP4	XP_012857943.1, XM_013002489.1
EguHP5	*Erythranthe guttata*	HP5	XP_012836634.1, XM_012981180.1
EguPHP6	*Erythranthe guttata*	PHP6	XP_012856268.1, XM_013000814.1
KdaHP	*Kalanchoë daigremontiana*	HP	MW682858
KfeHP0018	*Kalanchoë fedtschenkoi*	HP	Kaladp0087s0018.1
KfeHP0029	*Kalanchoë fedtschenkoi*	HP	Kaladp0021s0029.1
KfeHP0030	*Kalanchoë fedtschenkoi*	HP	Kaladp0021s0030.1
KfeHP0039	*Kalanchoë fedtschenkoi*	HP	Kaladp0020s0039.1

KfeHP0100	*Kalanchoë fedtschenkoi*	HP	Kaladp0030s0100.1
KfeHP0101	*Kalanchoë fedtschenkoi*	HP	Kaladp0030s0101.1
KfeHP0108	*Kalanchoë fedtschenkoi*	HP	Kaladp0058s0108.1
KfeHP0217	*Kalanchoë fedtschenkoi*	HP	Kaladp0092s0217.1
KfeHP0256	*Kalanchoë fedtschenkoi*	HP	Kaladp0024s0256.1
KfeHP0423	*Kalanchoë fedtschenkoi*	HP	Kaladp0011s0423.1
KfeHP0429	*Kalanchoë fedtschenkoi*	HP	Kaladp0045s0429.1
KfeHP0512	*Kalanchoë fedtschenkoi*	HP	Kaladp0095s0512.1
KlaHP0002	*Kalanchoë laxiflora*	HP	Kalax.1839s0002.1
KlaHP0003	*Kalanchoë laxiflora*	HP	Kalax.1071s0003.1
KlaHP0007	*Kalanchoë laxiflora*	HP	Kalax.0280s0007.1
KlaHP0011	*Kalanchoë laxiflora*	HP	Kalax.0454s0011.1
KlaHP0014	*Kalanchoë laxiflora*	HP	Kalax.0587s0014.1
KlaHP0015	*Kalanchoë laxiflora*	HP	Kalax.0917s0015.1
KlaHP0016	*Kalanchoë laxiflora*	HP	Kalax.0478s0016.1
KlaHP0017	*Kalanchoë laxiflora*	HP	Kalax.0112s0017.1
KlaHP0021	*Kalanchoë laxiflora*	HP	Kalax.0258s0021.1
KlaHP0022	*Kalanchoë laxiflora*	HP	Kalax.0028s0022.1
KlaHP0023	*Kalanchoë laxiflora*	HP	Kalax.0105s0023.1
KlaHP0045	*Kalanchoë laxiflora*	HP	Kalax.0038s0045.1
KlaHP0049	*Kalanchoë laxiflora*	HP	Kalax.0102s0049.1
KlaHP0058	*Kalanchoë laxiflora*	HP	Kalax.0100s0058.1
KlaHP0115	*Kalanchoë laxiflora*	HP	Kalax.0006s0115.1
KlaHP0235	*Kalanchoë laxiflora*	HP	Kalax.0235s0021.1
NcoPHP6	*Nymphaea colorata*	PHP6	XP_031488814.1, XM_031632954.1
NnuHP1	*Nelumbo nucifera*	HP1	XP_010242575.1, XM_010244273.2
NnuPHP6	*Nelumbo nucifera*	PHP6	XP_010250154.1, XM_010251852.2
NnuYPD1	*Nelumbo nucifera*	YPD1	XP_010242575.1, XM_010244273.1
OsaHP1	*Oryza sativa*	HP1	XP_015648297.1, XM_015792811.2
OsaHP2	*Oryza sativa*	HP2	XP_015611768.1, XM_015756282.2
OsaPHP1	*Oryza sativa*	PHP1	BAF06135.2, AP008207.2
OsaPHP2	*Oryza sativa*	PHP2	XP_015637666.1, XM_015782180.2
OsaPHP5	*Oryza sativa*	PHP5	XP_015639479.1, XM_015783993.2
PpaHP2	*Physcomitrium patens*	HP2	PNR29348, ABEU02000023.1
PpaYPD1	*Physcomitrium patens*	YPD1	PNR59838.1, ABEU02000002.1
PsiPHP6	*Picea sitchensis*	PHP6	ABK25839.1, EF086581.1
PtrHP1	*Populus trichocarpa*	HP1	XM_002314406.3, XP_002314442.1
PtrHP2/3	*Populus trichocarpa*	HP2/3	XM_002309091.2, XP_002309127.1
PtrHP4	*Populus trichocarpa*	HP4	XM_024595858.1, XP_024451626.1
PtrHP5	*Populus trichocarpa*	HP5	XM_002323530.2, XP_002323566.1
PtrPHP6	*Populus trichocarpa*	PHP6	XM_002298214.3, XP_002298250.1
PtrYPD1	*Populus trichocarpa*	YPD1	XP_006382659.1, XM_006382597
SmoYPD1	*Selaginella moellendorffii*	YPD1	XP_002965866, XM_002965820.2
VviHP1	*Vitis vinifera*	HP1	XM_002278375.4, XP_002278411.1
VviHP2/3	*Vitis vinifera*	HP2/3	XM_002272117.4, XP_002272153.2
VviHP4	*Vitis vinifera*	HP4	XM_002283650.3, XP_002283686.1
VviHP5	*Vitis vinifera*	HP5	XM_002272117.4, XP_002272153.2

VviPHP6	*Vitis vinifera*	PHP6	XM_002265407.3, XP_002265443.1
VviYPD1	*Vitis vinifera*	YPD1	XP_002265307.1, XM_002265271.4
ZmaHP1	*Zea mays*	HP1	ONM04120, CM007647.1
ZmaHP2	*Zea mays*	HP2	NP_001104850.1, NM_001111380.3
ZmaHP3	*Zea mays*	HP3	AQK51658, CM000780.4
ZmaHP5	*Zea mays*	HP5	ACG39348.1, EU967230.1
ZmaHP6	*Zea mays*	PHP6	NP_001147413.1, NM_001153941.1
ZmaPHP2	*Zea mays*	PHP2	XP_008649423.1, XM_008651201.2

4.3.2. Plant materials

Wild-type *K. daigremontiana* plants were cultivated at 23^{o}C with a long day condition (16h light/8h dark) in a growth chamber. All plant materials were harvested using sterile razor blades.

4.3.3. RNA-sequencing and expression analysis

Total RNAs of plantlets at different developmental stages were extracted using RNeasy® Plant Mini kit (Qiagen, UK) according to the manufacturer's protocol with slight modifications. For each 100 mg plant materials, 10 mg polyvinylpyrrolidone (PVP) (molecular weight 40,000) was added to RLC buffer and incubated at 56 ^{o}C before use. After mixing disrupted the plant materials with RLC buffer, the mixture was incubated 56 ^{o}C before proceeding to the subsequent steps. 1 µg of purified RNA samples were sequenced using Sanger sequencing by Illumina HiSeq 2000 technology at The University of Manchester Sequencing Facility. Prior to cDNA synthesis using Tetro cDNA synthesis kit (Bioline, UK), RNA was treated with RQ1 RNase-free DNase (Promega, UK). Reverse transcriptase-PCR (RT-PCR) were performed using Q5® High-Fidelity DNA Polymerase (New England Biolabs, USA) and BIOTAQ™ DNA Polymerase in a T100™ Thermal Cycler (Biorad, UK). The reaction mixture and conditions used were as described in the BIOTAQ polymerase datasheet. *Kda18s* and *KdaHP* were amplified at 58 ^{o}C with 32 cycles whereas the other genes were amplified at 56 ^{o}C with 40 cycles. SensiFAST SYBR® Hi-ROX Mix (Bioline, UK) and StepOne™ Real-Time PCR System (Applied Biosystems, UK) was used for performing quantitative real-time PCR (qRT-PCR). StepOne™ and StepOnePlus™ Software v4.3 (Thermo Fisher Scientific, UK) was used for template design and analysis. An annealing temperature of 60 °C was used, with 40 cycles and *K. daigremontiana GLYCERALDEYHDE-3-PHOSPHATE DEHYDROGENAS* (*KdaGAPDH*) as a reference gene.

GraphPad Prism 8 was used to generate all the graphs and to perform non-parametric Kruskal-Wallis statistical tests and Dunn's multiple comparison tests.

Table 4.2 List of primers used for reverse transcriptase PCR and quantitative real-time PCR.
Expected band size for the PCR products amplified using either cDNA or genomic DNA for each gene and its corresponding primers used for semi-quantitative PCR and quantitative real-time PCR. Kda, *K. daigremontiana*; *GAPDH, GLYCERALDEYHDE-3-PHOSPHATE DEHYDROGENASE; HP*, *PUTATIVE PSEUDO HISTIDINE-CONTAINING PHOSPHOTRANSFER PROTEIN*; *STM*, SHOOT *MERISTEMLESS*; *LEC1*, *LEAFY COTYLEDON 1*; *WUS*, *WUSCHEL*; *CLV1*, *CLAVATA1*; *CLV2*, *CLAVATA2*; *YUC1*, *YUCCA1*; *TPL*, *TOPLESS.*

Gene	5'-3' primer sequence	With cDNA (bp)	With gDNA (bp)
KdaGAPDH	GGAGCAGAGATAACAACCTTC TCCATTCATCAACACAGACTAC	290	290
Kda18s	AGAAACGGCTACCACATCCAAG GACTCATTGAGCCCGGTATTGT	104	104
KdaHP	ACTTCGTGATGGAGGTGGTG GTATTCGCTGCTGAGGACTTG	274	1073
KdaSTM	GGATCAGTTCATGGAGGCTTAC CTTGAACTGGGACTCAATCCTC	112	112
KdaLEC1	GTCGGAGTATATCGGCTTCATC TGTATCGGTGCAGGTACAGAGT	135	135
KdaWUS	CCTCCAAATACTCAGACATCAACAA CATCCCTCCTTTAGCCCAAC	146	930
KdaCLV1	ATTGCTCTCCGCCGATTCT CTTCCGACCCGTTATCAGC	248	339
KdaCLV2	GGTGTTTCCAGTTACTCGCTTTG TTGGCAATGGCGTCGTTC	217	217
KdaYUC1	GAGCATTCAAGAAACAGAGCATC GAAGTTCATCAGCGGGAGC	277	277
KdaTPL	GACGACATTTATGCCTCCTCC AGCCCCTGATGAAACTAGAACA	211	302

4.3.4. Genotyping analysis

For genotyping the *KdaHP* antisense plants, the primers 5'-GTGGTCTCTGGTGGC TGCTGCCCTTCAACTG-3' and 5'-GTGGTCTCAAGCGGGTGATCTGGATTTTAGTACTGG-3' were used. The primers used to amplify *NPTII* were 5'- CACAACAGACAATCGGCTGC-3' and 5'-GCACGAGGAAGCGGTCAG-3'. The genomic DNA used for genotyping and as control samples was extracted following the protocol "Quick DNA Prep for PCR" from (Weigel and Glazebrook, 2002). The genotyping reaction were performed using Q5® High-Fidelity DNA Polymerase (New England Biolabs, USA) and BIOTAQ™ DNA Polymerase at 56 ^{o}C in a T100™ Thermal Cycler (Biorad, UK). The reaction mixture and conditions used were as described in the BIOTAQ

polymerase datasheet. All electrophoresis gels were visualised using ChemiDoc™ XRS+ Imager (Bio-Rad, UK) and Image Lab 5.1 (Bio-Rad, UK).

4.3.5. Making transgenic plants

KdaHP was isolated from genomic DNA of wild-type *K. daigremontiana* using primers 5'-GTGGTCTCTAAGCCGACTACACCAACTCCCTC-3' and 5'- GTGGTCTCTGGTGGCTGCTGCCCTTC AACTG-3'. The genomic DNA was extracted following the protocol (Garcês and Sinha, 2009e). The 249 bp *KdaHP* sequence was isolated using Q5® High-Fidelity DNA Polymerase (New England Biolabs, USA) at the melting temperature 58 ^{o}C. The reaction mixture and conditions used were as described in the Q5 polymerase datasheet. The primers were designed using NCBI Primer-Blast and Premier Biosoft Net Primer (Premier Biosoft, USA) based on the sequences from *K. fedtschenkoi* and *K. laxiflora.* The sequences were obtained from Phytozome v12.1 (JGI, USA). The amplified sequence was ligated into pGEM®-T Easy (Promega, USA) after gel extraction using Nucleospin® gel and PCR Clean-Up Kit (Macherey-Nagel, Germany). The sequence of synthetic promoter TCSn was obtained from Tao et al., 2017 and synthesised by GENEWIZ®, Germany. The *35S*::antisense-*KdaHP* construct was formed by ligating *Kda*HP antisense sequence with cauliflower mosaic virus (CaMV) 35S promoter and terminator into a modified *pBI121* vector. The *TCSn*::*GUS* cytokinin reporter construct were formed by ligating the *TCSn* promoter sequence with *GUS* coding region and *Nopaline Synthase* (*Nos*) Terminator into a modified *pBI121* vector. The *DR5*::*GFP* auxin reporter construct were formed by ligating the *DR5* promoter sequence with GFP-tagged histone H2B coding sequence, and *Nopaline Synthase* (*Nos*) Terminator into a modified *pBI121* vector. All constructs were formed *via* golden gate assembly, then transformed into *Escherichia coli* strain *DH5α*. The sequences of each construct were checked before transforming into *Agrobacterium tumefaciens* strain *LBA4404* through electroporation. The transformation of *K. daigremontiana* plants was performed with reference to the protocol from (Garcês and Sinha, 2009d).

4.3.6. Phenotype analysis

GUS staining was performed using GUS staining solution with final concentration of 100 mM Sodium phosphate buffer pH 7.2, 10 mM EDTA pH 8.0, 0.1% Triton X-100, 1 mM Potassium Ferricyanide, 1 mM Potassium Ferrocyanide and 2 mM X-gluc. All GUS staining images were taken using Leica S8 APO microscope (Leica Microsystems, Germany) with a GX-CAM-Eclipse camera (GT Vision, UK) attached. All photographs of live plants were taken using an iPhone 8 or using Leica S8 APO microscope (Leica Microsystems, Germany) with a GX-CAM-Eclipse camera (GT Vision, UK) attached. All graphs for quantitative analysis of transgenic plant phenotypes were generated using GraphPad Prism 8. The same software was used to perform non-parametric Kruskal-Wallis statistical tests and Dunn's multiple comparison tests. All fluorescent *DR5*::*GFP* images and *PIN1*::*PIN1-GFP* images (in Fig. 5.6A-F) were taken with Leica M205 FA Stereo fluorescence microscope (Leica Microsystems, Germany). *PIN1*::*PIN1-GFP* images (Fig. 5.6G-O) were taken with Leica SP8 upright confocal laser scanning microscope (Leica Microsystems, Germany).

4.4. **Results**

4.4.1. *Kalanchoë* histidine-containing phosphotransfer proteins (HP) evolved differently

To study the importance of cytokinin during plantlet formation, we attempted to generate transgenic *K. daigremontiana* with reduced expression of cytokinin signalling inhibitor, pseudo histidine-containing phosphotransfer protein 6 (PHP6). To identify PHP6 homolog in *Kalanchoë*, a phylogenetic tree consisting predicted HPs from *K. fedtschenkoi* and *K. laxiflora* and known HPs from a few angiosperm species were built (Fig. 4.1). The nucleotide tree showed a group of *Kalanchoë* genes, *KfeHp0423*, *KlaHp0021* and *KlaHp0023* sharing a common ancestor with *PHP6* genes of other angiosperm species, indicating that these genes might be the homologous *PHP6* gene in *Kalanchoë* (Fig. 4.1A). However, the same evolutionary relationship was not observed in the protein tree (Fig. 4.1B). The protein tree showed the same group of proteins KfeHP0423, KlaHP0021 and KlaHP0023 belong to the same clade as other groups of *Kalanchoë* HP and most importantly with all HP1, HP2, HP3, HP5, PHP6 from other angiosperm species. This latter observation was also consistent with comparative sequence analyses of all the nucleotide and protein sequences used for the phylogenetic analyses. Sequence analyses showed that among the *Kalanchoë* sequences, both nucleotide and protein sequences of *KfeHp0423*, *KlaHp0021* and *KlaHp0023* shared the highest sequence similarity, identity and Global Similarity (Blosum62) analyses to HP1, HP2, HP3, HP5, PHP6 of other angiosperm species. This suggests that perhaps these HP paralogs did not diverge or evolve from this group of *Kalanchoë* sequences.

To test our hypothesis that HP paralogs may not diverge in the *Kalanchoë* clade, phylogenetic trees encompassing these all HP *Kalanchoë* sequences in Fig. 4.1 and HP homologs from other angiosperm species were generated (Fig. 4.2). The nucleotide sequences of *KfeHp0423*, *KlaHp0021* and *KlaHp0023* were in the same clade as *VviYPD1* and *PtrYPD1* (Fig. 4.2A) but the protein sequences did not group with any other HP sequences (Fig. 4.2B). According to protein blast of these protein sequences, the protein sequences with the highest scores were signal transduction histidine kinase of *Macleaya cordata* and HP1 and HP1-like proteins in other plant species such as *Ricinus communis*, *Quercus suber* and *Carica papaya*.

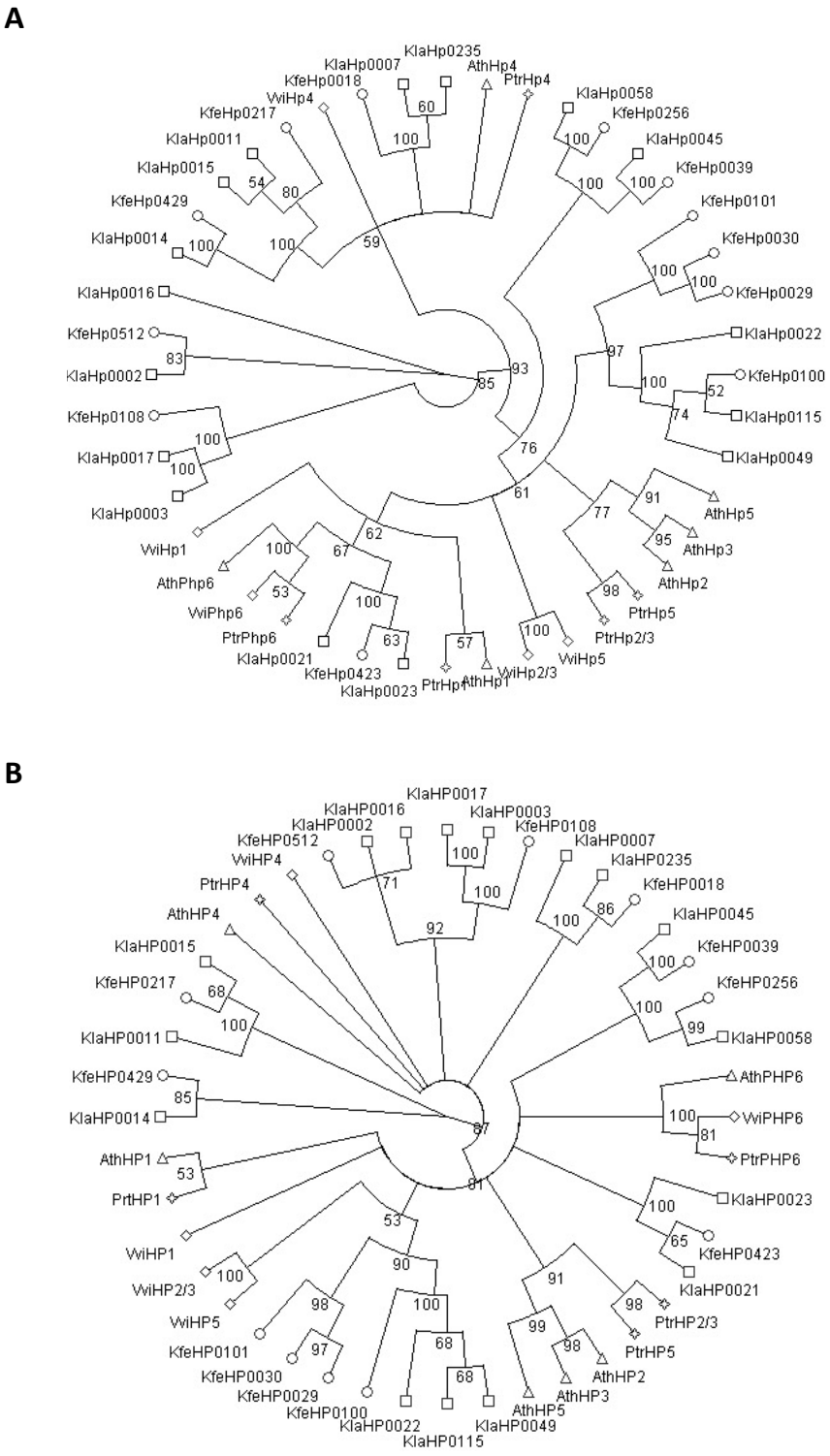

Figure 4.1 Phylogeny of full-length nucleotide and amino acid sequences of histidine-containing phosphotransfer proteins (HP) from *Kalanchoë* and three other angiosperm species.

(A) Nucleotide tree and (B) protein tree obtained using maximum-likelihood estimate model with 0.03 bootstrapping cutoff value. A group of potential homologous pseudo histidine-containing phosphotransfer proteins (PHP6) in *Kalanchoë* is highlighted in grey. Number on the edge represents bootstrap values. Edges with bootstrap values less than 50 were contracted. Each shape at the terminal node corresponds to a specific species. Ath, *Arabidopsis thaliana* (triangle); Kfe, *Kalanchoë fedtschenkoi* (circular); Kla, *Kalanchoë laxiflora* (rectangle); Ptr, *Populus trichocarpa* (star); Vvi, *Vitis vinifera* (diamond).

A

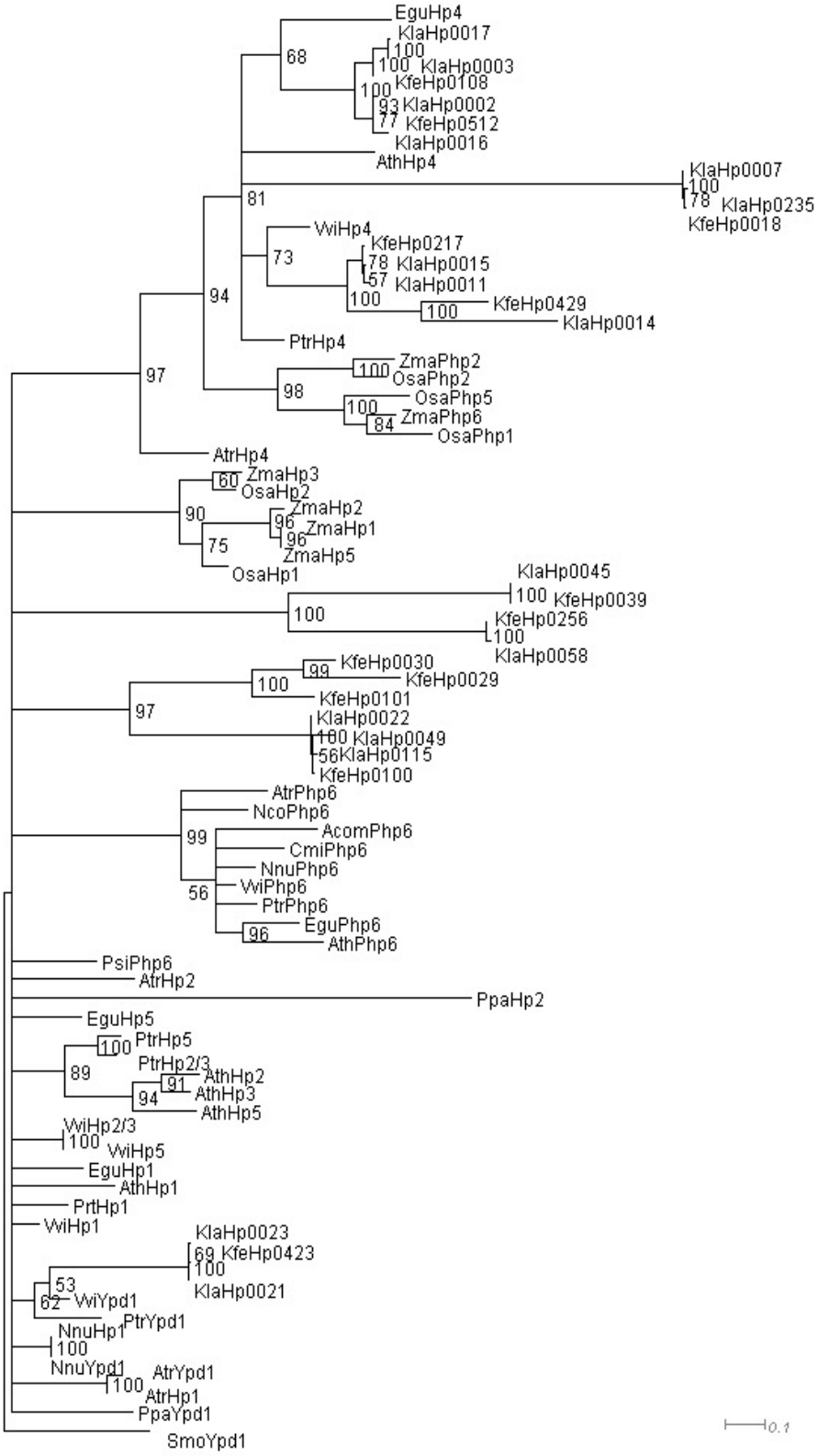
EguHp4
KlaHp0017
68
100
100 KlaHp0003
100 KfeHp0108
93 KlaHp0002
77 KfeHp0512
KlaHp0016
AthHp4
KlaHp0007
100
78 KlaHp0235
KfeHp0018
81
VviHp4
73
KfeHp0217
78 KlaHp0015
57 KlaHp0011
100
100 KfeHp0429
KlaHp0014
94
PtrHp4
97
100 ZmaPhp2
OsaPhp2
98
OsaPhp5
100
84 ZmaPhp6
OsaPhp1
AtrHp4
60 ZmaHp3
OsaHp2
90
ZmaHp2
96 ZmaHp1
96
75
ZmaHp5
OsaHp1
KlaHp0045
100 KfeHp0039
100
KfeHp0256
100
KlaHp0058
99 KfeHp0030
100
KfeHp0029
KfeHp0101
97
KlaHp0022
100 KlaHp0049
56KlaHp0115
KfeHp0100
AtrPhp6
NcoPhp6
99
AcomPhp6
CmiPhp6
NnuPhp6
56
VviPhp6
PtrPhp6
EguPhp6
96
AthPhp6
PsiPhp6
AtrHp2
PpaHp2
EguHp5
100 PtrHp5
89
PtrHp2/3
91 AthHp2
94
AthHp3
AthHp5
VviHp2/3
100 VviHp5
EguHp1
AthHp1
PrtHp1
VviHp1
KlaHp0023
69 KfeHp0423
100
53
62 VviYpd1
KlaHp0021
PtrYpd1
NnuHp1
100
NnuYpd1
100 AtrYpd1
AtrHp1
PpaYpd1
SmoYpd1
0.1

B

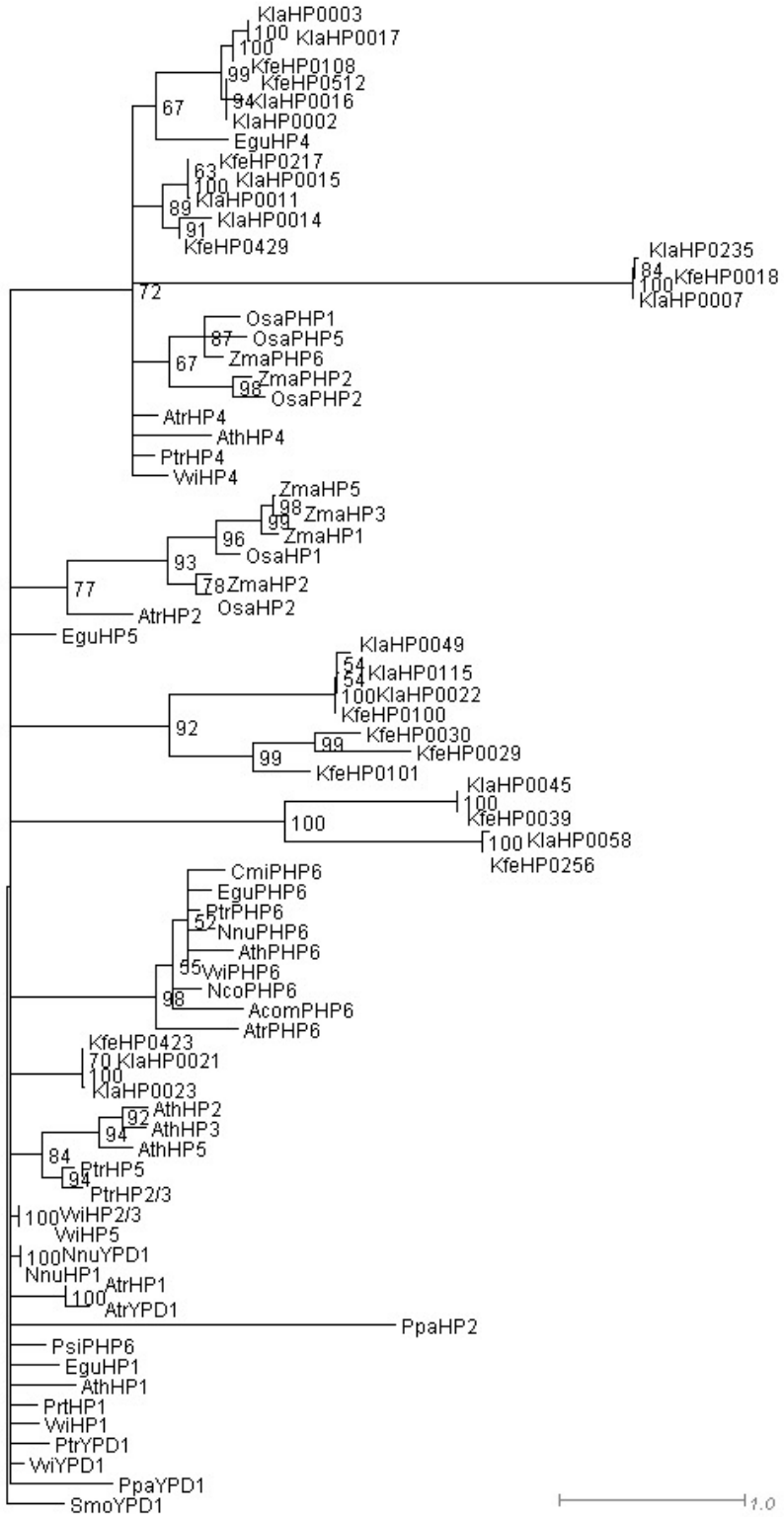

Figure 4.2 Phylogeny of nucleotide and amino acid sequences of histidine-containing phosphotransfer proteins (HP) from *Kalanchoë* and HP paralogs from other angiosperm species.

(A) Gene tree and (B) protein tree obtained using maximum-likelihood estimate model with 0.03 bootstrapping cutoff value. Grey-highlighted region shows a group of potential homologous *Kalanchoë* pseudo histidine-containing phosphotransfer proteins (PHP6). Number on the edge represent bootstrap values. Edges with bootstrap values less than 50 were contracted. Length of the edges represents evolutionary distance.

Phylogenetic analysis of *Kalanchoë* HPs showed that there was no clear distinction of HP paralogs in *Kalanchoë* but high similarity of KfeHP0423, KlaHP0021 and KlaHP0023 nucleotide and protein sequences to other HP paralogs suggest that this group of genes might be involved in some elements of cytokinin signalling. Compared to other putative *Kalanchoë* HP sequences, KfeHP0423, KlaHP0021 and KlaHP0023 also shared the highest sequence identity and similarity to AthPHP6, VviPHP6 and PtrPHP6. Hence, we decided to isolate and study the function of *K. daigremontiana* HP that is homologous to KfeHP0423, KlaHP0021 and KlaHP0023. A 222 bp nucleotide sequence was isolated from *K. daigremontiana* (*KdaHP*) and aligned with the sequences at the same region from *KfeHp0423*, *KlaHp0021* and *KlaHp0023* (Fig. 4.3A). Between these sequences, only 3 out of 222 nucleotide bases were not conserved. The *KdaHP* nucleotide sequence shared very high sequence similarity of 98.65 % to *KlaHp0021*, 99.1 % to *KfeHp0423* and 99.55 % to *KlaHp0021* (Fig. 4.3C). When the nucleotide sequence was translated to amino acid sequence, KdaHP exhibited one amino acid difference compared to other *Kalanchoë* sequences (Fig. 4.3B). This difference also translated into a 98.64 % amino acid sequence similarity compared to KfeHP0423, KlaHP0021 and KlaHP0023 (Fig. 4.3D). After the sequence was isolated, these *Kalanchoë* HP sequences were aligned with known HP and PHP paralogs in selected angiosperm sequences (Fig. 4.3E). This analysis was performed to examine whether these *Kalanchoë* HP sequences contain histidine at the canonical phosphorylation site as PHP6 is known to lack this conserved histidine, which caused its inability to accept a phosphoryl group (Mähönen et al., 2006). The multiple sequence alignment showed that all HP paralogs contain a histidine at this site, whereas all PHPs did not, apart from ZmaPHP2 (Fig. 4.3E).

A

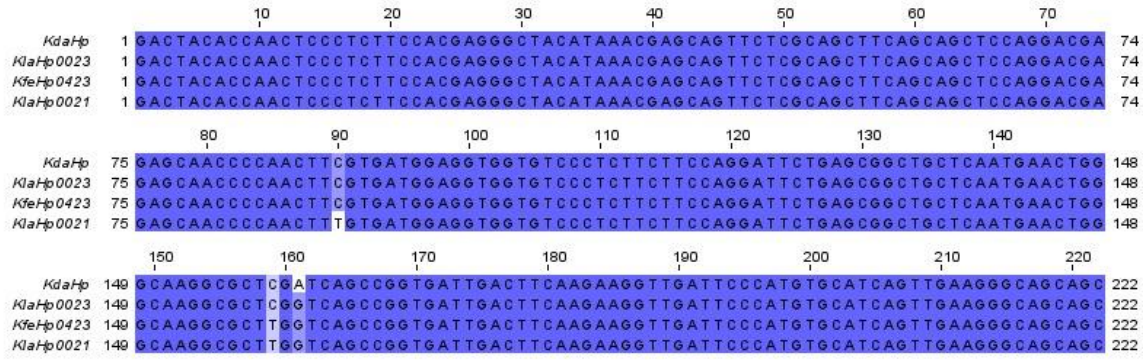

B

C

	Kfe	*Kla21*	*Kla23*	*Kda*
Kfe	100			
Kla21	99.55	100		
Kla23	99.55	99.1	100	
Kda	99.1	98.65	99.55	100

D

	Kfe	Kla21	Kla23	Kda
Kfe	100			
Kla21	100	100		
Kla23	100	100	100	
Kda	98.64	98.64	98.64	100

E

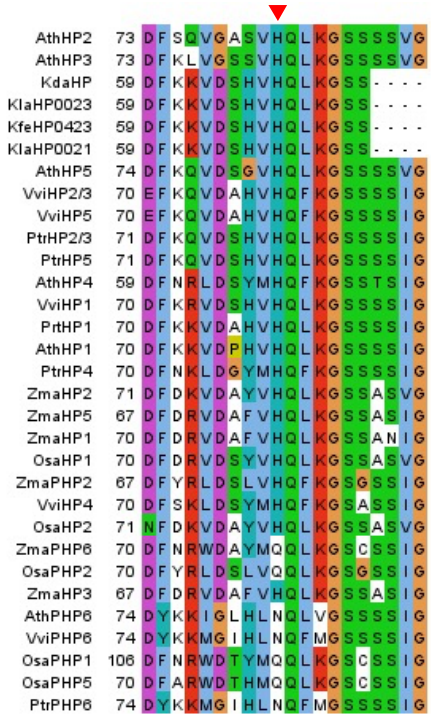

Figure 4.3 Sequence analysis of putative *Kalanchoë* PHP sequences.
Multiple sequence alignment of putative *Kalanchoë* pseudo histidine-containing phosphotransfer protein (PHP) nucleotide sequences (A) and amino acid sequences (B). Percentage sequence similarity of the same nucleotide sequence (C) and amino acid sequence (D) in (A) and (B) respectively. For C and D, Kfe represents KfeHP0423, Kla21 represents KlaHP0021, Kla23 represents KlaHP0023 and Kda represents the same protein homolog isolated from *K. daigremontiana*. (E) Multiple sequence alignment of putative *Kalanchoë* PHP sequences, HP paralogs and PHP from selected angiosperm species. Inverted triangle indicates conserved histidine phosphorylation site for HP. Ath, *Arabidopsis thaliana*; Kfe, *Kalanchoë fedtschenkoi*; Kla, *Kalanchoë laxiflora*; Osa, *Oryza sativa*, Ptr, *Populus trichocarpa*; Vvi, *Vitis vinifera*, Zma, *Zea mays*.

4.4.2. High expression of homologous *K. daigremontiana* HP and cytokinin activity was present during plantlet formation

RNA-sequencing data (Fig. 4.4A) revealed that *KdaHP*, homologous gene of *KfeHp0423*, *KlaHp0021* and *KlaHp0023* in *K. daigremontiana* was highly expressed across different plantlet developmental stages. However, the difference in expression level across these stages was not statistically significant. Quantitative real-time PCR (qRT-PCR) showed different *KdaHP* expression levels across selected plantlet developmental stages and the SAM (Fig. 4.4B). *KdaHP* expression of young leaf margins (control) are higher than SAM tissues. At stage S0, its expression dropped substantially, lower than its expression in the SAM and young leaf margin (control) but remained similar at stage S1. At plantlet stage S2, *KdaHP* expression increased dramatically to its highest compared to other plantlet stages or leaf maturity. This increase in expression of *KdaHP* at stage S2 was statistically significant ($P \leq 0.05$) compared to S0.

To visualise the innate activity of cytokinin during plantlet development, transgenic *K. daigremontiana TCSn::GUS* reporter lines were generated. TCSn (Two Component Signalling Sensor new) is an artificially designed promoter sequence, based on the DNA consensus sequence recognised by type-B ARABIDOPSIS RESPONSE REGULATORS (ARRs) involved in initial transcriptional response to cytokinin (Argyros et al., 2008; Hosoda et al., 2002; Imamura et al., 2003; Ishida et al., 2008; Sakai et al., 2000; Zürcher et al., 2013). *TCSn::GUS* reporter lines has been successfully used to visualise cyctokinin accumulation *in planta* (Liu and Müller, 2017; Zürcher et al., 2013). GUS activity was seen at the hydathode of leaves that starts to develop or have formed pedestal at the leaf indentation (Fig. 4.4C). Prior to emergence of the plantlet, GUS activity can already be observed in the enclosed pedestal (Fig. 4.4D). At the later stage, strong GUS staining reflected high cytokinin activity in the plantlet primordium (Fig. 4.4E). However, GUS staining was limited in emerging cotyledons of the heart-stage plantlet, which might indicate a decrease in cytokinin activity (Fig. 4.4F). As the cotyledons emerged, GUS activity was observed only at the proximal bottom-half of the cotyledon (Fig. 4.4G). As the plantlet developed, GUS activity diminished and was localised only at the hydathode of cotyledons and at the mid-bottom (hypocotyl) region of the plantlet (Fig. 4.4H). Later, GUS staining was present at the hydathode and developing vasculature of the cotyledon (Fig. 4.4I). The stain was also observed at basal region of the plantlet where root primordium was

emerging (Fig. 4.4I). Once the plantlet was mature, very faint GUS staining persisted throughout the leaf vasculature, but very strong staining was present at the root tip and vascular strand of the root (Fig. 4.4J). Guard cells on mature leaves of transgenic *K. daigremontiana TCSn::GUS* reporter lines also exhibited staining (Fig. 4.4K).

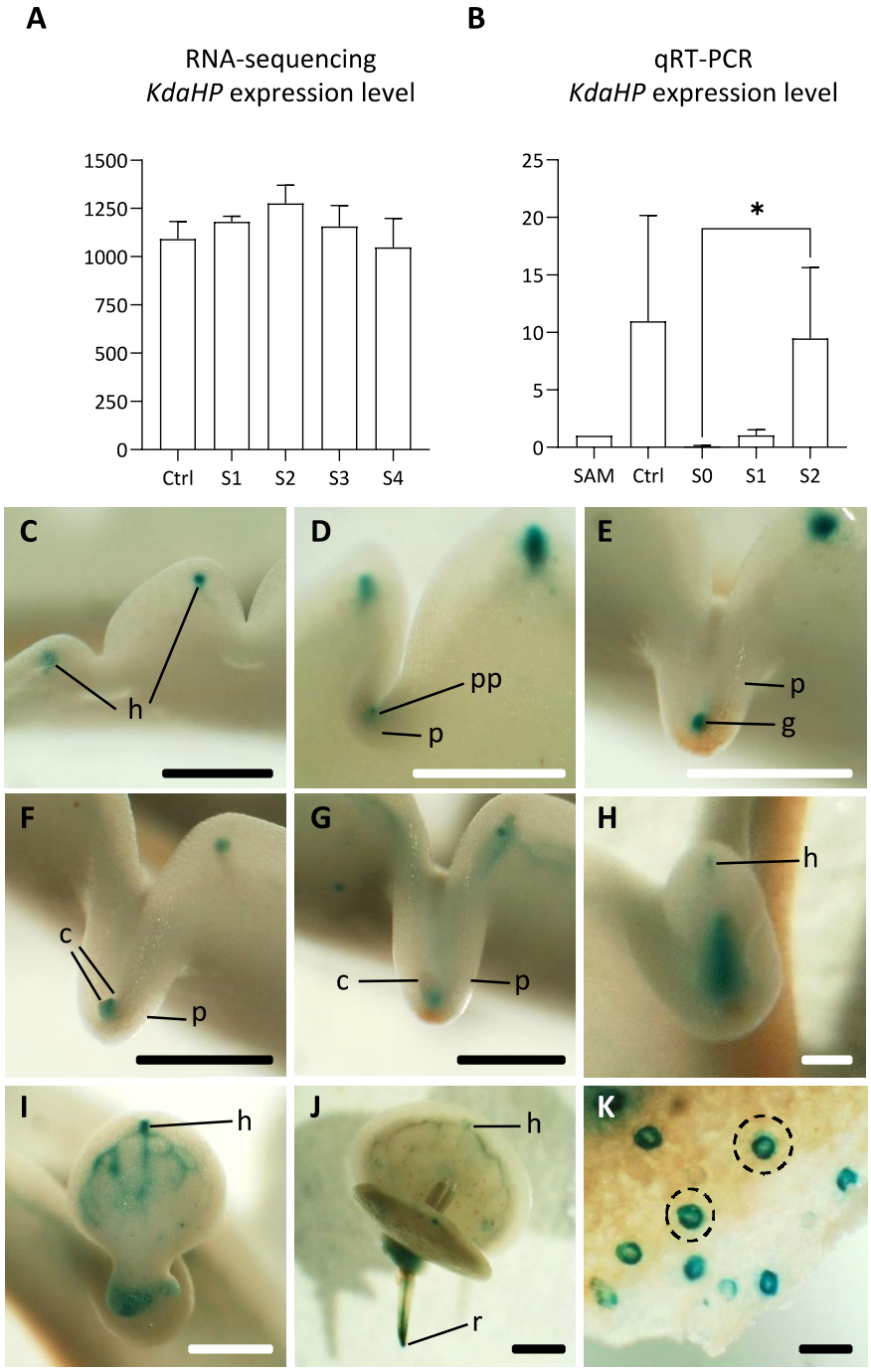

Figure 4.4 *KdaHP* expression during wild-type plantlet development and GUS activity of cytokinin reporter line. (A) RNA-sequencing analysis showing normalised *KdaHP* expression level in Ctrl samples and plantlet stages S1-S4. (B) Quantitative real-time PCR (qRT-PCR) of *KdaHP* expression in the shoot apical meristem (SAM), Ctrl samples and plantlet stages S0-S2. Kruskal Wallis test with Dunn's multiple comparison test indicate statistical significance, *P≤0.05. (C-I) GUS-staining of cytokinin reporter line *TCSn*::*GUS* in *K. daigremontiana*. GUS staining is observed (C) at hydathode of the leaf margin; (D) plantlet primordium; (E) globular-stage plantlet; (F) heart-stage plantlet; (G) basal-half of young cotyledon; (H) basal region of mature cotyledon, then including the hydathode and (I) vasculature as the cotyledon continues to mature; (J) hydathode, vasculature and roots of mature plantlet; (K) guard cells. Scale bars are 1 mm for image (C-J) and 0.1 mm for image (K). SAM, shoot apical meristem; Ctrl, leaf margin of 1-2 cm leaves; S0, indentation without pedestal of young leaf reaching maturity; S1, indentation without pedestal of mature leaf producing plantlets; S2, leaf indentation with pedestal; S3, leaf indentation with plantlet primordium; S4, plantlet with cotyledons at leaf indentation; c, cotyledon; h, hydathode; p, pedestal; pp; plantlet primordium; r, root.

4.4.3. Auxin activity was observed in initiation and outgrowth of plantlet primordia

To understand the role of auxin in plantlet formation, transgenic *K. daigremontiana* bearing the auxin response promoter construct, *DR5*::*GFP* was generated. DR5 is a synthetic auxin response element (AuxRE) promoter, designed based on natural composite AuxRE of soybean, and has been used to visualise the auxin activity in different tissues and of various species (Bensmihen, 2015; Friml et al., 2003; Izhaki and Bowman, 2007; Ulmasov et al., 1997b). GFP fluorescence representing auxin localisation was visible in the developing vasculature (Fig. 4.5A) and at the hydathode (Fig. 4.5A, B) of very young leaves. Strong fluorescence was observed at plantlet primordium site prior to emergence from the pedestal (Fig. 4.5C). Later, GFP signal was present strongly at the cotyledon tips of heart-stage plantlet (Fig. 4.5D). Gradually, the fluorescence became more localised at the hydathode and central region of the plantlet cotyledon (Fig. 4.5E). However, the fluorescence eventually became present only at the hydathode of the cotyledons (Fig. 4.5F). Similar observation in which fluorescence was present only at the hydathode persisted at later stages of the plantlet growth (Fig. 4.5G, H). Mature plantlet only exhibited fluorescence at its root tips and emerging root primordia (Fig. 4.5I).

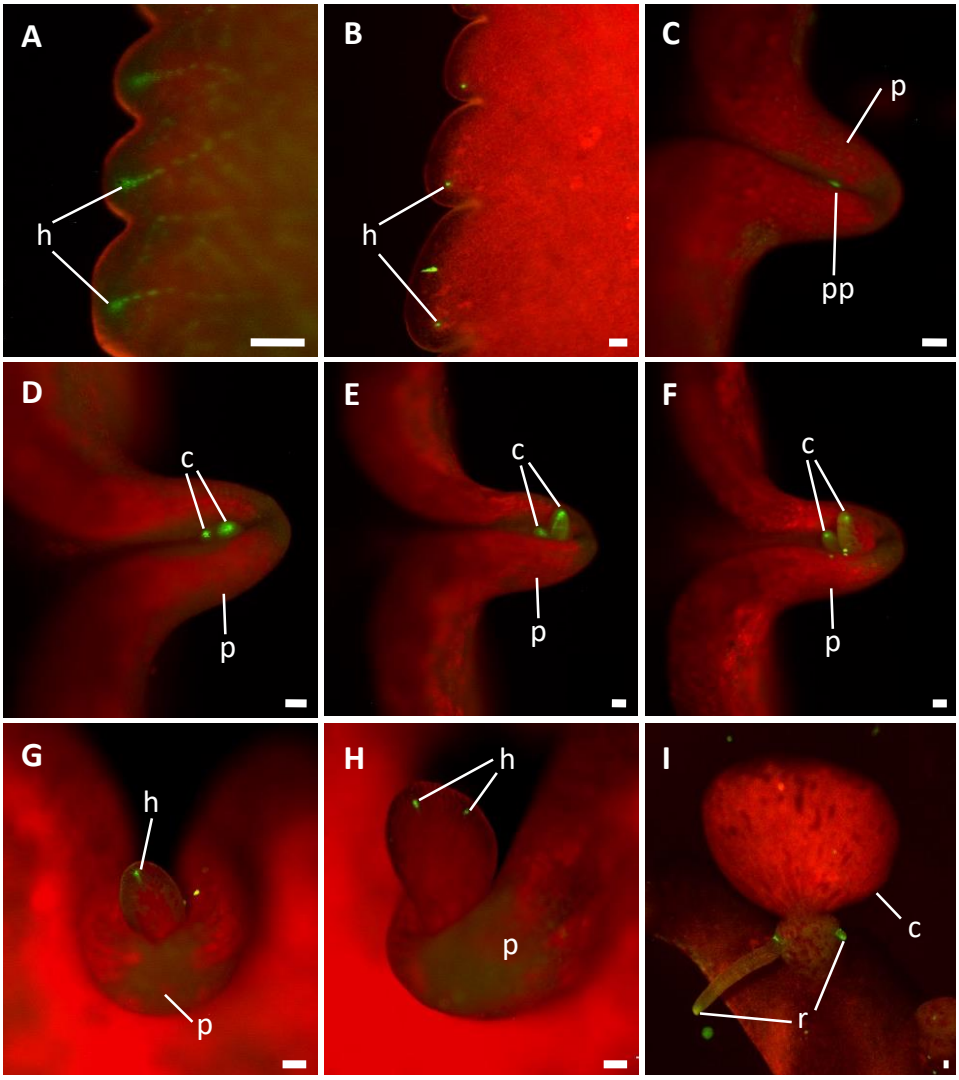

Figure 4.5 Auxin activity reflected by GFP activity of synthetic auxin response element promoter DR5.
GFP fluorescence activity was present at vasculature (A) and hydathode (A, B) of 1 cm young leaves; (C) emerging plantlet primordium still enclosed in pedestal; (D) emerging young cotyledon tips of heart-stage plantlet; (E) hydathode and mid-central region of emerging cotyledon; (F, G, H) only at hydathode(s) of cotyledons and (I) at root tips of mature plantlet. Scale bars are 1 mm for image (A-H) and 0.1 mm for image (I). c, cotyledon; h, hydathode; p, pedestal; pp, plantlet primordium; r, root.

To examine whether the auxin localisation observed was synthesised locally or transported from another region, *PIN1*::*PIN1-GFP* reporter lines of *K. daigremontiana* were generated. The presence of fluorescence visualised localisation of PIN1 transporter protein. No fluorescence was present during formation of pedestal (Fig. 4.6A). Then, during transition from globular to heart-stage, the plantlet exhibited strong fluorescence (Fig. 4.6B). At heart-stage, the fluorescence pattern formed a "v" shape, displaying *PIN1* localisation at the tips and outer edges of cotyledon primordia (Fig. 4.6C) This was unlike in *DR5*::*GFP* plants that showed fluorescence restricted only to the cotyledon primordia tips (Fig. 4.5D). As the cotyledons

continued to emerge and extend from the pedestal, the fluorescence retracted from the cotyledon tips and became localised at the edges of bottom-half of the plantlet (Fig. 4.6D). Eventually, faint fluorescence was present at the bottom of the plantlet where it was attached to the pedestal (Fig. 4.6E). From stages at Fig. 4.6C to Fig. 4.6E, the fluorescence at the pedestal also gradually became stronger. When the plantlet was mature, only the root tips exhibited fluorescence (Fig. 4.6F).

The presence of PIN1 transporter protein was strong, particularly during early stages of plantlet formation. Hence, a confocal fluorescence microscope was then used to determine whether localisation of PIN1 transporter protein was polarised at the single cell level to direct the polar auxin flow to the plantlet primordia at the early stages. When viewing the leaf notch from the direction of Fig. 4.6P1 prior to pedestal formation, fluorescence was detected specifically at and around the site where the plantlet primordium was about to emerge (Fig. 4.6G). A zoom-in image of the region in which fluorescence was observed showed that there was polarised accumulation of PIN1 transporter protein in some cells (Fig. 4.6H, arrows). When the leaf notch was viewed from the abaxial side (Fig. 4.6P2), strong fluorescence was present at the surrounding region of the leaf notch albeit polarisation was not obvious (Fig. 4.6I). Images Fig. 4.6J-L and Fig. 4.6N-O were viewed from direction of Fig. 4.6P4, whereas Fig. 4.6M was viewed from direction Fig. 4.6P3. Along with the outgrowth of pedestal, the fluorescence was seen increasing from outer edges of pedestal (Fig. 4.6J) to the outer region of site of plantlet formation (Fig. 4.6K). Prior to emergence of the plantlet, the plantlet primordium exhibited strong fluorescence (Fig. 4.6L). At the same time, fluorescence was detected in the pedestal region surrounding the plantlet primordium (Fig. 4.6L). At globular stage, the plantlet only has fluorescence on its L1 and L2 layers and the pedestal still expressed fluorescence (Fig. 4.6M). Compared to the stage shown in Fig. 4.6L, the heart-stage plantlet displayed stronger fluorescence in the protruding cotyledons (Fig. 4.6N), which eventually becomes more strongly localised at the distal tip of the cotyledons (Fig. 4.6O). From heart-stage plantlet onwards, the fluorescence decreased and retracted towards outer region of pedestal (Fig. 4.6N, O).

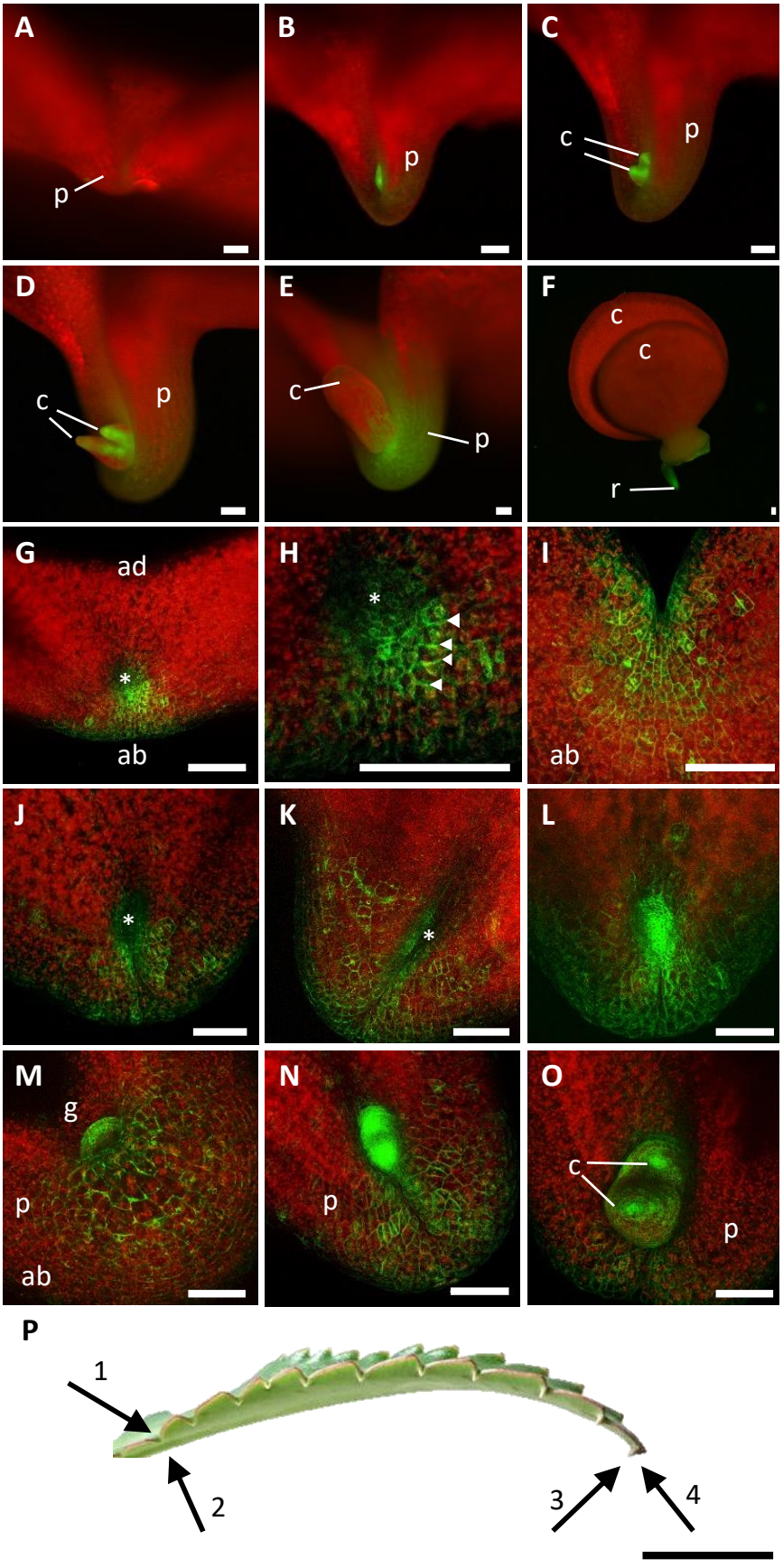

Figure 4.6 Distribution of PIN1 auxin efflux transporter as shown by GFP fluorescence activity of *PIN1*::*PIN1-GFP*.
(A) No GFP fluorescence during formation of pedestal and prior to plantlet formation at the leaf notch. (B) GFP signal was present at plantlet transitioning from globular to heart-stage; (C,D) distal tips heart-stage plantlet emerging cotyledons but GFP expression was eventually limited to the basal half of the cotyledon (D). GFP signal was observed at (E) pedestal of more mature cotyledon and (F) root tips of mature plantlet. (G-O) Confocal images showing *PIN1*::*PIN1-GFP* activity at higher magnification. When viewed from direction P1, GFP signal was observed at (G) site of plantlet formation before pedestal formation. (H) A close-up image of (G). (I) When viewed from P2, GFP fluorescence was visible at the region surrounding the leaf notch. GFP expression was visible at (J,K) the pedestal and site of plantlet formation; (L) the plantlet primordia; (M) outer edge (L1 and L2 layers) globular-stage plantlet; (N) heart-stage plantlet and (O) emerging cotyledons. Images (J-L, N, O) was viewed from direction P4; image (M) was viewed from direction P3. (P) Side view of a *K. daigremontiana* leaf showing leaf notches with and without pedestal. Scale bars are 1 mm for images (A-F), 0.1 mm for images (G-O) and 1 cm for image (P). asterisk, plantlet primordium; ab, abaxial; ad, adaxial; c, cotyledon; g, globular-stage plantlet; p, pedestal; r, root.

4.4.4. Reduced expression of *KdaHP* disrupted plantlet development

Based on the sequence and phylogenetic analyses mentioned above, it was not possible to identify a PHP6 homolog in *Kalanchoë*. However, due to high sequence identity and similarity of the *Kalanchoë* sequences *KfeHp0423*, *KlaHp0021* and *KlaHp0023* to PHP6 sequences in other species, we decided to isolate and to study the homologous sequence of this gene in *K. daigremontiana*. After the sequence *KdaHP* was isolated, an antisense *KdaHP* construct was generated. A construct encompassing the constitutive 35S promoter, antisense sequence of the isolated *KdaHP* and 35S terminator was generated and transformed into *K. daigremontiana*. The presence of the antisense transgene and *NEOMYCIN PHOSPHOTRANSFERASE II* (*NPTII*) gene of the transformation vector in *KdaHP* antisense plants implies that transformation was successful (Fig. 4.7A, B). Semi-quantitative reverse transcriptase PCR (RT-PCR) analysis showed that out of the four independent antisense lines that displayed altered phenotype, three showed reduced *KdaHP* transcript expression (Fig. 4.7C).

To determine whether down-regulation of *KdaHP* affected known meristem and embryogenesis genes, semi-quantitative RT-PCR were performed. The results showed that the expression of *KdaSTM*, *KdaLEC1*, *KdaCLAVATA1* (*KdaCLV1*) and *KdaTOPLESS* (*KdaTPL*) were not noticeably changed in all antisense lines compared to wild-type (Fig. 4.7C). The expression of *KdaWUS* was slightly higher in transformed plants than in wild-type (Fig. 4.7C). In addition, out of four transformed plant lines, line E exhibited lower *KdaCLV2* expression, whereas the other lines exhibited slightly higher expression compared to wild-type (Fig. 4.7C). In the case of *KdaYUC1*, its expression was varied depending on the lines: the lowest in line K, followed by E, L and F. Line K and E showed a similar level of expression, whereas line L and F showed a higher *KdaYUC1* expression than that of wild type.

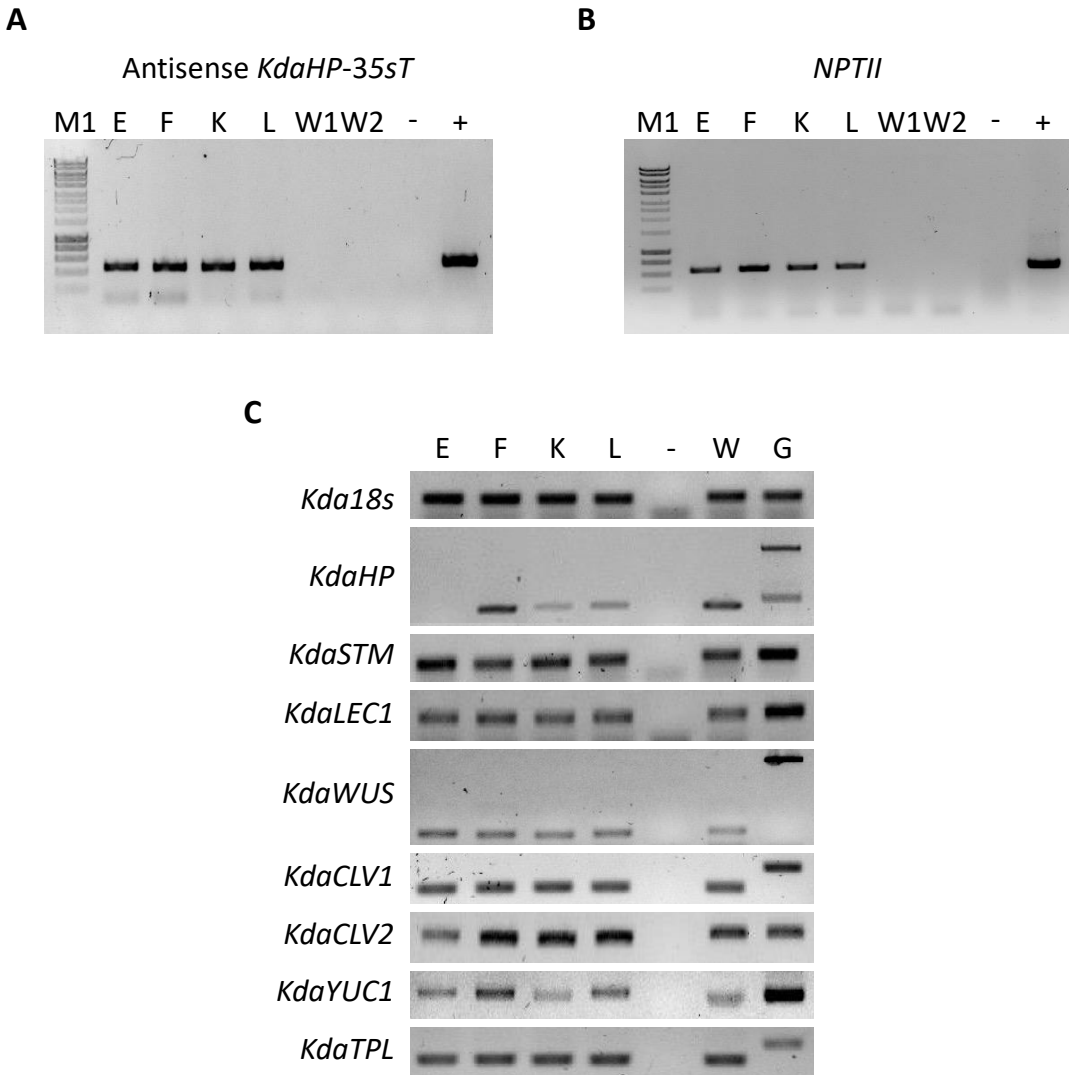

Figure 4.7 Genotyping and expression analysis of *KdaHP* antisense transformed plants.
(A) and (B) are gel electrophoresis images showing the presence of the antisense transgene (A) and *NEOMYCIN PHOSPHOTRANSFERASE II* (*NPTII*) gene of transformation vector in genomic DNA of the transgenic plants. M1, molecular marker; E, F, K, L, antisense lines; W1, wild-type sample 1; W2, wild-type sample 2; -, negative control using water; +, positive control using plasmid containing the antisense construct. The expected band size is 654 bp for *NPTII* and 493 bp for *antisense KdaHP-35ST*. (C) Semi-quantitative RT-PCR analysis of *KdaHP* and other meristem and embryogenesis genes in the transgenic plants. The expression level of each gene in the transgenic plants is relative to the expression level of the same gene in wild-type. E, F, K, L, antisense lines; -, water; W, wild-type; G, wild-type genomic DNA. *STM*, SHOOT *MERISTEMLESS*; *LEC1*, *LEAFY COTYLEDON 1*; *WUS*, *WUSCHEL*; *CLV1*, *CLAVATA1*; *CLV2*, *CLAVATA2*; *YUC1*, *YUCCA1*; *TPL*, *TOPLESS*, *Kda*, *K. daigremontiana*.

To understand the function of *KdaHP* and cytokinin signalling in plantlet formation, we examined various phenotypes of the three transgenic *KdaHP* antisense lines with reduced *KdaHP* expression. In contrast to the wild-type plants (Fig. 4.8A, B), the antisense plants appeared shorter, harbouring leaves that were smaller and with irregular shapes and surfaces (Fig. 4.8E, F). The uneven leaf margin presumably resulted in inconsistent positioning of leaf indentation, and thus asymmetrical distribution of plantlets along leaf margin (Fig. 4.8G, H).

This contrasted with wild-type *K. daigremontiana* leaves that showed consistent and regular positioning of leaf indentation and formation of plantlets along the leaf margin (Fig. 4.8C, D). In transgenic plantlets, downregulation of *KdaHP* affected various plantlet morphology and development. The altered leaf phyllotaxy shown by *KdaHP* antisense plantlets included formation of single cotyledon (Fig. 4.8I), single leaf (Fig. 4.8J) or three cotyledons and leaves (Fig. 4.8K). These antisense plants often formed plantlet with irregular-shape and sinuated cotyledon and leaves (Fig. 4.8L, N) and shallow pedestals (Fig. 4.8P). Some *KdaHP* antisense plantlets developed two meristems (Fig. 4.8N, O), and in some cases two plantlets developed on the same pedestal (Fig. 4.8M). Quantitative measurement also showed that the number of plantlets and lobes per leaf were significantly lower in transformed plants (Fig. 4.8Q, R) compared to wild-type but the depth of leaf indentation was statistically significantly lower only in line F, K and L (Fig. 4.8S). Wild-type plants develop an average of 68 plantlets but the antisense plants only developed an average of 17 plantlets which is only 25% of the number of plantlets in wild-type (Fig. 4.8Q). The average number of lobes per leaf of wild-type was 42 but for the antisense plants, it was 23, almost half of the number of lobes per leaf of wild-type (Fig. 4.8R). The wild-type leaves had indentations of 0.18 cm on average whereas the antisense plants (line E, K, L) had indentations of only 0.12 cm on average (Fig. 4.8S).

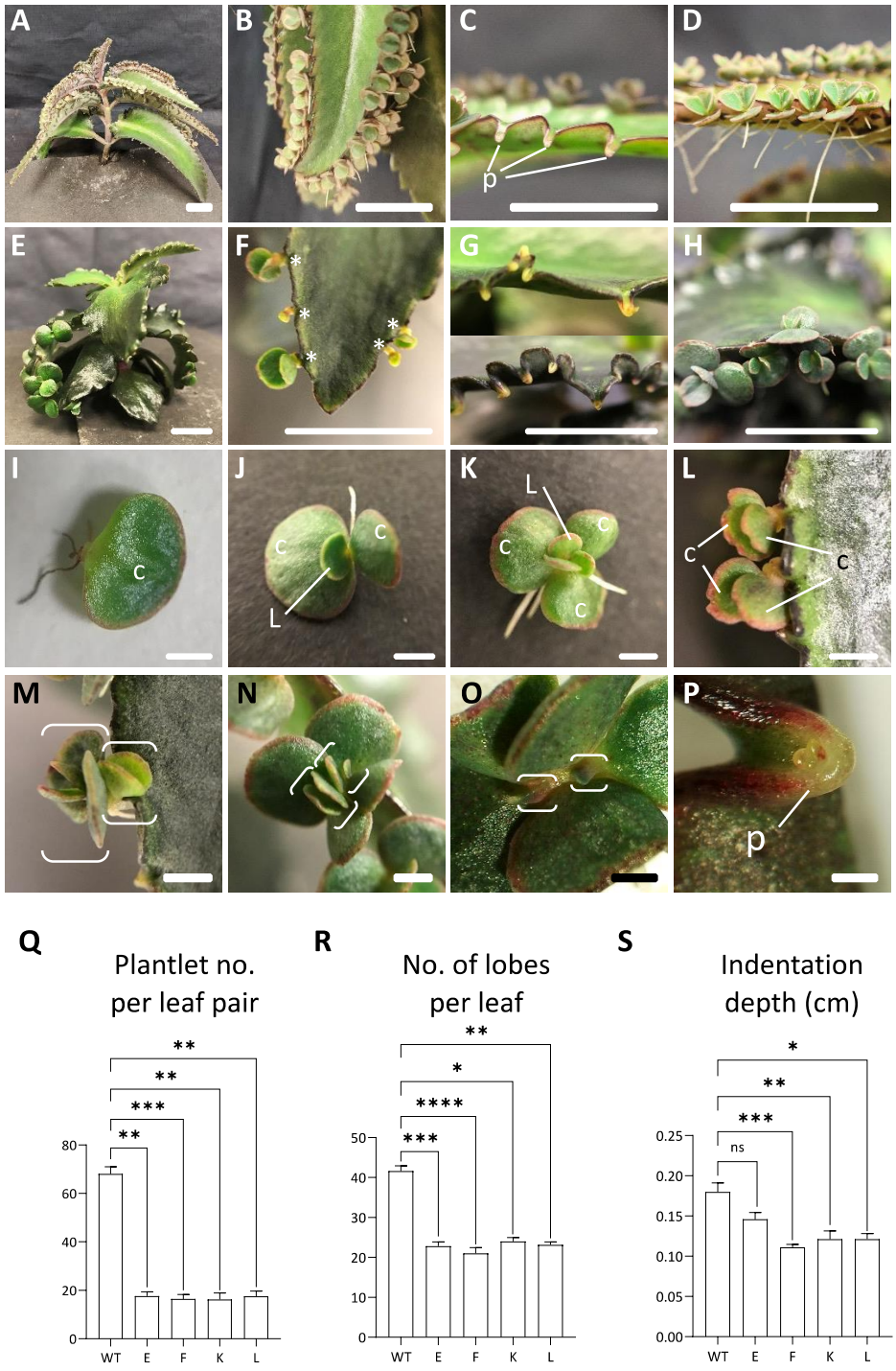

Figure 4.8 Images of whole plant, leaves and plantlets of wild-type and *KdaHP* antisense plants.
Wild-type (WT) (A) whole plant; (B) mature leaf; (C) leaf indentations with pedestals; (D) mature plantlets on leaf margin. (E) Whole antisense plant. (F) Leaf of antisense plant showing asymmetrical plantlet formation. (G, H) Unusual positioning of indentations due to distorted leaf margin. Antisense plantlet (I) with only one cotyledon; (J) forming only one leaf; (K) with 3 cotyledons and 3 leaves; (L) with cotyledons showing irregular indentations. Antisense plants with (M) two plantlets formed on the same pedestal; (N) plantlet with two shoot apical meristems; (O) a close-up image of meristems of a plantlet; (P) formation of plantlet on a shallow pedestal. Scale bars are 1 cm for (A, E), 1 mm for other images. (Q) Plantlet number on a pair of leaves. (R) Number of lobes on one leaf. (S) Depth of individual indentation on the leaves. E, F, K, L, *KdaHP* antisense plants. Kruskal Wallis test with Dunn's multiple comparison test indicate statistical significance, *P≤0.05; **P≤0.005; ***P≤0.0005; ****P≤0.0001. Error bar represents standard error.

4.5. **Discussion**

Cytokinin regulates various developmental processes in plants and through exogenous cytokinin application, cytokinin activity and function during plantlet formation have yet to be clearly demonstrated. Cytokinin signalling is mediated by histidine phosphotransfer proteins (Hutchison et al., 2006) such as AHP1-6 in *Arabidopsis*. Apart from AHP6, AHP1-5 contain conserved histidine residue that allows the proteins to be phosphorylated and relay cytokinin signalling (Suzuki et al., 2000). AHP6, conversely, has lost this conserved histidine residue, which resulted in its inability to act as a true phosphotransfer protein. Hence, AHP6 is known as a pseudo histidine-containing phosphotransfer protein that inhibits cytokinin signalling (Mähönen et al., 2006). This study attempted to generate transgenic plants deprived of cytokinin signalling inhibitor, PHP6 by first identifying its homolog in *Kalanchoë*. Preliminary phylogenetic analysis (Fig. 4.1) revealed that a group of *Kalanchoë* genes clustered with *PHP6* nucleotide sequences but not PHP6 protein sequences. Multiple sequence analyses also showed that among all predicted HP *Kalanchoë* sequences, this groups of sequences were most closely similar to all HP1, HP2, HP3, HP5, PHP6 angiosperm paralogs. Addition of sequences from greater range of angiosperm species did not illustrate the presence of distinct HP1, HP2, HP3, HP5, PHP6 paralogs in *Kalanchoë* (Fig. 4.2). These results suggest that HP paralogs such as HP1, 2, 3, 5 and PHP6 might not have diverged from this group of *Kalanchoë* sequences. Due to the high sequence similarity of KfeHP0423, KlaHP0021 and KlaHP0023 to all HP1, HP2, HP3, HP5, PHP6 angiosperm paralogs, these *Kalanchoë* sequences might be able to perform certain functions of HP in cytokinin signalling. Hence, the homolog of KfeHP0423, KlaHP0021 and KlaHP0023 in *K. daigremontiana* were studied. Multiple sequence alignments suggest that the isolated sequence KdaHP is indeed the correct homolog as its sequences were at least 98.6% identical to KfeHP0423, KlaHP0021 and KlaHP0023 nucleotide and protein sequences (Fig. 4.3A-D). This inference is supported by current literatures which stated that homology is recognised if the sequences are at least 30% similar for nucleotides and at least 40% similar for protein (Do and Katoh, 2008; Pearson, 2013). Nonetheless, there is one difference in amino acid between KdaHP and other *Kalanchoë* peptide sequences. Further investigation into the structure of KdaHP is needed to understand the consequence of a change from the amino acid G (glycine) to D (aspartic acid). If the position is at a catalytic domain, a

change in function may arise due to differences in properties of the amino acids (Betts and Russell, 2003).

A recent study showed that PHPs first arise in gymnosperms but evolved independently in monocots and dicots (Vaughan-Hirsch et al., 2021). In addition, there are also more than one copy of PHP in rice and maize (Fig. 4.2). Hence, *Kalanchoë* PHP and other HP paralogs might have evolved differently in the *Kalanchoë* clade, compared to other angiosperm species. Although this group of *Kalanchoë* sequences contain histidine at the canonical phosphorylation site, this information is not sufficient to rule out its function as a negative regulator of cytokinin signalling as *Arabidopsis HP4* was shown to negatively affect cytokinin response (Hutchison et al., 2006). Unexpectedly, maize ZmaPHP2 also contains histidine at the phosphorylation site (Fig. 4.3E) but the sequence used in this study is inconsistent with ZmaPHP2 sequence used in a recent study (Vaughan-Hirsch et al., 2021). As the ZmaPHP2 sequence used in this study was annotated based on computational prediction methods, the sequence might not be inaccurate. Nonetheless, to determine whether KfeHP0423, KlaHP0021, KlaHP0023 and the isolated homolog from *K. daigremontiana* can act as PHP, detailed examination of the protein structure is required, and phosphorylation activity of purified homologous KdaHP proteins can be performed by using *in vitro* phosphotransfer assay (Mähönen et al., 2006; Vaughan-Hirsch et al., 2021; Verma et al., 2013).

The analysis of *KdaHP* expression using RNA-sequencing and qRT-PCR data did not yield a consensus in changes of *KdaHP* expression pattern across plantlet developmental stages (Fig. 4.4A, B). However, both analyses showed highest *KdaHP* expression at S2 stage plantlet. Due to limitation of harvesting with naked eyes, S2 samples include a wide range of stages of plantlet development (after formation of pedestal and before emergence of cotyledons). Thereby, rendering impossible to distinguish *KdaHP* expression at globular-stage or heart-stage plantlet. Nonetheless, the results presented are of the first to show *KdaHP* expression in embryo-equivalent stages of plantlet formation, which might suggest control of endogenous cytokinin activity in plantlet development. The existing literatures have shown expression of *PHP6* in zygotic embryo, gynoecium, roots and the SAM (Andersen et al., 2018; Besnard et al., 2014a; Durán-Medina et al., 2017b; Mähönen et al., 2006; Moreira et al., 2013; Reyes-Olalde

et al., 2017), which agrees with the qRT-PCR data (Fig. 4.4B) that detected *KdaHP* expression at the SAM. Assuming that KdaHP inhibits the cytokinin signalling, high expression of *KdaHP* in stage S2 plantlets suggest that cytokinin signalling should be at its lowest, compared to plantlet stages S0, S1 and other tissues such as the SAM and young leaf margin. It might be possible that the qRT-PCR data might have captured high expression of *KdaHP* specifically from the heart-stage plantlets, which was reflected by reduced GUS activity of *TCSn*::*GUS* heart-stage plantlets (Fig. 4.4F). In order to understand whether *KdaHP* was directly regulating cytokinin activity during plantlet formation, it might require studying cytokinin activity across plantlet developmental stages in plants with reduced *KdaHP* expression.

To study the participation of cytokinin in plantlet formation, *K. daigremontina TCSn*::*GUS* transgenic plants were generated. *TCSn* is a synthetic promoter designed to reflect transcriptional activity of type-B response regulators involved in cytokinin signalling (Zürcher et al., 2013). *GFP* expression of *TCSn*::*GFP* were demonstrated in various *Arabidopsis* and maize developmental contexts such as in SAM, leaf vasculature, seedling roots, pavement cells, guard cells, ovule, and at different stages of zygotic embryo (Steiner et al., 2020; Zürcher et al., 2013). The presence of GUS activity in guard cells and leaf hydathodes of *TCSn*::*GUS* transgenic plants (Fig. 4.4C,K) confirms conservation of *TCSn* promoter activity in *K. daigremontina*. GUS staining of *TCSn*::*GUS* to illustrate endogenous cytokinin activity showed strong staining in the emerging plantlet (Fig. 4.4D). However, GUS staining of heart-stage plantlets was greatly diminished compared to globular-stage plantlet (Fig. 4.4E). Based on current literature, cytokinin activity localises only at hypophysis and suspensor of globular-stage *Arabidopsis* embryo (Müller and Sheen, 2008; Zürcher et al., 2013). Hence, the cytokinin activity observed in our results might indicate novel function of cytokinin in early plantlet formation or somatic embryogenesis. Nonetheless, the cytokinin activity observed at heart-stage plantlets (Fig. 4.4F) seems to be similar to localisation of cytokinin activity at centre region of heart-stage zygotic and somatic embryos, which might be transient signal for the prospective SAM (Müller and Sheen, 2008; Su et al., 2015; Zürcher et al., 2013, 2016). Similarity in cytokinin expression during plantlet formation suggest that the function of cytokinin signalling in specification of shoot meristem and marginal leaf serrations are recruited during plantlet formation (Meng et al., 2017; Shani et al., 2010; Xie et al., 2018; Zhang et al., 2017c; Zubo et al., 2017).

Apart from cytokinin, auxin is another major hormone that regulates many developmental events in plants and similarly its effect on plantlet formation remains contradictory. Hence, we used *DR5*::*GFP* and *PIN1*::*PIN1-GFP* reporter lines and revealed auxin activity and transport during plantlet formation. DR5 was designed as a synthetic auxin response element (AuxRE) promoter to reflect auxin activity by incorporating the auxin-response TGTCTC sequence (Ulmasov et al., 1997b). DR5 promoter was used to illustrate auxin activity in different tissues and of various species (Bensmihen, 2015; Friml et al., 2003; Izhaki and Bowman, 2007; Ulmasov et al., 1997b). The presence of auxin activity in hydathode and vasculature of young *K. daigremontiana* leaves was expected as auxin is known to mediate leaf vasculature patterning (Biedroń and Banasiak, 2018). The reduction of DR5 activity at the hydathode as shown in Fig. 4.5E-H was also observed in *Arabidopsis* embryo (Izhaki and Bowman, 2007; Mattsson et al., 2003; Möller and Weijers, 2009). The presence of stronger GFP activity at the hydathode compared to the rest of the vasculature was also consistent with GUS staining and schematic diagram illustrating DR5 activity in developing *Arabidopsis* leaf (Biedroń and Banasiak, 2018; Mattsson et al., 2003; Steynen and Schultz, 2003). DR5 activity during plantlet development also correlates to existing studies that illustrate DR5 activity at the globular-stage embryo proper (Fig. 4.5C) and developing cotyledon primordia of heart-stage plantlet (Fig. 4.5D) (Chandler et al., 2007; Mattsson et al., 2003; Möller and Weijers, 2009; Xiang et al., 2011). During *Arabidopsis* zygotic embryogenesis, auxin is present at high concentration at the apical cell of the 2-cell stage and the cells that it subsequently give rise to, until the 16-cell stage (Friml et al., 2003; Robert et al., 2013). Due to strong fluorescence exhibited by the plantlet primordium that was enclosed in the pedestal, it is very likely the plantlet primordia represented early embryo proper (Fig. 4.5C). This indicates that at this stage, auxin localisation at the plantlet primordium was specifying its fate to become an embryo, as is in the case of *Arabidopsis* embryo proper (Friml et al., 2003). Beyond the 16-cell stage of *Arabidopsis* zygotic embryo, auxin accumulates at hypophysis to determine its fate of giving rise to RAM (Friml et al., 2003; Robert et al., 2013). In the case of *K. daigremontiana* plantlet, no such accumulation was seen, but this was not sufficient to rule out the role of auxin in specification of plantlet RAM. The localisation of DR5 activity at the cotyledon tips and provascular tissues of heart-stage plantlet (Fig. 4.5D) is similar to as seen at heart-stage *Arabidopsis* embryo. This suggests

that, similar to transition of zygotic embryo from globular to heart-stage, redistribution of auxin caused radial symmetry of the plantlet changed into a bilateral symmetry, initiating outgrowth of cotyledons (Benková et al., 2003).

In the case of *PIN1*::*PIN1-GFP* reporter lines, PIN1 auxin efflux transporter was homogenously distributed at plantlet primordia transitioning from globular to heart-stage before localising specifically to the cotyledon primordia and vascular initials (Fig. 4.6B,C,N). At later stage, PIN1 distribution gradually reduced and became localised only at vasculature precursor of the plantlet (Fig. 4.6D). These patterns of PIN1 localisation in *K. daigremontiana* plantlet is very similar to PIN1 expression in *Arabidopsis* zygote (Benková et al., 2003; Huang et al., 2010; Izhaki and Bowman, 2007; Xiang et al., 2011). The similarity in expression of DR5 and PIN1 during plantlet formation to *Arabidopsis* zygotic embryogenesis provided further evidence that plantlet developmental stages are equivalent to embryogenesis (Benková et al., 2003; Reinhardt et al., 2003; Scarpella et al., 2006). This also suggest that auxin plays a similar role in plantlet formation as zygotic embryogenesis, possibly involved specification of early cell fate, phyllotaxy and vein patterning of plantlet (Benková et al., 2003; Reinhardt et al., 2003; Scarpella et al., 2006). If these speculations were true, presence of auxin at globular-stage plantlet would be the results of auxin transport by PIN7 and distribution by PIN1. In subsequent stages, PIN1 proteins also distribute auxin and lead to auxin accumulation at cotyledon primordia and precursor vasculature tissues (Benková et al., 2003; Reinhardt et al., 2003; Scarpella et al., 2006). With confocal images, it seems that the activity of auxin transport around the pedestal is at its highest during development of heart-stage plantlet (Fig. 4.6L) but the localisation of PIN1 is not clear enough to indicate specific directional transport of auxin. Nonetheless, the presence of PIN1 localisation around the pedestal is unique and is even higher after formation of cotyledons (Fig. 4.6E). An explanation for this observation is that perhaps PIN1 proteins are directing auxin to accumulate at basal region of plantlet to specify root outgrowth as PIN1 was previously shown to be a good marker for root meristem activity (Omelyanchuk et al., 2016). The most fascinating finding is the presence of PIN1 prior to pedestal formation at the site of plantlet formation and at the abaxial side of the leaf notch (Fig. 4.6G-I). These observations suggest that auxin might be transported from abaxial side of the leaf to the site of plantlet formation to stimulate plantlet initiation. Although more detailed

examination is required to clearly illustrate directional auxin transport, observations from *DR5*::*GFP* and *PIN1*::*PIN1-GFP* activities provided further evidence that *K. daigremontiana* plantlet developmental stages are comparable to zygotic embryo-equivalent and recruits similar auxin signalling during this process (Garcês et al., 2007).

As cytokinin is known to participate in different aspects of plant development development (Wybouw and Rybel, 2019), reduced expression of *KdaHP* has unsurprisingly led to exhibition of a wide range of phenotypic changes (Fig. 4.8). If KdaHP is indeed a PHP6 ortholog, reduction in its expression signifies decline in cytokinin signalling inhibition, and thus, the phenotypes observed might be the results of increased cytokinin activity. When compared to gain-of-function mutants of cytokinin receptors (Bartrina et al., 2017), *KdaHP* antisense lines also developed enlarged cotyledons (Fig. 4.8E) but the mature leaves of *KdaHP* antisense plants were not larger than wild-type (Fig. 4.8A). However, *KdaHP* antisense leaves were thicker than wild-type *K. daigremontiana* and exhibited uneven leaf surface (Fig. 4.8C, G). This might be due to incomplete suppression of *KdaHP*, resulting in slightly enhanced cell expansion and proliferation due to increased cytokinin activity but the effect was insufficient to cause significant change in length of leaves (Holst et al., 2011; Skalák et al., 2019). The phenotypes might also be a consequence of reduced cytokinin signalling as KdaHP might be a cytokinin signalling regulator similar to AHP1-5. Although single or double *AHP* mutants are usually similar to wild-type due to their redundancy, this redundancy might not exist in *K. daigremontiana* as KdaHP might be the only HP homolog (Hutchison et al., 2006; Nishiyama et al., 2013). However, *ahp* triple mutants were found to have smaller leaves relative to wild-type homolog (Hutchison et al., 2006; Nishiyama et al., 2013). The uneven leaf surface might have led to irregular localisation of the leaf indentation and thus asymmetrical positioning of the plantlets along the leaf margin (Fig. 4.8G, H). The alteration in cell expansion and proliferation might also have caused the change in shape of the pedestal (Fig. 4.8P), forming a more exposed pedestal, which might impact physical protection of the plantlet during early development. To measure the effect of *KdaHP* suppression on various aspects of leaf development, an array of tools is available to study leaf morphogenesis (Bar and Ori, 2014).

Apart from general leaf shape and thickness, indentation depth and number of lobes on the leaves of *KdaHP* antisense plants was also affected (Fig. 4.8R, S). Research on formation of leaf serrations revealed that KNOX I proteins activates cytokinin biosynthesis, which then inhibits synthesis of gibberellic acid (Shani et al., 2010; Yanai et al., 2005). Gibberellic acid signalling has been associated with reducing leaf serration of tomato leaflets and *Arabidopsis* overexpressing KNOX I proteins (Hay et al., 2002; Jasinski et al., 2008). From these findings, if *KdaHP* is a PHP, *KdaHP* suppression should lead to increased cytokinin activity, reduced gibberellic acid signalling and increased leaf serrations. However, quantitative measurements showed that *KdaHP* antisense plants have lower indentation depth and number of lobes per leaf (Fig. 4.8R, S). If considering *KdaHP* as a HP that mediates cytokinin signalling, this observation would be expected as downregulation of *KdaHP* should lead to increase gibberellic acid signalling and reduced leaf serrations. The pathway suggested above might also not be the actual pathway opted during formation of leaf serration as a direct link between KNOX I transcription factor and *CUP-SHAPED COTYLEDON* (*CUC*) gene has been shown to play a role of evolution of leaf shape (Hasson et al., 2011; Spinelli et al., 2011). There is no evidence of association between *CUC* genes and cytokinin in regulating leaf serration, however, *CUC* genes and cytokinin were reported to regulate flower development and ovule number in *Arabidopsis* (Cucinotta et al., 2018; Li et al., 2010). *Arabidopsis* leaf serrations are formed due to alternating region of growth restriction by *CUC2* activity and growth promotion by auxin maxima (Bilsborough et al., 2011). *CUC2* promotes PIN1 expression that leads to the auxin accumulation whilst auxin represses *CUC2* expression (Bilsborough et al., 2011). As cytokinin was shown to control PIN1-dependent polar auxin transport, perhaps cytokinin signalling is indirectly regulating the role of *CUC2* in *K. daigremontiana* leaf serration by mediating polar auxin transport (Marhavý et al., 2014).

Cytokinin signalling might also mediate sources of auxin as changes of auxin biosynthesis flavin monooxygenase enzyme gene *KdaYUC1* expression in *KdaHP* antisense plants was observed. At this stage, it is not possible to determine how *KdaHP* impacted *KdaYUC1* expression, but it is extremely common to observe interaction and influence between auxin and cytokinin (Bielach et al., 2017; Kurepa et al., 2019; Müller et al., 2017). During gynoecium development, cytokinin was found to positively regulates auxin signalling by promoting auxin biosynthesis

components such as *YUC1*. During this process, auxin signalling also triggers *AHP6* to repress cytokinin signalling (Müller et al., 2017). Hence, the difference in *KdaYUC1* expression might be the result of the complexity of auxin-cytokinin crosstalk and the multiple roles of *YUC1* (Cao et al., 2019; Chen et al., 2016; Müller and Sheen, 2008; Uc-Chuc et al., 2020). The loss of leaf indentation indicated by number of lobes per leaf might also have directly impacted in reduction of plantlet number per leaf pair (Fig. 4.8Q). If this was not true, we would have expected to observe formation of plantlet on the leaf margin even when indentation is not present. However, this inference is likely to be true as similar observation was made when *KdSOC1* was overexpressed in *K. daigremontiana* (Zhu et al., 2017). The influence of cytokinin signalling on auxin biosynthesis might also be the reason behind the loss of sequencing basipetal (distal to proximal) formation of plantlets along the leaf margin (Fig. 4.8F). A recent study showed that auxin biosynthesis creates a basipetal gradient of growth and proliferation to aid the outgrowth and form of *Arabidopsis* leaves (Zhang et al., 2020). This is achieved by promoting proximal lateral growth and inhibiting distal growth (by inducing differentiation) (Zhang et al., 2020). This also requires local activation of *YUC* genes such as *YUC1* near the leaf margin (Zhang et al., 2020). *Arabidopsis yuc* mutants developed abnormal leaf margin development and narrower leaves (Wang et al., 2011; Zhang et al., 2020), similar to what was also observed in *Kda*HP antisense plants (Fig. 4.8E). As plantlet formation is stimulated only during leaf growth and maturation, changes in *KdYUC1* expression might have resulted in disruption of this basipetal gradient which is required not only for leaf blade growth but also as a cue for plantlet initiation. Hence, leaves of *KdaHP* antisense plants were uneven in thickness and plantlet is initiated inconsistently along the leaf margin (Fig. 4.8E, F).

KdaHP antisense plants also exhibited inconsistent plantlet leaf phyllotaxy (Fig. 4.8I-K), which might be due to the role of cytokinin in organ formation through interaction with *STM* and through the action of *AHP6* (Besnard et al., 2014; Rupp et al., 1999). *STM* is needed to separate the organs from the SAM during the organ outgrowth (Landrein et al., 2015). If *KdaHP* is a cytokinin signalling mediator, reduction of its expression should lead to decreased *STM* expression as cytokinin is known to upregulate *STM* expression. However, *KdaSTM* expression seems to be stronger in *KdaHP* antisense plants compared to wild-type. Organ initiation occurs as a result of local auxin accumulation mediated through auxin efflux transporter PIN1 at the

region of incipient organ primordia and auxin depletion at its periphery (Jönsson et al., 2006; Reinhardt et al., 2003; de Reuille et al., 2006; Smith et al., 2006; Vernoux et al., 2011). Organ initiation also depends on synergistic effect of auxin and cytokinin signalling (Besnard et al., 2014a; Yoshida et al., 2011). The peripheral region of auxin depletion coincides with AHP6 activity which forms the organ inhibitory field (Besnard et al., 2014a). *Arabidopsis ahp6* mutant meristems developed pairs or triplets of young organs unlike in wild-type which makes individual organ following specific phyllotaxis (Besnard et al., 2014b). If *KdaHP* is a cytokinin signalling inhibitor, the loss or weakened *KdaHP* might have resulted in expansion in auxin and cytokinin signalling as seen in *ahp6* mutants, thus, causing formation of plantlets with multiple cotyledon or leaf (Fig. 4.8K). Ectopic formation of an additional plantlet on the same pedestal and presence of multiple meristems on a plantlet was also observed in *KdaHP* antisense plants. This phenomenon might be explained by slight upregulation of *KdaWUS* in these plants (Fig. 4.7C) as *WUS* overexpression has resulted in ectopic meristem formation and somatic embryos (Bouchabké-Coussa et al., 2013; Gallois et al., 2004; Zuo et al., 2002). It was as expected to observe upregulation of *KdaWUS* because if KdaHP is indeed a cytokinin signalling inhibitor, reduced KdaHP should increase cytokinin signalling; and as cytokinin is a positive regulator of *WUS* (Gordon et al., 2007), increased cytokinin signalling lead to elevated *KdaWUS* expression. It is well known that *WUS* work with *CLV* genes to regulate organogenesis (Somssich et al., 2016) and that *WUS-CLV* pathway is reinforced by direct transcriptional activation of *CLV1* expression by WUS (Busch et al., 2010). However, increase in *KdaWUS* expression does not correlate with changes in *KdaCLV1* and *KdaCLV2* expression (Fig. 4.7C). The reason for this might be *WUS* induction through CLV-independent pathway after cytokinin treatment (Gordon et al., 2009). Nonetheless, *KdaCLV2* expression decreased in one of the *KdaHP* antisense line, indicating that increased cytokinin signalling might have indirectly inhibited *KdaCLV2* expression. This finding is intriguing because *clv2* mutants have shown to increase *AHP6* expression during protoxylem vessel formation, but not *vice versa* (Kondo et al., 2011).

4.6. **Conclusion**

In conclusion, the present results have offered novel insight into auxin and cytokinin activity during *K. daigremontiana* plantlet formation. In particular, our results illustrated auxin efflux transporter PIN1 activity at site of pedestal and plantlet formation, which suggest the potential role of auxin in initiating plantlet formation. Cytokinin activity was also present during early plantlet formation, a phenomenon not observed in zygotic embryos. Exhibition of auxin and cytokinin activity similar to zygotic embryogenesis in plantlets at later stages, indicating reuse of the same mechanisms for plantlet development. Our data has also shed light onto the independent evolution of components involved in cytokinin signalling as HP paralogs apart from HP4 were absent in *Kalanchoë.* Nonetheless, a putative cytokinin signalling regulator in *K. daigremontiana*, *KdaHP* that was highly expressed during plantlet development severely affected plantlet formation when its expression was reduced. Phenotype analysis and expression analysis of other genes in *KdaHP* antisense plants raised the possibility of complex auxin-cytokinin crosstalk in plantlet formation. Further investigation into the mechanisms of hormonal control of plantlet initiation and development will be of ease as we have established useful transgenic plants. Future experiments might contribute to how hormonal regulation ties in with molecular mechanisms such as embryogenesis, organogenesis and flowering that were shown to be recruited during plantlet development. This knowledge will also facilitate our understanding towards other asexual reproductive strategies in plants.

CHAPTER 5

RESULTS 4

University of Manchester sequencing facility sequenced *Kalanchoë pinnata* and *Kalanchoë daigremontiana* RNA samples prepared by FJB and JPO respectively. The RNA samples were sequenced by the University of Manchester Genomic Technologies Core Facility. PCA, Heat map, clustering data and volcano plots were generated by LZ. FJB produced all text in introduction and results; JPO performed gene ontology analyses and produced all final figures in this chapter. Discussion in this chapter was written by both FJB and JPO. Images in Fig. 5.1A were taken by Victoria Spencer.

5. Comparative Transcriptome Analysis of Two *Kalanchoë* Species During Plantlet Formation

Francisco Jácome-Blásquez[1], Joo Phin Ooi[1], Leo A. H. Zeef[2] and Minsung Kim[1*]

[1]School of Biological Sciences, Faculty of Biology, Medicine and Health, University of Manchester, Manchester, M13 9PT, United Kingdom

[2]Bioinformatics Core Facility, Faculty of Biology, Medicine and Health, University of Manchester, Manchester, M13 9PT, United Kingdom

*Corresponding author: Minsung.kim@manchester.ac.uk

Key words: Asexual Reproduction, *Kalanchoë*, plantlet formation, organogenesis, embryogenesis, plantlets.

5.1. Abstract

Some species in the *Kalanchoë* genus form plantlets on their leaf margins as an asexual reproduction strategy. The limited molecular studies on plantlet formation showed that an organogenesis gene, *SHOOTMERISTEMLESS* (*STM*) and embryogenesis genes such as *LEAFY COTYLEDON1* (*LEC1*) and *FUSCA3* are recruited during plantlet formation. To understand the mechanisms of two *Kalanchoë* plantlet-forming species with slightly different mode of plantlet formation, RNA-sequencing analysis was performed. Our results showed the expression pattern of most genes that were significantly differentially changed can be categorise into 8 or 12 clusters in *K. daigremontiana* and *K. pinnata* respectively. Out of these gene clusters, GO terms such as signalling, response to wounding, reproduction, regulation of hormone level and response to karrikin that may be involved in plantlet formation of both species are overrepresented. Compared to the common GO terms, there were more unique GO terms overrepresented during plantlet formation of each species. More in-depth investigation is needed to understand how these GO terms are participating in plantlet formation. Nonetheless, this transcriptome analysis is presented as a reliable basis for future studies on plantlet formation and development in two plantlet-forming *Kalanchoë* species.

5.2. **Introduction**

Flowering plants (angiosperms) reproduce sexually or asexually by numerous and complex ways (Klimeš et al., 1997; de Meeûs et al., 2007; Yang and Kim, 2016). Selective preference for either sexual or asexual reproduction and the specific strategy used depends on the species and external environmental conditions (Yang and Kim, 2016). While sexual reproduction in plants involves many traits and developmental events (*e.g.* flower morphology, pollination, fertilization, seed and fruit development and dispersal mechanisms) (Barrett, 2008), asexual reproduction (vegetative, clonal) is relatively simple and fewer traits are involved. Asexual reproduction is particularly advantageous when a species is already in a niche of favourable conditions as it is rapid and allows the progeny to integrate earlier to existing populations (Barrett, 2015; Klimeš et al., 1997). However, asexual reproduction could lead to a low genetic diversity in the population, leading to lack of traits to combat sudden change in environmental conditions or introduction of pathogens or diseases (de Meeûs et al., 2007; Yang and Kim, 2016). Plants have evolved several different forms of asexual reproduction strategies, including but not limited to apomixis, stolon, corms, rhizomes and adventitious buds (Barrett, 2015). Apomixis is an asexual seed formation without gametes fusion in which meiosis and fertilization are bypassed (Enriquez-quiroz and Morales-nieto, 2010). The other ways of vegetative reproduction consist of formation of new plants connected to the mother plant by tubers, rhizomes or stolons (Yoshida et al., 2016). It was suggested that vegetative reproduction only involves plant body growth rather than a real reproduction process (Harper, 1977). Although asexual reproduction strategies are common among perennial plants, molecular and genetic mechanisms controlling the asexual reproduction is still elusive.

Kalanchoë is a genus native to Madagascar and Africa, which evolved a unique asexual reproduction strategy (Allorge-Boiteau, 1996). Many *Kalanchoë* species have acquired the ability to reproduce asexually by forming new baby plants (plantlets) on the margin of the leaves. Phylogenetic analysis of *Kalanchoë* revealed an evolutionary trajectory of the plantlet formation strategies. While *Kalanchoë* species in the basal group such as *Kalanchoë tomentosa* and *K. marmorata*, are unable to form plantlets in leaf margins (Garcês et al., 2007; Gorelick, 2015), species in derived clades such as *K. daigremontiana* and *K. tubiflora* form plantlets on the margin constitutively under a long-day condition (Abdel-Raouf, 2012; Garcês et al., 2007).

Intriguingly, an evolutionary transition is also seen in the clades flanked between basal and derived clades. *Kalanchoë* species (*e.g.*, *K. fedschenkoi*, *K. prolifera*, *K. pinnata*, *K. streptantha* and *K. gastonis-bonnieri*) in these transitory clades, only form plantlets after leaves are damaged or detached from the mother plant, and thus it is called inducible plantlet formation (Allorge-Boiteau, 1996; Garcês et al., 2007). Interestingly, in *Kalanchoë*, asexual reproduction strategies *via* plantlet formation appears to evolve as a trade-off with regular sexual reproduction. While inducible and non-plantlet-forming species produce perfectly viable seeds, constitutive plantlet-forming species generate non-viable seeds and has lost the ability to reproduce sexually (Garcês and Sinha, 2009d; Garcês et al., 2007). While plantlet formation in constitutive and inducible species appears to be superficially similar, developmental mechanism(s) in these *Kalanchoë* groups is suggested to be different. An inducible plantlet-forming species, *K. pinnata*, develops epiphyllous buds during leaf formation, which remain dormant until leaves are excised from the plant, due to presumably a disruption of hormones supply that triggers shoots initiation (Jaiswal and Sawhney, 2006b; Sawhney et al., 1994). In some cases, bud dormancy does not affect roots initiation as adventitious-like roots emerge when leaves are still attached to the plant (Garcês and Sinha, 2009a). On the other hand, plantlet formation in constitutive plantlet-forming species *K. daigremontiana* resembles zygotic embryogenesis, but skipping dormancy and seedling stage (Garcês et al., 2014). In contrast with inducible plantlet-forming species, constitutive plantlet-forming species form pedestal structures in the notches, in which plantlet primordia emerge from. Once the plantlets are fully formed, excision sites are established at the plantlets base, allowing them to fall onto the ground and start growing independently (Garcês et al., 2007).

To date, little is known about genetic mechanism(s) modulating the plantlet formation in *Kalanchoë* leaves. Ectopic expression of a class 1 *KNOTTED-LIKE HOMEOBOX1* (*KNOX1*) gene, *SHOOTMERISTEMLESS* (*STM*) in leaf notches was proven to be required for the formation of plantlets. *STM*-downregulated *K. daigremontiana* transgenic plants were unable to develop plantlets (Garcês et al., 2007). *STM* is normally expressed in the shoot apical meristem (SAM) where it maintains pluripotent stem cells (Endrizzi et al., 1996). In *Arabidopsis*, *STM* is required to develop and maintain a functional SAM and its ectopic expression induces *de novo* meristem formation (Scofield et al., 2014). *stm*-silenced *Arabidopsis* mutants failed to organise a SAM

during embryogenesis (Long et al., 1996). Consistent to the fact that *STM* expression on the leaves of *Kalanchoë* plantlet-forming species is required for plantlet formation, *STM* was not expressed in leaves of non-plantlet forming species (Garcês et al., 2007). This suggest that plantlet formation is facilitated by meristematic pathways. In addition, two embryogenesis genes, *LEAFY COTYLEDON1* (*LEC1*) and *FUSCA3* (*FUS3*) also were found to be expressed in the leaf margin and plantlet primordia of constitutively plantlet-forming *K. daigremontiana* (Garcês et al., 2007). *LEC1*-downregulation did not affect plantlet formation in transgenic *K. daigremontiana* because LEC1 protein was truncated and unfunctional. This also allow plantlet primordia to bypass dormancy but also make zygotic seeds unviable (Garcês et al., 2014). A functional *Arabidopsis thaliana LEC1* expressed in *K. daigremontiana* made plantlet primordia behave like seeds, going through dormancy and accumulating oils, ultimately impeding normal plantlet development in the leaves (Garcês et al., 2014).

Transcriptome analyses are useful to reveal gene expression from specific cells or tissues at a given developmental stage or process (Ward et al., 2012). RNA-sequencing (RNA-seq) and DNA microarrays are the most common methods for broad gene expression quantification (Wang et al., 2009). RNA-seq analysis has been established as an essential tool for the study of transcriptomes (Garber et al., 2011; Kukurba and Montgomery, 2015). It allows the identification of novel genes related to specific processes or pathways, quantification of gene expression under different conditions, visualization of expression trends and comparison of transcriptomes between different species and cultivars in model and non-model plants (Arick and Hsu, 2018; Begara-Morales et al., 2014; Garg and Jain, 2013). In particular, comparative approaches of transcriptomic analyses have been performed in evolutionary, crop yield performance and specific traits studies. An RNA-seq analysis in crested wheatgrass (*Agropyron cristatum* L.) provided a robust molecular basis of floral initiation and development, identifying 113 flowering time-associated genes, 123 *MADS-box* genes and 22 *CONSTANS-LIKE* (*COL*) candidate genes (Zeng et al., 2017). In grape (*Vitis vinifera*), an RNA-seq analysis allowed the detection of differentially expressed transcripts related to gibberellic acid (GA) and abscisic acid (ABA) pathways during paradormancy, endodormancy and summer budding (Khalil-Ur-Rehman et al., 2017). An RNA-seq analysis was also implemented to compare transcriptomes from wild *Agave deserti*, *A. sisalana* and domesticated *A. tequilana*, in order to track

phylogenetic relationships and traits evolution, finding numerous key candidate unigenes modulating fructan, fibre and stress response-related pathways (Huang et al., 2018).

This study aims to detect biological processes and genes involved during plantlet formation in constitutive (*K. daigremontiana*) and inducible (*K. pinnata*) *Kalanchoë* species through the use of RNA-sequencing. Based on the differences in mode of plantlet formation and morphological structure of plantlets, we selected specific plantlet stages and time points to harvest tissues for our experiment. Technical analysis of our experiment and biological replicates indicate that our data is highly consistent and reliable. In both species, a large number of genes are involved during plantlet initiation and development. However, the changes in expression of these genes can be categorised into only 8 and 12 patterns in *K. daigremontiana* and *K. pinnata* respectively. From this dataset, we compared and contrasted unique and shared GO terms overrepresented during plantlet formation in each species. We found more unique GO terms overrepresented during plantlet formation in *K. pinnata* compared to *K. daigremontiana*. In *K. daigremontiana,* these GO terms include response to stress, cellularization and whereas in *K. pinnata*, the terms were immune system process, stem cell population maintenance and response to inorganic substance. Our results also detected common overrepresented pathways in both species, from which, we highlighted the ones that might be implicated during plantlet formation such as: signalling, regulation of hormone levels, reproduction and response to karrikin. Functions of genes involved in these pathways provided clues towards mechanisms recruited in plantlet formation of both *Kalanchoë* species. However, the conclusions we have arrived at are still preliminary due to the absence of further experimental evidence. Nonetheless, our study serves as a pioneering source of molecular insight into plantlet formation and development in two plantlet-forming *Kalanchoë* species.

5.3. **Materials & Methods**

5.3.1. Plant Materials and Growth Conditions

Wild-type *K. daigremontiana* plants were grown in SANYO versatile environmental test chamber MLR-351 at 23˚C with a photoperiod of 16 hour/8 hour with 50 µmol $m^{-2}s^{-1}$ light and 60 % humidity. Wild-type *K. pinnata* plants were grown in Percival Scientific growth chamber AR-60L at 23 ˚C with a photoperiod of 8 hour/16 hour with 30 µmol $m^{-2}s^{-1}$ light and 60% humidity. The plants were grown in a mixture of 6 parts Levington® F2 Seed & Modular Compost (The Scotts Company, UK), 1 part Vermiculite V3 medium (Sinclair Pro, UK) and 1 part Perlite P35 standard (Sinclair Pro, UK). Four distinct stages of plantlet formation in wild-type *K. daigremontiana* were identified to include stages of plantlet initiation (Fig. 5.1A). Leaves exhibiting at least three of these stages of plantlet maturation along its leaf margin are carefully selected for use. The leaves were removed using a razor blade and 0.3 cm^2 tissues at the leaf notches were harvested using the blade. The control samples were whole margin of leaves of about 1-2cm long when measured from base to tip of each leaf. As for *K. pinnata*, four time points after leaf detachment (0 h, 4 h, 24 h, 48 h) were selected. 0.3 cm^2 tissues at the leaf notches were harvested with a razor blade from unattached leaves (0 h) and from leaves detached after 4 hours, 24 hours and 48 hours. No major morphological changes were present during these time points. All samples harvested were immediately frozen in liquid nitrogen and stored at -80 °C until RNA extraction. Images in Fig. 1A were taken using a S8AP0 Stereo Microscope (Leica Microsystems, Germany) with a Digital D3100 camera (Nikon, Japan) attached. Images in Fig. 1B were taken using the same microscope but with a GX-CAM-Eclipse camera (GT Vision, UK) attached. All images were also processed with ImageJ 1.48V to include a scale bar.

5.3.2. RNA extraction and RNA-Sequencing

Total RNAs from each sample was extracted with Qiagen RNeasy Plant Mini Kit (Qiagen, UK) according to the manufacture's protocol with modification. For *K. daigremontiana* samples, 600 µl of RLC buffer with 10 mg of Polyvinylpyrrolidone (PVP) with molecular weight 40,000 was used for a maximum of 100 mg tissue powder. For *K. pinnata* samples, 600 µl of RLC buffer with 10 mg of Polyethylene glycol (PEG) with molecular weight 40,000 was used for a maximum of 100 mg tissue powder. The mixed solution of samples from *K. daigremontiana* or *K. pinnata*

was then vortexed and incubated for 1 minute at 56 °C and 80 °C respectively before following the subsequent steps of the kit's protocol. Purified RNA samples were sent for Sanger sequencing by Illumina HiSeq 2000 technology (The University of Manchester Sequencing Facility). Several quality checks on the RNA-sequencing reads were performed with FastQC (Babraham Bioinformatics, UK). DESeq2 (Bioconductor, Canada) was used to generate a PCA plot (Fig. 5.1C) and differential gene expression reading between samples.

5.3.3. Expression Profiling and Clustering Analysis

Based on the differential gene expression readings, volcano plots (Fig. 5.5) were subsequently generated using DESeq2 to show proportion of genes that are significant and up- or downregulated between samples of different stages or time points. The dataset was trimmed by using adjusted p value ≤ 0.05, and log2 fold change> |0.6| for *K. daigremontiana* and log2 fold change > |1.585| for *K. pinnata*. The means were calculated for each condition in log scale and Z-transformed (a normalisation where for each gene the average of the 5 means was set to zero and the standard deviation set to 1). A heat map was then generated with DESeq2 to cluster genes with similar expression profiles (Fig. 5.2). The trimmed dataset was used to identify genes that are differentially expressed from one stage to another. Venn diagrams (Fig. 5.4) showing the number of differentially expressed genes and whether these genes overlapped between different comparisons were generated using http://bioinformatics.psb.ugent.be/webtools/Venn/. The average expression level of genes from each cluster was used to generate line graphs using Microsoft Excel to illustrate changes in expression pattern of genes in each cluster. Gene clusters with similar trend was collated onto the same graph and presented in Fig. 5.3.

5.3.4. Gene Ontology Enrichment Analysis

Gene ontology (GO) enrichment analysis was performed on each of the gene clusters from *K. daigremontiana* & *K. pinnata*. The list of genes in each cluster were analysed for biological processes that are overrepresented using http://geneontology.org/. ReviGO was used to remove redundant GO terms that are enriched in each cluster. Only terms with 0 dispensability are presented in Supplementary table 5.1. A multiple list comparator tool (http://www.molbiotools.com/listcompare.html) was used to determine whether

overrepresented terms with 0% dispensability from each cluster overlaps or is exclusive to each species. The overlapping GO terms are presented in Table 5.1. GO terms with more specific biological functions and that are more relevant to plantlet formation were selected. Genes present in selected GO terms are presented in Table 5.2. The number of genes in these GO terms and whether these genes overlap between different gene clusters were generated using http://www.molbiotools.com/listcompare.html and are shown in Fig. 5.7. GO terms exclusively present only in one species and not the other are shown in Table 5.3.

5.4. **Results**

5.4.1. Morphology of plantlet formation and clustering of samples from selected plantlet formation stages and time-points

The process of plantlet formation in *K. daigremontiana* and *K. pinnata* is superficially analogous, both species have the ability to produce progeny from specialised structures located on the leaf margins. These structures were more prominent in *K. daigremontiana*, they resembled pedestals holding developing somatic embryos (Fig. 5.1A). Before *K. daigremontiana* plantlet was morphologically visible, a pedestal was formed (Fig. 5.1A, S2) from the leaf notch localised between leaf serrations (Fig. 5.1A, S1). As the pedestal continued to develop, plantlet primordium grew and emerged from the pedestal (Fig. 5.1A, S3). As the plantlet matures and formed cotyledons, it continued to remain on the pedestal (Fig. 5.1A, S4). Once the plantlets were fully formed, they detached from the pedestals. In the case of *K. pinnata*, the plantlet primordium emerged from a bud-like structure (Fig. 5.1B, S1). As the plantlet developed and formed cotyledons, the bud-like structure became less visible (Fig. 5.1B, S2). Eventually, roots started to grow out of the plantlet base (Fig. 5.1B, S3). Beyond this stage, the cotyledons and roots continued developing as the plantlet matures (Fig. 5.1B, S4). The plantlets stayed attached to the senescent leaves until these were decomposed.

Molecular studies on plantlet formation have been limited, hence, an RNA-sequencing analysis was conducted to capture genes and biological processes involved in the initiation and development of plantlets in *K. daigremontiana* and *K. pinnata*. *K. daigremontiana* and *K. pinnata* have different modes of plantlet formation; *K. daigremontiana* produce plantlets continuously under long-day condition whereas *K. pinnata* leaves form plantlets upon detachment or aging (Garcês and Sinha, 2009a). Hence, tissues of four different *K. daigremontiana* plantlets stages (S1, S2, S3, S4) were selected and harvested for the RNA-sequencing experiment (Fig. 5.1A). The control samples (Con) in *K. daigremontiana* were young 1 to 2 cm leaf margins. For *K. pinnata*, tissues at the notches (N) of post-detachment leaves across four time points (0 h, 4 h, 24 h, 48 h) were used. The mid-section (M) of leaves after 48 h post-detachment was used as control samples. Principal component analyses (PCA) were performed, and two graphs were generated to illustrate two factors PC1 and PC2 that captured the most variance among the samples. The PCA of *K. daigremontiana* tissues showed high

consistency between the biological replicates as evident from the tight clustering of replicates (Fig. 5.1C). In *K. daigremontiana*, there was no overlapping of samples across PC2, suggesting differences according to the different stages. Across PC1, there was a slight overlap between stage 3 (S3) and stage 4 (S4). This indicates less changes between the last two stages of plantlet formation in *K. daigremontiana* and more changes occurred during the formation of the pedestal from stage S1 to S2. Nonetheless, due to the lack of overlapping between samples, this indicates that these developmental stages were very distinct from each other and that PC1 and PC2 represent specific factors representing differences due to the developmental stages. On the other hand, for *K. pinnata,* the biological replicates were grouped perhaps according to different time points after leaf detachment and to the type of tissues (Fig. 5.1D). PC1, which covered 41 % variance might have captured variation between the different time points. 0 hours (0hN) compared to 4 hours (4hN) and 0hN compared to 24 hours (24hN) showed similar variation percentage, but these variations were smaller than the one found between 4hN and 24hN. Variations between 24hN and 48 hours (48hN) were the smallest between all comparisons, suggesting that major changes occurred within the first 24 hours after leaf detachment. Samples of 48 hours after leaf detachment on the mid-section of the leaves (48hM) separated from the rest at PC2, probably because the tissue came from the mid-section of the leaves where no plantlet formation occurred. In addition, unlike *K. daigremontiana* where the variations among developmental stages showed a directional gradual progression for both PC1 and PC2, in *K. pinnata* variations in 4hN showed an opposite trend to 24hN and 48hN samples. PC2 covered 26 % of variations might have represented the difference between the source of tissue: notches and the mid-section of the leaf. In both plant species, the replicates grouping together showed consistency and reliability of our results.

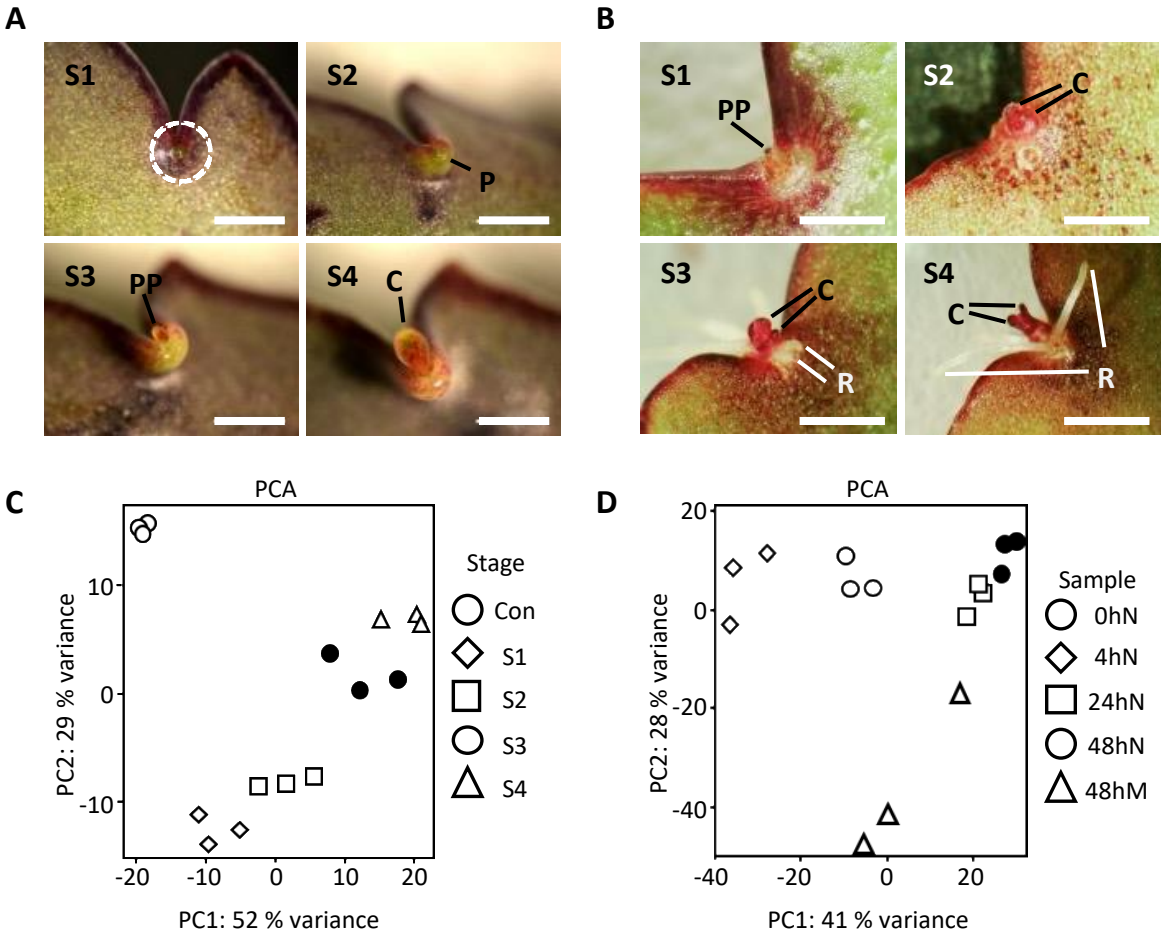

Figure 5.1 *K. daigremontiana* and *K. pinnata* plantlet analyses and principle component analysis (PCA). (A) Four distinctive stages of plantlet formation in *K. daigremontiana* selected for RNA-sequencing experiment. (Stage 1, S1) Leaf notch without pedestal formation; (Stage 2, S2) leaf notch with pedestal formation; (Stage 3, S3) leaf notch with pedestal and with an emerging plantlet primordium; (Stage 4, S4) leaf notch with plantlet primordium with visible cotyledons. (B) Plantlet formation in *K. pinnata*. (S1) plantlet primordium emerging from leaf notch; (S2) plantlet primordium with visible cotyledons emerging from leaf notch; (S3) plantlet with emerging root primordia; (S4) plantlet with extended root formation. The scale bar is 1 mm. C, cotyledon; P, pedestal; PP, plantlet primordium; R, root. (C-D) PCA of RNA samples harvested from leaf notches of *K. daigremontiana* at stages (A) and of *K. pinnata* at time points 0 hour (h), 4 h, 24 h and 48 h. Margins of young 1-2 cm leaves were used as control samples (Con) for *K. daigremontiana* whereas for the control samples were *K. pinnata* mid-section of detached leaves after 48hM. Three biological replicates were generated for each developmental stage or time point. Con, Control; N, Leaf notches; M, Leaf mid-section.

5.4.2. Heat map and graphical representation of expression of genes in different clusters during plantlet formation

Transcriptomic analyses revealed a total of 4,594 genes in *K. daigremontiana* and 5,706 in *K. pinnata* that were significantly differentially expressed during plantlet formation. Genes with similar expression profiles were hierarchically clustered: 8 clusters for *K. daigremontiana* and 12 for *K. pinnata* (Fig. 5.2). At first glance, *K. daigremontiana* gene clusters in comparison to *K. pinnata,* exhibited either very high or very low expression, as suggested by greater number of

concentrated blue or red regions. In the control samples (C), *K. daigremontiana* gene cluster 1, 2 and 6 showed the lowest expression levels, followed by cluster 8, then cluster 7 and 4 whereas gene clusters 3 and 5 showed the highest expression levels (Fig. 5.2A). At stage S1, gene clusters 1 and 7 showed the highest expression level, followed by cluster 2, then 3 and 4, 5 whilst clusters 4 and 8 had the lowest expression level. At stage S2, genes in cluster 1, 2, 6 and 7 exhibited higher expression level than the other clusters. However, at later stages, S3 and S4, genes within each cluster exhibited greater differences in expression level, as suggested by a display of different colours along the spectrum. In contrast to *K. pinnata*, this was observed in all gene clusters across most time points (Fig. 5.2B). In *K. pinnata*, the highest expression level was in gene cluster 1 at 48hM; cluster 3 at 4hN; cluster 11 at 0hN and cluster 12 at 48hN. This was unlike *K. daigremontiana* as the highest expression level occurred at the same stage C (Fig. 5.2A). Gene clusters in *K. pinnata* with the lowest expression level were gene cluster 4 at 4hN, cluster 6 and 8 at 48hM and cluster 10 at 0hN (Fig. 5.2B). Apart from gene cluster 12 at 48hN, the expression level of all gene clusters at 24hN and 48hN were fairly similar.

Gene clusters with similar expression pattern during plantlet formation in *K. daigremontiana* and *K. pinnata* were contrasted on the same graph (Fig. 5.3). Clusters 1, 2 and 7 in *K. daigremontiana* showed a noticeable upregulation between Con and S1, but their expression decreased gradually during S3 and S4 (Fig. 5.3A). This expression pattern was similar to clusters 1 and 7 in *K. pinnata* (Fig. 5.3E). *K. pinnata* clusters 3 and 6 initially behaved similarly but there was an upregulation between 24 and 48 hours after leaf detachment (Fig. 5.3I). In *K. daigremontiana*, expression of gene clusters 4, 5 and 8 dramatically dropped between Con and S1 but were upregulated again after S1 (Fig. 5.3B). A similar expression pattern was seen in clusters 8 and 12 in *K. pinnata* (Fig. 5.3F, J). Clusters 4 and 9 also showed a similar expression pattern during the first few time points but the genes were downregulated again at 24 hours after leaf detachment (Fig. 5.3F). A steady upregulation was observed in expression of genes in cluster 6 of *K. daigremontiana*, in which the same observation applies to clusters 5 and 10 in *K. pinnata* (Fig. 5.3C and G). In cluster 3 of *K. daigremontiana* and clusters 2 and 11 of *K. pinnata*, an opposite expression trend was observed, where a progressive downregulation was seen from the starting point to the last stage (Fig. 5.3D and H).

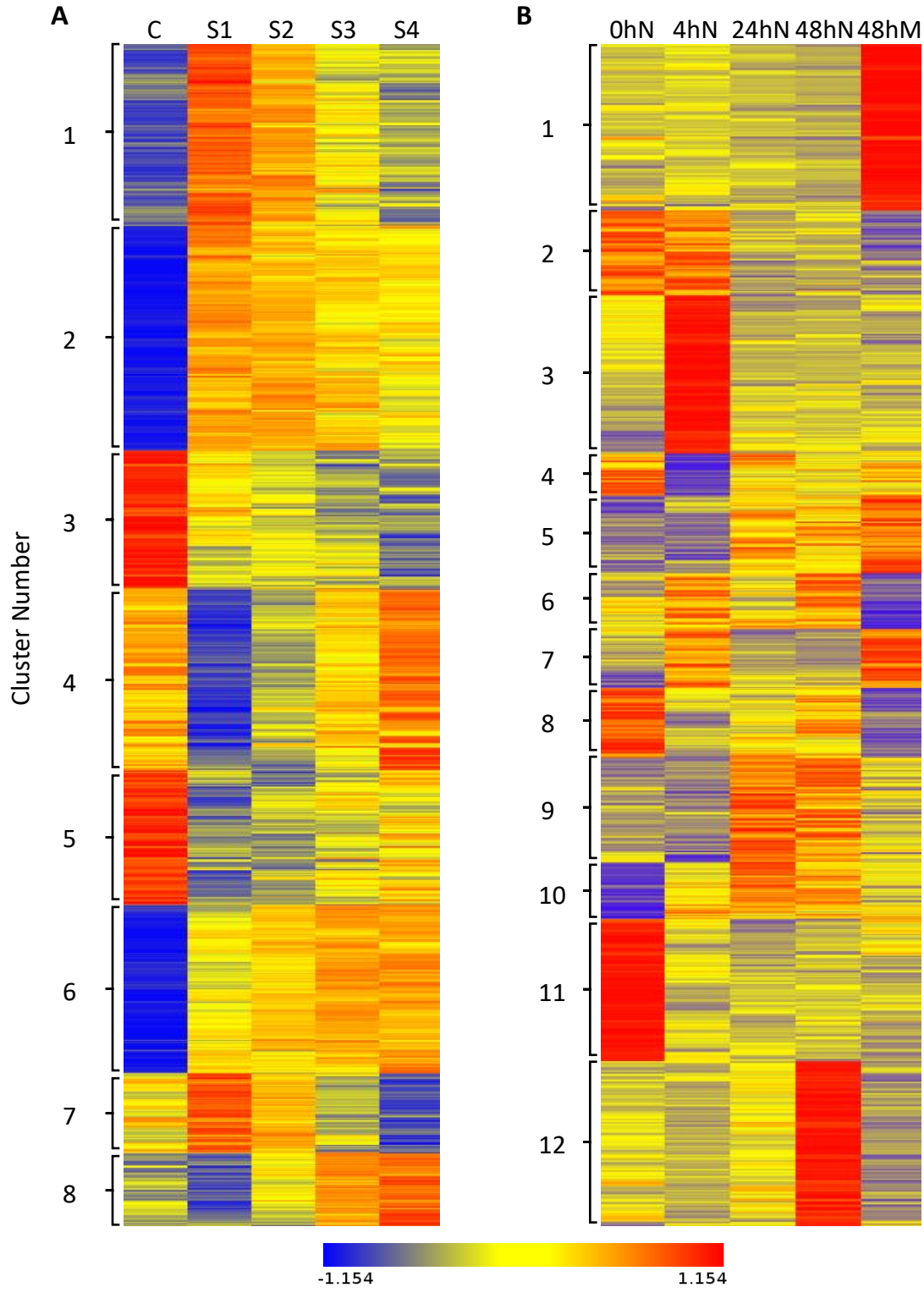

Figure 5.2 Heat Map shows hierarchical clustering of genes with similar expression profiles.
(A) Heat map shows a total of 4,594 differentially expressed genes in *K. daigremontiana*, which groups into 8 clusters with similar expression profiles. Only genes with adjusted p value ≤ 0.05 and log2 foldchange > |0.6| were selected. C, Control; S1, stage 1; S2, stage 2; S3, stage 3; S4, stage 4. (B) Heat map shows a total of 5,706 differentially genes in *K. pinnata*, which groups into 12 clusters with similar expression profiles. Only genes with adjusted p value ≤ 0.05 and log2foldchange > |1.585| were selected. N, Leaf notches; M, leaf mid-section. Colour range of blue-yellow-red indicates expression level from low to high.

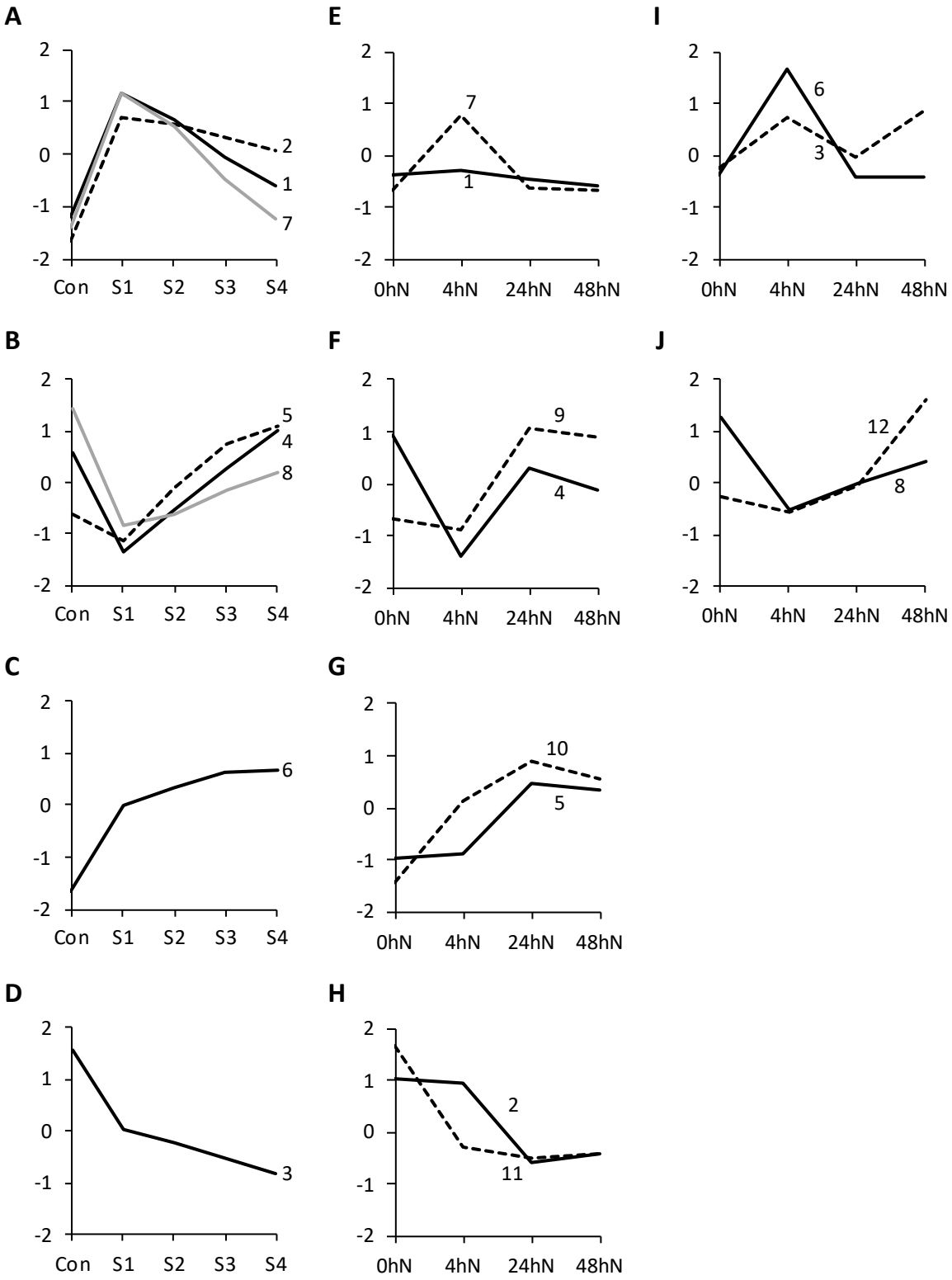

Figure 5.3 Graphical representation of average change in expression of genes in different gene clusters.
(A-D) The expression pattern of 8 gene clusters in *K. daigremontiana* across different plantlet developmental stages. (E-J) The expression pattern of 12 gene clusters across different time points after detachment of *K. pinnata* leaf. Clusters of genes with similar trend of changes in expression are visualised on the same graph. Number adjacent to each graph line corresponds to the number of gene cluster in figure 5.2. Con, Control; S1, stage 1; S2, stage 2; S3, stage 3; S4, stage 4; N, leaf notches.

5.4.3. Number of significant differentially expressed genes during plantlet formation

Among the significant differentially expressed genes (DEG), shared and unique expression was detected between the different stages (Fig. 5.4) in each species. The largest number of uniquely expressed genes were observed at the initiation of plantlet formation, between stage 1 and 2 in *K. daigremontiana* (n=3,104) (Fig. 5.4A), and in the first 4 hours after leaf detachment in *K. pinnata* (n=302) (Fig. 5.4B). This indicates that the initiation of plantlet formation for both species involves many more DEG than at the later stages. In *K. pinnata*, there was also a large number of DEG between 48 hours after leaf detachment in notches and mid-section of the leaves (n=560), however, this was more likely to represent genes that are important for development of different tissues rather than for plantlet initiation as there was no plantlet formation in the mid-section of leaves. In *K. daigremontiana*, 3,104 genes were specific to S1 vs Con, 84 genes to S2 vs S1 and 183 genes were shared between Con, S1 and S2. 79 genes were unique to S3 vs S2 and 79 genes to S4 vs S3, from these, 15 genes were shared between S2, S3 and S4. 115 genes were shared between all the stages in *K. daigremontiana*. *In K. pinnata*, 302 genes were specific to 4hN vs 0hN, 273 genes to 24hN vs 4hN and 259 genes were shared in 0hN, 4hN and 24hN. 209 genes were unique to 24hN vs 0hN, 156 genes to 48hN vs 0hN and 198 genes were shared between 0hN, 24hN and 48hN. 560 genes were unique to 48hM VS 48hN and 70 genes were shared between all the time points. To investigate shared and unique genes for plantlet formation between *K. daigremontiana* and *K. pinnata*, we compared DEGs in earlier stages of plantlet formation in these species (Fig. 5.4C). Between the two species, 114 genes were overlapped, while 2,179 genes were unique to *K. pinnata* and 2,316 to *K. daigremontiana*. Among *K. daigremontiana* specific DEGs, 2,013 genes were unique for Con vs S1, 84 genes were unique for S2 vs S1 and 219 genes were shared for Con, S1 and S2. Among *K. pinnata* specific DEGs, 1,116 genes were unique for 4hN vs 0hN, 588 genes were unique for 24hN vs 4hN and 475 genes were shared for 0hN, 4hN and 24hN.

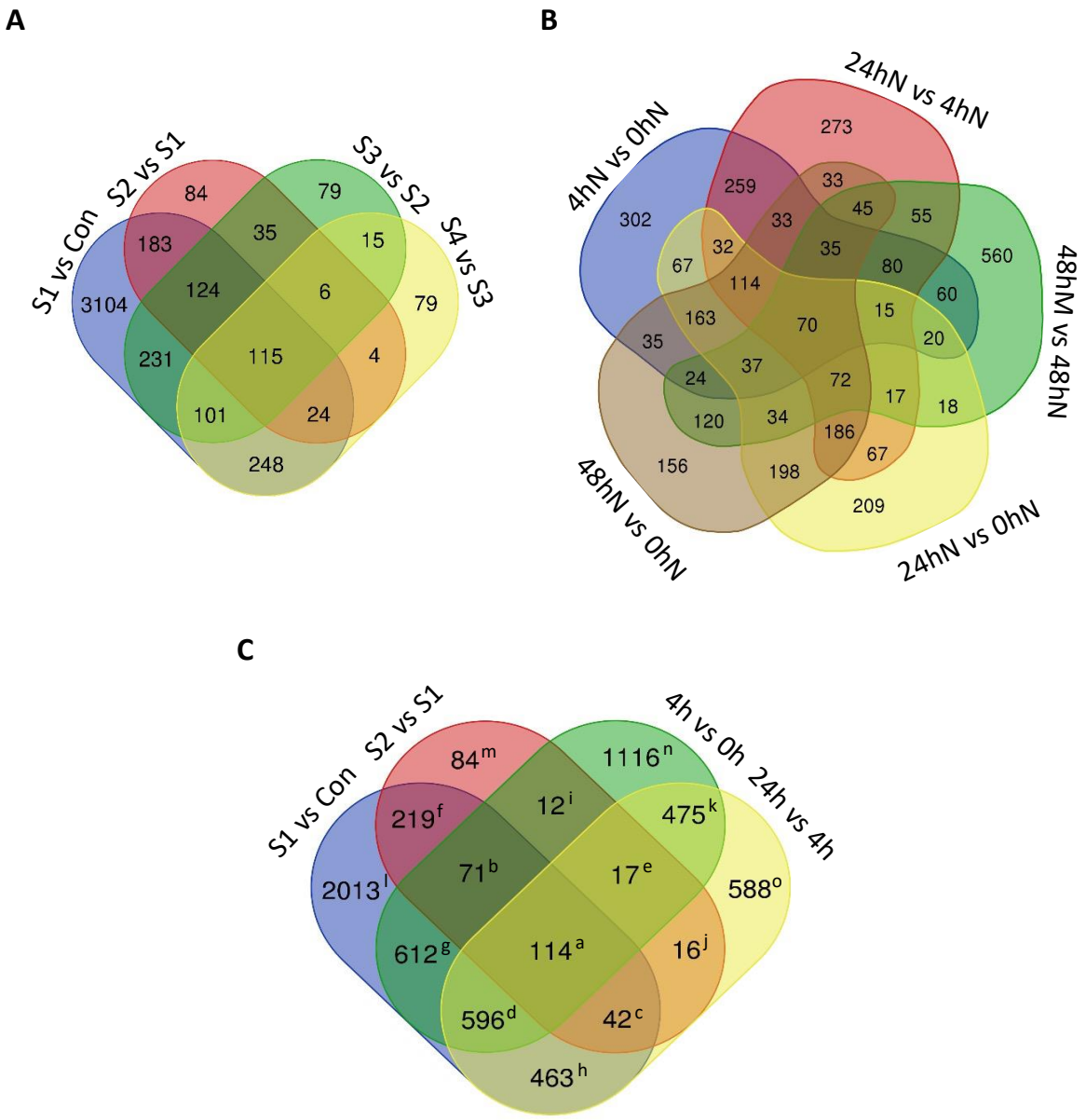

Figure 5.4 Venn diagrams showing number of differentially expressed genes (DEG) during plantlet formation. Number of DEG overlapped from comparison of (A) different plantlet developmental stages from *K. daigremontiana* or (B) samples harvested at specific time points upon *K. pinnata* leaf detachment. (C) Number of exclusive and overlapping differentially expressed genes between selected plantlet stages from (A) and time potins from (B). Con, Control; S1, stage 1; s2, Stage 2; S3, stage 3; S4, stage 4; N, leaf notches; M, leaf mid-section. Superscript alphabets correspond to the lists of genes in Supplementary table 5.1.

5.4.4. Statistical significance of DEG during plantlet formation

The RNA-sequencing experiment captured many DEG during plantlet formation in both *K. daigremontiana* and *K.* pinnata, however only certain proportions of DEG exhibit statistically significant change in expression (Fig. 5.5). Both species showed a similar amount of significantly up and downregulated genes between the first two samples (Fig. 5.5A, E). Some of these genes had a higher statistical significance in *K. daigremontiana* compared to *K. pinnata* as seen from presence of DEG having a $-\log_{10}$(p value) more than 60 which is highest than the most significant DEG in *K. pinnata*. The overall symmetry of the volcano plots showed slightly different tendencies in significant DEG between the two species. Taking into consideration only the statistically significant DEG, across all comparisons, up-regulated genes displayed higher statistical significance than down-regulated genes in *K. daigremontiana* (Fig. 5.5B-D); whereas in *K. pinnata*, up-regulated and down-regulated genes were of fairly similar statistical significance (Fig. 5.5E, F, J-L). In *K. daigremontiana*, there was a larger proportion of upregulated genes that were statistically significant when comparing gene expression between S1, S2 and S3 (Fig. 5.5B, C) and there were more non-significantly changed genes between S3 and S4 (Fig. 5.5D). On the other hand, in *K. pinnata*, between 4 h and 24 h after leaf detachment (Fig. 5.5F), there was a similar amount of significantly up and downregulated genes. The expression of almost all genes did not change significantly between 24 h and 48 h after leaf detachment (Fig. 5.5G). However, when comparing 24 h and 0 h control (Fig. 5J, K), an upregulation and downregulation of genes were noticed, with some genes being more significative similar to what was observed in 0 h and 48 h. We also compared DEG for the mid-section of leaf 48 h after leaf detachment, finding roughly the same amount of up and downregulated genes (Fig. 5.5L). This suggests that overall, for both species, gene expression changes were more significant in the early stage or time point, that that of later stages.

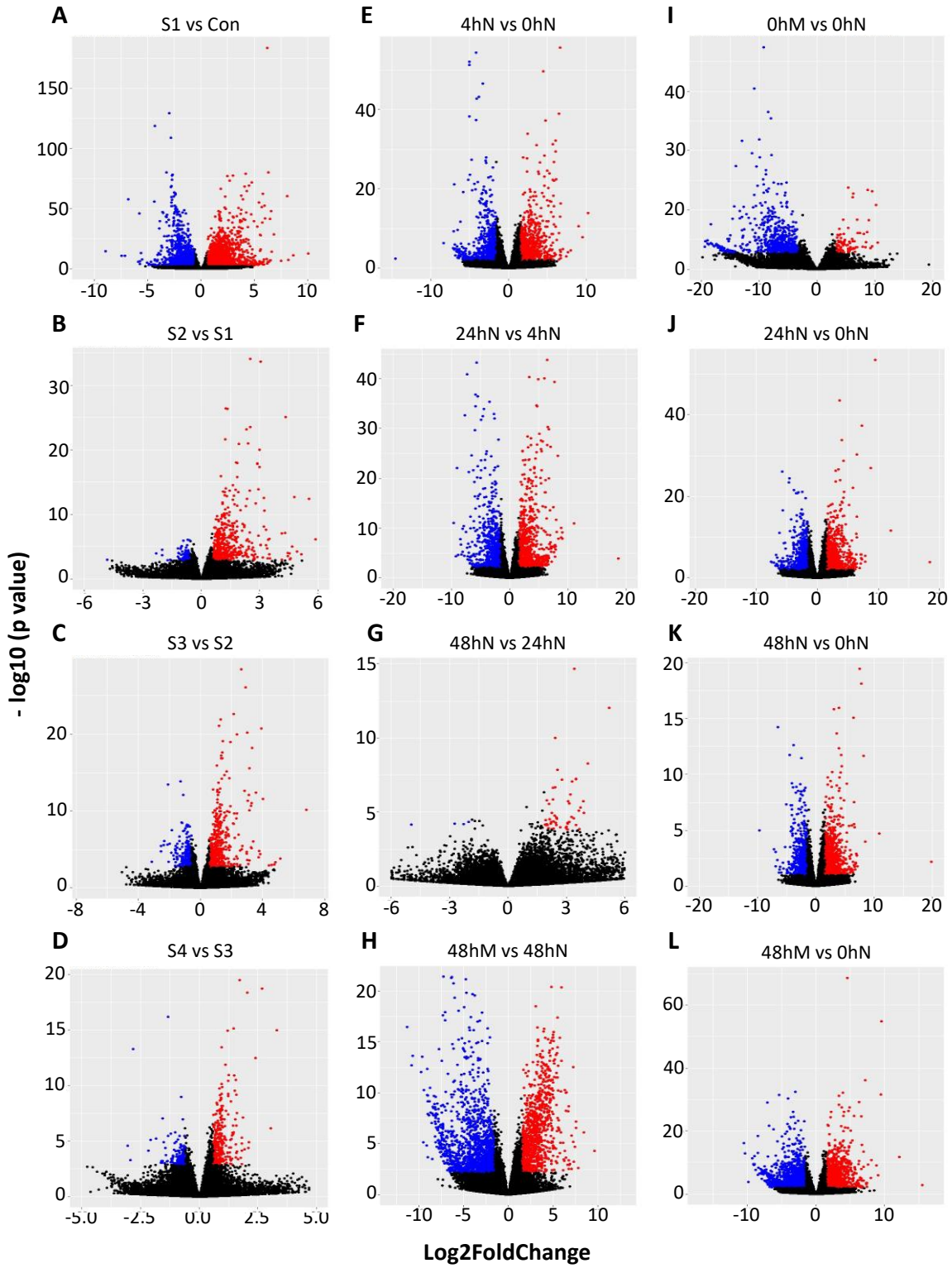

Figure 5.5 Volcano plots showing statistical significance of changes in gene expression and their fold-change in expression during plantlet formation.

Each plot shows comparison between two developmental stages of plantlet formation in *K. daigremontiana* (A-D) or between two time points post-detachment of *K. pinnata* leaves (E-L). Each plot shows -log10 (p value) against log2 foldchange. Blue, False discovery rate (FDR) ≤ 0.05, log2 foldchange ≤ -0.6 for A-D, log2 foldchange ≤ -1.585 for E-L; Red, FDR≤0.05, Log2 foldchange > 0.6 for A-D, log2 foldchange > 1.585 for E-L; Black, not significant. Con, control; S1, stage 1; S2, stage 2; S3, stage 3; S4, stage 4; N, leaf notches; M, leaf mid-section.

5.4.5. Biological processes during *Kalanchoë* plantlet formation

Gene ontology (GO) enrichment analysis was performed on the clustering data to analyse the biological processes during plantlet formation of both *K. daigremontiana* and *K. pinnata* species. Overrepresented GO terms in both species are shown in Table 5.1. 'Response to stimulus', 'cellular process', 'developmental process', 'multicellular organismal process', 'biological regulation', 'metabolic process', 'regulation of hormone levels', 'reproduction', 'response to wounding', 'signalling' and 'gene expression' were found to be the most overrepresented GO terms in both *Kalanchoë* species. Genes in the GO term 'Response to stimulus' exhibited all eight trends of expression patterns presented in our dataset. Genes involved in 'cellular process' displayed all but expression trends 5 and 8. For genes functioning in 'developmental process' and 'multicellular organismal process', they were expressed in three patterns of trends 3, 5 and 8. Genes responsible for 'biological function' were expressed following trends 1, 3, 5 and 8 whereas 'metabolic process' genes were expressed following trends 1, 2, 6 and 7. Genes in both 'regulation of hormone levels' and 'reproduction' were expressed according to trend 3, showing upregulation between the first two stages and then downregulation in the subsequent stages. Genes in 'regulation of hormone levels' were also continuously upregulated across all stages (trend 5). Apart from expression trend 5, genes involved in 'response to wounding' also displayed expression trends 1 and 2 in which the genes were upregulated then downregulated in the first few stages. Similarly, 'signalling' and 'gene expression' genes were also expressed following trend 1 and 2, with the final stages down- and up-regulated respectively. As for genes with a role in 'response to karrikin', they exhibited expression trend 1 and 4, in which the latter trend of expression fluctuated from downregulation to upregulation and then downregulation again. From this list of GO terms, we shortlisted overrepresented GO terms that might be associated to plantlet formation: 'signalling', 'reproduction', 'response to wounding', 'regulation of hormone levels' and 'response to karrikin'. The number of unique and shared genes between gene clusters from *K. daigremontiana* and *K. pinnata* was shown in Fig. 5.6. In the 'signalling' GO term, there was 29 shared genes between *K. daigremontiana* and *K. pinnata* (Fig. 5.6A); 'response to wounding' and 'reproduction' had 9 and 5 shared genes respectively (Fig. 5.6B, C); 'regulation of hormone levels' shared 9 genes (Fig. 5.6D); and 'response to karrikin' shared 3 genes between the two species studied (Fig. 5.6E).

Table 5.1 List of overrepresented GO terms that overlap between gene clusters and its corresponding expression trend during plantlet formation in *K. daigremontiana* (Kd) and *K. pinnata* (Kp).

Number that follows the species name symbol Kd or Kp represents the cluster number derived from the heat map in Fig. 5.2 that categorised all genes into clusters based on similarity in expression patterns across different plantlet developmental stages or time points. There are 8 distinct expression trends exhibited by these genes (see Fig. 5.3 for graphical representation of expression trends). ↘ indicates the genes were downregulated, ↗ indicates the genes were upregulated from one stage or time point to the next. The occurrence records the frequency of gene clusters in which the GO term is overrepresented. The highlighted boxes show that the specific GO term is overrepresented in gene clusters of either *K. daigremontiana* (Kd), highlighted in grey and/or *K. pinnata* (Kp), highlighted in black.

			Expression Trend																		
			1					2		3					4		5	6		7	8	
GO Term	**GO ID**	**Occur-rence**	Kd1	Kd2	Kd7	Kp1	Kp7	Kp3	Kp6	Kd4	Kd5	Kd8	Kp8	Kp12	Kp4	Kp9	Kd6	Kp5	Kp10	Kd3	Kp2	Kp11
Response to stimulus	GO:0050896	12																				
Cellular process	GO:0009987	9																				
Developmental process	GO:0032502	6																				
Multicellular organismal process	GO:0032501	6																				
Biological regulation	GO:0065007	5																				
Metabolic process	GO:0008152	5																				
Regulation of hormone levels	GO:0010817	3																				
Reproduction	GO:0000003	3																				
Response to wounding	GO:0009611	3																				
Signalling	GO:0023052	3																				
Gene expression	GO:0010467	2																				
Response to karrikin	GO:0080167	2																				

Expression trend (Based on Figure 5.3)

Trend 1 ↗↘↘	Trend 2 ↗↘↗	Trend 3 ↘↗↗	Trend 4 ↘↗↘	Trend 5 ↗↗↗	Trend 6 ↗↗↘	Trend 7 ↘↘↘	Trend 8 ↘↘↗

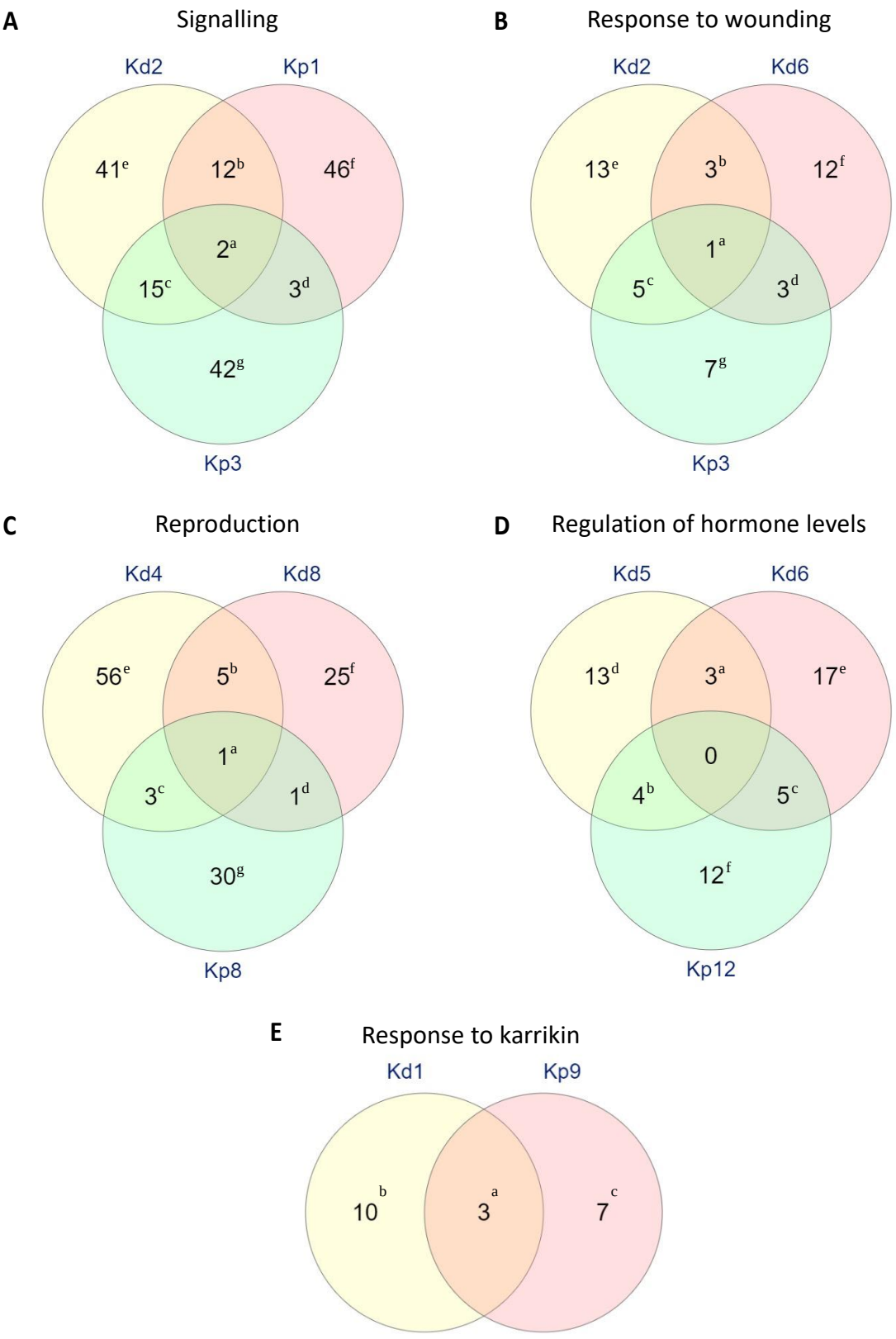

Figure 5.6 Number of genes in selected GO terms that are overlapped between different clusters of two *Kalanchoë* species.

Kd, *K. daigremontiana*; Kp, *K. pinnata*. Numerical value next to the species name symbol (Kd, Kp) represent the corresponding gene cluster in Figure 5.2. Numerical value in the Venn diagrams represents the number of genes. Superscript alphabets correspond to the lists of genes in Supplementary table 5.2.

5.4.6. Specific functions of DEG in selected biological processes

Upon further analysis, we recorded the function of DEGs in the GO terms shown in Fig. 5.6 on Table 5.2. The functions described for each gene was included based on its relevance to the GO term and possible participation to plantlet formation, thus the list of functions is not exclusive. Most of the genes in 'Signalling GO:0023052' play a role in response to different types of stress. The biotic stress described includes pathogen, disease and wounding and the abiotic stress includes heat, salt, drought, oxidative and endoplasmic reticulum (ER) stress. Among these genes, there were those involved in regulating abscisic acid (ABA) signalling during seedling germination and growth, such as *CALMODULIN 5* (*CAM5*), *PYRABACTIN RESISTANCE-LIKE 4* (*PYL4*), *DEHYDRATION-RESPONSIVE ELEMENT-BINDING 2C* (*DREB2C*), *RING AND DOMAIN OF UNKNOWN FUNCTION 1* (*RDUF1*), *PROTEIN PHOSPHATASE 2C FAMILY PROTEIN 5* (*PP2C5*), *RING-H2 FINGER A2* (*RHA2A*), *C2 DOMAIN PROTEIN* (*C2*) and *CBL-INTERACTING SERINE/THREONINE-PROTEIN KINASE 11* (*CIPK11*). For the GO term, 'Response to wounding GO:0009611', genes belonging to the same clusters Kd2 and Kp3 were also over-represented in the GO term, 'Signalling GO:0023052'. Hence, some of these genes are also involved in similar stress responses. *PHATOGENESIS-RELATED PROTEIN 3* (*PR3*) and *JASMONIC ACID CARBOXYL METHYLTRANSFERASE* (*JMT*) were over-represented in both 'Signalling GO:0023052' and 'Response to wounding GO:0009611'. Most of the genes over-represented in 'Response to wounding GO:0009611' are involved in either jasmonic acid (JA) synthesis or dependent on JA signalling. Over-represented genes in the GO terms, 'Reproduction GO:0000003', functions as the name suggests, in reproduction, which includes formation of reproductive structures such as flowers, siliques, pollen tube and seeds. The GO term, 'Regulation of hormone levels GO:0010817', contained 12 over-represented genes, in which all but 3 genes are associated with auxin hormone.

Table 5.2 List of overrepresented genes in selected GO terms that are shared between two or more gene clusters in *K. daigremontiana* and *K. pinnata.*

The gene ID represents Locus TAIR object ID. Gene description is adapted from TAIR locus description. The gene function is described exclusively based on its functional relevance to plantlet formation. Kd, *K. daigremontiana*; Kp, *K. pinnata*.

Signalling GO:0023052					
Gene ID	Gene Symbol	Description	Cluster in Kd	Cluster in Kp	Gene Function & Reference
AT1G21326		MAP kinase 4 substrate 1 (MKS1) homolog	2	1	Pathogen defence (Andreasson et al., 2005)
AT1G42990	BZIP60	Basic region/leucine zipper motif 60	2	1	ER stress (Gayral et al., 2020)
AT2G23460	XLG1	Extra-large G protein 1	2	1	Stress response (Liang et al., 2017), disease resistance (Zhu et al., 2009)
AT2G30360	CIPK11	A member of the CBL-interacting protein kinase, SOS2-like protein	2	1	Salt stress (Yang et al., 2019b), drought stress (Ma et al., 2019), Alkaline stress (Xu et al., 2012), ABA signalling (Zhou et al., 2015)
AT2G40180	PP2C5	MAPK phosphatase	2	1	Stress response (Schweighofer et al., 2004), seed germination (Brock et al., 2010)
AT3G17510	CIPK1	CBL-interacting protein kinase 1	2	1	Nutrient deficiency (Lu et al., 2020), osmotic stress (Cho et al., 2018)
AT3G25070	RIN4	RPM1 interacting protein 4, a member of R protein complex	2	1	ER stress (Chakraborty et al., 2020), pathogen defence (Prokchorchik et al., 2020; Ray et al., 2019)
AT3G46620	RDUF1	RING domain-containing E3 ligase	2	1	Salt stress (Li et al., 2013), drought stress (Kim et al., 2012), ABA-mediated germination (Kim et al., 2012)
AT4G15800	RALFL33	Rapid Alkalinization Factor-like 33	2	1	-
AT4G34410	ERF109	Ethylene response factor 109	2	1	Wounding (Ye et al., 2020), seedling growth (Dong et al., 2020), salt stress (Bahieldin et al., 2018)
AT5G47910	RBOHD	Respiratory burst oxidase homologue D	2	1	Oxidative stress (Cui et al., 2020; Kimura et al., 2020)
AT5G48150	PAT1	Phytochrome A signal transduction 1	2	1	Light perception (Torres-Galea et al., 2013)
AT2G20900	DGK5	Diacylglycerol kinase 5	-	1,3	Freezing stress (Tan et al., 2018)
AT3G17980	C2	C2 domain	-	1,3	ABA sensitivity (Rodriguez et al., 2014), salt & oxidative stress (Cheung et al., 2013)
AT5G20480	EFR	EF-TU receptor	-	1,3	Pathogen defence (Spears et al., 2019)
AT2G03440	NRP1	Nodulin-related protein 1	2	1,3	Heat stress (Fu et al., 2010), ER stress (Reis et al., 2016; Wang et al., 2019)
AT3G12500	PR3	Pathogenesis-related protein 3, encodes basic chitinase	2	1,3	Pathogen defence (Dinolfo et al., 2017; Martin-Rivilla et al., 2019)
AT1G12110	NRT1	Nitrate transporter 1	2	3	Salt stress (Liu et al., 2020b)
AT1G13260	RAV1	Related to ABI3/VP1 1	2	3	Dehydration stress (Sengupta et al., 2020)

AT1G15100	RHA2A	Ring-H2 finger A2A	2	3	ABA signalling & drought stress (Li et al., 2011)
AT1G19640	JMT	Jasmonic acid carboxyl methyltransferase	2	3	Drought stress (Kim et al., 2009), cold stress (Li et al., 2017)
AT1G25560	TEM1	Tempranillo 1	2	3	Salt tolerance (Osnato et al., 2020), flowering (Osnato et al., 2012; Sgamma et al., 2014)
AT2G27030	CAM5	Calmodulin 5	2	3	Pathogen defence (Lv et al., 2019), heat shock (Niu et al., 2020), ABA inhibition during seed germination & seedling growth (Zhou et al., 2018)
AT2G38310	PYL4	Pyrabactin resistance-like 4	2	3	ABA signalling during germination (Wang et al., 2020c)
AT2G40340	DREB2C	Dehydration-responsive element-binding protein 2C	2	3	Oxidative stress (Hwang et al., 2012), heat stress (Chen et al., 2010), salt stress (Song et al., 2014), ABA biosynthesis during germination (Je et al., 2014)
AT4G26150	CGA1	Cytokinin-responsive GATA factor 1	2	3	Chloroplast development (Chiang et al., 2012; Hudson et al., 2011), flowering (Mara and Irish, 2008; Richter et al., 2013)
AT5G02810	PRR7	Pseudo-response regulator 7	2	3	Heat stress (Blair et al., 2019)
AT5G07580	ERF106	Ethylene response factor 106	2	3	Pathogen resistance (Fröschel et al., 2019), seedling growth (Zhu et al., 2020)
AT5G25190	ESE3	Ethylene and salt inducible 3	2	3	Salt stress during germination and seedling development (Zhang et al., 2011)
AT5G36930	NLR	Disease resistance protein (TIR-NBS-LRR class) family	2	3	Disease resistance (Tan et al., 2007)
AT5G47120	BI1	Bax inhibitor 1	2	3	ER stress (Ruberti et al., 2018), drought stress(Ramiro et al., 2016)
AT5G66730	IDD1	Indeterminate domain 1	2	3	Promote germination (Feurtado et al., 2011)
Response to wounding GO:0009611					
Gene ID	Gene Symbol	Gene Description	Cluster in Kd	Cluster in Kp	Gene Function & Reference
AT1G17840	ABCG11	ATP-binding cassette G11	2	3	Cutin transport (Panikashvili et al., 2010), vascular development
AT1G67560	LOX6	Lipoxygenase 6	2	3	JA synthesis, wounding response (Chauvin et al., 2013), stress resistance (Grebner et al., 2013)
AT3G12500	PR3	Pathogenesis-related protein 3, encodes basic chitinase	2	3	JA-mediated pathogen defense (Dinolfo et al., 2017; Martin-Rivilla et al., 2019)
AT3G45140	LOX2	Lipoxygenase 2	2	3	wounding response (Mochizuki et al., 2016), JA synthesis, senescence (Seltmann et al., 2010)
AT4G15440	HPL1	Hydroperoxide Lyase 1	2	3	JA signalling stress response (Nilsson et al., 2016; Ribot et al., 2008; Scala et al., 2013)

AT3G14840	LIK1	LYSM RLK1-interacting kinase 1	6	3	JA-dependent pathogen defense (Le et al., 2014)
AT4G20140	GSO1	GASSHO1, receptor-like kinase	6	3	Embryonic cuticle formation (Creff et al., 2019; Moussu et al., 2017)
AT5G46050	PTR3	Wound-induced peptide transporter	6	3	JA-mediated wounding response, pathogen defense (Karim et al., 2007), salt stress (Karim et al., 2005)
AT1G27730	ZAT10	Cys2/His2-type zinc finger protein	2,6	-	Drought stress, osmotic stress, heat stress, salt stress (Mittler et al., 2006; Sakamoto et al., 2004)
AT1G32920		Hypothetical protein	2,6	-	-
AT3G25250	AGC2-1	AGC2 kinase 1	2,6	-	Oxidative stress (Rentel et al., 2004; Shumbe et al., 2016), pathogen defense (Petersen et al., 2009)
AT1G19640	JMT	Jasmonic acid carboxyl methyltransferase	2,6	3	Drought stress (Kim et al., 2009), cold stress (Li et al., 2017)
Reproduction GO:0000003					
Gene ID	Gene Symbol	Gene Description	Cluster in Kd	Cluster in Kp	Gene Function & Reference
AT2G44190	EDE1	Microtubule-associated protein, Endosperm defective 1	4	8	Microtubule function during seed development (Pignocchi et al., 2009)
AT4G13560	UNE15	Late embryogenesis abundant proteins, Unfertilised embryo sac 15	4	8	Stress response (Hundertmark and Hincha, 2008)
AT5G10510	AIL6	Aintegumenta-like 6	4	8	Auxin-mediated flower development (Krizek, 2011)
AT5G66730	IDD1	Indeterminate domain 1	8	8	Promote germination (Feurtado et al., 2011)
AT1G60420	NRX1	Nucleoredoxin 1	4,8	-	Pollen tube growth (Qin et al., 2009)
AT1G64625	LHL 3	Lonesome highway like 3	4,8	-	Meiotic synchrony during reproduction (Li et al., 2015), root development (Ohashi-Ito and Bergmann, 2007)
AT4G24580	REN1	ROP1 enhancer	4,8	-	Pollen tube development (Chen et al., 2018; Hwang et al., 2008)
AT4G37750	ANT	Aintegumenta	4,8	-	Plant defense (Krizek et al., 2016), Auxin-mediated flower development (Krizek et al., 2020)
AT5G66460	MAN7	Endo-beta-mannase 7	4,8	-	seed germination (Iglesias-Fernández et al., 2011), silique dehiscence (He et al., 2018)
AT4G24660	HB22	Homeobox protein 22	4,8	8	Embryo development (Pagnussat et al., 2005), seed tolerance (Bueso et al., 2017)
Regulation of hormone levels GO:0010817					
Gene ID	Gene Symbol	Gene Description	Cluster in Kd	Cluster in Kp	Gene Function & Reference

AT1G73590	PIN1	Auxin efflux carrier, PIN-formed 1	5	12	Establish embryo axis (Friml et al., 2003), Shoot and root development (Zhou and Luo, 2018)
AT4G09160	PATL5	Patellin protein 5	5	12	Embryo patterning, organgenesis, Stress response (Tejos et al., 2018; Zhou et al., 2019)
AT5G55540	TRN1	Tornado 1	5	12	Leaf patterning (Cnops et al., 2006), root epidermal patterning (Kwak et al., 2015), auxin transport (Carland and McHale, 1996)
AT5G65640	bHLH093	Beta HLH protein 93	5	12	Gibberellin-mediated reproductive growth (Poirier et al., 2018; Sharma et al., 2016)
AT1G19790	SRS7	Shi-related sequence 7	6	12	Flower development (Kim et al., 2010; Kuusk et al., 2006)
AT1G68320	MYB62	MYB domain protein 62	6	12	Phosphate starvation response, gibberellin biosynthesis (Devaiah et al., 2009)
AT1G75520	SRS5	Shi-related sequence 5	6	12	promotes photomorphogenesis (Yuan et al., 2018), flower development (Estornell et al., 2018; Kuusk et al., 2006), lateral root formation (Yuan et al., 2020)
AT2G26710	BAS1	PhyB activation tagged suppressor	6	12	Brassinosteroids metabolism (Neff et al., 1999; Turk et al., 2005)
AT3G51060	STY1	Stylish 1	6	12	Auxin biosynthesis (Eklund et al., 2010), flower development (Estornell et al., 2018; Ståldal et al., 2012)
AT2G34650	PID	Pinoid	5,6	-	Positive regulator of cellular auxin efflux (Kleine-Vehn et al., 2009), negative regulator of auxin signalling (Saini et al., 2017)
AT2G47260	WRKY23	WRKY DNA-binding protein	5,6	-	Mediates PIN polarity (Prát et al., 2018), embryo development (Grunewald et al., 2013)
AT4G33090	APM1	Aminopeptidase M1	5,6	-	Auxin polar transport (Peer et al., 2009)
Response to karrikin GO:0080167					
Gene ID	Gene Symbol	Gene Description	Cluster in Kd	Cluster in Kp	Gene Function & Reference
AT1G06520	GPAT1	Glycerol-3-phosphate sn-2-acyltransferase	1	9	Pollen development (Zheng et al., 2003), seed development (Bai et al., 2021; Lei et al., 2018)
AT3G11600	GIR2	Plant-specific adapter protein	1	9	Root hair development (Wu and Citovsky, 2017a), promote histone deacetylation (Wu and Citovsky, 2017b)
AT3G47600	MYB94	Putative transcription factor	1	9	Cuticle formation (Lee and Suh, 2015; Lee et al., 2016)

5.4.7. Unique GO terms in *K. daigremontiana* or *K. pinnata* plantlet formation

Apart from recording GO terms and genes that were overrepresented in both species, we also recorded overrepresented GO terms that were unique to one *Kalanchoë* species or the other in Table 5.3. The table records the cluster in which these terms was overrepresented and the expression trend of genes in each cluster. There were more unique GO terms overrepresented in *K. pinnata* compared to *K. daigremontiana*. Genes in *K. pinnata* unique GO terms exhibited all trends of expression observed in our dataset whereas in *K. daigremontiana*, the genes only showed expression trends 1, 3, 5 and 7. There was a great range of gene counts in these GO terms and there was no association between the gene count and overrepresented GO terms in each gene cluster.

Table 5.3 List of unique GO terms that are overrepresented in gene clusters of one species but not the other.

Kd, *K. daigremontiana;* Kp, *K. pinnata*. Trend represents specific expression pattern of genes in different cluster (See Fig. 5.3 for graphical representation of expression trends). ↘ indicates the genes were downregulated, ↗ indicates the genes were upregulated from one stage or time point to the next.

Kd Cluster	GO Term	GO ID	P value	Gene count	Trend	GO Term	GO ID	P value	Gene count	Kp cluster
2	Regulation of signalling	GO:0023051	2.04E-04	19	1	Immune system process	GO:0002376	1.13E-12	36	1
						Multi-organism process	GO:0051704	6.65E-11	83	
	Cellular protein-containing complex assembly	GO:0034622	3.03E-04	1		Response to drug	GO:0042493	8.40E-10	36	
						Regulation of multi-organism process	GO:0043900	1.54E-06	21	
	Carbohydrate metabolic process	GO:0005975	3.89E-04	44		Biological process	GO:0008150	1.98E-05	521	
						Organelle organization	GO:0006996	1.42E-04	14	
7	Protein-chromophore linkage	GO:0018298	6.89E-14	12		Collagen catabolic process	GO:0030574	4.51E-04	3	
						Multi-organism process	GO:0051704	7.96E-06	32	7
	Response to radiation	GO:0009314	2.01E-07	23		Response to oxygen levels	GO:0070482	4.13E-05	11	
						Immune system process	GO:0002376	5.00E-05	13	
					2	Defence response	GO:0006952	1.71E-04	53	3
						Intracellular transport	GO:0046907	3.01E-04	3	
						Drug metabolic process	GO:0017144	7.25E-04	26	
						Regulation of biosynthetic process	GO:0009889	3.60E-05	40	6
						Xylem development	GO:0010089	6.54E-05	5	
4	Cellularization	GO:0007349	5.48E-05	4	3	Regulation of biological process	GO:0050789	2.14E-06	85	8
	Ribosome biogenesis	GO:0042254	3.65E-04	19		Nitrogen compound metabolic process	GO:0006807	2.71E-05	30	
	Sulphur compound metabolic process	GO:0006790	8.77E-04	19		Stem cell population maintenance	GO:0019827	3.33E-04	5	
	Regulation of signalling	GO:0023051	9.05E-04	16		Flavonoid biosynthetic process	GO:0009813	2.02E-09	13	12
5	Localization	GO:0051179	9.05E-04	67		Cell wall organization or biogenesis	GO:0071554	1.87E-08	33	
	Water transport	GO:0006833	2.06E-04	5		Response to auxin	GO:0009733	1.91E-06	24	
	RNA processing	GO:0006396	2.22E-04	2		Multi-organism process	GO:0051704	4.26E-04	59	
	Response to fructose	GO:0009750	2.68E-04	4		Multicellular organismal reproductive process	GO:0048609	5.49E-04	13	
8	Response to chemical	GO:0042221	3.72E-04	45		Plant organ formation	GO:1905393	6.09E-04	10	

	Response to stress	GO:0006950	3.75E-04	52		Ribonucleoprotein complex biogenesis	GO:0022613	9.80E-04	1	
						Establishment of protein localization	GO:0045184	1.07E-03	5	
					4	Protein folding	GO:0006457	1.24E-10	13	4
						Pigment biosynthetic process	GO:0046148	1.34E-05	7	
						Response to virus	GO:0009615	1.80E-04	5	
						Wax biosynthetic process	GO:0010025	1.55E-07	7	9
6	Carbohydrate transport	GO:0008643	6.57E-05	10	5					
					6	Response to inorganic substance	GO:0010035	1.87E-07	31	5
						Wax biosynthetic process	GO:0010025	1.42E-05	5	
						Positive regulation of seed germination	GO:0010030	1.71E-05	5	
						Protein complex oligomerization	GO:0051259	2.05E-05	6	
						Ion transport	GO:0006811	2.40E-04	20	
						Proteasomal ubiquitin-independent protein catabolic process	GO:0010499	6.10E-06	5	10
						Cellular component organization or biogenesis	GO:0071840	2.34E-04	43	
						Response to inorganic substance	GO:0010035	3.26E-04	19	
3	Plastid organization	GO:0009657	2.88E-07	19	7					
	Water transport	GO:0006833	2.28E-05	6						
	Regulation of flavonoid biosynthetic process	GO:0009962	1.29E-04	5						
	Response to abiotic stimulus	GO:0009628	1.52E-04	59						
					8	Terpenoid metabolic process	GO:0006721	3.53E-05	10	2
						Regulation of biological process	GO:0050789	4.56E-05	95	
						Cellular response to endogenous stimulus	GO:0071495	1.06E-04	25	
						Response to light stimulus	GO:0009416	7.05E-06	32	11
						Shoot system development	GO:0048367	1.96E-04	30	
						Multi-organism cellular process	GO:0044764	3.35E-04	8	

Expression trend (Based on Figure 5.3)

Trend 1 ↗↘↘	Trend 2 ↗↘↗	Trend 3 ↘↗↗	Trend 4 ↘↗↘	Trend 5 ↗↗↗	Trend 6 ↗↗↘	Trend 7 ↘↘↘	Trend 8 ↘↘↗

5.5. **Discussion**

This study contrasts the transcriptome during plantlet formation in *K. daigremontiana* and *K. pinnata*, which represents constitutive and inducible plantlet-forming *Kalanchoë* species respectively. Plantlet formation in both species seem to be analogous, however, it has been proposed that constitutive species recruit embryogenesis programme whereas inducible species carry out organogenesis initiation after induction (Garcês et al., 2007). These were established based on molecular evidence such as the expression of embryonic genes *LEC1* and *FUS3* on the leaf notches of *K. daigremontiana*, and the resemblance of triggering apical meristematic competence with the expression of *STM* in all plantlet-forming species (constitutive and inducible) (Garcês et al., 2007, 2014). In the case of inducible plantlet-forming species, plantlets originate from pre-existent primordia located on the leaf crenulations, which remain dormant probably under hormonal influence and reactivated until external stimuli breaks that dormancy (Kulka, 2008). In the case of *K. daigremontiana*, plantlets emerge from pedestal structures, where somatic embryos are formed and then develop into fully-formed plants (Garcês and Sinha, 2009a). These studies suggested plantlet formation mechanism(s) in each species may differ, however, studies were limited to only a few genes or to anatomical analyses. To better identify the genetic mechanism of plantlet formation for both species, we performed an RNA-seq analysis that allowed us to identify biological processes and differentially expressed genes, which may play important roles in modulating the asexual reproduction for *K. daigremontiana* and *K. pinnata*. Little is known about the mechanism of embryonic and meristematic competency acquirements that led to a successful asexual reproductive strategy. These two species are suitable models to study somatic embryogenesis and organogenesis, but also dormancy and stress response.

Most of the genes represented in 'Signalling GO:0023052' are overlapped between a *K. daigremontiana* cluster Kd2 and *K. pinnata* cluster Kp1 and Kp3. According to the GO database AmiGO2, this specific GO term 'Signalling GO:0023052' includes genes involved in signal transduction within a biological system. These clusters exhibited a similar expression trend in which there is an upregulation followed by a downregulation, suggesting that genes in these clusters might be important for the initiation or early stages of plantlet formation in both species (Table. 5.1, Fig. 5.6A). In terms of the functions of these genes, most of them are

involved in regulating and sensing biotic and abiotic stress (Table 5.2). This observation is predictable as rate of plantlet formation in *K. daigremontiana* is enhanced by drought stress (Zhong et al., 2013). Some plants also developed preference for asexual reproduction under certain stress conditions (Takahashi and Mikami, 2017; Yang and Kim, 2016). In addition, *K. daigremontiana* plantlet formation is triggered only under long-day condition (Hershey, 2002). With evidence of light-dependent selective preference for asexual or sexual reproduction (Yang and Kim, 2016), light or light-associated stress response might be regulating plantlet initiation of *K. daigremontiana*. Apart from that, the likely mechanism for plantlet formation in *K. daigremontiana*, somatic embryogenesis, is a consequence of stress response (Fehér, 2015; Zavattieri et al., 2010). Existing research has shown that various stresses such as osmotic stress, oxidative stress, heavy metal stress, temperature and nutrients play a role in stimulating somatic embryogenesis (Castander-Olarieta et al., 2020; Khattak et al., 2017; Krishnan and Siril, 2017; Nic-Can et al., 2016; Pandey and Chaudhary, 2014; Yang et al., 2020). Somatic embryogenesis involves induction of totipotency or embryogenic competence of differentiated plant cells (Fehér, 2015). The fact that embryogenesis genes *LEC1* and *FUS3* are expressed at leaf margin of *K. daigremontiana* mother leaves and that plantlets exhibit embryo-like morphological features during early development, it was postulated that differentiated cells at the leaf notches undergo somatic embryogenesis to develop into plantlets (Batygina et al., 1996; Garcês et al., 2007). From *in vitro* culture of *Kalanchoë* tissues, different salinity concentration of media affected the number and weight of callus (Obaid et al., 2019).

Although all plantlet-forming *Kalanchoë* species expresses *STM* gene that is responsible for embryonic shoot meristem specification, but in plantlet-inducible species such as *K. pinnata*, *LEC1* expression is not present (Garcês et al., 2007). This led to the speculation that plantlet formation of plantlet-inducible species is primarily regulated via organogenesis as *LEC1* is known as the master regulator of late embryogenesis. Study on another constitutive plantlet-forming species, *K. laetivirens* revealed presence of pre-existing stem cells at site of plantlet formation and expression of *WUSCHEL*, regulator of stem cell homeostasis at different stages of plantlet formation (Guo et al., 2015). As major post-embryonic development of plants originates from SAM, capability to respond and adapt to stress is vital (Lee, 2018). Similar to

somatic embryogenesis, stem cell signalling also involves phytohormones and reactive oxygen species, which contributes to oxidative stress if present at elevated level (Huang et al., 2019; Lee, 2018; Zhou et al., 2016). Although detailed mechanism of stress-induced plantlet formation has yet to be elucidated, oxidative stress was shown to affect *K. pinnata* plantlet formation *via* nitric oxide (Abat and Deswal, 2013). In the constitutive plantlet-forming species *K. tubiflora*, antioxidant defence of plantlets was reduced compared to mother plant leaves (Luo et al., 2015). The same study also showed that plantlets invest more energy to prevent water loss. Osmotic stress was shown to affect plantlet formation as addition of sucrose overcome cytokinin inhibition of *K. marnierianum in vitro* plantlet formation (Kulka, 2006). Though the direct impact on plantlet formation was not illustrated, increased drought tolerance and water stress that influence survival of *Kalanchoë* plants is expected to contribute to stimulation or inhibition of plantlet formation (Kefu et al., 2003; Luo et al., 2014; Malwattage et al., 2020). Induction of *K. pinnata* plantlet through leaf aging or detachment (Howe, 1931; Jaiswal and Sawhney, 2006a; Yarbrough, 1932) might also be achieved through activating senescence that occurs via integration of stress signals (Bata Gouda et al., 2020; Jibran et al., 2013; Pogson and Morris, 2004).

From the list of genes in 'Signalling GO:0023052', genes such as *CAM5*, *PYL4*, *DREB2C*, *RDUF1*, *PP2C5*, *RHA2A, C2* and *CIPK11* act *via* regulating abscisic acid (ABA) signalling during seed germination and seedling growth. This provides evidence that ABA might be involved in maintenance of plantlet dormancy even though a previous experiment showed that application of ABA did not release plantlets with functional *KdLEC1* from dormancy (Garcês et al., 2014). The authors suggested that the window for ABA signalling to act on plantlet dormancy might be narrow (Garcês et al., 2014). However, our data suggest that ABA signalling is regulated by multiple genes, hence, this might explain that application of ABA is not sufficient to bypass complexity of ABA signalling regulation to exert its effect on plantlet formation. These results indicate that the plantlet developmental stages of the tissues may be analogous to seed germination and seedling growth. It is not unexpected to observe association of stress response during this stage because seeds need to be sensitive to its environment to ensure that conditions are optimal to induce germination.

The over-represented genes in the GO term 'Response to wounding GO:0009611', are overlapped between *K. daigremontiana* clusters Kd2 and Kd6 and a *K. pinnata* cluster, Kp3. Genes in these clusters were upregulated only at the earliest stages, then genes in cluster Kd2 and Kp3 decrease their expression, however, genes in Kd6 continued to upregulate until later stages of the plantlet development (Table. 5.2, Fig. 5.3). Among these genes in this GO term, two genes, *ATP-BINDING CASSETTE G11* (*ABCG11*) and *GASSHO1* (*GSO1*) provide a clue to explain participation of these genes during early plantlet formation. *GSO1* encodes an embryonically expressed receptor kinase that are essential for embryonic cuticle formation (Tsuwamoto et al., 2008; Xing et al., 2013) whereas *ABCG11* encodes an ATP binding cassette (ABC) transporter involved in secretion of cuticular lipid that are required for cuticle formation (Luo et al., 2007; Panikashvili et al., 2007). The cuticle layer formed through *ABCG11* mediation acts as a protective sheath against high stress conditions for vegetative tissues, reproductive organs, embryo epidermis and the endosperm tissue of developing seeds (Bird et al., 2007; Luo et al., 2007; Panikashvili et al., 2010). Hence, the cuticle layer might act to prevent tissues from losing water during plantlet formation and in the case of *K. pinnata*, to slow down leaf drying while plantlets are being formed. During germination, seeds undergo a process known as testa rupture after hydration, followed by endosperm rupture and radicle protrusion (Nonogaki, 2008). During these events, the structures of cellular membranes are damaged, thus, triggering various repair mechanisms (Weitbrecht et al., 2011), possibly those involved in wounding and stress responses. Apart from that, most of these genes are either involved in jasmonic acid (JA) synthesis or dependent on JA signalling. Based on existing literature, JA signalling induces germination during wounding and stress responses (Campos et al., 2014; Singh et al., 2017; Yang et al., 2019a). Hence, in the case of plantlet formation in *K. daigremontiana* and *K. pinnata*, the formation of indentation and pedestal prior to emergence of plantlet might be presented as damage to the surrounding tissues, which in turns triggered JA signalling to break dormancy and induce plantlet formation.

Genes that are overrepresented in 'Reproduction GO:0000003' belonged to either *K. daigremontiana* cluster Kd4 and Kd8 or *K. pinnata* cluster Kp8. Genes in all three clusters have the same expression pattern in which the genes were initially downregulated and then upregulated for the subsequent stages (Table 5.2, Fig. 5.3). The expression trend indicates that

these genes might not be required for the initiation of plantlet formation, but they may be important for plantlet development. It was not surprising to observe activity of these reproduction-associated genes during early plantlet development as *K. daigremontiana* plantlet developments morphologically resembles embryo development and that *LEC1* and *FUS3* were expressed in *K. daigremontiana* plantlets (Garcês et al., 2007). It was suggested that *K. pinnata* plantlet develops possibly recruit only organogenesis as *LEC1* expression was not present in *K. pinnata* leaves (Garcês et al., 2007). However, this is insufficient to rule out whether other parts of embryogenesis pathways are recruited during *K. pinnata* plantlet formation. Our results suggest that this might be the case, with embryogenesis route recruited during *K. pinnata* plantlet initiation as expression of genes involved in embryo development such as *ENDOSPERM DEFECTIVE 1* (*EDE1*) and *UNFERTILISED EMBRYO SAC 15* (*UNE15*) were differentially significantly expressed. Although the specific function of *UNE15* is yet to be demonstrated but it is known to be accumulate during late embryogenesis and is associated with stress response (Hundertmark and Hincha, 2008). As for *EDE1*, it was shown to interact with microtubules to regulate formation of *Arabidopsis* endosperm and embryo (Pignocchi et al., 2009). The upregulation of these genes in subsequent stages of plantlet development was particularly intriguing, because in later stages of tissues harvested, the cotyledons were already present (See Fig. 5.1), indicating seedling-equivalent stage of plantlet maturity. The only plausible explanation is that these genes might have different functions during the seedling stages. Further research into the role of these genes during plantlet formation and whether other embryogenesis genes are involved in the process is needed to obtain conclusive evidence on the participation of embryogenesis during *Kalanchoë* plantlet formation.

The GO term, 'Regulation of hormone levels GO:0010817' includes genes that are involved in regulation of hormone levels. These genes belong to *K. daigremontiana* cluster Kd5 and Kd6 and *K. pinnata* cluster Kp12. Cluster of genes in Kd5 and Kp12 exhibit the same expression pattern as genes in the reproduction GO term, being downregulated between the first two stages, then continual increase in expression in subsequent stages. Genes in cluster Kd6, however, continued to rise in expression since the beginning (Table 5.2, Fig. 5.3). From the expression trend, it seems that these genes might be more involved in the later stages but a lower expression of genes in Kd6 does not indicate less importance. It is expected to observe

gene controlling hormone level to be involved during plantlet formation, as hormones are known to play a major role in proper plant growth and development (Bhattacharya, 2019; Dilworth et al., 2017). Plant hormones such as auxin, have been extensively studied, and is known to affect various aspects of plant development (Zhao, 2010). Hence, it was not surprising to observe that most of the genes in this GO terms are either involved in auxin transport (*PIN-FORMED 1* [*PIN1*] , *AMINOPEPTIDASE M1* [*APM1*], *PINOID* [*PID*], *TORNADO 1* [*TRN1*], *PATELLIN PROTEIN 5* [*PATL5*], *WRKY DNA-BINDING PROTEIN* [*WRKY23*], auxin biosynthesis (*STYLISH 1* [*STY1*]) or is regulated by auxin (*SHI-RELATED SEQUENCE 5* [*SRS5*], *SRS7*) (Estornell et al., 2018; Yuan et al., 2020). There are also recent publication discussing the role of auxin on seed development and stress response (Blakeslee et al., 2019; Figueiredo and Köhler, 2018; Korver et al., 2018). This finding provided further support on the significance of auxin on plantlet formation in addition to our results in Chapter 4 of this thesis that illustrated strong expression of *PIN1* auxin efflux transporter and auxin response during plantlet development. Our data includes a novel finding showing *PIN1* expression before *K. daigremontiana* pedestal formation, indicating participation of auxin in plantlet initiation.

The last GO term selected for further analysis is 'Response in karrikin GO:0080167', in which only 3 genes, *GLYCEROL-3-PHOSPHATE SN-2-ACYLTRANSFERASE* (*GPAT1*), *GIR2*, *MYB DOMAIN PROTEIN 94* (*MYB94*) are overlapped between the two gene clusters showing overrepresentation of this GO term. These genes were overrepresented in *K. daigremontiana* cluster Kd1 and *K. pinnata* cluster Kp9. In the first few stages, Kd1 and Kp9 have opposite trend of expression in which genes in Kd1 are upregulated and then downregulated, whilst the vice versa was true for genes in Kp9. At the final stages, however, both Kd1 and Kp9 clusters of genes were downregulated. At first glance, these expression patterns suggest that these genes exhibit opposite function in *K. daigremontiana* and *K. pinnata*. However, to date, karrikins are known to trigger seed germination and seedling establishment (Nelson et al., 2009; Yao and Waters, 2020). Hence, it is also possible that the stages in which expression of genes in these clusters are upregulated signify seed germination-equivalent stage of plantlet development. Even though existing studies showed that *GPAT1*, *GIR2* and *MYB94* function differently (See Table 5.2), the fact that these genes are overrepresented in both species suggest that these genes might be important elements during plantlet development. *GIR2* promotes histone

deacetylation to regulate root hair development, *MYB94* inhibits auxin-induced callus formation mediated via a root developmental pathway and *GPAT1* is involve in differentiation of tapetal cells, which are nutritive cells in anthers (Dai et al., 2020; Wu and Citovsky, 2017b; Zheng et al., 2003). In cooperation with auxin, *GIR2* might be changing chromatin structure of cells of plantlet primordia to allow access of embryogenesis program, *MYB94* might be modulating change in cell fate of the cells and with *GPAT1* regulating local nutrient availability for plantlet formation (Dai et al., 2020; Wang et al., 2020a; Wu and Citovsky, 2017b; Zheng et al., 2003).

Compared to the number of overlapping GO terms, gene ontology analysis revealed that there are more unique GO terms associated with each of the species studied (Table 5.3). It was not unexpected because *K. daigremontiana* and *K. pinnata* have different modes of plantlet formation (Batygina et al., 1996; Garcês et al., 2007). In the case of *K. daigremontiana*, there were 5 GO terms over-represented in gene cluster 2 and 7, exhibiting the same expression pattern of trend 1. This means that these genes were upregulated in S1 stage of plantlet formation when compared to young leaf margins. Then, these genes continued to decrease in their expression level across the subsequent plantlet developmental stages (Fig. 5.3). Apart from 'response to radiation GO:0009314', over-representation of these GO terms was expected, as these terms signify general processes that occur during plantlet development the since samples contained developing young leaves and plantlets. The 'response to radiation GO:0009314' might have indicated that as developing leaves mature, the plants actively respond to electromagnetic radiation, including light stimulus. The developing leaves might be responding to radiation to obtain sufficient light for growth, but also to protect from radiation damage (Dotto and Casati, 2017; Vanhaelewyn et al., 2020). At the same time, the plants might be detecting whether there is sufficient light exposure for plantlet formation as plantlet formation occurs only under long-day condition (Hershey, 2002). Plantlet formation in response to light is specific to constitutive plantlet-forming species such as *K. daigremontiana* as other plantlet-inducible species such as *K. pinnata* forms plantlets upon leaf aging or excision and does not require long-day condition to form plantlets.

The GO terms that share similar expression pattern of trend 3, belong to gene clusters 4, 5 and 8. Genes in these GO terms have the exact opposite expression trend as the previously mentioned for other GO terms. These genes exhibit downregulation from young leaf margin stage or S1 plantlet stage and then upregulation across subsequent plantlet formation stages (Fig. 5.3). The most fascinating term that was over-represented in cluster 4 and was uniquely present in *K. daigremontiana* is 'cellularization GO:0007349'. In plants, cellularisation is the process in which the multi-nucleated syncytium separates into individual cells and develops into seed endosperm (Boisnard-Lorig et al., 2001). As plantlets are not seeds, it is interesting to observe participation of cellurization, and particularly during later stages of plantlet formation and not during the initiation phase. This points out the need to look at the function of individual genes in each term as these genes might only indirectly affect cellurization and are not major players in the process. Apart from 'cellularization GO:0007349', the overrepresentation of the other GO terms was not surprising because these biological processes are required to manufacture essential proteins, to position cellular components, and to respond to abiotic and biotic factors, in order to support the developing plantlets. A similar explanation might be applicable to 'carbohydrate transport GO:0008643' because developing young leaves and plantlets will require nutrients in the form of carbohydrates and some carbohydrate transporters are also known to regulate plant-pathogen interaction (Breia et al., 2021; Durand et al., 2018). However, genes in this GO term are upregulated since the development of young leaf margins until the final stage of plantlet formation examined.

The last group of unique GO terms overrepresented during *K. daigremontiana* plantlet formation belongs to cluster 3, in which its gene expression was downregulated since the development of young leaves. The downregulation of 'plastid organization GO:0009657' suggests that the arrangement of plastids, also known as sites of photosynthesis are not necessary for developing young leaves and plantlets (Powikrowska et al., 2014). As *K. daigremontiana* plantlet formation is assumed to occur *via* somatic embryogenesis, this is expected because as the somatic cells dedifferentiate, their photosynthetic ability is lost (Neelakandan and Wang, 2012). 'Regulation of flavonoid biosynthetic process GO:0009962' is the process of regulating biosynthesis of flavonoids which are low-molecular-weight phenolic compounds produced by plants for bacterial defence (Havsteen, 2002). The downregulation of

‘regulation of flavonoid biosynthetic process GO:0009962’ and ‘response to abiotic stimulus GO:0009628’ was unexpected because GO terms associated with response to more specific stimuli were upregulated at different stages of plantlet formation. Nonetheless, this might be an attempt for plants to balance the energy required for both growth and response to stimuli (Wasternack, 2017).

K. pinnata clusters 1 and 7 include genes that were upregulated at the leaf notches 4 hours after leaf detachment but were gradually downregulated after this stage. GO terms that were overrepresented in these clusters included large number of genes compared to the number of genes in overrepresented GO terms of *K. daigremontiana*. To identify genes that might be more relevant towards plantlet formation, the p value act as a useful tool to narrow down the list of genes as a smaller p value indicates a higher significance. It might also be more useful to examine GO terms that are more specific, such as, in clusters 1 and 7, ‘immune system process GO:0002376’, ‘response to drug GO:0042493’ and ‘response to oxygen levels GO:0070482’. According to the GO database AmiGO2, ‘immune system process GO:0002376’ refers to processes involving the immune system in response to potential internal or invasive threats caused by both biotic and abiotic factors. This GO term was overrepresented possibly due to the wounding caused by harvesting the leaf notches. The same explanation might apply to the overrepresentation of ‘response to oxygen levels GO:0070482’. Changes in oxygen level might have occurred during the process and triggered *K. pinnata* plantlet formation. A previous study has shown that oxidative stress imposed by nitric oxide can affect *K. pinnata* plantlet formation (Abat and Deswal, 2013). The plantlets of *K. tubiflora,* a constitutive plantlet-forming species, has lower antioxidant defence compared to the mother leaves (Luo et al., 2015). ‘Response to drug GO:0042493’ refers to responses stimulated by drugs used in the diagnosis, treatment or prevention of a disease. As the plants were not treated with any substances that could potentially be identified as drugs, genes in this GO term might have been overrepresented due to its indirect effect on this process. Unique overrepresented GO terms for *K. pinnata* in cluster 3 and 6 include genes which were upregulated at the initial stages, downregulated after 4 hours of leaf detachment, and upregulated after 24 hours. ‘Defence response GO:0006952’ usually denotes response to an injury, which results in a structural damage to the organism, that in this case might be leaf detachment. ‘Regulation of biosynthetic process GO:0009889’

include genes that mediate the synthesis of substances, probably result of carbohydrates metabolism to retrieve energy. The overrepresentation of 'Drug metabolic process GO:0017144' was unusual; however, it has been reported that bufadienolides compounds that have anticancer and antiviral effects are present in the leaves of *K. pinnata* (Kolodziejczyk-Czepas and Stochmal, 2017). This GO term might be overrepresented as a result of degradation of these compounds after leaf detachment.

Gene clusters 8 and 12 that exhibited expression trend 3 in *K. pinnata* include downregulated genes that were upregulated after leaf detachment and remained upregulated in subsequent time points. Overrepresented GO terms in these clusters were: 'response to inorganic substance GO:0010035 genes', that might have changed its expression in response to water deprivation after leaf was excised from the mother plant. 'Wax biosynthetic process GO:0010025' contained genes possibly playing a role in preventing water evaporation from removed leaves, as it was seen that plantlets appear after 9 days of leaf detachment. 'Stem cell population maintenance GO:0019827' genes were also found to be overrepresented in trend 3. Stem cells in plants are usually maintained in the SAM, RAM, and vascular meristems for growth, as plants develop post-embryonically (Aichinger et al., 2012). These cells also contribute for the regeneration of lost organs through organogenesis routes because of biotic or abiotic stress (Lup et al., 2016). At cellular level, growth, development, and regeneration share the same genetic pathways (Perez-Garcia and Moreno-Risueno, 2018). The epiphyllous buds in *K. pinnata* require the presence and maintenance of a stem cell niche from where plantlets will emerge. The regeneration of whole new plants from specialised structures in *Kalanchoë* already represents a reproductive strategy. 'Cell wall organization or biogenesis GO:0071554' GO term found in cluster 12 could feasibly be playing important roles during cell divisions leading to generate new plantlets. 'Response to auxin' GO term was also overrepresented and included genes involved in the organogenesis pathway of plantlet formation. Auxin plays key role in essential developmental processes in plants such as: embryogenesis, gametogenesis, vascular pattering, and flowering (Zhao, 2010). Auxin accumulation promotes lateral organ initiation in the SAM, and it is carried via polar transport, facilitated by PIN1 protein (Reinhardt et al., 2003). Auxin is also present in the central zone in the SAM, and it has been reported that auxin signalling in stem cells is mediated by *AUXIN*

RESPOSE FACTORS (*ARFs*) to positively regulate *CLAVATA 3* (*CLV3*) (Luo et al., 2018). It has been reported that auxin plays a key role in plantlet formation in *K. marnierianum* (Kulka, 2008). Upregulation of 'plant organ formation GO:1905393' genes were found after leaf excision, possibly facilitating plantlet formation. The expression of organogenesis genes in subsequent time points after leaf detachment was expected, as inducible plantlet-forming species are known to form plantlets through organogenesis routes (Garcês et al., 2007).

'Positive regulation of seed germination GO:0010030' term includes genes in trend 6, which was upregulated after leaf detachment and downregulated 48 hours after leaf detachment. This GO term is involved in the activation of seed germination processes. This suggests that *K. pinnata* plantlet formation activates the same pathways recruited in seed germination. Interestingly, the presence of seed and embryo genes has only been reported for constitutively plantlet-forming *K. daigremontiana* (Garcês et al., 2007). 'Cellular response to endogenous stimulus GO:0071495' and 'shoot system development GO:0048367' were uniquely overrepresented in *K. pinnata*. These genes follow trend 8, where upregulation occurs only 48 hours after leaf detachment. Signals to the epiphyllous buds from within the plant and meristematic activity in the buds expressed simultaneously on inducible plantlet-forming species, *K. pinnata.* When epiphyllous buds initiate plantlet formation, the first visible structure is the SAM, and it becomes visible 9 days after leaf was excised from the mother plant. Surprisingly, 'shoot system development GO:0048367' GO term is present only two days after inducing plantlet formation in *K. pinnata*. Plantlet formation in *K. pinnata* is activated by the detachment of leaves. According to our data, the set of upregulated genes within the first 4 hours possibly more relevant to the vegetative reproductive process were: 'immune system process GO:0002376', 'defence response GO:0006952', 'regulation of biosynthetic process GO:0009889', 'wax biosynthetic process GO:0010025', 'cellular component organization or biogenesis GO:0071840'. These GO terms indicated the sensing of mechanical damage to the plant integrity after leaf excision. Plants being sessile organisms acquired the ability to quickly respond to damage by activating protective mechanisms (Savatin et al., 2014). After the plant recognised and responded to leaf damage, the set of genes upregulated within 24 hours of leaf included: 'stem cell population maintenance GO:0019827', 'cell wall organization or biogenesis GO:0071554', 'multicellular organismal reproductive process GO:0048609', 'plant organ

formation GO:1905393'. The upregulation of these genes 24 hours following leaves detachment from the mother plant could possibly mean that the epiphyllous buds were at this point already initiating an organogenesis programme to form plantlets. Furthermore, 'shoot system development GO:0048367 term', which includes specific organogenesis genes designated to shape the SAM was upregulated 48 hours after leaf detachment.

5.6. **Conclusion**

This study is the first global transcriptome analysis of plantlet formation. Based on the different mode of plantlet formation and plantlet morphological structures, we successfully selected tissues with almost exclusively distinctive plantlet stages and time points to conduct our experiment. Clustering of biological replicates of our tissue samples signify that our results are very consistent and thus, highly reliable. Our data suggests that plantlet formation in *K. daigremontiana* and *K. pinnata* are largely unique as suggested by greater number of unique genes and GO terms overrepresented in each species. However, overrepresentation of the same GO terms in both species suggests plantlet formation in *K. daigremontiana* and *K. pinnata* relies on participation of pathways involved in signalling, wounding response, hormone regulation, reproduction and response to karrikin. It is not clear yet how the unique GO terms are recruited during plantlet formation specific to each species. Our findings remain preliminary and still requires extensive validation and experiments to understand molecular mechanisms involved in plantlet formation. Nonetheless, our analysis will be a pioneer for future research on *Kalanchoë* plantlet formation. A greater knowledge in this field will accelerate our understanding towards the varied asexual reproduction strategies in plants.

CHAPTER 6

GENERAL DISCUSSION

6. GENERAL DISCUSSION

Most plants can choose to reproduce sexual or asexually based on their environmental conditions (Eckert, 2002; Lei, 2010; Silvertown, 2008; Winkler and Fischer, 2001). However, plants in the *Kalancho*ë genus seemed to have evolved a preference towards asexual reproduction (Garcês et al., 2007). This asexual reproduction strategy in *Kalancho*ë species is known as plantlet formation in which miniature version of the adult plants are formed on the leaf margin of mother leaves (Garcês et al., 2007). It has been speculated that plantlet formation is induced by somatic embryogenesis which stimulates somatic leaf cells at leaf indentations to revert to a state of pluripotency or totipotency. This event involves dedifferentiation of somatic cells and acquiring embryonic potential that allows them to develop into an embryo (Garcês et al., 2007; Zhu et al., 2017). Molecular studies revealed that *Kalancho*ë *daigremontiana* (*K. daigremontiana*), a *Kalancho*ë species that makes plantlets constitutively in favourable conditions, recruits embryogenesis, organogenesis and flowering pathways during plantlet formation (Garcês et al., 2007, 2014; Liu et al., 2016; Zhu et al., 2017). Earlier studies also showed that plant hormones such as auxin and cytokinin are also involved in plantlet formation, but their effects remain contradictory (Heide, 1965; Henson and Wareing, 1977; Yazgan and Vardar, 1977). This research project sets out to investigate detailed mechanisms involved in plantlet formation, particularly on triggered pluripotency of plantlet precursor cells.

6.1. **Embryogenesis**

6.1.1. Early Embryogenesis

Zygotic embryogenesis is initiated through the entrance of sperm cell into the ovule, bringing in *SHORT-SUSPENSOR* (*SSP*) transcripts that was translated into SSP proteins which then activates the *YODA* signalling pathways (Bayer et al., 2009; Neu et al., 2019). This leads to activation of mitogen-activated protein kinase (MAPK) signalling cascade that ultimately results in zygote elongation and development of the basal cell lineage (Lukowitz et al., 2004; Musielak and Bayer, 2014). *YODA* also activates WRKY DNA-BINDING PROTEIN (WRKY2) that upregulates expression of *WUSCHEL-RELATED HOMEOBOX* (*WOX*) transcription factors (Ueda et al., 2017). During early embryogenesis, *WOX2*, *WOX8* and *WOX9* are expressed in the zygote to establish embryo polarity (Haecker et al., 2004; Ueda et al., 2011). Although somatic

embryogenesis and *Kalancho*ë plantlet formation do not involve fertilisation, the expression of *WOX* transcription factors were present during somatic embryogenesis of several different species (Bueno et al., 2021; Gambino et al., 2011; Tvorogova et al., 2015). Our RNA-sequencing analysis showed that expression of *WRKY2* and *WOX* genes are present during plantlet formation, indicating similar mechanisms are recruited to pattern early plantlet formation. However, the expression data were not statistically significant, hence, further quantitative validation is required. The *WOX* genes might be suitable candidates to study based on their role in early embryogenesis but their functional redundance and low expression level present a challenge in visualisation of expression and phenotypic analysis (Ueda et al., 2011).

Although the genetic mechanisms that trigger plantlet formation is yet to be illustrated, it is very likely that the plantlet formation is initiated by auxin. This is suggested by strong expression of auxin efflux transporter PIN-FORMED1 (PIN1), at the leaf notches prior to formation of pedestals. Auxin's role in initiating plantlets is also supported by auxin activity visualised in *DR5*::*GFP* plants. In these plants, auxin activity was localised in the same region of PIN1 expression. The similarity in expression of auxin activity and auxin efflux transporter *KdPIN1* during plantlet formation is analogous to that of *Arabidopsis* zygotic embryogenesis (Benková et al., 2003; Reinhardt et al., 2003; Scarpella et al., 2006). This also indicates that auxin is likely to be involved in determining early cell fate, phyllotaxy and vein patterning of plantlet (Benková et al., 2003; Reinhardt et al., 2003; Scarpella et al., 2006). Based on RNA-sequencing analysis, *PIN1* expression was also differentially regulated significantly during *K. daigremontiana* plantlet development. Its expression was downregulated from young leaf margins (Ctrl) to leaf notches prior to pedestal formation (S1) but was then upregulated in subsequent plantlet developmental stages. In combination with PIN1 localisation data, this suggests that plantlet initiation might have occurred in very young leaves, prior to any sign of pedestal formation. Then, as the leaves reaches a certain maturity and are under a long-day condition, plantlet development is stimulated.

6.1.2. Meristem

In zygotic embryogenesis, establishment of meristems occurs after determination of apical-basal polarity and cell fate. Only at this point, cytokinin signalling is recruited to specify shoot

and root stem cell niches. The presence of cytokinin activity is first visible only at the hypophysis of a globular-stage zygotic embryo for specification of root stem cells (Müller and Sheen, 2008; Zürcher et al., 2013). Our data showed strong cytokinin activity throughout the embryo proper of globular-stage plantlet, suggesting a potential role of cytokinin in early plantlet formation. After this stage, cytokinin activity during plantlet formation was similar to what was observed during zygotic embryogenesis, indicating that cytokinin signalling is also used to specify the shoot apical meristem (SAM) of *K. daigremontiana* plantlets (Meng et al., 2017; Shani et al., 2010; Xie et al., 2018; Zhang et al., 2017c; Zubo et al., 2017). Reduced expression of a putative cytokinin signalling regulator in *K. daigremontiana* (*KdaHP*) resulted in defective plantlet morphology and reduced plantlet number, suggesting that cytokinin signalling is important for plantlet initiation and development. These plants were accompanied by inconsistent change in auxin biosynthesis enzyme gene *YUCCA1* (*YUC1*) expression, suggesting that complex cytokinin-auxin crosstalk is recruited to regulate plantlet formation.

KdaHP antisense plants also showed *WUS* upregulation and *CLV2* downregulation, implying that cytokinin signalling is also interacting with organogenesis pathway to regulate plantlet formation. Cytokinin signalling mediates function of another organogenesis gene *SHOOTMERISTEMLESS* (*STM*) to initiate SAM formation of a zygotic embryo (Jasinski et al., 2005; Yanai et al., 2005). When *K. daigremontiana* homolog of *SHOOTMERISTEMLESS* (*KdSTM*) gene was downregulated, plantlet formation was completely inhibited (Garcês et al., 2007). This suggests that plantlet formation requires KdSTM activity, and that organogenesis pathways might be involved in initiation or maintenance of stem cells at site of plantlet formation. To understand whether organogenesis pathways are involved, *K. daigremontiana* transgenic plants with reduced expression in other organogenesis genes *WUSCHEL* (*WUS*) and *CLAVATA* (*CLV*) were generated. These transgenic plants, along with *KdaHP* antisense plants had significantly reduced number of plantlets and leaf serration, accompanied by irregular leaf phyllotaxy and shape. Changes in *YUC1* expression in these plants suggest that auxin biosynthesis might be disrupted, leading to loss of basipetal arrangement of pedestal and plantlet and defective formation of leaf serration (Bilsborough et al., 2011). Formation of leaf serrations depends on alternating localisation of auxin maxima promoting outgrowth of serration tips and regions of growth retardation activity of CUP-SHAPED COTYLDEON 2 (CUC2)

(Bilsborough et al., 2011). However, *KdYUC1* expression level was inconsistent in *KdaHP*, *KdWUS* and *KdCLV1* antisense transgenic plants; perhaps the leaf serration defect was due to *CUC* activity that was directly affected by cytokinin signalling or WUS-CLV pathway. The presence of plantlets with cylinder or cone-shaped cotyledon in *KdWUS* antisense plants similar to *cuc* mutants supports the idea that WUS-CLV might affect the *CUC* activity (Aida et al., 1997). Apart from this, auxin biosynthesis was known to form an auxin gradient to regulate basipetal outgrowth of leaf blade. Moreover, plantlet only develops as the leaf grows. Hence, changes in *KdYUC1* might have disrupted leaf formation and also basipetal and symmetrical formation of pedestals and plantlets along the leaf margin. As discussed above, the presence of PIN1 at the site of pedestal and plantlet formation suggests that auxin acts as a signal for plantlet initiation.

6.1.3. Late Embryogenesis

During late embryogenesis, a zygotic embryo matures and transits to dormancy primarily under the regulation of *LAFL* network of genes, *LEAFY COTYLEDON 1* (*LEC1*), *LEC1-LIKE* (*L1L*), *ABSCISIC ACID INSENSITIVE3* (*ABI3*), *FUSCA3* (*FUS3*) and *LEC2* (Giraudat et al., 1992; Jia et al., 2013; Kwong et al., 2003; Lotan et al., 1998; Luerßen et al., 1998; Stone et al., 2001). Plantlet developmental process morphologically resembles *Arabidopsis* zygotic embryogenesis, and *KdLEC1* and *KdFUS3* are expressed during *K. daigremontiana* plantlet formation (Garcês et al., 2007). These observations indicate that embryogenesis is recruited during plantlet formation. However, KdLEC1 is truncated and non-functional due to a 20-nucleotide deletion at its B domain. Moreover, loss of KdLEC1 function is required to bypass dormancy to allow plantlet growth in constitutive plantlet-forming species, *K. daigremontiana* (Garcês et al., 2014). This led to the speculation that other embryogenesis gene such as *KdFUS3* might have evolved to replace essential embryogenesis function of *LEC1* during plantlet formation. Although the data obtained is insufficient to confirm this speculation, *KdFUS3* is functionally important during plantlet formation as downregulation of *KdFUS3* resulted in various phenotypes such as defective pedestal formation, plantlet initiation and arrested plantlet development. These phenotypes are similar to *K. daigremontiana* plants with downregulated *KdSTM* which was also downregulated in *KdFUS3* plants. *KdWUS* was also downregulated in these plants, hence, perhaps *KdFUS3* function might be integrated into organogenesis pathways (Garcês et al.,

2007). *KdFUS3* B3 domain was found to be highly conserved among angiosperm species The spatial and temporal expression domain of *KdFUS3* overlaps with that of *KdLEC1* during early plantlet formation. *KdFUS3* expression persisted until later stages of plantlet formation similar to *Arabidopsis FUS3* expression. This indicates that *KdFUS3* might have evolved to replace some functions of *KdLEC1* whilst retaining its original function similar to *Arabidopsis FUS3.* Extensive mutual regulatory interactions among *LAFL* genes (Boulard et al., 2018; Pelletier et al., 2017; Tian et al., 2020b; Wang and Perry, 2013) and differences in their expression in *K. daigremontiana* compared to *Arabidopsis* embryogenesis suggest that *LAFL* gene network might have evolved over time to exert its function during plantlet formation.

6.1.4. Somatic Embryogenesis

K. daigremontiana plantlet formation appears to share mechanism(s) with somatic embryogenesis, in which somatic leaf cells at the leaf notches dedifferentiate to regain embryonic potency and grow into a plantlet (Fehér, 2006). This switch in cell fate involves chromatin remodelling to increase accessibility and allow large-scale transcriptional activation of embryogenic genes (De-la-Peña et al., 2015; Florentin et al., 2013; Kumar and Staden, 2017; Wang et al., 2020a). The presence of shoot meristem-like cells at leaf notches of very young *K. daigremontiana* leaves suggests that somatic embryogenesis might have occurred as new leaf notches develop (Guo et al., 2015). The severity of plantlet defects observed from *K. daigremontiana* antisense lines of organogenesis genes (*STM, WUS, CLV1*) and embryogenesis gene (*FUS3)* seems to support the use of somatic embryogenesis during plantlet formation. Compared to *WUS* and *CLV1* antisense plants, *STM* and *FUS3* antisense plants plantlet formation was more severely affected as plantlet formation was almost abolished and initiated plantlets were eventually aborted (Garcês et al., 2007). Similarity in these phenotypes in *STM* and *FUS3* antisense plants suggest that *STM* and *FUS3* might have affected the same pathway, such as somatic embryogenesis. *FUS3* overexpression in *Arabidopsis* only triggered mild phenotypes of leaves developing cotyledon-like traits, and that *STM* overexpression only enhanced efficiency of indirect somatic embryogenesis (Elhiti et al., 2010; Gazzarrini et al., 2004). This suggest that *FUS3* and *STM* might be involved in regulating somatic embryogenesis but are not key players in the process. Hence, when its expression was reduced, some transgenic plants were obtained. This is in contrast to our leaky *KdWUS* antisense transgenic

plants with very mild downregulation of *KdWUS* expression. The inability to obtain *KdWUS* antisense lines with greater reduction in expression implies that *KdWUS* is important for somatic embryogenesis for *in vitro* regeneration of *K. daigremontiana* tissues. *FUS3* and *STM* might have affected somatic embryogenesis required for plantlet formation by affecting other genes needed for the process. *FUS3* and *STM* have shown to interact with genes that induce somatic embryogenesis when overexpressed. These genes are *LAFL* genes such as *LEC1* and *LEC2* that mutually regulates each other with *FUS3* and *WUS* that can regulate *STM* expression (Lotan et al., 1998; Stone et al., 2001; Su et al., 2020; Wang and Perry, 2013).

6.2. **Environmental cues**

6.2.1. Light

As sessile organisms, plants need to detect and respond to the rapidly changing environment for survival. These environmental factors include light and other stresses such as drought, temperature and pathogens. In the case of *K. daigremontiana*, exposure to at least 12 hours of light over a period of time is required to initiate plantlet formation (Heide, 1965; Hershey, 2002). However, *K. daigremontiana* detached leaves produce plantlets independent of day length (Heide, 1965; Yazgan and Vardar, 1977). This is similar to a stress-inducible plantlet forming species *K. pinnata*, which makes plantlets only on detached leaves, even under short-day condition or in the dark (Heide, 1965; Paterson and Rost, 1979). As stress-induced plantlet-forming *Kalanchoë* species are more ancestral in *Kalanchoë* genus evolution, this suggests that over evolutionary time, light was incorporated into stimulation of plantlet formation in constitutive plantlet-forming species (Garcês et al., 2007). RNA-sequencing data revealed that the GO term 'response to radiation GO:0009314' was over-represented during *K. daigremontiana* plantlet formation. All genes in this GO term were upregulated across the stages corresponding to plantlet initiation phase and also belong to the GO term 'response to light stimulus GO:0009416'. This GO term 'response to light stimulus GO:0009416' was over-represented during *K. pinnata* plantlet formation, however, the genes were continuously downregulated upon leaf detachment until 24 hours after detachment. This correlates with the fact that light-sensing is not needed in stress-induced plantlet-forming *Kalanchoë* species to initiate plantlet formation and the *vice versa* applies to constitutive plantlet-forming species.

With limited molecular studies on plantlet formation, the mechanisms on photoperiod stimulation of plantlet formation are yet to be elucidated. Nonetheless, participation of a flowering signal integrator gene *SUPPRESSOR OF CONSTANS OVEREXPRESSION 1* (*KdSOC1*) in *K. daigremontiana* plantlet formation suggests that photoperiodism might be mediating plantlet formation through recruitment of flowering pathways during plantlet formation (Lee and Lee, 2010; Zhu et al., 2017). Existing studies have shown that *SOC1* can integrate photoperiodism and actions of phytohormones such as gibberellic acid into flowering genetic pathways to regulate flowering (Kinoshita et al., 2020; Lee and Park, 2015). Apart from that, *SOC1* was shown to affect dormancy break, hence, perhaps *SOC1* is also responsible for maintaining dormancy of *Kalancho*ë plantlet (Trainin et al., 2013; Voogd et al., 2015). A recent study showed that overexpression of *KdSOC1* in *K. daigremontiana* led to increase in auxin concentration and *KdPIN1* expression (Zhu et al., 2017). This indicates that *KdSOC1* is acting upstream of *KdPIN1* and auxin activity which, according to our data, might be involved in plantlet initiation. Based on known functions of *SOC1*, *KdSOC1* is a likely candidate to act early in plantlet initiation, however, this speculation still requires extensive studies. As light remains as the primary trigger for plantlet formation particularly in constitutive plantlet-forming species such as *K. daigremontiana*, evidence on mechanism of photoperiodism in plantlet formation will contribute to understanding on plantlet initiation, integration of flowering pathways and embryogenesis and evolution of *Kalancho*ë asexual reproduction.

6.2.2. Stress factors

*Kalancho*ë plantlet formation is activated upon leaf detachment and incision of leaf blade (Garcês and Sinha, 2009a). Hence, plantlet formation is assumed to be a consequence of stress response. Though this physiological response is well-observed (Kulka, 2006; Viana and Nováis, 1970; Warden, 1969), studies on molecular mechanisms of how different stress factors stimulate plantlet formation remains very limited. In the case of constitutive plantlet-forming species such as *K. daigremontiana* and *K. tubiflora*, plantlet formation is also accelerated by drought stress (Luo et al., 2014; Zhong et al., 2013). In *K. tubiflora*, this is accompanied by increased reaction oxygen species and sugar content, indicating that oxidative stress and salinity stress are involved in inducing plantlet formation (Luo et al., 2014). Based on our RNA-sequencing data, stress detection and response seemed to play a role in plantlet formation,

particularly during the early stages. This is shown by overrepresentation of many stress-sensing and -regulating genes during plantlet formation of both *K. daigremontiana* and *K. pinnata*, which are upregulated during the first two stages examined. Somatic embryogenesis and stem cell signalling has both been shown to be stimulated by stress response (Castander-Olarieta et al., 2020; Huang et al., 2019; Khattak et al., 2017; Krishnan and Siril, 2017; Lee, 2018; Nic-Can et al., 2016; Pandey and Chaudhary, 2014; Yang et al., 2020; Zhou et al., 2016). Hence, these stress responses might have triggered somatic embryogenesis, the likely mechanism of *K. daigremontiana* plantlet formation. However, in the case of *K. pinnata*, stress response might be triggering organogenesis as embryogenesis does not appear to be recruited in stress-inducible plantlet-forming species (Garcês et al., 2007). Compared to light, other stress factors seem to be the more dominant and ancient trigger for plantlet formation. This is because only the most recently evolved constitutive plant-forming species depends on light to make plantlets whereas plantlet formation in all *Kalancho*ë plant-forming species is induced by stress (Garcês and Sinha, 2009a; Garcês et al., 2007). Hence, understanding the integration of stress signals during plantlet formation might revealed molecular mechanisms that initiates plantlet formation in all *Kalancho*ë plantlet-forming species.

6.2.3. Mechanical forces

Apart from the different types of stress discussed above, stresses can also come in the form of mechanical stress. Plants can experience external and internal mechanical forces that affect various cellular processes such as growth, polarity, and gene expression (Landrein and Ingram, 2019). The intrinsic cause of mechanical stress in plant arises from internal turgor pressure as plant cells are structures containing content under compression enveloped by the rigid cell wall under tension (Moulia et al., 2015; Peters and Tomos, 1996). Previous studies have shown that softening cell wall using expansin or auxin-dependent pectin demethylesterification can promote organogenesis in the SAM (Braybrook and Peaucelle, 2013; Fleming et al., 1997; Peaucelle et al., 2011). In addition, high anisotropic mechanical stress changes microtubule orientation of cells at the boundary domain of the SAM to channel growth direction and promotes tissue folding (Burian et al., 2013; Hamant et al., 2008; Louveaux et al., 2016). Mechanical stresses has also shown to influence orientation and polarity of auxin efflux transporter PIN1 at the SAM, leading to auxin repartition and subsequently alters the growth

rate and organ shape (Heisler et al., 2010; Landrein et al., 2015; Nakayama et al., 2012). These consequences can also be affected by induction of *STM* expression *via* micromechanical perturbations at the boundary domain (Landrein et al., 2015). The same study showed that the correlation of *STM* expression with the curvature in the saddle-shaped boundary domain of the SAM and is required for organ separation (Landrein et al., 2015). The curvature is similar to the site of plantlet formation in which two fast-growing leaf lobes meet. Hence, the mechanical pressure generated by the curvature might have induced *KdSTM* expression and PIN1 at the plantlet formation site. PIN1 localisation observed at the leaf notch prior to pedestal formation might lead to auxin accumulation at the leaf notch to induce somatic embryogenesis (Tang et al., 2020). *KdSTM* expression might then functions to separate the outgrowth of pedestal from the leaf notch, similar to the organ separation at *Arabidopsis* SAM (Landrein et al., 2015). Outgrowth of pedestal might exerts mechanical stress that in turn induce *KdSTM* expression to regulate plantlet development (Garcês et al., 2007; Landrein et al., 2015). Existing literatures illustrating how mechanical pressure affect *STM* expression, PIN1 localisation and auxin will serve as a good starting point to study the role of mechanical stress in stimulating formation of pedestal or plantlet.

6.3. **Conclusion**

Gathering the information discussed above, this research project has uncovered genetic and hormonal control behind different stages of plantlet developmental process in *K. daigremontiana*. These stages include pedestal formation, plantlet initiation and plantlet development. We showed that similar mechanisms in patterning zygotic embryo might be reused in patterning plantlet. Through visualisation of auxin efflux transport PIN1, we showed that auxin accumulation might be involved in triggering pedestal outgrowth and plantlet initiation. Presence of cytokinin activity during plantlet development, and defective plantlet formation in *KdaHP* antisense plants suggests that cytokinin also participates in early and later stages of plantlet formation. The data also showed possible integration between auxin and cytokinin with embryogenesis and organogenesis pathways. Nonetheless, some data still requires validation and further studies are needed to obtain more concrete and conclusive evidence. A better understanding of *Kalancho*ë plantlet formation will expand our knowledge on triggered pluripotency in plants. This will aid our understanding of plant asexual reproduction and plant developmental plasticity. The knowledge will in turn serve as a reference to enhance production of economically and agriculturally important plant species.

Supplementary Figures and Tables

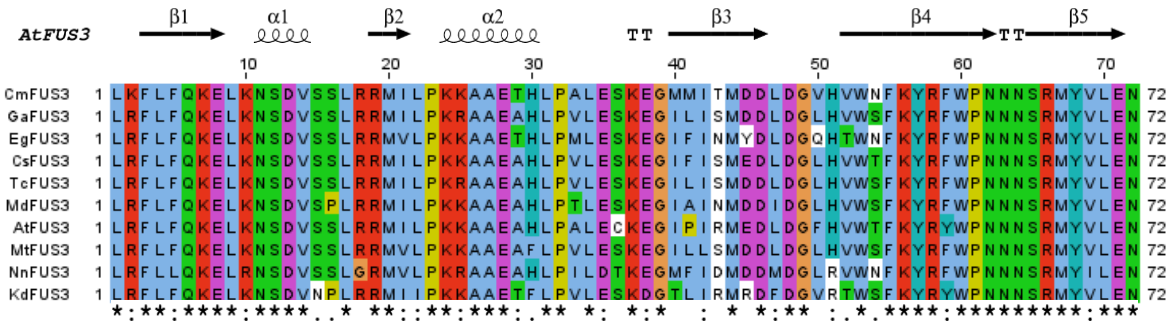

Supplementary Figure 2.1. Multiple sequence alignment of FUS3 B3 domain peptide sequences. "*" indicates conservation of the same amino acid, ":" indicates conservation of amino acids with strong similarity, "." Indicates conservation of amino acids with weak similarity, absence of symbol indicates no conservation of amino acid at the position. The secondary structure of the sequences with reference to *AtFUS3* is shown at the top of the alignment. The position of each amino acid is indicated by the value directly above the alignment.

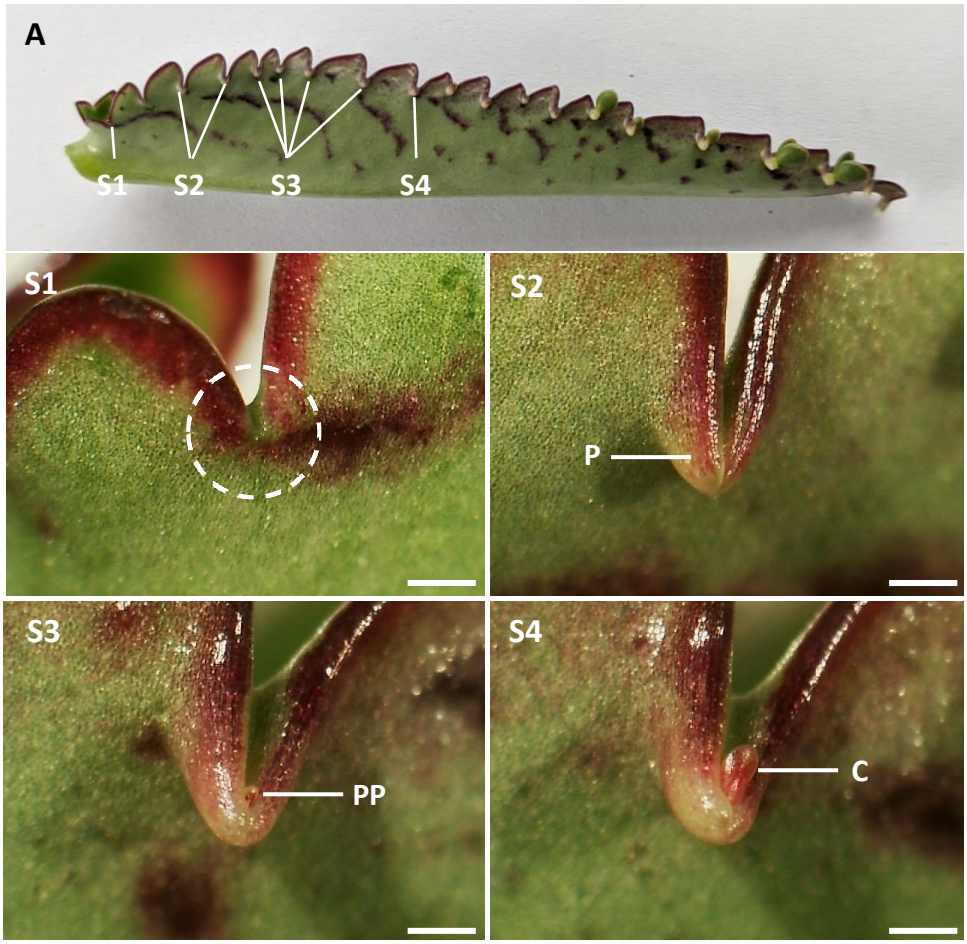

Supplementary Figure 2.2. Stages of plantlet formation selected for RNA-sequencing. (A) A mature plantlet-forming *K. daigremontiana* leaf with the selected stages of plantlet formation. (Stage 1, S1) Leaf notch without pedestal formation. (Stage 2, S2) Leaf notch with pedestal (P) but without morphologically visible plantlet. (Stage 3, S3) Leaf notch with pedestal enveloping an emerging plantlet primordium (PP). (Stage 4, S4) Leaf notch with pedestal supporting a plantlet forming cotyledon (C). Scale bar represents 1 mm.

Supplementary Table 5.1 List of exclusive and overlapping differentially expressed genes between selected plantlet stages from *K. daigremontiana* and post-detachment time points of *K. pinnata* leaves.

	TAIR ID						No. of genes
a	AT2G47260.1	AT1G70830.1	AT1G30270.1	AT3G60030.1	AT4G02520.1	AT5G36930.2	114
	AT2G30770.1	AT1G22340.1	AT4G38620.1	AT4G33790.1	AT3G19540.1	AT3G22810.1	
	AT1G09380.1	AT1G03440.1	AT3G51630.1	AT4G20140.1	AT1G02170.1	AT1G62990.1	
	AT3G18490.1	AT3G18830.1	AT1G79420.1	AT2G34060.1	AT1G23820.1	AT1G03840.1	
	AT4G39790.1	AT3G22840.1	AT1G63100.1	AT1G58440.1	AT3G45850.1	AT5G50210.1	
	AT5G47070.1	AT1G23790.1	AT5G54190.1	AT5G06300.1	AT1G08440.1	AT4G22680.1	
	AT4G35070.1	AT3G25400.1	AT5G57260.1	AT4G22920.1	AT5G57340.1	AT5G53130.1	
	AT1G68570.1	AT5G66730.1	AT1G50010.1	AT1G70880.1	AT5G64330.1	AT5G47060.1	
	AT5G52510.1	AT4G30960.1	AT1G80830.1	AT1G29670.1	AT4G12500.1	AT1G30040.1	
	AT4G33270.1	AT5G49620.1	AT5G20740.1	AT1G80130.1	AT3G51970.1	AT3G51060.1	
	AT2G04570.1	AT4G31940.1	AT1G76490.1	AT1G75900.1	AT3G12500.1	AT2G15760.1	
	AT2G22620.1	AT5G54160.1	AT4G39720.1	AT2G34190.1	AT5G19650.1	AT4G35100.1	
	AT4G15560.1	AT5G62360.1	AT1G30360.1	AT5G25610.1	AT2G36830.1	AT2G01190.1	
	AT1G04820.1	AT2G44670.1	AT1G15100.1	AT5G20860.1	AT5G54670.1	AT2G47500.1	
	AT5G53390.1	AT1G19870.1	AT3G24240.1	AT4G14960.1	AT1G60420.1	AT1G08470.1	
	AT3G51280.1	AT2G44480.1	AT2G36530.1	AT3G19640.1	AT5G33320.1	AT2G32280.1	
	AT5G14180.1	AT3G17510.1	AT4G02340.1	AT2G21060.1	AT5G23660.1	AT4G11080.1	
	AT5G53660.1	AT3G12870.1	AT5G01870.1	AT2G34700.1	AT3G61490.3	AT1G29930.1	
	AT4G33400.1 AT1G09950.1 AT1G59970.1 AT5G53970.1 AT2G40610.1 AT2G27030.3						
b	AT5G48850.1	AT1G20450.1	AT5G62040.1	AT3G51740.1	AT5G23860.2	AT4G17000.1	71
	AT2G44940.1	AT2G36200.1	AT1G61260.1	AT3G01860.1	AT1G04150.1	AT3G57830.1	
	AT5G49650.1	AT1G78610.1	AT1G67480.1	AT3G54250.1	AT1G27510.1	AT2G38740.1	
	AT1G04770.1	AT3G52710.1	AT2G05940.1	AT5G19860.1	AT5G63860.1	AT2G19770.1	
	AT2G40010.1	AT4G16780.1	AT2G42520.1	AT3G10180.1	AT4G14150.1	AT3G23890.2	
	AT3G22670.1	AT1G73620.1	AT4G34530.1	AT4G24460.1	AT5G59420.1	AT5G57123.1	
	AT1G28100.3	AT4G35160.1	AT4G12420.2	AT2G30140.1	AT4G22860.1	AT2G30150.1	
	AT1G65710.1	AT4G03100.1	AT3G52990.1	AT2G26310.1	AT1G61350.1	AT5G46230.1	
	AT1G19640.1	AT3G25150.2	AT3G15550.1	AT3G22540.1	AT2G36750.1	AT1G75820.1	
	AT4G35470.1	AT5G26667.1	AT4G37750.1	AT1G70850.1	AT5G24650.1	AT1G07090.1	
	AT5G13000.1	AT5G60150.1	AT5G67270.1	AT4G21280.1	AT3G22830.1	AT5G48820.1	
	AT1G46264.1 AT3G22142.1 AT1G18370.1 AT2G03090.1 AT1G32580.1						
c	AT3G20650.1	AT5G63160.1	AT3G52610.1	AT5G13870.1	AT4G17240.1	AT1G08465.1	42
	AT1G11910.1	AT4G21620.1	AT1G09450.1	AT1G75250.1	AT3G22550.1	AT2G31390.1	
	AT2G40890.1	AT2G46660.1	AT2G38620.2	AT1G78110.1	AT5G25190.1	AT5G66460.1	
	AT5G58320.2	AT2G23380.1	AT2G17500.3	AT2G29120.1	AT4G12080.1	AT4G28390.1	
	AT2G30490.1	AT3G07880.1	AT1G56430.1	AT1G69970.2	AT2G16580.1	AT4G00820.1	
	AT5G39950.1	AT4G18960.1	AT3G53190.1	AT1G10070.1	AT4G33090.1	AT4G36180.1	
	AT5G24270.1 AT5G49100.1 AT3G56680.1 AT1G22400.1 AT1G18650.1 AT1G60060.1						
d	AT5G02890.1	AT4G18750.1	AT3G15630.1	AT3G48310.1	AT5G17540.1	AT3G54890.1	596
	AT1G08070.1	AT2G44600.1	AT3G13960.1	AT5G19730.1	AT1G15690.1	AT3G14470.1	
	AT3G21700.3	AT4G27310.1	AT4G10080.1	AT1G61065.1	AT4G16730.1	AT4G23500.1	
	AT1G52855.1	AT1G67970.1	AT2G14910.1	AT2G21100.1	AT2G19130.1	AT4G38970.1	
	AT5G17230.2	AT4G35190.1	AT1G32450.1	AT1G03590.1	AT3G49220.1	AT3G07040.1	
	AT1G62750.1	AT4G17900.1	AT3G18080.1	AT5G64230.1	AT2G46710.1	AT2G20835.1	
	AT1G28220.1	AT1G05590.1	AT3G25140.1	AT3G47570.1	AT5G62100.2	AT1G16030.1	
	AT2G45980.1	AT2G39518.1	AT1G19910.1	AT1G47128.1	AT4G17940.1	AT5G52860.1	
	AT4G39780.1	AT5G66060.1	AT4G01900.1	AT5G10510.2	AT5G65380.1	AT3G26170.1	
	AT1G15210.1	AT2G01220.1	AT4G14540.1	AT5G12020.1	AT4G21440.1	AT2G20880.1	
	AT2G20990.2	AT1G03220.1	AT3G11780.1	AT5G67300.1	AT2G48020.2	AT2G39210.1	
	AT4G28140.1	AT1G70850.3	AT1G68820.1	AT5G47770.1	AT2G36870.1	AT5G05950.1	
	AT5G50570.2	AT1G68370.1	AT1G61800.1	AT3G26690.1	AT5G48810.1	AT5G36110.1	
	AT1G78900.1	AT4G37850.1	AT4G34500.1	AT2G15900.1	AT3G26310.1	AT2G29730.1	

	AT2G28570.1	AT4G31860.1	AT1G15670.1	AT2G46680.1	AT4G39120.1	AT1G70950.1	
	AT5G12230.1	AT3G17020.1	AT5G47120.1	AT1G31330.1	AT3G46640.1	AT5G59320.1	
	AT3G63250.1	AT1G11260.1	AT2G45590.1	AT2G46600.1	AT5G23230.1	AT2G32210.1	
	AT5G20270.1	AT2G32720.1	AT3G03280.1	AT5G10170.1	AT5G19940.1	AT1G45688.1	
	AT5G57660.1	AT3G50330.1	AT5G18980.1	AT5G64440.1	AT4G37790.1	AT5G55180.1	
	AT4G22260.1	AT3G06810.1	AT2G40080.1	AT5G39670.1	AT5G15948.1	AT5G17310.2	
	AT5G40240.1	AT3G47730.1	AT3G26050.1	AT2G26850.1	AT3G54070.1	AT4G30190.1	
	AT2G20570.1	AT2G32010.2	AT2G36080.1	AT1G49740.1	AT3G24190.1	AT2G34500.1	
	AT5G05510.1	AT5G20410.1	AT1G09430.1	AT4G39010.1	AT4G02980.1	AT5G14370.1	
	AT1G78380.1	AT3G18370.1	AT3G14460.1	AT5G19140.1	AT5G64920.1	AT1G66370.1	
	AT3G48360.1	AT5G64510.1	AT5G62910.1	AT1G21980.1	AT4G22990.2	AT3G61650.1	
	AT5G48300.1	AT4G12300.1	AT4G02940.1	AT3G52450.1	AT2G21520.1	AT1G06620.1	
	AT2G16630.1	AT2G13560.1	AT4G15960.1	AT2G16120.1	AT1G17870.1	AT1G12663.1	
	AT5G35320.1	AT3G11510.1	AT5G56980.1	AT3G01750.1	AT1G68390.1	AT5G40250.1	
	AT2G41560.1	AT5G09590.1	AT4G15530.6	AT1G15380.2	AT5G14040.1	AT1G52240.2	
	AT2G26150.1	AT5G26230.1	AT4G01970.1	AT5G59760.1	AT1G62760.1	AT3G04590.2	
	AT5G04440.1	AT4G35350.2	AT2G22430.1	AT3G52105.1	AT3G15850.1	AT5G47900.1	
	AT4G01150.1	AT2G39420.1	AT3G14225.1	AT5G22740.1	AT5G49700.1	AT3G45140.1	
	AT2G18910.1	AT3G20300.1	AT5G56030.1	AT2G38530.1	AT2G07180.2	AT4G14550.1	
	AT5G46330.1	AT5G49360.1	AT1G04760.1	AT5G39450.1	AT2G29510.1	AT5G33370.1	
	AT3G25780.1	AT3G05950.1	AT1G17080.1	AT4G00570.1	AT1G01800.1	AT1G72330.1	
	AT2G21210.1	AT5G42110.1	AT2G45180.1	AT2G25760.1	AT5G05280.1	AT5G49015.2	
	AT1G27170.1	AT3G62980.1	AT4G08685.1	AT3G26320.1	AT1G11750.1	AT5G46050.1	
	AT1G07430.1	AT5G06700.1	AT1G13080.1	AT5G48630.1	AT1G53035.1	AT5G11000.1	
	AT3G46510.1	AT5G16390.1	AT1G77380.1	AT2G27310.1	AT3G14680.1	AT2G21660.1	
	AT1G75130.1	AT4G01370.1	AT4G10265.1	AT1G78950.1	AT1G53910.1	AT4G00230.1	
	AT1G12110.1	AT4G38060.2	AT3G43520.1	AT5G57150.1	AT4G35230.1	AT4G33420.1	
	AT4G00360.1	AT3G50760.1	AT1G50590.1	AT4G38960.1	AT1G02520.1	AT2G33500.2	
	AT5G65790.1	AT3G45010.1	AT2G24820.1	AT5G23530.1	AT2G22240.1	AT5G46970.1	
	AT4G32190.1	AT5G66320.2	AT2G01570.1	AT1G53540.1	AT1G28330.4	AT2G45550.1	
	AT1G23850.1	AT5G05480.1	AT2G24230.1	AT3G14840.2	AT5G54165.1	AT2G22420.1	
	AT2G39650.1	AT3G16030.1	AT1G22360.1	AT1G02610.1	AT2G42490.1	AT3G13870.1	
	AT1G62790.1	AT1G79870.1	AT3G14660.1	AT5G22480.1	AT1G49230.1	AT5G10770.1	
	AT3G45780.2	AT1G59650.1	AT3G03620.1	AT4G18570.1	AT4G21320.1	AT2G16570.1	
	AT5G09530.1	AT1G56290.1	AT1G13260.1	AT5G56000.1	AT4G34950.1	AT4G03420.1	
	AT2G26170.1	AT5G10550.1	AT5G57710.1	AT2G39770.2	AT3G02540.3	AT3G09270.1	
	AT1G53210.1	AT2G28000.1	AT1G80160.1	AT2G38090.1	AT3G47420.1	AT1G73590.1	
	AT4G13395.1	AT4G05200.1	AT5G17860.1	AT5G62350.1	AT3G45600.1	AT2G05100.1	
	AT5G67470.1	AT4G33920.1	AT3G10700.1	AT5G05500.1	AT2G43130.1	AT3G54420.1	
	AT5G59300.1	AT1G61520.3	AT1G68400.1	AT1G52190.1	AT5G58700.1	AT4G37450.1	
	AT5G65710.1	AT1G20550.1	AT2G01150.1	AT4G24240.1	AT3G23820.1	AT1G67730.1	
	AT2G17820.1	AT5G62470.2	AT5G66880.1	AT3G07310.1	AT4G30950.1	AT1G55490.1	
	AT5G04550.1	AT5G27690.1	AT3G62270.1	AT3G48710.1	AT4G36360.1	AT5G47550.1	
	AT5G22930.1	AT2G37970.1	AT5G13720.1	AT1G24540.1	AT5G53750.1	AT3G11600.1	
	AT5G06060.1	AT1G72820.1	AT2G14740.1	AT1G51700.1	AT1G20080.1	AT1G68050.1	
	AT5G42740.1	AT1G15520.1	AT4G12730.1	AT4G26150.1	AT3G57450.1	AT4G32350.1	
	AT1G13570.1	AT5G25140.1	AT5G20480.1	AT3G54140.1	AT3G54820.1	AT1G20030.2	
	AT5G42610.1	AT1G17200.1	AT5G60920.1	AT1G55360.1	AT1G44170.2	AT5G61890.1	
	AT4G21870.1	AT4G25700.1	AT4G36670.1	AT2G38310.1	AT1G08250.1	AT1G01260.3	
	AT5G49820.1	AT1G30380.1	AT4G08570.1	AT4G12510.1	AT5G66750.1	AT1G67980.1	
	AT4G01950.1	AT4G27870.1	AT1G24360.1	AT5G15950.2	AT4G30100.1	AT3G47470.1	
	AT3G62660.1	AT2G36460.1	AT5G42200.1	AT1G69780.1	AT1G65560.1	AT1G74640.1	
	AT4G24510.1	AT5G19770.1	AT3G23810.1	AT3G22970.1	AT1G18390.2	AT1G08380.1	
	AT1G23710.1	AT3G54660.1	AT4G01470.1	AT1G72110.1	AT1G52580.1	AT5G11590.1	
	AT3G17640.1	AT3G52070.1	AT3G13160.1	AT1G17020.1	AT3G25800.1	AT5G02500.1	
	AT4G02800.1	AT5G57560.1	AT2G23790.1	AT1G06680.1	AT3G04350.1	AT1G79750.1	

	AT1G29100.1	AT1G29050.1	AT4G27435.1	AT3G14230.3	AT1G80460.1	AT4G35530.1	
	AT2G39980.1	AT3G61770.1	AT5G49665.1	AT1G31350.1	AT4G16144.1	AT3G03820.1	
	AT5G49910.1	AT1G61560.1	AT1G01630.1	AT3G05500.1	AT4G03510.1	AT3G25520.1	
	AT5G07010.1	AT5G60390.1	AT1G12330.1	AT5G59500.1	AT2G04039.1	AT5G41790.1	
	AT5G43010.1	AT3G46220.1	AT1G12060.1	AT4G23180.1	AT1G71900.1	AT5G36230.1	
	AT3G23050.1	AT2G25890.1	AT4G37260.1	AT1G12450.1	AT5G34930.1	AT1G75780.1	
	AT2G38940.1	AT1G26880.1	AT1G14560.1	AT3G09320.1	AT3G59140.1	AT1G29140.1	
	AT2G30360.1	AT5G39660.1	AT4G25040.1	AT1G32900.1	AT1G44790.1	AT2G40320.1	
	AT3G18570.1	AT2G01290.1	AT3G48280.1	AT5G42900.3	AT3G55410.1	AT5G05140.1	
	AT5G14210.1	AT2G20740.1	AT4G15470.1	AT5G10160.1	AT5G04070.1	AT1G19180.1	
	AT5G57330.1	AT5G51050.1	AT4G25200.1	AT3G47500.1	AT4G15530.2	AT1G32780.1	
	AT1G55530.1	AT3G48740.1	AT1G09310.1	AT4G11150.1	AT5G04530.1	AT5G48485.1	
	AT5G49720.1	AT3G22060.1	AT1G15760.1	AT3G24060.1	AT5G35370.1	AT5G65020.1	
	AT5G67360.1	AT2G45900.1	AT1G77720.1	AT1G12780.1	AT1G07350.1	AT4G36250.1	
	AT3G21690.1	AT1G49820.1	AT5G03760.1	AT5G10600.1	AT2G27190.1	AT4G23990.1	
	AT1G76880.1	AT1G76560.1	AT5G45890.1	AT5G11150.1	AT2G17230.1	AT5G45670.1	
	AT4G00430.1	AT5G14690.1	AT5G54630.1	AT1G55340.2	AT5G64750.1	AT3G14690.1	
	AT2G02240.1	AT1G12770.1	AT3G29360.1	AT4G34760.1	AT5G14280.1	AT4G39210.1	
	AT5G14120.1	AT2G20260.1	AT4G19390.1	AT5G60710.1	AT3G15840.1	AT4G21860.3	
	AT4G12750.1	AT1G78300.1	AT4G37360.1	AT3G52420.1	AT3G11170.1	AT5G50450.1	
	AT1G32190.1	AT5G60520.1	AT4G24900.1	AT2G46690.1	AT3G13310.1	AT5G19760.1	
	AT4G21990.1	AT1G05850.1	AT2G28840.1	AT1G07570.1	AT1G76080.1	AT4G22130.1	
	AT2G21590.1	AT4G01070.1	AT3G05010.1	AT1G06520.1	AT5G02810.1	AT1G67070.1	
	AT1G64660.1	AT1G22840.1	AT3G46970.1	AT1G53380.2	AT1G25480.1	AT4G21380.1	
	AT1G27150.1	AT5G48370.1	AT3G09390.1	AT5G22340.2	AT2G38270.1	AT4G02920.1	
	AT5G43060.1	AT5G61430.1	AT3G17000.1	AT4G15800.1	AT4G32940.1	AT1G68760.1	
	AT1G52920.1	AT5G59880.1	AT2G31980.1	AT1G42960.1	AT3G10640.1	AT3G13600.1	
	AT5G54770.1	AT5G64040.1	AT2G46100.1	AT2G17480.1	AT3G25110.1	AT5G42000.1	
	AT5G60580.1	AT1G27650.1	AT3G57680.1	AT2G20560.1	AT3G52590.1	AT3G10760.1	
	AT3G23410.1 AT1G12260.1						
e	AT3G28920.1	AT5G65140.1	AT2G45430.1	AT5G64260.1	AT3G16240.1	AT1G14790.1	17
	AT1G35190.1	AT5G16370.1	AT1G76690.1	AT1G66950.1	AT1G58340.1	AT3G08860.1	
	AT5G16990.1 AT2G29290.2 AT5G60680.1 AT2G22170.1 AT4G32551.1						
f	AT5G13120.1	AT3G28857.1	AT5G02440.1	AT2G45190.1	AT5G21920.1	AT1G20930.1	219
	AT1G19600.1	AT2G42110.1	AT4G02810.1	AT5G51850.1	AT2G37460.1	AT5G45700.1	
	AT1G03940.1	AT5G38970.1	AT2G18470.1	AT1G14030.1	AT3G63010.1	AT3G05220.1	
	AT5G11600.1	AT3G26590.1	AT5G07670.1	AT5G14940.1	AT4G37510.1	AT5G10150.1	
	AT5G23210.1	AT4G31980.1	AT4G34770.1	AT1G75390.1	AT4G12540.1	AT5G63100.1	
	AT3G13510.1	AT1G64625.2	AT4G32830.1	AT1G75520.1	AT1G03870.1	AT4G08150.1	
	AT3G23670.1	AT1G70210.1	AT1G12150.1	AT4G02390.1	AT5G22090.1	AT1G27660.1	
	AT5G26330.1	AT4G32480.1	AT5G18520.1	AT1G18590.1	AT5G64620.1	AT1G48405.1	
	AT3G26700.1	AT5G51410.2	AT3G43210.1	AT3G48410.1	AT4G14723.1	AT4G31690.1	
	AT4G20230.1	AT4G39980.1	AT1G69740.2	AT2G04700.1	AT2G19070.1	AT1G51220.1	
	AT1G68060.1	AT1G28130.1	AT3G55470.1	AT3G14420.2	AT3G25130.1	AT4G22010.1	
	AT1G75710.1	AT5G64980.1	AT5G66055.1	AT5G61850.1	AT3G07130.1	AT1G14600.1	
	AT1G28200.1	AT2G38860.2	AT3G52910.1	AT3G27850.1	AT1G15270.1	AT2G02860.1	
	AT1G22380.1	AT5G01660.1	AT4G02290.1	AT3G15990.1	AT3G01710.2	AT2G42800.1	
	AT4G28230.1	AT3G11090.1	AT5G50150.1	AT1G54820.1	AT1G64080.1	AT1G08560.1	
	AT1G34355.1	AT3G48040.1	AT3G50410.1	AT3G25410.1	AT5G63950.1	AT5G47820.2	
	AT1G06830.1	AT5G48600.2	AT5G56220.1	AT2G33560.1	AT5G66230.1	AT5G02030.1	
	AT1G49870.1	AT2G36026.1	AT3G15190.1	AT4G15140.1	AT2G18890.1	AT5G67260.1	
	AT1G12790.1	AT4G33040.1	AT5G13840.1	AT3G26744.1	AT1G09000.1	AT1G65810.1	
	AT4G04350.1	AT3G55370.3	AT1G62360.1	AT1G72310.1	AT5G48040.1	AT4G13370.1	
	AT3G58610.2	AT3G21420.1	AT5G24800.1	AT1G75430.1	AT3G20290.2	AT2G19780.1	
	AT5G06150.1	AT2G25880.1	AT2G33450.1	AT3G58880.1	AT3G61640.1	AT1G20330.1	
	AT1G65620.4	AT2G34650.1	AT3G49200.1	AT2G45490.1	AT4G14330.1	AT3G05600.1	

	AT5G50915.1	AT1G76660.1	AT5G42340.1	AT5G24490.1	AT1G18660.4	AT2G36630.1	
	AT1G80080.1	AT5G07050.1	AT1G75388.1	AT5G05240.1	AT3G03660.1	AT1G54780.1	
	AT3G15353.1	AT5G15510.1	AT4G01310.1	AT1G44110.1	AT5G53030.1	AT3G54400.1	
	AT2G17650.1	AT4G09060.1	AT4G16447.1	AT4G13940.1	AT1G31310.1	AT1G70710.1	
	AT1G75540.1	AT2G40490.1	AT3G16490.1	AT2G40110.1	AT5G01990.1	AT4G21760.1	
	AT5G09760.1	AT4G01730.1	AT1G11120.2	AT1G26680.1	AT2G41870.1	AT4G16740.2	
	AT5G28640.1	AT5G57390.1	AT5G11320.1	AT2G23450.1	AT5G62710.1	AT1G27680.1	
	AT5G25280.1	AT2G39830.1	AT3G20150.1	AT5G55960.1	AT3G25810.1	AT5G20630.1	
	AT2G31160.1	AT1G04880.1	AT5G05940.1	AT3G29300.1	AT2G25060.1	AT5G53950.1	
	AT2G44920.2	AT1G53860.1	AT4G24710.1	AT3G20060.1	AT1G59540.1	AT4G19840.1	
	AT3G19184.1	AT3G09290.1	AT5G23960.2	AT2G01630.1	AT1G52790.1	AT5G01590.1	
	AT4G10630.1	AT4G32730.1	AT2G18196.1	AT1G68320.1	AT4G34290.1	AT1G20610.1	
	AT1G68350.1	AT5G36890.1	AT5G23520.1	AT3G02875.1	AT1G69870.1	AT1G16070.1	
	AT2G27770.1	AT2G01420.1	AT4G03210.1				
g	AT1G62850.3	AT4G25050.1	AT2G43460.1	AT2G35605.1	AT5G16520.1	AT2G20490.1	612
	AT3G63240.1	AT1G75180.1	AT4G24570.1	AT5G42990.1	AT1G52740.1	AT5G35090.1	
	AT1G22780.1	AT3G51550.1	AT4G16720.1	AT2G37330.1	AT1G75950.1	AT5G12890.1	
	AT4G18040.1	AT2G35736.1	AT2G09990.1	AT1G22310.2	AT1G47200.1	AT1G22450.1	
	AT1G26170.1	AT3G17090.1	AT1G30135.1	AT2G40660.1	AT1G68550.2	AT3G50660.1	
	AT1G02130.1	AT5G02960.1	AT5G27470.1	AT2G37500.1	AT2G20760.1	AT2G44620.1	
	AT3G56760.1	AT1G56070.1	AT5G25620.1	AT3G10985.1	AT5G13930.1	AT1G49570.1	
	AT4G19460.1	AT4G36710.1	AT4G25970.1	AT2G34660.2	AT1G63850.1	AT5G11200.1	
	AT3G26330.1	AT3G15670.1	AT3G18600.1	AT3G27310.1	AT1G09330.1	AT2G25580.1	
	AT3G06430.1	AT1G09812.1	AT3G49010.1	AT2G15695.1	AT1G31220.1	AT3G10410.1	
	AT3G23620.1	AT5G25560.1	AT4G16563.1	AT3G27830.1	AT1G24020.2	AT3G46100.1	
	AT3G13670.1	AT4G33760.1	AT2G42500.1	AT1G23300.1	AT4G38460.1	AT4G14420.1	
	AT1G75170.1	AT2G31200.1	AT4G14090.1	AT3G10210.1	AT2G29620.1	AT1G10720.1	
	AT3G15460.1	AT1G22020.1	AT5G25170.1	AT3G23160.1	AT3G15470.1	AT1G60590.1	
	AT1G17070.1	AT1G13450.1	AT2G21050.1	AT5G61980.1	AT1G56560.1	AT5G59820.1	
	AT4G31890.1	AT4G25170.1	AT1G04480.1	AT5G42080.1	AT3G48100.1	AT5G42470.1	
	AT2G25737.1	AT2G40950.1	AT5G24580.1	AT5G17230.3	AT4G39080.1	AT5G11260.1	
	AT5G04800.1	AT1G47980.1	AT5G14640.1	AT3G16060.1	AT1G03905.1	AT4G02370.1	
	AT2G36885.1	AT4G15802.1	AT3G61440.1	AT3G08020.1	AT3G08760.1	AT1G04260.1	
	AT2G19520.1	AT1G10380.1	AT1G74050.1	AT5G20930.1	AT1G67940.1	AT5G60960.1	
	AT4G36470.1	AT5G53170.1	AT3G03810.1	AT3G51730.1	AT1G53310.1	AT1G58170.1	
	AT1G67430.1	AT3G10040.1	AT5G57160.1	AT3G15810.1	AT3G16720.1	AT1G05680.1	
	AT1G09280.1	AT2G34670.2	AT5G23340.1	AT3G56810.1	AT3G50770.1	AT3G22960.1	
	AT1G20696.3	AT2G16595.1	AT3G03450.1	AT3G66654.1	AT1G66240.1	AT4G17030.1	
	AT3G62760.1	AT2G45510.1	AT1G22410.1	AT5G61510.1	AT3G61050.2	AT3G57290.1	
	AT5G03455.1	AT1G73500.1	AT3G48900.2	AT3G54510.2	AT2G42740.1	AT3G28970.1	
	AT5G46240.1	AT5G27920.1	AT5G44060.1	AT3G48610.1	AT5G42570.1	AT1G76760.1	
	AT1G49780.1	AT2G40340.1	AT2G47470.1	AT1G18080.1	AT5G61960.2	AT3G55830.1	
	AT2G41840.1	AT4G15910.1	AT3G15920.1	AT5G35732.1	AT3G06370.1	AT3G50530.1	
	AT2G27510.1	AT1G69360.1	AT4G34460.1	AT1G78870.2	AT1G12310.1	AT5G55940.1	
	AT2G03890.1	AT4G02110.1	AT2G18950.1	AT1G68140.1	AT2G04690.1	AT5G20150.1	
	AT1G47250.1	AT3G63480.2	AT3G60540.2	AT3G10050.1	AT2G26640.1	AT3G06680.1	
	AT4G25740.1	AT1G72890.2	AT4G05530.1	AT3G01680.1	AT3G06670.1	AT3G42170.1	
	AT3G14980.1	AT3G09650.1	AT4G32800.1	AT1G68560.1	AT3G12390.1	AT5G49630.1	
	AT2G16920.1	AT4G37680.1	AT5G37490.1	AT4G23950.1	AT3G06130.1	AT1G07630.1	
	AT5G09570.1	AT1G23540.1	AT5G59240.1	AT4G23420.2	AT3G12120.1	AT3G16780.1	
	AT3G62870.1	AT3G13920.1	AT2G02130.1	AT4G31780.2	AT2G32260.1	AT2G20340.1	
	AT5G08415.1	AT3G49260.1	AT5G61170.1	AT2G32060.3	AT5G17840.1	AT2G22900.1	
	AT5G58420.1	AT2G45960.2	AT5G35200.1	AT5G27390.1	AT1G64230.1	AT5G27850.1	
	AT5G09500.1	AT5G53980.1	AT2G30950.1	AT2G20450.1	AT4G17530.1	AT2G35680.1	
	AT5G11040.1	AT3G49780.1	AT5G58070.1	AT1G55740.1	AT4G27270.1	AT1G75290.1	
	AT1G49760.2	AT5G59400.1	AT2G36170.1	AT4G21510.1	AT4G38040.1	AT3G19050.1	

	AT2G26340.1	AT5G55160.1	AT1G09010.1	AT5G46020.1	AT1G09850.1	AT3G13460.1	
	AT2G37150.3	AT3G27010.1	AT1G70600.1	AT1G70280.2	AT5G50810.1	AT3G49470.1	
	AT1G76410.1	AT4G34040.1	AT5G21080.1	AT5G45775.2	AT5G20060.2	AT2G26570.1	
	AT5G01410.1	AT4G32850.9	AT5G58710.1	AT4G30420.1	AT1G51060.1	AT2G38610.2	
	AT3G53420.2	AT4G14240.1	AT4G17520.1	AT4G33800.1	AT1G34575.1	AT5G26780.1	
	AT5G56760.1	AT5G43260.1	AT1G79810.1	AT2G33150.1	AT3G51620.2	AT5G25900.1	
	AT5G64130.1	AT3G09630.1	AT2G39390.1	AT1G68490.1	AT1G15125.1	AT4G39955.1	
	AT2G01950.1	AT3G04400.1	AT2G17360.2	AT3G60390.1	AT4G18830.1	AT1G72490.1	
	AT1G64230.2	AT3G52740.1	AT1G48600.2	AT1G61680.1	AT4G20260.1	AT5G49660.1	
	AT1G23410.1	AT3G57520.1	AT1G61580.1	AT4G34110.1	AT4G24020.1	AT1G70780.1	
	AT1G74690.1	AT2G34480.1	AT2G02050.1	AT5G51190.1	AT5G64140.1	AT5G32440.3	
	AT1G74720.1	AT4G35270.1	AT3G10090.1	AT1G49470.1	AT1G02860.1	AT5G20350.1	
	AT1G06950.1	AT3G18930.1	AT1G49620.1	AT3G14630.1	AT3G06030.1	AT2G26770.1	
	AT3G26580.1	AT2G27710.4	AT4G33030.1	AT1G32120.1	AT1G07070.1	AT4G09800.1	
	AT1G53025.1	AT2G21300.2	AT1G67710.1	AT2G35290.1	AT1G65820.1	AT1G09200.1	
	AT2G39340.1	AT5G26667.2	AT5G26340.1	AT1G09540.1	AT1G44350.1	AT2G36570.1	
	AT1G54580.1	AT5G25450.1	AT4G29390.1	AT3G28430.1	AT5G20060.3	AT5G56190.2	
	AT3G02550.1	AT1G16120.1	AT2G39220.1	AT1G54410.1	AT3G60450.1	AT4G30210.2	
	AT5G51940.1	AT4G32330.3	AT4G16480.1	AT3G52520.1	AT5G13100.1	AT4G36910.1	
	AT1G79380.1	AT2G40510.1	AT1G15390.1	AT4G14300.1	AT3G60200.1	AT1G48830.2	
	AT1G77510.1	AT2G44970.1	AT5G04810.1	AT1G24510.1	AT2G33845.1	AT4G29840.1	
	AT4G24210.1	AT1G49510.1	AT1G70090.1	AT3G15820.1	AT1G80230.1	AT3G06400.2	
	AT1G72370.1	AT1G31660.1	AT5G53850.2	AT1G28290.1	AT2G18340.1	AT1G33780.1	
	AT4G22970.1	AT2G44610.1	AT2G37210.1	AT5G47750.1	AT1G76710.1	AT4G13250.1	
	AT3G58040.1	AT5G43470.2	AT5G16010.1	AT4G28880.1	AT1G19920.1	AT1G25520.1	
	AT4G02740.1	AT1G75380.2	AT1G07050.1	AT2G47270.1	AT1G66670.1	AT5G47500.1	
	AT2G20190.1	AT1G57860.1	AT3G53340.1	AT1G28440.1	AT3G44540.1	AT1G80710.1	
	AT4G40030.2	AT5G11910.1	AT3G04770.2	AT1G15250.1	AT5G54800.1	AT3G47300.1	
	AT5G25110.1	AT1G51540.1	AT3G16500.1	AT3G11530.1	AT1G67960.1	AT5G27700.1	
	AT4G38580.1	AT1G09530.2	AT1G32928.1	AT5G64530.1	AT1G63120.1	AT2G43970.1	
	AT5G11880.1	AT1G05940.1	AT3G51800.3	AT3G50820.1	AT1G22030.1	AT5G26220.1	
	AT5G40610.1	AT1G60600.2	AT5G47450.1	AT5G10360.1	AT1G26910.1	AT3G04290.1	
	AT4G24700.1	AT1G33240.1	AT2G01850.1	AT1G73670.1	AT1G60990.2	AT2G30070.1	
	AT5G54790.1	AT1G56600.1	AT1G48280.1	AT1G17120.1	AT5G63050.1	AT5G23060.1	
	AT1G44920.1	AT3G54440.1	AT5G49480.1	AT1G15820.1	AT4G15440.1	AT4G08850.1	
	AT2G19170.1	AT1G55265.1	AT5G10870.1	AT3G49950.1	AT3G62550.1	AT2G41380.1	
	AT2G23520.1	AT1G75580.1	AT1G65295.1	AT4G36130.1	AT2G28120.1	AT5G57630.1	
	AT3G49910.1	AT3G06190.1	AT4G21700.1	AT2G29990.1	AT2G34300.1	AT3G61620.2	
	AT3G50830.1	AT4G34670.1	AT2G06040.1	AT2G23620.1	AT3G16090.1	AT2G03440.1	
	AT1G21690.1	AT5G54530.1	AT5G54680.1	AT1G13990.1	AT4G20980.2	AT3G53740.2	
	AT5G03300.1	AT2G17265.1	AT1G51710.1	AT4G19810.1	AT2G16800.1	AT5G06390.1	
	AT4G03400.1	AT4G26260.2	AT2G46280.2	AT5G23740.1	AT1G69440.1	AT3G45980.1	
	AT5G55190.1	AT3G07270.2	AT3G07470.1	AT1G48040.1	AT5G50460.1	AT5G50600.1	
	AT5G63190.2	AT5G17620.1	AT4G40060.1	AT5G17330.1	AT1G29150.1	AT4G36660.1	
	AT4G16450.1	AT2G45700.1	AT5G65430.1	AT1G33140.1	AT5G14450.1	AT2G37250.1	
	AT2G28470.1	AT4G02100.1	AT2G26600.1	AT4G31985.1	AT5G63470.2	AT4G39680.2	
	AT3G62200.1	AT1G11330.2	AT2G34830.1	AT5G54580.1	AT3G21570.1	AT5G67050.1	
	AT1G36240.1	AT1G68070.1	AT4G25540.1	AT4G31340.1	AT2G02570.1	AT5G57190.1	
	AT2G10940.1	AT3G04730.1	AT4G18770.1	AT5G11580.1	AT5G46170.1	AT5G42250.1	
	AT1G08650.1	AT2G32590.1	AT3G29360.2	AT2G36620.1	AT2G43000.1	AT4G35240.2	
	AT3G62840.1	AT1G72410.1	AT2G33570.1	AT2G15680.1	AT4G13420.1	AT5G62865.1	
	AT4G13850.1	AT5G51300.1	AT3G10950.1	AT1G13245.1	AT1G78560.1	AT3G49010.3	
	AT1G48330.1	AT5G57760.1	AT4G04320.1	AT4G22730.1	AT1G75140.1	AT3G05890.1	
	AT3G28460.1	AT1G75350.1	AT4G32400.1	AT1G56050.1	AT5G54170.1	AT1G69760.1	
	AT5G50320.1	AT5G60640.1	AT5G05690.1	AT3G48890.1	AT5G45390.1	AT2G37400.1	
	AT3G45900.1	AT3G18410.1	AT2G25310.1	AT4G17040.1	AT2G26180.1	AT3G08720.1	

	AT2G03810.1	AT5G08130.5	AT4G39090.1	AT1G51130.1	AT1G62640.1	AT3G19570.2	
	AT2G24970.1	AT1G52150.1	AT2G32560.1	AT2G19830.1	AT3G61880.2	AT2G39730.1	
	AT1G48440.1	AT5G39850.1	AT4G29000.1	AT4G00165.2	AT3G62240.1	AT4G39490.1	
	AT4G32850.5 AT4G14900.1 AT3G13980.1 AT4G24820.2 AT1G75500.2 AT1G26480.1						
h	AT2G41140.1	AT4G31240.2	AT1G66430.1	AT2G03200.1	AT5G05850.1	AT5G14740.2	463
	AT5G03280.1	AT2G28260.1	AT2G38550.1	AT5G52830.1	AT5G20720.1	AT3G02750.1	
	AT4G38520.2	AT1G79620.1	AT1G66680.1	AT5G62180.1	AT4G23470.1	AT2G46870.1	
	AT3G27210.1	AT1G14820.3	AT1G54050.1	AT4G08950.1	AT5G17050.1	AT5G01950.1	
	AT1G72970.1	AT5G48450.1	AT3G15030.3	AT3G23940.1	AT5G37570.1	AT3G14940.1	
	AT5G27930.2	AT5G28960.1	AT2G27830.1	AT2G35010.2	AT2G44500.1	AT4G39840.1	
	AT4G32300.1	AT1G55370.2	AT4G33150.3	AT5G65730.1	AT5G24314.1	AT3G27890.1	
	AT3G21240.1	AT2G28320.1	AT5G59020.1	AT3G23390.1	AT5G43080.1	AT4G13010.1	
	AT1G51630.1	AT5G65520.1	AT5G48500.1	AT1G19850.1	AT1G71140.1	AT2G46420.1	
	AT4G39260.3	AT5G08640.2	AT2G19210.1	AT2G20680.1	AT1G70170.1	AT5G35360.1	
	AT2G29970.1	AT2G38060.1	AT5G66330.1	AT1G22470.1	AT2G38040.2	AT4G14440.1	
	AT2G34930.1	AT1G15000.1	AT4G11560.1	AT5G07990.1	AT5G65660.1	AT2G45580.1	
	AT3G20230.1	AT4G27430.2	AT4G18910.1	AT2G38540.1	AT1G21670.1	AT5G25360.1	
	AT1G53300.1	AT4G04450.1	AT3G17611.1	AT3G49800.1	AT3G50910.1	AT4G19380.1	
	AT5G60200.1	AT5G04310.1	AT1G32920.1	AT4G16580.1	AT2G48110.1	AT4G16380.1	
	AT1G12680.1	AT3G59420.1	AT4G28610.1	AT2G02380.1	AT1G09220.1	AT4G30220.1	
	AT1G14290.1	AT2G40200.1	AT5G08350.1	AT3G23830.1	AT1G02180.1	AT5G42210.1	
	AT2G23770.1	AT4G17920.1	AT3G05570.1	AT1G33540.1	AT2G26440.1	AT5G40840.1	
	AT4G19170.1	AT2G30440.1	AT4G14640.1	AT1G28280.1	AT4G10710.1	AT3G08030.1	
	AT3G26040.1	AT1G18250.1	AT1G75890.1	AT5G53588.1	AT1G59960.1	AT5G51920.1	
	AT1G60730.1	AT1G56300.1	AT4G33050.3	AT5G39360.1	AT4G37340.1	AT4G34880.1	
	AT2G37040.1	AT4G39795.1	AT4G36750.1	AT5G58230.1	AT3G08670.1	AT3G20390.1	
	AT5G20250.4	AT4G08500.1	AT5G57685.1	AT5G30510.1	AT3G02720.1	AT1G72430.1	
	AT3G17810.1	AT3G18280.1	AT4G26790.1	AT3G16950.2	AT2G16720.1	AT1G10500.1	
	AT4G34160.1	AT2G47180.1	AT3G46290.1	AT5G55530.3	AT1G52780.1	AT1G70630.1	
	AT4G36760.1	AT3G55760.2	AT2G35980.1	AT2G05620.1	AT4G10500.1	AT5G45910.1	
	AT4G39520.1	AT1G27950.1	AT5G20670.1	AT2G47360.1	AT4G13710.1	AT4G17170.1	
	AT3G05700.1	AT5G66440.1	AT3G06240.1	AT1G11545.1	AT5G50011.1	AT1G16630.1	
	AT5G21482.1	AT2G33400.1	AT1G63260.2	AT5G14930.2	AT5G43850.1	AT5G48910.1	
	AT1G48520.1	AT3G20240.1	AT4G05320.4	AT1G07080.1	AT5G46760.1	AT3G15580.1	
	AT5G52920.1	AT3G03760.1	AT5G11700.2	AT2G38290.1	AT4G21210.1	AT5G14460.1	
	AT3G21760.1	AT4G28250.1	AT1G13360.1	AT5G54540.1	AT3G20860.1	AT4G34050.1	
	AT4G31800.2	AT3G02050.1	AT5G45960.1	AT5G14700.1	AT5G49525.1	AT4G01840.1	
	AT3G22530.1	AT1G13440.1	AT2G40130.2	AT3G11820.2	AT2G02980.1	AT2G04220.1	
	AT3G06650.1	AT2G21710.1	AT1G75420.1	AT2G01300.1	AT5G15900.1	AT3G03960.1	
	AT5G06560.1	AT5G60790.1	AT1G15130.1	AT2G24490.2	AT3G11660.1	AT2G30630.1	
	AT4G23850.1	AT1G68530.1	AT3G51240.1	AT3G07010.1	AT1G29750.2	AT5G19260.1	
	AT1G25270.1	AT3G47520.1	AT2G32030.1	AT2G26730.1	AT4G30920.1	AT4G34320.1	
	AT3G06070.1	AT3G16770.1	AT5G01340.1	AT5G19290.1	AT2G43940.1	AT3G24480.1	
	AT3G62630.1	AT2G34840.1	AT2G41740.1	AT3G53260.1	AT4G00150.1	AT3G61510.1	
	AT4G11280.1	AT3G55990.1	AT1G62280.1	AT2G22590.1	AT1G52200.1	AT5G40780.1	
	AT4G35830.1	AT1G60010.1	AT3G47600.1	AT5G13170.1	AT3G05980.1	AT4G32530.1	
	AT1G75270.1	AT3G01660.1	AT5G12080.1	AT3G19450.1	AT1G71160.1	AT4G06744.1	
	AT4G25960.1	AT1G55020.1	AT2G41430.2	AT3G49550.1	AT2G03880.1	AT4G16600.1	
	AT5G22000.3	AT4G00110.1	AT3G06720.1	AT5G10190.1	AT1G10850.1	AT4G14380.1	
	AT5G56500.1	AT5G05830.1	AT5G64350.1	AT1G24130.1	AT1G64720.1	AT1G12710.1	
	AT3G23730.1	AT2G30980.1	AT2G23070.1	AT2G36840.1	AT2G44050.1	AT5G25930.1	
	AT5G07580.1	AT2G02500.1	AT1G10270.1	AT2G15890.1	AT5G24470.1	AT3G16360.2	
	AT1G47670.1	AT2G36880.2	AT1G63820.1	AT5G19900.1	AT1G17720.1	AT1G51800.1	
	AT3G52880.1	AT4G15630.1	AT4G13180.1	AT4G13830.2	AT1G70370.2	AT2G39710.1	
	AT3G23790.1	AT1G08970.1	AT1G48420.1	AT1G67560.1	AT3G12630.1	AT1G63610.1	
	AT1G30260.1	AT1G25560.1	AT5G38160.1	AT1G26810.1	AT2G39770.1	AT1G13250.1	

	AT3G04870.1	AT1G24735.2	AT1G28360.1	AT4G21200.1	AT5G02770.1	AT4G17500.1	
	AT2G02540.1	AT4G39400.1	AT2G40475.1	AT2G05990.1	AT4G29400.1	AT3G22790.1	
	AT5G66910.1	AT1G72230.1	AT4G08290.1	AT4G04020.1	AT4G11600.1	AT5G14320.1	
	AT1G78955.1	AT1G43710.1	AT3G07940.1	AT1G02205.2	AT1G17840.1	AT5G42890.1	
	AT3G45300.1	AT2G26550.2	AT2G40000.1	AT3G48530.1	AT3G55010.2	AT5G16970.1	
	AT2G20370.1	AT5G42650.1	AT4G02715.1	AT5G15310.1	AT1G17147.1	AT1G09920.1	
	AT4G00355.2	AT1G55270.1	AT1G31420.2	AT5G54600.1	AT1G21910.1	AT4G13360.1	
	AT3G03150.1	AT2G35880.1	AT2G35930.1	AT1G28960.1	AT1G63650.2	AT5G05350.1	
	AT1G28310.2	AT2G38320.1	AT5G46290.1	AT5G55360.1	AT1G31812.1	AT5G23100.1	
	AT5G63980.1	AT2G15290.1	AT5G67400.1	AT1G75380.1	AT5G41315.1	AT5G42146.1	
	AT2G21250.1	AT1G67570.1	AT4G28706.3	AT1G22710.1	AT1G26220.1	AT1G74790.1	
	AT4G36640.1	AT4G20780.1	AT5G17990.1	AT3G52780.1	AT2G16990.2	AT2G26900.1	
	AT1G03475.1	AT1G26830.1	AT2G33390.1	AT2G44870.1	AT1G65730.1	AT3G03550.1	
	AT5G42760.1	AT5G58620.1	AT2G47730.1	AT1G27520.1	AT5G20280.1	AT4G36040.1	
	AT5G48930.1	AT4G26570.1	AT3G01930.2	AT4G17840.1	AT1G20980.1	AT5G39220.1	
	AT4G25260.1	AT3G53180.1	AT1G18470.1	AT5G64667.1	AT3G18670.1	AT4G01870.1	
	AT3G23250.1	AT2G26330.1	AT4G27250.1	AT1G80920.1	AT1G01200.1	AT3G58610.1	
	AT4G00530.1	AT3G13540.1	AT4G35840.1	AT5G08640.1	AT4G27670.1	AT1G76420.1	
	AT1G06980.1	AT2G16600.1	AT5G42750.1	AT1G14900.1	AT3G26100.2	AT2G47590.1	
	AT3G03190.1	AT1G06870.1	AT3G16660.1	AT2G32600.1	AT5G57655.2	AT5G59120.1	
	AT3G62150.1	AT4G23810.1	AT4G15920.1	AT2G05920.1	AT1G78060.1	AT1G72300.1	
	AT5G49890.1	AT3G21090.1	AT3G25860.1	AT5G23670.1	AT5G58600.1	AT5G58920.1	
	AT1G77280.1	AT2G28900.1	AT1G75170.2	AT3G25500.1	AT4G02880.2	AT4G32330.2	
	AT5G20720.2	AT4G21410.1	AT1G25440.1	AT5G14680.1	AT3G29575.3	AT3G07760.1	
	AT1G29700.1	AT1G64160.1	AT2G26700.1	AT1G05805.1	AT4G35300.1	AT1G07220.1	
	AT2G23810.1						
i	AT5G13180.1	AT1G55850.1	AT1G11700.1	AT1G61590.1	AT1G02630.1	AT4G15760.1	12
	AT4G17980.1 AT2G42840.1 AT3G62650.1 AT4G29670.1 AT1G64355.1 AT2G02070.1						
j	AT1G49320.1	AT1G03310.1	AT2G18540.1	AT1G64625.3	AT5G66760.1	AT1G54100.1	16
	AT1G79630.1	AT5G14920.1	AT1G68640.1	AT5G50380.1	AT4G36990.1	AT1G03310.2	
	AT1G52820.1 AT1G70830.3 AT2G02950.1 AT5G59310.1						
k	AT3G15180.2	AT1G20560.1	AT1G09610.1	AT3G10960.1	AT5G10840.1	AT1G52640.1	475
	AT1G55365.1	AT1G10385.1	AT1G71010.1	AT2G16090.1	AT1G21070.1	AT5G09810.1	
	AT3G19000.1	AT1G79690.1	AT4G10955.1	AT3G07150.1	AT5G40240.2	AT3G24420.1	
	AT3G29090.1	AT3G59970.3	AT4G16442.1	AT3G07970.1	AT1G47710.1	AT3G14130.1	
	AT4G02750.1	AT5G05600.1	AT5G51820.1	AT4G34200.1	AT2G28420.1	AT4G28400.1	
	AT3G02420.1	AT2G30310.1	AT1G04430.1	AT5G47635.1	AT1G71695.1	AT3G15730.1	
	AT4G03490.2	AT3G51895.1	AT3G27090.1	AT5G04410.1	AT4G21470.1	AT3G25160.1	
	AT2G26780.1	AT5G67020.1	AT4G35030.3	AT2G36090.1	AT1G33170.1	AT3G05840.2	
	AT4G36650.1	AT4G29190.1	AT2G27290.1	AT5G17920.1	AT4G00730.1	AT1G68830.1	
	AT3G03310.1	AT3G02130.1	AT5G09900.2	AT3G25030.1	AT1G11330.1	AT5G15250.1	
	AT3G22600.1	AT5G42710.1	AT2G28250.2	AT1G65980.1	AT3G49190.1	AT4G00750.1	
	AT2G43870.1	AT5G54960.1	AT5G35160.2	AT3G05530.1	AT2G38905.1	AT1G60890.2	
	AT1G69490.1	AT3G55020.1	AT1G69570.1	AT1G10740.1	AT2G04305.1	AT4G13870.2	
	AT5G48580.1	AT4G08320.1	AT4G24000.1	AT5G13800.1	AT1G56060.1	AT2G17450.1	
	AT1G07650.2	AT2G21120.1	AT3G46530.1	AT1G55310.3	AT5G36290.2	AT4G31130.1	
	AT4G03120.1	AT1G24430.1	AT3G02230.1	AT1G63800.1	AT5G11650.1	AT4G01050.1	
	AT1G14870.1	AT3G12100.1	AT1G80940.1	AT5G50990.1	AT3G23600.1	AT5G41610.1	
	AT2G16030.1	AT2G33620.1	AT5G57345.1	AT2G30520.1	AT1G01580.1	AT1G02500.1	
	AT1G52570.1	AT1G55460.1	AT4G04910.1	AT2G13820.1	AT4G18700.1	AT3G19040.1	
	AT4G13020.4	AT1G74310.1	AT4G29510.1	AT1G70480.2	AT5G52400.1	AT5G18460.1	
	AT5G03560.1	AT2G25140.1	AT5G22460.2	AT5G24930.1	AT2G15980.1	AT5G54260.1	
	AT3G62370.1	AT4G37280.1	AT1G52720.1	AT5G47530.1	AT5G35525.1	AT5G64370.1	
	AT3G61660.1	AT4G23860.2	AT4G28850.1	AT2G29380.1	AT1G11310.1	AT5G14260.1	
	AT3G17080.1	AT2G26980.4	AT1G73850.1	AT2G44260.2	AT3G29240.2	AT4G13480.1	
	AT3G61310.1	AT3G02630.1	AT1G05500.1	AT3G11010.1	AT4G15248.1	AT5G35170.1	

	AT3G57280.1	AT4G34740.1	AT1G62300.1	AT4G17090.1	AT2G35760.1	AT2G25590.1	
	AT4G34610.1	AT4G28300.1	AT4G34000.2	AT4G04930.1	AT5G65290.1	AT1G25370.1	
	AT5G46860.1	AT2G34590.1	AT4G05150.1	AT1G62740.1	AT1G08200.1	AT2G40330.1	
	AT5G62600.1	AT1G64380.1	AT5G13220.1	AT1G11050.1	AT1G68040.1	AT1G23730.1	
	AT5G64460.6	AT4G16520.2	AT5G15450.1	AT1G45249.1	AT5G16000.1	AT3G16230.2	
	AT3G18400.1	AT3G58970.1	AT3G25805.1	AT4G14690.1	AT2G05830.1	AT2G47800.1	
	AT4G28556.1	AT3G62830.1	AT5G01270.2	AT3G13790.1	AT4G21120.1	AT1G23100.1	
	AT3G07090.1	AT5G09880.1	AT5G07475.1	AT3G01470.1	AT3G17240.3	AT2G27980.1	
	AT5G55050.1	AT5G15050.1	AT3G47150.1	AT5G64030.1	AT4G16490.1	AT5G53000.1	
	AT2G28100.1	AT2G04030.1	AT3G53950.1	AT2G41820.1	AT5G14410.1	AT3G19270.1	
	AT2G33310.2	AT1G68220.1	AT2G23690.1	AT4G33300.1	AT5G22140.1	AT5G17520.1	
	AT5G27020.1	AT5G45820.1	AT5G23860.1	AT1G55730.1	AT1G44446.1	AT4G17230.1	
	AT3G56940.1	AT3G15210.1	AT3G46790.1	AT2G20540.1	AT3G11210.1	AT4G04770.1	
	AT1G16950.1	AT5G11420.1	AT4G36650.2	AT3G02870.1	AT2G28200.1	AT3G25640.1	
	AT4G34480.1	AT2G39350.1	AT2G40720.1	AT3G59940.1	AT1G13360.3	AT2G22540.1	
	AT5G39660.2	AT1G69530.1	AT1G03700.1	AT2G01970.1	AT5G60840.1	AT1G66340.1	
	AT4G23030.1	AT4G24620.1	AT4G10200.1	AT3G09470.2	AT5G57490.1	AT2G41010.1	
	AT1G50575.1	AT1G31790.1	AT4G09510.1	AT5G16940.1	AT5G02540.1	AT3G01060.1	
	AT3G43740.1	AT5G52420.1	AT2G31670.1	AT1G25500.2	AT1G71060.1	AT1G25380.1	
	AT3G16510.1	AT3G14310.1	AT2G46050.1	AT4G33170.1	AT4G29990.1	AT2G37620.1	
	AT4G35320.1	AT2G01505.1	AT2G46270.1	AT2G17220.2	AT5G40010.1	AT3G55290.1	
	AT3G26570.2	AT4G04040.1	AT3G17980.1	AT3G12320.1	AT5G14750.1	AT1G64110.3	
	AT5G12210.1	AT3G03990.1	AT5G49970.1	AT5G45630.1	AT5G27410.2	AT1G78860.1	
	AT5G19790.1	AT5G01710.1	AT2G36210.1	AT3G63520.1	AT3G24320.1	AT1G22930.1	
	AT3G16180.1	AT3G56200.1	AT1G07200.2	AT2G30210.1	AT5G41800.1	AT1G18860.1	
	AT2G21600.1	AT4G02040.1	AT5G53160.2	AT5G07350.1	AT1G78310.1	AT2G48030.1	
	AT5G40410.1	AT3G45160.1	AT1G68630.1	AT2G32120.1	AT5G65840.1	AT2G17730.1	
	AT3G24090.1	AT3G01550.1	AT3G24520.1	AT3G05420.2	AT1G61250.1	AT4G10340.1	
	AT3G13560.3	AT4G18530.1	AT3G22104.1	AT4G35260.1	AT2G02990.1	AT1G74460.1	
	AT1G48110.2	AT4G24280.1	AT2G20900.2	AT4G26470.1	AT1G28190.1	AT5G59100.1	
	AT3G03860.1	AT1G03140.1	AT3G43850.1	AT3G13620.1	AT5G06860.1	AT4G27720.1	
	AT1G64700.1	AT1G67440.1	AT5G22060.1	AT5G05820.1	AT3G11430.1	AT4G26490.1	
	AT1G63460.1	AT2G37620.2	AT2G42690.1	AT2G42760.1	AT1G10630.1	AT4G20930.1	
	AT4G00720.1	AT4G05120.1	AT4G36730.1	AT2G33680.1	AT1G58520.1	AT1G02700.1	
	AT1G27290.1	AT5G05340.1	AT5G09430.1	AT5G13700.1	AT5G08790.1	AT4G16130.1	
	AT5G15650.1	AT2G26250.1	AT1G24330.1	AT4G22290.1	AT3G57430.1	AT4G17720.1	
	AT5G64940.2	AT3G11220.1	AT3G62580.1	AT3G49760.1	AT5G21090.1	AT1G47960.1	
	AT3G13062.2	AT4G25210.1	AT5G56310.1	AT1G28260.1	AT2G44880.1	AT3G11670.1	
	AT1G07570.2	AT1G36160.1	AT1G69450.2	AT5G22580.1	AT1G18000.1	AT1G14670.1	
	AT5G47730.1	AT3G11150.1	AT2G17120.1	AT2G26670.1	AT5G50530.1	AT1G66330.1	
	AT5G65670.1	AT4G04470.1	AT5G14540.1	AT4G35780.1	AT5G23670.2	AT5G54270.1	
	AT1G67600.1	AT2G32510.1	AT1G75280.1	AT1G25530.1	AT5G51720.1	AT4G09900.1	
	AT3G25230.1	AT3G05020.1	AT4G26200.1	AT3G27960.1	AT5G50360.1	AT3G61470.1	
	AT3G07080.1	AT3G48660.1	AT5G17300.1	AT2G18660.1	AT1G16770.1	AT3G52050.3	
	AT5G62890.1	AT1G24530.1	AT5G52190.1	AT2G46830.2	AT5G20380.1	AT1G78960.1	
	AT1G69850.1	AT5G07220.1	AT5G49690.1	AT2G27690.1	AT2G15530.4	AT5G60910.1	
	AT5G22010.1	AT5G62680.1	AT3G61610.1	AT5G63290.1	AT2G29090.1	AT3G49720.1	
	AT2G45440.1	AT2G32120.2	AT1G68080.3	AT3G12060.1	AT5G16400.1	AT5G16860.1	
	AT1G57680.2	AT1G72030.1	AT1G53280.1	AT2G41250.1	AT5G36930.1	AT5G21222.1	
	AT4G32060.1	AT5G19530.1	AT5G10930.1	AT2G17630.1	AT3G11760.1	AT1G20780.1	
	AT5G47560.1	AT5G09520.1	AT1G08510.1	AT2G44530.2	AT3G60340.1	AT1G18330.2	
	AT3G08840.2	AT4G09320.1	AT2G48020.1	AT4G39230.1	AT5G13630.1	AT5G50120.1	
	AT4G21790.1	AT5G23240.1	AT1G63380.2	AT2G33735.1	AT4G03560.1	AT3G01120.1	
	AT3G48520.1	AT1G52340.1	AT3G47780.1	AT1G70670.1	AT5G64940.1	AT4G02610.1	
	AT1G01120.1						

I	AT1G17860.1	AT1G27850.1	AT3G22480.1	AT1G67830.1	AT1G68010.1	AT3G01490.1	2013
	AT3G22370.1	AT4G39200.1	AT1G13330.1	AT5G04830.1	AT3G12090.1	AT1G25260.1	
	AT3G08790.1	AT5G45870.1	AT1G49760.1	AT4G24730.1	AT4G12970.1	AT1G29370.1	
	AT4G23330.2	AT1G56200.1	AT4G37130.1	AT5G22640.1	AT3G45970.1	AT5G46750.1	
	AT4G12680.1	AT1G65590.1	AT1G14620.1	AT3G16850.1	AT2G42620.1	AT5G53380.1	
	AT1G09210.1	AT1G70820.1	AT5G47080.1	AT3G04340.1	AT2G32500.1	AT1G11080.2	
	AT1G03350.1	AT1G68590.1	AT1G22770.1	AT2G13290.1	AT5G47230.1	AT2G01660.1	
	AT5G04950.1	AT5G54910.1	AT2G03620.2	AT3G13224.2	AT2G38040.1	AT4G17440.2	
	AT3G57000.1	AT5G35460.1	AT5G47780.1	AT2G02470.1	AT2G35190.1	AT5G22120.1	
	AT5G59250.1	AT3G52150.2	AT5G52580.1	AT4G35930.1	AT4G25310.1	AT5G16110.1	
	AT1G65660.1	AT2G25430.1	AT2G24490.1	AT4G31320.1	AT3G59510.1	ATCG00150.1	
	AT1G18170.1	AT1G78530.1	AT5G08500.1	AT1G52770.1	AT2G37790.1	AT5G20370.1	
	AT5G01320.1	AT1G65770.1	AT5G54510.1	AT2G47880.1	AT4G21310.1	AT4G37630.2	
	AT3G18110.1	AT4G38890.1	AT4G02600.2	AT5G40340.1	AT5G36970.1	AT1G56020.1	
	AT5G61350.1	AT2G03120.1	AT3G61530.2	AT2G41680.1	AT2G13840.1	AT5G12180.1	
	AT1G07890.8	AT1G11680.1	AT5G51330.1	AT1G70890.1	AT4G24380.1	AT5G10440.1	
	AT1G11125.1	AT5G60740.1	AT1G78570.1	AT3G48200.1	AT1G26760.1	AT3G27950.1	
	AT1G18140.1	AT4G31590.1	AT1G23890.2	AT1G22050.1	AT2G05310.1	AT4G39370.3	
	AT1G56570.1	AT3G52110.2	AT5G24500.1	AT4G03080.1	AT1G29350.1	AT1G76310.1	
	AT2G25080.1	AT4G21920.1	AT4G24265.1	AT5G43600.1	AT2G36330.1	AT3G52170.1	
	AT4G12440.2	AT1G61415.2	AT4G24690.1	AT1G29070.1	AT1G14860.1	AT4G00755.2	
	AT2G21340.1	AT4G18340.1	AT3G19720.1	AT3G63130.2	AT5G01530.1	AT5G43960.1	
	AT3G13110.1	AT1G72210.1	AT2G30570.1	AT4G24780.2	AT1G15910.1	AT5G59190.1	
	AT3G14860.2	AT2G02220.1	AT4G28950.1	AT1G19080.1	AT5G15380.1	AT3G02580.1	
	AT5G59360.1	AT3G50780.1	AT1G80560.1	AT1G54220.2	AT2G29900.1	AT1G44960.1	
	AT4G14465.1	AT4G36810.1	AT1G71530.1	AT2G38600.1	AT1G11530.1	AT1G43790.1	
	AT5G52210.1	AT3G27640.1	AT5G23870.3	AT3G05910.1	AT5G41850.1	AT1G34190.1	
	AT5G46700.1	AT3G16800.2	AT5G09550.1	AT3G45650.1	AT1G19840.1	AT1G13290.1	
	AT4G20060.1	AT3G05560.3	AT2G29740.1	AT4G23460.1	AT3G12040.1	AT4G05160.1	
	AT1G08860.1	AT1G75380.3	AT1G27730.1	AT3G30390.2	AT4G34660.1	AT1G68800.1	
	AT1G02150.1	AT5G23040.1	AT4G22120.4	AT2G06520.1	AT5G59510.1	AT4G31450.1	
	AT2G40180.1	AT5G60930.1	AT5G47470.1	AT3G27100.1	AT2G44830.1	AT3G06860.1	
	AT5G11680.1	AT5G47030.1	AT3G24570.1	AT5G40645.1	AT2G26520.1	AT4G35020.1	
	AT1G56220.1	AT3G56160.1	AT5G65205.1	AT3G17170.1	AT5G60850.1	AT1G22140.1	
	AT1G74670.1	AT2G36680.1	AT5G18570.1	AT2G30620.1	AT1G51440.1	AT2G02910.1	
	AT4G28100.1	AT2G14900.1	AT5G11510.1	AT4G33910.1	AT1G01710.1	AT4G23540.1	
	AT3G54210.1	AT4G10120.2	AT2G25940.1	AT5G22000.1	AT2G46810.1	AT4G29720.1	
	AT1G12980.1	AT3G03770.2	AT3G24660.1	AT1G06150.1	AT3G52500.1	AT3G62720.1	
	AT5G01970.1	AT5G10270.1	AT5G23390.1	AT4G27745.1	AT1G48910.1	AT1G78680.1	
	AT3G26120.1	AT3G05510.1	AT4G01100.1	AT5G51010.1	AT2G25680.1	AT1G13700.1	
	AT1G30330.1	AT5G54690.1	AT2G35390.2	AT2G04160.1	AT2G42280.1	AT3G16730.1	
	AT5G57360.1	AT4G15240.1	AT1G23040.1	AT1G51200.3	AT1G61050.1	AT3G59030.1	
	AT5G37780.2	AT3G01810.3	AT2G16530.1	AT2G42940.1	AT1G54320.1	AT1G04520.1	
	AT1G49520.1	AT2G37585.1	AT5G58610.1	AT2G26140.1	AT5G46390.2	AT5G43270.2	
	AT4G34490.1	AT5G53210.1	AT1G21500.1	AT4G13650.1	AT2G04845.1	AT5G58020.1	
	AT1G26550.1	AT2G01210.1	AT4G02725.1	AT4G24120.1	AT4G12290.1	AT4G17905.1	
	AT1G10840.1	AT5G28750.1	AT5G04660.1	AT1G29390.1	AT5G50610.1	AT5G65640.1	
	AT1G03130.1	AT4G05030.1	AT1G04330.1	AT5G53860.2	AT2G06925.1	AT3G62830.2	
	AT2G43020.1	AT4G04960.1	AT3G26980.1	AT2G03150.1	AT5G39380.1	AT4G36000.1	
	AT3G54620.1	AT1G10910.1	AT4G20090.1	AT4G15430.1	AT5G13520.1	AT2G38400.1	
	AT3G05030.1	AT2G43990.1	AT2G21280.1	AT1G34640.1	AT2G20230.1	AT4G40010.1	
	AT1G18640.2	AT1G74970.1	AT1G51745.1	AT3G20190.1	AT1G27500.1	AT4G28760.1	
	AT2G15490.3	AT3G50870.1	AT5G03650.1	AT5G02950.1	AT1G52760.1	AT5G23400.1	
	AT4G15563.1	AT1G77580.2	AT5G62220.1	AT5G58060.1	AT1G04360.1	AT5G47720.2	
	AT5G07720.1	AT3G48700.1	AT1G12740.1	AT5G15240.1	AT4G27130.1	AT5G23810.1	
	AT5G65220.1	AT2G14095.1	AT5G03170.1	AT3G49810.1	AT5G21910.1	AT5G65700.1	

	AT2G42910.1	AT5G06290.1	AT4G36390.1	AT5G25310.1	AT2G45630.2	AT5G43180.1	
	AT5G45380.1	AT1G66150.1	AT5G18630.1	AT3G09830.1	AT1G73880.1	AT2G39840.1	
	AT5G24910.1	AT4G13030.1	AT1G54610.2	AT4G10770.1	AT1G32490.1	AT3G49290.1	
	AT5G04960.1	AT1G20225.1	AT3G23280.2	AT3G54700.1	AT1G24405.1	AT2G18670.1	
	AT2G17350.1	AT1G05070.1	AT1G02640.1	AT4G23690.1	AT2G40480.1	AT2G40860.1	
	AT4G24220.1	AT5G03870.1	AT3G59440.1	AT3G51710.1	AT3G04710.3	AT5G46150.1	
	AT1G53885.1	AT1G79610.1	AT1G06730.1	AT3G56590.1	AT1G79800.1	AT5G67460.1	
	AT3G23490.1	AT5G27400.1	AT3G55040.1	AT5G64380.1	AT1G79050.1	AT1G49710.1	
	AT5G19160.1	AT1G09740.1	AT4G02790.1	AT5G18940.1	AT5G43500.2	AT2G33860.1	
	AT4G22120.3	AT3G09280.1	AT4G01690.1	AT5G04620.2	AT2G20860.1	AT1G75300.1	
	AT1G21830.1	AT3G07350.1	AT1G32440.1	AT5G55220.1	AT5G01750.2	AT4G27840.1	
	AT1G09070.1	AT4G17300.1	AT3G13227.1	AT4G26100.1	AT1G63500.1	AT1G08280.1	
	AT2G31840.1	AT1G54180.2	AT5G60370.1	AT1G50200.1	AT1G54220.1	AT1G20020.1	
	AT3G21215.1	AT5G52290.1	AT1G11870.2	AT5G50010.1	AT2G44640.1	AT5G42480.1	
	AT3G17560.1	AT3G46740.1	AT1G51450.1	AT3G58680.1	AT3G50940.1	AT4G39870.2	
	AT2G39630.1	AT5G28040.1	AT3G25100.1	AT4G11740.1	AT1G51520.1	AT5G11950.1	
	AT4G07960.1	AT4G17380.1	AT1G23750.1	AT2G42380.2	AT5G42700.1	AT3G51830.1	
	AT1G11112.1	AT5G13710.2	AT3G24160.1	AT2G33670.1	AT1G75450.1	AT2G47840.1	
	AT5G17010.1	AT4G31850.1	AT1G72710.1	AT1G18500.1	AT3G08570.1	AT3G57990.1	
	AT4G38070.1	AT5G05930.1	AT4G29210.1	AT5G11550.1	AT1G32200.1	AT3G61530.1	
	AT5G63660.1	AT2G45340.1	AT2G47820.2	AT3G27550.1	AT2G27460.1	AT4G38130.1	
	AT3G06880.2	AT3G62910.1	AT5G65250.1	AT5G40500.2	AT4G22756.1	AT5G57960.1	
	AT4G38800.1	AT2G31810.1	AT5G08400.2	AT1G71090.1	AT4G33480.1	AT4G29830.1	
	AT5G08770.1	AT5G16490.1	AT1G07480.2	AT3G27200.1	AT1G76870.1	AT5G44210.1	
	AT1G68810.1	AT5G55860.1	AT2G26790.1	AT4G16820.1	AT5G08540.1	AT4G25800.2	
	AT4G24680.1	AT3G61260.1	AT5G50250.1	AT5G56030.2	AT2G47580.1	AT5G01090.1	
	AT1G62710.1	AT5G16810.1	AT3G52180.1	AT2G46220.1	AT1G64390.1	AT5G19750.1	
	AT1G73020.1	AT3G23610.3	AT1G23965.1	AT2G31040.1	AT5G38530.1	AT2G37570.1	
	AT5G64270.1	AT2G22360.1	AT1G76065.1	AT3G57080.1	AT4G32890.1	AT1G11600.1	
	AT5G09280.1	AT2G20300.1	AT5G38260.1	AT3G06930.1	AT1G08520.1	AT1G19715.3	
	AT2G03420.1	AT4G33350.1	AT1G32500.1	AT3G17940.1	AT3G13410.1	AT1G19980.1	
	AT3G14870.3	AT1G30810.2	AT5G50375.1	AT3G06260.1	AT3G14080.2	AT4G33950.1	
	AT2G41060.2	AT3G15680.1	AT1G55550.1	AT2G23150.1	AT2G47790.1	AT4G03390.1	
	AT5G48960.1	AT1G67340.1	AT1G76890.2	AT1G16820.1	AT5G65490.1	AT5G25940.1	
	AT3G14160.1	AT2G24070.2	AT4G02590.1	AT5G59130.2	AT2G17710.1	AT5G56260.1	
	AT1G23170.2	AT4G00210.1	AT5G07960.1	AT4G20380.7	AT1G02070.1	AT1G80360.1	
	AT2G31880.1	AT3G49940.1	AT5G43400.1	AT1G56700.1	AT5G40990.1	AT4G22810.1	
	AT3G16785.1	AT1G80600.1	AT5G16620.1	AT3G19660.1	AT5G58560.1	AT3G27027.1	
	AT2G26660.1	AT4G12560.1	AT5G28060.1	AT5G53490.1	AT3G20898.1	AT3G27730.1	
	AT2G45290.1	AT5G10790.1	AT5G56040.2	AT1G26670.1	AT1G17455.2	AT5G14890.1	
	AT4G35750.1	AT4G21520.1	AT2G27040.2	AT4G24330.1	AT4G18270.1	AT2G06530.1	
	AT5G66770.1	AT5G62050.1	AT2G05710.1	AT3G47550.6	AT5G56690.1	AT1G07670.1	
	AT4G24880.1	AT4G10140.1	AT1G06660.1	AT1G62670.1	AT1G30100.1	AT5G04885.1	
	AT5G01910.1	AT5G11890.1	AT2G27660.1	AT3G48730.1	AT4G22240.1	AT4G07990.1	
	AT3G42050.1	AT3G27750.1	AT5G06710.1	AT5G14780.1	AT4G12560.2	AT2G44190.1	
	AT5G08520.1	AT3G06580.1	AT3G14350.1	AT5G01020.1	AT3G58100.1	AT5G44030.1	
	AT2G13810.1	AT3G15880.2	AT1G26850.2	AT4G32700.2	AT3G11830.1	AT1G07250.1	
	AT3G20830.1	AT2G01900.1	AT4G18780.1	AT2G41835.1	AT4G21540.1	AT1G74780.1	
	AT2G47390.1	AT4G12800.1	AT3G19300.1	AT2G46080.1	AT4G14320.1	AT1G72670.1	
	AT1G69200.1	AT1G08080.1	AT5G58490.1	AT3G28715.1	AT1G06340.1	AT1G54290.1	
	AT2G40410.2	AT5G42300.1	AT5G50900.1	AT4G30810.1	AT1G30210.1	AT1G51560.1	
	AT5G16710.1	AT1G07850.1	AT3G12680.1	AT1G56580.1	AT3G49750.1	ATCG00130.1	
	AT3G56910.1	AT1G04410.1	AT1G21010.1	AT5G57870.1	AT2G47460.1	AT3G13080.1	
	AT1G18450.1	AT2G42200.1	AT5G55090.1	AT1G07520.1	AT5G52960.1	AT1G08600.4	
	AT2G28315.1	AT4G27680.1	AT3G48140.1	AT2G42790.1	AT5G24690.1	AT5G39030.1	
	AT1G48030.1	AT3G22070.1	AT4G32590.1	AT4G14720.1	AT1G78390.1	AT5G35770.1	

	AT4G10760.1	AT2G30200.1	AT3G15410.1	AT5G48270.1	AT4G36010.2	AT5G51150.1	
	AT5G65760.1	AT1G61680.2	AT5G19875.1	AT3G20050.1	AT3G55550.1	AT5G44500.2	
	AT1G62390.1	AT3G61550.1	AT3G04760.1	AT3G17120.2	AT2G14520.1	AT5G58630.1	
	AT1G79780.1	AT3G17040.1	AT5G58440.1	AT4G18030.1	AT2G01140.1	AT4G25230.1	
	AT1G79840.1	AT1G72470.1	AT1G69210.1	AT1G25580.1	AT3G18550.2	AT1G52320.2	
	AT5G48170.1	AT4G15510.1	AT4G19120.1	AT2G13620.1	AT5G42600.1	AT2G33800.1	
	AT2G24580.1	AT4G34150.1	AT3G61220.2	AT1G12064.1	AT2G36130.1	AT4G34410.1	
	AT1G70460.1	AT1G49540.1	AT1G69580.2	AT1G05870.2	AT5G03450.1	AT3G10620.1	
	AT5G47000.1	AT4G24970.1	AT1G04970.1	AT5G09360.1	AT2G28105.1	AT5G65920.1	
	AT4G35000.1	AT2G46560.1	AT4G18460.1	AT5G03990.1	AT4G34830.1	AT2G38610.1	
	AT4G27030.1	AT5G13510.1	AT5G45290.1	AT5G04700.1	AT4G20430.1	AT5G42380.1	
	AT1G45207.2	AT1G54570.1	AT3G01560.1	AT5G55510.1	AT4G35410.2	AT1G04830.1	
	AT2G40650.1	AT4G04900.1	AT5G19390.3	AT3G01720.1	AT2G33260.1	AT2G15580.1	
	AT4G23140.1	AT3G14770.1	AT5G43870.1	AT5G12900.1	AT5G60020.1	AT1G16916.1	
	AT2G27970.1	AT4G05460.1	AT2G47810.1	ATCG00720.1	AT1G09290.1	AT5G37630.1	
	AT5G46840.1	AT3G45310.1	AT2G15820.1	AT3G50845.1	AT3G25717.1	AT3G21550.1	
	AT5G23420.1	AT3G10405.1	AT2G19740.1	AT3G07410.1	AT3G26180.2	AT2G07715.1	
	AT3G05510.2	AT1G06190.1	AT1G67510.1	AT1G17160.1	AT2G36850.1	AT2G35230.1	
	AT5G56630.1	AT3G60670.1	AT5G39940.1	AT3G17930.1	AT3G05520.2	AT4G35140.1	
	AT5G05000.3	AT1G71000.1	AT1G02850.2	AT4G30410.1	AT5G37020.1	AT2G32940.1	
	AT5G59090.1	AT4G19020.1	AT2G29670.1	AT4G25910.1	AT3G53160.1	AT5G61280.1	
	AT3G11050.1	AT1G72160.1	AT2G35470.1	AT5G41330.1	AT2G22480.1	AT2G39130.1	
	AT3G62190.1	AT5G13400.1	AT3G28510.1	AT3G14390.1	AT3G48160.2	AT1G54385.2	
	AT3G19210.1	AT1G80310.1	AT1G45230.1	AT4G27090.1	AT4G37480.1	AT2G45850.2	
	AT3G06980.1	AT5G28050.1	AT1G05310.1	AT1G26330.2	AT1G28110.2	AT5G16080.1	
	AT5G58760.1	AT1G71190.1	AT4G32030.1	AT2G23740.2	AT1G07320.1	AT4G19003.1	
	AT3G15760.1	AT3G07370.1	AT4G02840.1	AT1G14150.1	AT4G16710.1	AT1G32550.1	
	AT3G19990.1	AT5G54490.1	AT5G58940.1	AT4G33540.1	AT5G13190.1	AT4G33865.1	
	AT5G56540.1	AT1G08170.1	AT3G21300.1	AT5G63090.1	AT2G02160.1	AT3G47450.2	
	AT3G26410.1	AT5G14050.1	AT1G05270.1	AT1G79340.1	AT5G62410.1	AT2G26870.1	
	AT3G28860.1	AT1G30090.1	AT3G18040.1	AT2G30970.2	AT1G67120.1	AT2G15325.1	
	ATCG00470.1	AT4G14385.1	ATCG00140.1	AT2G25290.1	AT2G21350.1	AT5G64580.1	
	AT2G17760.1	AT3G24500.1	AT1G08840.2	AT1G10950.1	AT5G67090.1	AT4G38090.1	
	AT3G52380.1	AT1G72100.1	AT2G46420.2	AT1G05420.1	AT3G50560.1	AT2G22690.1	
	AT5G50740.3	AT5G53920.1	AT1G76250.1	AT1G04120.1	AT3G48260.1	AT1G10070.2	
	AT1G29200.2	AT1G14810.1	AT2G01130.1	AT3G04720.1	AT1G34380.2	AT3G42630.1	
	AT5G10290.1	AT2G22660.2	AT3G63490.1	AT4G02080.1	AT3G03130.1	AT4G26550.1	
	AT5G57140.1	AT3G21200.1	AT5G66390.1	AT5G22470.1	AT2G07050.1	AT5G66840.1	
	AT5G13080.1	AT5G51100.1	AT5G03610.1	AT4G16440.1	AT1G31800.1	AT5G53620.1	
	AT3G02660.1	AT5G54250.2	AT1G71210.1	AT2G40430.1	AT5G10745.1	AT4G36740.1	
	AT2G01940.1	AT5G56580.1	AT1G52160.1	AT5G40740.1	AT5G23690.1	AT1G55350.4	
	AT3G60130.1	AT1G18790.1	AT3G16370.1	AT4G26140.1	AT4G22150.1	AT3G04030.3	
	AT4G37810.1	AT1G33100.1	AT3G08680.1	AT5G58530.1	AT5G50400.1	AT4G08350.1	
	AT2G14255.1	AT5G48385.1	AT1G55205.1	AT5G43900.3	AT3G58140.1	AT3G55000.1	
	AT1G35720.1	AT4G22120.1	AT4G29310.1	AT1G03160.1	AT1G60160.1	AT1G21730.1	
	AT3G24590.1	AT1G10522.1	AT1G22990.1	AT3G47990.1	AT2G16050.1	AT3G48690.1	
	AT5G33280.1	AT2G37050.3	AT4G01130.1	AT5G57690.1	AT1G48480.1	AT3G14240.1	
	AT4G23440.1	AT1G32240.1	AT3G25070.1	AT5G15210.1	AT1G32100.1	AT2G46225.3	
	AT2G40840.1	AT3G04310.1	AT2G33420.1	AT1G09800.1	AT2G39430.1	AT1G20350.1	
	AT2G16850.1	AT2G13440.1	AT5G23950.1	AT2G01590.1	AT4G33110.2	AT3G10650.1	
	AT3G58730.1	AT2G13610.1	AT5G39785.1	AT5G03460.1	AT1G28070.1	AT1G23220.1	
	AT2G24090.1	AT1G07360.1	AT5G17920.2	AT4G21300.1	AT2G28085.1	AT2G01100.2	
	AT4G25980.1	AT5G65930.2	AT5G65925.1	AT2G44910.1	AT1G76340.1	AT3G08890.2	
	AT3G15610.1	AT1G25340.1	AT5G26742.2	AT2G19810.1	AT3G18380.1	AT5G13890.3	
	AT5G18600.1	AT1G32990.1	AT5G62550.1	AT1G69040.2	AT1G74960.2	AT1G02400.1	
	AT4G23060.1	AT1G73920.1	AT3G28180.1	AT1G74390.1	AT1G73530.1	AT3G28345.1	

	AT4G19230.1	AT5G17650.1	AT1G11290.1	AT1G56190.1	AT5G07040.1	AT1G17410.1	
	AT1G32360.1	AT2G41990.1	AT5G01075.1	AT5G57000.2	AT3G57670.1	AT5G42090.1	
	AT1G53050.1	AT2G36050.1	AT4G18640.1	AT2G21110.1	AT3G24050.1	AT1G17180.1	
	AT5G55970.1	ATCG00220.1	AT2G47900.3	AT5G12130.1	AT3G57240.1	AT2G25220.1	
	AT5G17630.1	AT4G08170.2	AT2G16390.1	AT1G76160.1	AT5G16630.2	AT3G07510.2	
	AT5G43190.1	AT4G32270.1	AT3G44850.1	AT1G60710.1	AT2G34460.1	AT5G02420.1	
	AT5G08680.1	AT2G04360.1	AT1G22870.1	AT3G01980.3	AT5G04820.1	AT1G21360.1	
	AT1G49770.1	AT2G23840.1	AT4G18170.1	AT5G11930.1	AT5G16730.1	AT1G06920.1	
	AT4G20360.1	AT3G47670.1	AT1G72040.1	AT2G32230.1	AT1G45170.1	AT5G16420.1	
	AT2G35490.1	AT3G05070.1	AT3G20930.1	AT2G34585.1	AT2G28800.1	AT5G57590.1	
	AT2G46500.1	AT2G21890.1	AT2G46860.1	AT3G20540.2	AT3G58180.1	AT2G39370.1	
	AT5G42180.1	AT1G27200.1	AT2G06025.1	AT1G19520.1	AT1G79080.1	AT1G69420.1	
	AT3G59110.1	AT4G30410.2	AT3G12670.1	AT5G27440.1	AT5G55830.1	AT1G32470.1	
	AT2G36740.1	AT2G26260.1	AT3G53750.1	AT5G24760.1	AT3G04880.1	AT5G64320.1	
	AT4G24660.1	AT4G16835.1	AT1G74320.1	AT3G61870.1	AT5G17780.1	AT3G25920.1	
	AT5G62890.3	AT3G11590.1	AT5G08420.1	AT5G51260.1	AT3G09070.1	AT5G27330.1	
	AT5G19090.1	AT5G48120.1	AT5G08180.2	AT3G54900.1	AT4G25070.2	AT3G56080.1	
	AT1G34580.1	AT2G23780.1	AT1G05000.1	AT5G48150.2	AT2G24550.1	AT5G15330.1	
	AT1G30755.1	AT1G05190.1	AT5G08050.1	AT1G21090.1	AT3G09860.1	AT5G08380.1	
	AT5G54855.1	AT4G22360.1	AT4G16520.1	AT1G53570.4	AT2G28740.1	AT5G22400.1	
	AT3G27060.1	AT4G05400.2	AT1G20640.1	AT5G57860.3	AT1G28530.2	AT1G75880.2	
	AT2G41020.1	AT1G68710.1	AT3G19590.1	AT2G05790.1	AT1G19790.2	AT2G20562.1	
	AT2G37860.3	AT4G31170.1	AT1G07230.1	AT3G61250.1	AT1G55120.1	AT2G19440.1	
	AT3G56850.1	AT1G10510.1	AT2G39470.1	AT1G65520.1	AT3G51890.1	AT5G15630.1	
	AT1G29980.1	AT3G60245.1	AT5G40760.1	AT4G00090.1	AT2G45650.1	AT1G68750.1	
	AT3G56500.1	AT1G73010.1	AT1G61170.1	AT5G14090.1	AT1G33250.1	AT4G15090.1	
	AT2G25605.1	AT4G16790.1	AT4G21960.1	AT1G63680.1	AT1G18260.1	AT3G63140.1	
	AT3G04380.1	AT4G10030.1	AT5G10350.1	AT3G61200.1	AT4G35550.1	AT4G38900.2	
	AT2G23060.1	AT5G61210.1	AT1G30330.2	AT1G11240.1	AT5G14270.2	AT2G39930.1	
	AT3G06778.1	AT1G19330.2	AT4G25770.1	AT5G48760.1	AT1G74520.1	AT5G64050.1	
	AT2G28400.1	AT5G15510.2	AT3G63110.1	AT3G14930.2	AT1G29900.1	AT1G57770.1	
	AT3G14050.1	AT5G47240.1	AT1G69510.2	AT1G15550.1	AT3G20680.1	AT5G20650.1	
	AT4G03510.2	AT5G59980.2	AT1G76510.1	AT2G45470.1	AT5G22830.1	AT5G22950.1	
	AT5G26800.1	ATCG00340.1	AT3G18420.1	AT4G33220.1	AT4G36870.1	AT1G01650.1	
	AT1G18580.1	AT4G00990.1	AT3G53990.1	AT5G07120.1	AT5G14910.1	AT5G63135.1	
	AT4G32390.1	AT1G68580.2	AT1G51690.1	AT3G18660.2	AT4G37980.1	AT1G12760.1	
	AT4G39952.1	AT1G65840.1	AT4G01037.1	AT2G38790.1	AT1G07040.1	AT4G04670.1	
	AT4G21445.1	AT4G28210.1	AT1G26270.1	AT1G24625.1	AT5G50710.1	AT1G08720.1	
	AT5G54130.2	AT1G63930.1	AT1G07890.5	AT4G32760.2	AT3G45660.1	AT2G04530.1	
	AT3G20600.1	AT2G39780.2	AT1G03470.2	AT1G64760.2	AT4G28365.1	AT5G16630.1	
	AT1G70610.1	AT2G40435.1	AT1G32330.1	AT1G17880.1	AT1G36990.1	AT2G24300.2	
	ATCG00020.1	AT5G05930.2	AT3G14900.1	AT5G10750.1	AT4G31820.1	AT1G05385.1	
	AT1G71780.1	AT4G18010.2	AT1G08600.2	AT1G17730.1	AT2G28680.1	AT3G51390.1	
	AT5G40640.1	AT1G06800.1	AT1G67350.1	AT5G17280.1	AT1G50000.1	AT5G40460.1	
	AT5G45860.1	AT3G62950.1	AT5G26680.2	AT1G22960.1	AT5G09260.1	AT5G05520.1	
	AT3G51430.1	AT1G14730.1	AT4G22330.1	AT4G37740.1	AT5G13650.1	AT3G48000.1	
	AT3G19020.1	AT2G41200.1	AT3G54500.1	AT1G06020.1	AT4G15890.1	AT1G53250.1	
	AT2G20000.1	AT1G30470.1	AT5G59010.1	AT5G24430.1	AT1G24610.1	AT2G41950.1	
	AT3G57040.1	AT4G28700.1	AT5G49470.3	AT5G05365.1	AT5G19620.1	AT2G25270.1	
	AT5G17210.1	AT1G73030.1	AT3G63200.1	AT3G60720.1	AT1G25510.1	AT1G01610.1	
	AT4G33360.1	AT5G23980.1	AT1G27920.1	AT5G56120.1	AT3G15620.1	AT5G61930.2	
	AT5G17060.1	AT4G02620.1	AT2G47710.1	AT5G10240.1	AT1G71500.1	AT1G77860.1	
	AT3G09920.2	AT4G18160.1	AT4G11450.1	AT3G57610.1	AT4G14965.1	AT3G61490.1	
	AT1G71890.1	AT5G19850.1	AT3G28040.1	AT5G59160.3	AT5G03680.1	AT1G79120.1	
	AT1G02820.1	AT1G12020.1	AT1G07480.1	AT1G72220.1	AT3G26020.1	AT1G02920.1	
	AT1G48950.1	AT2G43945.1	AT5G59750.2	AT1G69310.1	AT2G01440.1	AT4G09160.1	

	AT3G20770.1	AT3G02780.1	AT1G55910.1	AT4G17790.1	AT5G27600.1	AT4G39280.2	
	AT3G24180.2	AT4G13560.1	AT2G13360.2	AT5G08550.1	AT1G62050.1	AT1G70840.1	
	AT5G67570.1	AT2G28671.1	AT2G26840.1	AT4G28000.1	AT2G07170.1	AT5G38200.1	
	AT4G15110.1	AT2G41350.1	AT5G42765.1	AT1G02380.1	AT3G24450.1	AT4G24940.1	
	AT1G52540.1	AT5G41780.1	AT2G41040.1	AT4G38140.1	AT5G60870.1	AT2G27810.1	
	AT4G37890.2	AT5G52390.1	AT1G05440.1	AT4G22690.1	AT1G08500.1	AT3G23150.1	
	AT4G28840.1	AT1G67540.2	AT5G20680.3	AT3G26710.1	AT1G03900.1	AT2G37480.1	
	AT5G57800.1	AT4G31510.1	AT3G45070.1	AT3G05710.2	AT2G47485.1	AT5G62230.1	
	AT5G17910.1	AT1G08090.1	AT4G30850.2	AT1G62040.2	AT3G59340.1	AT1G01490.1	
	AT3G19760.1	AT4G39130.1	AT2G27775.1	AT5G67150.1	AT3G04550.1	AT1G32910.1	
	AT5G15230.1	AT3G13490.1	AT1G23280.1	AT5G03540.1	AT1G64510.1	AT1G65720.1	
	AT3G49500.1	AT2G17410.1	AT2G45680.1	AT1G55840.1	AT1G61550.1	AT2G17240.1	
	AT2G35612.1	AT5G05070.1	AT2G17570.1	AT3G05470.1	AT3G13130.1	AT3G05625.1	
	AT4G30400.1	AT1G10210.1	AT5G02370.1	AT3G58720.2	AT5G20850.1	AT1G19210.1	
	AT5G24710.1	AT4G28030.1	AT3G24180.1	AT1G51940.1	AT5G23760.1	AT1G60490.1	
	AT5G06800.1	AT5G64390.3	AT5G18930.1	AT3G10130.1	AT1G17270.1	AT3G02640.1	
	AT3G15090.1	AT4G03130.1	AT5G62390.1	AT3G44380.1	AT5G03740.1	AT2G40880.1	
	AT2G18245.1	AT4G37540.1	AT2G18220.1	AT1G67360.2	AT4G27070.1	AT5G47910.1	
	AT5G20110.1	AT2G43290.1	AT5G04050.1	AT1G29160.1	AT1G75810.1	AT4G09680.1	
	AT4G35220.1	AT2G38480.1	AT1G24764.1	AT3G03680.1	AT1G09020.1	AT1G11090.1	
	AT5G65720.1	AT1G50240.2	AT5G03810.1	AT1G78790.1	AT2G15430.1	AT4G10120.1	
	AT5G06350.1	AT1G50480.1	AT4G36280.1	AT2G40116.1	AT4G26260.1	AT5G53620.3	
	AT1G78620.1	AT5G54010.1	AT4G12280.1	AT2G16430.2	AT2G28410.1	AT5G46580.1	
	AT4G32210.1	AT5G60620.1	AT4G24610.1	AT4G38660.1	AT5G47740.1	AT2G18420.1	
	AT5G42390.1	AT1G74100.1	AT2G44300.1	AT2G27920.1	AT3G57150.1	AT2G14170.1	
	AT4G24560.1	AT3G08500.1	AT5G04670.1	AT5G38690.1	AT1G23080.1	AT5G27280.1	
	AT3G47000.1	AT1G55610.1	AT1G21310.1	AT2G24700.1	AT1G17500.1	AT5G59350.1	
	AT3G03220.1	AT5G45780.1	AT1G30280.1	AT1G09560.1	AT3G16857.2	AT1G08970.2	
	AT1G68020.2	AT5G63810.1	AT4G33650.1	AT1G09640.1	AT1G35780.1	AT2G43030.1	
	AT2G37550.1	AT5G32470.1	AT1G32400.2	AT2G32800.1	AT3G16520.3	AT1G61100.1	
	AT4G14305.1	AT5G61040.1	AT3G52230.1	AT4G37640.1	AT1G63770.5	AT2G35360.1	
	AT4G25160.1	AT5G43270.1	AT5G48310.2	AT3G06780.1	AT1G05920.1	AT1G18670.1	
	AT5G45650.1	AT4G16360.3	AT5G51210.1	AT5G56230.1	AT1G48410.1	AT3G10060.1	
	AT5G05130.1	AT4G24580.1	AT4G12910.1	AT3G62420.1	AT1G80530.1	AT5G20010.1	
	AT1G27620.1	AT5G56140.1	AT5G12380.1	AT2G22850.1	AT5G42800.1	AT2G15320.1	
	AT2G02740.2	AT5G23070.1	AT1G48130.1	AT2G17980.1	AT2G05760.1	AT5G06210.1	
	AT1G54990.1	AT3G17380.1	AT2G30170.1	AT2G45000.1	AT4G14710.1	AT3G05545.1	
	AT1G11360.2	AT1G08490.1	AT1G35680.1	AT3G25250.1	AT5G04420.3	AT1G31130.1	
	AT3G08750.1	AT3G60190.1	AT5G14990.1	AT5G02010.1	AT5G53280.1	AT1G77220.1	
	AT1G06930.1	AT3G11750.1	AT2G38370.1	AT3G17700.1	AT5G17670.1	AT1G51405.1	
	AT5G25265.1	AT5G03910.1	AT1G59580.1	AT5G06660.1	AT1G09900.1	AT1G12700.1	
	AT3G48860.2	AT1G15110.1	AT2G23460.1	AT3G56370.1	AT1G23740.1	AT4G33980.2	
	AT2G15690.1	AT3G04790.1	AT2G28310.1	AT5G06770.1	AT4G02380.1	AT4G39235.1	
	AT2G45450.1	AT4G19860.1	AT4G00300.2	AT3G15000.1	AT3G53390.1	AT5G49710.3	
	AT2G30260.1	AT1G07120.1	AT5G52970.1	AT2G43250.1	AT4G33670.1	AT2G18500.1	
	AT1G70000.2	AT2G03780.1	AT5G45680.1	AT1G22490.1	AT1G02460.1	AT1G08780.1	
	AT2G05910.1	AT1G64970.1	AT1G15260.1	AT5G26570.1	AT4G14890.1	AT5G66160.1	
	AT1G63220.1	AT2G43710.1	AT5G48880.3	AT1G07280.3	AT3G01280.1	AT3G10610.1	
	AT5G59830.2	AT3G54710.1	AT3G17430.1	AT2G03720.1	AT3G55530.1	AT3G18165.1	
	AT5G40820.1	AT3G17350.1	AT3G15430.1	AT5G52380.1	AT3G52850.1	AT5G40200.1	
	AT5G25510.1	AT3G17690.1	AT3G10740.1	AT5G55540.1	AT1G79950.1	AT5G20920.3	
	AT5G41040.1	AT2G46620.1	AT1G05170.1	AT5G51990.1	AT3G57880.1	AT1G06590.1	
	AT1G74040.1	AT3G53580.1	AT3G23920.1	AT5G11520.1	AT1G19000.2	AT5G64670.1	
	AT5G42240.1	AT5G09320.1	AT3G07320.1	AT5G25770.3	AT3G43660.1	AT1G27190.1	
	AT5G55630.1	AT5G58100.1	AT1G55200.1	AT1G50420.1	AT5G35180.1	AT2G46490.1	
	AT5G40510.1	AT3G52900.1	AT5G22860.1	AT1G12500.1	AT1G40390.1	AT3G60270.1	

	AT1G64770.3 AT5G05170.1 AT4G28720.1 AT5G51570.1 AT3G06470.1 AT2G40095.1 AT4G36530.2 AT5G01420.1 AT1G52980.1 AT5G07590.1 AT3G19010.1 AT2G05170.1 AT4G30080.1 AT1G74850.1 AT5G51800.1 AT2G16250.1 AT5G12150.1 AT2G20875.1 AT2G39570.1 AT2G38970.1 AT4G32180.3 AT2G32680.1 AT1G03610.1 AT1G67260.1 AT1G60940.1 AT4G24730.3 AT3G61050.1 AT2G38130.2 AT5G54290.2 AT5G18290.2 AT4G38160.2 AT5G10530.1 AT1G13580.1 AT5G12870.1 AT3G54630.1 AT1G28470.1 AT3G14580.1 AT3G18010.1 AT4G36520.1 AT1G67190.2 AT3G01670.1 AT4G35090.1 AT2G24020.1 AT2G15730.1 AT2G01170.1 AT5G38830.1 AT3G15070.2 AT1G63470.1 AT1G80290.2 AT4G39110.1 AT1G02790.1 AT4G19070.1 ATMG01320.1 AT3G11490.1 AT3G46620.1 AT4G14930.1 AT2G38560.1 AT1G64610.1 AT3G09950.1 AT5G51600.1 AT4G21065.1 AT3G15250.1 AT4G13930.1 AT3G16190.1 AT5G67210.1 AT5G17780.2 AT1G68740.1 AT1G48350.1 AT1G52140.1 AT1G12410.1 AT2G01510.1 AT3G21400.1 AT2G39700.1 AT1G53840.1 AT1G75690.1 AT3G07890.2 AT3G63430.1 AT1G54540.1 AT3G20015.1 AT1G03050.1 AT2G40140.2 AT5G03700.1 AT5G59910.1 AT5G46080.1 AT2G22450.1 AT5G19090.2 AT1G77610.1 AT3G23240.1 AT4G30720.1 AT3G51930.1 AT1G34245.1 AT5G42310.1 AT2G31500.1 AT2G43180.1 AT3G62770.1 AT5G63905.1 AT1G10810.1 AT1G12950.1 AT1G67410.1 AT3G12900.1 AT1G17140.2 AT5G35520.1 AT1G70080.1 AT2G27080.1 AT3G26430.1 AT3G01860.2 AT5G17770.1 AT2G19090.1 AT4G40080.1 AT3G48270.1 AT4G33650.2 AT1G50140.1 AT1G09340.1 AT1G28760.1 AT3G13235.3 AT3G51580.2 AT1G02660.1 AT4G02680.1 AT4G08790.1 AT2G38720.1 AT2G32150.1 AT4G22120.5 AT5G46570.1 AT1G77800.2 AT5G52780.1 AT3G21530.1 AT4G34710.1 AT5G13710.1 AT5G59030.1 AT5G25220.2 AT5G66580.1 AT3G44260.1 AT3G16270.1 AT2G26710.1 AT1G21880.2 AT2G20520.1 AT5G38840.1 AT2G14820.1 AT5G04890.1 AT2G46780.1 AT5G06260.1 AT3G10300.3 AT5G27450.3 AT5G18130.1 AT1G19880.1 AT3G12600.1 AT5G38700.1 AT5G03420.1 AT4G00710.1 AT5G40600.1 AT2G38070.1 AT1G27300.1 AT4G00100.1 AT5G40330.1 AT2G39690.1 AT3G53970.1 AT1G24650.1 AT4G12230.1 AT4G22550.1 AT3G55150.1 AT5G12110.1 AT3G21810.1 AT4G35900.1 AT2G38440.1 AT1G21326.1 AT5G10230.1 AT1G19350.3 AT1G21600.2 AT2G16890.2 AT3G53960.1 AT3G60660.1 AT5G47980.1 AT4G31430.2 AT2G45050.1 AT3G10840.1 AT4G27760.1 AT5G53590.1 AT2G26510.1 AT3G17580.1 AT1G22590.2 AT4G35730.1 AT4G26270.1 AT3G55070.1 AT2G45130.1 AT5G23940.1 AT1G15800.1 AT1G16250.1 AT5G05780.1 AT1G61670.1 AT3G06730.1 AT3G02450.1 AT4G04980.1 AT5G16280.1 AT1G62500.1 AT3G21460.1 AT3G15352.1 AT5G45110.1 AT1G09815.1 AT4G36850.1 AT5G05810.1 AT1G14720.1 AT1G29300.1 AT1G14270.1 AT4G00050.1 AT3G25560.1 AT2G16730.1 AT1G72175.1 AT1G31910.1 AT2G27040.1 AT5G24090.1 AT3G52770.1 AT5G04770.1 AT1G78700.1 AT1G42990.1 AT1G29195.1 AT1G01690.1 AT5G50890.1 AT3G54440.3 AT5G67350.1 AT3G21430.2 AT1G80840.1 AT2G36800.1 AT1G04290.1 AT1G22660.1 AT4G04330.1 AT4G38510.5 ATCG00270.1 AT3G22160.1 AT2G28110.1 AT2G04410.1 AT3G01930.1 AT5G03670.1 AT4G14310.1 AT2G40260.1 AT1G20650.1 AT4G05090.1 AT1G78630.1 AT5G11460.1 AT1G44000.1 AT5G08480.1 AT2G27600.1 AT5G02750.1 AT3G54320.1 AT3G23000.1 AT5G49330.1 AT3G48180.1 AT2G39970.1 AT3G07490.1 AT1G56310.1 AT2G24370.1 AT1G68550.1 ATCG00360.1 AT3G10380.1 AT2G47600.1 AT5G22920.1 AT4G25360.2 AT5G42620.2 AT4G25390.1 AT2G29650.1 AT4G04870.1 AT5G20050.1 AT4G17350.1 AT5G18560.1 AT3G44610.1 AT1G15410.1 AT5G03905.1 AT2G02180.1 AT5G43230.1 AT1G64100.2 AT2G28190.1 AT3G08947.1 AT1G73940.1 AT1G03080.1 AT4G24910.1 AT3G03850.1 AT3G57340.2 AT2G37080.1 AT2G19580.1 AT4G24610.2 AT1G18550.1 AT3G13780.1 AT1G14650.2 AT3G25680.1 AT5G20520.1 AT1G19990.1 AT1G69350.1 AT1G59900.1 AT2G37690.1 AT5G39250.1 AT1G04110.1 AT2G01820.1 AT3G60580.1 AT5G25270.1 AT1G10690.1 AT3G58030.2 AT5G48460.1 AT5G11530.1 AT1G58110.1 AT3G11980.1 AT2G26800.1 AT1G32160.1 AT4G28310.1 AT5G20510.1 AT2G47490.1 AT1G01110.2 AT4G29090.1 AT1G09760.1 AT3G22750.1 AT5G03260.1 AT2G32300.1 AT1G61570.1 AT5G64080.2 AT4G30440.1 AT3G27160.1 AT1G16520.1 AT1G10930.1 AT5G12330.4 AT1G33811.1 AT2G44770.1 AT3G01820.1 AT3G29320.1 AT5G40930.1 AT1G77660.1 AT3G44830.1 AT3G32930.1 AT1G64690.1 AT4G37000.1 AT1G23780.1 AT4G40090.1 AT3G44735.1 AT4G35580.2 AT4G28360.1 AT3G14870.1	

m	AT3G19500.1	AT4G24060.1	AT5G19050.1	AT2G42610.1	AT2G02850.1	AT2G41940.1	84
	AT3G10970.2	AT5G44600.1	AT4G31890.2	AT5G58250.1	AT2G25810.1	AT5G15350.1	
	AT5G65165.1	AT2G38870.1	AT2G36000.1	AT3G14110.1	AT3G57090.1	AT5G59790.1	
	AT1G11380.1	AT2G37470.1	AT1G01300.1	AT3G50070.1	AT2G18193.1	AT3G59040.1	
	AT3G55780.1	AT5G17380.1	AT1G09970.1	AT3G55270.1	AT3G12750.1	AT1G22240.1	
	AT1G09520.1	AT4G31360.1	AT3G53900.2	AT1G69560.1	AT5G17870.1	AT2G33430.1	
	AT4G02590.2	AT1G19900.1	AT2G01730.1	AT5G51020.1	AT3G61940.1	AT5G46880.1	
	AT1G78780.2	AT5G07620.1	AT5G65530.1	AT4G10300.1	AT1G64450.1	AT1G61610.1	
	AT1G63440.1	AT1G69770.1	AT4G29020.1	AT5G66800.1	AT3G53460.1	AT2G38640.1	
	AT5G16530.1	AT2G26540.1	AT1G71691.2	AT1G26120.1	AT5G52010.1	AT3G54770.1	
	AT3G12930.1	AT1G60550.1	AT3G24020.1	AT5G38450.1	AT4G34588.1	AT3G19090.1	
	AT2G19330.1	AT3G17668.1	AT3G19820.2	AT2G40540.1	AT1G24490.1	AT4G39730.1	
	AT5G24530.1	AT2G26580.1	AT2G43900.1	AT1G19690.1	AT5G63450.1	AT5G08280.1	
	AT3G61700.2 AT4G17770.1 AT2G46530.1 AT1G11430.1 AT2G28830.1 AT2G42610.2						
n	AT3G11400.1	AT5G15540.1	AT5G57290.1	AT1G17210.1	AT1G04390.1	AT4G38100.1	1116
	AT3G12270.1	AT3G02710.1	AT5G42930.1	AT3G50670.1	AT5G62760.4	AT1G07780.1	
	AT3G63340.1	AT2G19530.1	AT3G06483.1	AT1G35210.1	AT5G19440.1	AT2G43010.1	
	AT3G07660.1	AT2G04280.1	AT1G72650.2	AT2G37190.1	AT4G21105.1	AT3G54130.1	
	AT2G35330.1	AT2G23610.1	AT1G26300.1	AT1G15230.1	AT4G23900.1	AT1G22860.1	
	AT1G26150.1	AT1G75080.1	AT1G03060.1	AT5G03415.1	AT1G09830.1	AT5G64660.1	
	AT2G39960.1	AT2G17030.1	AT4G18465.1	AT3G50610.1	AT3G63340.2	AT5G24510.1	
	AT1G51190.1	AT2G33840.1	AT4G30010.1	AT2G04540.1	AT3G60800.1	AT3G03490.1	
	AT3G19490.1	AT3G15095.1	AT2G44740.1	AT1G71260.1	AT3G47700.1	AT4G20840.1	
	AT5G06680.1	AT5G19820.1	AT5G41760.2	AT1G27970.1	AT4G37830.1	AT5G43670.1	
	AT3G26340.1	AT1G58030.1	AT3G07750.1	AT3G48190.1	AT3G08800.1	AT1G58290.1	
	AT2G17420.1	AT5G18380.1	AT3G17850.1	AT3G13060.2	AT2G19450.1	AT5G59810.1	
	AT3G58120.1	AT3G26400.1	AT2G02870.3	AT1G09270.2	AT5G43860.1	AT2G27430.1	
	AT4G12570.1	AT5G18070.1	AT2G26690.1	AT3G52260.2	AT5G52660.2	AT3G22930.1	
	AT3G43860.1	AT2G46290.1	AT5G44250.2	AT5G56340.1	AT5G10070.1	AT3G48050.2	
	AT1G10150.1	AT1G70520.1	AT5G40390.1	AT3G19360.1	AT5G03940.1	AT1G79490.1	
	AT5G59900.1	AT5G17370.1	AT5G62670.1	AT5G23280.1	AT2G33847.1	AT1G34160.1	
	AT2G33590.1	AT4G17140.3	AT1G22150.1	AT4G17890.1	AT5G28840.1	AT4G20260.2	
	AT2G03350.1	AT4G24160.2	AT1G31340.1	AT5G60540.1	AT1G03000.1	AT4G33700.1	
	AT3G29200.1	AT2G32440.1	AT3G18860.1	AT2G45500.1	AT1G32050.1	AT1G24420.1	
	AT2G39730.2	AT3G25840.1	AT2G35940.3	AT3G09840.1	AT5G22040.3	AT4G25130.1	
	AT5G57970.2	AT3G23750.1	AT1G53240.1	AT4G27500.1	AT2G15630.1	AT3G28030.1	
	AT4G05390.1	AT5G18610.1	AT2G37025.1	AT1G08450.1	AT5G23535.1	AT1G20580.1	
	AT4G37670.2	AT4G24015.1	AT2G41130.1	AT4G26510.2	AT2G30050.1	AT3G05590.1	
	AT3G29290.1	AT1G47640.1	AT4G17440.1	AT4G35920.3	AT5G60700.1	AT4G32420.1	
	AT3G18020.1	AT4G14990.1	AT5G14080.1	AT3G20250.1	AT5G10010.1	AT1G18280.1	
	AT1G09645.1	AT3G12160.1	AT2G44710.1	AT5G35620.1	AT3G26230.1	AT5G18580.1	
	AT2G03140.2	AT2G34790.1	AT2G22780.1	AT1G65270.3	AT3G27325.2	AT2G39760.1	
	AT2G39795.1	AT4G19710.2	AT1G68620.1	AT2G37510.1	AT1G60770.1	AT1G03380.1	
	AT1G79020.1	AT5G07840.1	AT2G24290.1	AT1G32090.1	AT2G45620.1	AT3G17465.1	
	AT1G63000.1	AT3G20890.1	AT5G43970.1	AT1G49010.1	AT5G47890.1	AT2G04520.1	
	AT3G04600.1	AT5G24660.1	AT3G16480.1	AT3G19510.1	AT5G62850.1	AT3G23340.1	
	AT3G60400.1	AT2G48060.1	AT1G71830.1	AT2G19480.3	AT1G55890.1	AT5G07710.1	
	AT1G53750.1	AT3G02160.1	AT1G08680.1	AT3G22910.1	AT1G55340.1	AT4G08520.1	
	AT1G10660.4	AT2G33220.1	AT3G51030.1	AT5G15140.1	AT5G40770.1	AT3G02260.1	
	AT4G16800.1	AT5G50200.2	AT4G19110.2	AT3G13860.1	AT2G45260.1	AT1G69523.1	
	AT4G11260.1	AT2G45760.1	AT4G21970.1	AT1G13560.1	AT5G26990.1	AT3G08610.1	
	AT1G65380.1	AT2G23180.1	AT2G25050.1	AT2G25570.1	AT1G29860.1	AT1G78240.1	
	AT3G09740.1	AT5G06740.1	AT1G19490.1	AT1G71960.1	AT4G38200.1	AT1G69500.1	
	AT1G80520.1	AT5G38630.1	AT5G11980.1	AT1G77370.1	AT3G51780.1	AT2G28940.2	
	AT1G17370.1	AT2G25760.2	AT1G33390.1	AT1G71730.1	AT3G21480.1	AT1G78810.1	
	AT3G51880.2	AT5G15120.1	AT5G44250.1	AT5G03290.1	AT3G27870.1	AT3G52720.1	

	AT5G39740.1	AT5G22760.1	AT3G24800.1	AT5G38660.2	AT5G53930.1	AT4G24230.6	
	AT5G08430.1	AT1G02816.1	AT4G27410.2	AT3G26690.2	AT3G09520.1	AT1G31810.1	
	AT1G70940.1	AT5G51880.1	AT1G01720.1	AT4G20970.1	AT1G64980.1	AT1G67580.1	
	AT3G26770.1	AT1G67680.1	AT1G08590.1	AT1G55190.1	AT1G22810.1	AT1G45050.1	
	AT1G58350.2	AT3G61130.1	AT5G58140.1	AT4G15000.1	AT5G21070.1	AT1G16760.1	
	AT1G28140.1	AT4G00590.1	AT4G16650.1	AT5G22850.1	AT4G33467.1	AT4G14960.2	
	AT1G21750.1	AT3G01090.2	AT5G40670.1	AT4G21860.1	AT1G14700.1	AT4G34910.1	
	AT1G77010.1	AT4G38690.1	AT4G27290.1	AT4G29520.1	AT1G16040.1	AT4G32160.1	
	AT1G22260.1	AT1G23149.1	AT2G46915.1	AT2G25320.1	AT5G62440.1	AT1G73100.1	
	AT4G12590.1	AT5G26030.1	AT2G30350.2	AT5G25390.2	AT5G60590.2	AT2G22475.1	
	AT3G07230.1	AT3G20640.1	AT4G25420.1	AT3G55090.1	AT5G14440.1	AT5G37260.1	
	AT2G47190.1	AT5G59850.1	AT4G37100.1	AT1G67920.1	AT5G19130.1	AT2G25625.1	
	AT1G80170.1	AT5G57250.1	AT3G22780.1	AT5G51300.3	AT2G18110.1	AT1G35620.1	
	AT2G28760.2	AT5G66010.1	AT4G24175.1	AT3G62920.1	AT2G29210.1	AT4G18130.1	
	AT1G49380.1	AT4G20020.1	AT5G15890.1	AT1G19290.1	AT1G16840.1	AT3G05170.1	
	AT5G60160.1	AT4G23340.1	AT1G80270.2	AT1G02870.1	AT3G29060.1	AT5G41110.1	
	AT4G31160.1	AT2G20390.1	AT5G45800.1	AT3G24315.1	AT1G70330.1	AT1G06460.1	
	AT2G28290.3	AT1G36050.2	AT4G25000.1	AT1G60200.1	AT5G62790.1	AT2G41720.1	
	AT5G45030.2	AT4G29410.2	AT5G29000.4	AT5G05660.1	AT5G23250.1	AT1G64520.1	
	AT5G58290.1	AT5G18280.1	AT5G40810.1	AT5G41410.1	AT5G06160.1	AT5G18480.1	
	AT4G02570.4	AT3G63088.1	AT2G17110.1	AT5G21950.1	AT5G61310.4	AT3G56400.1	
	AT1G65030.1	AT3G57030.1	AT2G32900.1	AT2G21390.1	AT1G78660.2	AT4G30390.1	
	AT1G69450.1	AT1G16930.1	AT5G67590.1	AT5G62000.3	AT4G00550.1	AT4G01040.1	
	AT3G21820.1	AT3G16200.1	AT5G49610.1	AT3G62600.1	AT3G26130.1	AT5G48780.1	
	AT1G70770.2	AT5G04280.1	AT1G63830.2	AT3G07950.1	AT4G16850.1	AT3G11460.1	
	AT5G27720.1	AT2G40760.1	AT5G58000.1	AT5G42150.1	AT3G02650.1	AT1G30440.1	
	AT5G18200.1	AT1G12480.1	AT5G10940.2	AT5G11790.1	AT2G02960.2	AT4G02580.1	
	AT2G21190.1	AT5G53400.1	AT5G27300.1	AT5G18400.3	AT3G08940.2	AT2G01050.1	
	AT5G47390.1	AT1G73170.1	AT5G32440.1	AT5G63640.1	AT2G28370.1	AT5G35910.1	
	AT1G07990.1	AT2G19540.1	AT3G46560.1	AT1G80810.2	AT5G50090.1	AT3G58110.1	
	AT3G04500.1	AT1G68920.2	AT2G02410.1	AT5G15400.1	AT2G48010.1	AT5G67630.1	
	AT3G46350.1	AT2G24530.1	AT2G38250.1	AT2G46090.1	AT5G57120.1	AT4G28200.1	
	AT2G27020.1	AT2G06500.1	AT4G30310.2	AT5G05210.1	AT5G43630.1	AT1G21760.1	
	AT4G11970.1	AT3G44330.1	AT1G19110.1	AT5G53880.1	AT2G27090.1	AT2G45600.1	
	AT1G74630.1	AT1G12390.1	AT2G33470.2	AT3G57490.1	AT4G24820.1	AT4G27490.1	
	AT5G52800.2	AT3G19508.1	AT3G02310.1	AT1G19530.1	AT1G05010.1	AT2G47430.1	
	AT2G25730.2	AT5G16820.2	AT5G26660.1	AT1G47830.1	AT5G02870.1	AT2G31580.1	
	AT4G00660.2	AT5G57020.1	AT5G20320.1	AT1G12360.1	AT3G16110.1	AT5G10710.1	
	AT1G13130.1	AT1G51965.1	AT3G43980.1	AT5G37475.1	AT4G18800.1	AT1G04140.1	
	AT4G34890.1	AT4G32820.2	AT4G10940.1	AT1G09060.2	AT5G05670.1	AT2G21490.1	
	AT1G44910.1	AT1G80000.2	AT1G18800.1	AT4G17330.1	AT1G70090.2	AT4G37170.1	
	AT1G58122.1	AT4G35500.1	AT2G41620.1	AT4G24140.1	AT1G17680.1	AT2G46410.1	
	AT3G49080.1	AT1G14360.1	AT1G52565.1	AT5G35930.1	AT3G45830.1	AT5G15550.1	
	AT5G06850.1	AT4G22580.1	AT1G21770.1	AT3G20740.1	AT2G35790.1	AT3G15420.1	
	AT2G40750.1	AT5G14740.5	AT1G55760.1	AT2G39380.1	AT1G26740.1	AT3G29170.1	
	AT1G10290.1	AT4G08940.1	AT5G43130.1	AT1G63310.1	AT4G31700.1	AT3G61110.1	
	AT4G25120.1	AT2G35060.2	AT5G53500.1	AT3G20790.1	AT2G25950.1	AT4G14920.1	
	AT1G79180.1	AT3G09060.1	AT5G02600.2	AT2G38080.1	AT3G18260.1	AT1G74440.1	
	AT3G20340.1	AT2G04880.2	AT1G21650.3	AT3G55140.1	AT1G27350.1	AT1G17890.1	
	AT5G35410.1	AT1G17720.2	AT2G16790.1	AT1G74330.1	AT4G31500.1	AT2G19720.1	
	AT4G04640.1	AT1G64650.1	AT4G31750.1	AT2G29200.1	AT3G61890.1	AT1G74700.1	
	AT3G19160.1	AT4G34640.1	AT1G20140.1	AT5G07900.1	AT5G10780.1	AT4G30260.1	
	AT1G60670.2	AT4G01560.1	AT4G01940.1	AT2G30400.1	AT2G34250.2	AT5G04800.4	
	AT5G50960.1	AT3G51100.1	AT5G10370.1	AT1G58250.1	AT5G49530.1	AT1G13980.2	
	AT1G77800.1	AT1G50430.1	AT5G64200.2	AT1G32210.1	AT4G35650.1	AT4G33780.1	
	AT2G31750.1	AT5G50390.1	AT2G24860.1	AT5G66920.1	AT4G16280.2	AT5G23570.1	

	AT2G34520.1	AT1G73720.1	AT3G22845.1	AT1G06515.2	AT1G61900.1	AT4G29790.1	
	AT2G26650.1	AT5G05310.2	AT1G70580.1	AT5G39680.1	AT3G24490.1	AT3G06035.1	
	AT4G38370.1	AT5G50110.1	AT5G64360.1	AT5G48030.1	AT2G04780.2	AT1G03190.1	
	AT1G06410.1	AT5G25752.1	AT1G47900.2	AT2G31600.1	AT1G72020.1	AT5G16850.1	
	AT5G20490.1	AT1G10140.1	AT1G28510.1	AT4G00060.1	AT3G50430.1	AT5G41970.1	
	AT4G32820.1	AT3G15200.1	AT3G57930.2	AT3G26850.2	AT3G17300.1	AT1G30420.1	
	AT3G12020.1	AT5G26860.1	AT5G14710.1	AT3G26360.1	AT3G15800.1	AT3G18820.1	
	AT5G57240.1	AT4G14820.1	AT1G16130.1	AT1G69330.1	AT1G52530.1	AT2G45200.2	
	AT2G36930.1	AT3G20000.1	AT1G07870.2	AT3G60830.1	AT5G01220.1	AT5G27380.1	
	AT1G43690.1	AT3G47110.1	AT3G49990.1	AT5G20910.1	AT3G07930.3	AT5G61770.3	
	AT4G03150.1	AT4G18370.1	AT5G44180.1	AT3G54760.1	AT3G04480.1	AT3G08640.1	
	AT1G30580.1	AT3G25690.2	AT5G56600.1	AT4G07390.1	AT3G20720.2	AT3G14720.1	
	AT1G18850.1	AT5G42960.1	AT1G24706.1	AT3G54560.1	AT3G21780.1	AT5G65170.1	
	AT2G43090.1	AT5G08720.1	AT5G49370.1	AT1G29880.1	AT5G58040.1	AT5G55310.1	
	AT4G17895.1	AT2G03500.1	AT1G35160.1	AT3G20620.1	AT3G54670.1	AT4G11400.1	
	AT1G50740.1	AT2G43370.1	AT1G26340.1	AT4G32600.1	AT2G03430.1	AT1G01770.1	
	AT1G30970.1	AT3G12580.1	AT1G06570.1	AT4G27010.1	AT2G44100.1	AT2G34660.1	
	AT1G08130.1	AT3G16890.1	AT1G15215.2	AT5G02970.1	AT2G25870.1	AT3G07050.1	
	AT4G37710.1	AT4G15180.1	AT1G17760.1	AT1G15120.1	AT2G16485.1	AT3G49645.1	
	AT3G26780.1	AT1G09570.1	AT4G31440.1	AT1G48540.1	AT4G10100.1	AT3G44620.1	
	AT3G24860.1	AT3G25690.1	AT1G72280.1	AT3G21740.1	AT4G37090.1	AT1G30320.1	
	AT3G02150.2	AT1G16780.1	AT1G66350.1	AT2G37270.2	AT4G33470.1	AT3G08910.1	
	AT3G52250.1	AT4G21900.1	AT1G02140.1	AT4G29120.1	AT3G56190.1	AT4G15770.1	
	AT4G37820.1	AT5G40370.1	AT1G79730.1	AT2G31955.1	AT3G60820.1	AT4G33600.1	
	AT4G20010.1	AT5G04140.2	AT3G55620.1	AT5G19910.1	AT2G34150.2	AT4G17080.1	
	AT5G06460.1	AT1G67370.1	AT2G30060.1	AT3G46780.1	AT5G63460.1	AT5G50860.1	
	AT2G37540.1	AT5G03250.1	AT5G61840.1	AT5G42660.1	AT5G02130.1	AT5G30495.2	
	AT3G48240.1	AT5G47940.1	AT1G22520.1	AT3G57050.1	AT2G25710.1	AT4G28510.1	
	AT2G03820.1	AT4G14170.1	AT1G29290.1	AT5G19320.1	AT1G76010.1	AT4G11670.1	
	AT3G55605.1	AT2G40930.1	AT3G06050.1	AT3G12650.1	AT2G45060.1	AT5G49160.1	
	AT4G14350.3	AT1G21790.1	AT4G28730.1	AT1G62420.1	AT1G14830.1	AT3G24495.1	
	AT1G62930.1	AT1G19580.1	AT4G01680.2	AT3G05620.1	AT1G74600.1	AT5G05987.1	
	AT2G46540.1	AT1G65950.1	AT4G30360.1	AT1G55915.1	AT1G01040.2	AT5G64840.1	
	AT4G28650.1	AT5G61970.1	AT2G37270.1	AT5G24350.1	AT5G16690.1	AT2G35658.1	
	AT3G12340.1	AT5G25220.1	AT3G05210.1	AT1G72480.1	AT5G03720.1	AT4G38790.1	
	AT4G28240.1	AT3G03580.1	AT2G35120.1	AT5G59600.1	AT5G41010.1	AT1G19940.1	
	AT4G08910.1	AT5G66680.1	AT1G09150.1	AT4G01250.1	AT2G33850.1	AT2G47510.2	
	AT5G13450.1	AT1G80010.1	AT5G40380.1	AT5G45620.1	AT2G15230.1	AT5G22360.1	
	AT4G09010.1	AT4G35790.2	AT5G24165.1	AT1G03457.1	AT1G07410.1	AT4G35240.1	
	AT4G10810.1	AT5G56090.1	AT1G61790.1	AT3G06040.3	AT2G34040.1	AT1G35530.2	
	AT2G36780.1	AT1G55475.1	AT3G27080.1	AT2G28440.1	AT1G02410.1	AT4G28320.1	
	AT1G70260.1	AT5G48240.1	AT4G19600.1	AT5G42680.2	AT2G04550.1	AT1G51090.1	
	AT5G10060.1	AT2G27940.1	AT2G45910.1	AT1G59720.1	AT4G14100.1	AT5G06530.1	
	AT4G21570.1	AT4G35890.1	AT3G51580.1	AT1G78990.1	AT3G50380.1	AT5G10050.1	
	AT2G10940.2	AT5G63620.1	AT3G11500.1	AT2G41790.1	AT1G36980.1	AT1G33055.1	
	AT5G38710.1	AT3G07810.2	AT5G17190.1	AT5G32450.1	AT1G51200.4	AT5G11330.1	
	AT1G60780.1	AT2G37120.1	AT4G17830.1	AT5G10310.1	AT5G13780.1	AT1G10170.1	
	AT5G46090.1	AT5G11090.1	AT5G03340.1	AT3G05410.2	AT1G04960.1	AT4G25290.1	
	AT3G02200.2	AT5G43790.1	AT3G56040.1	AT4G33500.1	AT2G46550.1	AT5G14660.2	
	AT2G40765.1	AT5G58030.1	AT5G13050.1	AT1G03400.1	AT1G24040.2	AT3G13440.1	
	AT1G09195.2	AT1G10200.1	AT3G24760.1	AT1G60030.1	AT5G46630.1	AT4G25030.2	
	AT3G48030.1	AT3G03600.1	AT5G16450.1	AT5G65160.1	AT2G17695.2	AT3G25040.1	
	AT1G77180.2	AT5G42400.1	AT4G16566.1	AT5G45320.1	AT4G31180.1	AT2G44410.1	
	AT4G34540.1	AT5G52230.2	AT1G77710.1	AT5G14250.1	AT3G47120.1	AT5G27430.1	
	AT5G35530.1	AT4G29950.1	AT1G32750.1	AT2G43010.2	AT1G08640.1	AT3G45890.1	
	AT5G51970.1	AT5G24870.1	AT3G15010.1	AT4G26750.1	AT3G55440.1	AT4G16340.1	

	AT4G26620.1	AT1G26160.1	AT2G33855.1	AT1G54740.1	AT2G44950.1	AT2G41700.1	
	AT3G61780.1	AT2G28520.1	AT1G71800.1	AT1G52230.1	AT1G42480.1	AT4G25470.1	
	AT4G10970.2	AT3G01800.1	AT2G01320.3	AT5G42130.1	AT2G27300.1	AT5G41950.1	
	AT4G30160.1	AT2G38050.1	AT2G35630.1	AT3G09890.1	AT1G80930.1	AT2G35030.1	
	AT1G74900.1	AT1G53490.1	AT5G12430.1	AT4G31180.2	AT1G10522.2	AT3G26630.1	
	AT4G20350.2	AT3G12260.1	AT5G45190.2	AT2G24610.1	AT5G39890.1	AT4G34630.1	
	AT2G32380.1	AT5G55390.1	AT4G30790.1	AT1G07950.1	AT2G14860.1	AT4G12400.2	
	AT3G16760.1	AT4G26910.1	AT3G54690.1	AT4G20325.1	AT2G44060.1	AT1G23550.1	
	AT2G25970.1	AT5G27740.1	AT5G11560.1	AT3G22890.1	AT2G33790.1	AT1G09575.1	
	AT1G07770.1	AT3G51140.1	AT1G67930.1	AT4G31250.1	AT1G12050.1	AT3G58570.1	
	AT4G09570.1	AT1G79250.2	AT4G15830.1	AT3G04240.1	AT4G21430.1	AT1G51350.1	
	AT1G07150.2	AT3G51120.1	AT2G46210.1	AT4G29430.1	AT1G15460.1	AT4G02900.1	
	AT3G03305.1	AT2G40850.1	AT1G64940.1	AT4G37470.1	AT5G66360.2	AT1G18740.1	
	AT2G37110.1	AT3G11930.2	AT1G13690.1	AT5G51030.1	AT5G24750.1	AT5G63830.1	
	AT3G06620.1	AT5G60860.1	AT1G74060.1	AT1G78010.1	AT4G12770.2	AT3G25570.1	
	AT5G12470.1	AT5G04190.1	AT4G16160.2	AT5G57480.1	AT1G14040.1	AT2G45970.1	
	AT3G26618.1	AT5G23540.1	AT4G35790.1	AT3G57660.1	AT5G53900.2	AT2G01470.1	
	AT2G20710.1	AT1G10610.1	AT5G21930.1	AT3G20870.1	AT2G01770.1	AT5G11500.1	
	AT2G31130.1	AT4G25840.1	AT2G24220.1	AT1G53200.1	AT4G37380.1	AT1G17630.1	
	AT1G19485.2	AT5G62290.2	AT2G21290.1	AT2G17390.1	AT4G34940.1	AT1G24030.2	
	AT2G03630.1	AT1G26110.2	AT4G02330.1	AT1G68720.1	AT5G47430.1	AT2G42900.1	
	AT2G13370.1	AT1G04080.1	AT4G32850.10	AT1G11200.1	AT3G52560.1	AT5G05080.2	
	AT4G13460.1	AT3G27540.1	AT3G15010.2	AT3G12170.1	AT2G37260.1	AT2G30395.1	
	AT3G04570.1	AT1G31930.2	AT5G11480.1	AT5G16510.2	AT3G47890.1	AT5G60390.3	
	AT1G13960.1	AT5G56680.1	AT1G65930.1	AT1G07830.1	AT1G04040.1	AT1G69340.1	
	AT1G17450.2	AT1G58120.1	AT1G18210.2	AT1G80000.1	AT1G31920.1	AT3G55260.1	
	AT5G59870.1	AT2G26890.1	AT5G60600.1	AT3G52950.2	AT4G04180.1	AT3G01370.1	
	AT2G46630.1	AT4G39920.1	AT5G40580.1	AT5G24300.1	AT2G40290.1	AT4G29680.1	
	AT4G14950.1	AT3G13230.1	AT2G33610.1	AT2G25110.1	AT5G67500.1	AT4G35600.1	
	AT2G28500.1	AT5G16660.1	AT5G22750.1	AT2G30130.1	AT5G45550.1	AT4G31480.1	
	AT5G14030.1	AT1G04270.1	AT1G12420.1	AT4G24490.1	AT5G47300.1	AT1G06840.1	
	AT1G26761.1 AT4G18975.1 AT2G19560.1 AT2G26910.1 AT3G17910.1 AT1G23360.1						
o	AT3G60290.1	AT3G14280.1	AT3G03770.1	AT2G32990.1	AT3G51370.1	AT1G56140.1	588
	AT3G63030.1	AT5G35100.1	AT2G39445.1	AT1G05170.2	AT2G33810.1	AT1G54790.3	
	AT1G59820.1	AT1G02680.1	AT2G24100.1	AT4G04860.1	AT4G34350.1	AT3G53730.1	
	AT1G78520.1	AT5G53560.1	AT3G55420.1	AT3G19553.1	AT2G40390.1	AT3G12910.1	
	AT4G14880.1	AT3G02460.1	AT5G47490.1	AT5G41761.1	AT4G26900.1	AT4G35420.1	
	AT1G21720.1	AT3G50690.1	AT5G55260.1	AT4G13990.1	AT2G39200.1	AT5G56290.1	
	AT1G77210.1	AT5G66900.1	AT5G23130.1	AT1G16470.1	AT4G13260.1	AT4G33925.1	
	AT4G25780.1	AT5G43700.1	AT1G44130.1	AT4G31020.1	AT2G45220.1	AT4G33945.1	
	AT3G54300.1	AT5G26880.2	AT1G03560.1	AT3G52290.1	AT1G15730.1	AT1G80133.1	
	AT2G27610.1	AT3G27360.1	AT5G47570.1	AT4G24830.1	AT1G53670.1	AT1G03280.1	
	AT5G06280.1	AT1G75250.2	AT1G19250.1	AT1G26560.1	AT1G14590.1	AT3G12050.1	
	AT4G18520.1	AT1G79570.1	AT4G28570.1	AT5G26770.1	AT3G29130.2	AT1G28280.2	
	AT1G51340.2	AT5G58430.1	AT1G11190.1	AT3G48990.1	AT1G77930.1	AT4G31870.1	
	AT4G16370.1	AT5G38280.1	AT4G32770.1	AT4G11820.2	AT2G21150.1	AT1G70680.1	
	AT1G27385.1	AT4G35560.2	AT4G21500.1	AT2G22795.1	AT1G70250.1	AT1G15190.1	
	AT4G21192.1	AT5G63380.1	AT3G13610.1	AT5G16720.1	AT3G59400.1	AT3G57650.1	
	AT1G26610.1	AT5G42020.1	AT2G47830.1	AT1G06790.1	AT1G26520.1	AT1G73020.2	
	AT3G48750.1	AT3G44680.1	AT3G26420.1	AT2G38170.2	AT2G37680.1	AT5G14740.3	
	AT4G36720.1	AT1G79440.1	AT1G11790.1	AT4G00960.1	AT1G76405.2	AT1G12570.1	
	AT1G66920.2	AT1G33260.2	AT3G12490.2	AT1G31830.1	AT4G35590.1	AT2G45360.1	
	AT1G36940.1	AT5G13490.2	AT1G64000.1	AT1G77740.1	AT3G17205.3	AT3G02110.1	
	AT5G14520.1	AT2G26810.2	AT5G27730.1	AT3G15395.3	AT4G14710.2	AT3G18620.1	
	AT3G04530.1	AT3G63380.1	AT1G24110.1	AT3G18580.1	AT1G55790.1	AT5G18610.2	
	AT3G45080.1	AT1G02840.3	AT3G22320.1	AT3G14590.2	AT4G19110.1	AT4G29910.1	

	AT5G09310.1	AT1G09820.1	AT1G02060.1	AT2G18360.1	AT3G23330.1	AT1G47420.1	
	AT5G55560.1	AT1G76040.2	AT3G50360.1	AT4G09580.1	AT4G16640.1	AT1G53600.1	
	AT3G56970.1	AT1G01090.1	AT5G19990.1	AT3G14067.1	AT1G19780.1	AT2G35200.1	
	AT1G01940.1	AT3G25620.2	AT1G37130.1	AT5G38720.1	AT3G58810.1	AT1G20630.1	
	AT2G01710.1	AT3G29230.1	AT5G50790.1	AT4G34560.1	AT1G09580.1	AT3G51520.1	
	AT2G46940.1	AT3G17030.1	AT5G19890.1	AT2G17070.1	AT1G25540.1	AT5G49010.1	
	AT2G30270.1	AT3G11410.1	AT3G48950.1	AT1G27450.1	AT5G47400.1	AT5G47180.2	
	AT2G04790.2	AT1G18910.1	AT3G46430.1	AT3G43590.1	AT1G71040.1	AT1G30845.1	
	AT2G45010.1	AT3G20410.1	AT3G46730.1	AT4G02830.1	AT1G27930.1	AT2G26810.3	
	AT4G12320.1	AT3G52525.1	AT3G23840.1	AT5G12340.1	AT1G58350.1	AT1G18890.1	
	AT5G35970.1	AT1G64500.1	AT1G08230.2	AT3G17470.1	AT1G45976.1	AT2G38280.2	
	AT1G31930.1	AT4G35360.1	AT3G05610.1	AT5G67290.1	AT4G26090.1	AT3G54480.1	
	AT3G55120.1	AT5G42050.1	AT5G62200.1	AT3G56290.1	AT3G03330.1	AT1G68585.1	
	AT1G04580.1	AT5G56960.1	AT1G33410.1	AT2G37560.1	AT3G47833.1	AT5G05390.1	
	AT4G00340.1	AT5G61660.1	AT1G06130.1	AT4G28530.1	AT1G35180.1	AT1G22330.1	
	AT1G64060.1	AT4G34131.1	AT3G14440.1	AT3G21640.1	AT2G23450.2	AT1G38131.1	
	AT1G16300.1	AT3G11450.1	AT4G15620.1	AT3G16050.1	AT5G11710.1	AT5G13490.1	
	AT1G53330.1	AT5G25050.1	AT2G20980.1	AT4G10430.1	AT1G74360.1	AT1G20960.2	
	AT4G26690.1	AT5G12080.2	AT4G32140.1	AT3G55610.1	AT2G06050.1	AT4G02630.1	
	AT5G62150.1	AT1G05990.1	AT3G11110.1	AT1G09880.1	AT5G58960.2	AT5G54390.1	
	AT3G51480.1	AT4G37900.1	AT5G55630.2	AT1G10020.1	AT5G06900.1	AT3G52905.1	
	AT5G05730.1	AT4G18540.1	AT2G37678.1	AT1G66510.1	AT4G27540.1	AT5G15530.1	
	AT3G62800.2	AT3G22330.1	AT4G30230.1	AT4G34450.1	AT2G23970.1	AT1G04570.1	
	AT1G16350.1	AT3G50810.1	AT3G60220.1	AT4G33940.1	AT1G04540.1	AT2G31110.2	
	AT1G60190.1	AT3G06670.2	AT3G47840.1	AT1G49970.1	AT3G55360.1	AT2G25180.1	
	AT1G28710.3	AT1G17420.1	AT2G48120.1	AT3G05340.1	AT1G25450.1	AT4G22200.1	
	AT2G19160.1	AT3G09760.1	AT4G12840.1	AT1G55730.2	AT1G06820.1	AT4G21490.1	
	AT4G27730.1	AT1G64090.1	AT4G31270.1	AT2G35380.1	AT5G61340.1	AT5G05460.1	
	AT3G22640.1	AT2G20320.1	AT5G10730.1	AT1G11610.1	AT3G54460.1	AT1G47330.1	
	AT5G10480.1	AT4G31410.2	AT3G56230.1	AT1G17620.1	AT4G01200.1	AT2G29760.1	
	AT1G34430.1	AT3G24550.1	AT5G63400.1	AT5G05220.1	AT1G27760.3	AT4G24130.1	
	AT1G51760.1	AT1G21460.1	AT1G03910.1	AT5G52840.1	AT2G38150.1	AT3G08820.1	
	AT3G15518.1	AT1G53440.1	AT3G59760.1	AT1G67856.1	AT4G36380.1	AT4G13440.1	
	AT4G36220.1	AT3G28370.1	AT1G79210.1	AT3G06200.1	AT5G44790.1	AT1G11755.1	
	AT5G24030.1	AT1G11360.4	AT3G09640.2	AT1G32220.1	AT2G32190.1	AT1G59860.1	
	AT1G68930.1	AT5G05270.1	AT4G10270.1	AT2G43630.1	AT1G34780.1	AT5G11860.4	
	AT4G21580.1	AT5G20610.1	AT2G23910.1	AT4G19191.1	AT5G19180.1	AT3G09780.1	
	AT1G18720.1	AT1G23870.1	AT4G22890.1	AT2G24430.1	AT5G57510.1	AT2G37060.2	
	AT3G21790.1	ATCG00065.1	AT2G42040.1	AT5G19120.1	AT5G02120.1	AT3G59290.1	
	AT5G14240.1	AT3G18430.1	AT3G19080.1	AT1G56720.2	AT5G45130.1	AT1G12520.1	
	AT3G57510.1	AT3G15350.1	AT3G03610.1	AT1G05450.2	AT1G65060.1	AT2G22880.1	
	AT5G54570.1	AT5G61820.1	AT3G27180.1	AT5G35110.1	AT3G46550.1	AT1G56130.1	
	AT3G11730.1	AT2G42920.1	AT4G10250.1	AT2G26560.1	AT2G02390.1	AT2G02870.1	
	AT5G24560.1	AT5G09460.1	AT2G14750.1	AT2G48130.1	AT2G46150.1	AT3G20500.1	
	AT1G20230.1	AT3G26210.1	AT2G36650.1	AT4G32410.1	AT3G54300.2	AT1G55170.1	
	AT2G38110.1	AT3G11130.1	AT5G15300.1	AT3G57260.1	AT3G07250.1	AT3G56440.1	
	AT2G37130.1	AT3G04090.1	AT4G11980.1	AT1G10340.1	AT3G46940.1	AT5G37680.1	
	AT4G12420.1	AT1G09600.1	AT3G21800.1	AT3G23990.1	AT4G01240.1	AT5G63910.1	
	AT2G32070.1	AT3G47620.1	AT1G70230.1	AT1G33350.1	AT4G20050.2	AT2G22120.2	
	AT3G52620.1	AT5G56550.1	AT5G04250.1	AT3G48330.1	AT1G22460.1	AT5G02230.2	
	AT1G19300.1	AT5G58800.1	AT1G02305.1	AT1G07420.1	AT3G56130.1	AT1G78080.1	
	AT5G07330.1	AT1G71720.1	AT3G58610.3	AT3G02430.1	AT2G24940.1	AT4G37250.1	
	AT4G14040.1	AT2G16070.2	AT3G14880.2	AT5G47540.1	AT5G54380.1	AT1G79700.2	
	AT4G21250.1	AT1G56450.1	AT1G21065.1	AT5G14340.1	AT2G28720.1	AT4G36790.1	
	AT5G13640.1	AT2G40620.1	AT3G53540.1	AT3G20480.1	AT5G25400.1	AT3G61040.1	
	AT1G65260.1	AT2G23540.1	AT4G23100.3	AT3G05250.1	AT5G04220.2	AT1G33590.1	

	AT4G32430.1	AT4G22220.1	AT5G43430.1	AT1G63270.1	AT1G59640.1	AT4G17550.1	
	AT4G02010.1	AT3G56490.1	AT2G30580.1	AT2G48070.1	AT4G08960.1	AT5G28650.1	
	AT3G26810.1	AT4G16430.1	AT5G39410.1	AT1G35710.1	AT5G67030.1	AT5G35740.1	
	AT1G05120.1	AT3G52130.1	AT2G37660.1	AT3G01570.1	AT4G11070.1	AT3G05200.1	
	AT4G18140.2	AT4G11480.1	AT1G53580.1	AT5G03380.1	AT4G19185.1	AT2G06005.1	
	AT4G10160.1	AT5G46030.1	AT2G42360.1	AT1G19140.1	AT5G05840.1	AT1G47240.1	
	AT4G18470.1	AT1G14280.1	AT3G21720.1	AT2G27385.1	AT4G27360.1	AT3G18380.2	
	AT2G02450.2	AT5G57910.1	AT2G21970.1	AT1G68090.1	AT1G11300.1	AT3G20910.1	
	AT4G15780.1	AT2G20920.1	AT1G25280.1	AT3G51000.1	AT4G32870.1	AT5G24318.1	
	AT4G38170.1	AT3G18950.1	AT1G29280.1	AT5G55930.1	AT2G20530.2	AT3G17880.1	
	AT1G71790.1	AT5G23190.1	AT3G44880.1	AT2G33540.1	AT5G39270.1	AT2G41945.1	
	AT1G74940.1	AT1G28410.1	AT3G56120.1	AT1G05180.1	AT4G04940.1	AT5G50720.1	
	AT5G08460.1	AT5G47810.1	AT1G29000.1	AT5G35180.2	AT1G11930.2	AT2G32240.1	
	AT3G22630.1	AT3G47650.1	AT1G21270.1	AT1G78440.1	AT1G08960.1	AT1G16860.1	
	AT5G20790.1	AT5G65110.1	AT3G23325.1	AT3G49740.1	AT1G15400.3	AT5G20885.1	
	AT3G60890.2	AT2G41705.2	AT4G34700.1	AT1G62660.1	AT1G15950.1	AT1G77210.2	
	AT3G02010.1	AT1G20180.1	AT5G16770.2	AT5G27620.1	AT4G31300.1	AT1G05560.1	
	AT3G54860.1 AT5G61550.2 AT1G77590.1 AT1G15080.1 AT4G13950.1 AT1G19440.1						

Supplementary Table 5.2 List of exclusive and overlapping differentially expressed genes in selected GO terms overrepresented during both *K. daigremontiana* and *K. pinnata* plantlet formation.

Figure	Alphabet	TAIR ID	No. of genes
6A	a	AT2G03440 AT3G12500	2
	b	AT1G21326 AT2G40180 AT3G25070 AT4G15800 AT2G23460 AT2G30360 AT5G47910 AT5G48150 AT1G42990 AT3G46620 AT3G17510 AT4G34410	12
	c	AT1G15100 AT5G25190 AT2G38310 AT2G27030 AT4G26150 AT1G12110 AT1G25560 AT1G13260 AT5G36930 AT5G47120 AT5G02810 AT5G66730 AT5G07580 AT1G19640 AT2G40340	15
	d	AT2G20900 AT5G20480 AT3G17980	3
	e	AT1G75500 AT2G29900 AT4G17530 AT5G47230 AT5G51190 AT3G16857 AT2G17820 AT4G30080 AT3G59510 AT1G73500 AT2G44940 AT2G15320 AT3G51550 AT4G17500 AT2G23070 AT3G16770 AT3G07410 AT4G08500 AT1G79380 AT5G12180 AT1G67710 AT3G46510 AT3G15920 AT3G48360 AT2G43130 AT2G36460 AT3G46290 AT1G24625 AT1G03840 AT5G64330 AT3G24500 AT3G22370 AT5G59010 AT3G13980 AT5G60870 AT1G51940 AT2G16600 AT2G04410 AT3G29575 AT1G30330 AT5G40330	41
	f	AT5G05190 AT1G65800 AT4G14640 AT4G36950 AT5G21090 AT3G50930 AT4G13920 AT1G02130 AT2G32680 AT5G36970 AT2G33020 AT1G30755 AT1G19210 AT5G01550 AT5G24090 AT4G18700 AT1G14360 AT3G07360 AT3G21700 AT1G31930 AT3G46550 AT5G19450 AT5G64810 AT2G40950 AT3G56400 AT3G11820 AT4G24210 AT4G33430 AT3G21220 AT5G44510 AT4G22330 AT1G78080 AT3G25600 AT5G52020 AT5G28540 AT1G22810 AT1G51800 AT5G44210 AT5G47710 AT5G66210 AT1G32640 AT5G26170 AT3G18690 AT5G51990 AT2G32510 AT5G40645	46
	g	AT4G28720 AT2G25180 AT4G28140 AT1G19250 AT2G46680 AT2G33310 AT5G64750 AT3G43740 AT1G52340 AT1G52570 AT5G11260 AT3G12160 AT5G61890 AT3G22930 AT5G53160 AT1G07410 AT2G01150 AT1G63650 AT4G01370 AT2G40330 AT1G30270 AT5G52830 AT5G46760 AT1G05850 AT5G14920 AT5G25390 AT1G08650 AT4G03560 AT2G36830 AT5G11590	42

		AT2G22430 AT4G00720 AT1G78300 AT2G20880 AT1G62300 AT1G07150 AT4G32800 AT2G40080 AT5G67300 AT3G15730 AT2G37970 AT4G26470	
6B	a	AT1G19640	1
	b	AT1G27730 AT3G25250 AT1G32920	3
	c	AT1G67560 AT4G15440 AT3G12500 AT1G17840 AT3G45140	5
	d	AT5G46050 AT4G20140 AT3G14840	3
	e	AT3G44260 AT4G34710 AT4G32940 AT3G54420 AT3G48360 AT2G28900 AT4G08170 AT1G72300 AT5G47910 AT1G73500 AT4G08500 AT1G79380 AT5G13930	13
	f	AT4G32551 AT2G20340 AT5G24090 AT4G11280 AT1G74100 AT2G33150 AT3G23050 AT5G43470 AT1G80840 AT3G44540 AT2G32800 AT5G53750	12
	g	AT3G48520 AT5G09810 AT4G01370 AT2G02990 AT5G13220 AT4G21440 AT1G76690	7
6C	a	AT4G24660	1
	b	AT4G37750 AT1G64625 AT5G66460 AT1G60420 AT4G24580	5
	c	AT5G10510 AT4G13560 AT2G44190	3
	d	AT5G66730	1
	e	AT5G51330 AT5G20850 AT5G62410 AT5G67260 AT4G01370 AT5G51210 AT3G07130 AT5G16730 AT3G23890 AT5G37630 AT5G63980 AT1G13290 AT5G56580 AT2G36170 AT3G52590 AT2G33560 AT3G25100 AT5G42080 AT1G07430 AT5G11320 AT1G29300 AT4G24710 AT5G61850 AT4G13940 AT4G14300 AT1G50240 AT3G19590 AT4G15890 AT4G34160 AT3G43210 AT2G20000 AT4G17380 AT1G63930 AT1G23080 AT1G08840 AT4G04900 AT5G52290 AT5G05510 AT1G13330 AT1G09000 AT5G03800 AT5G15380 AT1G01690 AT5G64620 AT3G61650 AT4G18750 AT3G23670 AT3G26790 AT4G22810 AT4G14150 AT3G12670 AT4G22970 AT3G19210 AT4G32400 AT1G06660 AT3G16730	56
	f	AT3G63010 AT1G19900 AT1G65620 AT5G02030 AT3G13540 AT2G21060 AT4G25420 AT2G23380 AT5G16560 AT2G45190 AT5G22650 AT1G09540 AT2G45430 AT5G28640 AT1G49320 AT2G32280 AT4G20140 AT5G03790 AT4G34200 AT3G03810 AT1G24260 AT1G61610 AT1G77720 AT3G50070 AT1G69770	25
	g	AT4G00260 AT2G46660 AT1G69780 AT4G28650 AT1G67260 AT3G15510 AT3G61880 AT5G23660 AT2G34830 AT4G40060 AT2G41720 AT5G65700 AT1G05010 AT3G13730 AT2G15530 AT2G42200 AT2G35270 AT4G19180 AT2G22540 AT2G13680 AT1G52150 AT1G76500 AT2G45650 AT2G36880 AT2G31160 AT2G35510 AT2G02850 AT5G07280 AT5G24860 AT1G62360	30
6D	a	AT2G34650 AT4G33090 AT2G47260	3
	b	AT5G55540 AT5G65640 AT4G09160 AT1G73590	4
	c	AT1G19790 AT1G68320 AT1G75520 AT3G51060 AT2G26710	5
	d	AT1G55020 AT5G07010 AT1G48910 AT5G25620 AT5G11950 AT3G62150 AT5G48880 AT5G47750 AT2G33860 AT4G31820 AT1G15550 AT2G26170 AT5G25900	13
	e	AT4G35190 AT1G30040 AT4G36760 AT5G06300 AT3G25780 AT4G11280 AT1G19640 AT2G33150 AT4G30960 AT5G12330 AT5G16530 AT5G38970 AT2G24300 AT3G21420 AT4G25800 AT1G05680 AT1G62360	17
	f	AT2G37040 AT4G28720 AT4G39950 AT1G17140 AT1G73340 AT3G51670 AT4G37650 AT2G01420 AT3G02875 AT4G35160 AT5G54160 AT5G13930	12

6E	a	AT1G06520 AT3G11600 AT3G47600	3
	b	AT4G27030 AT5G57710 AT5G42900 AT5G20250 AT5G53660 AT1G22770 AT2G40080 AT2G41040 AT3G61220 AT2G01150	10
	c	AT4G14440 AT5G08640 AT2G39980 AT4G30400 AT5G48500 AT5G17050 AT3G55120	7

References

Abat, J.K., and Deswal, R. (2013). Nitric Oxide Modulates the Expression of Proteins and Promotes Epiphyllous Bud Differentiation in Kalanchoe pinnata. J Plant Growth Regul *32*, 92–101.

Abdel-Raouf, H.S. (2012). Anatomical traits of some species of Kalanchoe (Crassulaceae) and their taxonomic value. Annals of Agricultural Sciences *57*, 73–79.

Abebe, D., and Ayehu, A. (1993). Medicinal plants and enigmatic health practices of northern Ethiopia (B.S.P.E.).

Abrahamsson, M., Valladares, S., Larsson, E., Clapham, D., and von Arnold, S. (2012). Patterning during somatic embryogenesis in Scots pine in relation to polar auxin transport and programmed cell death. Plant Cell Tiss Organ Cult *109*, 391–400.

Agarwal, H., and Shanmugam, V.K. (2019). Anti-inflammatory activity screening of Kalanchoe pinnata methanol extract and its validation using a computational simulation approach. Informatics in Medicine Unlocked *14*, 6–14.

Ahammed, G.J., and Yu, J.-Q. (2016). Plant hormones under challenging environmental factors (Springer).

Aichinger, E., Kornet, N., Friedrich, T., and Laux, T. (2012). Plant Stem Cell Niches. Annual Review of Plant Biology *63*, 615–636.

Aida, M., Ishida, T., Fukaki, H., Fujisawa, H., and Tasaka, M. (1997). Genes involved in organ separation in Arabidopsis: an analysis of the cup-shaped cotyledon mutant. Plant Cell *9*, 841–857.

Aida, M., Ishida, T., and Tasaka, M. (1999). Shoot apical meristem and cotyledon formation during Arabidopsis embryogenesis: interaction among the CUP-SHAPED COTYLEDON and SHOOT MERISTEMLESS genes. Development *126*, 1563–1570.

Aida, M., Beis, D., Heidstra, R., Willemsen, V., Blilou, I., Galinha, C., Nussaume, L., Noh, Y.-S., Amasino, R., and Scheres, B. (2004). The PLETHORA Genes Mediate Patterning of the Arabidopsis Root Stem Cell Niche. Cell *119*, 109–120.

Alexandra Pila Quinga, L., Heringer, A.S., Pacheco de Freitas Fraga, H., do Nascimento Vieira, L., Silveira, V., Steinmacher, D.A., and Guerra, M.P. (2018). Insights into the conversion potential of Theobroma cacao L. somatic embryos using quantitative proteomic analysis. Scientia Horticulturae *229*, 65–76.

Allorge-Boiteau, L. (1996). Madagascar centre de speciation et d'origine du genre Kalanchoe (Crassulaceae). Biogeographie de Madagascar *8*, 137–145.

Al-Nami, S. (2020). Kalanchoe Blossfeldina Extract as a Green Corrosion Inhibitor for Carbon Steel in Na2S-polluted NaCl Solutions. International Journal of Electrochemical Science 535–547.

Altman, A., and Hasegawa, P.M. (2012). Plant Biotechnology and Agriculture: Prospects for the 21st Century (Academic Press).

Amin, A.B. (2019). Elucidating the Regulatory Role of the Obligate Crassulacean Acid Metabolism (CAM) Plant, Kalanchoe fedtschenkoi MYB Transcription Factor. M.S. University of South Dakota.

Andersen, T.G., Naseer, S., Ursache, R., Wybouw, B., Smet, W., De Rybel, B., Vermeer, J.E.M., and Geldner, N. (2018). Diffusible repression of cytokinin signalling produces endodermal symmetry and passage cells. Nature *555*, 529–533.

Andreasson, E., Jenkins, T., Brodersen, P., Thorgrimsen, S., Petersen, N.H., Zhu, S., Qiu, J.-L., Micheelsen, P., Rocher, A., Petersen, M., et al. (2005). The MAP kinase substrate MKS1 is a regulator of plant defense responses. The EMBO Journal *24*, 2579–2589.

Argyros, R.D., Mathews, D.E., Chiang, Y.-H., Palmer, C.M., Thibault, D.M., Etheridge, N., Argyros, D.A., Mason, M.G., Kieber, J.J., and Schaller, G.E. (2008). Type B Response Regulators of Arabidopsis Play Key Roles in Cytokinin Signaling and Plant Development. The Plant Cell *20*, 2102–2116.

Arick, M., and Hsu, C.-Y. (2018). Differential Gene Expression Analysis of Plants. pp. 279–298.

Arnao, M.B., and Hernández-Ruiz, J. (2020). Is Phytomelatonin a New Plant Hormone? Agronomy *10*, 95.

Arroyo-Herrera, A., Ku Gonzalez, A., Canche Moo, R., Quiroz-Figueroa, F.R., Loyola-Vargas, V.M., Rodriguez-Zapata, L.C., Burgeff D'Hondt, C., Suárez-Solís, V.M., and Castaño, E. (2008). Expression of WUSCHEL in Coffea canephora causes ectopic morphogenesis and increases somatic embryogenesis. Plant Cell Tiss Organ Cult *94*, 171–180.

Awada, R., Campa, C., Gibault, E., Déchamp, E., Georget, F., Lepelley, M., Abdallah, C., Erban, A., Martinez-Seidel, F., Kopka, J., et al. (2019). Unravelling the Metabolic and Hormonal Machinery During Key Steps of Somatic Embryogenesis: A Case Study in Coffee. International Journal of Molecular Sciences *20*, 4665.

Ayil-Gutiérrez, B., Galaz-Ávalos, R.M., Peña-Cabrera, E., and Loyola-Vargas, V.M. (2013). Dynamics of the concentration of IAA and some of its conjugates during the induction of somatic embryogenesis in Coffea canephora. Plant Signaling & Behavior *8*, e26998.

Bahieldin, A., Atef, A., Edris, S., Gadalla, N.O., Ramadan, A.M., Hassan, S.M., Al Attas, S.G., Al-Kordy, M.A., Al-Hajar, A.S.M., Sabir, J.S.M., et al. (2018). Multifunctional activities of ERF109 as affected by salt stress in Arabidopsis. Scientific Reports *8*, 6403.

Bai, B., Su, Y.H., Yuan, J., and Zhang, X.S. (2013). Induction of Somatic Embryos in Arabidopsis Requires Local YUCCA Expression Mediated by the Down-Regulation of Ethylene Biosynthesis. Molecular Plant *6*, 1247–1260.

Bai, Y., Shen, Y., Zhang, Z., Jia, Q., Xu, M., Zhang, T., Fang, H., Yu, X., Li, L., Liu, D., et al. (2021). A GPAT1 Mutation in Arabidopsis Enhances Plant Height but Impairs Seed Oil Biosynthesis. International Journal of Molecular Sciences *22*, 785.

Baldwin, J.T. (1938). Kalanchoe: the genus and its chromosomes. American Journal of Botany *25*, 572–579.

Balick, M.J., Kronenberg, F., Ososki, A.L., Reiff, M., Fugh-Berman, A., Bonnie, O., Roble, M., Lohr, P., and Atha, D. (2000). Medicinal plants used by latino healers for women's health conditions in New York CityPlantas medicinales usadas por curanderos latinos en el tratamiento de enfermedades femeninas en la ciudad de Nueva York. Econ Bot *54*, 344–357.

Bar, M., and Ori, N. (2014). Leaf development and morphogenesis. Development *141*, 4219–4230.

Barrett, S.C.H. (2008). Major Evolutionary Transitions in Flowering Plant Reproduction: An Overview. International Journal of Plant Sciences *169*, 1–5.

Barrett, S.C.H. (2015). Influences of clonality on plant sexual reproduction. Proceedings of the National Academy of Sciences of the United States of America *112*, 8859–8866.

Barton, M.K., and Poethig, R.S. (1993). Formation of the shoot apical meristem in Arabidopsis thaliana: an analysis of development in the wild type and in the shoot meristemless mutant. Development *119*, 823–831.

Bartrina, I., Jensen, H., Novák, O., Strnad, M., Werner, T., and Schmülling, T. (2017). Gain-of-Function Mutants of the Cytokinin Receptors AHK2 and AHK3 Regulate Plant Organ Size, Flowering Time and Plant Longevity. Plant Physiology *173*, 1783–1797.

Bata Gouda, M., Zhang, C., Wang, J., Peng, S., Chen, Y., Luo, H., and Yu, L. (2020). ROS and MAPK Cascades in the Post-harvest Senescence of Horticultural Products. Journal of Proteomics & Bioinformatics *13*.

Batygina, T., Bragina, E., and E. Titova, G. (1996). Morphogenesis of Propagules in Viviparous Species Bryophyllum Daigremontianum annd B. Calycinum. Acta Societatis Botanicorum Poloniae *65*, 127–133.

Bäumlein, H., Miséra, S., Luerßen, H., Kölle, K., Horstmann, C., Wobus, U., and Müller, A.J. (1994). The FUS3 gene of Arabidopsis thaliana is a regulator of gene expression during late embryogenesis. The Plant Journal *6*, 379–387.

Bayer, M., Nawy, T., Giglione, C., Galli, M., Meinnel, T., and Lukowitz, W. (2009). Paternal Control of Embryonic Patterning in Arabidopsis thaliana. Science *323*, 1485–1488.

Begara-Morales, J.C., Sánchez-Calvo, B., Luque, F., Leyva-Pérez, M.O., Leterrier, M., Corpas, F.J., and Barroso, J.B. (2014). Differential Transcriptomic Analysis by RNA-Seq of GSNO-Responsive Genes Between Arabidopsis Roots and Leaves. Plant and Cell Physiology *55*, 1080–1095.

Bell, A.D., and Bryan, A. (2008). Plant Form: An Illustrated Guide to Flowering Plant Morphology (Portland, Or: Timber Press).

Benková, E., Michniewicz, M., Sauer, M., Teichmann, T., Seifertová, D., Jürgens, G., and Friml, J. (2003). Local, Efflux-Dependent Auxin Gradients as a Common Module for Plant Organ Formation. Cell *115*, 591–602.

Bennett, T., Brockington, S.F., Rothfels, C., Graham, S.W., Stevenson, D., Kutchan, T., Rolf, M., Thomas, P., Wong, G.K.-S., Leyser, O., et al. (2014). Paralogous radiations of PIN proteins with multiple origins of noncanonical PIN structure. Mol. Biol. Evol. *31*, 2042–2060.

Bensmihen, S. (2015). Hormonal Control of Lateral Root and Nodule Development in Legumes. Plants *4*, 523–547.

Berg, A.R. (1972). Chapter 24 - Grass Reproduction. In The Biology and Utilization of Grasses, V.B. Younger, and C.M. McKell, eds. (Academic Press), pp. 334–347.

Berg, C. van den, Willemsen, V., Hendriks, G., Weisbeek, P., and Scheres, B. (1997). Short-range control of cell differentiation in the *Arabidopsis* root meristem. Nature *390*, 287.

Besnard, F., Rozier, F., and Vernoux, T. (2014a). The AHP6 cytokinin signaling inhibitor mediates an auxin-cytokinin crosstalk that regulates the timing of organ initiation at the shoot apical meristem. Plant Signal Behav *9*.

Besnard, F., Refahi, Y., Morin, V., Marteaux, B., Brunoud, G., Chambrier, P., Rozier, F., Mirabet, V., Legrand, J., Lainé, S., et al. (2014b). Cytokinin signalling inhibitory fields provide robustness to phyllotaxis. Nature *505*, 417–421.

Betsuyaku, S., Takahashi, F., Kinoshita, A., Miwa, H., Shinozaki, K., Fukuda, H., and Sawa, S. (2011). Mitogen-activated protein kinase regulated by the CLAVATA receptors contributes to shoot apical meristem homeostasis. Plant Cell Physiol *52*, 14–29.

Bharathan, G., Goliber, T.E., Moore, C., Kessler, S., Pham, T., and Sinha, N.R. (2002). Homologies in Leaf Form Inferred from KNOXI Gene Expression During Development. Science *296*, 1858–1860.

Bhattacharya, A. (2019). Chapter 6 - Effect of High-Temperature Stress on the Metabolism of Plant Growth Regulators. In Effect of High Temperature on Crop Productivity and Metabolism of Macro Molecules, A. Bhattacharya, ed. (Academic Press), pp. 485–591.

Biedroń, M., and Banasiak, A. (2018). Auxin-mediated regulation of vascular patterning in Arabidopsis thaliana leaves. Plant Cell Rep *37*, 1215–1229.

Bielach, A., Hrtyan, M., and Tognetti, V.B. (2017). Plants under Stress: Involvement of Auxin and Cytokinin. International Journal of Molecular Sciences *18*, 1427.

Bilsborough, G.D., Runions, A., Barkoulas, M., Jenkins, H.W., Hasson, A., Galinha, C., Laufs, P., Hay, A., Prusinkiewicz, P., and Tsiantis, M. (2011). Model for the regulation of Arabidopsis thaliana leaf margin development. PNAS *108*, 3424–3429.

Bird, D., Beisson, F., Brigham, A., Shin, J., Greer, S., Jetter, R., Kunst, L., Wu, X., Yephremov, A., and Samuels, L. (2007). Characterization of Arabidopsis ABCG11/WBC11, an ATP binding cassette (ABC) transporter that is required for cuticular lipid secretion†. The Plant Journal *52*, 485–498.

Blair, E.J., Bonnot, T., Hummel, M., Hay, E., Marzolino, J.M., Quijada, I.A., and Nagel, D.H. (2019). Contribution of time of day and the circadian clock to the heat stress responsive transcriptome in Arabidopsis. Scientific Reports *9*, 4814.

Blakeslee, J.J., Peer, W.A., and Murphy, A.S. (2005). Auxin transport. Curr. Opin. Plant Biol. *8*, 494–500.

Blakeslee, J.J., Spatola Rossi, T., and Kriechbaumer, V. (2019). Auxin biosynthesis: spatial regulation and adaptation to stress. Journal of Experimental Botany *70*, 5041–5049.

Bleckmann, A., Weidtkamp-Peters, S., Seidel, C.A.M., and Simon, R. (2010). Stem Cell Signaling in Arabidopsis Requires CRN to Localize CLV2 to the Plasma Membrane. Plant Physiol *152*, 166–176.

Bleecker, A.B., and Kende, H. (2000). Ethylene: a gaseous signal molecule in plants. Annu. Rev. Cell Dev. Biol. *16*, 1–18.

Bofkin, L., and Goldman, N. (2007). Variation in Evolutionary Processes at Different Codon Positions. Molecular Biology and Evolution *24*, 513–521.

Boisnard-Lorig, C., Colon-Carmona, A., Bauch, M., Hodge, S., Doerner, P., Bancharel, E., Dumas, C., Haseloff, J., and Berger, F. (2001). Dynamic Analyses of the Expression of the HISTONE::YFP Fusion Protein in Arabidopsis Show That Syncytial Endosperm Is Divided in Mitotic Domains. The Plant Cell *13*, 495–509.

Boiteau, P., and Allorge-Boiteau, L. (1995). Kalanchoe (Crassulacées) de Madagascar: systématique, écophysiologie et phytochimie (KARTHALA Editions).

Bouchabké-Coussa, O., Obellianne, M., Linderme, D., Montes, E., Maia-Grondard, A., Vilaine, F., and Pannetier, C. (2013). Wuschel overexpression promotes somatic embryogenesis and induces organogenesis in cotton (Gossypium hirsutum L.) tissues cultured in vitro. Plant Cell Rep *32*, 675–686.

Boulard, C., Thévenin, J., Tranquet, O., Laporte, V., Lepiniec, L., and Dubreucq, B. (2018). LEC1 (NF-YB9) directly interacts with LEC2 to control gene expression in seed. Biochimica et Biophysica Acta (BBA) - Gene Regulatory Mechanisms *1861*, 443–450.

Boutilier, K., Offringa, R., Sharma, V.K., Kieft, H., Ouellet, T., Zhang, L., Hattori, J., Liu, C.-M., van Lammeren, A.A.M., Miki, B.L.A., et al. (2002). Ectopic Expression of BABY BOOM Triggers a Conversion from Vegetative to Embryonic Growth. Plant Cell *14*, 1737–1749.

Bowman, J.L., and Eshed, Y. (2000). Formation and maintenance of the shoot apical meristem. Trends in Plant Science *5*, 110–115.

Brand, U., Grünewald, M., Hobe, M., and Simon, R. (2002). Regulation of CLV3 expression by two homeobox genes in Arabidopsis. Plant Physiol *129*, 565–575.

Brandt, R., Salla-Martret, M., Bou-Torrent, J., Musielak, T., Stahl, M., Lanz, C., Ott, F., Schmid, M., Greb, T., Schwarz, M., et al. (2012). Genome-wide binding-site analysis of REVOLUTA reveals a link between leaf patterning and light-mediated growth responses. The Plant Journal *72*, 31–42.

Braybrook, S.A., and Peaucelle, A. (2013). Mechano-Chemical Aspects of Organ Formation in Arabidopsis thaliana: The Relationship between Auxin and Pectin. PLOS ONE *8*, e57813.

Braybrook, S.A., Stone, S.L., Park, S., Bui, A.Q., Le, B.H., Fischer, R.L., Goldberg, R.B., and Harada, J.J. (2006). Genes directly regulated by LEAFY COTYLEDON2 provide insight into the control of embryo maturation and somatic embryogenesis. Proc Natl Acad Sci U S A *103*, 3468–3473.

Breia, R., Conde, A., Badim, H., Fortes, A.M., Gerós, H., and Granell, A. (2021). Plant SWEETs: from sugar transport to plant–pathogen interaction and more unexpected physiological roles. Plant Physiology *186*, 836–852.

Breuninger, H., Rikirsch, E., Hermann, M., Ueda, M., and Laux, T. (2008). Differential Expression of WOX Genes Mediates Apical-Basal Axis Formation in the Arabidopsis Embryo. Developmental Cell *14*, 867–876.

Brock, A.K., Willmann, R., Kolb, D., Grefen, L., Lajunen, H.M., Bethke, G., Lee, J., Nürnberger, T., and Gust, A.A. (2010). The Arabidopsis Mitogen-Activated Protein Kinase Phosphatase PP2C5 Affects Seed Germination, Stomatal Aperture, and Abscisic Acid-Inducible Gene Expression. Plant Physiology *153*, 1098–1111.

Broertjes, C., Haccius, B., and Weidlich, S. (1968). Adventitious bud formation on isolated leaves and its significance for mutation breeding. Euphytica *17*, 321–344.

Buchanan, B.B., Gruissem, W., and Jones, R.L. (2015). Biochemistry and Molecular Biology of Plants (John Wiley & Sons).

Bueno, N., Cuesta, C., Centeno, M.L., Ordás, R.J., and Alvarez, J.M. (2021). In Vitro Plant Regeneration in Conifers: The Role of WOX and KNOX Gene Families. Genes *12*, 438.

Bueso, E., Serrano, R., Pallás, V., and Sánchez-Navarro, J.A. (2017). Seed tolerance to deterioration in arabidopsis is affected by virus infection. Plant Physiology and Biochemistry *116*, 1–8.

Burian, A., Ludynia, M., Uyttewaal, M., Traas, J., Boudaoud, A., Hamant, O., and Kwiatkowska, D. (2013). A correlative microscopy approach relates microtubule behaviour, local organ geometry, and cell growth at the Arabidopsis shoot apical meristem. Journal of Experimental Botany *64*, 5753–5767.

Busch, W., Miotk, A., Ariel, F.D., Zhao, Z., Forner, J., Daum, G., Suzaki, T., Schuster, C., Schultheiss, S.J., Leibfried, A., et al. (2010). Transcriptional control of a plant stem cell niche. Dev Cell *18*, 849–861.

Byrne, M.E., Simorowski, J., and Martienssen, R.A. (2002). ASYMMETRIC LEAVES1 reveals knox gene redundancy in Arabidopsis. Development *129*, 1957–1965.

Cagliari, A., Turchetto-Zolet, A.C., Korbes, A.P., Maraschin, F.D.S., Margis, R., and Margis-Pinheiro, M. (2014). New insights on the evolution of Leafy cotyledon1 (LEC1) type genes in vascular plants. Genomics *103*, 380–387.

Callaghan, T.V. (1984). Growth and Translocation in a Clonal Southern Hemisphere Sedge, Uncinia Meridensis. Journal of Ecology *72*, 529–546.

Campos, M.L., Kang, J.-H., and Howe, G.A. (2014). Jasmonate-Triggered Plant Immunity. J Chem Ecol *40*, 657–675.

Cao, X., Yang, H., Shang, C., Ma, S., Liu, L., and Cheng, J. (2019). The Roles of Auxin Biosynthesis YUCCA Gene Family in Plants. Int J Mol Sci *20*.

Capron, A., Chatfield, S., Provart, N., and Berleth, T. (2009). Embryogenesis: Pattern Formation from a Single Cell. The Arabidopsis Book / American Society of Plant Biologists *7*, e0126.

Carland, F.M., and McHale, N.A. (1996). LOP1: a gene involved in auxin transport and vascular patterning in Arabidopsis. Development *122*, 1811–1819.

Carter, R., Woolfenden, H., Baillie, A., Amsbury, S., Carroll, S., Healicon, E., Sovatzoglou, S., Braybrook, S., Gray, J.E., Hobbs, J., et al. (2017). Stomatal Opening Involves Polar, Not Radial, Stiffening Of Guard Cells. Current Biology *0*.

Casson, S., Spencer, M., Walker, K., and Lindsey, K. (2005). Laser capture microdissection for the analysis of gene expression during embryogenesis of Arabidopsis. Plant J *42*, 111–123.

Castander-Olarieta, A., Pereira, C., Montalbán, I.A., Pěnčík, A., Petřík, I., Pavlović, I., Novák, O., Strnad, M., and Moncaleán, P. (2020). Quantification of endogenous aromatic cytokinins in Pinus radiata embryonal masses after application of heat stress during initiation of somatic embryogenesis. Trees.

Chakraborty, R., Uddin, S., Macoy, D.M., Park, S.O., Van Anh, D.T., Ryu, G.R., Kim, Y.H., Lee, J.-Y., Cha, J.-Y., Kim, W.-Y., et al. (2020). Inositol-requiring enzyme 1 (IRE1) plays for AvrRpt2-triggered immunity and RIN4 cleavage in Arabidopsis under endoplasmic reticulum (ER) stress. Plant Physiology and Biochemistry *156*, 105–114.

Chandler, J.W., Cole, M., Flier, A., Grewe, B., and Werr, W. (2007). The AP2 transcription factors DORNROSCHEN and DORNROSCHEN-LIKE redundantly control Arabidopsis embryo patterning via interaction with PHAVOLUTA. Development *134*, 1653–1662.

Chatfield, S.P., Capron, R., Severino, A., Penttila, P.-A., Alfred, S., Nahal, H., and Provart, N.J. (2013). Incipient stem cell niche conversion in tissue culture: using a systems approach to probe early events in WUSCHEL-dependent conversion of lateral root primordia into shoot meristems. Plant J. *73*, 798–813.

Chauvin, A., Caldelari, D., Wolfender, J.-L., and Farmer, E.E. (2013). Four 13-lipoxygenases contribute to rapid jasmonate synthesis in wounded Arabidopsis thaliana leaves: a role for lipoxygenase 6 in responses to long-distance wound signals. New Phytologist *197*, 566–575.

Chen, H., Hwang, J.E., Lim, C.J., Kim, D.Y., Lee, S.Y., and Lim, C.O. (2010). Arabidopsis DREB2C functions as a transcriptional activator of HsfA3 during the heat stress response. Biochemical and Biophysical Research Communications *401*, 238–244.

Chen, L., Tong, J., Xiao, L., Ruan, Y., Liu, J., Zeng, M., Huang, H., Wang, J.-W., and Xu, L. (2016). YUCCA-mediated auxin biogenesis is required for cell fate transition occurring during de novo root organogenesis in Arabidopsis. Journal of Experimental Botany *67*, 4273–4284.

Chen, S.-K., Kurdyukov, S., Kereszt, A., Wang, X.-D., Gresshoff, P.M., and Rose, R.J. (2009). The association of homeobox gene expression with stem cell formation and morphogenesis in cultured Medicago truncatula. Planta *230*, 827–840.

Chen, W., Gong, P., Guo, J., Li, H., Li, R., Xing, W., Yang, Z., and Guan, Y. (2018). Glycolysis regulates pollen tube polarity via Rho GTPase signaling. PLOS Genetics *14*, e1007373.

Cheng, W.-H., Zhu, H.-G., Tian, W.-G., Zhu, S.-H., Xiong, X.-P., Sun, Y.-Q., Zhu, Q.-H., and Sun, J. (2016). De novo transcriptome analysis reveals insights into dynamic homeostasis regulation of somatic embryogenesis in upland cotton (G. hirsutum L.). Plant Mol Biol *92*, 279–292.

Cheng, Y., Dai, X., and Zhao, Y. (2006). Auxin biosynthesis by the YUCCA flavin monooxygenases controls the formation of floral organs and vascular tissues in Arabidopsis. Genes Dev. *20*, 1790–1799.

Cheng, Y., Dai, X., and Zhao, Y. (2007). Auxin Synthesized by the YUCCA Flavin Monooxygenases Is Essential for Embryogenesis and Leaf Formation in Arabidopsis. The Plant Cell *19*, 2430–2439.

Chernetskyy, M. (2011). Problems in nomenclature and systematics in the subfamily Kalanchoideae (Crassulaceae) over the years. Acta Agrobotanica *64*, 67–73.

Cheung, M.-Y., Li, M.-W., Yung, Y.-L., Wen, C.-Q., and Lam, H.-M. (2013). The unconventional P-loop NTPase OsYchF1 and its regulator OsGAP1 play opposite roles in salinity stress tolerance. Plant, Cell & Environment *36*, 2008–2020.

Chiang, Y.-H., Zubo, Y.O., Tapken, W., Kim, H.J., Lavanway, A.M., Howard, L., Pilon, M., Kieber, J.J., and Schaller, G.E. (2012). Functional Characterization of the GATA Transcription Factors GNC and CGA1 Reveals Their Key Role in Chloroplast Development, Growth, and Division in Arabidopsis. Plant Physiology *160*, 332–348.

Chickarmane, V.S., Gordon, S.P., Tarr, P.T., Heisler, M.G., and Meyerowitz, E.M. (2012). Cytokinin signaling as a positional cue for patterning the apical–basal axis of the growing Arabidopsis shoot meristem. PNAS *109*, 4002–4007.

Chlyah-Arnason, A., and Van, M.T.T. (1968). Budding Capacity of Undetached Begonia rex Leaves. Nature *218*, 493–493.

Cho, J.H., Choi, M.N., Yoon, K.H., and Kim, K.-N. (2018). Ectopic Expression of SjCBL1, Calcineurin B-Like 1 Gene From Sedirea japonica, Rescues the Salt and Osmotic Stress Hypersensitivity in Arabidopsis cbl1 Mutant. Front. Plant Sci. *9*.

Chuck, G., Lincoln, C., and Hake, S. (1996). KNAT1 induces lobed leaves with ectopic meristems when overexpressed in Arabidopsis. Plant Cell *8*, 1277–1289.

Clark, S.E., Running, M.P., and Meyerowitz, E.M. (1993). CLAVATA1, a regulator of meristem and flower development in Arabidopsis. Development *119*, 397–418.

Clark, S.E., Jacobsen, S.E., Levin, J.Z., and Meyerowitz, E.M. (1996). The CLAVATA and SHOOT MERISTEMLESS loci competitively regulate meristem activity in Arabidopsis. Development *122*, 1567–1575.

Clark, S.E., Williams, R.W., and Meyerowitz, E.M. (1997). The CLAVATA1 gene encodes a putative receptor kinase that controls shoot and floral meristem size in Arabidopsis. Cell *89*, 575–585.

Cnops, G., Neyt, P., Raes, J., Petrarulo, M., Nelissen, H., Malenica, N., Luschnig, C., Tietz, O., Ditengou, F., Palme, K., et al. (2006). The TORNADO1 and TORNADO2 Genes Function in Several Patterning Processes during Early Leaf Development in Arabidopsis thaliana. The Plant Cell *18*, 852–866.

Cohen, J.D., Slovin, J.P., and Hendrickson, A.M. (2003). Two genetically discrete pathways convert tryptophan to auxin: more redundancy in auxin biosynthesis. Trends in Plant Science *8*, 197–199.

Condic, M.L. (2013). Totipotency: What It Is and What It Is Not. Stem Cells and Development *23*, 796–812.

Cosgrove, D.J. (2005). Growth of the plant cell wall. Nature Reviews Molecular Cell Biology *6*, 850.

Creff, A., Brocard, L., Joubès, J., Taconnat, L., Doll, N.M., Marsollier, A.-C., Pascal, S., Galletti, R., Boeuf, S., Moussu, S., et al. (2019). A stress-response-related inter-compartmental signalling pathway regulates embryonic cuticle integrity in Arabidopsis. PLOS Genetics *15*, e1007847.

Cucinotta, M., Manrique, S., Cuesta, C., Benkova, E., Novak, O., and Colombo, L. (2018). CUP-SHAPED COTYLEDON1 (CUC1) and CUC2 regulate cytokinin homeostasis to determine ovule number in Arabidopsis. Journal of Experimental Botany *69*, 5169–5176.

Cui, X., Zhao, P., Liang, W., Cheng, Q., Mu, B., Niu, F., Yan, J., Liu, C., Xie, H., Kav, N.N.V., et al. (2020). A Rapeseed WRKY Transcription Factor Phosphorylated by CPK Modulates Cell Death and Leaf Senescence by Regulating the Expression of ROS and SA-Synthesis-Related Genes. J. Agric. Food Chem. *68*, 7348–7359.

Dai, X., Liu, N., Wang, L., Li, J., Zheng, X., Xiang, F., and Liu, Z. (2020). MYB94 and MYB96 additively inhibit callus formation via directly repressing LBD29 expression in Arabidopsis thaliana. Plant Science *293*, 110323.

Dal Bosco, C., Dovzhenko, A., Liu, X., Woerner, N., Rensch, T., Eismann, M., Eimer, S., Hegermann, J., Paponov, I.A., Ruperti, B., et al. (2012). The endoplasmic reticulum localized PIN8 is a pollen-specific auxin carrier involved in intracellular auxin homeostasis. Plant J. *71*, 860–870.

Daum, G., Medzihradszky, A., Suzaki, T., and Lohmann, J.U. (2014). A mechanistic framework for noncell autonomous stem cell induction in Arabidopsis. Proc Natl Acad Sci U S A *111*, 14619–14624.

De-la-Peña, C., Nic-Can, G.I., Galaz-Ávalos, R.M., Avilez-Montalvo, R., and Loyola-Vargas, V.M. (2015). The role of chromatin modifications in somatic embryogenesis in plants. Front Plant Sci *6*.

Dello Ioio, R., Nakamura, K., Moubayidin, L., Perilli, S., Taniguchi, M., Morita, M.T., Aoyama, T., Costantino, P., and Sabatini, S. (2008). A genetic framework for the control of cell division and differentiation in the root meristem. Science *322*, 1380–1384.

Devaiah, B.N., Madhuvanthi, R., Karthikeyan, A.S., and Raghothama, K.G. (2009). Phosphate Starvation Responses and Gibberellic Acid Biosynthesis are Regulated by the MYB62 Transcription Factor in Arabidopsis. Molecular Plant *2*, 43–58.

DeYoung, B.J., and Clark, S.E. (2008). BAM Receptors Regulate Stem Cell Specification and Organ Development Through Complex Interactions With CLAVATA Signaling. Genetics *180*, 895–904.

van Dijk, A.D.J., Morabito, G., Fiers, M., van Ham, R.C.H.J., Angenent, G.C., and Immink, R.G.H. (2010). Sequence motifs in MADS transcription factors responsible for specificity and diversification of protein-protein interaction. PLoS Comput. Biol. *6*, e1001017.

Dilworth, L.L., Riley, C.K., and Stennett, D.K. (2017). Chapter 5 - Plant Constituents: Carbohydrates, Oils, Resins, Balsams, and Plant Hormones. In Pharmacognosy, S. Badal, and R. Delgoda, eds. (Boston: Academic Press), pp. 61–80.

Dinolfo, M.I., Castañares, E., and Stenglein, S.A. (2017). Resistance of Fusarium poae in Arabidopsis leaves requires mainly functional JA and ET signaling pathways. Fungal Biology *121*, 841–848.

Do, C.B., and Katoh, K. (2008). Protein Multiple Sequence Alignment. In Functional Proteomics: Methods and Protocols, J.D. Thompson, C. Schaeffer-Reiss, and M. Ueffing, eds. (Totowa, NJ: Humana Press), pp. 379–413.

Dolan, L., Janmaat, K., Willemsen, V., Linstead, P., Poethig, S., Roberts, K., and Scheres, B. (1993). Cellular organisation of the Arabidopsis thaliana root. Development *119*, 71–84.

Dong, X., Zhu, R., Kang, E., and Shang, Z. (2020). RRFT1 (Redox Responsive Transcription Factor 1) is involved in extracellular ATP-regulated gene expression in Arabidopsis thaliana seedlings. Plant Signaling & Behavior *15*, 1748282.

Dostál, R. (1970). Growth correlations in Bryophyllum leaves and exogenous growth regulators. Biol Plant *12*, 125–133.

Dotto, M., and Casati, P. (2017). Developmental reprogramming by UV-B radiation in plants. Plant Science *264*, 96–101.

Doust, L.L. (1981). Population Dynamics and Local Specialization in a Clonal Perennial (Ranunculus Repens): I. The Dynamics of Ramets in Contrasting Habitats. Journal of Ecology *69*, 743–755.

Dumais, J., and Kwiatkowska, D. (2002). Analysis of surface growth in shoot apices. Plant J. *31*, 229–241.

Durand, M., Mainson, D., Porcheron, B., Maurousset, L., Lemoine, R., and Pourtau, N. (2018). Carbon source–sink relationship in Arabidopsis thaliana: the role of sucrose transporters. Planta *247*, 587–611.

Durán-Medina, Y., Díaz-Ramírez, D., and Marsch-Martínez, N. (2017a). Cytokinins on the Move. Front. Plant Sci. *8*.

Durán-Medina, Y., Serwatowska, J., Reyes-Olalde, J.I., de Folter, S., and Marsch-Martínez, N. (2017b). The AP2/ERF Transcription Factor DRNL Modulates Gynoecium Development and Affects Its Response to Cytokinin. Front. Plant Sci. *8*.

Eckert, C.G. (2002). The loss of sex in clonal plants. In Ecology and Evolutionary Biology of Clonal Plants, (Springer, Dordrecht), pp. 279–298.

Efron, B., Halloran, E., and Holmes, S. (1996). Bootstrap confidence levels for phylogenetic trees. Proc Natl Acad Sci U S A *93*, 13429–13434.

Eggli, U. (2003). Illustrated Handbook of Succulent Plants: Crassulaceae.

Eklund, D.M., Ståldal, V., Valsecchi, I., Cierlik, I., Eriksson, C., Hiratsu, K., Ohme-Takagi, M., Sundström, J.F., Thelander, M., Ezcurra, I., et al. (2010). The Arabidopsis thaliana STYLISH1 Protein Acts as a Transcriptional Activator Regulating Auxin Biosynthesis. The Plant Cell *22*, 349–363.

Eklund, D.M., Ishizaki, K., Flores-Sandoval, E., Kikuchi, S., Takebayashi, Y., Tsukamoto, S., Hirakawa, Y., Nonomura, M., Kato, H., Kouno, M., et al. (2015). Auxin Produced by the Indole-3-Pyruvic Acid Pathway Regulates Development and Gemmae Dormancy in the Liverwort Marchantia polymorpha. The Plant Cell *27*, 1650–1669.

Elhiti, M., Tahir, M., Gulden, R.H., Khamiss, K., and Stasolla, C. (2010). Modulation of embryo-forming capacity in culture through the expression of Brassica genes involved in the regulation of the shoot apical meristem. J Exp Bot *61*, 4069–4085.

Elhiti, M., Stasolla, C., and Wang, A. (2013). Molecular regulation of plant somatic embryogenesis. In Vitro Cell.Dev.Biol.-Plant *49*, 631–642.

Endrizzi, K., Moussian, B., Haecker, A., Levin, J.Z., and Laux, T. (1996). The SHOOT MERISTEMLESS gene is required for maintenance of undifferentiated cells in Arabidopsis shoot and floral meristems and acts at a different regulatory level than the meristem genes WUSCHEL and ZWILLE. The Plant Journal *10*, 967–979.

Enriquez-quiroz, J., and Morales-nieto, C. (2010). Apomixis y su importancia en la selección y mejoramiento de gramineas forrajeras tropicales. Revisión. Revista Mexicana de Ciencias Pecuarias *1*, 25–42.

Espinosa-Leal, C.A., Puente-Garza, C.A., and García-Lara, S. (2018). In vitro plant tissue culture: means for production of biological active compounds. Planta *248*, 1–18.

Estornell, L.H., Landberg, K., Cierlik, I., and Sundberg, E. (2018). SHI/STY Genes Affect Pre- and Post-meiotic Anther Processes in Auxin Sensing Domains in Arabidopsis. Front. Plant Sci. *9*.

Fal, K., Landrein, B., and Hamant, O. (2015). Interplay between miRNA regulation and mechanical stress for CUC gene expression at the shoot apical meristem. Plant Signal Behav *11*.

Fanourakis, D., Hyldgaard, B., Giday, H., Bouranis, D., Körner, O., Nielsen, K.L., and Ottosen, C.-O. (2017). Differential effects of elevated air humidity on stomatal closing ability of Kalanchoë blossfeldiana between the C3 and CAM states. Environmental and Experimental Botany *143*, 115–124.

Fatihi, A., Boulard, C., Bouyer, D., Baud, S., Dubreucq, B., and Lepiniec, L. (2016). Deciphering and modifying LAFL transcriptional regulatory network in seed for improving yield and quality of storage compounds. Plant Sci *250*, 198–204.

Feeney, M., Frigerio, L., Cui, Y., and Menassa, R. (2013). Following vegetative to embryonic cellular changes in leaves of Arabidopsis overexpressing LEAFY COTYLEDON2. Plant Physiol *162*, 1881–1896.

Fehér, A. (2006). Why Somatic Plant Cells Start to form Embryos? In Somatic Embryogenesis, (Springer, Berlin, Heidelberg), pp. 85–101.

Fehér, A. (2015). Somatic embryogenesis — Stress-induced remodeling of plant cell fate. Biochimica et Biophysica Acta (BBA) - Gene Regulatory Mechanisms *1849*, 385–402.

Fehér, A. (2019). Callus, Dedifferentiation, Totipotency, Somatic Embryogenesis: What These Terms Mean in the Era of Molecular Plant Biology? Front. Plant Sci. *10*.

Felsenstein, J., and Kishino, H. (1993). Is there Something Wrong with the Bootstrap on Phylogenies? A Reply to Hillis and Bull. Systematic Biology *42*, 193–200.

Fernandez, R., Das, P., Mirabet, V., Moscardi, E., Traas, J., Verdeil, J.-L., Malandain, G., and Godin, C. (2010). Imaging plant growth in 4D: robust tissue reconstruction and lineaging at cell resolution. Nature Methods *7*, 547.

Feurtado, J.A., Huang, D., Wicki-Stordeur, L., Hemstock, L.E., Potentier, M.S., Tsang, E.W.T., and Cutler, A.J. (2011). The Arabidopsis C2H2 Zinc Finger INDETERMINATE DOMAIN1/ENHYDROUS Promotes the Transition to Germination by Regulating Light and Hormonal Signaling during Seed Maturation. The Plant Cell *23*, 1772–1794.

Figueiredo, D.D., and Köhler, C. (2018). Auxin: a molecular trigger of seed development. Genes Dev. *32*, 479–490.

Fleming, A.J., McQueen-Mason, S., Mandel, T., and Kuhlemeier, C. (1997). Induction of Leaf Primordia by the Cell Wall Protein Expansin. Science *276*, 1415–1418.

Fletcher, J.C. (2018). The CLV-WUS Stem Cell Signaling Pathway: A Roadmap to Crop Yield Optimization. Plants (Basel) *7*.

Fletcher, J.C., Brand, U., Running, M.P., Simon, R., and Meyerowitz, E.M. (1999). Signaling of cell fate decisions by CLAVATA3 in Arabidopsis shoot meristems. Science *283*, 1911–1914.

Florentin, A., Damri, M., and Grafi, G. (2013). Stress induces plant somatic cells to acquire some features of stem cells accompanied by selective chromatin reorganization. Dev. Dyn. *242*, 1121–1133.

Fricke, W., Jarvis, M.C., and Brett, C.T. (2000). Turgor pressure, membrane tension and the control of exocytosis in higher plants. Plant, Cell & Environment *23*, 999–1003.

Friml, J., Benková, E., Blilou, I., Wisniewska, J., Hamann, T., Ljung, K., Woody, S., Sandberg, G., Scheres, B., Jürgens, G., et al. (2002). AtPIN4 Mediates Sink-Driven Auxin Gradients and Root Patterning in Arabidopsis. Cell *108*, 661–673.

Friml, J., Vieten, A., Sauer, M., Weijers, D., Schwarz, H., Hamann, T., Offringa, R., and Jürgens, G. (2003). Efflux-dependent auxin gradients establish the apical–basal axis of Arabidopsis. Nature *426*, 147–153.

Fröschel, C., Iven, T., Walper, E., Bachmann, V., Weiste, C., and Dröge-Laser, W. (2019). A Gain-of-Function Screen Reveals Redundant ERF Transcription Factors Providing Opportunities for Resistance Breeding Toward the Vascular Fungal Pathogen Verticillium longisporum. MPMI *32*, 1095–1109.

Fu, Q., Li, S., and Yu, D. (2010). Identification of an Arabidopsis Nodulin-related protein in heat stress. Mol Cells *29*, 77–84.

Fuchs, M., and Lohmann, J.U. (2020). Aiming for the top: non-cell autonomous control of shoot stem cells in Arabidopsis. J Plant Res *133*, 297–309.

Gaillochet, C., and Lohmann, J.U. (2015). The never-ending story: from pluripotency to plant developmental plasticity. Development *142*, 2237–2249.

Galinha, C., Hofhuis, H., Luijten, M., Willemsen, V., Blilou, I., Heidstra, R., and Scheres, B. (2007). PLETHORA proteins as dose-dependent master regulators of *Arabidopsis* root development. Nature *449*, 1053–1057.

Gallois, J.-L., Woodward, C., Reddy, G.V., and Sablowski, R. (2002). Combined SHOOT MERISTEMLESS and WUSCHEL trigger ectopic organogenesis in Arabidopsis. Development *129*, 3207–3217.

Gallois, J.-L., Nora, F.R., Mizukami, Y., and Sablowski, R. (2004). WUSCHEL induces shoot stem cell activity and developmental plasticity in the root meristem. Genes Dev. *18*, 375–380.

Galvan-Ampudia, C.S., Cerutti, G., Legrand, J., Azais, R., Brunoud, G., Moussu, S., Wenzl, C., Lohmann, J.U., Godin, C., and Vernoux, T. (2018). From spatio-temporal morphogenetic gradients to rhythmic patterning at the shoot apex. BioRxiv 469718.

Galvan-Ampudia, C.S., Cerutti, G., Legrand, J., Brunoud, G., Martin-Arevalillo, R., Azais, R., Bayle, V., Moussu, S., Wenzl, C., Jaillais, Y., et al. (2020). Temporal integration of auxin information for the regulation of patterning. ELife *9*, e55832.

Gälweiler, L., Guan, C., Müller, A., Wisman, E., Mendgen, K., Yephremov, A., and Palme, K. (1998). Regulation of Polar Auxin Transport by AtPIN1 in Arabidopsis Vascular Tissue. Science *282*, 2226–2230.

Gambino, G., Minuto, M., Boccacci, P., Perrone, I., Vallania, R., and Gribaudo, I. (2011). Characterization of expression dynamics of WOX homeodomain transcription factors during somatic embryogenesis in Vitis vinifera. Journal of Experimental Botany *62*, 1089–1101.

Ganguly, A., Park, M., Kesawat, M.S., and Cho, H.-T. (2014). Functional Analysis of the Hydrophilic Loop in Intracellular Trafficking of Arabidopsis PIN-FORMED Proteins. The Plant Cell *26*, 1570–1585.

Garber, M., Grabherr, M.G., Guttman, M., and Trapnell, C. (2011). Computational methods for transcriptome annotation and quantification using RNA-seq. Nature Methods *8*, 469–477.

Garcês, H., and Sinha, N. (2009a). The “mother of thousands” (Kalanchoë daigremontiana): a plant model for asexual reproduction and CAM studies. Cold Spring Harb Protoc *2009*, pdb.emo133.

Garcês, H., and Sinha, N. (2009b). Fixing and sectioning tissue from the plant Kalanchoë daigremontiana. Cold Spring Harb Protoc *2009*, pdb.prot5301.

Garcês, H., and Sinha, N. (2009c). In situ hybridization in the plant Kalanchoë daigremontiana. Cold Spring Harb Protoc *2009*, pdb.prot5302.

Garcês, H., and Sinha, N. (2009d). Transformation of the plant Kalanchoë daigremontiana using Agrobacterium tumefaciens. Cold Spring Harb Protoc *2009*, pdb.prot5303.

Garcês, H., and Sinha, N. (2009e). Extraction of DNA from the plant Kalanchoë daigremontiana. Cold Spring Harb Protoc *2009*, pdb.prot5304.

Garcês, H., and Sinha, N. (2009f). Extraction of RNA from the plant Kalanchoë daigremontiana. Cold Spring Harb Protoc *2009*, pdb.prot5305.

Garcês, H.M.P., Champagne, C.E.M., Townsley, B.T., Park, S., Malhó, R., Pedroso, M.C., Harada, J.J., and Sinha, N.R. (2007). Evolution of asexual reproduction in leaves of the genus Kalanchoë. Proc Natl Acad Sci U S A *104*, 15578–15583.

Garcês, H.M.P., Koenig, D., Townsley, B.T., Kim, M., and Sinha, N.R. (2014). Truncation of LEAFY COTYLEDON1 protein is required for asexual reproduction in Kalanchoë daigremontiana. Plant Physiol. *165*, 196–206.

Garg, R., and Jain, M. (2013). RNA-Seq for Transcriptome Analysis in Non-model Plants. pp. 43–58.

Gayral, M., Gaguancela, O.A., Vasquez, E., Herath, V., Flores, F.J., Dickman, M.B., and Verchot, J. (2020). Multiple ER-to-nucleus stress signaling pathways are activated during Plantago asiatica mosaic virus and Turnip mosaic virus infection in Arabidopsis thaliana. The Plant Journal *103*, 1233–1245.

Gazzarrini, S., Tsuchiya, Y., Lumba, S., Okamoto, M., and McCourt, P. (2004). The Transcription Factor FUSCA3 Controls Developmental Timing in Arabidopsis through the Hormones Gibberellin and Abscisic Acid. Developmental Cell *7*, 373–385.

Gerashchenkov, G.A., and Rozhnova, N.A. (2013). The involvement of phytohormones in the plant sex regulation. Russ J Plant Physiol *60*, 597–610.

Gilroy, S. (2008). Plant tropisms. Current Biology *18*, R275–R277.

Giraudat, J., Hauge, B.M., Valon, C., Smalle, J., Parcy, F., and Goodman, H.M. (1992). Isolation of the Arabidopsis ABI3 gene by positional cloning. Plant Cell *4*, 1251–1261.

Gliwicka, M., Nowak, K., Balazadeh, S., Mueller-Roeber, B., and Gaj, M.D. (2013). Extensive Modulation of the Transcription Factor Transcriptome during Somatic Embryogenesis in Arabidopsis thaliana. PLOS ONE *8*, e69261.

Gordon, S.P., Heisler, M.G., Reddy, G.V., Ohno, C., Das, P., and Meyerowitz, E.M. (2007). Pattern formation during de novo assembly of the Arabidopsis shoot meristem. Development *134*, 3539–3548.

Gordon, S.P., Chickarmane, V.S., Ohno, C., and Meyerowitz, E.M. (2009). Multiple feedback loops through cytokinin signaling control stem cell number within the Arabidopsis shoot meristem. PNAS *106*, 16529–16534.

Gorelick, R. (2015). Why Vegetative Propagation of Leaf Cuttings is Possible in Succulent and Semi-Succulent Plants. Hase *2015*, 51–57.

Grace, J.B. (1993). The adaptive significance of clonal reproduction in angiosperms: an aquatic perspective. Aquatic Botany *44*, 159–180.

Grafi, G. (2004). How cells dedifferentiate: a lesson from plants. Developmental Biology *268*, 1–6.

Grafi, G., Florentin, A., Ransbotyn, V., and Morgenstern, Y. (2011). The Stem Cell State in Plant Development and in Response to Stress. Front. Plant Sci. *2*.

Grebner, W., Stingl, N.E., Oenel, A., Mueller, M.J., and Berger, S. (2013). Lipoxygenase6-Dependent Oxylipin Synthesis in Roots Is Required for Abiotic and Biotic Stress Resistance of Arabidopsis. Plant Physiology *161*, 2159–2170.

Green, P.B. (1999). Expression of pattern in plants: combining molecular and calculus-based biophysical paradigms. Am. J. Bot. *86*, 1059–1076.

Groner, M.G. (1974). Intraspecific Allelopathy in Kalanchoe daigremontiana. Botanical Gazette *135*, 73–79.

Grundy, W.N., and Naylor, G.J. (1999). Phylogenetic inference from conserved sites alignments. J Exp Zool *285*, 128–139.

Grunewald, W., De Smet, I., De Rybel, B., Robert, H.S., van de Cotte, B., Willemsen, V., Gheysen, G., Weijers, D., Friml, J., and Beeckman, T. (2013). Tightly controlled WRKY23 expression mediates Arabidopsis embryo development. EMBO Reports *14*, 1136–1142.

Guenot, B., Bayer, E., Kierzkowski, D., Smith, R., Mandel, T., Žádníková, P., Benková, E., and Kuhlemeier, C. (2012). PIN1-Independent Leaf Initiation in Arabidopsis. Plant Physiology *159*, 1501–1510.

Guerra-García, A., Golubov, J., and Mandujano, M.C. (2015). Invasion of Kalanchoe by clonal spread. Biol Invasions *17*, 1615–1622.

Gulzar, B., Mujib, A., Malik, M.Q., Sayeed, R., Mamgain, J., and Ejaz, B. (2020). Genes, proteins and other networks regulating somatic embryogenesis in plants. Journal of Genetic Engineering and Biotechnology *18*, 31.

Guo, F., Liu, C., Xia, H., Bi, Y., Zhao, C., Zhao, S., Hou, L., Li, F., and Wang, X. (2013). Induced expression of AtLEC1 and AtLEC2 differentially promotes somatic embryogenesis in transgenic tobacco plants. PLoS One *8*, e71714.

Guo, J., Liu, H., He, Y., Cui, X., Du, X., and Zhu, J. (2015). Origination of asexual plantlets in three species of Crassulaceae. Protoplasma *252*, 591–603.

Guo, Y., Han, L., Hymes, M., Denver, R., and Clark, S.E. (2010). CLAVATA2 forms a distinct CLE-binding receptor complex regulating Arabidopsis stem cell specification. Plant J *63*, 889–900.

Gupta, N., and Nath, U. (2020). Integration of light and hormone response during seedling establishment. J. Plant Biochem. Biotechnol. *29*, 652–664.

Haberlandt, G. (2003). Culturversuche mit isolierten Pflanzenzellen. In Plant Tissue Culture: 100 Years since Gottlieb Haberlandt, M. Laimer, and W. Rücker, eds. (Vienna: Springer), pp. 1–24.

Hadfi, K., Speth, V., and Neuhaus, G. (1998). Auxin-induced developmental patterns in Brassica juncea embryos. Development *125*, 879–887.

Haecker, A., Groß-Hardt, R., Geiges, B., Sarkar, A., Breuninger, H., Herrmann, M., and Laux, T. (2004). Expression dynamics of WOX genes mark cell fate decisions during early embryonic patterning in Arabidopsis thaliana. Development *131*, 657–668.

Hamant, O., and Haswell, E.S. (2017). Life behind the wall: sensing mechanical cues in plants. BMC Biology *15*, 59.

Hamant, O., Heisler, M.G., Jönsson, H., Krupinski, P., Uyttewaal, M., Bokov, P., Corson, F., Sahlin, P., Boudaoud, A., Meyerowitz, E.M., et al. (2008). Developmental Patterning by Mechanical Signals in Arabidopsis. Science *322*, 1650–1655.

Han, J.-D., Li, X., Jiang, C.-K., Wong, G.K.-S., Rothfels, C.J., and Rao, G.-Y. (2017). Evolutionary Analysis of the LAFL Genes Involved in the Land Plant Seed Maturation Program. Front. Plant Sci. *8*.

Hanemian, M., Barlet, X., Sorin, C., Yadeta, K.A., Keller, H., Favery, B., Simon, R., Thomma, B.P.H.J., Hartmann, C., Crespi, M., et al. (2016). Arabidopsis CLAVATA1 and CLAVATA2 receptors contribute to Ralstonia solanacearum pathogenicity through a miR169-dependent pathway. New Phytologist *211*, 502–515.

Hannan-Jones, M., and Playford, J. (2011). The biology of Australian weeds 40. Bryophyllum Salisb. species. *17*.

Harada, J.J., Belmonte, M.F., and Kwong, R.W. (2001). Plant Embryogenesis (Zygotic and Somatic). In ELS, (John Wiley & Sons, Ltd), p.

Harper, J.L. (1977). Population Biology of plants (London, UK: Academic Press).

Hasson, A., Plessis, A., Blein, T., Adroher, B., Grigg, S., Tsiantis, M., Boudaoud, A., Damerval, C., and Laufs, P. (2011). Evolution and Diverse Roles of the CUP-SHAPED COTYLEDON Genes in Arabidopsis Leaf Development. The Plant Cell *23*, 54–68.

Havsteen, B.H. (2002). The biochemistry and medical significance of the flavonoids. Pharmacology & Therapeutics *96*, 67–202.

Hay, A., Kaur, H., Phillips, A., Hedden, P., Hake, S., and Tsiantis, M. (2002). The gibberellin pathway mediates KNOTTED1-type homeobox function in plants with different body plans. Current Biology: CB *12*, 1557–1565.

He, H., Bai, M., Tong, P., Hu, Y., Yang, M., and Wu, H. (2018). CELLULASE6 and MANNANASE7 Affect Cell Differentiation and Silique Dehiscence. Plant Physiology *176*, 2186–2201.

Heide, O.M. (1965). Effects of 6-benzylamino-purine and 1-naphthaleneacetic acid on the epiphyllous bud formation in Bryophyllum. Planta *67*, 281–296.

Heidstra, R., Welch, D., and Scheres, B. (2004). Mosaic analyses using marked activation and deletion clones dissect Arabidopsis SCARECROW action in asymmetric cell division. Genes Dev *18*, 1964–1969.

Heisler, M.G., Hamant, O., Krupinski, P., Uyttewaal, M., Ohno, C., Jönsson, H., Traas, J., and Meyerowitz, E.M. (2010). Alignment between PIN1 Polarity and Microtubule Orientation in the Shoot Apical Meristem Reveals a Tight Coupling between Morphogenesis and Auxin Transport. PLOS Biology *8*, e1000516.

Helariutta, Y., Fukaki, H., Wysocka-Diller, J., Nakajima, K., Jung, J., Sena, G., Hauser, M.T., and Benfey, P.N. (2000). The SHORT-ROOT gene controls radial patterning of the Arabidopsis root through radial signaling. Cell *101*, 555–567.

Henson, I.E., and Wareing, P.F. (1976). Cytokinins in Xanthium strumarium L.: Distribution in the Plant and Production in the Root System. J Exp Bot *27*, 1268–1278.

Henson, I.E., and Wareing, P.F. (1977). Changes in the Levels of Endogenous Cytokinins and Indole-3-Acetic Acid During Epiphyllous Bud Formation in Bryophyllum Daigremontianum. New Phytologist *79*, 225–232.

Hernández-Hernández, V., Rueda, D., Caballero, L., Alvarez-Buylla, E.R., and Benítez, M. (2014). Mechanical forces as information: an integrated approach to plant and animal development. Front. Plant Sci. *5*.

Herrera, I., and Nassar, J.M. (2009). Reproductive and recruitment traits as indicators of the invasive potential of Kalanchoe daigremontiana (Crassulaceae) and Stapelia gigantea (Apocynaceae) in a Neotropical arid zone. Journal of Arid Environments *73*, 978–986.

Herrera, I., Hernandez, M.-J., Lampo, M., and Nassar, J.M. (2012). Plantlet recruitment is the key demographic transition in invasion by Kalanchoe daigremontiana. Popul Ecol *54*, 225–237.

Hershey, D.R. (2002). Using the Kalanchoe daigremontiana Plant to Show the Effects of Photoperiodism on Plantlet Formation. Science Activities: Classroom Projects and Curriculum Ideas *39*, 30–34.

Heyne, K. (1988). Tumbuhan berguna Indonesia (Yayasan Sarana Wana Jaya : Diedarkan oleh Koperasi Karyawan, Departemen Kehutanan).

Hibara, K., Karim, M.R., Takada, S., Taoka, K., Furutani, M., Aida, M., and Tasaka, M. (2006). Arabidopsis CUP-SHAPED COTYLEDON3 Regulates Postembryonic Shoot Meristem and Organ Boundary Formation. The Plant Cell *18*, 2946–2957.

Hillis, D.M., and Bull, J.J. (1993). An Empirical Test of Bootstrapping as a Method for Assessing Confidence in Phylogenetic Analysis. Systematic Biology *42*, 182–192.

Hirakawa, Y., Shinohara, H., Kondo, Y., Inoue, A., Nakanomyo, I., Ogawa, M., Sawa, S., Ohashi-Ito, K., Matsubayashi, Y., and Fukuda, H. (2008). Non-cell-autonomous control of vascular stem cell fate by a CLE peptide/receptor system. PNAS *105*, 15208–15213.

Hirakawa, Y., Kondo, Y., and Fukuda, H. (2010). TDIF Peptide Signaling Regulates Vascular Stem Cell Proliferation via the WOX4 Homeobox Gene in Arabidopsis[W]. Plant Cell *22*, 2618–2629.

Hirakawa, Y., Fujimoto, T., Ishida, S., Uchida, N., Sawa, S., Kiyosue, T., Ishizaki, K., Nishihama, R., Kohchi, T., and Bowman, J.L. (2020). Induction of Multichotomous Branching by CLAVATA Peptide in Marchantia polymorpha. Current Biology *30*, 3833-3840.e4.

Holst, K., Schmülling, T., and Werner, T. (2011). Enhanced cytokinin degradation in leaf primordia of transgenic Arabidopsis plants reduces leaf size and shoot organ primordia formation. Journal of Plant Physiology *168*, 1328–1334.

Horstman, A., Li, M., Heidmann, I., Weemen, M., Chen, B., Muiño, J.M., Angenent, G.C., and Boutilier, K. (2017a). The BABY BOOM transcription factor activates the LEC1-ABI3-FUS3-LEC2 network to induce somatic embryogenesis. Plant Physiology pp.00232.2017.

Horstman, A., Bemer, M., and Boutilier, K. (2017b). A transcriptional view on somatic embryogenesis. Regeneration (Oxf) *4*, 201–216.

Hosoda, K., Imamura, A., Katoh, E., Hatta, T., Tachiki, M., Yamada, H., Mizuno, T., and Yamazaki, T. (2002). Molecular structure of the GARP family of plant Myb-related DNA binding motifs of the Arabidopsis response regulators. Plant Cell *14*, 2015–2029.

Houck, D.F., and Rieseberg, L.H. (1983). Hormonal Regulation of Epiphyllous Bud Release and Development in Bryophyllum calycinum. American Journal of Botany *70*, 912–915.

Houghton, A.D. (1935). An interesting hybrid. Cactus and Succulent Journal *7*, 44.

Hove, C.A. ten, Lu, K.-J., and Weijers, D. (2015). Building a plant: cell fate specification in the early Arabidopsis embryo. Development *142*, 420–430.

Howe, M.D. (1931). A Morphological Study of the Leaf Notches of Bryophyllum calycinum. American Journal of Botany *18*, 387–390.

Hu, Y., Zhou, L., Huang, M., He, X., Yang, Y., Liu, X., Li, Y., and Hou, X. (2018). Gibberellins play an essential role in late embryogenesis of Arabidopsis. Nat Plants *4*, 289–298.

Huang, F., Zago, M., Abas, L., Marion, A., Galván-Ampudia, C., and Offringa, R. (2010). Phosphorylation of Conserved PIN Motifs Directs Arabidopsis PIN1 Polarity and Auxin Transport. The Plant Cell *22*, 1129–1142.

Huang, H., Ullah, F., Zhou, D.-X., Yi, M., and Zhao, Y. (2019). Mechanisms of ROS Regulation of Plant Development and Stress Responses. Front. Plant Sci. *10*.

Huang, M., Hu, Y., Liu, X., Li, Y., and Hou, X. (2015). Arabidopsis LEAFY COTYLEDON1 controls cell fate determination during post-embryonic development. Front Plant Sci *6*, 955.

Huang, X., Wang, B., Xi, J., Zhang, Y., He, C., Zheng, J., Gao, J., Chen, H., Zhang, S., Wu, W., et al. (2018). Transcriptome Comparison Reveals Distinct Selection Patterns in Domesticated and Wild Agave Species, the Important CAM Plants. International Journal of Genomics *2018*, 1–12.

Hudson, D., Guevara, D., Yaish, M.W., Hannam, C., Long, N., Clarke, J.D., Bi, Y.-M., and Rothstein, S.J. (2011). GNC and CGA1 Modulate Chlorophyll Biosynthesis and Glutamate Synthase (GLU1/Fd-GOGAT) Expression in Arabidopsis. PLOS ONE *6*, e26765.

Hundertmark, M., and Hincha, D.K. (2008). LEA (Late Embryogenesis Abundant) proteins and their encoding genes in Arabidopsis thaliana. BMC Genomics *9*, 118.

Hutchings, M.J. (1988). Differential foraging for resources, and structural plasticity in plants. Trends in Ecology & Evolution *3*, 200–204.

Hutchison, C.E., Li, J., Argueso, C., Gonzalez, M., Lee, E., Lewis, M.W., Maxwell, B.B., Perdue, T.D., Schaller, G.E., Alonso, J.M., et al. (2006). The Arabidopsis Histidine Phosphotransfer Proteins Are Redundant Positive Regulators of Cytokinin Signaling. The Plant Cell *18*, 3073–3087.

Hwang, J.E., Lim, C.J., Chen, H., Je, J., Song, C., and Lim, C.O. (2012). Overexpression of Arabidopsis dehydration-responsive element-binding protein 2C confers tolerance to oxidative stress. Mol Cells *33*, 135–140.

Hwang, J.-U., Vernoud, V., Szumlanski, A., Nielsen, E., and Yang, Z. (2008). A Tip-Localized RhoGAP Controls Cell Polarity by Globally Inhibiting Rho GTPase at the Cell Apex. Current Biology *18*, 1907–1916.

Iglesias-Fernández, R., Rodríguez-Gacio, M. del C., Barrero-Sicilia, C., Carbonero, P., and Matilla, A.J. (2011). Molecular analysis of endo-β-mannanase genes upon seed imbibition suggest a cross-talk between radicle and micropylar endosperm during germination of Arabidopsis thaliana. Plant Signaling & Behavior *6*, 80–82.

Ikeda, M., Mitsuda, N., and Ohme-Takagi, M. (2009). Arabidopsis WUSCHEL Is a Bifunctional Transcription Factor That Acts as a Repressor in Stem Cell Regulation and as an Activator in Floral Patterning. Plant Cell *21*, 3493–3505.

Ikeuchi, M., Ogawa, Y., Iwase, A., and Sugimoto, K. (2016). Plant regeneration: cellular origins and molecular mechanisms. Development *143*, 1442–1451.

Ikeuchi, M., Iwase, A., Rymen, B., Lambolez, A., Kojima, M., Takebayashi, Y., Heyman, J., Watanabe, S., Seo, M., Veylder, L.D., et al. (2017). Wounding Triggers Callus Formation via Dynamic Hormonal and Transcriptional Changes. Plant Physiology *175*, 1158–1174.

Ikeuchi, M., Favero, D.S., Sakamoto, Y., Iwase, A., Coleman, D., Rymen, B., and Sugimoto, K. (2019). Molecular Mechanisms of Plant Regeneration. Annu Rev Plant Biol *70*, 377–406.

Imamura, A., Kiba, T., Tajima, Y., Yamashino, T., and Mizuno, T. (2003). In Vivo and In Vitro Characterization of the ARR11 Response Regulator Implicated in the His-to-Asp Phosphorelay Signal Transduction in Arabidopsis thaliana. Plant and Cell Physiology *44*, 122–131.

Immink, R.G.H., Posé, D., Ferrario, S., Ott, F., Kaufmann, K., Valentim, F.L., de Folter, S., van der Wal, F., van Dijk, A.D.J., Schmid, M., et al. (2012). Characterization of SOC1's central role in

flowering by the identification of its upstream and downstream regulators. Plant Physiol. *160*, 433–449.

Innis, M.A., Gelfand, D.H., Sninsky, J.J., and White, T.J. (2012). PCR Protocols: A Guide to Methods and Applications (Academic Press).

Ishida, K., Yamashino, T., Yokoyama, A., and Mizuno, T. (2008). Three type-B response regulators, ARR1, ARR10 and ARR12, play essential but redundant roles in cytokinin signal transduction throughout the life cycle of Arabidopsis thaliana. Plant Cell Physiol *49*, 47–57.

Iwase, A., Harashima, H., Ikeuchi, M., Rymen, B., Ohnuma, M., Komaki, S., Morohashi, K., Kurata, T., Nakata, M., Ohme-Takagi, M., et al. (2017). WIND1 Promotes Shoot Regeneration through Transcriptional Activation of ENHANCER OF SHOOT REGENERATION1 in Arabidopsis. Plant Cell *29*, 54–69.

Iwase, A., Mita, K., Favero, D.S., Mitsuda, N., Sasaki, R., Kobayshi, M., Takebayashi, Y., Kojima, M., Kusano, M., Oikawa, A., et al. (2018). WIND1 induces dynamic metabolomic reprogramming during regeneration in Brassica napus. Developmental Biology *442*, 40–52.

Izhaki, A., and Bowman, J. (2007). KANADI and Class III HD-Zip Gene Families Regulate Embryo Patterning and Modulate Auxin Flow during Embryogenesis in Arabidopsis. The Plant Cell *19*, 495–508.

Izumi, K., Yamaguchi, I., Wada, A., Oshio, H., and Takahashi, N. (1984). Effects of a New Plant Growth Retardant (E)-1-(4-Chlorophenyl)-4,4-dimethyl-2-(1,2,4-triazol-1-yl)-1-penten-3-ol (S-3307) on the Growth and Gibberellin Content of Rice Plants. Plant and Cell Physiology *25*, 611–617.

Jackson, D., Veit, B., and Hake, S. (1994). Expression of maize KNOTTED1 related homeobox genes in the shoot apical meristem predicts patterns of morphogenesis in the vegetative shoot. Development *120*, 405–413.

Jaiswal, S., and Sawhney, S. (2006a). Correlation of epiphyllous bud differentiation with foliar senescence in crassulacean succulent Kalanchoe pinnata as revealed by thidiazuron and ethrel application. J. Plant Physiol. *163*, 717–722.

Jaiswal, S., and Sawhney, S. (2006b). Modulation of TDZ-induced morphogenetic responses by anti-auxin TIBA in bud-bearing foliar explants of Kalanchoe pinnata. Plant Cell, Tissue and Organ Culture *86*, 69–76.

Jasinski, S., Piazza, P., Craft, J., Hay, A., Woolley, L., Rieu, I., Phillips, A., Hedden, P., and Tsiantis, M. (2005). KNOX Action in Arabidopsis Is Mediated by Coordinate Regulation of Cytokinin and Gibberellin Activities. Current Biology *15*, 1560–1565.

Jasinski, S., Tattersall, A., Piazza, P., Hay, A., Martinez-Garcia, J.F., Schmitz, G., Theres, K., McCormick, S., and Tsiantis, M. (2008). PROCERA encodes a DELLA protein that mediates control of dissected leaf form in tomato. The Plant Journal: For Cell and Molecular Biology *56*, 603–612.

Je, J., Chen, H., Song, C., and Lim, C.O. (2014). Arabidopsis DREB2C modulates ABA biosynthesis during germination. Biochemical and Biophysical Research Communications *452*, 91–98.

Jeong, S., Trotochaud, A.E., and Clark, S.E. (1999). The Arabidopsis CLAVATA2 gene encodes a receptor-like protein required for the stability of the CLAVATA1 receptor-like kinase. Plant Cell *11*, 1925–1934.

Jia, H., McCarty, D.R., and Suzuki, M. (2013). Distinct roles of LAFL network genes in promoting the embryonic seedling fate in the absence of VAL repression. Plant Physiol. *163*, 1293–1305.

Jibran, R., A Hunter, D., and P Dijkwel, P. (2013). Hormonal regulation of leaf senescence through integration of developmental and stress signals. Plant Mol Biol *82*, 547–561.

Jiménez, V.M. (2005). Involvement of Plant Hormones and Plant Growth Regulators on in vitro Somatic Embryogenesis. Plant Growth Regul *47*, 91–110.

Jin, F., Hu, L., Yuan, D., Xu, J., Gao, W., He, L., Yang, X., and Zhang, X. (2014). Comparative transcriptome analysis between somatic embryos (SEs) and zygotic embryos in cotton: evidence for stress response functions in SE development. Plant Biotechnol. J. *12*, 161–173.

Jo, L., Pelletier, J.M., and Harada, J.J. (2019). Central role of the LEAFY COTYLEDON1 transcription factor in seed development. Journal of Integrative Plant Biology *61*, 564–580.

Johnson, M.A. (1934). The Origin of the Foliar Pseudo-Bulbils in Kalanchoe daigremontiana. Bulletin of the Torrey Botanical Club *61*, 355–366.

Jönsson, H., Heisler, M.G., Shapiro, B.E., Meyerowitz, E.M., and Mjolsness, E. (2006). An auxin-driven polarized transport model for phyllotaxis. Proc Natl Acad Sci U S A *103*, 1633–1638.

Joshi, B., Panda, S.K., Jouneghani, R.S., Liu, M., Parajuli, N., Leyssen, P., Neyts, J., and Luyten, W. (2020). Antibacterial, Antifungal, Antiviral, and Anthelmintic Activities of Medicinal Plants of Nepal Selected Based on Ethnobotanical Evidence.

Junker, A., Mönke, G., Rutten, T., Keilwagen, J., Seifert, M., Thi, T.M.N., Renou, J.-P., Balzergue, S., Viehöver, P., Hähnel, U., et al. (2012). Elongation-related functions of LEAFY COTYLEDON1 during the development of Arabidopsis thaliana. Plant J *71*, 427–442.

Jura-Morawiec, J., Tulik, M., and Iqbal, M. (2015). Lateral Meristems Responsible for Secondary Growth of the Monocotyledons: A Survey of the State of the Art. Bot. Rev. *81*, 150–161.

Jürgens, G., Torres Ruiz, R.A., and Berleth, T. (1994). Embryonic pattern formation in flowering plants. Annu. Rev. Genet. *28*, 351–371.

Jurkuta, R., Kaplinsky, N., Spindel, J., and Barton, M. (2009). Partitioning the Apical Domain of the Arabidopsis Embryo Requires the BOBBER1 NudC Domain Protein. The Plant Cell *21*, 1957–1971.

Kadri, A., Grenier De March, G., Guerineau, F., Cosson, V., and Ratet, P. (2021). WUSCHEL Overexpression Promotes Callogenesis and Somatic Embryogenesis in Medicago truncatula Gaertn. Plants *10*, 715.

Kagaya, Y., Ohmiya, K., and Hattori, T. (1999). RAV1, a novel DNA-binding protein, binds to bipartite recognition sequence through two distinct DNA-binding domains uniquely found in higher plants. Nucleic Acids Res *27*, 470–478.

Kagaya, Y., Toyoshima, R., Okuda, R., Usui, H., Yamamoto, A., and Hattori, T. (2005). LEAFY COTYLEDON1 Controls Seed Storage Protein Genes through Its Regulation of FUSCA3 and ABSCISIC ACID INSENSITIVE3. Plant Cell Physiol *46*, 399–406.

Karim, S., Lundh, D., Holmström, K.-O., Mandal, A., and Pirhonen, M. (2005). Structural and functional characterization of AtPTR3, a stress-induced peptide transporter of Arabidopsis. J Mol Model *11*, 226–236.

Karim, S., Holmström, K.-O., Mandal, A., Dahl, P., Hohmann, S., Brader, G., Palva, E.T., and Pirhonen, M. (2007). AtPTR3, a wound-induced peptide transporter needed for defence against virulent bacterial pathogens in Arabidopsis. Planta *225*, 1431–1445.

Kaufmann, K., Melzer, R., and Theissen, G. (2005). MIKC-type MADS-domain proteins: structural modularity, protein interactions and network evolution in land plants. Gene *347*, 183–198.

Kayes, J.M., and Clark, S.E. (1998). CLAVATA2, a regulator of meristem and organ development in Arabidopsis. Development *125*, 3843–3851.

Kefu, Z., Hai, F., San, Z., and Jie, S. (2003). Study on the salt and drought tolerance of Suaeda salsa and Kalanchoe claigremontiana under iso-osmotic salt and water stress. Plant Science *165*, 837–844.

Keith, K., Kraml, M., Dengler, N.G., and McCourt, P. (1994). fusca3: A Heterochronic Mutation Affecting Late Embryo Development in Arabidopsis. Plant Cell *6*, 589–600.

Kerstetter, R.A., Laudencia-Chingcuanco, D., Smith, L.G., and Hake, S. (1997). Loss-of-function mutations in the maize homeobox gene, knotted1, are defective in shoot meristem maintenance. Development *124*, 3045–3054.

Khalil-Ur-Rehman, M., Sun, L., Li, C.-X., Faheem, M., Wang, W., and Tao, J.-M. (2017). Comparative RNA-seq based transcriptomic analysis of bud dormancy in grape. BMC Plant Biology *17*, 18.

Khattak, M.S.K., Abiri, R., Valdiani, A., Atabaki, N., Shariat, M., Talei, D., and Maziah, M. (2017). SOMATIC EMBRYOGENESIS AND IN-VITRO REGENERATION OF RICE (ORYZA SATIVA L.) CULTIVARS UNDER ONE-STEP AND MULTIPLE-STEP SALINITY STRESSES. Journal of Plant Breeding and Genetics *5*, 75–89.

Kieber, J.J., and Schaller, G.E. (2018). Cytokinin signaling in plant development. Development *145*.

Kim, E.H., Kim, Y.S., Park, S.-H., Koo, Y.J., Choi, Y.D., Chung, Y.-Y., Lee, I.-J., and Kim, J.-K. (2009). Methyl Jasmonate Reduces Grain Yield by Mediating Stress Signals to Alter Spikelet Development in Rice. Plant Physiology *149*, 1751–1760.

Kim, J.I., Sharkhuu, A., Jin, J.B., Li, P., Jeong, J.C., Baek, D., Lee, S.Y., Blakeslee, J.J., Murphy, A.S., Bohnert, H.J., et al. (2007). yucca6, a Dominant Mutation in Arabidopsis, Affects Auxin Accumulation and Auxin-Related Phenotypes. Plant Physiology *145*, 722–735.

Kim, M., McCormick, S., Timmermans, M., and Sinha, N. (2003). The expression domain of PHANTASTICA determines leaflet placement in compound leaves. Nature *424*, 438–443.

Kim, S.-G., Lee, S., Kim, Y.-S., Yun, D.-J., Woo, J.-C., and Park, C.-M. (2010). Activation tagging of an Arabidopsis SHI-RELATED SEQUENCE gene produces abnormal anther dehiscence and floral development. Plant Mol Biol *74*, 337–351.

Kim, S.J., Ryu, M.Y., and Kim, W.T. (2012). Suppression of Arabidopsis RING-DUF1117 E3 ubiquitin ligases, AtRDUF1 and AtRDUF2, reduces tolerance to ABA-mediated drought stress. Biochemical and Biophysical Research Communications *420*, 141–147.

Kimura, S., Hunter, K., Vaahtera, L., Tran, H.C., Citterico, M., Vaattovaara, A., Rokka, A., Stolze, S.C., Harzen, A., Meißner, L., et al. (2020). CRK2 and C-terminal Phosphorylation of NADPH Oxidase RBOHD Regulate Reactive Oxygen Species Production in Arabidopsis. The Plant Cell *32*, 1063–1080.

Kinoshita, A., Vayssières, A., Richter, R., Sang, Q., Roggen, A., van Driel, A.D., Smith, R.S., and Coupland, G. (2020). Regulation of shoot meristem shape by photoperiodic signaling and phytohormones during floral induction of Arabidopsis. ELife *9*, e60661.

Kleine-Vehn, J., Huang, F., Naramoto, S., Zhang, J., Michniewicz, M., Offringa, R., and Friml, J. (2009). PIN Auxin Efflux Carrier Polarity Is Regulated by PINOID Kinase-Mediated Recruitment into GNOM-Independent Trafficking in Arabidopsis. Plant Cell *21*, 3839–3849.

Klepikova, A.V., Kasianov, A.S., Gerasimov, E.S., Logacheva, M.D., and Penin, A.A. (2016). A high resolution map of the Arabidopsis thaliana developmental transcriptome based on RNA-seq profiling. Plant J *88*, 1058–1070.

Klimeš, L., Klimešová, J., Hendriks, R., and van Groenendael, J. (1997). Clonal plant architecture: a comparative analysis of form and function. The Ecology and Evolution of Clonal Plants 1–29.

Kolodziejczyk-Czepas, J., and Stochmal, A. (2017). Bufadienolides of Kalanchoe species: an overview of chemical structure, biological activity and prospects for pharmacological use. Phytochem Rev 1–17.

Kondo, Y., Hirakawa, Y., Kieber, J.J., and Fukuda, H. (2011). CLE peptides can negatively regulate protoxylem vessel formation via cytokinin signaling. Plant Cell Physiol *52*, 37–48.

Korver, R.A., Koevoets, I.T., and Testerink, C. (2018). Out of Shape During Stress: A Key Role for Auxin. Trends in Plant Science *23*, 783–793.

Krishnan, S.R.S., and Siril, E.A. (2017). Auxin and nutritional stress coupled somatic embryogenesis in Oldenlandia umbellata L. Physiology and Molecular Biology of Plants *23*, 471–475.

Krizek, B.A. (2011). Aintegumenta and Aintegumenta-Like6 regulate auxin-mediated flower development in Arabidopsis. BMC Research Notes *4*, 176.

Krizek, B.A., Bequette, C.J., Xu, K., Blakley, I.C., Fu, Z.Q., Stratmann, J.W., and Loraine, A.E. (2016). RNA-Seq Links the Transcription Factors AINTEGUMENTA and AINTEGUMENTA-LIKE6 to Cell Wall Remodeling and Plant Defense Pathways. Plant Physiology *171*, 2069–2084.

Krizek, B.A., Blakley, I.C., Ho, Y.-Y., Freese, N., and Loraine, A.E. (2020). The Arabidopsis transcription factor AINTEGUMENTA orchestrates patterning genes and auxin signaling in the establishment of floral growth and form. The Plant Journal *103*, 752–768.

Kroj, T., Savino, G., Valon, C., Giraudat, J., and Parcy, F. (2003). Regulation of storage protein gene expression in Arabidopsis. Development *130*, 6065–6073.

Kukurba, K.R., and Montgomery, S.B. (2015). RNA Sequencing and Analysis. Cold Spring Harbor Protocols *2015*, pdb.top084970.

Kulka, R.G. (2006). Cytokinins inhibit epiphyllous plantlet development on leaves of Bryophyllum (Kalanchoë) marnierianum. J Exp Bot *57*, 4089–4098.

Kulka, R.G. (2008). Hormonal control of root development on epiphyllous plantlets of Bryophyllum (Kalanchoë) marnierianum: role of auxin and ethylene. J Exp Bot *59*, 2361–2370.

Kumar, V., and Staden, J.V. (2017). New insights into plant somatic embryogenesis: an epigenetic view. Acta Physiol Plant *39*, 194.

Kurakawa, T., Ueda, N., Maekawa, M., Kobayashi, K., Kojima, M., Nagato, Y., Sakakibara, H., and Kyozuka, J. (2007). Direct control of shoot meristem activity by a cytokinin-activating enzyme. Nature *445*, 652–655.

Kurepa, J., Shull, T.E., and Smalle, J.A. (2019). Antagonistic activity of auxin and cytokinin in shoot and root organs. Plant Direct *3*, e00121.

Kuusk, S., Sohlberg, J.J., Magnus Eklund, D., and Sundberg, E. (2006). Functionally redundant SHI family genes regulate Arabidopsis gynoecium development in a dose-dependent manner. Plant J *47*, 99–111.

Kwak, S.-H., Song, S.-K., Lee, M.M., and Schiefelbein, J. (2015). TORNADO1 regulates root epidermal patterning through the WEREWOLF pathway in Arabidopsis thaliana. Plant Signaling & Behavior *10*, e1103407.

Kwiatkowska, D. (2008). Flowering and apical meristem growth dynamics. Journal of Experimental Botany *59*, 187–201.

Kwong, R.W., Bui, A.Q., Lee, H., Kwong, L.W., Fischer, R.L., Goldberg, R.B., and Harada, J.J. (2003). LEAFY COTYLEDON1-LIKE Defines a Class of Regulators Essential for Embryo Development. The Plant Cell *15*, 5–18.

Landrein, B., and Ingram, G. (2019). Connected through the force: mechanical signals in plant development. Journal of Experimental Botany *70*, 3507–3519.

Landrein, B., Kiss, A., Sassi, M., Chauvet, A., Das, P., Cortizo, M., Laufs, P., Takeda, S., Aida, M., Traas, J., et al. (2015). Mechanical stress contributes to the expression of the STM homeobox gene in Arabidopsis shoot meristems. ELife *4*, e07811.

Laufs, P., Peaucelle, A., Morin, H., and Traas, J. (2004). MicroRNA regulation of the CUC genes is required for boundary size control in Arabidopsis meristems. Development *131*, 4311–4322.

Laura, M., Borghi, C., Regis, C., Cassetti, A., and Allavena, A. (2013). Ectopic expression of Kxhkn5 in the viviparous species Kalanchoe × Houghtonii induces a novel pattern of epiphyll development. Transgenic Res *22*, 59–74.

Laux, T., and Mayer, K.F.X. (1998). Cell fate regulation in the shoot meristem. Seminars in Cell & Developmental Biology *9*, 195–200.

Laux, T., Mayer, K.F., Berger, J., and Jurgens, G. (1996). The WUSCHEL gene is required for shoot and floral meristem integrity in Arabidopsis. Development *122*, 87–96.

Laux, T., Würschum, T., and Breuninger, H. (2004). Genetic Regulation of Embryonic Pattern Formation. The Plant Cell *16*, S190–S202.

Le, B.H., Cheng, C., Bui, A.Q., Wagmaister, J.A., Henry, K.F., Pelletier, J., Kwong, L., Belmonte, M., Kirkbride, R., Horvath, S., et al. (2010). Global analysis of gene activity during Arabidopsis seed development and identification of seed-specific transcription factors. Proc Natl Acad Sci U S A *107*, 8063–8070.

Le, M.H., Cao, Y., Zhang, X.-C., and Stacey, G. (2014). LIK1, A CERK1-Interacting Kinase, Regulates Plant Immune Responses in Arabidopsis. PLOS ONE *9*, e102245.

Ledwoń, A., and Gaj, M.D. (2011). LEAFY COTYLEDON1, FUSCA3 expression and auxin treatment in relation to somatic embryogenesis induction in Arabidopsis. Plant Growth Regul *65*, 157–167.

Lee, H. (2018). Stem Cell Maintenance and Abiotic Stress Response in Shoot Apical Meristem for Developmental Plasticity. J. Plant Biol. *61*, 358–365.

Lee, J., and Lee, I. (2010). Regulation and function of SOC1, a flowering pathway integrator. J Exp Bot *61*, 2247–2254.

Lee, J.-H., and Park, C.-M. (2015). Integration of photoperiod and cold temperature signals into flowering genetic pathways in Arabidopsis. Plant Signaling & Behavior *10*, e1089373.

Lee, S.B., and Suh, M.C. (2015). Cuticular Wax Biosynthesis is Up-Regulated by the MYB94 Transcription Factor in Arabidopsis. Plant and Cell Physiology *56*, 48–60.

Lee, H., Fischer, R.L., Goldberg, R.B., and Harada, J.J. (2003). Arabidopsis LEAFY COTYLEDON1 represents a functionally specialized subunit of the CCAAT binding transcription factor. Proc. Natl. Acad. Sci. U.S.A. *100*, 2152–2156.

Lee, S.B., Kim, H.U., and Suh, M.C. (2016). MYB94 and MYB96 Additively Activate Cuticular Wax Biosynthesis in Arabidopsis. Plant and Cell Physiology *57*, 2300–2311.

Lei, S.A. (2010). Benefits and Costs of Vegetative and Sexual Reproduction in Perennial Plants: A Review of Literature. Journal of the Arizona-Nevada Academy of Science *42*, 9–14.

Lei, J., Miao, Y., Lan, Y., Han, X., Liu, H., Gan, Y., Niu, L., Wang, Y., and Zheng, Z. (2018). A Novel Complementation Assay for Quick and Specific Screen of Genes Encoding Glycerol-3-Phosphate Acyltransferases. Front. Plant Sci. *9*.

Leibfried, A., To, J.P.C., Busch, W., Stehling, S., Kehle, A., Demar, M., Kieber, J.J., and Lohmann, J.U. (2005). WUSCHEL controls meristem function by direct regulation of cytokinin-inducible response regulators. Nature *438*, 1172.

Lenhard, M., Jürgens, G., and Laux, T. (2002). The WUSCHEL and SHOOTMERISTEMLESS genes fulfil complementary roles in Arabidopsis shoot meristem regulation. Development *129*, 3195–3206.

León-Martínez, G., and Vielle-Calzada, J.-P. (2019). Chapter Twenty - Apomixis in flowering plants: Developmental and evolutionary considerations. In Current Topics in Developmental Biology, U. Grossniklaus, ed. (Academic Press), pp. 565–604.

Lepiniec, L., Devic, M., Roscoe, T.J., Bouyer, D., Zhou, D.-X., Boulard, C., Baud, S., and Dubreucq, B. (2018). Molecular and epigenetic regulations and functions of the LAFL transcriptional regulators that control seed development. Plant Reprod *31*, 291–307.

Li, H., Jiang, H., Bu, Q., Zhao, Q., Sun, J., Xie, Q., and Li, C. (2011). The Arabidopsis RING Finger E3 Ligase RHA2b Acts Additively with RHA2a in Regulating Abscisic Acid Signaling and Drought Response. Plant Physiology *156*, 550–563.

Li, H., Ye, K., Shi, Y., Cheng, J., Zhang, X., and Yang, S. (2017). BZR1 Positively Regulates Freezing Tolerance via CBF-Dependent and CBF-Independent Pathways in Arabidopsis. Molecular Plant *10*, 545–559.

Li, J., Han, Y., Zhao, Q., Li, C., Xie, Q., Chong, K., and Xu, Y. (2013). The E3 Ligase AtRDUF1 Positively Regulates Salt Stress Responses in Arabidopsis thaliana. PLOS ONE *8*, e71078.

Li, J., Dukowic-Schulze, S., Lindquist, I.E., Farmer, A.D., Kelly, B., Li, T., Smith, A.G., Retzel, E.F., Mudge, J., and Chen, C. (2015). The plant-specific protein FEHLSTART controls male meiotic entry, initializing meiotic synchronization in Arabidopsis. The Plant Journal *84*, 659–671.

Li, X.G., Su, Y.H., Zhao, X.Y., Li, W., Gao, X.Q., and Zhang, X.S. (2010). Cytokinin overproduction-caused alteration of flower development is partially mediated by CUC2 and CUC3 in Arabidopsis. Gene *450*, 109–120.

Li, X.-Y., Mantovani, R., Hooft van Huijsduijnen, R., Andre, I., Benoist, C., and Mathis, D. (1992). Evolutionary variation of the CCAAT-binding transcription factor NF-Y. Nucl Acids Res *20*, 1087–1091.

Lian, G., Ding, Z., Wang, Q., Zhang, D., and Xu, J. (2014). Origins and evolution of WUSCHEL-related homeobox protein family in plant kingdom. ScientificWorldJournal *2014*, 534140.

Liang, Y., Gao, Y., and Jones, A.M. (2017). Extra Large G-Protein Interactome Reveals Multiple Stress Response Function and Partner-Dependent XLG Subcellular Localization. Front. Plant Sci. *8*.

Lie, C., Kelsom, C., and Wu, X. (2012). WOX2 and STIMPY-LIKE/WOX8 promote cotyledon boundary formation in Arabidopsis. The Plant Journal *72*, 674–682.

Lincoln, C., Long, J., Yamaguchi, J., Serikawa, K., and Hake, S. (1994). A knotted1-like homeobox gene in Arabidopsis is expressed in the vegetative meristem and dramatically alters leaf morphology when overexpressed in transgenic plants. Plant Cell *6*, 1859–1876.

Liu, J., and Müller, B. (2017). Imaging TCSn::GFP, a Synthetic Cytokinin Reporter, in Arabidopsis thaliana. Methods Mol. Biol. *1497*, 81–90.

Liu, C., Xu, Z., and Chua, N. (1993). Auxin Polar Transport Is Essential for the Establishment of Bilateral Symmetry during Early Plant Embryogenesis. Plant Cell *5*, 621–630.

Liu, C., Zhu, C., and Zeng, H.M. (2016). Key KdSOC1 gene expression profiles during plantlet morphogenesis under hormone, photoperiod, and drought treatments. Genet Mol Res *15*.

Liu, G., David, B.T., Trawczynski, M., and Fessler, R.G. (2020a). Advances in Pluripotent Stem Cells: History, Mechanisms, Technologies, and Applications. Stem Cell Rev and Rep *16*, 3–32.

Liu, X., Dinh, T.T., Li, D., Shi, B., Li, Y., Cao, X., Guo, L., Pan, Y., Jiao, Y., and Chen, X. (2014). AUXIN RESPONSE FACTOR 3 integrates the functions of AGAMOUS and APETALA2 in floral meristem determinacy. The Plant Journal : For Cell and Molecular Biology *80*, 629.

Liu, X.X., Zhu, Y.X., Fang, X.Z., Ye, J.Y., Du, W.X., Zhu, Q.Y., Lin, X.Y., and Jin, C.W. (2020b). Ammonium aggravates salt stress in plants by entrapping them in a chloride over-accumulation state in an NRT1.1-dependent manner. Science of The Total Environment *746*, 141244.

Liu, Z., Yuan, L., Song, X., Yu, X., and Sundaresan, V. (2017). AHP2, AHP3, and AHP5 act downstream of CKI1 in Arabidopsis female gametophyte development. J Exp Bot *68*, 3365–3373.

Long, J.A., and Barton, M.K. (1998). The development of apical embryonic pattern in Arabidopsis. Development *125*, 3027–3035.

Long, J.A., Moan, E.I., Medford, J.I., and Barton, M.K. (1996). A member of the KNOTTED class of homeodomain proteins encoded by the STM gene of Arabidopsis. Nature *379*, 66–69.

Long, J.A., Ohno, C., Smith, Z.R., and Meyerowitz, E.M. (2006). TOPLESS Regulates Apical Embryonic Fate in Arabidopsis. Science *312*, 1520–1523.

Lotan, T., Ohto, M., Yee, K.M., West, M.A.L., Lo, R., Kwong, R.W., Yamagishi, K., Fischer, R.L., Goldberg, R.B., and Harada, J.J. (1998). Arabidopsis LEAFY COTYLEDON1 Is Sufficient to Induce Embryo Development in Vegetative Cells. Cell *93*, 1195–1205.

Louveaux, M., Julien, J.-D., Mirabet, V., Boudaoud, A., and Hamant, O. (2016). Cell division plane orientation based on tensile stress in Arabidopsis thaliana. PNAS *113*, E4294–E4303.

Lu, X., Li, X., Xie, D., Jiang, C., Wang, C., Li, L., Zhang, Y., Tian, H., Gao, H., and Wang, C. (2020). The Ca2+-regulated protein kinase CIPK1 integrates plant responses to phosphate deficiency in Arabidopsis thaliana. Plant Biology *22*, 753–760.

Luerßen, H., Kirik, V., Herrmann, P., and Miséra, S. (1998). FUSCA3 encodes a protein with a conserved VP1/ABI3-like B3 domain which is of functional importance for the regulation of seed maturation in Arabidopsis thaliana. The Plant Journal *15*, 755–764.

Lukowitz, W., Roeder, A., Parmenter, D., and Somerville, C. (2004). A MAPKK Kinase Gene Regulates Extra-Embryonic Cell Fate in Arabidopsis. Cell *116*, 109–119.

Luo, B., Xue, X.-Y., Hu, W.-L., Wang, L.-J., and Chen, X.-Y. (2007). An ABC Transporter Gene of Arabidopsis thaliana, AtWBC11, is Involved in Cuticle Development and Prevention of Organ Fusion. Plant Cell Physiol *48*, 1790–1802.

Luo, L., Zeng, J., Wu, H., Tian, Z., and Zhao, Z. (2018). A Molecular Framework for Auxin-Controlled Homeostasis of Shoot Stem Cells in Arabidopsis. Molecular Plant *11*, 899–913.

Luo, Y., Bi, T., Su, Z., Cui, X., and Lan, Q. (2014). Physiological response of Kalanchoe tubiflora leaves to drought stress and rewatering. Journal of Tropical and Subtropical Botany *22*, 391–398.

Luo, Y.L., Su, Z.L., Cui, X.L., and Lan, Q.Y. (2015). Water loss prevention plays a greater role than ROS scavenging in dehydration tolerance of Kalanchoe tubiflora epiphyllous buds. Israel Journal of Plant Sciences *62*, 153–159.

Lup, S.D., Tian, X., Xu, J., and Pérez-Pérez, J.M. (2016). Wound signaling of regenerative cell reprogramming. Plant Science *250*, 178–187.

Luschnig, C., and Vert, G. (2014). The dynamics of plant plasma membrane proteins: PINs and beyond. Development *141*, 2924–2938.

Lütken, H., Laura, M., Borghi, C., Ørgaard, M., Allavena, A., and Rasmussen, S.K. (2011). Expression of KxhKN4 and KxhKN5 genes in Kalanchoë blossfeldiana 'Molly' results in novel compact plant phenotypes: towards a cisgenesis alternative to growth retardants. Plant Cell Rep *30*, 2267–2279.

Lv, T., Li, X., Fan, T., Luo, H., Xie, C., Zhou, Y., and Tian, C. (2019). The Calmodulin-Binding Protein IQM1 Interacts with CATALASE2 to Affect Pathogen Defense. Plant Physiology *181*, 1314–1327.

Ma, H., McMullen, M.D., and Finer, J.J. (1994). Identification of a homeobox-containing gene with enhanced expression during soybean (Glycine max L.) somatic embryo development. Plant Mol. Biol. *24*, 465–473.

Ma, Y., Cao, J., Chen, Q., He, J., Liu, Z., Wang, J., Li, X., and Yang, Y. (2019). The Kinase CIPK11 Functions as a Negative Regulator in Drought Stress Response in Arabidopsis. International Journal of Molecular Sciences *20*, 2422.

Mähönen, A.P., Bishopp, A., Higuchi, M., Nieminen, K.M., Kinoshita, K., Törmäkangas, K., Ikeda, Y., Oka, A., Kakimoto, T., and Helariutta, Y. (2006). Cytokinin signaling and its inhibitor AHP6 regulate cell fate during vascular development. Science *311*, 94–98.

Malwattage, N.R.M., Garcia, T.M., Cushman, J.C., and Wone, B.W.M. (2020). Enhancing Abiotic Stress Response via a Kalanchoe fedtschenkoi NF-Y Transcription Factor in C3 Plants. The FASEB Journal *34*, 1–1.

Mara, C.D., and Irish, V.F. (2008). Two GATA Transcription Factors Are Downstream Effectors of Floral Homeotic Gene Action in Arabidopsis. Plant Physiology *147*, 707–718.

Marhavý, P., Duclercq, J., Weller, B., Feraru, E., Bielach, A., Offringa, R., Friml, J., Schwechheimer, C., Murphy, A., and Benková, E. (2014). Cytokinin Controls Polarity of PIN1-Dependent Auxin Transport during Lateral Root Organogenesis. Current Biology *24*, 1031–1037.

Marhavý, P., Montesinos, J.C., Abuzeineh, A., Damme, D.V., Vermeer, J.E.M., Duclercq, J., Rakusová, H., Nováková, P., Friml, J., Geldner, N., et al. (2016). Targeted cell elimination reveals an auxin-guided biphasic mode of lateral root initiation. Genes Dev. *30*, 471–483.

Márquez-López, R.E., Pérez-Hernández, C., Ku-González, Á., Galaz-Ávalos, R.M., and Loyola-Vargas, V.M. (2018). Localization and transport of indole-3-acetic acid during somatic embryogenesis in Coffea canephora. Protoplasma *255*, 695–708.

Marsch-Martinez, N., Greco, R., Van Arkel, G., Herrera-Estrella, L., and Pereira, A. (2002). Activation Tagging Using the En-I Maize Transposon System in Arabidopsis. Plant Physiol *129*, 1544–1556.

Marsch-Martínez, N., Ramos-Cruz, D., Reyes-Olalde, J.I., Lozano-Sotomayor, P., Zúñiga-Mayo, V.M., and Folter, S. de (2012). The role of cytokinin during Arabidopsis gynoecia and fruit morphogenesis and patterning. The Plant Journal *72*, 222–234.

Martin-Rivilla, H., Garcia-Villaraco, A., Ramos-Solano, B., Gutierrez-Mañero, F.J., and Lucas, J.A. (2019). Extracts from cultures of Pseudomonas fluorescens induce defensive patterns of gene expression and enzyme activity while depressing visible injury and reactive oxygen species in Arabidopsis thaliana challenged with pathogenic Pseudomonas syringae. AoB PLANTS *11*.

Mashiguchi, K., Tanaka, K., Sakai, T., Sugawara, S., Kawaide, H., Natsume, M., Hanada, A., Yaeno, T., Shirasu, K., Yao, H., et al. (2011). The main auxin biosynthesis pathway in Arabidopsis. Proc. Natl. Acad. Sci. U.S.A. *108*, 18512–18517.

Matthes, M.S., Best, N.B., Robil, J.M., Malcomber, S., Gallavotti, A., and McSteen, P. (2019). Auxin EvoDevo: Conservation and Diversification of Genes Regulating Auxin Biosynthesis, Transport, and Signaling. Molecular Plant *12*, 298–320.

Mattsson, J., Ckurshumova, W., and Berleth, T. (2003). Auxin Signaling in Arabidopsis Leaf Vascular Development. Plant Physiol *131*, 1327–1339.

Mayer, K.F., Schoof, H., Haecker, A., Lenhard, M., Jürgens, G., and Laux, T. (1998). Role of WUSCHEL in regulating stem cell fate in the Arabidopsis shoot meristem. Cell *95*, 805–815.

de Meeûs, T., Prugnolle, F., and Agnew, P. (2007). Asexual reproduction: genetics and evolutionary aspects. Cell. Mol. Life Sci. *64*, 1355–1372.

Meinke, D.W. (1992). A Homoeotic Mutant of Arabidopsis thaliana with Leafy Cotyledons. Science *258*, 1647–1650.

Meinke, D.W., Franzmann, L.H., Nickle, T.C., and Yeung, E.C. (1994). Leafy Cotyledon Mutants of Arabidopsis. The Plant Cell *6*, 1049–1064.

Melzer, S., Lens, F., Gennen, J., Vanneste, S., Rohde, A., and Beeckman, T. (2008). Flowering-time genes modulate meristem determinacy and growth form in Arabidopsis thaliana. Nat Genet *40*, 1489–1492.

Meng, W.J., Cheng, Z.J., Sang, Y.L., Zhang, M.M., Rong, X.F., Wang, Z.W., Tang, Y.Y., and Zhang, X.S. (2017). Type-B ARABIDOPSIS RESPONSE REGULATORs Specify the Shoot Stem Cell Niche by Dual Regulation of WUSCHEL. Plant Cell *29*, 1357–1372.

Michalczuk, L., Cooke, T.J., and Cohen, J.D. (1992). Auxin levels at different stages of carrot somatic embryogenesis. Phytochemistry *31*, 1097–1103.

Mirabet, V., Das, P., Boudaoud, A., and Hamant, O. (2011). The role of mechanical forces in plant morphogenesis. Annu Rev Plant Biol *62*, 365–385.

Mittler, R., Kim, Y., Song, L., Coutu, J., Coutu, A., Ciftci-Yilmaz, S., Lee, H., Stevenson, B., and Zhu, J.-K. (2006). Gain- and loss-of-function mutations in Zat10 enhance the tolerance of plants to abiotic stress. FEBS Letters *580*, 6537–6542.

Miyawaki, K., Matsumoto-Kitano, M., and Kakimoto, T. (2004). Expression of cytokinin biosynthetic isopentenyltransferase genes in Arabidopsis: tissue specificity and regulation by auxin, cytokinin, and nitrate. The Plant Journal *37*, 128–138.

Mochizuki, S., Sugimoto, K., Koeduka, T., and Matsui, K. (2016). Arabidopsis lipoxygenase 2 is essential for formation of green leaf volatiles and five-carbon volatiles. FEBS Letters *590*, 1017–1027.

Möller, B., and Weijers, D. (2009). Auxin Control of Embryo Patterning. Cold Spring Harb Perspect Biol *1*.

Monshausen, G.B., and Gilroy, S. (2009). Feeling green: mechanosensing in plants. Trends in Cell Biology *19*, 228–235.

Monshausen, G.B., and Haswell, E.S. (2013). A force of nature: molecular mechanisms of mechanoperception in plants. J Exp Bot *64*, 4663–4680.

Moon, J., Suh, S.-S., Lee, H., Choi, K.-R., Hong, C.B., Paek, N.-C., Kim, S.-G., and Lee, I. (2003). The SOC1 MADS-box gene integrates vernalization and gibberellin signals for flowering in Arabidopsis. Plant J. *35*, 613–623.

Morales, G., Campillo, G., Vélez, E., Osorio, J., Urquijo, J., and Andrés Velásquez, Á. (2019). Green synthesis of magnetic nanoparticles using leaf extracts of *Aloe vera* and *Kalanchoe daigremontiana* to remove divalent mercury from natural waters. J. Phys.: Conf. Ser. *1247*, 012021.

Moreira, S., Bishopp, A., Carvalho, H., and Campilho, A. (2013). AHP6 inhibits cytokinin signaling to regulate the orientation of pericycle cell division during lateral root initiation. PLoS ONE *8*, e56370.

Moubayidin, L., Perilli, S., Dello Ioio, R., Di Mambro, R., Costantino, P., and Sabatini, S. (2010). The rate of cell differentiation controls the Arabidopsis root meristem growth phase. Curr. Biol. *20*, 1138–1143.

Moulia, B., Coutand, C., and Julien, J.-L. (2015). Mechanosensitive control of plant growth: bearing the load, sensing, transducing, and responding. Front. Plant Sci. *6*.

Moulton, K., Diaz, S., Strother, A., and Hancock, C.N. (2020). A partial T-DNA insertion near KNAT1 results in lobed Arabidopsis thaliana leaves. MicroPublication Biology *2020*.

Moussu, S., Doll, N.M., Chamot, S., Brocard, L., Creff, A., Fourquin, C., Widiez, T., Nimchuk, Z.L., and Ingram, G. (2017). ZHOUPI and KERBEROS Mediate Embryo/Endosperm Separation by Promoting the Formation of an Extracuticular Sheath at the Embryo Surface. The Plant Cell *29*, 1642–1656.

Mozgová, I., Muñoz-Viana, R., and Hennig, L. (2017). PRC2 Represses Hormone-Induced Somatic Embryogenesis in Vegetative Tissue of Arabidopsis thaliana. PLOS Genetics *13*, e1006562.

Mravec, J., Skůpa, P., Bailly, A., Hoyerová, K., Krecek, P., Bielach, A., Petrásek, J., Zhang, J., Gaykova, V., Stierhof, Y.-D., et al. (2009). Subcellular homeostasis of phytohormone auxin is mediated by the ER-localized PIN5 transporter. Nature *459*, 1136–1140.

Mu, J., Tan, H., Zheng, Q., Fu, F., Liang, Y., Zhang, J., Yang, X., Wang, T., Chong, K., Wang, X.-J., et al. (2008). LEAFY COTYLEDON1 is a key regulator of fatty acid biosynthesis in Arabidopsis. Plant Physiol *148*, 1042–1054.

Müller, B., and Sheen, J. (2008). Cytokinin and auxin interplay in root stem-cell specification during early embryogenesis. Nature *453*, 1094–1097.

Müller, C.J., Larsson, E., Spíchal, L., and Sundberg, E. (2017). Cytokinin-Auxin Crosstalk in the Gynoecial Primordium Ensures Correct Domain Patterning. Plant Physiology *175*, 1144–1157.

Müller, R., Bleckmann, A., and Simon, R. (2008). The receptor kinase CORYNE of Arabidopsis transmits the stem cell-limiting signal CLAVATA3 independently of CLAVATA1. Plant Cell *20*, 934–946.

Murray, J.A.H., Jones, A., Godin, C., and Traas, J. (2012). Systems Analysis of Shoot Apical Meristem Growth and Development: Integrating Hormonal and Mechanical Signaling. The Plant Cell *24*, 3907–3919.

Musielak, T.J., and Bayer, M. (2014). YODA signalling in the early Arabidopsis embryo. Biochem Soc Trans *42*, 408–412.

Nagasawa, N., Miyoshi, M., Kitano, H., Satoh, H., and Nagato, Y. (1996). Mutations associated with floral organ number in rice. Planta *198*, 627–633.

Nakabayashi, K., Okamoto, M., Koshiba, T., Kamiya, Y., and Nambara, E. (2005). Genome-wide profiling of stored mRNA in Arabidopsis thaliana seed germination: epigenetic and genetic regulation of transcription in seed. Plant J *41*, 697–709.

Nakajima, K., Sena, G., Nawy, T., and Benfey, P.N. (2001). Intercellular movement of the putative transcription factor SHR in root patterning. Nature *413*, 307.

Nakayama, N., Smith, R.S., Mandel, T., Robinson, S., Kimura, S., Boudaoud, A., and Kuhlemeier, C. (2012). Mechanical Regulation of Auxin-Mediated Growth. Current Biology *22*, 1468–1476.

Nambara, E., Naito, S., and McCourt, P. (1992). A mutant of Arabidopsis which is defective in seed development and storage protein accumulation is a new abi3 allele. The Plant Journal *2*, 435–441.

Neff, M.M., Nguyen, S.M., Malancharuvil, E.J., Fujioka, S., Noguchi, T., Seto, H., Tsubuki, M., Honda, T., Takatsuto, S., Yoshida, S., et al. (1999). BAS1: A gene regulating brassinosteroid levels and light responsiveness in Arabidopsis. PNAS *96*, 15316–15323.

Negi, J., Hashimoto-Sugimoto, M., Kusumi, K., and Iba, K. (2014). New Approaches to the Biology of Stomatal Guard Cells. Plant Cell Physiol *55*, 241–250.

Neiman, M., Sharbel, T.F., and Schwander, T. (2014). Genetic causes of transitions from sexual reproduction to asexuality in plants and animals. J. Evol. Biol. *27*, 1346–1359.

Nelson, D.C., Riseborough, J.-A., Flematti, G.R., Stevens, J., Ghisalberti, E.L., Dixon, K.W., and Smith, S.M. (2009). Karrikins discovered in smoke trigger Arabidopsis seed germination by a mechanism requiring gibberellic acid synthesis and light. Plant Physiol. *149*, 863–873.

Neu, A., Eilbert, E., Asseck, L.Y., Slane, D., Henschen, A., Wang, K., Bürgel, P., Hildebrandt, M., Musielak, T.J., Kolb, M., et al. (2019). Constitutive signaling activity of a receptor-associated protein links fertilization with embryonic patterning in Arabidopsis thaliana. Proc Natl Acad Sci U S A *116*, 5795–5804.

Newton, M.A. (1995). Bootstrapping phylogenies: Large deviations and dispersion effects. Biometrika *83*, 315–328.

Nic-Can, G.I., López-Torres, A., Barredo-Pool, F., Wrobel, K., Loyola-Vargas, V.M., Rojas-Herrera, R., and De-la-Peña, C. (2013). New insights into somatic embryogenesis: leafy cotyledon1, baby boom1 and WUSCHEL-related homeobox4 are epigenetically regulated in Coffea canephora. PLoS One *8*, e72160.

Nic-Can, G.I., Avilez-Montalvo, J.R., Aviles-Montalvo, R.N., Márquez-López, R.E., Mellado-Mojica, E., Galaz-Ávalos, R.M., and Loyola-Vargas, V.M. (2016). The Relationship Between Stress and Somatic Embryogenesis. In Somatic Embryogenesis: Fundamental Aspects and Applications, V.M. Loyola-Vargas, and N. Ochoa-Alejo, eds. (Cham: Springer International Publishing), pp. 151–170.

Nick, P., and Opatrny, Z. (2014). Applied Plant Cell Biology: Cellular Tools and Approaches for Plant Biotechnology (Springer Science & Business Media).

Nieminen, K., Blomster, T., Helariutta, Y., and Mähönen, A.P. (2015). Vascular Cambium Development. Arabidopsis Book *13*.

Niklas, K.J., and Cobb, E.D. (2017). The evolutionary ecology (evo-eco) of plant asexual reproduction. Evol Ecol *31*, 317–332.

Nikovics, K., Blein, T., Peaucelle, A., Ishida, T., Morin, H., Aida, M., and Laufs, P. (2006). The balance between the MIR164A and CUC2 genes controls leaf margin serration in Arabidopsis. Plant Cell *18*, 2929–2945.

Nilsson, A.K., Fahlberg, P., Johansson, O.N., Hamberg, M., Andersson, M.X., and Ellerström, M. (2016). The activity of HYDROPEROXIDE LYASE 1 regulates accumulation of galactolipids containing 12-oxo-phytodienoic acid in Arabidopsis. J Exp Bot *67*, 5133–5144.

Nimchuk, Z.L. (2017). CLAVATA1 controls distinct signaling outputs that buffer shoot stem cell proliferation through a two-step transcriptional compensation loop. PLOS Genetics *13*, e1006681.

Nimchuk, Z.L., Zhou, Y., Tarr, P.T., Peterson, B.A., and Meyerowitz, E.M. (2015). Plant stem cell maintenance by transcriptional cross-regulation of related receptor kinases. Development *142*, 1043–1049.

Niu, W.-T., Han, X.-W., Wei, S.-S., Shang, Z.-L., Wang, J., Yang, D.-W., Fan, X., Gao, F., Zheng, S.-Z., Bai, J.-T., et al. (2020). Arabidopsis cyclic nucleotide-gated channel 6 is negatively modulated by multiple calmodulin isoforms during heat shock. J Exp Bot *71*, 90–104.

Nonogaki, H. (2008). Seed Germination and Reserve Mobilization. In ELS, (American Cancer Society), p.

Novák, O., Napier, R., and Ljung, K. (2017). Zooming In on Plant Hormone Analysis: Tissue- and Cell-Specific Approaches. Annual Review of Plant Biology *68*, 323–348.

Obaid, O.H., Reddy, S.K., and Sridhar, S. (2019). CALLUS INDUCTION AND PLANT REGENERATION FROM BRYOPHYLLUM LEAVES AND SALT STRESS EFFECT ON CALLUS CONTENT OF BRYOPHILIN A AND BRYOPHILIN C. 1483–1485.

Oberhauser, A.F., Marszalek, P.E., Erickson, H.P., and Fernandez, J.M. (1998). The molecular elasticity of the extracellular matrix protein tenascin. Nature *393*, 181.

Ogawa, M., Shinohara, H., Sakagami, Y., and Matsubayashi, Y. (2008). Arabidopsis CLV3 peptide directly binds CLV1 ectodomain. Science *319*, 294.

Ohashi-Ito, K., and Bergmann, D.C. (2007). Regulation of the Arabidopsis root vascular initial population by LONESOME HIGHWAY. Development *134*, 2959–2968.

Okada, K., Ueda, J., Komaki, M.K., Bell, C.J., and Shimura, Y. (1991). Requirement of the Auxin Polar Transport System in Early Stages of Arabidopsis Floral Bud Formation. The Plant Cell *3*, 677–684.

Ó'Maoiléidigh, D.S., Stewart, D., Zheng, B., Coupland, G., and Wellmer, F. (2018). Floral homeotic proteins modulate the genetic program for leaf development to suppress trichome formation in flowers. Development *145*.

Omelyanchuk, N.A., Kovrizhnykh, V.V., Oshchepkova, E.A., Pasternak, T., Palme, K., and Mironova, V.V. (2016). A detailed expression map of the PIN1 auxin transporter in Arabidopsis thaliana root. BMC Plant Biology *16*, 5.

O'Neill, J.P., Colon, K.T., and Jenik, P.D. (2019). The onset of embryo maturation in Arabidopsis is determined by its developmental stage and does not depend on endosperm cellularization. The Plant Journal *99*, 286–301.

Orłowska, A., and Kępczyńska, E. (2018). Identification of Polycomb Repressive Complex1, Trithorax group genes and their simultaneous expression with WUSCHEL, WUSCHEL-related Homeobox5 and SHOOT MERISTEMLESS during the induction phase of somatic embryogenesis in Medicago truncatula Gaertn. Plant Cell Tiss Organ Cult *134*, 345–356.

Orłowska, A., Igielski, R., Łagowska, K., and Kępczyńska, E. (2017). Identification of LEC1, L1L and Polycomb Repressive Complex 2 genes and their expression during the induction phase of Medicago truncatula Gaertn. somatic embryogenesis. Plant Cell Tiss Organ Cult *129*, 119–132.

Orr, A.W., Helmke, B.P., Blackman, B.R., and Schwartz, M.A. (2006). Mechanisms of Mechanotransduction. Developmental Cell *10*, 11–20.

Osmond, C.B., and Allaway, W.G. (1974). Pathways of CO2 Fixation in the CAM Plant Kalanchoe daigremontiana. I Patterns of 14CO2 Fixation in the Light. Functional Plant Biol. *1*, 503–511.

Osnato, M., Castillejo, C., Matías-Hernández, L., and Pelaz, S. (2012). TEMPRANILLO genes link photoperiod and gibberellin pathways to control flowering in Arabidopsis. Nature Communications *3*, 808.

Osnato, M., Cereijo, U., Sala, J., Matías-Hernández, L., Aguilar-Jaramillo, A.E., Rodríguez-Goberna, M.R., Riechmann, J.L., Rodríguez-Concepción, M., and Pelaz, S. (2020). The floral repressors TEMPRANILLO1 and 2 modulate salt tolerance by regulating hormonal components and photo-protection in *Arabidopsis*. Plant J tpj.15048.

Ottoline Leyser, H.M., and Furner, I.J. (1992). Characterisation of three shoot apical meristem mutants of Arabidopsis thaliana. Development *116*, 397–403.

Ozias-Akins, P., and Conner, J.A. (2020). Clonal Reproduction through Seeds in Sight for Crops. Trends in Genetics *36*, 215–226.

Pagnussat, G.C., Yu, H.-J., Ngo, Q.A., Rajani, S., Mayalagu, S., Johnson, C.S., Capron, A., Xie, L.-F., Ye, D., and Sundaresan, V. (2005). Genetic and molecular identification of genes required for female gametophyte development and function in Arabidopsis. Development *132*, 603–614.

Palovaara, J., and Hakman, I. (2008). Conifer WOX-related homeodomain transcription factors, developmental consideration and expression dynamic of WOX2 during Picea abies somatic embryogenesis. Plant Mol Biol *66*, 533–549.

Palovaara, J., Hallberg, H., Stasolla, C., and Hakman, I. (2010). Comparative expression pattern analysis of WUSCHEL-related homeobox 2 (WOX2) and WOX8/9 in developing seeds and somatic embryos of the gymnosperm Picea abies. The New Phytologist *188*, 122–135.

Pandey, D.K., and Chaudhary, B. (2014). Oxidative Stress Responsive SERK1 Gene Directs the Progression of Somatic Embryogenesis in Cotton (Gossypium hirsutum L. cv. Coker 310). American Journal of Plant Sciences *5*, 80–102.

Panikashvili, D., Savaldi-Goldstein, S., Mandel, T., Yifhar, T., Franke, R.B., Höfer, R., Schreiber, L., Chory, J., and Aharoni, A. (2007). The Arabidopsis DESPERADO/AtWBC11 Transporter Is Required for Cutin and Wax Secretion. Plant Physiology *145*, 1345–1360.

Panikashvili, D., Shi, J.X., Bocobza, S., Franke, R.B., Schreiber, L., and Aharoni, A. (2010). The Arabidopsis DSO/ABCG11 transporter affects cutin metabolism in reproductive organs and suberin in roots. Mol Plant *3*, 563–575.

Parcy, F., Valon, C., Raynal, M., Gaubier-Comella, P., Delseny, M., and Giraudat, J. (1994). Regulation of gene expression programs during Arabidopsis seed development: roles of the ABI3 locus and of endogenous abscisic acid. Plant Cell *6*, 1567–1582.

Parcy, F., Valon, C., Kohara, A., Miséra, S., and Giraudat, J. (1997). The ABSCISIC ACID-INSENSITIVE3, FUSCA3, and LEAFY COTYLEDON1 loci act in concert to control multiple aspects of Arabidopsis seed development. Plant Cell *9*, 1265–1277.

Paredez, A.R., Somerville, C.R., and Ehrhardt, D.W. (2006). Visualization of cellulose synthase demonstrates functional association with microtubules. Science *312*, 1491–1495.

Pasternak, T.P., Prinsen, E., Ayaydin, F., Miskolczi, P., Potters, G., Asard, H., Van Onckelen, H.A., Dudits, D., and Fehér, A. (2002). The Role of Auxin, pH, and Stress in the Activation of Embryogenic Cell Division in Leaf Protoplast-Derived Cells of Alfalfa. Plant Physiology *129*, 1807–1819.

Paterson, K.E., and Rost, T.L. (1979). Effects of Light and Hormones on Regeneration of Crassula argentea from Leaves. American Journal of Botany *66*, 463–470.

Pavlović, M., and Radotić, K. (2017). Lateral Meristems. In Animal and Plant Stem Cells: Concepts, Propagation and Engineering, M. Pavlović, and K. Radotić, eds. (Cham: Springer International Publishing), pp. 179–180.

Pearson, W.R. (2013). An Introduction to Sequence Similarity ("Homology") Searching. Curr Protoc Bioinformatics *0 3*.

Peaucelle, A., Braybrook, S.A., Le Guillou, L., Bron, E., Kuhlemeier, C., and Höfte, H. (2011). Pectin-Induced Changes in Cell Wall Mechanics Underlie Organ Initiation in Arabidopsis. Current Biology *21*, 1720–1726.

Peer, W.A., Hosein, F.N., Bandyopadhyay, A., Makam, S.N., Otegui, M.S., Lee, G.-J., Blakeslee, J.J., Cheng, Y., Titapiwatanakun, B., Yakubov, B., et al. (2009). Mutation of the Membrane-Associated M1 Protease APM1 Results in Distinct Embryonic and Seedling Developmental Defects in Arabidopsis. The Plant Cell *21*, 1693–1721.

Pelletier, J.M., Kwong, R.W., Park, S., Le, B.H., Baden, R., Cagliari, A., Hashimoto, M., Munoz, M.D., Fischer, R.L., Goldberg, R.B., et al. (2017). LEC1 sequentially regulates the transcription of genes involved in diverse developmental processes during seed development. PNAS *114*, E6710–E6719.

Perez-Garcia, P., and Moreno-Risueno, M.A. (2018). Stem cells and plant regeneration. Developmental Biology *442*, 3–12.

Perilli, S., Di Mambro, R., and Sabatini, S. (2012). Growth and development of the root apical meristem. Current Opinion in Plant Biology *15*, 17–23.

Pescador, R., Kerbauy, G.B., de Melo Ferreira, W., Purgatto, E., Suzuki, R.M., and Guerra, M.P. (2012). A hormonal misunderstanding in Acca sellowiana embryogenesis: levels of zygotic embryogenesis do not match those of somatic embryogenesis. Plant Growth Regul *68*, 67–76.

Peters, W.S., and Tomos, A.D. (1996). The History of Tissue Tension. Annals of Botany *77*, 657–665.

Petersen, L.N., Ingle, R.A., Knight, M.R., and Denby, K.J. (2009). OXI1 protein kinase is required for plant immunity against Pseudomonas syringae in Arabidopsis. J Exp Bot *60*, 3727–3735.

Pignocchi, C., Minns, G.E., Nesi, N., Koumproglou, R., Kitsios, G., Benning, C., Lloyd, C.W., Doonan, J.H., and Hills, M.J. (2009). ENDOSPERM DEFECTIVE1 Is a Novel Microtubule-Associated Protein Essential for Seed Development in Arabidopsis. The Plant Cell *21*, 90–105.

Pinon, V., Prasad, K., Grigg, S.P., Sanchez-Perez, G.F., and Scheres, B. (2013). Local auxin biosynthesis regulation by PLETHORA transcription factors controls phyllotaxis in Arabidopsis. PNAS *110*, 1107–1112.

Poethig, R.S., and Sussex, I.M. (1985). The developmental morphology and growth dynamics of the tobacco leaf. Planta *165*, 158–169.

Pogson, B.J., and Morris, S.C. (2004). 22 - Postharvest Senescence of Vegetables and its Regulation. In Plant Cell Death Processes, L.D. Noodén, ed. (San Diego: Academic Press), pp. 319–329.

Poirier, B.C., Feldman, M.J., and Lange, B.M. (2018). bHLH093/NFL and bHLH061 are required for apical meristem function in Arabidopsis thaliana. Plant Signaling & Behavior *13*, e1486146.

Powikrowska, M., Oetke, S., Jensen, P.E., and Krupinska, K. (2014). Dynamic composition, shaping and organization of plastid nucleoids. Front Plant Sci *5*.

Prát, T., Hajný, J., Grunewald, W., Vasileva, M., Molnár, G., Tejos, R., Schmid, M., Sauer, M., and Friml, J. (2018). WRKY23 is a component of the transcriptional network mediating auxin feedback on PIN polarity. PLOS Genetics *14*, e1007177.

Prigge, M.J., Otsuga, D., Alonso, J.M., Ecker, J.R., Drews, G.N., and Clark, S.E. (2005). Class III homeodomain-leucine zipper gene family members have overlapping, antagonistic, and distinct roles in Arabidopsis development. Plant Cell *17*, 61–76.

Prokchorchik, M., Choi, S., Chung, E.-H., Won, K., Dangl, J.L., and Sohn, K.H. (2020). A host target of a bacterial cysteine protease virulence effector plays a key role in convergent evolution of plant innate immune system receptors. New Phytologist *225*, 1327–1342.

Pulianmackal, A.J., Kareem, A.V.K., Durgaprasad, K., Trivedi, Z.B., and Prasad, K. (2014). Competence and regulatory interactions during regeneration in plants. Front Plant Sci *5*.

Putz, N. (1996). Underground plant movement. III. The corm of Sauromatum guttatum (Wall.) Schott (Araceae). Flora : Morphologie, Geobotanik, Oekophysiologie.

Qin, Y., Leydon, A.R., Manziello, A., Pandey, R., Mount, D., Denic, S., Vasic, B., Johnson, M.A., and Palanivelu, R. (2009). Penetration of the Stigma and Style Elicits a Novel Transcriptome in Pollen Tubes, Pointing to Genes Critical for Growth in a Pistil. PLOS Genetics *5*, e1000621.

Rabas, A.R., and Martin, C.E. (2003). Movement of Water from Old to Young Leaves in Three Species of Succulents. Ann Bot *92*, 529–536.

Rademacher, E.H., Möller, B., Lokerse, A.S., Llavata-Peris, C.I., van den Berg, W., and Weijers, D. (2011). A cellular expression map of the Arabidopsis AUXIN RESPONSE FACTOR gene family. Plant J *68*, 597–606.

Radoeva, T., and Weijers, D. (2014). A roadmap to embryo identity in plants. Trends in Plant Science *19*, 709–716.

Radoeva, T., Lokerse, A.S., Llavata-Peris, C.I., Wendrich, J.R., Xiang, D., Liao, C.-Y., Vlaar, L., Boekschoten, M., Hooiveld, G., Datla, R., et al. (2019). A Robust Auxin Response Network Controls Embryo and Suspensor Development through a Basic Helix Loop Helix Transcriptional Module. Plant Cell *31*, 52–67.

Ramírez-Mosqueda, M.A., Iglesias-Andreu, L.G., Sáenz, L., and Córdova, I. (2018). Preliminary molecular detection of the somatic embryogenesis receptor-like kinase (VpSERK) and knotted-like homeobox (VpKNOX1) genes during in vitro morphogenesis of Vanilla planifolia Jacks. 3 Biotech *8*, 94.

Ramiro, D.A., Melotto-Passarin, D.M., Barbosa, M. de A., Santos, F. dos, Gomez, S.G.P., Júnior, N.S.M., Lam, E., and Carrer, H. (2016). Expression of Arabidopsis Bax Inhibitor-1 in transgenic sugarcane confers drought tolerance. Plant Biotechnology Journal *14*, 1826–1837.

Rautiainen, P., Koivula, K., and Hyvärinen, M. (2004). The effect of within-genet and between-genet competition on sexual reproduction and vegetative spread in Potentilla anserina ssp. egedii. Journal of Ecology *92*, 505–511.

Ray, S.K., Macoy, D.M., Kim, W.-Y., Lee, S.Y., and Kim, and M.G. (2019). Role of RIN4 in Regulating PAMP-Triggered Immunity and Effector-Triggered Immunity: Current Status and Future Perspectives. Molecules and Cells *42*, 503–511.

Regla-Márquez, C.F., Avilés-Viñas, S.A., Canto-Flick, A., Muñoz-Ramírez, L.S., Peña-Yam, L.P., Valle-Gough, R.E., Osorio-Montalvo, P.M., Pérez-Pastrana, J., and Santana-Buzzy, N. (2019). Genes involved in the deformations of the shoot apical meristem in somatic embryos of Capsicum chinense Jacq. J. Genet. *98*.

Reinhardt, D., Mandel, T., and Kuhlemeier, C. (2000). Auxin Regulates the Initiation and Radial Position of Plant Lateral Organs. The Plant Cell *12*, 507–518.

Reinhardt, D., Pesce, E.-R., Stieger, P., Mandel, T., Baltensperger, K., Bennett, M., Traas, J., Friml, J., and Kuhlemeier, C. (2003). Regulation of phyllotaxis by polar auxin transport. Nature *426*, 255–260.

Reinhart, B.J., Liu, T., Newell, N.R., Magnani, E., Huang, T., Kerstetter, R., Michaels, S., and Barton, M.K. (2013). Establishing a framework for the Ad/abaxial regulatory network of Arabidopsis: ascertaining targets of class III homeodomain leucine zipper and KANADI regulation. Plant Cell *25*, 3228–3249.

Reis, P.A.B., Carpinetti, P.A., Freitas, P.P.J., Santos, E.G.D., Camargos, L.F., Oliveira, I.H.T., Silva, J.C.F., Carvalho, H.H., Dal-Bianco, M., Soares-Ramos, J.R.L., et al. (2016). Functional and regulatory conservation of the soybean ER stress-induced DCD/NRP-mediated cell death signaling in plants. BMC Plant Biology *16*, 156.

Rentel, M.C., Lecourieux, D., Ouaked, F., Usher, S.L., Petersen, L., Okamoto, H., Knight, H., Peck, S.C., Grierson, C.S., Hirt, H., et al. (2004). OXI1 kinase is necessary for oxidative burst-mediated signalling in Arabidopsis. Nature *427*, 858–861.

Replogle, A., Wang, J., Bleckmann, A., Hussey, R.S., Baum, T.J., Sawa, S., Davis, E.L., Wang, X., Simon, R., and Mitchum, M.G. (2011). Nematode CLE signaling in Arabidopsis requires CLAVATA2 and CORYNE. The Plant Journal *65*, 430–440.

de Reuille, P.B., Bohn-Courseau, I., Ljung, K., Morin, H., Carraro, N., Godin, C., and Traas, J. (2006). Computer simulations reveal properties of the cell-cell signaling network at the shoot apex in Arabidopsis. Proc Natl Acad Sci U S A *103*, 1627–1632.

Reyes-Olalde, J.I., Zúñiga-Mayo, V.M., Serwatowska, J., Montes, R.A.C., Lozano-Sotomayor, P., Herrera-Ubaldo, H., Gonzalez-Aguilera, K.L., Ballester, P., Ripoll, J.J., Ezquer, I., et al. (2017). The bHLH transcription factor SPATULA enables cytokinin signaling, and both activate auxin biosynthesis and transport genes at the medial domain of the gynoecium. PLOS Genetics *13*, e1006726.

Ribnicky, D.M., Cohen, J.D., Hu, W.-S., and Cooke, T.J. (2002). An auxin surge following fertilization in carrots: a mechanism for regulating plant totipotency. Planta *214*, 505–509.

Ribot, C., Zimmerli, C., Farmer, E.E., Reymond, P., and Poirier, Y. (2008). Induction of the Arabidopsis PHO1;H10 Gene by 12-Oxo-Phytodienoic Acid But Not Jasmonic Acid via a CORONATINE INSENSITIVE1-Dependent Pathway. Plant Physiology *147*, 696–706.

Richter, R., Bastakis, E., and Schwechheimer, C. (2013). Cross-Repressive Interactions between SOC1 and the GATAs GNC and GNL/CGA1 in the Control of Greening, Cold Tolerance, and Flowering Time in Arabidopsis. Plant Physiology *162*, 1992–2004.

Richter, R., Kinoshita, A., Vincent, C., Martinez-Gallegos, R., Gao, H., Driel, A.D. van, Hyun, Y., Mateos, J.L., and Coupland, G. (2019). Floral regulators FLC and SOC1 directly regulate expression of the B3-type transcription factor TARGET OF FLC AND SVP 1 at the Arabidopsis shoot apex via antagonistic chromatin modifications. PLOS Genetics *15*, e1008065.

Riefler, M., Novak, O., Strnad, M., and Schmülling, T. (2006). Arabidopsis Cytokinin Receptor Mutants Reveal Functions in Shoot Growth, Leaf Senescence, Seed Size, Germination, Root Development, and Cytokinin Metabolism. The Plant Cell *18*, 40–54.

Robert, X., and Gouet, P. (2014). Deciphering key features in protein structures with the new ENDscript server. Nucleic Acids Research *42*, W320–W324.

Robert, H.S., Grones, P., Stepanova, A.N., Robles, L.M., Lokerse, A.S., Alonso, J.M., Weijers, D., and Friml, J. (2013). Local Auxin Sources Orient the Apical-Basal Axis in Arabidopsis Embryos. Current Biology *23*, 2506–2512.

Robert, H.S., Grunewald, W., Sauer, M., Cannoot, B., Soriano, M., Swarup, R., Weijers, D., Bennett, M., Boutilier, K., and Friml, J. (2015a). Plant embryogenesis requires AUX/LAX-mediated auxin influx. Development *142*, 702–711.

Robert, H.S., Crhak Khaitova, L., Mroue, S., and Benková, E. (2015b). The importance of localized auxin production for morphogenesis of reproductive organs and embryos in Arabidopsis. Journal of Experimental Botany *66*, 5029–5042.

Robert, H.S., Park, C., Gutièrrez, C.L., Wójcikowska, B., Pěnčík, A., Novák, O., Chen, J., Grunewald, W., Dresselhaus, T., Friml, J., et al. (2018). Maternal auxin supply contributes to early embryo patterning in Arabidopsis. Nature Plants *4*, 548–553.

Rocha, D., and Carnier Dornelas, M. (2013). Molecular overview on plant somatic embryogenesis.

Rodriguez, L., Gonzalez-Guzman, M., Diaz, M., Rodrigues, A., Izquierdo-Garcia, A.C., Peirats-Llobet, M., Fernandez, M.A., Antoni, R., Fernandez, D., Marquez, J.A., et al. (2014). C2-Domain Abscisic Acid-Related Proteins Mediate the Interaction of PYR/PYL/RCAR Abscisic Acid Receptors with the Plasma Membrane and Regulate Abscisic Acid Sensitivity in Arabidopsis. The Plant Cell *26*, 4802–4820.

Rodríguez-Garay, B., J, G.-H., and Jm, R.-D. (2014). K. daigremontiana as a Model Plant for the Study of Auxin Effects in Plant Morphology. Journal of Plant Biochemistry & Physiology *2*.

Rojo, E., Sharma, V.K., Kovaleva, V., Raikhel, N.V., and Fletcher, J.C. (2002). CLV3 Is Localized to the Extracellular Space, Where It Activates the Arabidopsis CLAVATA Stem Cell Signaling Pathway. Plant Cell *14*, 969–977.

Rolland-Lagan, A.-G., Bangham, J.A., and Coen, E. (2003). Growth dynamics underlying petal shape and asymmetry. Nature *422*, 161.

Rong, X.F., Sang, Y.L., Wang, L., Meng, W.J., Zou, C.H., Dong, Y.X., Bie, X.M., Cheng, Z.J., and Zhang, X.S. (2018). Type-B ARRs Control Carpel Regeneration Through Mediating AGAMOUS Expression in Arabidopsis. Plant and Cell Physiology *59*, 761.

Rosspopoff, O., Chelysheva, L., Saffar, J., Lecorgne, L., Gey, D., Caillieux, E., Colot, V., Roudier, F., Hilson, P., Berthomé, R., et al. (2017). Direct conversion of root primordium into shoot meristem relies on timing of stem cell niche development. Development *144*, 1187–1200.

Ruberti, C., Lai, Y., and Brandizzi, F. (2018). Recovery from temporary endoplasmic reticulum stress in plants relies on the tissue-specific and largely independent roles of bZIP28 and bZIP60, as well as an antagonizing function of BAX-Inhibitor 1 upon the pro-adaptive signaling mediated by bZIP28. The Plant Journal *93*, 155–165.

Rupp, H.-M., Frank, M., Werner, T., Strnad, M., and Schmulling, T. (1999). Increased steady state mRNA levels of the STM and KNAT1 homeobox genes in cytokinin overproducing Arabidopsis thaliana indicate a role for cytokinins in the shoot apical meristem. The Plant Journal *18*, 557–563.

Sabatini, S., Heidstra, R., Wildwater, M., and Scheres, B. (2003). SCARECROW is involved in positioning the stem cell niche in the Arabidopsis root meristem. Genes Dev *17*, 354–358.

Saini, K., AbdElgawad, H., Markakis, M.N., Schoenaers, S., Asard, H., Prinsen, E., Beemster, G.T.S., and Vissenberg, K. (2017). Perturbation of Auxin Homeostasis and Signaling by PINOID Overexpression Induces Stress Responses in Arabidopsis. Front. Plant Sci. *8*.

Sakai, H., Aoyama, T., and Oka, A. (2000). Arabidopsis ARR1 and ARR2 response regulators operate as transcriptional activators. The Plant Journal *24*, 703–711.

Sakakibara, H. (2005). Cytokinin Biosynthesis and Regulation. In Vitamins & Hormones, G. Litwack, ed. (Academic Press), pp. 271–287.

Sakamoto, H., Maruyama, K., Sakuma, Y., Meshi, T., Iwabuchi, M., Shinozaki, K., and Yamaguchi-Shinozaki, K. (2004). Arabidopsis Cys2/His2-Type Zinc-Finger Proteins Function as Transcription Repressors under Drought, Cold, and High-Salinity Stress Conditions. Plant Physiology *136*, 2734–2746.

Santa-Catarina, C., de Oliveira, R.R., Cutri, L., Floh, E.I.S., and Dornelas, M.C. (2012). WUSCHEL-related genes are expressed during somatic embryogenesis of the basal angiosperm Ocotea catharinensis Mez. (Lauraceae). Trees *26*, 493–501.

Santos-Mendoza, M., Dubreucq, B., Baud, S., Parcy, F., Caboche, M., and Lepiniec, L. (2008). Deciphering gene regulatory networks that control seed development and maturation in Arabidopsis. Plant J. *54*, 608–620.

Savatin, D.V., Gramegna, G., Modesti, V., and Cervone, F. (2014). Wounding in the plant tissue: the defense of a dangerous passage. Front. Plant Sci. *5*.

Savini, G., Giorgi, V., Scarano, E., and Neri, D. (2008). Strawberry plant relationship through the stolon. Physiologia Plantarum *134*, 421–429.

Sawhney, S., Bansal, A., and Sawhney, N. (1994). Epiphyllous bud differentiation in Kalanchoe pinnata: a model developmental system. Indian Journal of Plant Physiology *37*, 229–236.

Scala, A., Mirabella, R., Mugo, C., Matsui, K., Haring, M.A., and Schuurink, R.C. (2013). E-2-hexenal promotes susceptibility to Pseudomonas syringae by activating jasmonic acid pathways in Arabidopsis. Front. Plant Sci. *4*.

Scarpella, E., Marcos, D., Friml, J., and Berleth, T. (2006). Control of leaf vascular patterning by polar auxin transport. Genes & Development *20*, 1015–1027.

Schaller, G.E., Kieber, J.J., and Shiu, S.-H. (2008). Two-Component Signaling Elements and Histidyl-Aspartyl Phosphorelays†. Arabidopsis Book *6*.

Schlereth, A., Möller, B., Liu, W., Kientz, M., Flipse, J., Rademacher, E.H., Schmid, M., Jürgens, G., and Weijers, D. (2010). MONOPTEROS controls embryonic root initiation by regulating a mobile transcription factor. Nature *464*, 913–916.

Schmid, M., Davison, T.S., Henz, S.R., Pape, U.J., Demar, M., Vingron, M., Schölkopf, B., Weigel, D., and Lohmann, J.U. (2005). A gene expression map of Arabidopsis thaliana development. Nat Genet *37*, 501–506.

Schmidt, A. (2020). Controlling Apomixis: Shared Features and Distinct Characteristics of Gene Regulation. Genes *11*, 329.

Schoof, H., Lenhard, M., Haecker, A., Mayer, K.F.X., Jürgens, G., and Laux, T. (2000). The Stem Cell Population of Arabidopsis Shoot Meristems Is Maintained by a Regulatory Loop between the CLAVATA and WUSCHEL Genes. Cell *100*, 635–644.

Schweighofer, A., Hirt, H., and Meskiene, I. (2004). Plant PP2C phosphatases: emerging functions in stress signaling. Trends in Plant Science *9*, 236–243.

Scofield, S., Dewitte, W., and Murray, J.A.H. (2007). The KNOX gene SHOOT MERISTEMLESS is required for the development of reproductive meristematic tissues in Arabidopsis. Plant J. *50*, 767–781.

Scofield, S., Dewitte, W., and Murray, J.A. (2014). STM sustains stem cell function in the Arabidopsis shoot apical meristem and controls KNOX gene expression independently of the transcriptional repressor AS1. Plant Signal Behav *9*.

Seltmann, M.A., Stingl, N.E., Lautenschlaeger, J.K., Krischke, M., Mueller, M.J., and Berger, S. (2010). Differential Impact of Lipoxygenase 2 and Jasmonates on Natural and Stress-Induced Senescence in Arabidopsis. Plant Physiology *152*, 1940–1950.

Sengupta, S., Ray, A., Mandal, D., and Nag Chaudhuri, R. (2020). ABI3 mediated repression of RAV1 gene expression promotes efficient dehydration stress response in Arabidopsis thaliana. Biochimica et Biophysica Acta (BBA) - Gene Regulatory Mechanisms *1863*, 194582.

Sgamma, T., Jackson, A., Muleo, R., Thomas, B., and Massiah, A. (2014). TEMPRANILLO is a regulator of juvenility in plants. Scientific Reports *4*, 3704.

Shani, E., Ben-Gera, H., Shleizer-Burko, S., Burko, Y., Weiss, D., and Ori, N. (2010). Cytokinin Regulates Compound Leaf Development in Tomato[C][W]. Plant Cell *22*, 3206–3217.

Sharma, N., Xin, R., Kim, D.-H., Sung, S., Lange, T., and Huq, E. (2016). NO FLOWERING IN SHORT DAY (NFL) is a bHLH transcription factor that promotes flowering specifically under short-day conditions in Arabidopsis. Development *143*, 682–690.

Shi, B., Guo, X., Wang, Y., Xiong, Y., Wang, J., Hayashi, K., Lei, J., Zhang, L., and Jiao, Y. (2018). Feedback from Lateral Organs Controls Shoot Apical Meristem Growth by Modulating Auxin Transport. Developmental Cell *44*, 204-216.e6.

Shinohara, H., and Matsubayashi, Y. (2015). Reevaluation of the CLV3-receptor interaction in the shoot apical meristem: dissection of the CLV3 signaling pathway from a direct ligand-binding point of view. The Plant Journal *82*, 328–336.

Shumbe, L., Chevalier, A., Legeret, B., Taconnat, L., Monnet, F., and Havaux, M. (2016). Singlet Oxygen-Induced Cell Death in Arabidopsis under High-Light Stress Is Controlled by OXI1 Kinase. Plant Physiology *170*, 1757–1771.

Silvertown, J. (2008). The Evolutionary Maintenance of Sexual Reproduction: Evidence from the Ecological Distribution of Asexual Reproduction in Clonal Plants. International Journal of Plant Sciences *169*, 157–168.

Singh, P., Dave, A., Vaistij, F.E., Worrall, D., Holroyd, G.H., Wells, J.G., Kaminski, F., Graham, I.A., and Roberts, M.R. (2017). Jasmonic acid-dependent regulation of seed dormancy following maternal herbivory in Arabidopsis. New Phytologist *214*, 1702–1711.

Skalák, J., Vercruyssen, L., Claeys, H., Hradilová, J., Černý, M., Novák, O., Plačková, L., Saiz-Fernández, I., Skaláková, P., Coppens, F., et al. (2019). Multifaceted activity of cytokinin in leaf development shapes its size and structure in Arabidopsis. The Plant Journal *97*, 805–824.

Skoog, F., and Miller, C.O. (1957). Chemical regulation of growth and organ formation in plant tissues cultured in vitro. Symp. Soc. Exp. Biol. *11*, 118–130.

Slack, J.M. (2017). Animal regeneration: ancestral character or evolutionary novelty? EMBO Reports *18*, 1497–1508.

Sloan, J., Hakenjos, J.P., Gebert, M., Ermakova, O., Gumiero, A., Stier, G., Wild, K., Sinning, I., and Lohmann, J.U. (2020). Structural basis for the complex DNA binding behavior of the plant stem cell regulator WUSCHEL. Nature Communications *11*, 2223.

Smaczniak, C., Immink, R.G.H., Angenent, G.C., and Kaufmann, K. (2012). Developmental and evolutionary diversity of plant MADS-domain factors: insights from recent studies. Development *139*, 3081–3098.

Smertenko, A., and Bozhkov, P.V. (2014). Somatic embryogenesis: life and death processes during apical-basal patterning. J Exp Bot *65*, 1343–1360.

Smet, I.D., Lau, S., Mayer, U., and Jürgens, G. (2010). Embryogenesis – the humble beginnings of plant life. The Plant Journal *61*, 959–970.

Smith, Z.R., and Long, J.A. (2010). Control of Arabidopsis apical–basal embryo polarity by antagonistic transcription factors. Nature *464*, 423–426.

Smith, G.F., Figueiredo, E., and Wyk, A.E. van (2019). Kalanchoe (Crassulaceae) in Southern Africa: Classification, Biology, and Cultivation (Academic Press).

Smith, L.G., Greene, B., Veit, B., and Hake, S. (1992). A dominant mutation in the maize homeobox gene, Knotted-1, causes its ectopic expression in leaf cells with altered fates. Development *116*, 21–30.

Smith, L.G., Jackson, D., and Hake, S. (1995). Expression of knotted1 marks shoot meristem formation during maize embryogenesis. Developmental Genetics *16*, 344–348.

Smith, R.S., Guyomarc'h, S., Mandel, T., Reinhardt, D., Kuhlemeier, C., and Prusinkiewicz, P. (2006). A plausible model of phyllotaxis. Proc Natl Acad Sci U S A *103*, 1301–1306.

Sogabe, S., Hatleberg, W.L., Kocot, K.M., Say, T.E., Stoupin, D., Roper, K.E., Fernandez-Valverde, S.L., Degnan, S.M., and Degnan, B.M. (2019). Pluripotency and the origin of animal multicellularity. Nature *570*, 519–522.

Soltis, P.S., and Soltis, D.E. (2003). Applying the Bootstrap in Phylogeny Reconstruction. Statistical Science *18*, 256–267.

Somssich, M., Je, B.I., Simon, R., and Jackson, D. (2016). CLAVATA-WUSCHEL signaling in the shoot meristem. Development *143*, 3238–3248.

Song, C., Je, J., Hong, J.K., and Lim, C.O. (2014). Ectopic expression of an Arabidopsis dehydration-responsive element-binding factor DREB2C improves salt stress tolerance in crucifers. Plant Cell Rep *33*, 1239–1254.

Spears, B.J., Howton, T.C., Gao, F., Garner, C.M., Mukhtar, M.S., and Gassmann, W. (2019). Direct Regulation of the EFR-Dependent Immune Response by Arabidopsis TCP Transcription Factors. Molecular Plant-Microbe Interactions.

Spinelli, S.V., Martin, A.P., Viola, I.L., Gonzalez, D.H., and Palatnik, J.F. (2011). A Mechanistic Link between STM and CUC1 during Arabidopsis Development1[C][W][OA]. Plant Physiol *156*, 1894–1904.

Ståldal, V., Cierlik, I., Chen, S., Landberg, K., Baylis, T., Myrenås, M., Sundström, J.F., Eklund, D.M., Ljung, K., and Sundberg, E. (2012). The Arabidopsis thaliana transcriptional activator STYLISH1 regulates genes affecting stamen development, cell expansion and timing of flowering. Plant Mol Biol *78*, 545–559.

Steiner, E., Israeli, A., Gupta, R., Shwartz, I., Nir, I., Leibman-Markus, M., Tal, L., Farber, M., Amsalem, Z., Ori, N., et al. (2020). Characterization of the cytokinin sensor TCSv2 in arabidopsis and tomato. Plant Methods *16*, 152.

Stepanova, A.N., Yun, J., Robles, L.M., Novak, O., He, W., Guo, H., Ljung, K., and Alonso, J.M. (2011). The Arabidopsis YUCCA1 flavin monooxygenase functions in the indole-3-pyruvic acid branch of auxin biosynthesis. Plant Cell *23*, 3961–3973.

Steynen, Q., and Schultz, E. (2003). The FORKED genes are essential for distal vein meeting in Arabidopsis. Development (Cambridge, England) *130*, 4695–4708.

Stone, S.L., Kwong, L.W., Yee, K.M., Pelletier, J., Lepiniec, L., Fischer, R.L., Goldberg, R.B., and Harada, J.J. (2001). LEAFY COTYLEDON2 encodes a B3 domain transcription factor that induces embryo development. PNAS *98*, 11806–11811.

Stone, S.L., Braybrook, S.A., Paula, S.L., Kwong, L.W., Meuser, J., Pelletier, J., Hsieh, T.-F., Fischer, R.L., Goldberg, R.B., and Harada, J.J. (2008). Arabidopsis LEAFY COTYLEDON2 induces maturation traits and auxin activity: Implications for somatic embryogenesis. Proc Natl Acad Sci U S A *105*, 3151–3156.

Strader, L.C., and Bartel, B. (2008). A new path to auxin. Nature Chemical Biology *4*, 337–339.

Su, Y.H., Zhao, X.Y., Liu, Y.B., Zhang, C.L., O'Neill, S.D., and Zhang, X.S. (2009). Auxin-induced WUS expression is essential for embryonic stem cell renewal during somatic embryogenesis in Arabidopsis. Plant J *59*, 448–460.

Su, Y.H., Liu, Y.B., Bai, B., and Zhang, X.S. (2015). Establishment of embryonic shoot–root axis is involved in auxin and cytokinin response during Arabidopsis somatic embryogenesis. Front. Plant Sci. *5*.

Su, Y.H., Zhou, C., Li, Y.J., Yu, Y., Tang, L.P., Zhang, W.J., Yao, W.J., Huang, R., Laux, T., and Zhang, X.S. (2020). Integration of pluripotency pathways regulates stem cell maintenance in the Arabidopsis shoot meristem. PNAS *117*, 22561–22571.

Sun, B., and Ito, T. (2015). Regulation of floral stem cell termination in Arabidopsis. Front. Plant Sci. *6*.

Suzaki, T., Sato, M., Ashikari, M., Miyoshi, M., Nagato, Y., and Hirano, H.-Y. (2004). The gene FLORAL ORGAN NUMBER1 regulates floral meristem size in rice and encodes a leucine-rich repeat receptor kinase orthologous to Arabidopsis CLAVATA1. Development *131*, 5649–5657.

Suzuki, M., and McCarty, D.R. (2008). Functional symmetry of the B3 network controlling seed development. Curr Opin Plant Biol *11*, 548–553.

Suzuki, M., Kao, C.Y., and McCarty, D.R. (1997). The conserved B3 domain of VIVIPAROUS1 has a cooperative DNA binding activity. Plant Cell *9*, 799–807.

Suzuki, T., Sakurai, K., Imamura, A., NAKAMURA, A., Ueguchi, C., and Mizuno, T. (2000). Compilation and Characterization of Histidine-Containing Phosphotransmitters Implicated in His-to-Asp Phosphorelay in Plants: AHP Signal Transducers of Arabidopsis thaliana. Bioscience, Biotechnology, and Biochemistry *64*, 2486–2489.

Swaminathan, K., Peterson, K., and Jack, T. (2008). The plant B3 superfamily. Trends in Plant Science *13*, 647–655.

Takada, S., Hibara, K., Ishida, T., and Tasaka, M. (2001). The CUP-SHAPED COTYLEDON1 gene of Arabidopsis regulates shoot apical meristem formation. Development *128*, 1127–1135.

Takahashi, M., and Mikami, K. (2017). Oxidative Stress Promotes Asexual Reproduction and Apogamy in the Red Seaweed Pyropia yezoensis. Front. Plant Sci. *8*.

Tamaki, T., Kubo, S., Shimomura, K., and Umehara, M. (2020). Effects of Gibberellin and Abscisic Acid on Asexual Reproduction from Graptopetalum paraguayense Leaves. Journal of Plant Growth Regulation 1–8.

Tan, W.-J., Yang, Y.-C., Zhou, Y., Huang, L.-P., Xu, L., Chen, Q.-F., Yu, L.-J., and Xiao, S. (2018). DIACYLGLYCEROL ACYLTRANSFERASE and DIACYLGLYCEROL KINASE Modulate Triacylglycerol and Phosphatidic Acid Production in the Plant Response to Freezing Stress. Plant Physiology *177*, 1303–1318.

Tan, X., Meyers, B.C., Kozik, A., West, M.A., Morgante, M., St Clair, D.A., Bent, A.F., and Michelmore, R.W. (2007). Global expression analysis of nucleotide binding site-leucine rich repeat-encoding and related genes in Arabidopsis. BMC Plant Biology *7*, 56.

Tang, L.P., Zhang, X.S., and Su, Y.H. (2020). Regulation of cell reprogramming by auxin during somatic embryogenesis. ABIOTECH *1*, 185–193.

Tao, J., Sun, H., Gu, P., Liang, Z., Chen, X., Lou, J., Xu, G., and Zhang, Y. (2017). A sensitive synthetic reporter for visualizing cytokinin signaling output in rice. Plant Methods *13*.

Tao, Y., Ferrer, J.-L., Ljung, K., Pojer, F., Hong, F., Long, J.A., Li, L., Moreno, J.E., Bowman, M.E., Ivans, L.J., et al. (2008). Rapid Synthesis of Auxin via a New Tryptophan-Dependent Pathway Is Required for Shade Avoidance in Plants. Cell *133*, 164–176.

Tejos, R., Rodriguez-Furlán, C., Adamowski, M., Sauer, M., Norambuena, L., and Friml, J. (2018). PATELLINS are regulators of auxin-mediated PIN1 relocation and plant development in Arabidopsis thaliana. J Cell Sci *131*.

Theissen, G., Kim, J.T., and Saedler, H. (1996). Classification and phylogeny of the MADS-box multigene family suggest defined roles of MADS-box gene subfamilies in the morphological evolution of eukaryotes. J. Mol. Evol. *43*, 484–516.

Thomas, C., Bronner, R., Molinier, J., Prinsen, E., van Onckelen, H., and Hahne, G. (2002). Immuno-cytochemical localization of indole-3-acetic acid during induction of somatic embryogenesis in cultured sunflower embryos. Planta *215*, 577–583.

Tian, R., Paul, P., Joshi, S., and Perry, S.E. (2020a). Genetic activity during early plant embryogenesis. Biochemical Journal *477*, 3743–3767.

Tian, R., Wang, F., Zheng, Q., Niza, V.M.A.G.E., Downie, A.B., and Perry, S.E. (2020b). Direct and indirect targets of the arabidopsis seed transcription factor ABSCISIC ACID INSENSITIVE3. The Plant Journal *103*, 1679–1694.

To, A., Valon, C., Savino, G., Guilleminot, J., Devic, M., Giraudat, J., and Parcy, F. (2006). A network of local and redundant gene regulation governs Arabidopsis seed maturation. Plant Cell *18*, 1642–1651.

Torres-Galea, P., Hirtreiter, B., and Bolle, C. (2013). Two GRAS Proteins, SCARECROW-LIKE21 and PHYTOCHROME A SIGNAL TRANSDUCTION1, Function Cooperatively in Phytochrome A Signal Transduction. Plant Physiology *161*, 291–304.

Trainin, T., Bar-Ya'akov, I., and Holland, D. (2013). ParSOC1, a MADS-box gene closely related to Arabidopsis AGL20/SOC1, is expressed in apricot leaves in a diurnal manner and is linked with chilling requirements for dormancy break. Tree Genetics & Genomes *9*, 753–766.

Truscott, M., and Nepveu, A. (2006). Homeodomains. In Encyclopedic Reference of Genomics and Proteomics in Molecular Medicine, (Berlin, Heidelberg: Springer), pp. 806–813.

Tsuchiya, Y., Nambara, E., Naito, S., and McCourt, P. (2004). The FUS3 transcription factor functions through the epidermal regulator TTG1 during embryogenesis in Arabidopsis. The Plant Journal *37*, 73–81.

Tsuwamoto, R., Fukuoka, H., and Takahata, Y. (2008). GASSHO1 and GASSHO2 encoding a putative leucine-rich repeat transmembrane-type receptor kinase are essential for the normal development of the epidermal surface in Arabidopsis embryos. The Plant Journal *54*, 30–42.

Tucker, M., Hinze, A., Tucker, E., Takada, S., Jürgens, G., and Laux, T. (2008). Vascular signalling mediated by ZWILLE potentiates WUSCHEL function during shoot meristem stem cell development in the Arabidopsis embryo. Development (Cambridge, England) *135*, 2839–2843.

Turk, E.M., Fujioka, S., Seto, H., Shimada, Y., Takatsuto, S., Yoshida, S., Wang, H., Torres, Q.I., Ward, J.M., Murthy, G., et al. (2005). BAS1 and SOB7 act redundantly to modulate Arabidopsis photomorphogenesis via unique brassinosteroid inactivation mechanisms. The Plant Journal *42*, 23–34.

Tvorogova, V.E., and Lutova, L.A. (2018). Genetic Regulation of Zygotic Embryogenesis in Angiosperm Plants. Russ J Plant Physiol *65*, 1–14.

Tvorogova, V.E., Lebedeva, M.A., and Lutova, L.A. (2015). Expression of WOX and PIN genes during somatic and zygotic embryogenesis in Medicago truncatula. Russ J Genet *51*, 1189–1198.

Uc-Chuc, M.A., Pérez-Hernández, C., Galaz-Ávalos, R.M., Brito-Argaez, L., Aguilar-Hernández, V., and Loyola-Vargas, V.M. (2020). YUCCA-Mediated Biosynthesis of the Auxin IAA Is Required during the Somatic Embryogenic Induction Process in Coffea canephora. International Journal of Molecular Sciences *21*, 4751.

Ueda, M., Zhang, Z., and Laux, T. (2011). Transcriptional Activation of Arabidopsis Axis Patterning Genes WOX8/9 Links Zygote Polarity to Embryo Development. Developmental Cell *20*, 264–270.

Ueda, M., Aichinger, E., Gong, W., Groot, E., Verstraeten, I., Vu, L.D., De Smet, I., Higashiyama, T., Umeda, M., and Laux, T. (2017). Transcriptional integration of paternal and maternal factors in the Arabidopsis zygote. Genes Dev *31*, 617–627.

Ulmasov, T., Hagen, G., and Guilfoyle, T.J. (1997a). ARF1, a transcription factor that binds to auxin response elements. Science *276*, 1865–1868.

Ulmasov, T., Murfett, J., Hagen, G., and Guilfoyle, T.J. (1997b). Aux/IAA proteins repress expression of reporter genes containing natural and highly active synthetic auxin response elements. The Plant Cell *9*, 1963–1971.

Vaishak, K.P., Yadukrishnan, P., Bakshi, S., Kushwaha, A.K., Ramachandran, H., Job, N., Babu, D., and Datta, S. (2019). The B-box bridge between light and hormones in plants. Journal of Photochemistry and Photobiology B: Biology *191*, 164–174.

Vanhaelewyn, L., Van Der Straeten, D., De Coninck, B., and Vandenbussche, F. (2020). Ultraviolet Radiation From a Plant Perspective: The Plant-Microorganism Context. Front. Plant Sci. *11*.

Vaughan-Hirsch, J., Tallerday, E.J., Burr, C.A., Hodgens, C., Boeshore, S.L., Beaver, K., Melling, A., Sari, K., Kerr, I.D., Šimura, J., et al. (2021). Function of the pseudo phosphotransfer proteins has diverged between rice and Arabidopsis. The Plant Journal *106*, 159–173.

Veale, D.J.H., Furman, K.I., and Oliver, D.W. (1992). South African traditional herbal medicines used during pregnancy and childbirth. Journal of Ethnopharmacology *36*, 185–191.

Venglat, S.P., Dumonceaux, T., Rozwadowski, K., Parnell, L., Babic, V., Keller, W., Martienssen, R., Selvaraj, G., and Datla, R. (2002). The homeobox gene BREVIPEDICELLUS is a key regulator of inflorescence architecture in Arabidopsis. Proc Natl Acad Sci U S A *99*, 4730–4735.

Verdeil, J.-L., Alemanno, L., Niemenak, N., and Tranbarger, T.J. (2007). Pluripotent versus totipotent plant stem cells: dependence versus autonomy? Trends Plant Sci. *12*, 245–252.

Verma, V., Sivaraman, J., and Kumar, P.P. (2013). Expression, purification, and characterization of cytokinin signaling intermediates: Arabidopsis histidine phosphotransfer protein 1 (AHP1) and AHP2. Plant Cell Rep *32*, 795–805.

Vermeer, J.E.M., Wangenheim, D. von, Barberon, M., Lee, Y., Stelzer, E.H.K., Maizel, A., and Geldner, N. (2014). A Spatial Accommodation by Neighboring Cells Is Required for Organ Initiation in Arabidopsis. Science *343*, 178–183.

Vernoux, T., Kronenberger, J., Grandjean, O., Laufs, P., and Traas, J. (2000). PIN-FORMED 1 regulates cell fate at the periphery of the shoot apical meristem. Development *127*, 5157–5165.

Vernoux, T., Brunoud, G., Farcot, E., Morin, V., Van den Daele, H., Legrand, J., Oliva, M., Das, P., Larrieu, A., Wells, D., et al. (2011). The auxin signalling network translates dynamic input into robust patterning at the shoot apex. Mol Syst Biol *7*, 508.

Viana, M.J., and Nováis, M.C. (1970). Influence of different light conditions on hormonal control of leaf-embryo development in Bryophyllum. Portugaliae Acta Biologica, Serie A. Morfologia, fisiologia, genetica e biologia geral *11*, 373–384.

Vogler, H., Felekis, D., Nelson, B.J., and Grossniklaus, U. (2015). Measuring the Mechanical Properties of Plant Cell Walls. Plants *4*, 167–182.

Vondrakova, Z., Dobrev, P.I., Pesek, B., Fischerova, L., Vagner, M., and Motyka, V. (2018). Profiles of Endogenous Phytohormones Over the Course of Norway Spruce Somatic Embryogenesis. Front Plant Sci *9*, 1283.

Voogd, C., Wang, T., and Varkonyi-Gasic, E. (2015). Functional and expression analyses of kiwifruit SOC1-like genes suggest that they may not have a role in the transition to flowering but may affect the duration of dormancy. J Exp Bot *66*, 4699–4710.

de Vries, S.C., and Weijers, D. (2017). Plant embryogenesis. Current Biology *27*, R870–R873.

Wang, F., and Perry, S.E. (2013). Identification of Direct Targets of FUSCA3, a Key Regulator of Arabidopsis Seed Development. Plant Physiology *161*, 1251–1264.

Wang, S., and Schiefelbein, J. (2014). Regulation of cell fate determination in plants. Front Plant Sci *5*.

Wang, F.-X., Shang, G.-D., Wu, L.-Y., Xu, Z.-G., Zhao, X.-Y., and Wang, J.-W. (2020a). Chromatin Accessibility Dynamics and a Hierarchical Transcriptional Regulatory Network Structure for Plant Somatic Embryogenesis. Developmental Cell *54*, 742-757.e8.

Wang, G., Ellendorff, U., Kemp, B., Mansfield, J.W., Forsyth, A., Mitchell, K., Bastas, K., Liu, C.-M., Woods-Tör, A., Zipfel, C., et al. (2008). A Genome-Wide Functional Investigation into the Roles of Receptor-Like Proteins in Arabidopsis. Plant Physiology *147*, 503–517.

Wang, G., Long, Y., Thomma, B.P.H.J., Wit, P.J.G.M. de, Angenent, G.C., and Fiers, M. (2010a). Functional Analyses of the CLAVATA2-Like Proteins and Their Domains That Contribute to CLAVATA2 Specificity. Plant Physiology *152*, 320–331.

Wang, G., Fiers, M., Ellendorff, U., Wang, Z., Wit, P.J.G.M. de, Angenent, G.C., and Thomma, B.P.H.J. (2010b). The Diverse Roles of Extracellular Leucine-rich Repeat-containing Receptor-like Proteins in Plants. Critical Reviews in Plant Sciences *29*, 285–299.

Wang, H., Ngwenyama, N., Liu, Y., Walker, J.C., and Zhang, S. (2007). Stomatal development and patterning are regulated by environmentally responsive mitogen-activated protein kinases in Arabidopsis. Plant Cell *19*, 63–73.

Wang, J., Tian, C., Zhang, C., Shi, B., Cao, X., Zhang, T.-Q., Zhao, Z., Wang, J.-W., and Jiao, Y. (2017). Cytokinin Signaling Activates WUSCHEL Expression during Axillary Meristem Initiation. Plant Cell *29*, 1373–1387.

Wang, K., Chen, H., Miao, Y., and Bayer, M. (2020b). Square one: zygote polarity and early embryogenesis in flowering plants. Current Opinion in Plant Biology *53*, 128–133.

Wang, Q., Kohlen, W., Rossmann, S., Vernoux, T., and Theres, K. (2014a). Auxin Depletion from the Leaf Axil Conditions Competence for Axillary Meristem Formation in *Arabidopsis* and Tomato. Plant Cell *26*, 2068–2079.

Wang, W., Xu, B., Wang, H., Li, J., Huang, H., and Xu, L. (2011). YUCCA Genes Are Expressed in Response to Leaf Adaxial-Abaxial Juxtaposition and Are Required for Leaf Margin Development. Plant Physiology *157*, 1805–1819.

Wang, W., Li, X., Zhu, M., Tang, X., Wang, Z., Guo, K., Zhou, Y., Sun, Y., Zhang, W., and Li, X. (2019). Arabidopsis GAAP1 to GAAP3 Play Redundant Role in Cell Death Inhibition by Suppressing the Upregulation of Salicylic Acid Pathway Under Endoplasmic Reticulum Stress. Front. Plant Sci. *10*.

Wang, X.-Q., Xu, W.-H., Ma, L.-G., Fu, Z.-M., Deng, X.-W., Li, J.-Y., and Wang, Y.-H. (2006). Requirement of KNAT1/BP for the Development of Abscission Zones in Arabidopsis thaliana. Journal of Integrative Plant Biology *48*, 15–26.

Wang, Y., Wang, J., Shi, B., Yu, T., Qi, J., Meyerowitz, E.M., and Jiao, Y. (2014b). The Stem Cell Niche in Leaf Axils Is Established by Auxin and Cytokinin in *Arabidopsis*. Plant Cell *26*, 2055–2067.

Wang, Z., Gerstein, M., and Snyder, M. (2009). RNA-Seq: a revolutionary tool for transcriptomics. Nature Reviews Genetics *10*, 57–63.

Wang, Z., Ren, Z., Cheng, C., Wang, T., Ji, H., Zhao, Y., Deng, Z., Zhi, L., Lu, J., Wu, X., et al. (2020c). Counteraction of ABA-Mediated Inhibition of Seed Germination and Seedling Establishment by ABA Signaling Terminator in Arabidopsis. Molecular Plant *13*, 1284–1297.

Ward, J.A., Ponnala, L., and Weber, C.A. (2012). Strategies for transcriptome analysis in nonmodel plants. American Journal of Botany *99*, 267–276.

Warden, J. (1969). Leaf-embryo dormancy in Bryophyllum crenatum under short day conditions; blocking of the factors controlling cell division and morphogenesis. Portugaliae Acta Biologica. Serie A.

Wasternack, C. (2017). A plant's balance of growth and defense – revisited. New Phytologist *215*, 1291–1294.

Weigel, D., and Glazebrook, J. (2002). Quick DNA Prep for PCR. In Arabidopsis: A Laboratory Manual, (CSHL Press), pp. 168–169.

Weitbrecht, K., Müller, K., and Leubner-Metzger, G. (2011). First off the mark: early seed germination. J Exp Bot *62*, 3289–3309.

Werner, T., Motyka, V., Laucou, V., Smets, R., Van Onckelen, H., and Schmülling, T. (2003). Cytokinin-Deficient Transgenic Arabidopsis Plants Show Multiple Developmental Alterations Indicating Opposite Functions of Cytokinins in the Regulation of Shoot and Root Meristem Activity. The Plant Cell *15*, 2532–2550.

Werner, T., Köllmer, I., Bartrina, I., Holst, K., and Schmülling, T. (2006). New Insights into the Biology of Cytokinin Degradation. Plant Biology *8*, 371–381.

West, M., Yee, K.M., Danao, J., Zimmerman, J.L., Fischer, R.L., Goldberg, R.B., and Harada, J.J. (1994). LEAFY COTYLEDON1 Is an Essential Regulator of Late Embryogenesis and Cotyledon Identity in Arabidopsis. The Plant Cell *6*, 1731–1745.

Wickramasuriya, A.M., and Dunwell, J.M. (2015). Global scale transcriptome analysis of Arabidopsis embryogenesis in vitro. BMC Genomics *16*, 301.

Williams, L., and Fletcher, J.C. (2005). Stem cell regulation in the Arabidopsis shoot apical meristem. Curr. Opin. Plant Biol. *8*, 582–586.

Winkelmann, T. (2016). Somatic Versus Zygotic Embryogenesis: Learning from Seeds. Methods Mol Biol *1359*, 25–46.

Winkler, E., and Fischer, M. (2001). The role of vegetative spread and seed dispersal for optimal life histories of clonal plants: a simulation study. Evolutionary Ecology *15*, 281–301.

Winter, D., Vinegar, B., Nahal, H., Ammar, R., Wilson, G.V., and Provart, N.J. (2007). An "Electronic Fluorescent Pictograph" Browser for Exploring and Analyzing Large-Scale Biological Data Sets. PLOS ONE *2*, e718.

Wojciechowska, N., Sobieszczuk-Nowicka, E., and Bagniewska-Zadworna, A. (2018). Plant organ senescence – regulation by manifold pathways. Plant Biology *20*, 167–181.

Wójcik, A.M., Wójcikowska, B., and Gaj, M.D. (2020). Current Perspectives on the Auxin-Mediated Genetic Network that Controls the Induction of Somatic Embryogenesis in Plants. International Journal of Molecular Sciences *21*, 1333.

Wójcikowska, B., Jaskóła, K., Gąsiorek, P., Meus, M., Nowak, K., and Gaj, M.D. (2013). LEAFY COTYLEDON2 (LEC2) promotes embryogenic induction in somatic tissues of Arabidopsis, via YUCCA-mediated auxin biosynthesis. Planta *238*, 425–440.

Woodward, C., Bemis, S.M., Hill, E.J., Sawa, S., Koshiba, T., and Torii, K.U. (2005). Interaction of Auxin and ERECTA in Elaborating Arabidopsis Inflorescence Architecture Revealed by the Activation Tagging of a New Member of the YUCCA Family Putative Flavin Monooxygenases. Plant Physiology *139*, 192–203.

Wu, R., and Citovsky, V. (2017a). Adaptor proteins GIR1 and GIR2. I. Interaction with the repressor GLABRA2 and regulation of root hair development. Biochemical and Biophysical Research Communications *488*, 547–553.

Wu, R., and Citovsky, V. (2017b). Adaptor proteins GIR1 and GIR2. II. Interaction with the co-repressor TOPLESS and promotion of histone deacetylation of target chromatin. Biochemical and Biophysical Research Communications *488*, 609–613.

Wu, C.-C., Li, F.-W., and Kramer, E.M. (2019). Large-scale phylogenomic analysis suggests three ancient superclades of the WUSCHEL-RELATED HOMEOBOX transcription factor family in plants. PLOS ONE *14*, e0223521.

Wu, J., Liu, Z., Zhang, Z., Lv, Y., Yang, N., Zhang, G., Wu, M., Lv, S., Pan, L., Joosten, M.H.A.J., et al. (2016). Transcriptional regulation of receptor-like protein genes by environmental stresses and hormones and their overexpression activities in Arabidopsis thaliana. Journal of Experimental Botany *67*, 3339–3351.

Wu, X., Chory, J., and Weigel, D. (2007). Combinations of WOX activities regulate tissue proliferation during Arabidopsis embryonic development. Developmental Biology *309*, 306–316.

Wybouw, B., and Rybel, B.D. (2019). Cytokinin – A Developing Story. Trends in Plant Science *24*, 177–185.

Xiang, D., Yang, H., Venglat, P., Cao, Y., Wen, R., Ren, M., Stone, S., Wang, E., Wang, H., Xiao, W., et al. (2011). POPCORN Functions in the Auxin Pathway to Regulate Embryonic Body Plan and Meristem Organization in Arabidopsis. The Plant Cell *23*, 4348–4367.

Xiao, Y., Chen, Y., Ding, Y., Wu, J., Wang, P., Yu, Y., Wei, X., Wang, Y., Zhang, C., Li, F., et al. (2018). Effects of GhWUS from upland cotton (Gossypium hirsutum L.) on somatic embryogenesis and shoot regeneration. Plant Science *270*, 157–165.

Xie, M., Chen, H., Huang, L., O'Neil, R.C., Shokhirev, M.N., and Ecker, J.R. (2018). A B-ARR-mediated cytokinin transcriptional network directs hormone cross-regulation and shoot development. Nat Commun *9*, 1604.

Xing, Q., Creff, A., Waters, A., Tanaka, H., Goodrich, J., and Ingram, G.C. (2013). ZHOUPI controls embryonic cuticle formation via a signalling pathway involving the subtilisin protease ABNORMAL LEAF-SHAPE1 and the receptor kinases GASSHO1 and GASSHO2. Development *140*, 770–779.

Xu, J.-J., Zhang, X.-F., and Xue, H.-W. (2016). Rice aleurone layer specific OsNF-YB1 regulates grain filling and endosperm development by interacting with an ERF transcription factor. J Exp Bot *67*, 6399–6411.

Xu, W., Jia, L., Baluška, F., Ding, G., Shi, W., Ye, N., and Zhang, J. (2012). PIN2 is required for the adaptation of Arabidopsis roots to alkaline stress by modulating proton secretion. J Exp Bot *63*, 6105–6114.

Yadav, R.K., Tavakkoli, M., and Reddy, G.V. (2010). WUSCHEL mediates stem cell homeostasis by regulating stem cell number and patterns of cell division and differentiation of stem cell progenitors. Development *137*, 3581–3589.

Yadav, R.K., Perales, M., Gruel, J., Girke, T., Jönsson, H., and Reddy, G.V. (2011). WUSCHEL protein movement mediates stem cell homeostasis in the Arabidopsis shoot apex. Genes Dev *25*, 2025–2030.

Yadav, R.K., Perales, M., Gruel, J., Ohno, C., Heisler, M., Girke, T., Jönsson, H., and Reddy, G.V. (2013). Plant stem cell maintenance involves direct transcriptional repression of differentiation program. Mol Syst Biol *9*, 654.

Yamaguchi, I., Cohen, J.D., Culler, A.H., Quint, M., Slovin, J.P., Nakajima, M., Yamaguchi, S., Sakakibara, H., Kuroha, T., Hirai, N., et al. (2010). 4.02 - Plant Hormones. In Comprehensive Natural Products II, H.-W. (Ben) Liu, and L. Mander, eds. (Oxford: Elsevier), pp. 9–125.

Yamamoto, A., Yoshii, M., Murase, S., Fujita, M., Kurata, N., Hobo, T., Kagaya, Y., Takeda, S., and Hattori, T. (2014). Cell-by-cell developmental transition from embryo to post-germination phase revealed by heterochronic gene expression and ER-body formation in Arabidopsis leafy cotyledon mutants. Plant Cell Physiol *55*, 2112–2125.

Yanai, O., Shani, E., Dolezal, K., Tarkowski, P., Sablowski, R., Sandberg, G., Samach, A., and Ori, N. (2005). Arabidopsis KNOXI Proteins Activate Cytokinin Biosynthesis. Current Biology *15*, 1566–1571.

Yang, X., and Zhang, X. (2010). Regulation of Somatic Embryogenesis in Higher Plants. Critical Reviews in Plant Sciences *29*, 36–57.

Yang, Y.Y., and Kim, J.G. (2016). The optimal balance between sexual and asexual reproduction in variable environments: a systematic review. J Ecology Environ *40*, 12.

Yang, J., Duan, G., Li, C., Liu, L., Han, G., Zhang, Y., and Wang, C. (2019a). The Crosstalks Between Jasmonic Acid and Other Plant Hormone Signaling Highlight the Involvement of Jasmonic Acid as a Core Component in Plant Response to Biotic and Abiotic Stresses. Front Plant Sci *10*.

Yang, L., Guo, H., Liu, Y., Zhang, D., Liu, H., and Shen, H. (2020). Relationship between H2O2 accumulation and NO synthesis during osmotic stress: promoted somatic embryogenesis of Fraxinus mandshurica. J. For. Res.

Yang, Z., Wang, C., Xue, Y., Liu, X., Chen, S., Song, C., Yang, Y., and Guo, Y. (2019b). Calcium-activated 14-3-3 proteins as a molecular switch in salt stress tolerance. Nature Communications *10*, 1199.

Yao, J., and Waters, M.T. (2020). Perception of karrikins by plants: a continuing enigma. J Exp Bot *71*, 1774–1781.

Yarbrough, J.A. (1932). Anatomical and Developmental Studies of the Foliar Embryos of Bryophyllum calycinum. American Journal of Botany *19*, 443–453.

Yazgan, M., and Vardar, Y. (1977). Studies on the effects of auxin-kinetin applications on the epiphyllous budding of Bryophyllum daigremontianumBerg. Zeitschrift Für Pflanzenphysiologie *84*, 203–211.

Ye, B.-B., Shang, G.-D., Pan, Y., Xu, Z.-G., Zhou, C.-M., Mao, Y.-B., Bao, N., Sun, L., Xu, T., and Wang, J.-W. (2020). AP2/ERF Transcription Factors Integrate Age and Wound Signals for Root Regeneration. The Plant Cell *32*, 226–241.

Yi, H., Chen, Y., Wang, J.Z., Puri, V.M., and Anderson, C.T. (2019). The stomatal flexoskeleton: how the biomechanics of guard cell walls animate an elastic pressure vessel. Journal of Experimental Botany *70*, 3561–3572.

Yoshida, A., Terada, Y., Toriba, T., Kose, K., Ashikari, M., and Kyozuka, J. (2016). Analysis of Rhizome Development in Oryza longistaminata , a Wild Rice Species. Plant and Cell Physiology *57*, 2213–2220.

Yoshida, S., Mandel, T., and Kuhlemeier, C. (2011). Stem cell activation by light guides plant organogenesis. Genes Dev *25*, 1439–1450.

Yoshii, M., Yamamoto, A., Kagaya, Y., Takeda, S., and Hattori, T. (2015). The Arabidopsis transcription factor NAI1 is required for enhancing the active histone mark but not for removing the repressive mark on PYK10, a seedling-specific gene upon embryonic-to-postgerminative developmental phase transition. Plant Signal Behav *10*, e1105418.

Yuan, L., Liu, Z., Song, X., Johnson, C., Yu, X., and Sundaresan, V. (2016). The CKI1 Histidine Kinase Specifies the Female Gametic Precursor of the Endosperm. Developmental Cell *37*, 34–46.

Yuan, T.-T., Xu, H.-H., Zhang, Q., Zhang, L.-Y., and Lu, Y.-T. (2018). The COP1 Target SHI-RELATED SEQUENCE5 Directly Activates Photomorphogenesis-Promoting Genes. The Plant Cell *30*, 2368–2382.

Yuan, T.-T., Xu, H.-H., Li, J., and Lu, Y.-T. (2020). Auxin abolishes SHI-RELATED SEQUENCE5-mediated inhibition of lateral root development in Arabidopsis. New Phytologist *225*, 297–309.

Yusuf, M. (2017). Computational Study of Bufadienolides from Indonesia's Kalanchoe Pinnata as Na /K -ATPase Inhibitor for Anticancer Agent. Journal of Young Pharmacists *9*, 475–479.

Zavattieri, M.A., Frederico, A.M., Lima, M., Sabino, R., and Arnholdt-Schmitt, B. (2010). Induction of somatic embryogenesis as an example of stress-related plant reactions. Electronic Journal of Biotechnology *13*, 12–13.

Zeng, F., Biligetu, B., Coulman, B., Schellenberg, M., and Fu, Y.-B. (2017). RNA-Seq Analysis of Plant Maturity in Crested Wheatgrass (Agropyron cristatum L.). Genes *8*, 291.

Zhang, Tucker, E., Hermann, M., and Laux, T. (2017a). A Molecular Framework for the Embryonic Initiation of Shoot Meristem Stem Cells. Developmental Cell *40*, 264-277.e4.

Zhang, H., Rider, S.D., Henderson, J.T., Fountain, M., Chuang, K., Kandachar, V., Simons, A., Edenberg, H.J., Romero-Severson, J., Muir, W.M., et al. (2008). The CHD3 remodeler PICKLE promotes trimethylation of histone H3 lysine 27. J Biol Chem *283*, 22637–22648.

Zhang, L., Li, Z., Quan, R., Li, G., Wang, R., and Huang, R. (2011). An AP2 Domain-Containing Gene, ESE1, Targeted by the Ethylene Signaling Component EIN3 Is Important for the Salt Response in Arabidopsis. Plant Physiology *157*, 854–865.

Zhang, M., Wu, H., Su, J., Wang, H., Zhu, Q., Liu, Y., Xu, J., Lukowitz, W., and Zhang, S. (2017b). Maternal control of embryogenesis by MPK6 and its upstream MKK4/MKK5 in Arabidopsis. The Plant Journal *92*, 1005–1019.

Zhang, S., Wong, L., Meng, L., and Lemaux, P.G. (2002). Similarity of expression patterns of knotted1 and ZmLEC1 during somatic and zygotic embryogenesis in maize (Zea mays L.). Planta *215*, 191–194.

Zhang, T.-Q., Lian, H., Zhou, C.-M., Xu, L., Jiao, Y., and Wang, J.-W. (2017c). A Two-Step Model for de Novo Activation of WUSCHEL during Plant Shoot Regeneration. Plant Cell *29*, 1073–1087.

Zhang, Z., Tucker, E., Hermann, M., and Laux, T. (2017d). A Molecular Framework for the Embryonic Initiation of Shoot Meristem Stem Cells. Developmental Cell *40*, 264-277.e4.

Zhang, Z., Runions, A., Mentink, R.A., Kierzkowski, D., Karady, M., Hashemi, B., Huijser, P., Strauss, S., Gan, X., Ljung, K., et al. (2020). A WOX/Auxin Biosynthesis Module Controls Growth to Shape Leaf Form. Current Biology *30*, 4857-4868.e6.

Zhao, Y. (2010). Auxin biosynthesis and its role in plant development. Annu Rev Plant Biol *61*, 49–64.

Zhao, Y. (2018). Essential Roles of Local Auxin Biosynthesis in Plant Development and in Adaptation to Environmental Changes. Annu. Rev. Plant Biol. *69*, 417–435.

Zhao, P., Begcy, K., Dresselhaus, T., and Sun, M.-X. (2017). Does Early Embryogenesis in Eudicots and Monocots Involve the Same Mechanism and Molecular Players? Plant Physiol *173*, 130–142.

Zhao, Y., Christensen, S.K., Fankhauser, C., Cashman, J.R., Cohen, J.D., Weigel, D., and Chory, J. (2001). A Role for Flavin Monooxygenase-Like Enzymes in Auxin Biosynthesis. Science *291*, 306–309.

Zheng, W., Zhang, X., Yang, Z., Wu, J., Li, F., Duan, L., Liu, C., Lu, L., Zhang, C., and Li, F. (2014). AtWuschel promotes formation of the embryogenic callus in Gossypium hirsutum. PLoS One *9*, e87502.

Zheng, Z., Xia, Q., Dauk, M., Shen, W., Selvaraj, G., and Zou, J. (2003). Arabidopsis AtGPAT1, a Member of the Membrane-Bound Glycerol-3-Phosphate Acyltransferase Gene Family, Is Essential for Tapetum Differentiation and Male Fertility. The Plant Cell *15*, 1872–1887.

Zhong, T., Zhu, C., Zeng, H., and Han, L. (2013). Analysis of gene expression in Kalanchoe daigremontiana leaves during plantlet formation under drought stress. Electronic Journal of Biotechnology *16*, 4–4.

Zhou, J.-J., and Luo, J. (2018). The PIN-FORMED Auxin Efflux Carriers in Plants. Int J Mol Sci *19*.

Zhou, H., Duan, H., Liu, Y., Sun, X., Zhao, J., and Lin, H. (2019). Patellin protein family functions in plant development and stress response. Journal of Plant Physiology *234–235*, 94–97.

Zhou, T., Yang, X., Guo, K., Deng, J., Xu, J., Gao, W., Lindsey, K., and Zhang, X. (2016). ROS Homeostasis Regulates Somatic Embryogenesis via the Regulation of Auxin Signaling in Cotton. Mol Cell Proteomics *15*, 2108–2124.

Zhou, X., Hao, H., Zhang, Y., Bai, Y., Zhu, W., Qin, Y., Yuan, F., Zhao, F., Wang, M., Hu, J., et al. (2015). SOS2-LIKE PROTEIN KINASE5, an SNF1-RELATED PROTEIN KINASE3-Type Protein Kinase, Is Important for Abscisic Acid Responses in Arabidopsis through Phosphorylation of ABSCISIC ACID-INSENSITIVE5. Plant Physiology *168*, 659–676.

Zhou, Y.P., Wu, J.H., Xiao, W.H., Chen, W., Chen, Q.H., Fan, T., Xie, C.P., and Tian, C.-E. (2018). Arabidopsis IQM4, a Novel Calmodulin-Binding Protein, Is Involved With Seed Dormancy and Germination in Arabidopsis. Front. Plant Sci. *9*.

Zhu, C., Wang, L., Chen, J., Liu, C., Zeng, H., and Wang, H. (2017). Over-expression of KdSOC1 gene affected plantlet morphogenesis in Kalanchoe daigremontiana. Sci Rep *7*, 5629.

Zhu, H., Li, G.-J., Ding, L., Cui, X., Berg, H., Assmann, S.M., and Xia, Y. (2009). Arabidopsis Extra Large G-Protein 2 (XLG2) Interacts with the Gβ Subunit of Heterotrimeric G Protein and Functions in Disease Resistance. Molecular Plant *2*, 513–525.

Zhu, R., Dong, X., Xue, Y., Xu, J., Zhang, A., Feng, M., Zhao, Q., Xia, S., Yin, Y., He, S., et al. (2020). Redox-Responsive Transcription Factor 1 (RRFT1) Is Involved in Extracellular ATP-Regulated Arabidopsis thaliana Seedling Growth. Plant Cell Physiol *61*, 685–698.

Zhu, Y., Wang, Y., Li, R., Song, X., Wang, Q., Huang, S., Jin, J.B., Liu, C.-M., and Lin, J. (2010). Analysis of interactions among the CLAVATA3 receptors reveals a direct interaction between CLAVATA2 and CORYNE in Arabidopsis. Plant J *61*, 223–233.

Zubo, Y.O., Blakley, I.C., Yamburenko, M.V., Worthen, J.M., Street, I.H., Franco-Zorrilla, J.M., Zhang, W., Hill, K., Raines, T., Solano, R., et al. (2017). Cytokinin induces genome-wide binding of the type-B response regulator ARR10 to regulate growth and development in Arabidopsis. Proc. Natl. Acad. Sci. U.S.A. *114*, E5995–E6004.

Zuo, J., Niu, Q.-W., Frugis, G., and Chua, N.-H. (2002). The WUSCHEL gene promotes vegetative-to-embryonic transition in Arabidopsis. The Plant Journal *30*, 349–359.

Zürcher, E., Tavor-Deslex, D., Lituiev, D., Enkerli, K., Tarr, P.T., and Müller, B. (2013). A Robust and Sensitive Synthetic Sensor to Monitor the Transcriptional Output of the Cytokinin Signaling Network in Planta1[C][W][OA]. Plant Physiol *161*, 1066–1075.

Zürcher, E., Liu, J., Donato, M. di, Geisler, M., and Müller, B. (2016). Plant development regulated by cytokinin sinks. Science *353*, 1027–1030.

Zwanenburg, B., and Blanco-Ania, D. (2018). Strigolactones: new plant hormones in the spotlight. J Exp Bot *69*, 2205–2218.